ENVIRONMENTAL RESEARCH

RESEARCH AND TECHNOLOGY BRANCH

Environment
Ontario
Jim Bradley, Minister

ISBN 0-7729-6205-7 (2 vol. set)
0-7729-6206-5 (vol. 1)

EFFECTS OF INCREASING AMOUNTS OF NON-POLAR ORGANIC LIQUIDS IN DOMESTIC WASTE LEACHATE ON THE HYDRAULIC CONDUCTIVITY OF CLAY LINERS IN SOUTHERN ONTARIO

R. A. C. PROJECT NO. 213 PL/364 G

VOLUME 1

Report prepared for Environment Ontario by:

Robert M. Quigley
and
Federico Fernandez

Faculty of Engineering Science
University of Western Ontario
London, Ontario   N6A 5B9

PRINTED: OCTOBER 1989
REPRINTED: DECEMBER 1989

RECYCLABLE

Copyright: Queen's Printer for Ontario, 1989
This publication may be reproduced for non-commercial purposes with appropriate attribution.

90-01834/

DISCLAIMER

This report has been reviewed by the Research Advisory Committee of Environment Ontario and approved for publication. Approval does not necessarily signify that the contents reflect the views nor does mention of trade names or commercial products constitute endorsement or recommendation for use.

FORWARD

Sanitary landfilling remains a viable alternative for disposal of ever increasing volumes of solid waste. Current landfill design practice requires the presence of a clay barrier (liner) that may consist of either a natural stratum or compacted clay borrow. The liner acts as a hydraulic barrier to control the flux of contaminants from the waste into the adjacent groundwater. In order to do this, clay liners are required to have a hydraulic conductivity, **k**, less than 10^{-7} or 10^{-8} cm/s, and testing may be required to prove that **k** will not increase during exposure to leachate.

This report presents the results of a three-year research study to assess of compatibility between a natural clay from Southern Ontario and domestic waste leachate containing increasing amounts of organic solvents. The objective was to simulate leachates where co-disposal practices might have taken place or accidental spills of concentrated organics might have occurred close to a water-wet barrier clay. The clay/leachate compatibility studies were performed using fixed-ring permeameters that permitted control of the applied confining effective stresses, measurement of volume changes in the soil specimen, and assessment of the chemistry of the influent and effluent permeants.

Two water-soluble organic liquids (ethanol and dioxane) were used in concentrated form and added to domestic waste leachate in various percentages.

The test permeants were then passed through water-compacted clays to assess the impact on hydraulic conductivity at effective stresses varying from 0 kPa (Project #213 PL) to 160 kPa (Project #364 G). A special set of experiments were also run on leachate-moulded clays to study the effects of pre-compaction flocculation on **k**. An executive summary precedes the main body of this report which includes a literature review as well as a large body of original research. Extensive use is made of Appendices for detailing the data leading to the results presented in the main text. This MOE sponsored work on soluble organics has been incorporated in the doctoral thesis of F. Fernandez, which included NSERC funded work on insoluble organics. The thesis in draft form was submitted to Mr. Maurice Goodwin as a final progress report in April 1989. A final copy of the bound thesis will also be presented to MOE.

The support of the Ontario Ministry of the Environment is greatly appreciated. In particular, the supportive role and the incisive, useful and critical comments of our Liaison Officer, Mr. Maurice Goodwin were much appreciated throughout the tenure of the grant.

EXECUTIVE SUMMARY

This research project was carried out to determine the effect that leachates containing increasing amounts of soluble organic liquids may have on the integrity of clay barriers used as liners for waste impoundment facilities. Such leachate mixtures presumably exist at old co-disposal sites and recent sites where illegal or accidental tipping may have occurred. The compatibility of clays with respect to waste leachates was studied using hydraulic conductivity, k, as the assessment tool. Testing was performed using a computer controlled, constant flow rate, fixed-ring permeameter apparatus. The equipment was specially designed to permit application of static effective stresses, to monitor volume changes in the soil during testing, and to allow for collection and chemical analysis of effluent permeants.

The test soils were obtained from a clay deposit near Sarnia, Ontario, and consisted of abundant illite, chlorite, quartz, feldspar, carbonate and a variable amount of smectite formed by oxidation weathering of chlorite. Based on its convenient availability, its high smectite content (up to 15%) and low hydraulic conductivity, the re-compacted, brown surface clay (0.3 m in depth) was selected as the principal test soil for this study. Selected additional tests were performed using undisturbed samples of grey, unweathered Sarnia clays containing less that 2% smectite, since they actually form the containment system for organic wastes in the Sarnia area.

The test permeants consisted of municipal solid waste leachate containing increasing amounts of soluble organic solvents. The leachate was collected at the Westminster Sanitary landfill, City of London, Ontario, and is considered to be representative of raw domestic waste leachate. Ethanol (ethyl alcohol) and dioxane (diethylene ether) were the two organic solvents selected for this study since they are both soluble in water and consequently can form a full range of leachate/organic mixtures. Furthermore, ethanol and dioxane are liquids of intermediate and very low polarity (and dielectric constant), thus covering the behaviour expected of most soluble organics.

The Sarnia clays appear to be compatible with municipal landfill leachate, even at low stress levels, since they underwent slight decreases in k on leachate permeation. This was in spite partial c-axis contraction caused by K^+ and NH_4^+ adsorption.

Concentrated ethanol and dioxane increased the hydraulic conductivity of water-compacted brown clays by 100 and 1000-fold, thus destroying their effectiveness as liners if permeated at low stress levels. The increases in k resulted from double layer contraction in the presence of low dielectric pore fluids, and the consequent creation of more "free" pore space for flow.

Leachates containing less than ~ 70% organics (ethanol and dioxane) showed no adverse effects on the hydraulic conductivity of water-compacted clays. In fact, significant decreases in k were observed that are related to increases in permeant viscosity which prevail over dielectric constant effects at the lower organic concentrations.

The addition of soluble organic liquid to leachate markedly alters the physico/chemical properties of the resultant permeant. The dielectric constant decreases steadily with increasing organic content, while the permeant viscosity increases to a maximum two or three times greater than that of water at intermediate organic contents before it decreases again to values typical of the added organic liquid.

Concentrations of organics greater than 80% caused increases in **k** at low confining stresses, resulting from double layer collapse and macropore development in the presence of low dielectric pore fluid as noted above for the pure organic liquids. These findings were confirmed by two special tests for leachate containing 40% and 85% dioxane, run at a constant hydraulic gradient of 20 using larger cells. Additional testing on undisturbed samples of unweathered, grey clay revealed that concentrated ethanol caused increases in **k** which were of much lower magnitude than those for the brown, weathered, smectitic, surface clays.

The application of static confining stresses to the water-wet soil samples may cause sufficient vertical consolidation and K_o induced lateral creep to close chemically enlarged flow paths, greatly reducing or preventing large increases in **k**. For ethanol, in-place static stresses, σ'_v, of only 40 kPa are needed to eliminate the increases in **k**, whereas for high concentrations of non-polar dioxane increases in **k** occurred even at σ'_v stresses of 160 kPa. Effective stresses applied subsequent to the large increases in **k** produced by concentrated dioxane at $\sigma'_v = 0$, failed to improve the soil. The exposure of clays to dioxane at low stresses causes the clay structure to strengthen so that "corrective" stresses produce little remedial consolidation and little reduction in **k**. This suggests that the confining stresses must be in place on the water-compacted barrier prior to contact with highly reactive organic liquids, in order that beneficial consolidation may occur.

A series of tests run on dried clays moulded with leachate/hydrocarbon mixtures prior to compaction have shown that flocculation effects are a dominant factor controlling the values of **k**. The flocculated soil structures result in significantly higher values of **k** than the water-compacted clays, suggesting that water and leachates contaminated with organics should not be used as the moulding liquid prior to clay liner compaction.

TABLE OF CONTENTS

Page

VOLUME 1:

FORWARD ii

EXECUTIVE SUMMARY iv

TABLE OF CONTENTS viii

CHAPTER 1 - INTRODUCTION 1

1.1 General 1
1.2 Options for Waste Management 2
1.3 Sanitary Landfills 3
1.4 Scope of the Project 5

CHAPTER 2 - HYDRAULIC CONDUCTIVITY OF CLAY BARRIERS: A REVIEW 9

2.1 General 9
2.2 Hydraulic Conductivity of Clays 10
2.2.1 Clay Minerals 10
2.2.2 Diffuse Double Layers 11
2.2.3 Soil Fabric and Hydraulic Conductivity 16
2.2.4 Hydraulic Conductivity of Compacted Clays 18
2.2.5 Laboratory Testing for Hydraulic Conductivity 21
2.2.6 The Influence of Testing Conditions on **k** 22
2.3 The Effect of Waste Leachates on **k** 24
2.3.1 Domestic Waste Leachate 27
2.3.2 Concentrated Organic Solvents 28
2.3.3 Aqueous Solutions of Organic Solvents 32
2.4 Concluding Remarks 33

CHAPTER 3 - HYDRAULIC CONDUCTIVITY TESTING EQUIPMENT .. 46

3.1 Introduction 46
3.2 Fixed-ring Permeameter 47
3.2.1 Cell Description 47
3.2.2 Soil Preparation 48
3.3 Constant Flow Hydraulic Conductivity Equipment 50
3.4 Constant Head Hydraulic Conductivity Equipment 53
3.5 Chemical Analyses of Influent and Effluent Samples 54
3.6 Post-testing Assessment 54
3.7 Concluding Remarks 55

Page

CHAPTER 4 - TESTING MATERIALS 68

4.1 Introduction 68
4.2 Soil Properties 68
4.3 Properties of the Permeants 72
4.3.1 Domestic Landfill Leachate 73
4.3.2 Aqueous Solutions of Hydrocarbons 74
4.3.3 Physico-chemical Stability of Leachate/Hydrocarbon Mixtures 76

CHAPTER 5 - PERMEATION OF CLAYS WITH DOMESTIC LEACHATE CONTAINING HYDROCARBON LIQUIDS 98

5.1 Introduction 98
5.2 Permeant Compacted Clays 99
5.2.1 Ethanol/Water/Clay Mixtures 100
5.2.2 Dioxane/Water/Clay Mixtures 101
5.2.3 Leachate/Hydrocarbon/Clay Mixtures 102
5.2.4 Discussion of the Data 102
5.3 Water-saturated Clays 105
5.3.1 Leachate/Ethanol Mixtures on Compacted Brown Clay 106
5.3.2 Leachate/Dioxane Mixtures on Compacted Brown Clay 108
5.3.3 The Importance of Effective Stress Levels 110
5.3.4 Leachate/Ethanol Mixtures on Undisturbed Grey Clay 115
5.4 Post-testing Sample Assessment 116

CHAPTER 6 - DISCUSSION AND INTERPRETATION OF RESULTS 145

6.1 Introduction 145
6.2 The Role of Permeant Viscosity 145
6.3 Exclusion of Non-polar Organics from Double Layers 147
6.4 Confirmation Tests Using Larger Cells and Lower Gradients 151

CHAPTER 7 - CONCLUSIONS 168

7.1 Summary and Conclusions 168

REFERENCES 172

* * * * * *

Page

VOLUME 2:

APPENDIX A - EVAPORATION CURVES FOR VARIOUS LIQUIDS 179

APPENDIX B - INTERCONVERSION FORMULAS FOR COMPOSITION OF LIQUID SOLUTIONS 183

APPENDIX C - MEASUREMENT OF DIELECTRIC CONSTANT OF LIQUID PERMEANTS 190

APPENDIX D - HYDRAULIC CONDUCTIVITY CURVES FOR PERMEANT/CLAY MIXTURES 194

APPENDIX E - HYDRAULIC CONDUCTIVITY CURVES FOR WATER-COMPACTED BROWN SARNIA CLAY PERMEATED WITH LEACHATE/ETHANOL MIXTURES 227

APPENDIX F - HYDRAULIC CONDUCTIVITY CURVES FOR WATER-COMPACTED BROWN SARNIA CLAY PERMEATED WITH LEACHATE/DIOXANE MIXTURES 253

APPENDIX G - HYDRAULIC CONDUCTIVITY CURVES FOR UNDISTURBED GREY SARNIA CLAY PERMEATED WITH LEACHATE/ETHANOL MIXTURES 271

APPENDIX H - EFFLUENT CONCENTRATION CURVES FOR INORGANIC SPECIES WATER-COMPACTED BROWN SARNIA CLAY PERMEATED WITH LEACHATE/ETHANOL MIXTURES 277

APPENDIX I - EFFLUENT CONCENTRATION CURVES FOR INORGANIC SPECIES WATER-COMPACTED BROWN SARNIA CLAY PERMEATED WITH LEACHATE/DIOXANE MIXTURES 285

APPENDIX J - PORE SIZE DISTRIBUTION CURVES OBTAINED BY MERCURY INTRUSION POROSIMETRY 297

CHAPTER 1

INTRODUCTION

1.1 GENERAL

From the beginning man has intruded on the environment using water, fire and tools, which have allowed him to evolve and control nature beyond any other species on earth. However, the damaging impact of man's activities on the environment has become, during recent years, a subject of growing concern among all sectors of the community. This increased awareness is driven by abundant sources of information available to the general public, and by advanced technologies that enable detection of environmental stresses that in the past would have occurred unnoticed.

One of the major issues in the overall environmental problem is the disposal of man's waste products. The highly industrialized societies of today generate enormous quantities of waste that challenge the ability of nature to accommodate them. During the last two decades the amount of solid waste produced in North America has doubled, with significant increases in the per-capita rates. The United States produces over 160 million tonnes of municipal solid waste per year (Kohn and Pinyan, 1987). This figure corresponds to a per capita production of about 2 kg/day, which is estimated to apply to Canada as well.

1.2 OPTIONS FOR WASTE MANAGEMENT

Traditional methods of waste disposal, such as open dumping or burning, have been practised for centuries with little impact on the environment. However, during recent years both techniques have become environmentally unacceptable due to the increased volumes and the increasingly complex nature of wastes. Incineration of wastes requires temperatures greater than 800°C to 1100°C and residence times between 0.5 and 2 seconds to achieve complete combustion of the waste. Low combustion temperatures and short dwelling times may result in some very toxic, highly stable, organic compounds (such as dioxins) being released into the atmosphere. Uncontrolled land disposal of wastes has produced numerous cases of groundwater contamination. In most cases, the problem was detected only after large areas of soil were affected, making remedial efforts very costly and of limited success.

Ocean dumping is defined as the placement of waste in deep marine sediments. This method relies on two mechanisms for attenuation of pollutants: massive dilution by the large body of water and degradation of the pollutants by natural processes. The sea disposal option is strongly criticized by ecological groups, due to the uncertainties around the long-term effects on fishing and sea life in general.

Deep well injection into permeable geological formations has been used extensively by the oil industry for disposal of pumpable liquid wastes. This practise requires thorough knowledge of the geological formations and the hydrogeological regime, to ensure that the waste is permanently confined.

Other waste management options such as chemical or biological treatments are only applicable to specific types of waste, in order to be cost-effective. Examples of chemical treatments are neutralization, precipitation, oxidation, reduction and photolysis. Biological methods are applied to organic materials that can be degraded into innocuous components by the action of naturally occurring micro-organisms. Biological methods offer excellent results provided that the concentration of the contaminants remains below inhibitory levels.

The ultimate goal in waste management is summarized by the "4 R's" (Sibul, 1988); **reduction, recycling, recovery** and **re-use** of waste materials. Today, these ideal practices have major limitations, but are likely to grow with sound economic/environmental compromises. In the meantime, the most widespread option for disposal of solid waste in North America is sanitary landfilling: a relatively inexpensive and safe practice.

1.3 SANITARY LANDFILLS

Sanitary landfills are engineered earth structures, where the waste is spread in layers, compacted, and covered with soil at the end of each working day. Covering the waste prevents proliferation of insects, rodents and other pests, reducing odours and the probability of fires initiated by spontaneous combustion or arson. Landfills can be constructed above ground surface or in an excavated trench, and ideally the waste they accommodate should be inert or biodegradable. Some landfill facilities, however, may be licensed to receive hazardous wastes, primarily from industrial sources.

Figure 1.1 shows the schematic cross-sectional view of a typical, pumped, landfill facility. Water from snow and rain percolates through the waste, forming an aqueous solution of soluble waste constituents called "leachate". The composition and volumes of leachate are largely dependent on climate and type of wastes. Since contaminants are carried by the leachate, it is important to reduce the quantity of leachate generation. This is achieved by placing an impermeable soil cover on top of the waste. Vegetation is commonly placed on the final soil cover for aesthetic reasons and also to preserve the integrity of the soil (i.e. resist erosion). The soil cover also prevents leachate discharge to surface water streams and it allows for the collection or controlled release of gases formed during decomposition of the waste. A compacted clay liner, typically 1 to 4 metres in thickness (Quigley et al., 1984), serves as a barrier to limit the migration of contaminants into the surrounding hydrogeologic environment. The leachate collection system maintains low hydraulic gradients across the liner, thus reducing the advective transport of contaminants and often limiting the chemical flux to diffusion processes. The collected leachate is normally treated at a sewage treatment plant.

The effectiveness of a clay liner as a barrier for contaminants can be dramatically reduced by exposure to certain waste liquids. Recent studies by various investigators have shown that some organic liquids, less polar than water, can increase the hydraulic conductivity of clayey soils to values typical of sands. These liquids are commonly used by industries as metal cleaners, dyes, intermediary chemicals, etc. A study by Proctor and Redfern (1982) estimates that the total waste produced by industries in Ontario during 1981 was 1.5 million tonnes. As shown in Figure 1.2, organic liquid waste amounts to 16.5% (224,800 tonnes), including spent solvents, oils, greases and aqueous solutions of organics.

1.4 SCOPE OF THE PROJECT

This report presents the results of studies carried out to assess the effect mixtures of domestic landfill leachate and organic solvents on the hydraulic conductivity of natural clays from southern Ontario. The testing program was carried out under controlled conditions in the laboratory in a manner designed to define the mechanisms of interaction between clay and permeant liquids.

The report consists of seven chapters and ten appendices. The first chapter introduces the project and is followed by a general literature review on the hydraulic conductivity of clays in relation to waste leachates (Chapter 2). The testing equipment and materials are described in Chapter 3 and 4, respectively.

Chapters 5 presents the results of clay/permeant compatibility studies involving domestic leachate containing increasing amounts of organics. A general discussion is presented in Chapter 6, followed by a summary and conclusions in Chapter 7. Finally, supplementary information is given in Appendices A to J.

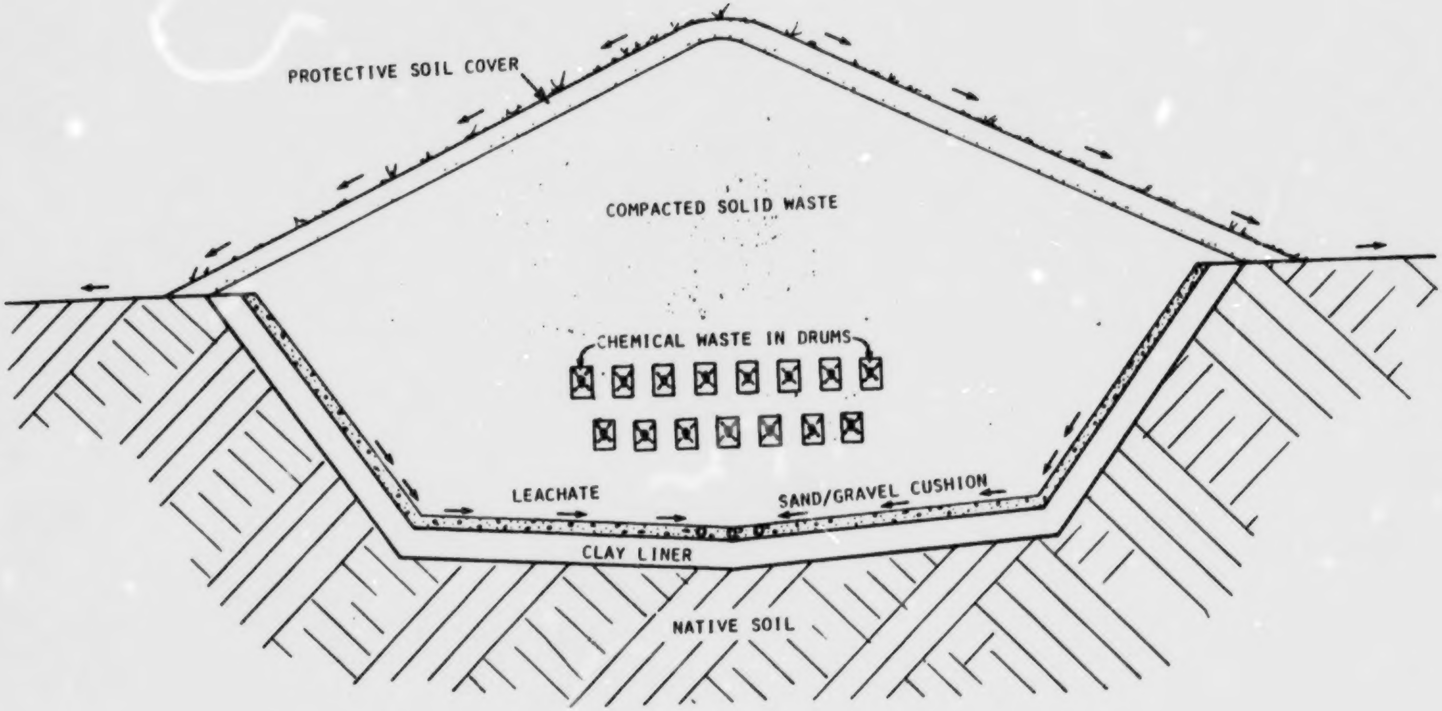
PROTECTIVE SOIL COVER
COMPACTED SOLID WASTE
CHEMICAL WASTE IN DRUMS
LEACHATE
SAND/GRAVEL CUSHION
CLAY LINER
NATIVE SOIL

FIGURE 1.1 SCHEMATIC CROSS SECTION OF A TYPICAL, SANITARY LANDFILL CELL WITH A LEACHATE COLLECTION SYSTEM (adapted from Montague, 1982)

Source: Proctor and Redfern Ltd. (1982)

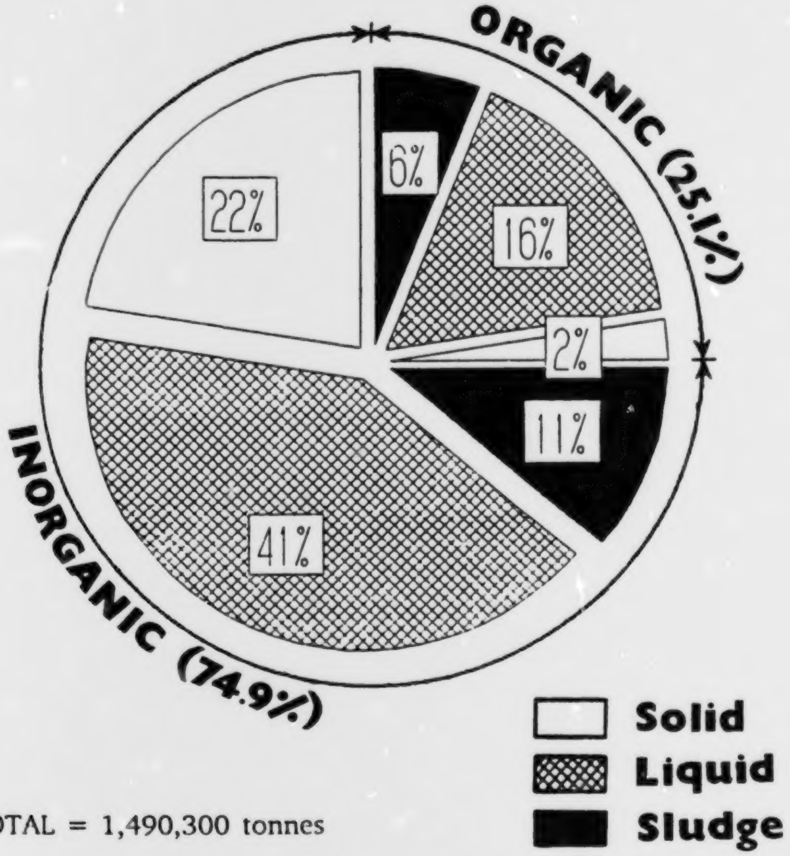

TOTAL = 1,490,300 tonnes

FIGURE 1.2 ESTIMATED WASTE GENERATED BY INDUSTRIES IN ONTARIO DURING 1981

CHAPTER 2

HYDRAULIC CONDUCTIVITY OF CLAY BARRIERS: A REVIEW

2.1 GENERAL

The hydraulic conductivity, **k**, is a fundamental property of soils that measures the ease with which a specific fluid can flow through the soil mass. Based on his laboratory work on sands, Darcy (1856) proposed an empirical relationship describing the hydraulic flow through porous media:

$$v = \mathbf{k}\, i$$

where the discharge velocity (rate of flow), v, is directly proportional to the hydraulic gradient (driving force), i.

The importance of **k** in geotechnical problems involving consolidation, stability and seepage has been long recognized, and various testing techniques were developed for its measurement. However, clayey soils have been traditionally regarded as "impervious" for most practical applications and would seldom be subjected to permeability testing. More recent applications of clays, such as hydraulic barriers for hazardous waste and other impoundments, has often required the geotechnical engineers to evaluate the hydraulic conductivity of fine grained soils and to understand the factors controlling it.

This chapter presents a review of fundamental concepts related to the hydraulic conductivity of clays. This is followed by a description of the published clay/leachate compatibility studies involving domestic landfill leachate and organic solvents.

2.2 HYDRAULIC CONDUCTIVITY OF CLAYS

Clays are fine-grained soils containing enough clay mineral particles to exhibit plastic and cohesive behaviour. Clay particles are very small, have large surface areas and consequently their behaviour is controlled by physico-chemical interactions among particle surfaces. Thus, while the hydraulic conductivity of coarse-grained soils is controlled mainly by particle sizes, various other factors such as mineral composition and soil fabric influence the hydraulic conductivity of clays.

2.2.1 Clay Minerals

Clay minerals are hydrous aluminum silicates carrying a net negative charge resulting from imperfection in their crystal structures. Clay minerals are commonly formed from weathering of parent materials such as rocks and occur in particles of small size. In geotechnical practise the clay fraction of a soil refers to the particles smaller than 2 μm (M.I.T. soil classification system). The clay fraction of a soil may not coincide with its clay mineral content, due to the presence of non-clay minerals (such as rock flower) finer than 2 μm or clay mineral particles coarser than 2 μm (Mitchell, 1976).

The structure of most clay minerals consists of stacks of crystal sheets. The two types of crystal sheets in clay minerals are the tetrahedral or silica and the octahedral or alumina sheets. The tetrahedral sheet consists of silicon atoms tetrahedrally coordinated with oxygen atoms, and the octahedral sheet consists of aluminum atoms octahedrally coordinated with six oxygens or hydroxyls. Isomorphous substitution of different cations in the crystal sheets leads to the formation of different clay minerals, depending on the type and amount of cations involved. Kaolinite, illite, smectite and chlorite are the main clay minerals groups, characterized by the arrangement of the crystal sheets and by the type of cations they contain. For detailed descriptions of the clay mineral groups the reader is referred to Grim (1953) and Mitchell (1976).

Typical isomorphous substitutions in clay minerals include aluminum (Al^{3+}) for silicon (Si^{4+}) in the tetrahedral sheet, and magnesium (Mg^{2+}) for aluminum (Al^{3+}) in the octahedral sheet. Such replacements result in charge deficiency and a net negative charge within and at the surface of the clay particle. The magnitude of the surface charge density, σ, ranges from 36,200 esu/cm^2 for montmorillonite to 115,900 esu/cm^2 for chlorite (Table 2.1).

2.2.2 Diffuse Double Layers

In a soil system, the cations present in the pore water are electrostatically attracted to the negatively charged surfaces of clay particles. At the same time, these cations tend to diffuse back to the bulk pore fluid, where their concentration is smaller (van Olphen, 1963). These two opposite trends give rise to a spacial ionic distribution (ionic layer) in the liquid surrounding the charged surface (charge layer), called the diffuse Gouy double layer. The distribution of ions adjacent to a clay particle surface is shown in Figure 2.1 (Mitchell, 1976). Cation concentrations decrease with the distance from the clay particle surface, while anion concentrations increase towards the bulk pore fluid. The electric potential, ψ, decreases exponentially with the distance, x, perpendicular to the particle surface, and for $\psi << 25$ mV can be expressed as follows:

$$\psi = \psi_o e^{-Kx}$$

where: ψ_o = electric potential at surface of clay particle

$K = \sqrt{(8\pi e^2 n z^2)/(\epsilon k T)}$ (cm^{-1})

ϵ = dielectric constant of the pore liquid

k = Boltzmann's constant (1.38×10^{-16} erg/°K)

T = absolute temperature (°K)

e = elementary (electron) charge (4.803×10^{-10} esu)

n = number of cations per cm^3 of bulk pore fluid

z = valence of cations

The value 1/K is known as the Debye characteristic length and represents the thickness of the double layer (van Olphen, 1963) and its magnitude is dependent upon the pore fluid properties; electrolyte concentration (n), cation valence (n), dielectric constant (ϵ) and temperature (T).

A general expression can be obtained (Bolt, 1955) describing a roughly exponential decay of electric potential in the double layer:

$$\psi = -\frac{k\,T}{e\,Z} \ln\left[\coth^2(Kx/2)\right]^{1}$$

The surface of a clay particle exhibits a constant surface charge density, σ, resulting from isomorphous substitution within the structure of the clay mineral. The electric potential at the surface of the clay particle, ψ_o, is determined by the properties of the pore fluid (n, z, ϵ and T). The magnitude of ψ_o can be obtained using the following equation, derived from Poisson's potential function (van Olphen, 1963):

$$\psi_o = \frac{k\,T}{e\,Z} \operatorname{arcsinh}\left[\sigma \sqrt{(\pi/2n\epsilon kT)}\right]^{1}$$

This equation is based on the Gouy model of electric double layers, where ions are considered as point charges. Ions have a finite size and therefore their maximum concentration near the clay particle surface is limited by the size of these ions. The Stern model considers a more realistic case where the electric

---

[1] A potential of 1 esu is equivalent to 299,790 mV

potential across a layer of closely packed ions (Stern layer) decreases linearly with distance from ψ_o to ψ_δ. The size of the Stern layers increases with the size of the adsorbed ionic species, projecting the double layers further into the pore fluid.

A quantitative description of the influence of the soil system variables on the values of ψ_o and 1/K is presented in Table 2.1. These values were calculated using the formulas described above (Gouy model) for montmorillonite and chlorite clays and pore liquids ranging from water to benzene. For a given pore liquid the electric surface potential of chlorite is larger than that of montmorillonite, reflecting the higher charge density of chlorite. The values of ψ_o decrease with increasing electrolyte concentration, decreasing cation valence and decreasing dielectric constant. For all other variables held constant, the double layer "thickness" (1/K) shows significant decreases with decreasing dielectric constant, increasing cation valence and increasing electrolyte concentration.

The results of a quantitative assessment of electric potential distribution in double layers using the equations previously described are summarized in Figure 2.2. A dilute (10^{-4} Molar) solution of monovalent ions in water at 20°C exhibits the electric potential distribution shown in Figure 2.2a. The electric potential approaches infinity at an imaginary plane corresponding to $x = 0$. The surface of the clay particle corresponds to the plane located at $x = x_o$, where the electric potential has a finite value equal to ψ_o. It is evident that for dilute electrolyte concentrations the distance x_o is very small relative to the double layer size. Therefore, according to the Gouy model the distribution of electric potential and double layer thickness (1/K) are practically independent of the clay mineral type. However, the clay mineral may influence the type of cation being adsorbed and thus affect the Stern layer and double layer size.

The curves in Figures 2.2b to 2.2c describe dramatic decreases in electric potential with increasing electrolyte concentration, increasing valence and decreasing dielectric constant. An increase in temperature causes an increase in electric potential across the double layer. However, in most fluids ϵ decreases with increasing temperature and thus the dielectric constant effect counteracts the temperature effect on the double layers (Mitchell, 1976). For the range of permeants used in this project it is estimated that a temperature variation of 60°C would alter the double layer thickness by less than 10%.

While the clay mineral type may have little effect on the double layer thickness, the amount of adsorbed water in the double layers relative to the total volume of pores varies greatly with the mineral type. The following example illustrates the volumes of water adsorbed in 1 nm thick double layers for saturated clays at a void ratio of 2.5:

CLAY MINERAL	SPECIFIC SURFACE (m^2/g)	VOLUME OF ADSORBED WATER IN DOUBLE LAYERS (% Pore Volume)
Kaolinite	20	~ 2%
Illite	100	~ 9%
Montmorillonite	800	~ 70%

The water molecules that hydrate cations in the double layers of a clayey soil are less mobile than the water in the bulk pore fluid. Consequently, the "adsorbed" water reduces the cross-sectional area available for permeant flow. It is evident that double layer contraction due to changes in the pore fluid chemistry can cause large increases in the hydraulic conductivity of the soil. The effect is more pronounced for clays where double layers occupy a large portion of their pores, i.e. clays having large specific surfaces.

2.2.3 Soil Fabric and Hydraulic Conductivity

Soils are multiphase systems, containing solid, liquid and gas. The solid phase is generally made up of particles of different minerals, while water and air are the usual components of the liquid and gas phases filling the soil pores. The fabric of a soil refers to the arrangement of particles, groups of particle and pore spaces, and it exerts a strong influence on the physical properties of the soil system, in particular its hydraulic conductivity. Van Olphen (1963) classified the fabric of clay suspensions based on the arrangement of the individual particles (dispersed or aggregated), and the arrangement of particle groups or aggregates (flocculated or deflocculated). Examples of three possible clay fabrics follow:

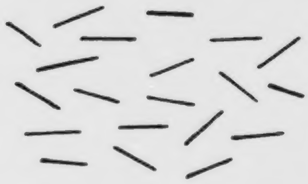
a) Dispersed and deflocculated

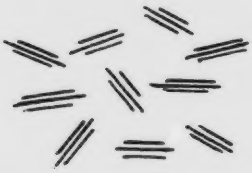
b) Aggregated and deflocculated

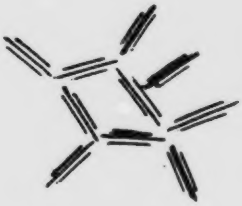
c) Aggregated and flocculated

The size of the pore spaces is significantly affected by the clay soil fabric. The dispersed and deflocculated clay (a) shows a large number of small pores, whereas the aggregated and flocculated clay (c) shows a lesser number of larger open pores. Since **k** increases with the square of the pore diameter, the flocculated clay is expected to be significantly more pervious than the dispersed clay at the same void ratio. The more dispersed the particles, i.e., the more nearly parallel they are, the more tortuous the paths for flow normal to the particles (Lambe and Whitman, 1979).

The fabric of a clayey soil is determined by forces of interaction between particles. The double layer repulsion and van der Waals attraction are the two main forces acting among the clay particles of a soil. Repulsive interparticle forces result from the electrostatic interaction of two or more adjacent double layers. The energy of repulsion decreases roughly exponentially with particle separation, and is largely affected by the properties of the pore liquid (n, z, ϵ and T). Van der Waals attractive forces result from charge fluctuations within individual atoms. The attractive energy decays rapidly with distance and is sensitive only to changes in dielectric constant and temperature (Mitchell, 1976).

In conclusion, either flocculation or dispersion of clay particles is promoted depending on whether the net energy of particle interaction is attractive or repulsive. The fabric of a clayey soil, and its hydraulic conductivity, are therefore very sensitive to changes in the chemistry of the system.

2.2.4 Hydraulic Conductivity of Compacted Clays

Compaction is the application of mechanical energy to a soil in order to increase its density. Cohesionless soils are most efficiently compacted under vibratory loads, while clayey soils require "kneading" action to alter its fabric. Compaction has traditionally aimed to improve the structural stability of a soil mass, i.e. increase its strength and reduce its susceptibility to undesirable volume changes (settlement, swelling, frost action, etc). Since compaction alters the soil fabric, it strongly affects the hydraulic conductivity of fine grained soils.

A thorough review of the factors affecting the permeability of compacted clay was presented by Mitchell, Hooper and Campanella (1965), following up the work by Lambe (1954) and Bjerrium and Huder (1957). Figure 2.3 illustrates the influence on dry density and permeability of the water content and energy of compaction. For a given energy of compaction, the dry density of the soil reaches a maximum value ($\rho_{d\,max}$) at the "optimum" water content (ω_{opt}). On the dry side of optimum, increasing water contents reduce the amount of air-filled voids, thus increasing both the saturation and density of the soil. The degree of saturation wet of optimum remains practically unchanged (typically S > 90%), and at increasing water contents the added water replaces solids, decreasing the soil density. Figure 2.3b shows that the density/water content relationship depends upon the energy of kneading compaction; the optimum water content decreases from ~ 20% for curve A (low energy) to ~ 16% for curve C (high energy). Additional energy applied dry of optimum is used to overcome capillary forces acting between particles of the unsaturated soil and to rearrange the soil particles into a denser configuration. On the wet side of optimum, however, the additional energy is absorbed by the water phase, resulting in transient excess pore water pressures without affecting the soil density.

The influence of moulding water content and amount of compactive effort on the hydraulic conductivity of cohesive soils is illustrated in Figure 2.3a, from Mitchell et al. (1965). The large variations in hydraulic conductivity at a given energy of compaction (over three orders of magnitude) reflects the strong control that the moulding water content has over the effect of compaction on soil fabric. For clays compacted dry of optimum the clay particles and aggregates are flocculated and resist rearrangement during compaction (Mitchell, 1976), yielding large values of **k**. Greatly decreased hydraulic conductivities are obtained at wet of optimum, where high shear strains by kneading compaction produce a more dispersed soil structure. Increasing energy of kneading compaction improves the degree of particle dispersion, resulting in lower **k**. For instance, samples compacted at a water content of 19% show a decrease of up to 10,000-fold with increasing compactive effort. At lower water contents (dry of optimum), the decreases in **k** are less pronounced suggesting that the soil fabric remains flocculated even after high energy kneading compaction.

The fabric of compacted clayey soils may change with time into a more flocculated state causing "thixotropic hardening" with increases in strength and hydraulic conductivity. Mitchell et al. (1965) reported significant increases (up to six-fold) in the **k** values of compacted silty clay after aging for 21 days.

2.2.5 Laboratory Testing for Hydraulic Conductivity

Laboratory measurements of hydraulic conductivity provide quantitative estimates of the suitability of clays as hydraulic barriers. Large numbers of laboratory **k** tests can be performed in relatively short times and at low costs to determine the influences of variables pertaining to both soil and permeant. The basic principal in a laboratory **k** test is to contain the test soil in a permeability cell and impose flow conditions upon the soil. The most common cell types include consolidation, fixed-wall and flexible-wall permeameters, and the tests can be run under conditions of constant head, falling head or constant flow.

A thorough discussion on the advantages and limitations of the different permeameter cells has been presented by Daniel et al. (1985). Briefly, the consolidation cells allow for testing of undisturbed samples under confining stresses with accurate measurements of changes in the sample volume. Fixed-wall (compaction mould) permeameters are extensively used for **k** measurements on compacted clays. This type of permeameter is usually not equipped for stress control or volume change measurement and has potential for side-wall leakage. Triaxial (flexible-wall) cells are suitable for testing of undisturbed samples, allowing for backpressure saturation, stress control and volume change measurements. Flexible wall tests are usually more costly and may lead to underestimating the **k** values of fractured or compressible clays.

Constant head tests are run by maintaining a constant hydraulic gradient through the soil sample and measuring the resultant flow rate. The main advantage of the constant head tests is the simplicity of interpretation of test results. In the falling head test, the hydraulic gradient decreases with time and the amount of flow is calculated from the head drop. The constant flow tests consist of forcing a known flow rate through the soil while measuring the induced hydraulic gradient across the sample by means of a pressure transducer. This testing technique allows for rapid and accurate measurements of **k** values.

2.2.6 The Influence of Testing Conditions on k

Laboratory testing conditions should be representative of actual field conditions. However, practical limitations of space and time often require a compromise. The following factors could contribute to significant discrepancies between laboratory and field values of hydraulic conductivity:

a) Sample Size and Disturbance: The sample size should be large enough so that all features of the tested soil are represented. Small samples could result in the exclusion of some features affecting the values of **k** such as grain size, soil layering, fissures, faults and open root holes.
Sample disturbance could also lead to discrepancies between laboratory and field values of **k**. Disturbance of clayey soils could cause particle orientation by shear, possible closure of fractures and consolidation on stress application that would cause lower values of **k**. In the case of stiff clays, fracture

opening would probably be the main problem, leading to large values of **k**.

b) Hydraulic Gradient: In most field situations hydraulic gradients acting on clay barriers are lower than 10. In order to reduce testing time, laboratory testing of fine-grained soils is often performed using gradients in excess of 100. High gradients produce large seepage forces that may result in particle migration and soil consolidation, leading to significant decreases in **k**.

c) Effective Confining Stress: Confining effective stresses may have an important effect on **k** by closing macropores and consolidating the test soil. Figure 2.4 shows the results of flexible-wall **k** tests on clays under variable confining stresses, reported by Daniel et al. (1985). The application of up to ~ 100 kPa confining stress to a clay sample containing desiccation cracks decreased **k** by a factor of 40. The same confining stresses applied to a similar sample of unfractured clay decreased **k** to about one third of its original value.

d) Degree of Saturation: Hydraulic conductivity decreases with decreasing degrees of saturation since the increasing gas phase in the soil reduces the pore space available for flow. Evidence of such behaviour in clayey soils has been presented by Bjerrium and Huder, 1957, Mitchell et al. (1965), and Olson and Daniel (1981). Therefore, testing performed using high hydraulic gradients or backpressure may overestimate the values of **k**, since the degree of saturation may be significantly increased.

e) Physical and Chemical Equilibria: Laboratory testing is performed to obtain short-term evaluations of **k** for fine grained soils. However, tests should not be terminated until all changes resulting from interactions between the permeant and the clay are completed. Large seepage stresses associated with permeation at high gradients may induce significant changes in the sample volume that could affect the initial flow measurements. The degree of saturation is likely to increase as permeation progresses, leading to higher **k**. Permeants of different composition than the original pore water may require long testing times to reach chemical equilibrium. In order to obtain more representative values of **k** the permeant should have the same chemistry as the initial pore water. This can be achieved by using pore water squeezed from the soil as permeant, or by matching the chemical composition of the pore water by dissolving selected salts in the permeant. The use of distilled water as permeant can lead to low values of **k** resulting from dispersion, particle migration and clogging of the pores (Olson and Daniel, 1981).

2.3 THE EFFECT OF WASTE LEACHATES ON k

The compatibility between waste leachate and clays is often evaluated by performing hydraulic conductivity tests. Since the chemical composition of leachates is usually radically different from the composition of the soil pore fluid, leachate permeation is likely to alter **k**. It is therefore essential to run the hydraulic conductivity testing long enough to ensure that the soil system has reached chemical equilibrium. That requirement can only be met by determining the chemical composition of both the influent and effluent permeant.

The effluent chemistry of laboratory k-tests for clay/leachate compatibility studies can be conveniently presented using "breakthrough curves". These curves describe the concentration of a chemical in effluent samples (C) relative to the initial concentration of that species in the influent permeant (C_o), plotted against the number of pore volumes of flow through the specimen. The location of the $C/C_o = 0.5$ point relative to one pore volume is often regarded as an indicator of the extent of retardation of chemicals. Figure 2.5 illustrates some typical shapes of breakthrough curves for contaminant flow through porous media. For simplicity it is assumed that the concentration of the chemical species in the pore fluid prior to permeation is zero. The following curves are shown:

1) Piston flow: This curve describes uniform, unretarded, non-dispersive flow fully displacing the original pore fluid. The values of C/C_o remain equal to zero until exactly one pore volume has passed through the sample. At this point the breakthrough curve follows a vertical line reaching $C/C_o = 1$ and remains constant until the end of permeation.

2) Unretarded dispersive flow: Curve 2 demonstrates the effect of dispersion on the effluent chemistry of an unretarded species. Dispersion causes a nearly symmetrical spread of the chemical front with $C/C_o = 0.5$ located at exactly one pore volume of flow.

3) Incomplete displacement flow: Curve 3 describes a case where the original pore fluid is only partially displaced by the permeant. The C/C_o values reach 0.5 at about half a pore volume of flow, suggesting early arrival of the chemical. This type of behaviour is shown by immiscible flow where part of the original pore liquid is retained around the soil particles.

4) Fracture flow: Early arrival of contaminants followed by "tailing" is characteristic of rapid flow through macropores along with diffusion into the adjacent soil peds (micropores). Tailing is the slow increase in the concentration ratios approaching $C/C_o = 1$. Two curves are shown, 4a for little diffusion and very early arrival and curve 4b for less early arrival resulting from diffusive losses.

5) Desorption: Curve 5 reflects negative attenuation or desorption of a chemical species often observed for calcium and magnesium displaced by sodium and potassium in the influent leachate. Excess effluent concentrations may also result from minerals such as gypsum and carbonates being dissolved in the permeating leachate. Desorption is characterized by early arrival followed by effluent concentrations that exceed the influent values. The

effluent concentrations drop towards the influent values ($C/C_o \rightarrow 1$) as the chemical reaction equilibrates throughout the sample.

6) Retardation: Curve 6 represents a strongly retarded species as C/C_o reaches a value of 0.5 at 2.5 pore volumes of leachate permeation. This behaviour is often observed for monovalent cations such as K^+ and NH_4^+ that are adsorbed onto the soil in place of divalent cations.

During recent years the effect of waste leachates on the hydraulic conductivity of clayey soils has become a crucial subject related to the design of liners for waste disposal facilities. Numerous investigations have been undertaken by researchers at different universities using various clay types and permeants including leachate from domestic landfill facilities and organic solvents. The published work, however, includes conflicting results, which are probably caused by the use of different testing procedures, soil types or soil preparation techniques. The following sections present a brief review of the most significant studies reported in the literature.

2.3.1 Domestic Waste Leachate

An extensive study to assess the effect of a sanitary landfill leachate on kaolinite, illite and montmorillonite clay/sand mixtures was reported by Griffin et al. (1976). Natural or sterilized leachate from a 15 year old municipal landfill near Chicago (Illinois) was passed through 44 soil columns. The resulting hydraulic conductivity data are presented in Figure 2.6 and show very consistent reductions in **k** after leachate permeation. The columns permeated with natural leachate experienced greater reductions in **k** than those permeated with sterile leachate, reflecting the effect of bacterial growth clogging the soil pores. The study included detailed analyses of effluent samples for chloride, sodium, potassium, calcium, magnesium, aluminum, silicon, ammonium, zinc, lead, cadmium, iron, mercury, manganese, boron, chemical oxygen demand, Eh and pH. The results from these analyses indicated that metals such as Fe, Pb, Zn, Cd and Hg were attenuated probably by precipitation as metal hydroxides or carbonates. Cations such as Na, K, NH_4 and Mg were attenuated by cation exchange resulting in desorption of calcium. The extent of attenuation was proportional to the cation exchange capacity of the soil (montmorillonite > illite > kaolinite).

In more recent studies, domestic waste leachate has been reported to cause little change (usually a decrease) in **k** for compacted clays (Daniel and Liljestrand, 1984, Brunelle et al., 1987, and Quigley et. al, 1988).

2.3.2 Concentrated Organic Solvents

The influence of organic chemicals on the hydraulic conductivity of clayey soils has been the subject of numerous studies. Major fundamental research dates back to Michaels and Lin (1954) who measured the permeability of kaolinite to water, methanol, dioxane, cyclohexane and nitrogen gas. Their work is replotted in Figure 2.7 to show values of intrinsic permeability K (cm^2) versus void ratio. The intrinsic or specific permeability is a very useful parameter to evaluate changes in the porous medium and results from correcting the values of **k** for effects of density and viscosity of the permeant:

$$K = \frac{\mathbf{k}\,\mu}{\rho\,g} = \mathbf{k}\frac{\mu}{\gamma} = \mathbf{k}\frac{\nu}{g}$$

where: μ = dynamic viscosity of the permeant fluid (g/(cm · s) = P (poise))

ρ = density of the permeant (g/cm^3)

g = gravitational constant = 981 cm/s^2

$\gamma = \rho\, g$ = unit weight of the permeant (g/(cm$^2 \cdot$ s^2))

$\nu = \mu/\rho$ = kinematic viscosity of the permeant (cm^2/s = St (stokes))

The results shown in Figure 2.7a correspond to samples of dry kaolinite clay sedimented in the permeant fluid and statically compacted (permeant-compacted) to various void ratios. Although the increases are only by a factor of 2 to 8, the trend of increasing K with decreasing ϵ is very clear. A second set of tests was carried out for kaolinite consolidated in distilled water (water-compacted) and subsequently permeated with water, dioxane, acetone and nitrogen gas. The results of these tests are summarized in Figure 2.7b and show that at a given void ratio the non-aqueous permeants caused increases in permeability. However, the increases in K for water-compacted clays (Figure

2.7b) were less pronounced than those for permeant-compacted clays (Figure 2.7a).

A very clear picture of the transmissive properties of permeant-compacted clays was presented by Mesri and Olson (1971). Figure 2.8 describes the ranges in the values of **k** calculated from results of consolidation tests on kaolinite, illite and smectite samples moulded with various liquids. The trend of increasing **k** with decreasing polarity of the moulding fluid agrees with the work of Michaels and Lin. At a given void ratio smectite shows enormous increases in **k** as the dielectric constant of the moulding fluid decreases from $\epsilon \sim 80$ (water) to $\epsilon \sim 2$ (benzene or carbon tetrachloride). The authors attributed the high values of **k** for low dielectric fluids to the opening of flow channels as a result of double layer contraction, which also promoted the formation of aggregates of clay particles with large flow channels. The validity of these conclusions were confirmed by Fernandez and Quigley (1985) for natural clays from southwestern Ontario and a variety of liquid permeants.

Recent studies carried out to assess the effects of organic solvents on the integrity of water-compacted clays have produced some controversial results. Green et al. (1981) reported decreases in **k** with various solvents of lower dielectric constant than water. The authors proposed an empirical relation where **k** increases as the dielectric constant of the pore fluid increases. This proposal is in direct conflict with the findings of Michael and Lin (1954) and

Mersi and Olson (1971). The validity of the work of Green and co-workers appears questionable from the viewpoint of experimental procedures (Dunn, 1983) and interpretation of equilibrium (Research Triangle Institute, 1986).

Extensive laboratory studies carried out by Brown and his co-workers (Brown and Anderson, 1980; Anderson and Brown, 1981; Anderson et al., 1982; Brown et al., 1983) showed that a variety of concentrated organic solvents produced spectacular increases in the hydraulic conductivity of water-compacted clays. Figure 2.9 shows the results of two typical tests where the values of **k** for water increased by more than 1000-fold after just over one pore volume of xylene or acetone was passed through the soil. The large increases in **k** were attributed to piping, shrinkage cracks and opening of pores as a result of double layer collapse. This work received a great deal of attention from the regulatory agency U.S.E.P.A., ultimately resulting in the required use of alternative liner materials such as synthetic membranes. However, the testing procedures employed by Brown and his colleagues may not have provided adequate control of the contact between the soil sample and the fixed-wall (compaction mould) permeameter. It is therefore possible that the large increases in **k** could reflect rapid flow of the concentrated solvents through channels formed along the soil/mould contact (side-wall leakage), without necessarily reflecting alterations in the core of the clay samples.

Later studies published by researchers at different universities have shown that forced permeation of insoluble organic permeants do not necessarily cause increases in **k** if adequate precautions were taken to prevent side-wall leakage. The permeant liquids studied include benzene and nitrobenzene (Acar et al., 1985), benzene, cyclohexane and xylene (Fernandez and Quigley, 1985), heptane (Foreman and Daniel, 1986), and aniline and xylene (Uppot and Stephenson, 1989). These insoluble hydrocarbons displaced only ~ 10% of the original water resident in the pores, suggesting that flow of the non-polar liquids was confined to channels formed by displacement of free interpedal water, without significantly altering the soil structure (Fernandez, 1984). Permeation with water soluble organic solvents resulted in much larger displacement of the water in the pores along with increases in hydraulic conductivity. The magnitude of the increases in **k** is largely affected by the permeameter type and the level of confining stresses (Anderson et al., 1985; Acar et al., 1985; Foreman and Daniel, 1986).

2.3.3 Aqueous Solutions of Organic Solvents

In practice, exposure of clay barriers to concentrated water-insoluble hydrocarbons could take place in cases of spills or leaking tanks (Mitchell and Madsen, 1987). Soluble organics, on the other hand, are likely to reach the clay liners in dilute forms. Brown et al. (1984) measured the hydraulic conductivity of compacted clays to various aqueous solutions of acetone. The permeants containing less than 75% acetone yielded values of **k** that did not exceed the values for water. Bowders et al. (1986) permeated compacted kaolinite samples with several water/methanol mixtures. The tests performed using fixed-wall and flexible-wall cells are described in Figure 2.10 and show that no significant increases in **k** took place for alcohol contents below ~ 80%.

2.4 CONCLUDING REMARKS

Major fundamental work on the effect of permeant properties on the hydraulic conductivity of clayey soils dates back several decades. During the past ten years, numerous studies have been reported on the effect of waste leachates on the integrity of clay barriers. Recent comprehensive reviews of the published work have been presented by Mitchell and Madsen (1987) and Research Triangle Institute (1986). The following general comments can be made:

1) Domestic landfill leachate produces little effect on the hydraulic conductivity of clayey barriers. Cation exchange and precipitation may play important roles in the attenuation of some chemical species. However, inadequate attention may have been paid to high charge clays such as vermiculite.

2) Concentrated, water-soluble organic solvents may cause dramatic increases in the hydraulic conductivity of clays. The magnitude of the increases in **k** varies with the testing procedure employed.

3) Water-insoluble, pure hydrocarbons appear to have little effect on water-compacted clays. Large discrepancies reported in the literature are related to different testing procedures (permeameter type, saturation, etc).

4) Little information is available on the effect of aqueous solutions of organics on the hydraulic conductivity of clays. The published data suggest that dilute concentrations of organics do not increase the hydraulic conductivity of water-compacted clays.

TABLE 2.1 SURFACE ELECTRIC POTENTIAL AND DOUBLE LAYER THICKNESS FOR VARIOUS CLAYS AND PORE LIQUIDS.

CLAY MINERAL	PORE LIQUID	ELECTROLYTE CONCENTRATION	VALENCE	ψ_0 (mV)	1/K (nm)
MONTMORILLONITE:	Water	10^{-4} M	1	268.9	30.52
Cation Exchange Capacity = 100 meq/100 g	Water	10^{-3} M	1	210.8	9.65
	Water	10^{-2} M	1	152.7	3.05
Specific Surface = 800 m^2/g	Water	10^{-1} M	1	95.6	0.965
	Water	10^{-4} M	2	134.5	15.26
Surface Charge Density = 36,200 esu/cm^2	Ethanol	10^{-4} M	1	297.6	17.29
	Benzene	10^{-4} M	1	358.9	5.14
CHLORITE:	Water	10^{-4} M	1	327.7	30.52
Cation Exchange Capacity = 20 meq/100 g	Water	10^{-3} M	1	269.6	9.65
	Water	10^{-2} M	1	211.4	3.05
Specific Surface = 50 m^2/g	Water	10^{-1} M	1	153.4	0.965
	Water	10^{-4} M	2	163.9	15.26
Surface Charge Density = 115,900 esu/cm^2	Ethanol	10^{-4} M	1	356.4	17.29
	Benzene	10^{-4} M	1	417.7	5.14

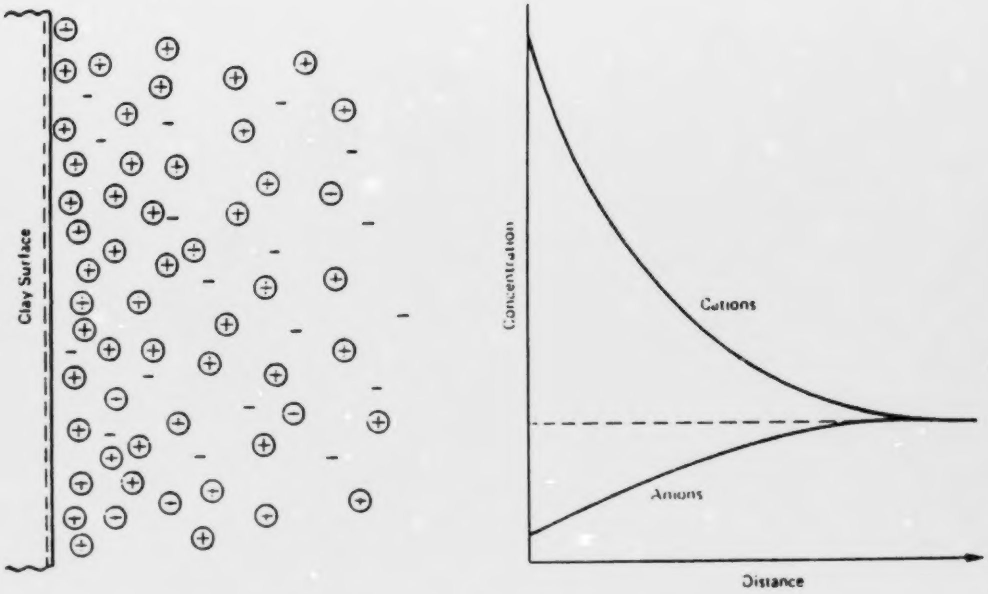
Clay Surface
Concentration
Cations
Anions
Distance

FIGURE 2.1 DISTRIBUTION OF IONS IN THE DIFFUSE DOUBLE LAYER (J.K. Mitchell, 1976)

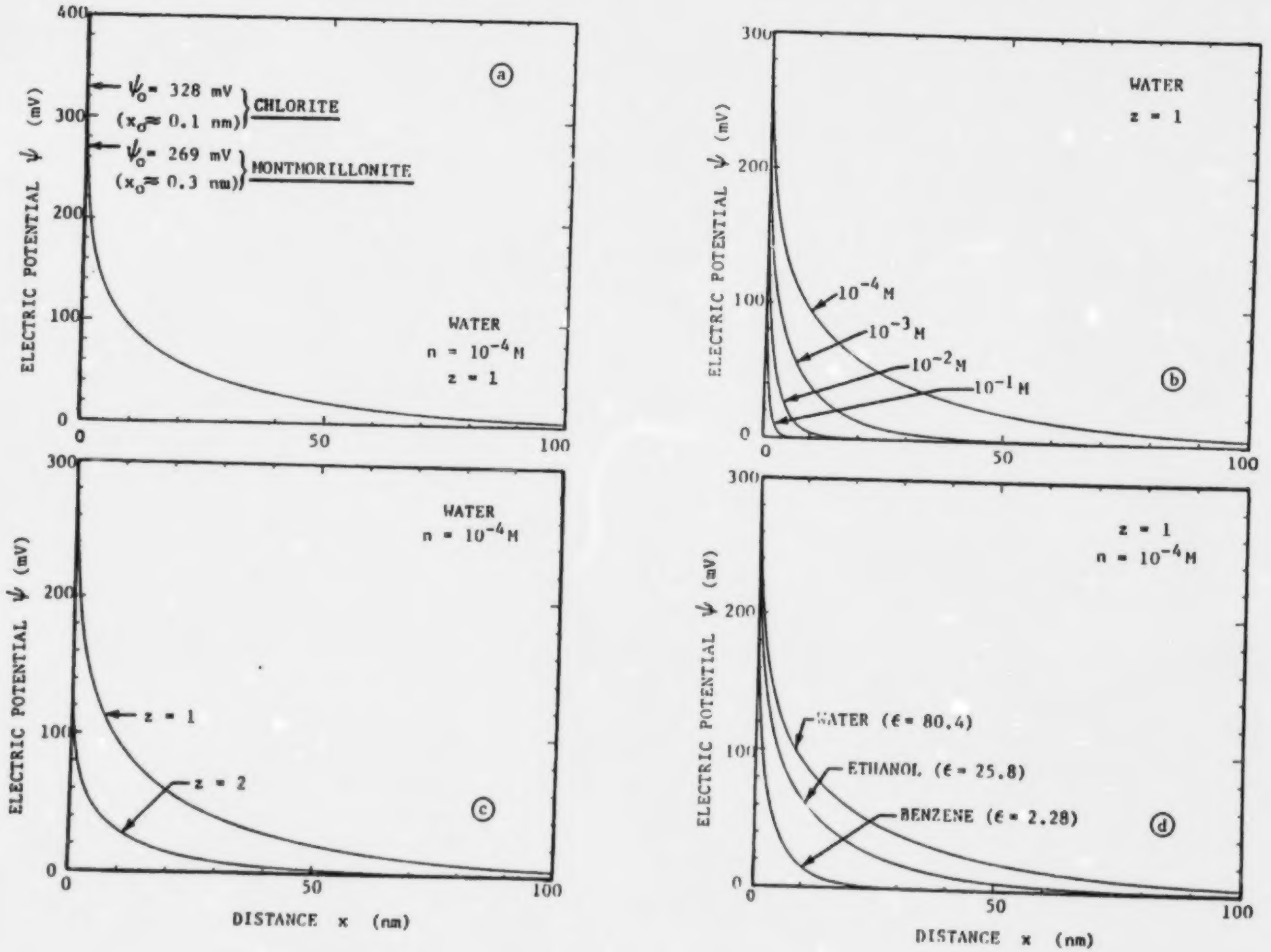

FIGURE 2.2 DISTRIBUTION OF ELECTRIC POTENTIAL IN DOUBLE LAYERS AFFECTED BY: a) CLAY MINERAL; b) ELECTROLYTE CONCENTRATION; c) ELECTROLYTE VALENCE; d) DIELECTRIC CONSTANT

Adapted from Mitchell et al. (1965)

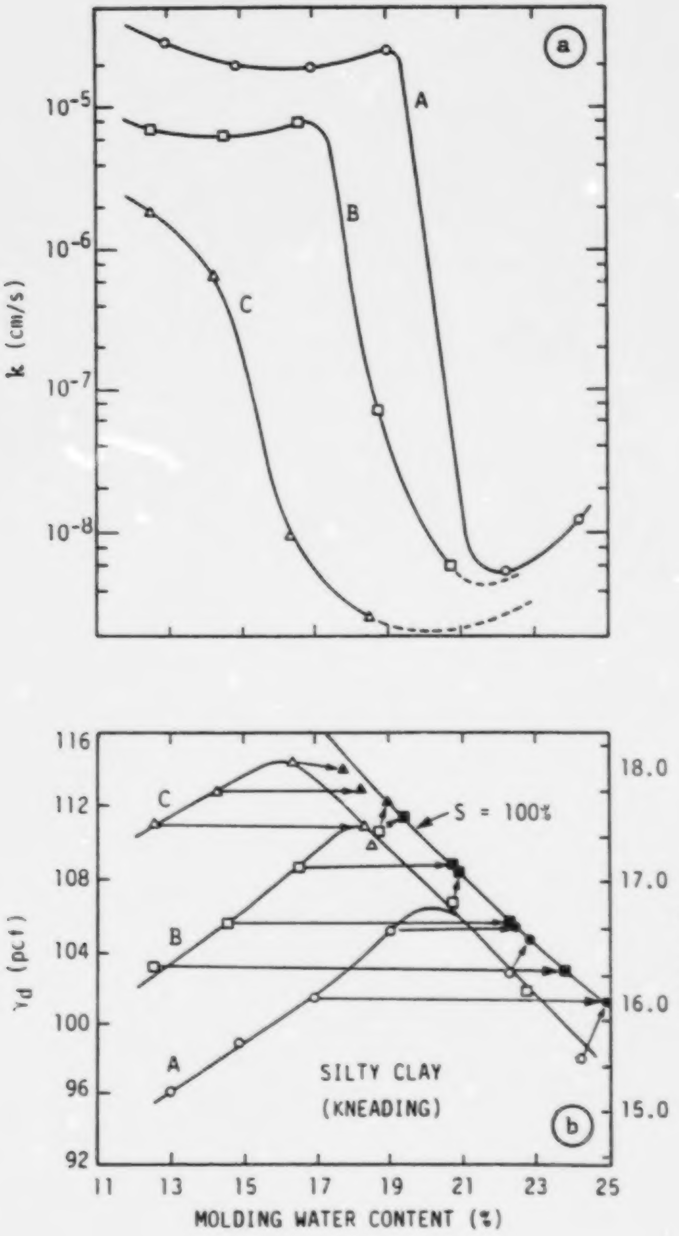

FIGURE 2.3 HYDRAULIC CONDUCTIVITY (a) AND DRY UNIT WEIGHT (b) VS WATER CONTENT (Mitchell et al., 1965).

Kneading compaction: A = 10 layers, 15 tamps, 30 lb/tamp
B = 10 layers, 15 tamps, 45 lb/tamp
C = 20 layers, 25 tamps, 50 lb/tamp

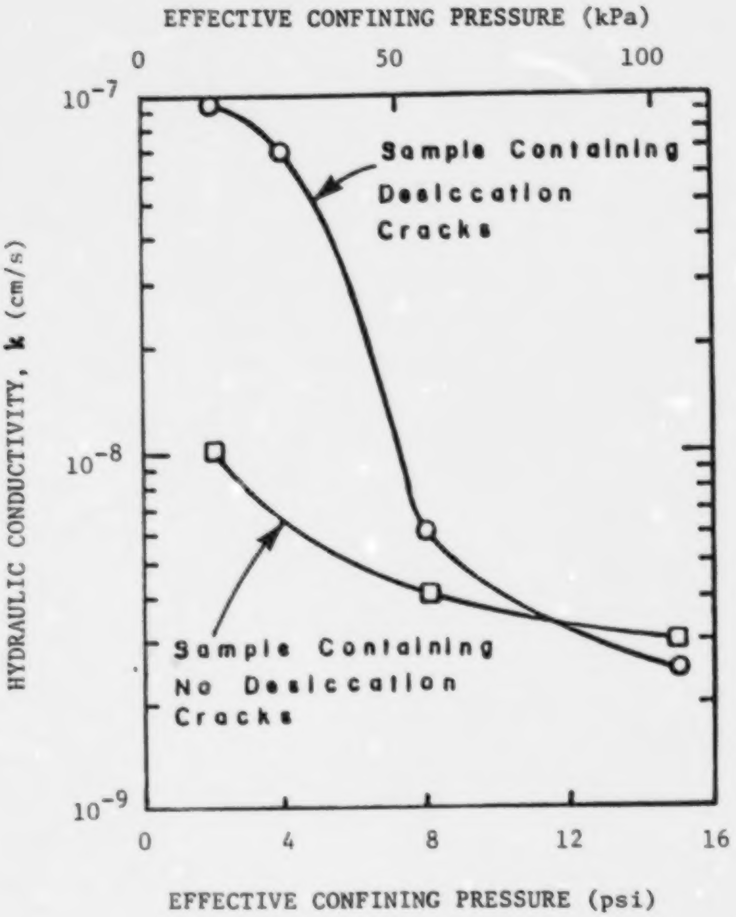

FIGURE 2.4 HYDRAULIC CONDUCTIVITY VS EFFECTIVE CONFINING PRESSURE (Daniel et al., 1985)

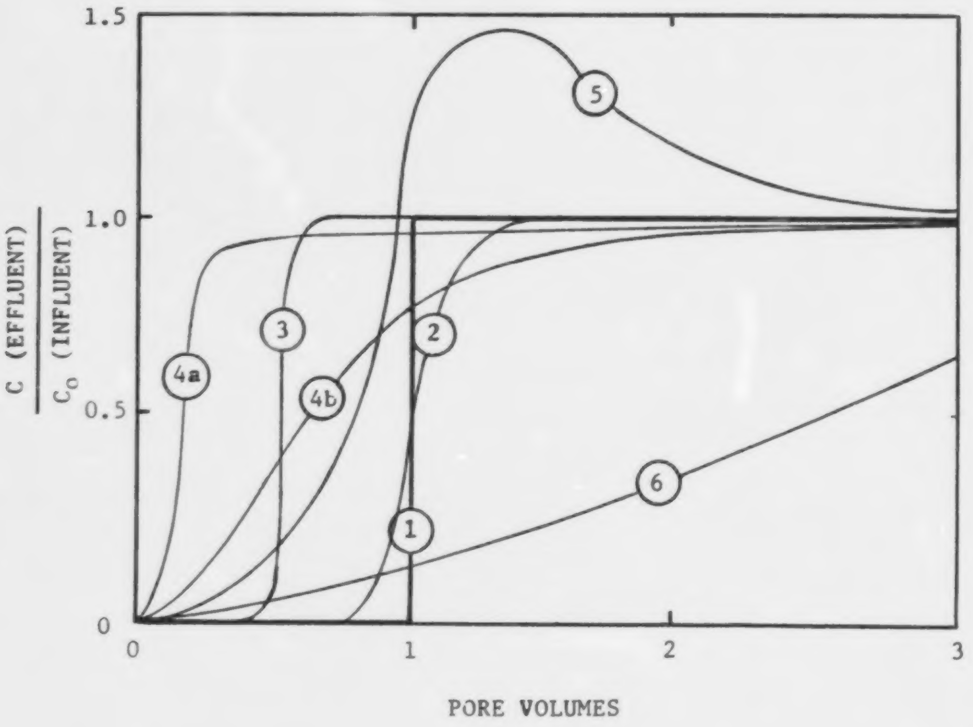

FIGURE 2.5 TYPICAL CURVES OF EFFLUENT CHEMISTRY VERSUS PORE VOLUMES (BREAKTHROUGH CURVES)

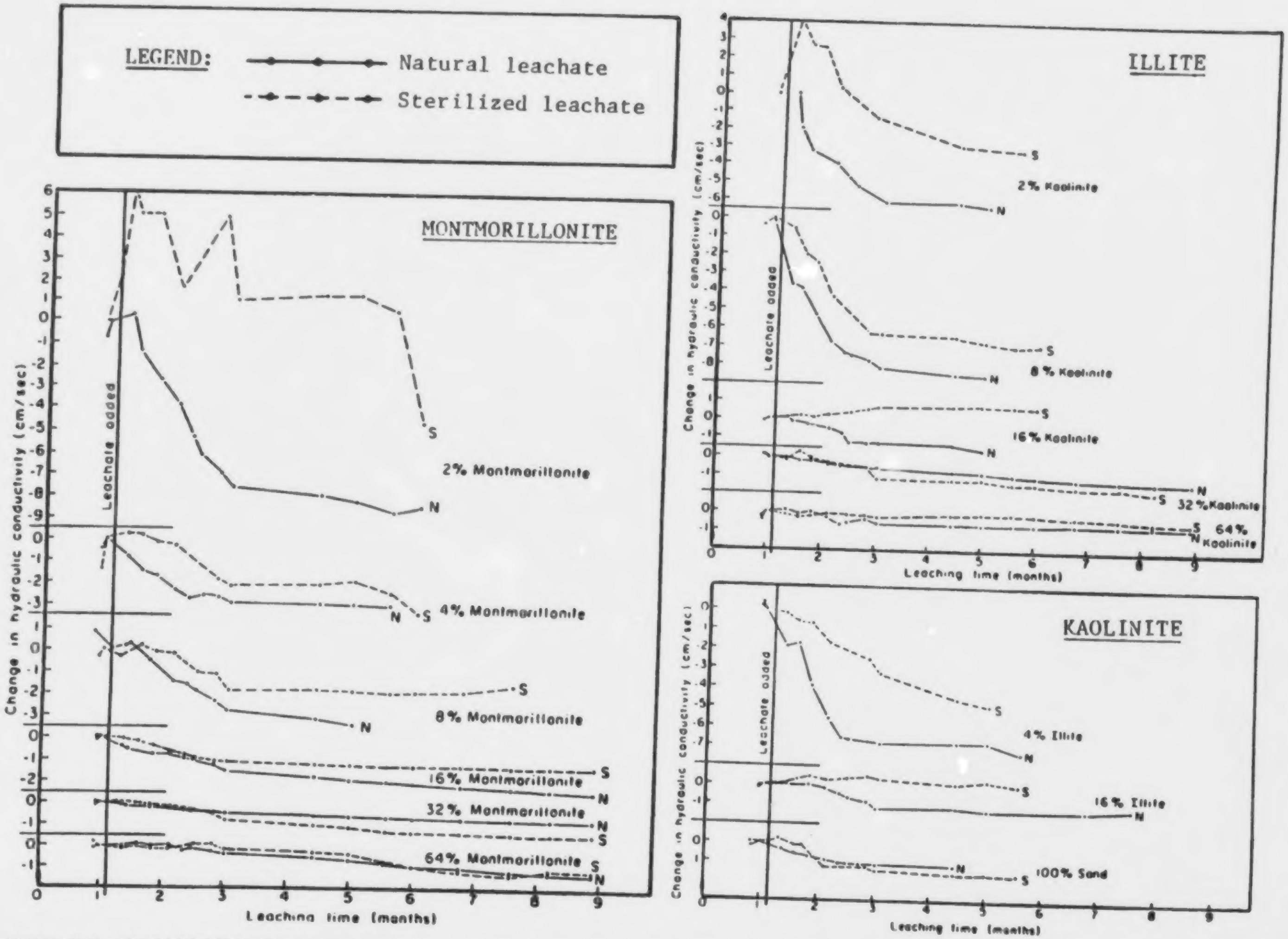

FIGURE 2.6 CHANGES IN HYDRAULIC CONDUCTIVITY OF CLAY/SAND COLUMNS PERMEATED WITH MUNICIPAL LANDFILL LEACHATE (Griffin et al., 1976)

Adapted from Michaels & Lin (1954)

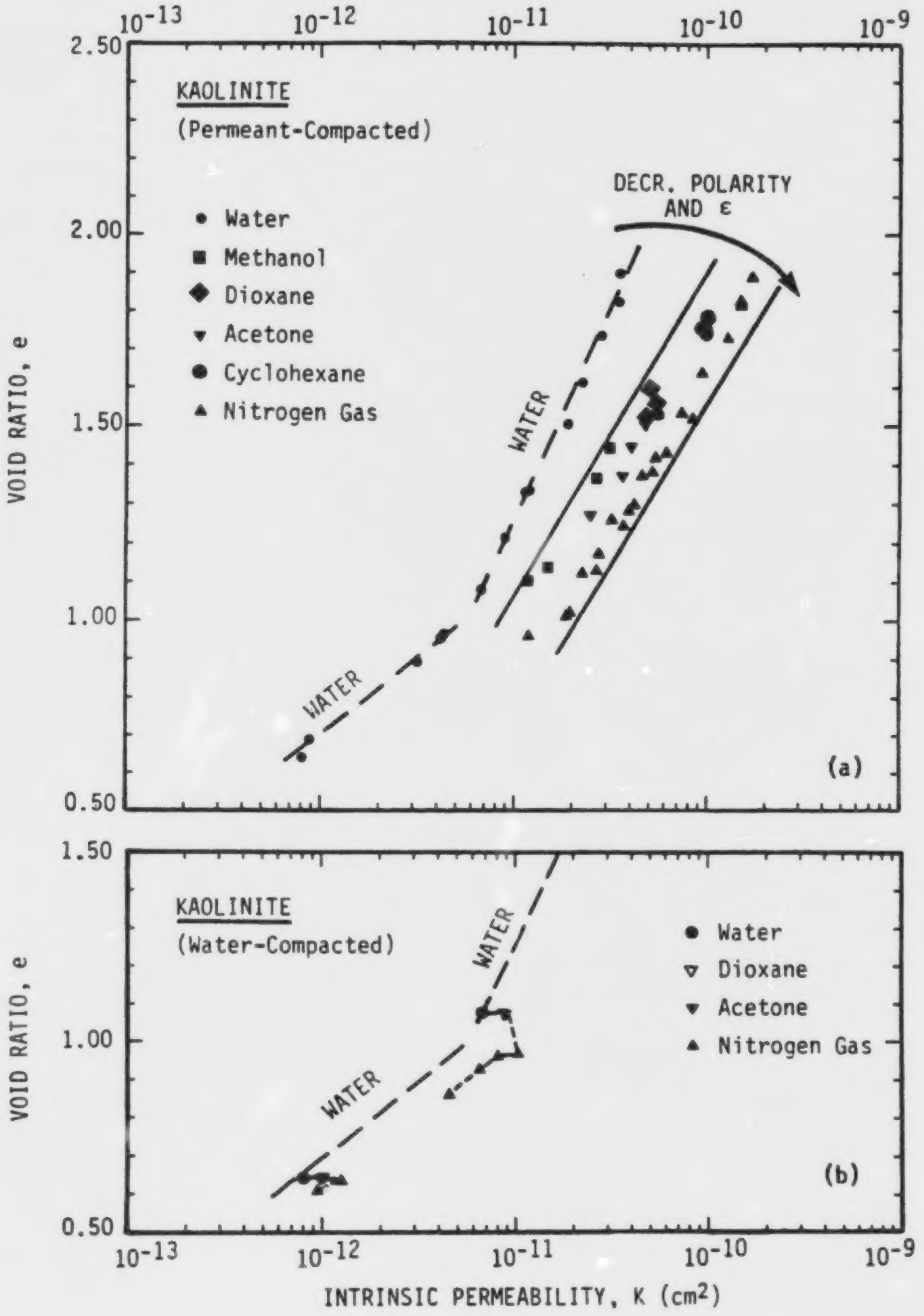

FIGURE 2.7 INTRINSIC PERMEABILITY VS VOID RATIO FOR KAOLINITE (Michaels and Lin, 1954):
(a) Compacted and permeated with the fluid indicated
(b) Water-compacted and permeated with the fluid indicated

Adapted from Mesri and Olson (1971)

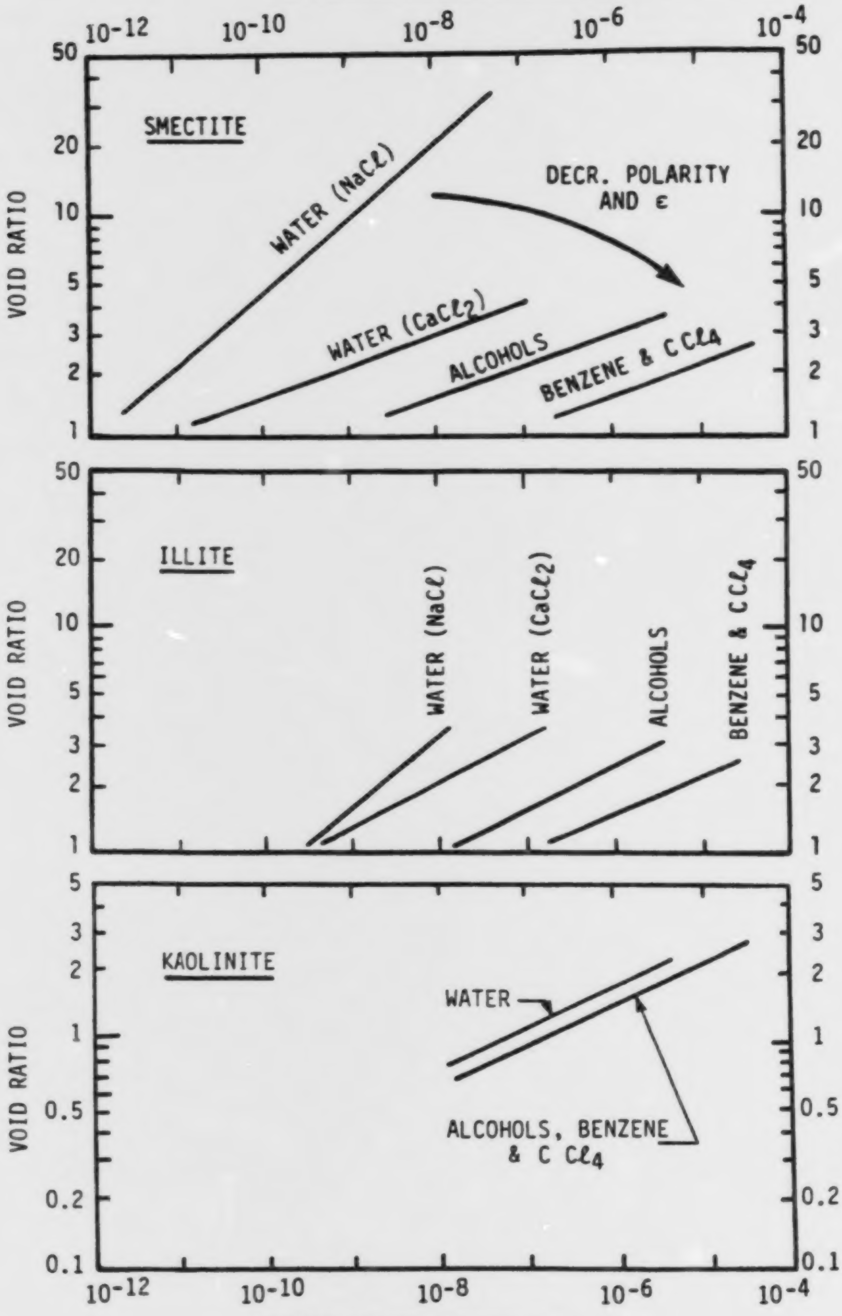

FIGURE 2.8 HYDRAULIC CONDUCTIVITY VS VOID RATIO FOR SMECTITE, ILLITE AND KAOLINITE (Mesri and Olson, 1971)

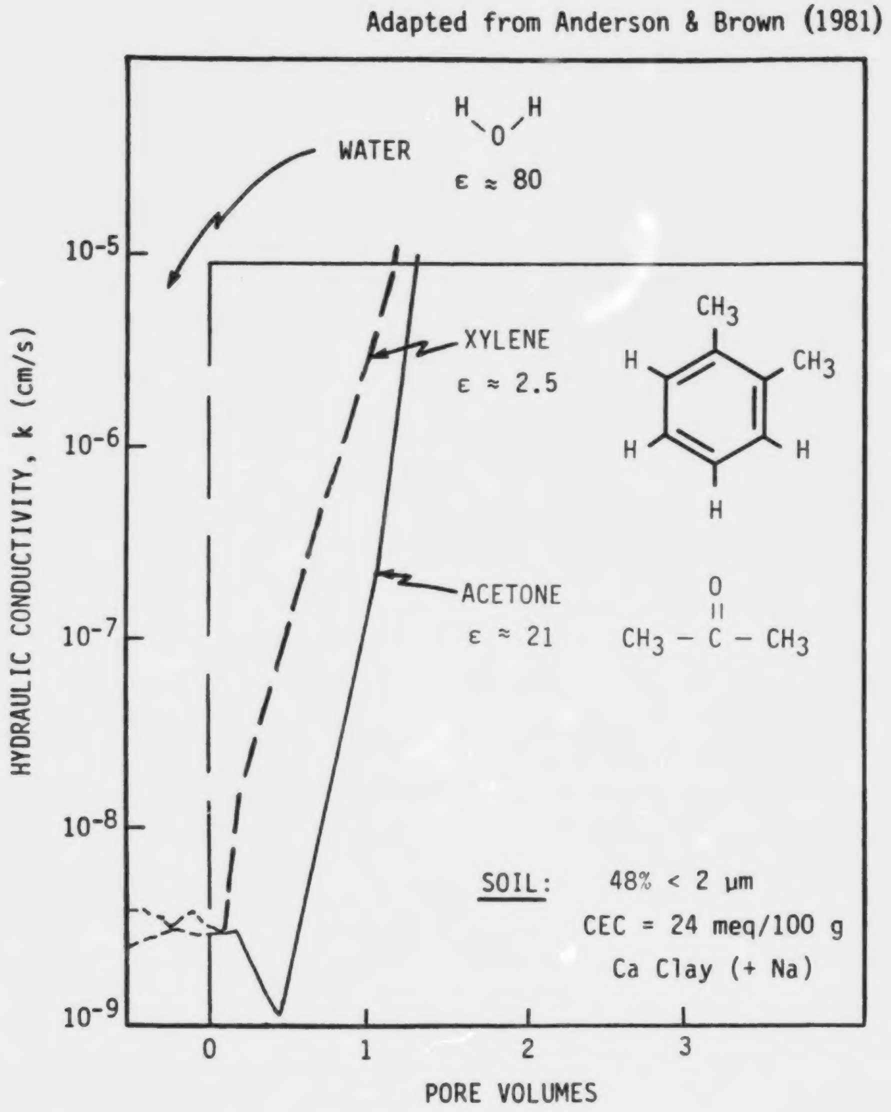

FIGURE 2.9 HYDRAULIC CONDUCTIVITY VS PORE VOLUMES FOR WATER-COMPACTED CLAYS PERMEATED WITH ACETONE AND XYLENE (Anderson and Brown, 1981)

Directly from Bowders (1985)

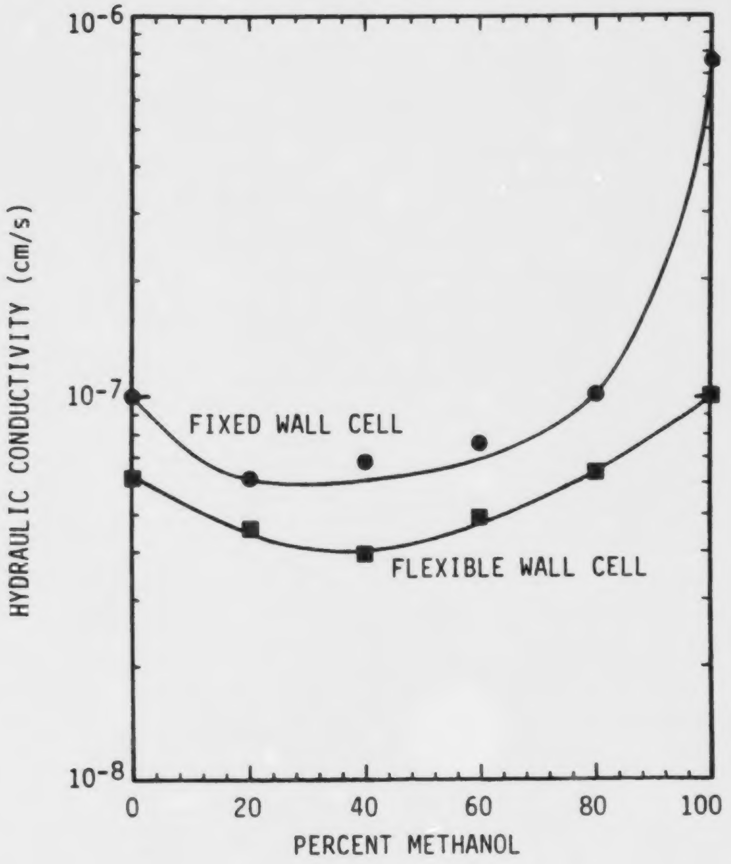

FIGURE 2.10 HYDRAULIC CONDUCTIVITY OF COMPACTED KAOLINITE TO AQUEOUS SOLUTIONS OF METHANOL (Bowders et al., 1985)

CHAPTER 3

HYDRAULIC CONDUCTIVITY TESTING EQUIPMENT

3.1 INTRODUCTION

This chapter describes the hydraulic conductivity equipment especially designed for clay/permeant compatibility studies. The results of such studies may be strongly dependent on the equipment and testing techniques employed and therefore a detailed description of both items is essential. The equipment is an improved version of that described by the author (Fernandez, 1984), and can operate under conditions of either constant flow or constant head.

The equipment consists of eight fixed-ring permeameters equipped with individual settlement monitoring and effluent collection systems. Vertical stresses of up to 320 kPa can be applied by means of spring loaded devices acting on the soil surface. All parts of the system exposed to the permeant are made either of stainless steel or glass, which are corrosion resistant to most organic solvents. During testing the permeant cylinders and cell reservoirs are safely sealed to prevent loss of volatile permeants that might be toxic. Samples of the effluent permeant are collected in glass bottles especially designed to minimize evaporation losses. These samples are chemically analyzed for both organic and inorganic species to obtain data that is important for interpretation of clay/leachate compatibility studies.

3.2 FIXED-RING PERMEAMETER

3.2.1 Cell Description

A permeability cell, illustrated in Figure 3.1, consists of a stainless steel cylinder (A) 5.40 cm in internal diameter and of variable height. Both ends of the cylinder are machined to contain viton O-rings (B) sealing the contact between the cylinder and the cell caps (C). The cell is held together by four threaded rods (D) fixed to the base.

The fluid inlet (E) leads the permeant into the fluid chamber (F) which supplies the flow through the soil sample. The fluid outlet (G) allows collection of the effluent permeant for flow assessment or chemical analysis. Stainless steel porous disks (H) are placed on top and below the soil sample with filter papers in between. The upper porous disk is 3.2 mm (1/8") thick with a pore diameter of 100 μm (porosity, n ~ 0.6), and the lower disk has a thickness of 2.0 mm (5/64") and a 40 μm pore size (n ~ 0.5). Two filter papers with a pore diameter of 20 μm are placed between the soil and the steel porous disks.

A group of springs (I) acting against the upper cell cap (C) and the porous disk (H) apply vertical effective stresses on the soil sample. A dial gauge placed on top of the settlement rod (J) monitors the volume change in the soil sample during testing. Figure 3.2 shows photographs of a fixed-ring permeameter in operation, a group of four springs, and a cell cylinder.

The effluent permeant is collected in 20 mL glass bottles fixed to the fluid outlet tube. The bottle caps are made of teflon and contain viton O-rings seals. Stainless steel tubing (1/16" O.D.) pierced through the teflon caps provides vents for displacing the air as the bottles fill-up with permeant. Teflon tips attached to the steel tubing reduce the aperture of the vents to 0.33 mm. Evaporation rates for water, dioxane, ethanol and cyclohexane in the effluent collection bottles are summarized in Table 3.1 and the details of test results are presented in Appendix A. The teflon tips reduce the losses of organics due to evaporation to less than 1% of the effluent mass, even at flow rates as low as 5×10^{-6} mL/s.

3.2.2 Soil Preparation

The test soils are obtained by removing the particles greater than 2 mm are removed from the air dried stock by passing it through a sieve # 10. The soil is then wetted with distilled water to the desired moisture content and allowed to sit overnight. A 12.5 mm diameter Harvard miniature rod mounted with a 0.142 kN (32 lb) spring is used to compact the test soil directly into the permeameter cells. Compaction is done in three layers ~ 8 mm thick, using 30 prods per layer. The compaction energy per mass of soil is similar to that employed in the Harvard miniature compaction test. However, the geometry of soil layers compacted in the **k** cell is quite different from those compacted in the Harvard cell, and may result in greater degree of compaction as discussed in

Section 4.2.

Once the soil is in the cell the upper surface is trimmed to the desired thickness (normally 20 mm) by rotating a trimming plate on top of the soil. This trimming method provides a flat and smooth surface for samples compacted at relatively high water contents.

After trimming, the fluid chamber is filled with permeant and a static effective stress, σ'_v, can be applied to the top of the sample by means of the spring loaded cap. Figure 3.3 shows a typical deflection curve for a static load of 160 kPa applied on a compacted and trimmed specimen of brown Sarnia clay. The deflection values are measured by the dial gauge mounted on the permeability cell. However, since the load builds up as the cell is assembled, the initial "seating" deflection is estimated by extrapolation of the straight portion of the curve, in analogy to Taylor's method for consolidation (Taylor, 1948). Vertical stresses of up to 320 kPa can be applied depending on the compressed length and number of springs. The applied stresses improve the contact between the soil sample and the cell walls and, to some extent, close fractures such as those created during sample trimming. Calibration curves for two spring groups are shown in Figure 3.4 yielding an individual spring constant of 5.41 N/mm, compared to the manufacturer's value of 5.53 N/mm. For the permeability cells described, this is equivalent to 2.36 kPa per spring per millimetre of spring compression.

3.3 CONSTANT FLOW HYDRAULIC CONDUCTIVITY EQUIPMENT

The computer controlled, constant flow, hydraulic conductivity equipment is shown during operation in Figure 3.5. The constant flow testing procedure was extensively described by Olsen (1965, 1966, 1972) and is particularly suitable for working with toxic liquid hydrocarbons which are safely concealed in the syringes. A displacement transducer is used for measuring the influent flow rate. The syringes have a capacity of ~ 60 mL and the loading frame generates flow rates, q, that can be varied from 6×10^{-6} to 1.5×10^{-2} mL/s. Figure 3.6 illustrates the range of hydraulic conductivities, flow rates and hydraulic gradients covered by the equipment.

A schematic of one circuit is shown in Figure 3.7 along with diagrams of seepage stresses and head distribution during testing. A pressure transducer monitors the permeant pressure, u_A, at the inlet side of the specimen (point A). The pressure head (h_{pA}) is equal to the pressure u_A divided by the unit weight of the permeant, γ, i.e. $h_{pA} = u_A/\gamma$. The pressure head at the outlet end is taken as zero, since it is open to the atmosphere and capillary effects in the 1/8" tubing amount to less than 1 cm. Then, the head drop across the sample, Δh_t, is then calculated as the sum of pressure and elevation heads at point A ($\Delta h_t = h_{tA} = h_{pA} + h_{eA}$). The hydraulic conductivity is calculated in accordance to Darcy's law as follows:

$$\mathbf{k} = \frac{q\ L}{\Delta h_t\ A}$$

where L and A are the thickness and cross-sectional area of the soil sample, respectively.

As the permeant flows through the soil mass the total head is gradually transferred to the soil skeleton through frictional drag, j, producing seepage (effective) stresses, J, in the direction of the flow. The seepage stresses (Figure 3.7) have a maximum value, J_{max}, at the outlet end of the soil sample:

$$J_{max} = j\ L = i\ \gamma\ L = \gamma\ \Delta h_t$$

where i is the hydraulic gradient, $i = \Delta h_t/L$

Seepage induced stresses may produce significant vertical consolidation during a hydraulic conductivity run using high hydraulic gradients.

The results of a typical hydraulic conductivity test are presented in Figure 3.8. A constant, forced flow rate of 5.9×10^{-5} mL/s through the soil induces a total head drop across the sample. The lag time required for the head drop (and the calculated values of **k**) to reach equilibrium is related to saturation problems of both equipment and soil and the expansion or compliance of the system as a whole. To reduce this effect all tubing and fittings are made of stainless steel and the tubing lengths are kept to a minimum. Another compliance problem is created by sudden changes in room temperature producing deviations in pressure head which in turn affects the values of k. The tendency of permeants to expand (contract) following an increase (decrease) in temperature results in pressure fluctuations that dissipate primarily through the soil sample. The effect is therefore more pronounced for permeants having high thermal expansivity and for soils of low permeability.

The results of a typical soil/permeant compatibility assessment based on hydraulic conductivity testing is shown in Figure 3.9. The test was performed on a water-compacted silty clay sample sequentially permeated by water and dioxane under a vertical effective stress σ'_v = 160 kPa. The test results are plotted as a function of the amount of flow passed through the sample, expressed as the number of pore volumes. The upper graph shows the hydraulic conductivity values and it can be observed that the temperature induced fluctuations become more pronounced during dioxane permeation. This is explained by dioxane's high coefficient of thermal expansivity, α, (approximately four times greater than water). The settlement of the soil during testing is illustrated in the central plot. The application of 160 kPa as a static effective stress caused settlement (ρ_{static}) of about 0.45 mm, as previously shown in Figure 3.3. Subsequent permeation with water followed by dioxane caused seepage settlements ($\rho_{seepage}$) amounting to a total of 0.339 mm. The lower plot in Figure 3.9 presents the concentration of dioxane in the effluent throughout the testing. The "Bottle" value, marked with a single asterisk, represents the initial source concentration (C_o) which in this case was 100% dioxane. The final reservoir value (98% dioxane) is marked with a double asterisk and represents the composition of the permeant directly above the soil at the end of testing. The final pore fluid composition was not obtained for this particular test.

3.4 CONSTANT HEAD HYDRAULIC CONDUCTIVITY EQUIPMENT

The fixed-ring permeameters can alternatively be connected to a constant head system as shown in Figure 3.10. The influent flow is measured by the displacement of a permeant/air meniscus along a graded glass tube located at the same elevation as the end of the effluent outlet tube. Consequently, the total head drop, Δh_t, is obtained by correcting the difference in water levels between the pressure pots (Z) for the permeant density, as follows:

$$\Delta h_t = Z \frac{\rho_{water}}{\rho}$$

Fluctuations in room temperature may affect the influent flow readings, particularly for soils of low permeability. The permeant expands (contracts) as the room temperature rises (drops), thus decreasing (increasing) the flow rate measured at the influent end of the sample. This source of inaccuracy can be minimized by spreading the time interval between flow readings.

The effluent flow can be measured by monitoring the weight of the effluent collection bottles during testing. However, effluent samples are obtained primarily for chemical analysis.

3.5 CHEMICAL ANALYSES OF INFLUENT AND EFFLUENT SAMPLES

The samples of effluent and influent permeant, collected during testing, may be chemically analyzed for organic and inorganic components. Inorganic species such as sodium, potassium, calcium, magnesium and total iron, are analyzed by atomic absorption spectroscopy (AAS). Chloride concentrations are obtained using a specific ion electrode connected to a multi-purpose meter. Organic components, on the other hand, are analyzed by gas chromatography (GC).

3.6 POST-TESTING ASSESSMENT

After completion of the hydraulic conductivity testing the soil samples are extruded from the permeameter cells and visually inspected for evidence of physical changes. Sub-samples of the soil may be used to obtain moisture content, mineralogical and chemical analyses, bacterial counts, pore size distribution by mercury intrusion and micro-fabric studies by scanning electron microscopy (SEM). The pore fluid of the tested specimens can be extracted using the mini-distillation apparatus described in Figure 3.11. The organic contents of the liquid extracts are then determined using gas chromatography.

Each one of these items, as well as the deflection and effluent chemistry during testing, may prove to be particularly useful for the interpretation of changes in the hydraulic conductivity of the tested soil.

3.7 CONCLUDING REMARKS

The fixed-ring permeameters for all hydraulic conductivity testing presented in this report have been thoroughly described. The permeameters can operate using a constant flow or a constant head technique. In both cases accurate measurements of **k** in fine grained soils can be made even for volatile permeants. The closed, sealed circuits permit safe testing of toxic permeants.

The computer controlled constant flow system is especially suitable for long term soil/permeant compatibility studies allowing continuous monitoring of hydraulic conductivity as well as soil settlement and effluent chemical composition. All are useful tools for the study of interactions between permeants and soils.

TABLE 3.1 EVAPORATION RATES FOR VARIOUS PERMEANTS IN EFFLUENT COLLECTION BOTTLES

PERMEANT	EVAPORATION RATE (g/day)		
	Open bottle (Φ = 21)	Steel tube (Φ = 1)	Teflon tip (Φ = 0.33)
Water	0.29	< 0.001	< 0.001
Dioxane	0.88	0.004	0.002
Ethanol	0.96	0.005	0.002
Cyclohexane	2.06	0.011	0.005

Note: Φ = venting aperture (mm)

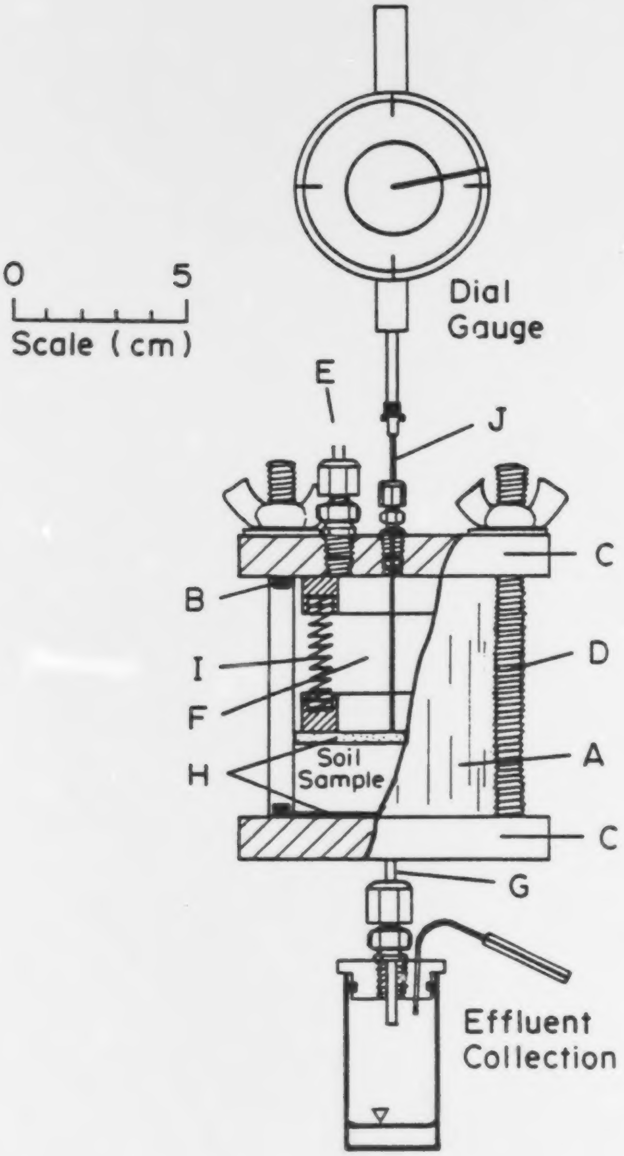
0
5
Scale (cm)
Dial
Gauge
E
J
C
B
D
I
F
A
H
Soil
Sample
C
G
Effluent
Collection

FIGURE 3.1 SCHEMATIC OF FIXED-RING PERMEAMETER

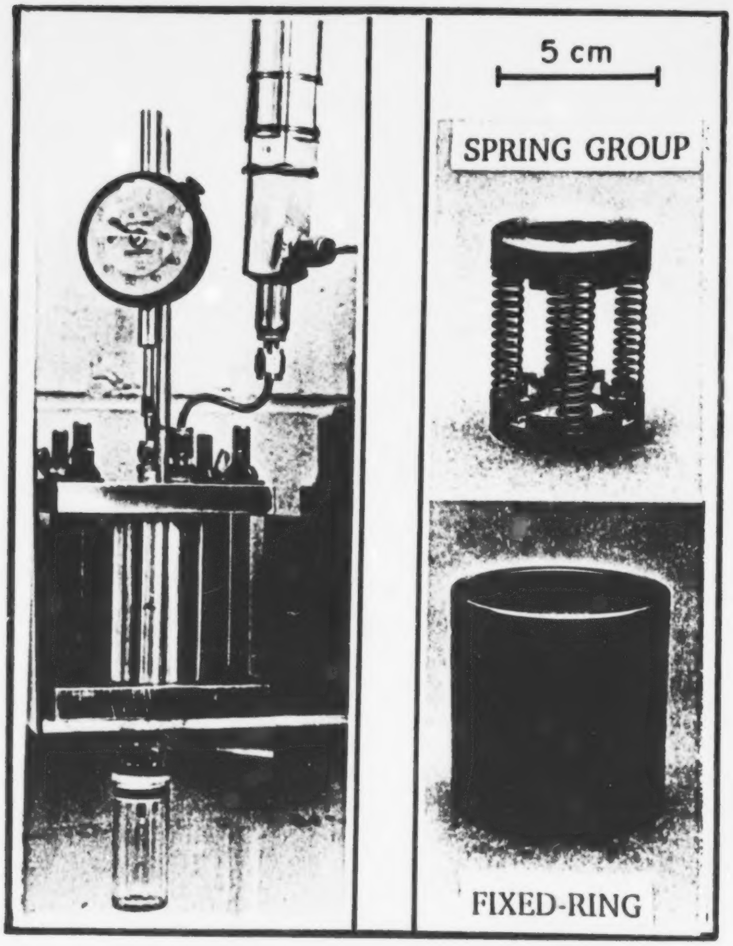
5 cm
SPRING GROUP
FIXED-RING

FIGURE 3.2 FIXED-RING PERMEAMETER

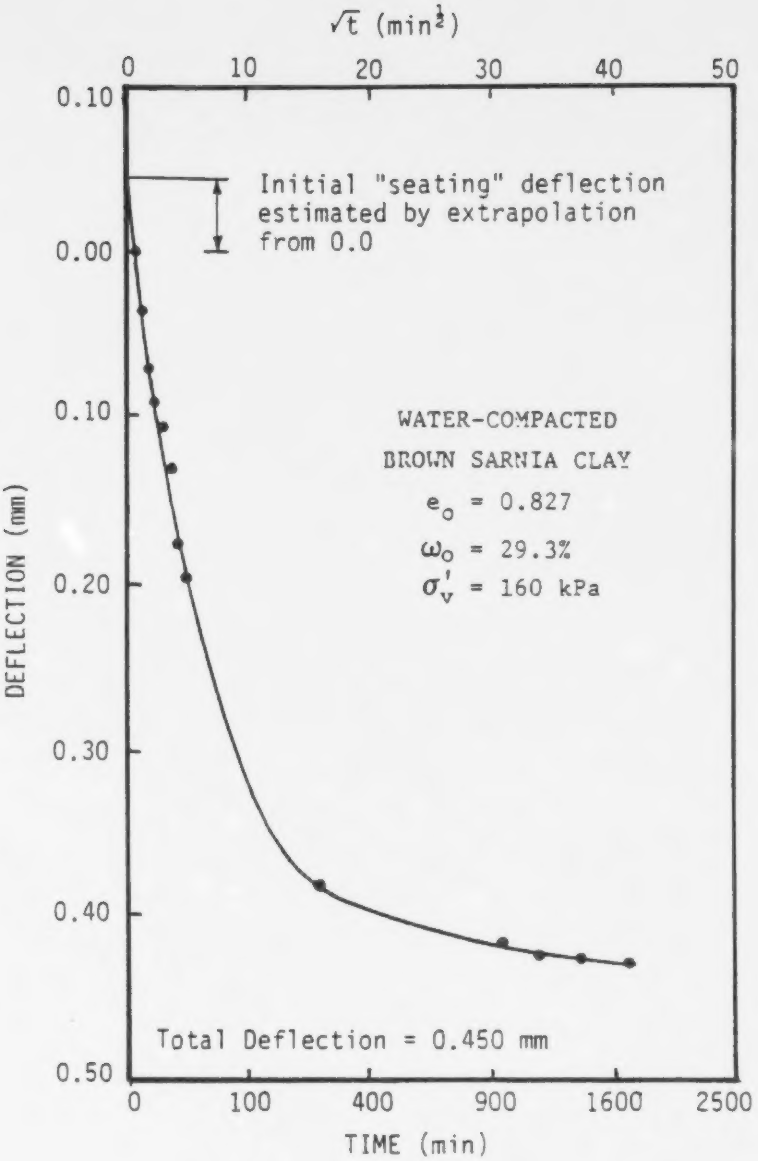

FIGURE 3.3 TYPICAL DEFLECTION-TIME CURVE FOR INITIAL STATIC LOADING

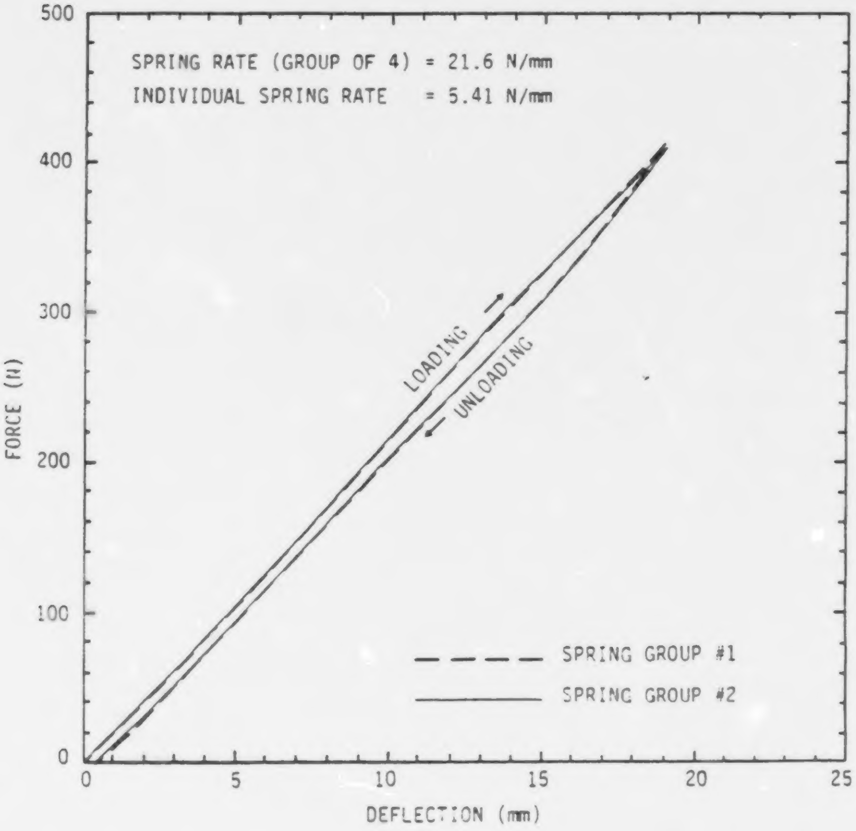

FIGURE 3.4 CALIBRATION CURVE FOR SPRING GROUPS

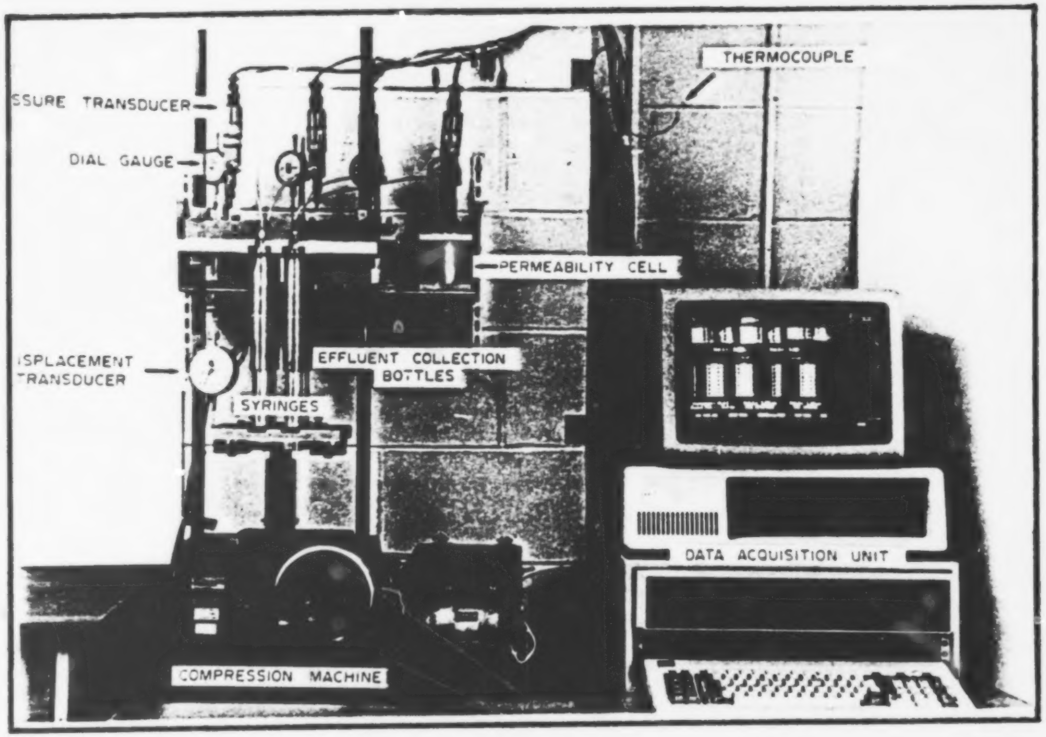
SSURE TRANSDUCER
DIAL GAUGE
ISPLACEMENT TRANSDUCER
SYRINGES
EFFLUENT COLLECTION BOTTLES
PERMEABILITY CELL
THERMOCOUPLE
DATA ACQUISITION UNIT
COMPRESSION MACHINE

FIGURE 3.5 COMPUTER CONTROLLED, CONSTANT FLOW HYDRAULIC CONDUCTIVITY EQUIPMENT IN OPERATION

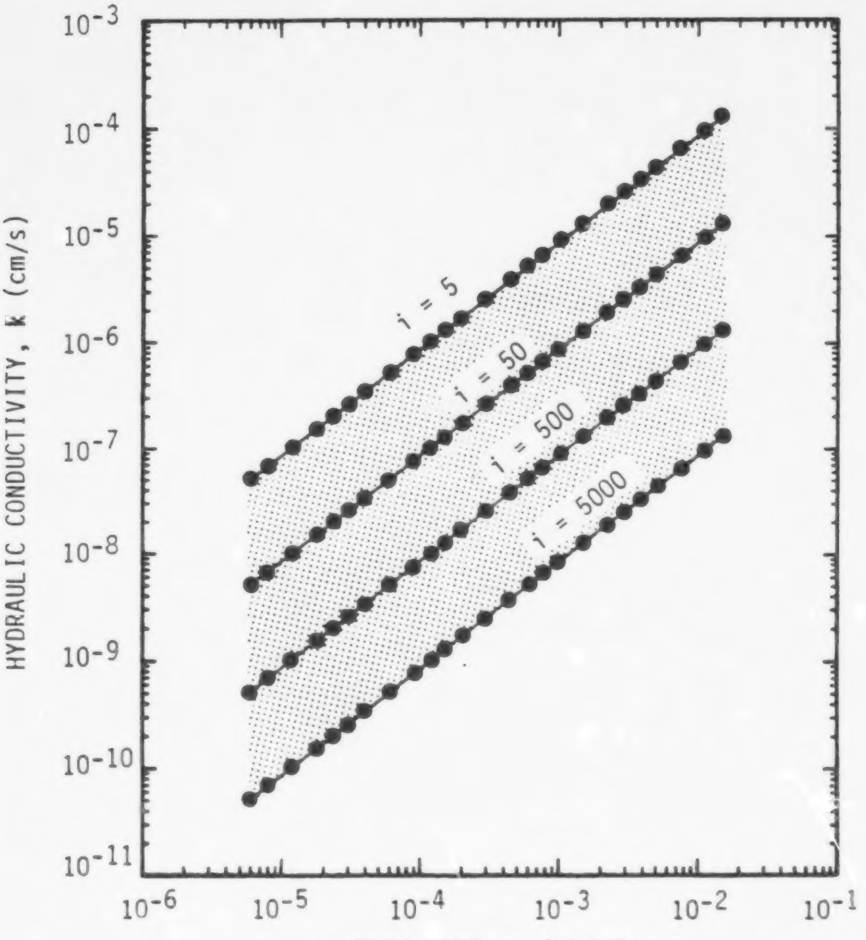

FIGURE 3.6 OPERATIONAL RANGE OF THE CONSTANT FLOW RATE HYDRAULIC CONDUCTIVITY EQUIPMENT

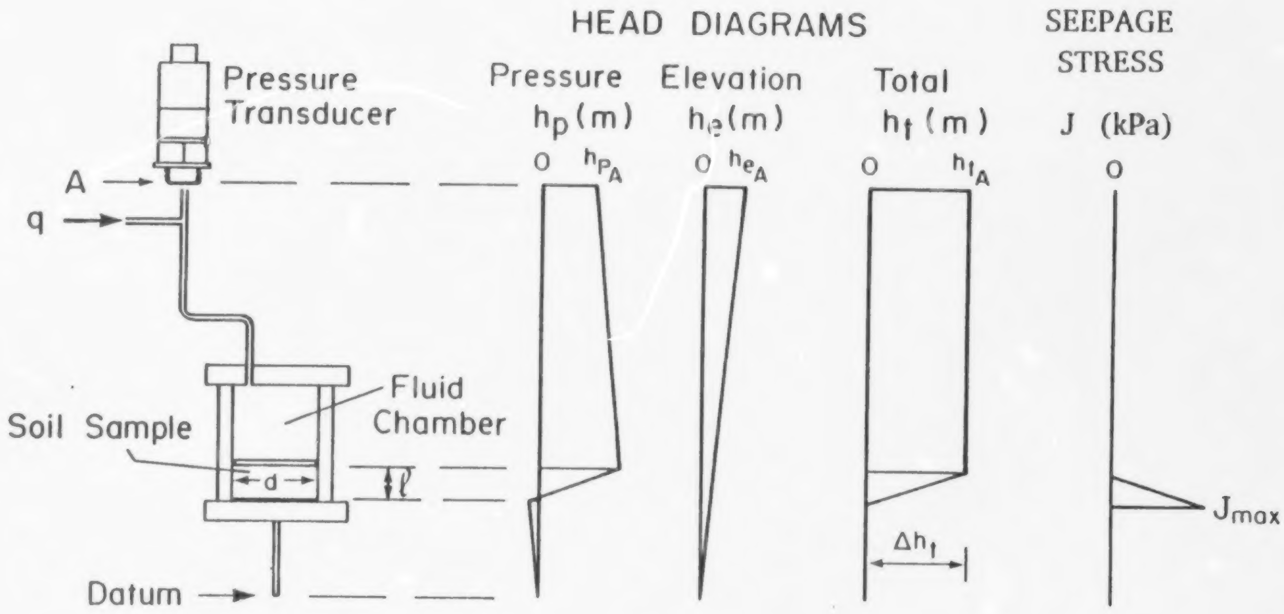
HEAD DIAGRAMS
SEEPAGE STRESS
Pressure Transducer
A
q
Fluid Chamber
Soil Sample
d
ℓ
Datum
Pressure h_p(m)
Elevation h_e(m)
Total h_t(m)
J (kPa)
0
h_{p_A}
h_{e_A}
h_{t_A}
Δh_t
J_{max}

$$k = \frac{q\ell}{\Delta h_t} \frac{4}{\pi d^2} \qquad \Delta h_t = h_{p_A} + h_{e_A}$$

$$J_{max} = i \gamma \ell = \Delta h_t \gamma$$

FIGURE 3.7 SCHEMATIC OF HEAD DIAGRAMS AND SEEPAGE FORCES FOR CONSTANT FLOW PERMEAMETER

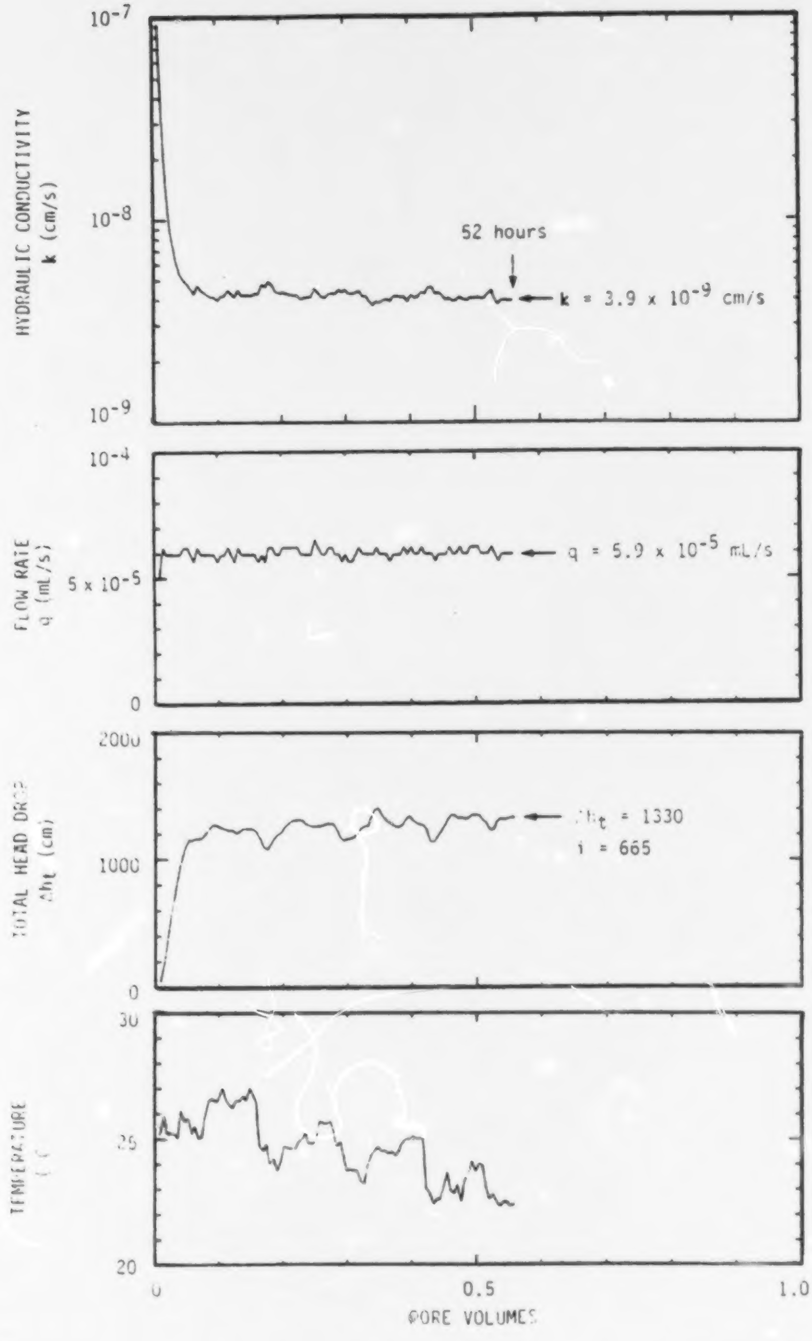

FIGURE 3.8 TYPICAL COMPLIANCE CURVES FOR HYDRAULIC CONDUCTIVITY, FLOW RATE, TOTAL HEAD DROP AND TEMPERATURE

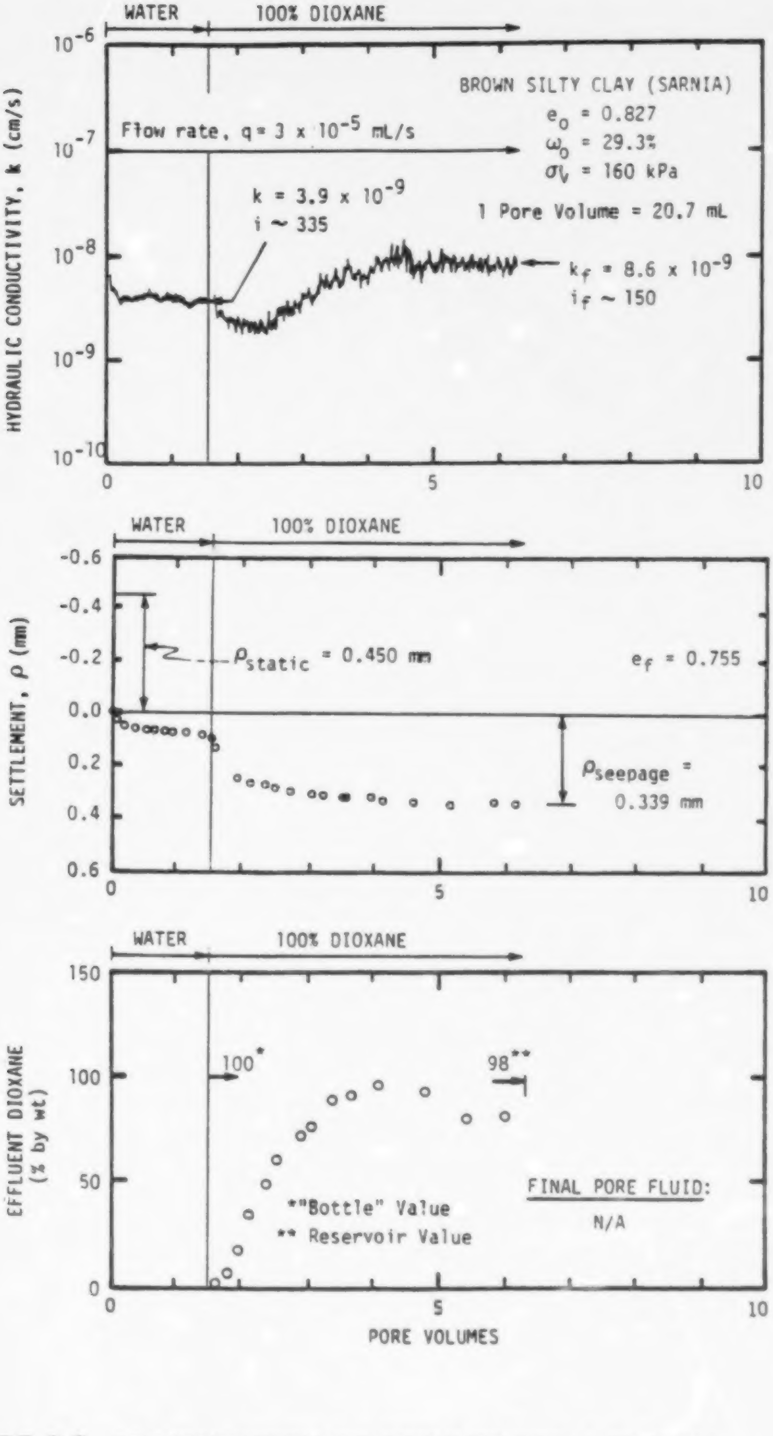

FIGURE 3.9 PRESENTATION OF RESULTS FOR A TYPICAL CLAY/LEACHATE COMPATIBILITY STUDY

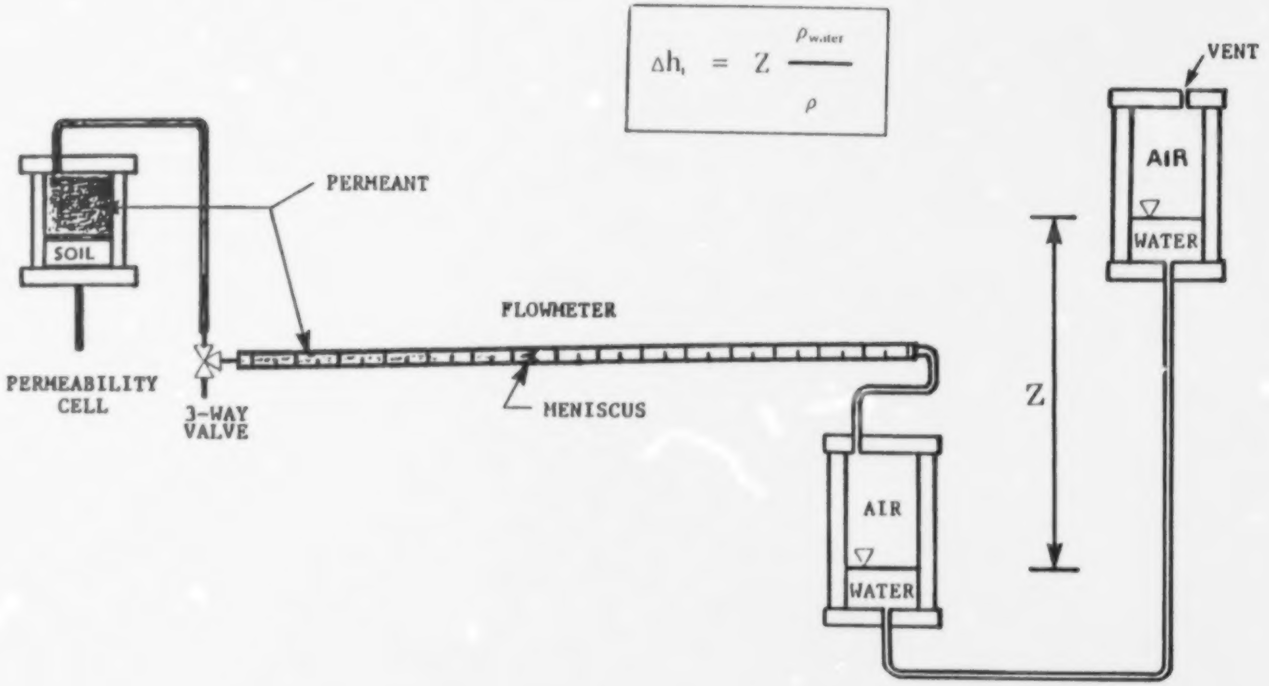

$$\Delta h_t = Z \frac{\rho_{water}}{\rho}$$

VENT
AIR
WATER
PERMEANT
SOIL
PERMEABILITY CELL
3-WAY VALVE
FLOWMETER
MENISCUS
Z
AIR
WATER

FIGURE 3.10 SCHEMATIC OF CONSTANT HEAD HYDRAULIC CONDUCTIVITY EQUIPMENT

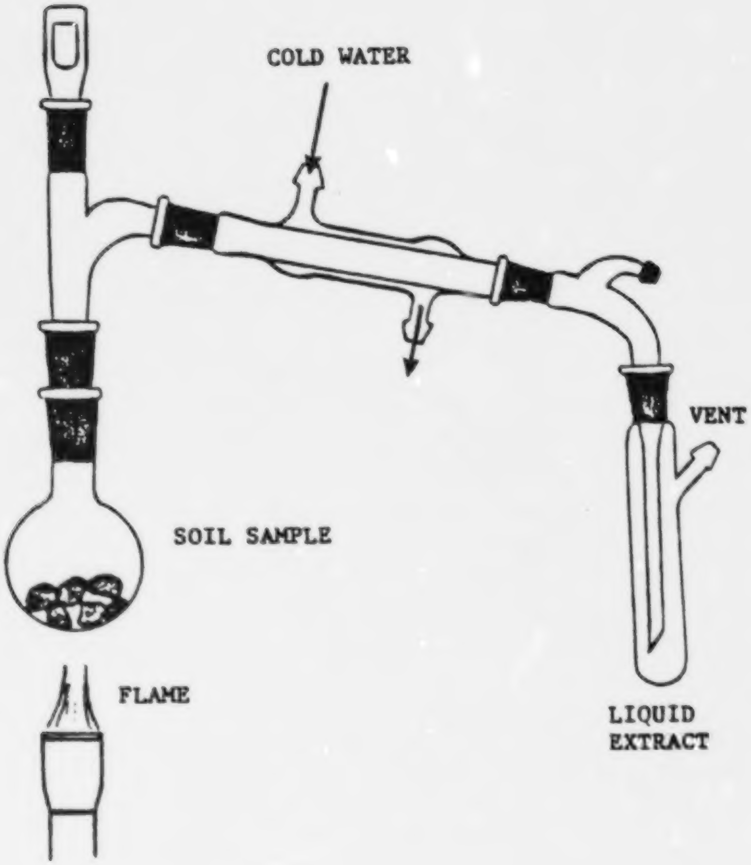
COLD WATER
VENT
SOIL SAMPLE
FLAME
LIQUID
EXTRACT

FIGURE 3.11 SCHEMATIC OF MINI-DISTILLATION APPARATUS

CHAPTER 4

TESTING MATERIALS

4.1 INTRODUCTION

This chapter describes the properties and characteristics of the soil specimens and liquid permeants used in the present research project. Separate sections are dedicated to the description of soils and permeants as unrelated materials, while the soil/permeant systems are described in the upcoming chapters.

The soils studied are considered to be representative of candidate soils for natural or compacted hydraulic barriers underlying sanitary landfill sites. The majority of the project was done using soil from the brown surface crust of a thick clay deposit in southwestern Ontario. Selected tests were extended to deeper samples of grey, less weathered regional clayey soils. The permeants used include water, leachate from a domestic waste landfill and organic liquids representing chemical industrial waste.

4.2 SOIL PROPERTIES

Clay samples were obtained from an excavation site at Courtright, Ontario, located fifteen kilometres south of the city of Sarnia. The samples were air dried, crushed and passed through sieve # 10 (2 mm) and stored in plastic bags.

The mineralogical composition and index properties of the Courtright soil were described by the author (Fernandez, 1984) and are summarized in Table 4.1. Having liquid limits around 40% and predominantly clayey texture, the Courtright soil can be classified as inorganic clay of low to medium plasticity (CL), according to the Unified Soil Classification System. The geology and composition of soils from the region of Sarnia have been described by Ogunbadejo (1973) and Quigley and Ogunbadejo (1976). They consist of an ~ 40 m thick deposit of water-lain clay till derived from the underlying limestones and shales. Table 4.1 shows that illite is the main clay mineral in both Courtright soils, followed by chlorite and variable amounts of carbonates and smectites. Up to 15% smecite is present in the brown surface soil, compared to ~ 2% in the deeper grey soil, resulting from oxidation weathering of unstable iron chlorite. Carbonates have been leached out from the brown surface soil during weathering, as observed by Ogunbadejo (1973) and Di Nardo (1977) for Sarnia clays.

Also listed in Table 4.1 are the cation exchange capacity (CEC) and the specific surface for the < 74 μm fractions of both soils. CEC values of 33 and 22 meq/100 g were obtained for the brown and grey clay, using a silver thiourea exchange method (Chabbra, 1975). These values are about 3 and 7 units higher than expected from the mineralogy of each soil (Table 4.1), the excess being mainly calcium from dissolution of calcite in silver thiourea. Specific surfaces of 120 and 55 m^2/g were estimated from measured glycol retention values of 37 and 17 mg/g for the brown and grey soils, respectively.

Compaction tests carried out on the < 2 mm Courtright soils are presented in Figure 4.1. Harvard miniature compaction in the Harvard mould (33.3 mm diameter by 71.5 mm high) was done in five layers of 20 tamps, using a 32 lb (0.142 kN) spring. This method resulted in a maximum dry density of 1.635 Mg/m^3 at an optimum water content of 21.5% for the brown clay and a maximum dry density of 1.708 Mg/m^3 at a water content of 20.5% for the grey clay. The results of a Standard Proctor test on the brown clay compare satisfactorily with the Harvard miniature results. However, both soil types compacted in the permeameter cells with a Harvard miniature tamper (3 layers, 30 tamps/layer, 0.142 kN/tamp) exhibit greater degree of compaction even though similar energy per unit mass of compacted soil was used. The larger area and reduced thickness of the layers in the **k** cell relative to the Harvard mould results in more soil being affected by the compaction rod and, consequently, more efficient compaction.

The influence of compaction on the hydraulic conductivity of the Courtright soils is shown in Figures 4.2 and 4.3. Compaction dry of optimum results in incomplete breakdown of soil lumps as the compaction effort is resisted by strong capillary forces. The resultant soil samples have large values of **k** (up to

1.6 x 10^{-6} cm/s), reflecting flow through large channels between soil peds. During permeation the dry samples gain moisture and swell, resulting in lower values of dry density (Tables 4.2 and 4.3). Sharp decreases in **k** to minimum values of 3.1 x 10^{-9} and 6.1 x 10^{-9} cm/s are shown by the brown and grey clays, at water contents 3% and 2% greater than their respective optimum values for compaction. The greatly reduced values of **k** are due to increased degrees of ped destruction and particle dispersion by mechanical kneading and wetting, reducing the average pore size. For samples compacted significantly wet of optimum, the values of **k** directly reflect the increase in void ratio with increasing water content. These important trends of hydraulic conductivity versus moulding water content were reported long ago for clayey soils by Lambe (1954), Bjerrium and Huder (1957) and Mitchell et al. (1965).

Based on its low hydraulic conductivity, its 15% smectite content and its convenient availability, the surface brown Courtright clay was selected as the prime test soil for this project. The samples were compacted at water contents close to 30%, which help to produce a uniform, well dispersed, ped-free and fracture-free soil structure.

Additional studies were carried out on undisturbed samples of grey, unweathered clay, obtained from a depth of 11 metres at the Confederation Road Landfill site, located 6.4 km southeast from the city of Sarnia, Ontario. The soil composition at the site has been described in several thesis studies at the University of Western Ontario (Ogunbadejo, 1973; Goodall, 1975; Crooks, 1981; and Yanful, 1986). Briefly, the water-laid till consists of a stiff, highly weathered, brown silty clay deposit approximately 4 m thick, underlain by grey, unweathered silty clay to a depth of about 40 m. Illite and Chlorite are the dominant clay minerals in the unweathered zone, while the smectite content is in the order of ~ 2%.

4.3 PROPERTIES OF THE PERMEANTS

Reference values of hydraulic conductivity for fine-grained soils should be obtained using natural pore water, since permeants of different chemical composition may yield erroneous values of **k**. For example, the use of distilled water as reference permeant may cause double layer expansion and consequently decrease **k** (Olson and Daniel, 1981; Dunn and Mitchell, 1984). Alternatively, the chemistry of the actual pore water may be closely duplicated to obtain an artificial pore water for use as a reference permeant. Throughout this thesis a standard solution of calcium sulphate in distilled water (0.01 N $CaSO_4$) was used to obtain reference values of **k** (water) prior to permeation with waste leachates. The concentration range of 0.01 N is believed to represent salt concentrations typically found in natural soils (Brown and Anderson, 1983). Furthermore, the calcium sulphate solution has been used as a control permeant on soil/permeant compatibility studies by numerous investigators (Anderson and Brown, 1980; Brown et al., 1983; Acar et al., 1985; Foreman and Daniel, 1986).

The waste leachate permeants used in this project consist of domestic landfill leachate, concentrated organic solvents and landfill leachate containing various amounts of organic solvents. The properties of these permeants are presented in separate sections following.

4.3.1 Domestic Landfill Leachate

Leachate was collected in dark plastic bottles from the leachate collection system at the Westminster Sanitary Landfill, City of London, Ontario, and is considered to be representative of raw domestic waste leachate. The fresh leachate has a salinity of ~ 5 g/L and could be described as a clear grey liquid with a pungent odour. Table 4.4 describes the composition of the Westminster landfill leachate, however the values may show a wide range in seasonal variation from dry to wet periods. The leachate composition is also largely dependent on the storage conditions. Exposure to oxygen turns the leachate brownish, whereas upon anaerobic storage at room temperature (22° ± 3°C) the leachate becomes black after a few days forming a black slimy substance. Reducing bacteria present in the leachate in counts of 6.2×10^9 colony-forming units per litre are believed to cause the slime formation. The chemical instability of leachate stored at room temperature may have significant implications in prolonged laboratory studies on clay/leachate compatibility. For further discussion on the subject the reader is referred to a recent study by Yanful, Fernandez and Quigley (1987).

4.3.2 Aqueous Solutions of Hydrocarbons

This section describes the properties of permeants used to assess the effect of increasing amounts of organic liquids in landfill leachates on the integrity of clays. The permeants were prepared by spiking Westminster landfill leachate with hycrocarbon liquids. Hydrocarbons are organic compounds consisting only carbon and hydrogen. At certain location in this report substances such as dioxane or alcohols, which also contain oxygen, may be referenced to as a hydrocarbon liquids for convenience of presentation, even though it is not strictly correct. Ethanol and dioxane were selected for this study, since they are both completely soluble in water and consequently can form a full range of leachate/hydrocarbon solutions. Furthermore, these two liquids represent solvents of intermediate and very low polarity respectively.

The hydrocarbon content of aqueous solutions can be expressed in terms of mass %, volume % and mole %. Although none of the three forms is inherently superior, the mass % (or % by wt) was selected to express the organic content of liquid samples throughout this report. The selection was made on the belief that the mass % is the least ambiguous and the simplest form for the geotechnical engineer. Interconversion formulas are derived in

Appendix B.

The dielectric constants of aqueous solutions of soluble organic liquids (methanol, ethanol, acetone and dioxane) are shown in Figure 4.4. All liquids show a steady decrease in ϵ with hydrocarbon content, from ~ 78 for pure water to the values for each concentrated solvent. The curves are close to linear when the hydrocarbon contents are expressed as Mass % or Volume %. In the molar scale, however, all curves exhibit a rapid decrease in ϵ at low hydrocarbon contents, reflecting predominant control of the less polar molecules on ϵ.

Plots of kinematic viscosity versus hydrocarbon content of aqueous solutions are shown in Figure 4.5. The addition of methanol, ethanol, acetone or dioxane to water promotes structural order, increasing the viscosity of the solutions. The maximum values of ν surpass the value of pure water by a factor ranging from ~ 1.5 (acetone) to ~ 3 (ethanol). Beyond these points the viscosity decreases to values typical of the concentrated solvents.

Figure 4.6 shows the equipment used for measurement of viscosity and dielectric constant of the test permeants. The kinematic viscosity was measured using a Cannon-Fenske routine viscometer placed in a constant temperature bath at 20°C. The dynamic viscosity was then obtained by multiplying the values of kinematic viscosity by the density of the liquid ($\mu = \nu \rho$). The measured viscosities of solutions of ethanol and dioxane in water and leachate are shown in Figure 4.7 and their values are detailed in Tables 4.5 to 4.8.

The dielectric constant of solutions of ethanol and dioxane in water are presented in Figure 4.8. The values were calculated from the capacitance of a specially designed capacitor (Figure 4.6a) filled with the liquid mixtures. Details of the calculations and the measured values of dielectric constant are given in Appendix C.

Table 4.9 shows the results of bacterial analyses on some of the permeants, performed by the Department of Microbiology and Immunology, University of Western Ontario. Small samples (0.1 mL) of the permeants were spread on agar plates and incubated aerobically and anaerobically for one week. The bacterial counts were then determined by enumerating the colonies of bacteria growing on each agar plate. Since the results are expressed as colony forming units per litre, values smaller than 10^4 indicate that growth of individual colonies was not observed. The data in Table 4.9 indicates that the addition of ethanol and dioxane produced significant decreases in both the aerobic and anaerobic bacterial population.

4.3.3 Physico-chemical Stability of Leachate/Hydrocarbon Mixtures

The addition of hydrocarbons to the Westminster landfill leachate resulted in rapid flocculation of the otherwise stable suspended matter. Figure 4.9

shows leachate/hydrocarbon mixtures after a sitting time of approximately one hour.

The flocs which formed in the ethanol/leachate mixtures settled to the bottom of the sample. The ethanol/leachate mixture containing benzene formed an unstable emulsion (by shaking) that rapidly separated in two phases: an upper "benzene-rich" phase and a lower aqueous phase. In this case the flocs were dragged upwards by benzene droplets separating out of the emulsion.

Upon addition of non-polar dioxane to the leachate, sediments concentrated at the top of the mixtures, and gradually sank to the bottom. It is speculated that the affinity of the flocs for non-polar phases is related to their content of organic matter including carboxylic acids, known to be common in landfill leachates (Chian, 1977; Crooks, 1981).

Concentrations of chloride, sodium, potassium, calcium, magnesium, and iron ions dissolved in the ethanol/leachate and dioxane/leachate mixtures are plotted in Figure 4.10. In spite of some scatter, the cation concentrations are predominantly lower than the expected values due to dilution upon addition of the organics. Chloride, on the other hand, appears at concentrations higher than the expected values due to dilution. Chemical analyses of the acid digested flocs revealed that they contain up to 20% calcium, ~ 10% iron, ~ 5% sodium, ~ 3% potassium, ~ 3% magnesium, and no chloride. It appears that the addition of organic solvents produces some salt dumping (nucleation and precipitation of dissolved ionic species) in the leachate.

TABLE 4.1 DESCRIPTION OF COURTRIGHT TEST SOILS

Test soil	Brown	Grey
Depth (m)	0.3	4.25
(1)Texture:		
clay (< 2 μm)	57%	57%
silt (2 μm - 74 μm)	33%	37%
sand (74 μm - 2 mm)	10%	6%
Plastic limit, ω_P	23%	21%
Liquid limit, ω_L	48%	40%
Specific gravity, G_s	2.75	2.74
(2)Maximum dry density, $\rho_{d_{max}}$ (g/cc)	1.635	1.708
(2)Water content at $\rho_{d_{max}}$	21.5%	20.5%
(2)Void ratio at $\rho_{d_{max}}$	0.682	0.604
Mineralogy:		
quartz and feldspar	~ 20%	~ 18%
carbonate	~ 6%	~ 20%
illite	~ 50%	~ 40%
chlorite	~ 8%	~ 20%
smectite	~ 15%	~ 2%
(3)Cation exchange capacity (meq/100g)	~ 30	~ 15
(3)Specific Surface (m^2/g)	120	55

Notes: (1) Sizes greater than 2 mm removed from bulk soil to obtain test soil.

(2) Values obtained from Harvard miniature compaction.

(3) Measured on < 74 μm soil fraction.

TABLE 4.2 HYDRAULIC CONDUCTIVITY TEST DATA FOR BROWN SILTY CLAY

MOISTURE CONTENT (%)		DRY DENSITY (Mg/m^3)		VOLUME (cc)		VOID RATIO		DEGREE OF SATURATION (%)		P.V.	i	k (cm/s)
ω_o	ω_f	ρ_{d_o}	ρ_{d_f}	V_o	V_f	e_o	e_f	S_o	S_f			
8.0	31.7	1.600	1.468	45.8	49.9	0.718	0.873	30.6	100	1.8	9	5.0×10^{-7}
9.9	29.2	1.624	1.526	45.8	48.7	0.693	0.802	39.3	100	2.2	61	1.6×10^{-6}
14.7	29.2	1.638	1.525	45.8	49.2	0.679	0.803	59.5	100	2.3	63	1.55×10^{-6}
17.1	30.2	1.692	1.496	45.8	51.8	0.625	0.838	75.4	99.0	1.9	270	9.7×10^{-9}
18.2	21.7	1.766	1.724	45.8	46.9	0.557	0.595	89.8	100	2.0	505	7.7×10^{-9}
22.9	24.2	1.642	1.651	45.8	45.5	0.675	0.665	93.2	100	1.9	1255	3.1×10^{-9}
28.5	29.4	1.505	1.518	45.8	45.4	0.827	0.812	94.8	99.5	1.0	745	5.2×10^{-9}
33.5	33.7	1.395	1.428	45.8	44.7	0.972	0.926	94.9	100	1.0	395	9.8×10^{-9}
37.1	36.9	1.332	1.354	45.8	45.1	1.065	1.031	95.9	98.4	0.9	210	1.85×10^{-8}
40.4	40.5	1.257	1.282	45.8	45.0	1.188	1.148	93.5	97.0	1.1	134	2.9×10^{-8}

TABLE 4.3 HYDRAULIC CONDUCTIVITY TEST DATA FOR GREY SILTY CLAY

MOISTURE CONTENT (%)		DRY DENSITY (Mg/m^3)		VOLUME (cc)		VOID RATIO		DEGREE OF SATURATION (%)		P.V.	i	k (cm/s)
ω_o	ω_f	ρ_{d_o}	ρ_{d_f}	V_o	V_f	e_o	e_f	S_o	S_f			
3.7	31.8	1.535	1.461	45.8	48.1	0.785	0.876	12.9	99.6	2.1	19	2.1×10^{-7}
7.2	28.4	1.586	1.526	45.8	47.6	0.727	0.795	27.2	97.9	2.2	22	1.75×10^{-7}
11.2	31.2	1.590	1.452	45.8	50.1	0.726	0.887	42.4	96.3	2.2	13	3.05×10^{-7}
18.5	22.3	1.779	1.708	45.8	47.7	0.540	0.605	93.9	100	2.2	320	8.2×10^{-9}
23.3	23.8	1.636	1.654	45.8	45.3	0.675	0.657	94.6	99.2	1.3	437	8.9×10^{-9}
25.9	26.8	1.562	1.578	45.8	45.3	0.754	0.736	94.3	99.9	1.2	288	1.35×10^{-8}
30.5	30.5	1.441	1.465	45.8	45.0	0.902	0.871	92.6	96.0	1.1	78	5.0×10^{-8}
35.3	34.3	1.345	1.379	45.8	44.7	1.038	0.987	93.1	95.2	1.0	97	4.0×10^{-8}

TABLE 4.4 CHEMICAL COMPOSITION OF LEACHATE FROM THE WESTMINSTER LANDFILL (CITY OF LONDON, ONTARIO)

	CONSTITUENT	TYPICAL VALUE
	pH	6.7 to 7
(1)	Ammonium - NH_4^+	1260 mg/L
	Alkalinity (as $CaCO_3$)	4200 mg/L
(1)	Sodium	955 mg/L
	Potassium	400 mg/L
	Calcium	250 mg/L
	Magnesium	290 mg/L
	Chloride	1000 mg/L
	Sulphate - $SO_4^{=}$	< 0.01 mg/L
	Sulphide - $S^{=}$	10.8 mg/L
(1)	Manganese	2.4 mg/L
	Iron	160 mg/L
	Lead	0.3 mg/L
	Zinc	4.1 mg/L
	Copper	0.1 mg/L
	Cadmium	0.05 mg/L
	Suspended Solids	97 mg/L
	Total Carbon in Susp. Solids	16 %
	Dissolved Inorganic Carbon (DIC)	77.5 mg/L
	Dissolved Organic Carbon (DOC)	3550 mg/L
(1)	Biological Oxygen Demand (BOD)	3876 mg/L
	Bacterial Count:-	
	Aerobic	3.2×10^9 cfu/L(2)
	Anaerobic	2.6×10^9 cfu/L

Notes: (1) Source: Barone et al. (1989)
(2) cfu/L = colony forming units per litre

TABLE 4.5 DENSITY AND VISCOSITY OF WATER/ETHANOL MIXTURES
(all values measured at 20°C)

ETHANOL CONTENT (% by wt)	DENSITY (ρ) (g/cm^3)	VISCOSITY	
		DYNAMIC (μ) (cP)	KINEMATIC (ν) (cS)
0	1.00123	1.00123	1.00000
10	0.98429	1.43892	1.46189
20	0.97223	2.00342	2.06064
35	0.95082	2.59662	2.73093
50	0.92297	2.71435	2.94088
65	0.89128	2.49363	2.79781
80	0.85762	2.09202	2.43933
90	0.83463	1.74463	2.15317
100	0.81026	1.46300	1.80559

TABLE 4.6 DENSITY AND VISCOSITY OF WATER/DIOXANE MIXTURES
(all values measured at 20°C)

DIOXANE CONTENT (% by wt)	DENSITY (ρ) (g/cm^3)	VISCOSITY	
		DYNAMIC (μ) (cP)	KINEMATIC (ν) (cS)
0	1.00123	1.00123	1.00000
10	1.00807	1.20999	1.20031
20	1.01640	1.43455	1.41140
35	1.02568	1.77479	1.73035
50	1.03398	2.09823	2.02928
65	1.04008	2.16991	2.08629
80	1.03920	1.88785	1.81664
90	1.03830	1.55825	1.50077
100	1.03373	1.27970	1.23795

TABLE 4.7 DENSITY AND VISCOSITY OF LEACHATE/ETHANOL MIXTURES
(all values measured at 20°C)

ETHANOL CONTENT (% by wt)	DENSITY (ρ) (g/cm^3)	VISCOSITY	
		DYNAMIC (μ) (cP)	KINEMATIC (ν) (cS)
0	1.00405	1.05089	1.04665
10	0.98901	1.46447	1.48074
20	0.97347	2.11194	2.16949
35	0.93643	2.76456	2.95223
50	0.90458	2.71513	3.00154
65	0.89094	2.56162	2.87519
80	0.85901	2.17995	2.53775
90	0.83662	1.82319	2.18028
100	0.81026	1.46300	1.80559

TABLE 4.8 DENSITY AND VISCOSITY OF LEACHATE/DIOXANE MIXTURES (all values measured at 20°C)

DIOXANE CONTENT (% by wt)	DENSITY (ρ) (g/cm^3)	VISCOSITY	
		DYNAMIC (μ) (cP)	KINEMATIC (ν) (cS)
0	1.00405	1.00123	1.04665
10	1.01150	1.28758	1.27294
20	1.01914	1.51365	1.48523
40	1.03164	1.97022	1.90980
70	1.04194	2.16976	2.08243
90	1.03549	1.57444	1.52048
100	1.03373	1.27970	1.23795

TABLE 4.9 BACTERIAL POPULATIONS OF LEACHATE/HYDROCARBON MIXTURES

HYDROCARBON CONTENT	BACTERIAL COUNT (cfu/L)	
	Anaerobic	Aerobic
0 %	3.2×10^9	2.6×10^9
Ethanol:		
20 %	1.5×10^4	10×10^4
40 %	(1) 1×10^4	1×10^4
Dioxane:		
10 %	(2) N/G	1×10^4
20 %	N/G	0.5×10^4
40 %	2×10^5	N/G
70 %	1×10^4	N/G

Notes: (1) A count of 1×10^4 cfu/L refers to one colony on the agar growth plate.

(2) Colony growth not observed.

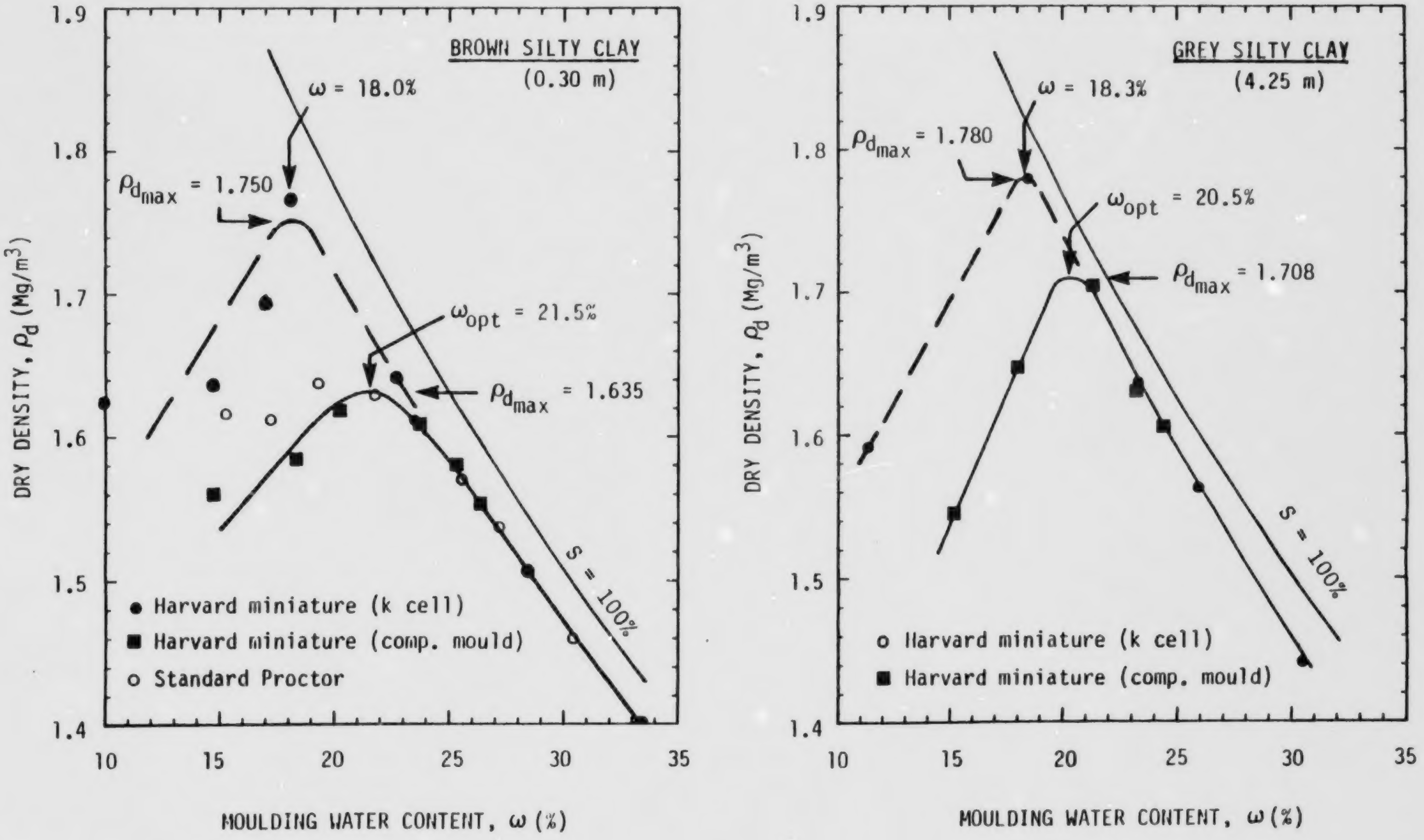

FIGURE 4.1 COMPACTION CURVES FOR COURTRIGHT TEST SOILS

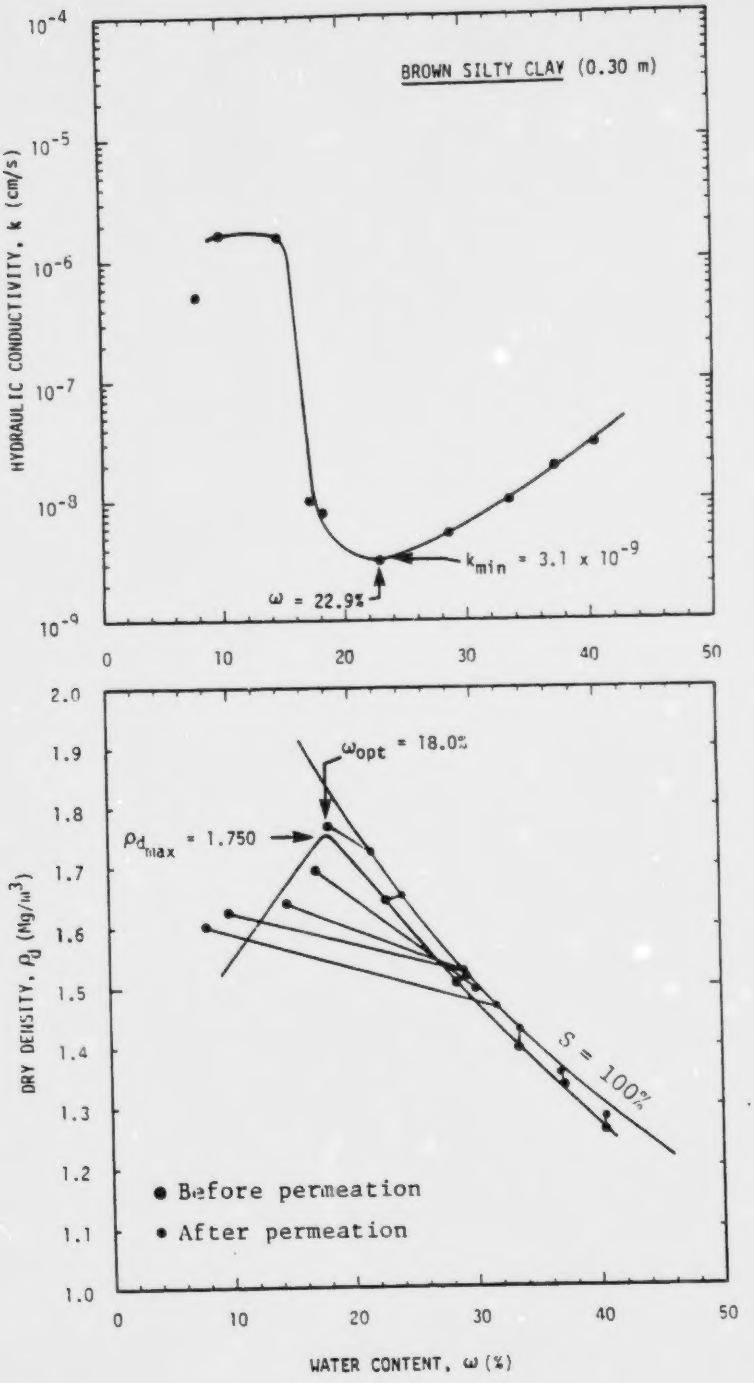

FIGURE 4.2 HYDRAULIC CONDUCTIVITY AND COMPACTION CURVES FOR BROWN COURTRIGHT SILTY CLAY

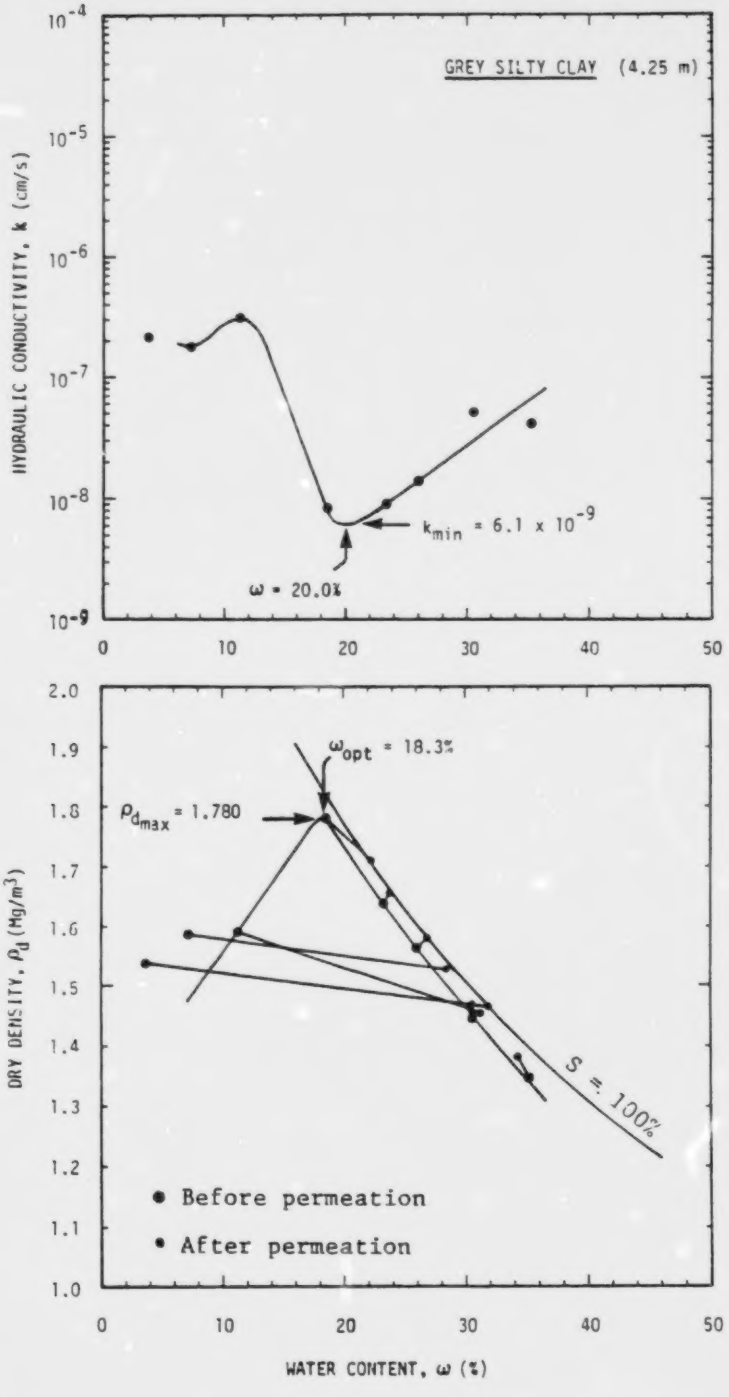

FIGURE 4.3 HYDRAULIC CONDUCTIVITY AND COMPACTION CURVES FOR GREY COURTRIGHT SILTY CLAY

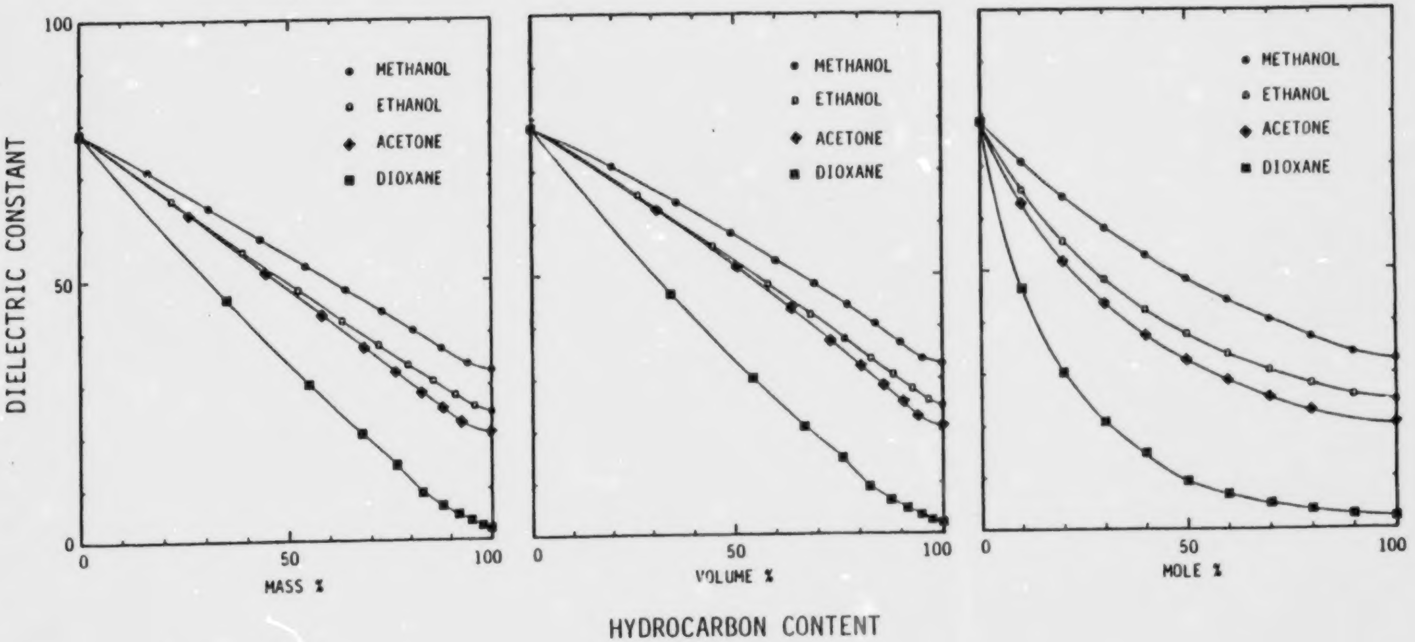

Source: Marcus, 1985

FIGURE 4.4 DIELECTRIC CONSTANT OF AQUEOUS SOLUTIONS CONTAINING HYDROCARBON LIQUIDS AT 25 °C (Source Marcus, 1985)

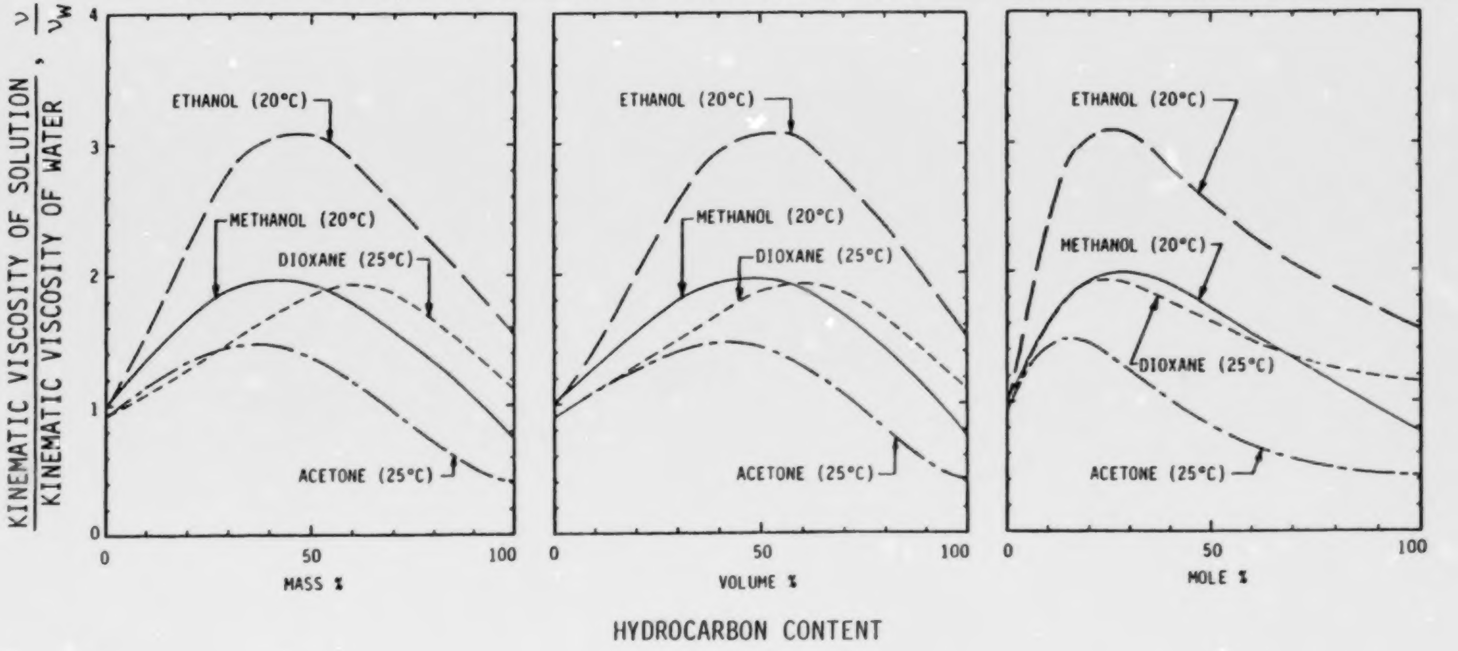

Sources: Weast, 1984 (Ethanol and Methanol); Flick, 1985 (Acetone); Janz, 1972 (Dioxane)

FIGURE 4.5 KINEMATIC VISCOSITY OF AQUEOUS SOLUTIONS CONTAINING HYDROCARBON LIQUIDS (Varied sources)
[All values relative to pure water]

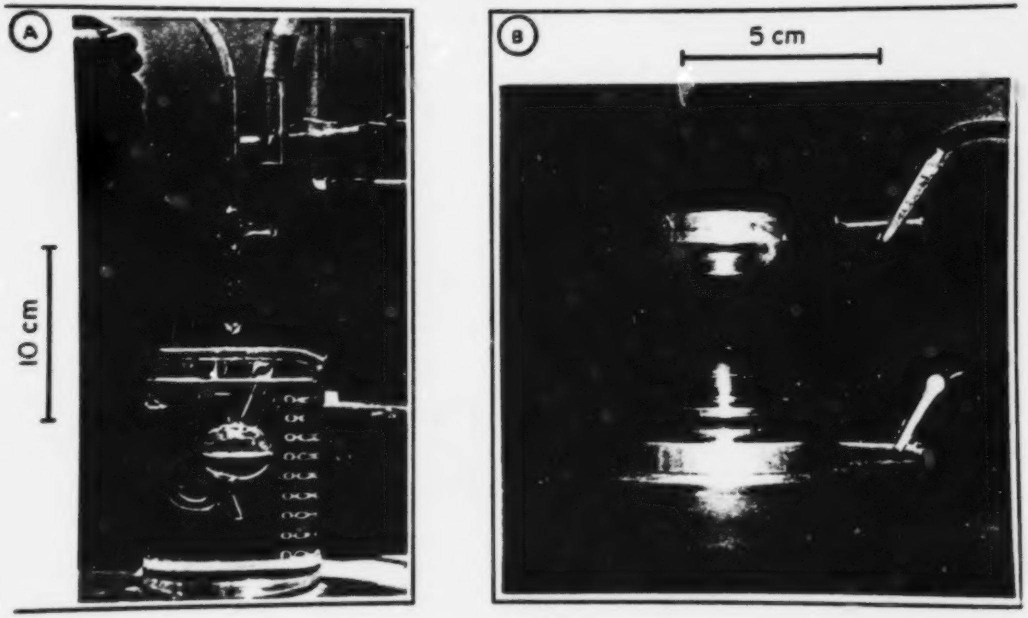

FIGURE 4.6 MEASUREMENT OF KINEMATIC VISCOSITY (a) AND DIELECTRIC CONSTANT (b)

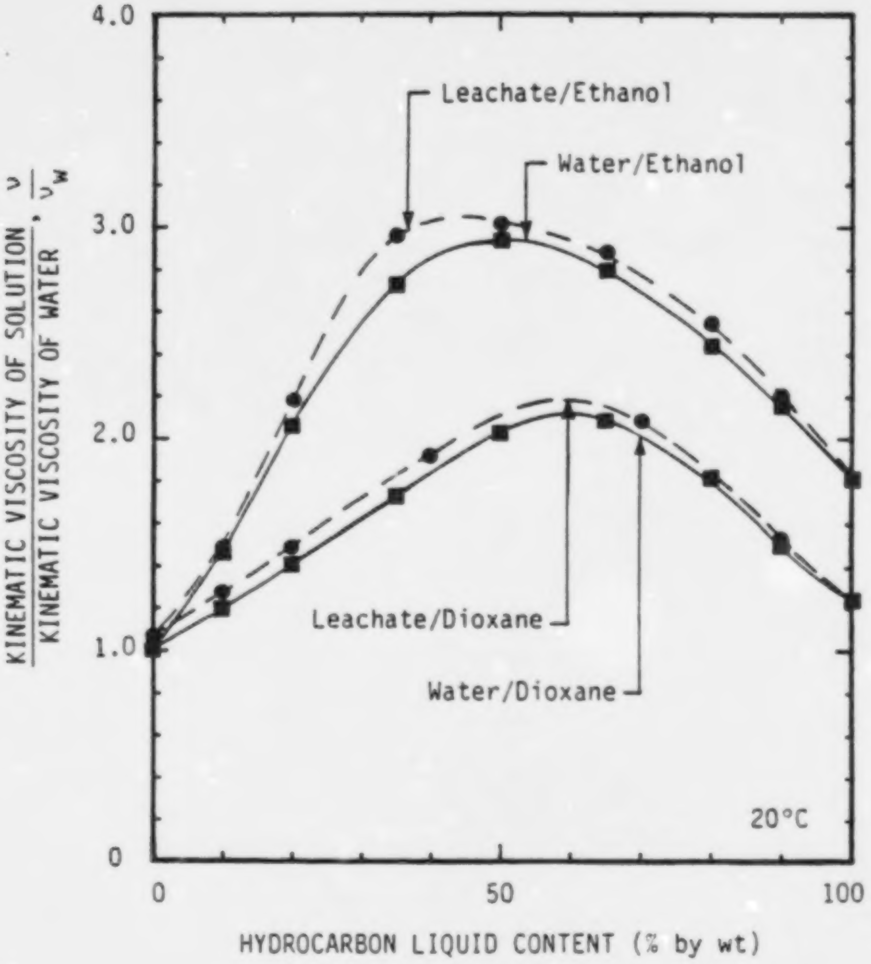

FIGURE 4.7 MEASURED VISCOSITY OF AQUEOUS SOLUTIONS CONTAINING HYDROCARBON LIQUIDS

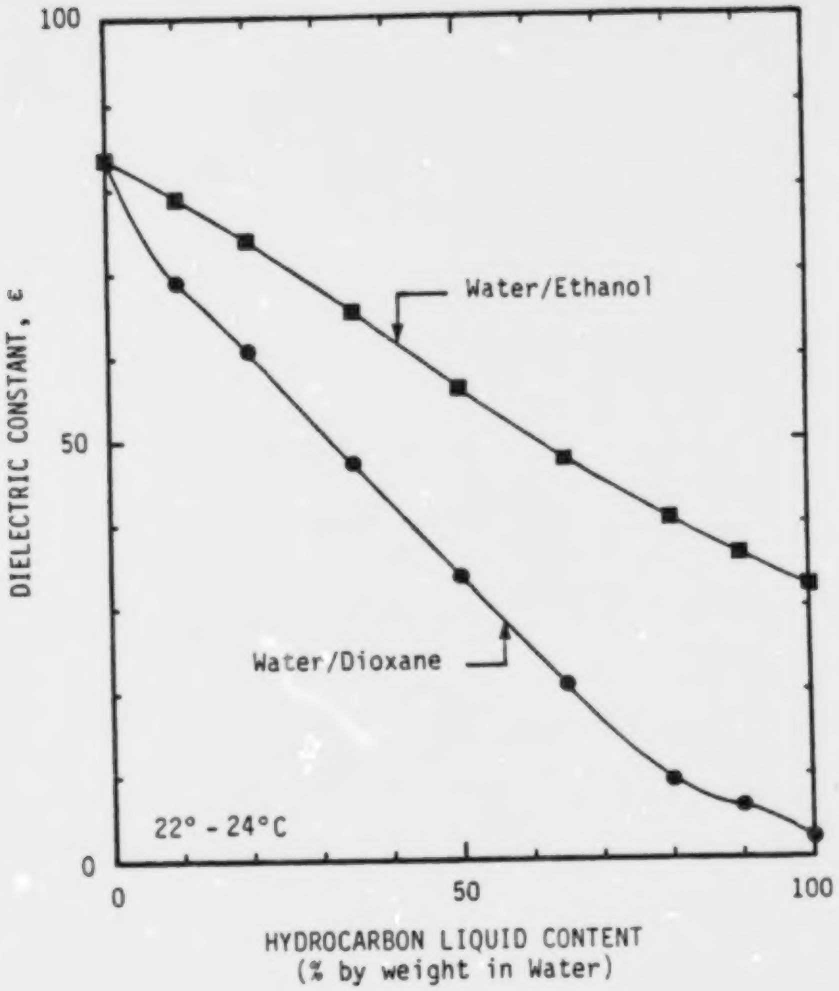

FIGURE 4.8 MEASURED DIELECTRIC CONSTANTS OF AQUEOUS SOLUTIONS CONTAINING HYDROCARBON LIQUIDS

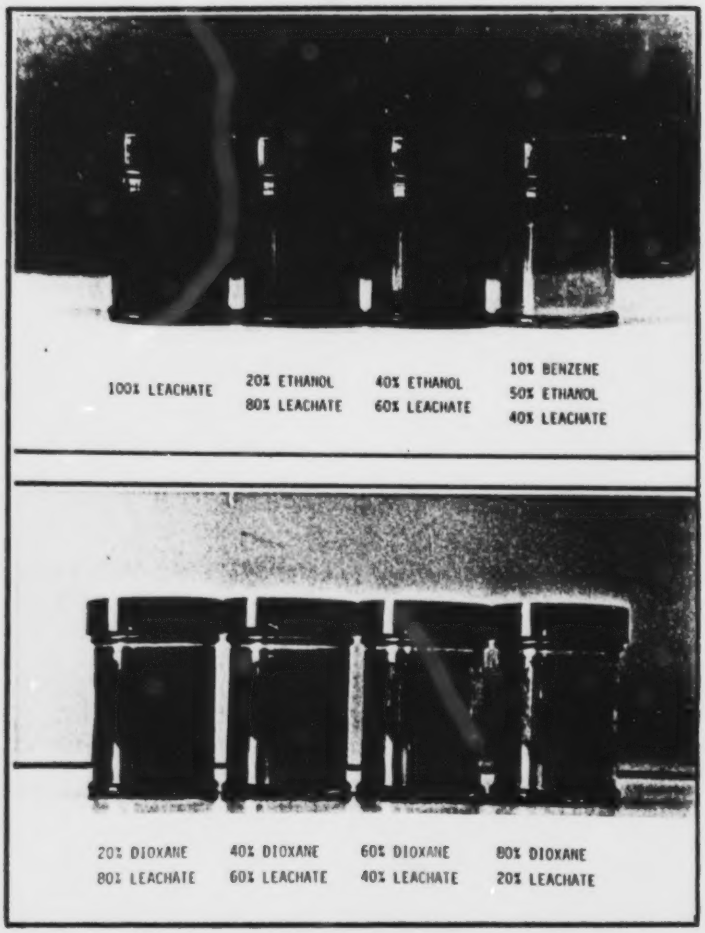
100% LEACHATE
20% ETHANOL
80% LEACHATE
40% ETHANOL
60% LEACHATE
10% BENZENE
50% ETHANOL
40% LEACHATE
20% DIOXANE
80% LEACHATE
40% DIOXANE
60% LEACHATE
60% DIOXANE
40% LEACHATE
80% DIOXANE
20% LEACHATE

FIGURE 4.9 INSTABILITY OF DOMESTIC WASTE LEACHATE UPON ADDITION OF ORGANIC LIQUIDS

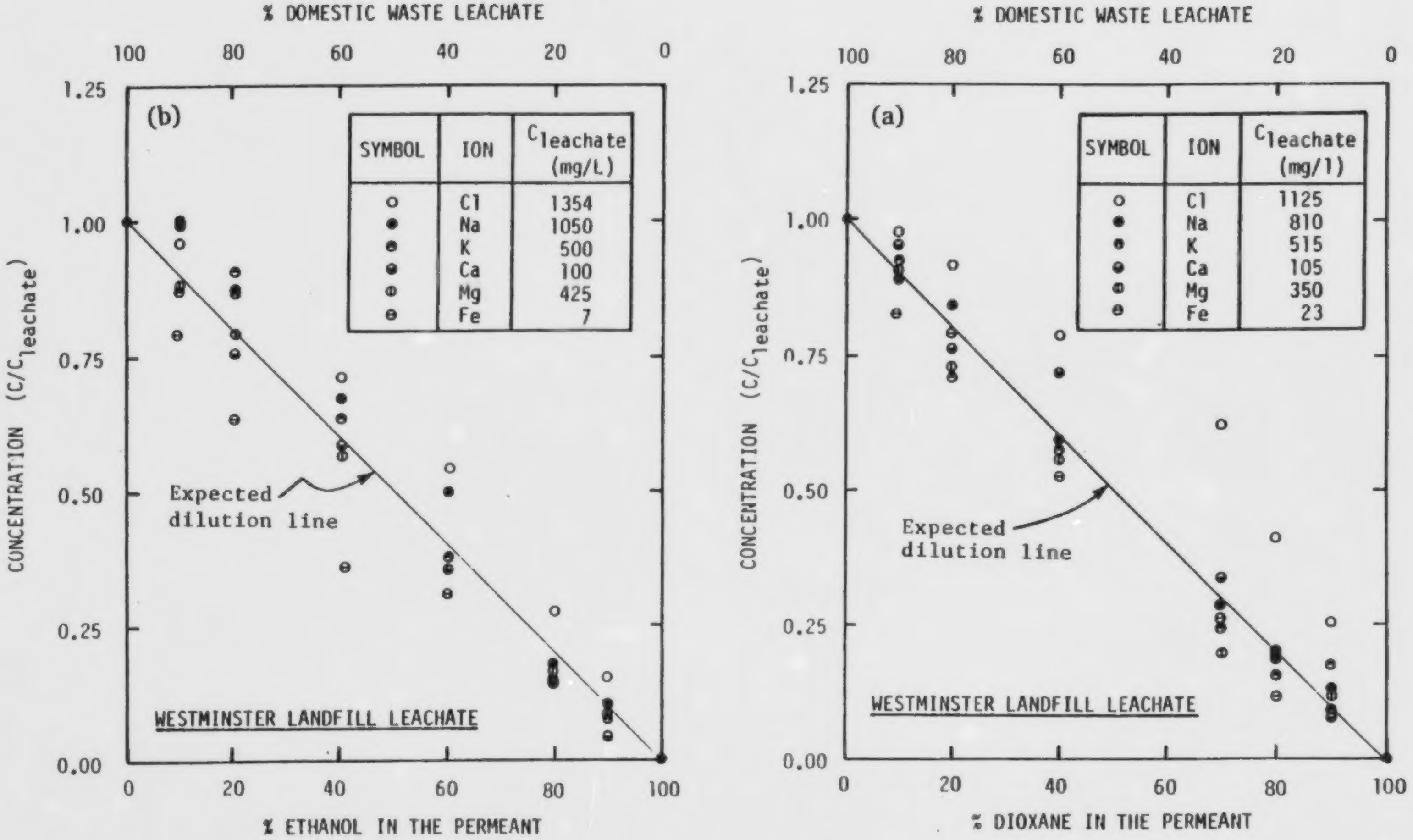

FIGURE 4.10 RELATIVE CONCENTRATIONS OF DISSOLVED INORGANIC SPECIES IN ETHANOL/LEACHATE AND DIOXANE/LEACHATE MIXTURES

CHAPTER 5

PERMEATION OF CLAYS WITH DOMESTIC LEACHATE CONTAINING HYDROCARBON LIQUIDS

5.1 INTRODUCTION

This chapter summarizes the results of a laboratory study on the effects of water-soluble organic liquids in domestic waste leachate on the hydraulic conductivity of the weathered Sarnia test clay. The purpose of the study was to assess the possibility of damage to clayey barriers at old codisposal sites, or domestic landfill locations where accidental or illegal dumping of organic solvents might have occurred. Ethanol (ethyl alcohol) and dioxane (diethylene ether) were used as the organic liquids since both are completely soluble in water and in aqueous domestic leachate and since they represent solvents of intermediate and very low dielectric constant, respectively. Furthermore, as reported by the authors elsewhere (Fernandez and Quigley, 1985), the water-soluble varieties of organic solvents are the most likely to increase the hydraulic conductivity of water-compacted clays.

The hydraulic conductivity test results are presented in two separate sections corresponding to two different methods of sample preparation and testing used. The first section describes fundamental studies carried out on dry clays mixed and permeated with aqueous solutions of ethanol and dioxane. An attempt is made to illustrate the interrelated roles of double layer collapse, soil flocculation and permeant viscosity on the measured values of **k**. The second section presents the hydraulic conductivity tests performed on water-compacted brown Sarnia clay permeated with domestic waste leachate mixed with a complete concentration range of ethanol or dioxane. The role of effective stresses in minimizing increases in **k** is illustrated by the results of testing performed using vertical static effective stresses of 0, 40, 80 and 160 kPa. This section also includes the hydraulic conductivity testing of undisturbed grey Sarnia clays permeated with mixtures of leachate and ethanol at zero static effective stresses.

5.2 PERMEANT COMPACTED CLAYS

Hydraulic conductivity testing of clays mixed and compacted with the ultimate permeant has been suggested as having the apparent advantage that the soil is closer to "chemical equilibrium" with the permeant at the start of testing. This should reduce permeation times and is occasionally advocated as a suitable procedure for studies of clay/leachate compatibility. Since the soils are thoroughly mixed with the permeants, significant permeant influence on the soil fabric (normally flocculation) is produced during sample preparation, rather than during permeation. Although the resulting **k** values are generally much higher than for water compacted clays, this type of testing can yield useful information on the behaviour of clay/organic liquid systems, if properly interpreted.

The following sections describe the results of more than sixty hydraulic conductivity tests performed on dry clays mixed with various aqueous solutions of liquid hydrocarbons. The results are shown in the form of summary figures, while individual curves showing hydraulic conductivity versus pore volumes are detailed in Appendix D.

5.2.1 Ethanol/Water/Clay Mixtures

Figure 5.1a shows the results of two sets of **k** tests for brown Sarnia clay, moulded and permeated with water/ethanol mixtures at void ratios of 0.8 and 1.2. The values of **k** for pure water at the low and high void ratios were 1.05 x 10^{-8} and 1.9 x 10^{-7} cm/s, respectively. For both cases, slight decreases in **k** were observed in the low (10%) to moderate (50%) ethanol concentration range. Above 50% the **k** values increase up to maximum values of 8.95 x 10^{-8} cm/s (e = 0.8) and 6.35 x 10^{-6} cm/s (e = 1.2) for concentrated ethanol. The same data, adjusted for viscosity/density effects, are shown in Figure 5.1b as intrinsic permeability values. Both K curves show steady increases with increasing ethanol content throughout the whole concentration range. The rate of increase in K (as indicated by the slope of the dashed lines) is significantly higher in the high ethanol concentration range (> 50%).

The results of reference **k**-tests for kaolinite and montmorillonite clays mixed and permeated with aqueous solutions of ethanol, are shown in Figure 5.2, relative to the brown Sarnia clay. Kaolinite exhibits a hydraulic conductivity of 2.05 x 10^{-8} cm/s for pure water, decreasing to 0.95 x 10^{-8} cm/s at ~ 40% ethanol. Beyond this point the values of **k** increase with ethanol content to a maximum value of 2.8 x 10^{-8} cm/s for concentrated ethanol. The values of **k** for montmorillonite, decrease from 3.5 x 10^{-10} cm/s (water) to 7.5 x 10^{-11} cm/s at 35% ethanol. This is followed by a spectacular rate of increase in **k** with alcohol content to 1.5 x 10^{-6} cm/s for concentrated ethanol. The curves in Figure 5.2a show very slight and gradual increase in the intrinsic permeability of kaolinite from 2.1 x 10^{-13} cm^2 (water) to 5.2 x 10^{-13} cm^2 (100% ethanol). Montmorillonite, on the other hand, shows spectacular increases in K from ~ 3 x 10^{-15} cm^2 (for ethanol contents up to 35%) to a maximum value of 2.8 x 10^{-11} cm^2, for 100% ethanol.

5.2.2 Dioxane/Water/Clay Mixtures

The results of **k** tests for brown Sarnia clay moulded and permeated with dioxane/water mixtures at e = 0.8 are shown in Figure 5.3, relative to similar tests with ethanol/water mixtures. The dioxane mixtures show a rapid increase in **k** with increasing hydrocarbon content from 1.05 x 10^{-8} cm/s (water) to 2.2 x 10^{-5} cm/s (pure dioxane). The values of intrinsic permeability also increase rapidly with dioxane content (Figure 5.3b). The maximum value of K for pure dioxane has increased 2600-fold above the K value for water, relative to a

15-fold increase shown by commercial ethanol.

5.2.3 Leachate/Hydrocarbon/Clay Mixtures

The test results for Sarnia clay samples moulded and permeated with leachate/ethanol and leachate/dioxane mixtures are presented in Figures 5.4 and 5.5. The figures also show the corresponding data for water/hydrocarbon mixtures. The ethanol mixtures yield minimum values of **k** for low to intermediate alcohol contents, followed by increases of up to 10-fold at high ethanol contents (Figure 5.4). The intrinsic permeability, K, exhibit gradual increases with increasing alcohol contents. In the 30% to 60% ethanol range, the leachate/ethanol mixtures appear to yield higher values of both **k** and K, relative to the water/ethanol mixtures. For the case of dioxane (Figure 5.5), there are no significant differences between the test results for leachate and water solutions. Both sets of permeants exhibit rapid increases in **k** and K with dioxane content.

5.2.4 Discussion of the Data

The present study has addressed several variables that affect the hydraulic conductivity of permeant-compacted clays. They include permeant specific properties such as viscosity and dielectric constant, as well as soil mineralogy and void ratio of compaction. The results reveal the interrelated roles of viscosity, dielectric constant and soil fabric on **k**:

a) Permeant Viscosity: As discussed in Chapter 4, soluble hydrocarbons such as ethanol and dioxane, mixed with water (or domestic leachate) produce two to three-fold increases in kinematic viscosity at concentrations of 40 to 60% (Figure 4.7). The hydraulic conductivity of the clay samples tested with aqueous solutions of ethanol (Figures 5.1a and 5.2a) decreases in a manner that mirrors the increases in the viscosity of the permeants. The results are adjusted for viscosity effects and expressed as intrinsic permeability, K, on Figures 5.1b and 5.2b, showing that the viscosity correction eliminates the decreases in **k** observed. It is therefore concluded that the decreases in hydraulic conductivity for the dilute to moderate range of alcohol contents are caused by the enhanced resistance to flow by viscous permeants.

b) Dielectric Constant: Ethanol and dioxane when mixed with water cause the dielectric constant of the mixtures to decrease as the hydrocarbon contents increase (Figure 4.8). As discussed in Chapter 2, decreases in the dielectric constant of the pore fluid causes progressive contraction of the double layers surrounding the clay particles. The clay/permeant system formed under such conditions, offers less resistance to flow than the corresponding clay/water system with expanded double layers. Thus the increases in **k** observed for high ethanol contents in Figures 5.1 and 5.2 are directly or indirectly related to double layer contraction in the presence of less polar permeants (see next section of soil fabric).

A summary plot of intrinsic permeability versus dielectric constant of the permeant is presented in Figure 5.6. This figure includes data from Figures 5.1 and 5.2 and data reported by the author (Fernandez 1984) for clay mixed and permeated with pure organic solvents. The values of K for brown Sarnia clay at a void ratio of 0.8 increase from ~ 10^{-13} to 10^{-9} cm^2 as the dielectric constant of the permeant decreases from ~ 80 to ~ 2. This trend applies consistently to a variety of pure solvents and the ethanol/water mixtures, confirming that the increases in permeability are caused by double layer contraction in the presence of low dielectric media. The relationship between K and ϵ, however, appears to be unique for each soil type; the values of K for kaolinite show little increase, whereas montmorillonite shows very large increases in K as ϵ reaches values below 50.

c) Soil Fabric: The "structure" or arrangement of the clay particles within soil samples is known to have strong effects on the values of **k** (Lambe, 1954). For a constant void ratio, a flocculated (aggregated) clay is likely to have larger pores than a dispersed clay, and consequently much larger **k**. Double layer contraction in the presence of a low dielectric pore fluid decreases the magnitude of repulsive forces between clay particles, thus promoting flocculation. Pore size distributions of the **k** tested samples, obtained by mercury intrusion porosimetry on freeze-dried specimens, are summarized in Figure 5.7. The brown Sarnia clays moulded with water/ethanol mixtures experienced progressive flocculation with increasing alcohol content. This is suggested by the gradual shift in the dominant pore diameter from 0.11 μm (water or leachate) to 0.32 μm (100% ethanol). The water/ethanol mixtures appear to have little effect on the pore size distribution of kaolinite. In all cases, the variations in dominant pore size exhibit a very close correlation with the values of intrinsic permeability.

In summary, the hydraulic conductivity of dried clays mixed and permeated with aqueous solutions of hydrocarbons is jointly controlled by the viscosity and dielectric constant the permeants. Decreases in k, resulting from the resistance to flow by viscous permeants, were typically observed for hydrocarbon contents of up to 50%. On the other hand, the drop in dielectric constant with increasing hydrocarbon content promoted flocculation of the clay fabric, resulting in increases in **k**, which become predominant at high hydrocarbon contents.

5.3 WATER-SATURATED CLAYS

The work presented in Section 5.2 illustrated the complex effect that aqueous solutions of hydrocarbons may have on the hydraulic conductivity of clays. It must be kept in mind that the clay samples were thoroughly dried and remoulded with the permeants prior to permeation, thus allowing for maximum control of the permeant on the clay fabric. In the field, however, clay barriers for containment of pollutants are compacted using water as the moulding fluid, and organic contaminants may contact the barrier only after the "water-compaction" is completed.

The hydraulic conductivity studies presented in this section correspond to water saturated Sarnia clays permeated with a reference solution (0.01 N $CaSO_4$ in water), followed by the leachate/hydrocarbon mixtures of interest. The soils include brown, weathered, 0.3 meters deep compacted clays, and grey, unweathered, 11 metres deep clays. The brown clays were moulded in water wet of optimum and compacted to obtain a low **k** material representative of clay liners. The grey subsurface clays were tested undisturbed as they constitute the native material underlying many regional sanitary landfill facilities. The results are presented as summary figures, while individual curves showing hydraulic conductivity, settlement and effluent chemistry versus pore volumes are detailed in Appendixes E to G. The values of void ratio, settlement and **k** for each test are summarized in Tables 5.1 to 5.3.

5.3.1 Leachate/Ethanol Mixtures on Compacted Brown Clay

Figure 5.8 shows the hydraulic conductivity test results at zero static effective stresses for compacted brown Sarnia clay permeated with leachate containing 0, 20, 40, 60, 80 and 100% ethanol. Reference **k** values for water used as the initial permeant (circles) are shown along with the final equilibrium **k** values for the organic permeants (triangles). Figure 5.8a shows that significant decreases in **k** occurred for ethanol contents of up to 60% with a minimum value of 1.7 x 10^{-9} cm/s at 40% ethanol. The sample permeated with 80% ethanol had doubled the **k** value for water and the sample permeated with concentrated ethanol had a **k** of 6.2 x 10^{-7} cm/s; more than 100 times the **k** for water. Figure 5.8b presents the same data expressed as intrinsic permeability, K, and illustrates that the permeants containing up to 40% ethanol produced very slight increases in K, followed by large increases in K as the amount of ethanol in the permeant rose above 40%.

The decrease in **k** observed in the "dilute" range of ethanol concentrations are directly related to the increased viscosity of the permeant. This is clearly supported by the complete removal of the decreases in permeability after the results were corrected for viscosity effects (Figure 5.8b). The large increases in **k** and K at ethanol contents greater than 50% result from progressive double layer contraction as the dielectric constant of the permeant is significantly reduced. It appears that the permeants containing less than 40% ethanol are incapable of collapsing the double layers of water and are thus incapable of increasing the permeability of the clay.

The results of hydraulic conductivity tests on similar soil samples permeated with leachate/ethanol mixtures under static effective vertical stresses of 40, 80 and 160 kPa are summarized in Figures 5.9 to 5.11. All permeants containing ethanol produced substantial decreases in the values of **k**, while the values of intrinsic permeability remained practically unchanged for all samples under static stresses. The application of static stresses prevented the large increases in **k** observed for samples permeated with high alcohol contents under zero static stress. Table 5.1 shows that the vertical stresses produced seepage consolidation of up to 5% of the sample volume for permeants containing high ethanol contents. The vertical consolidation combined with K_o effects that would close any shrinkage cracks that develop as a result of double layer contraction, prevent any large increases in permeability. Furthermore, the hydraulic conductivity of the clay samples are significantly reduced due to the large viscosity of the permeant mixtures.

5.3.2 Leachate/Dioxane Mixtures on Compacted Brown Clay

The results of **k** tests run at $\sigma'_v = 0$ kPa on compacted samples of brown Sarnia clay permeated with domestic waste leachate/dioxane mixtures (10, 20, 40, 70, 85, and 100%) are shown in Figure 5.12. The permeants containing up to 70% dioxane produced significant decreases in **k** (Figure 5.12a), whereas increases in **k** of 2 and 3 orders of magnitude were produced by 85% and 100% dioxane, respectively. The data are replotted on Figure 5.12b in terms of intrinsic permeability and show that the values of K remain practically unaltered by the permeants containing up to 70% dioxane, followed by large increases in K at higher dioxane contents.

The spectacular increases in both **k** and K for the samples permeated with 85 and 100% dioxane are evidence of double layer contraction in the high concentration range. The decreases in **k** observed at dioxane contents below 70% are caused by the increased viscosity of the permeants, since the "viscosity corrected" values of K remained unchanged during permeation. These values also show no evidence of double layer contraction at dioxane contents lower than 70%, suggesting that dioxane might be excluded from the cation-laden double layers of water. This hypothesis is based on the known strong affinity of double layer cations for polar water and is further discussed in Section 6.3.

The application of static vertical effective stresses of 40, 80 and 160 kPa to the water-compacted clay samples gradually suppressed the large increases in **k** at high dioxane contents (Figures 5.13 to 5.15). Table 5.2 shows that the stresses caused consolidation concurrent with permeation of up to ~ 3% of the initial sample volume. Vertical consolidation and K_o effects appear to have restricted the development of macropores or shrinkage cracks and prevented the large increases in **k** that take place without the presence of static stresses.

5.3.3 The Importance of Effective Stress Levels

Effective stresses play an important role in minimizing increases in the **k** of water-compacted clays permeated with soluble concentrated organics. Figures 5.16 and 5.17 illustrate the interrelationships between **k** and the static stresses level, σ'_v, for ethanol and dioxane permeation. In all cases σ'_v was in place on the water-compacted clay before permeation of the organics.

Figure 5.16 shows that a static vertical effective stress of only 20 kPa is required to prevent any increase in **k** during permeation of ethanol at a void ratio of about 0.85. At 40 kPa a significant decrease occurs. Dioxane permeation, on the other hand, induces net increases in **k** that are much less inhibited by the in-place effective stresses. Even at σ'_v values of up to 160 kPa, small increases in **k** are apparent for dioxane permeation (Figure 5.17).

If in-place stresses prevent the large increases in **k** noted at $\sigma'_v = 0$, the question arises whether post-damage application of stresses will heal a damaged liner. The data on Figures 5.18 and 5.19 illustrate attempts to restore low permeabilities to damaged, water-compacted clay by applying static effective stresses after permeation of ethanol and dioxane. Effective stresses applied subsequent to large increases in **k** produced by ethanol permeation at $\sigma'_v = 0$ seem to be capable of fully restoring the low values of **k** characteristic of water-compacted clays (Figure 5.18a). Original water permeation produced a **k** value of 5.95×10^{-9} cm/s ($\mathbf{k}_{ow}$) followed by a large increase after ethanol permeation to $\mathbf{k}_{0E}$ = 6.2 x 10^{-7} cm/s. Subsequent application of effective stresses of 40 and 80 kPa reduced **k** to values below the reference water ($\mathbf{k}_{80E}$ = 4 x 10^{-9} cm/s). At higher stresses of up to 320 kPa, the values of **k** were further reduced to $\mathbf{k}_{320E}$ = 1.5 x 10^{-9} cm/s. The settlement plot on Figure 5.18b shows clearly that the healing process involves large settlements. The total settlement after permeation at 320 kPa was 1.655 mm, which corresponds to ~ 8% of the initial sample volume.

The large decreases in **k** produced by dioxane permeation at zero static effective stress are only partially reduced by subsequent stress application. As shown on Figure 5.19a, water permeation at $\sigma'_v = 0$ yielded a **k** value of 6.25 x 10^{-9} cm/s ($\mathbf{k}_{0W}$), followed by a large increase after dioxane permeation to $\mathbf{k}_{0D}$ = 1.35 x 10^{-6} cm/s. Subsequent application of static effective stresses of 40, 80, 120, 160 and 320 kPa resulted in only partial reduction of **k**. Even at 320 kPa, the hydraulic conductivity ($\mathbf{k}_{320D}$ = 4 x 10^{-7}) remained about 65 times greater than that of water ($\mathbf{k}_{0W}$). The total settlement for the dioxane permeated sample amounted to 4.9% of the initial sample volume (Figure 5.19b), suggesting that dioxane apparently caused some strengthening of the clay structure relative to ethanol. This prevented some of the beneficial consolidation so that the sample could not be healed even by stresses of 320 kPa. The data for $\mathbf{k}_{40D}$ = 7.2 x 10^{-6} cm/s seems incorrect since $\mathbf{k}_{40D}$ is greater than $\mathbf{k}_{0D}$. This is interpreted as indicating incomplete reaction between the soil and dioxane during permeation at $\sigma'_v = 0$.

Summary plots showing the dramatic influence of effective stress on **k** for water-compacted clays permeated with ethanol and dioxane are presented on Figures 5.20 and 5.21. Each graph consists of four curves, describing the following data:

1) Reference **k** for water, with stress application immediately after compaction.

2) **k** obtained by organic permeation of pre-stressed samples (labelled pre-damage stresses).

3) **k** obtained on organic damaged clay (by permeation at $\sigma'_v = 0$), followed by stress application and measurement of **k** (labelled post-damage stresses).

4) **k** obtained on dry clay/organic mixtures stressed to the level indicated for measurement of **k** (labelled post-mixing stresses, dry clay/ethanol or dioxane.

The significance of each summary plot is discussed separately for ethanol and dioxane:

a) Ethanol (Figure 5.20): The reference values of **k** for ~ 1 pore volume of water permeation (solid circles) decrease from 5.95×10^{-9} to 2.25×10^{-9} cm/s as the applied stresses are increased from 0 to 160 kPa. At zero effective stress, subsequent permeation with ethanol produced a 100-fold increase in **k** to a value of 6.2×10^{-7} cm/s. This value is about 10 times larger than that for the dry clay/ethanol mixture at a similar void ratio. This suggests that clay sample shrinkage, macropore development and probable "leakage" along the sides of the fixed-ring permeameter may be major causes of the very large values of **k** at zero effective stresses.

The presence of in-place effective stresses of only 20 kPa is enough to prevent increases in **k** on ethanol permeation. The contact between the clay and the rigid walls of the permeameter is kept closed due to K_o effects, eliminating side wall flow. In such cases, the final values of **k** after ethanol permeation are lower than the values for water, which is due to the high viscosity of ethanol (about 80% higher than pure water) as well as the reduction in void ratio by consolidation during seepage.

The large increase in **k** at $\sigma'_v = 0$ was eliminated by post-damage application of stresses in excess of 80 kPa. The values of total settlement (due to static and seepage stresses) for each test are described in Table 5.1 and Figure 5.20b and indicate that the combined chemical and stress-induced consolidation of the water-compacted clays is a major factor in the elimination of the "damage" and reduction of **k**. The flocculated dry clay/ethanol mixtures exhibit maximum settlement of about 5% of the initial sample volume (1.03 mm) at 160 kPa. The water-compacted clays showed settlements of over 7% of the initial sample volume at 160 kPa (both pre- and post-damage), resulting in lower values of **k**.

b) Dioxane (Figure 5.21): Permeation with pure dioxane results in increases in **k** that are more difficult to control and eliminate by application of static effective stresses. The reference values of **k** after one pore volume of water permeation decrease from ~ 6.25 x 10^{-9} to a value between 3.9 x 10^{-9} cm/s as the applied stresses are increased from 0 to 160 kPa. At zero effective stress, subsequent permeation with dioxane produced a rapid increase in **k** to a value of 1.35 x 10^{-6} cm/s. This value about 13 times smaller than that for the highly flocculated dry clay/dioxane mixture at a similar void ratio.

In-place effective stresses of 40, 80, 120 and 160 kPa, on the water-compacted clay restricted the increases in **k** in proportion to the applied stress, although some increase occurred even at 160 kPa. Effective stresses applied subsequent to dioxane permeation and damage at σ'_v = 0 kPa (post-damage stresses) failed to reduce the **k** values significantly. The values of total settlement shown in Figure 5.21b and Table 5.2, indicate that the post-damage stresses resulted in settlements of ~ 3% of the original sample volume, with only small reductions in **k**. Pre-damage stresses produced more settlement (up to ~ 5% of the initial sample volume) and significantly lower increases in **k**. Overall, the values of settlement for the dioxane permeated samples are lower than those for ethanol, reflecting relative strengthening of the soil in the presence of low dielectric constant liquids.

5.3.4 Leachate/Ethanol Mixtures on Undisturbed Grey Clay

This final section describes the studies carried out to assess the effect of leachate/hydrocarbon mixtures on water-saturated grey, unweathered clays. Figure 5.22 summarizes the results of a series of tests run at $\sigma'_v = 0$, on undisturbed samples of grey Sarnia clay at their natural water content of ~ 20.5%.

Permeation with reference 0.01 N $CaSO_4$ (water) for close to two pore volumes yielded values of **k** ranging from 1.3×10^{-8} to 1.8×10^{-8} cm/s. Subsequent permeation by 40% ethanol decreased **k** to 5.6×10^{-9} cm/s, while increases in **k** to 1.7×10^{-8} and 2.0×10^{-8} cm/s were produced by 80% and 100% ethanol, respectively. The changes in void ratio, settlement and hydraulic conductivity of the clay samples during permeation are presented in Table 5.3. The sample permeated with 40% ethanol experienced the most consolidation (~ 1.4% of the initial sample volume), in response to seepage stresses (J_{max} ~ 125 kPa) that developed during testing.

The interpretation shown in Figure 5.22a shows that significant (viscosity related) decreases in **k** took place for ethanol contents of up to 70%. The values of intrinsic permeability increased only at high alcohol contents, and ratios of increase were less than four-fold. These increases in K are small relative to the more than 180-fold increases observed for the water-compacted brown Sarnia clay (Figure 5.8b). This is a reflection of the lower activity of the unweathered grey clay which contains only 1 or 2% of smectite compared to ~ 15% for the brown clay.

5.4 POST-TESTING SAMPLE ASSESSMENT

After completion of hydraulic conductivity studies the pore fluids of the tested samples were extracted (Section 3.6) and chemically analyzed, yielding the values presented in Table 5.4. Two general observation can be made: Firstly, the hydrocarbon contents of the pore fluids were lower than influent permeants, even though most tests were run long enough to ensure that the organic contents of the effluent and influent liquids were similar. This is interpreted to reflect the chemical exclusion of hydrocarbons from the double layers of water. Secondly, effective stresses in place on samples permeated with high hydrocarbon contents seem to have increased the degree of water removal from the pore fluid. It is suggested that the applied stresses promote uniform flow through the soil mass by preventing the development of macropores, especially along the fixed walls of the permeameter. This would result in a more thorough displacement of the resident pore water.

The results of mercury intrusion porosimetry studies performed on samples of compacted brown Sarnia clay after permeation with leachate/dioxane mixtures are summarized in Figure 5.23. The water-compacted clay exhibits two dominant pore size modes centred at ~ 0.1 μm and ~ 3 μm. Increasing dioxane contents produced a gradual removal of the larger pore mode, while strengthening the smaller mode. The apparent contraction of the pores does not correlate with the measured volume changes (Table 5.2) or the intrinsic permeability values (Figure 5.12b). The results are therefore difficult to explain and could have been affected by artifacts created during freeze drying of the specimens.

TABLE 5.1 VOID RATIO, SETTLEMENT AND HYDRAULIC CONDUCTIVITY OF BROWN WATER-COMPACTED CLAY PERMEATED WITH LEACHATE/ETHANOL MIXTURES

σ'_v (kPa)	Ethanol %	Void Ratio		Settlement (mm)		k (cm/s)	
		e_o	e_f	ρ_{static}	$\rho_{seepage}$	k_o	k_f
0	0	0.796	0.756	0	0.446	$6.1\text{x}10^{-9}$	$4.8\text{x}10^{-9}$
	20	0.862	0.836	0	0.275	$5.4\text{x}10^{-9}$	$3.3\text{x}10^{-9}$
	40	0.766	0.714	0	0.591	$4.6\text{x}10^{-9}$	$1.7\text{x}10^{-9}$
	60	0.790	0.752	0	0.428	$4.9\text{x}10^{-9}$	$3.5\text{x}10^{-9}$
	80	0.792	0.755	0	0.418	$5.0\text{x}10^{-9}$	$1.1\text{x}10^{-8}$
	100	0.803	0.767	0	0.397	$5.95\text{x}10^{-9}$	$6.2\text{x}10^{-7}$
10	100	0.844	0.794	0.047	0.503	$4.95\text{x}10^{-9}$	$8.4\text{x}10^{-9}$
20	100	0.843	0.769	0.120	0.686	$4.8\text{x}10^{-9}$	$6.1\text{x}10^{-9}$
40	0	0.772	0.734	0.080	0.353	$3.7\text{x}10^{-9}$	$3.3\text{x}10^{-9}$
	40	0.765	0.685	0.116	0.795	$3.3\text{x}10^{-9}$	$1.1\text{x}10^{-9}$
	80	0.766	0.682	0.132	0.820	$3.7\text{x}10^{-9}$	$1.35\text{x}10^{-9}$
	100	0.770	0.682	0.132	0.862	$3.6\text{x}10^{-9}$	$1.8\text{x}10^{-9}$
80	0	0.803	0.725	0.357	0.507	$3.6\text{x}10^{-9}$	$3.55\text{x}10^{-9}$
	40	0.800	0.698	0.329	0.800	$3.35\text{x}10^{-9}$	$1.3\text{x}10^{-9}$
	80	0.800	0.717	0.348	0.922	$3.05\text{x}10^{-9}$	$1.4\text{x}10^{-9}$
	100	0.809	0.692	0.346	0.954	$2.6\text{x}10^{-9}$	$1.4\text{x}10^{-9}$
120	100	0.795	0.675	0.476	0.869	$2.5\text{x}10^{-9}$	$1.7\text{x}10^{-9}$
160	0	0.754	0.682	0.449	0.375	$2.9\text{x}10^{-9}$	$2.75\text{x}10^{-9}$
	40	0.768	0.662	0.473	0.727	$2.6\text{x}10^{-9}$	$1.05\text{x}10^{-9}$
	80	0.768	0.654	0.502	0.784	$2.6\text{x}10^{-9}$	$9.5\text{x}10^{-10}$
	100	0.795	0.664	0.692	0.772	$2.25\text{x}10^{-9}$	$1.35\text{x}10^{-9}$

TABLE 5.2 VOID RATIO, SETTLEMENT AND HYDRAULIC CONDUCTIVITY OF BROWN WATER-COMPACTED CLAY PERMEATED WITH LEACHATE/DIOXANE MIXTURES

σ'_v (kPa)	Ethanol %	Void Ratio		Settlement (mm)		k (cm/s)	
		e_o	e_f	ρ_{static}	$\rho_{seepage}$	k_o	k_f
0	0	0.796	0.756	0	0.446	6.1x10^{-9}	4.8x10^{-9}
	10	0.819	0.780	0	0.424	9.2x10^{-9}	6.4x10^{-9}
	20	0.831	0.798	0	0.366	9.0x10^{-9}	6.1x10^{-9}
	40	0.836	0.812	0	0.267	9.2x10^{-9}	4.4x10^{-9}
	70	0.831	0.821	0	0.190	1.0x10^{-8}	6.1x10^{-9}
	85	0.795	0.777	0	0.193	1.05x10^{-8}	4.2x10^{-7}
	100	0.802	0.786	0	0.177	6.25x10^{-9}	1.35x10^{-6}
40	0	0.772	0.734	0.080	0.353	3.7x10^{-9}	3.3x10^{-9}
	40	0.859	0.772	0.265	0.674	4.9x10^{-9}	3.2x10^{-9}
	80	0.845	0.764	0.200	0.674	4.6x10^{-9}	2.8x10^{-9}
	100	0.805	0.744	0.104	0.569	4.95x10^{-9}	3.9x10^{-7}
80	0	0.803	0.725	0.357	0.507	3.6x10^{-9}	3.55x10^{-9}
	40	0.895	0.790	0.511	0.594	5.15x10^{-9}	3.05x10^{-9}
	80	0.896	0.805	0.627	0.503	5.5x10^{-9}	5.2x10^{-9}
	100	0.804	0.731	0.270	0.547	4.2x10^{-9}	1.8x10^{-7}
120	100	0.891	0.768	0.693	0.628	4.2x10^{-9}	1.25x10^{-8}
160	0	0.754	0.682	0.449	0.375	2.9x10^{-9}	2.75x10^{-9}
	40	0.882	0.769	0.725	0.510	3.85x10^{-9}	2.15x10^{-9}
	80	0.884	0.757	0.782	0.635	3.9x10^{-9}	1.9x10^{-9}
	100	0.827	0.755	0.450	0.339	3.9x10^{-9}	8.6x10^{-9}

TABLE 5.3 VOID RATIO, SETTLEMENT AND HYDRAULIC CONDUCTIVITY OF UNDISTURBED SAMPLES OF GREY SARNIA CLAY PERMEATED WITH LEACHATE/ETHANOL MIXTURES

σ'_v (kPa)	Ethanol %	Void Ratio		Settlement (mm)		k (cm/s)	
		e_o	e_f	ρ_{static}	$\rho_{seepage}$	k_o	k_f
0	0	0.588	0.582	0	0.084	1.8×10^{-8}	1.5×10^{-8}
	40	0.559	0.538	0	0.274	1.7×10^{-8}	5.6×10^{-9}
	80	0.587	0.574	0	0.154	1.35×10^{-8}	1.7×10^{-8}
	100	0.546	0.537	0	0.120	1.3×10^{-8}	2.0×10^{-8}

TABLE 5.4 HYDROCARBON CONTENT OF INFLUENT PERMEANT AND PORE FLUID AT END OF TESTING [Water-compacted brown Sarnia clay permeated with leachate/hydrocarbon mixtures]

σ'_v (kPa)	ETHANOL (%)		DIOXANE (%)	
	Permeant	Pore Fluid	Permeant	Pore Fluid
0			10	14
	20	16	20	18
	40	39	40	31
	60	59	70	67
	80	74	85	60
	100	70	100	86
40	40	35	40	35
	80	70	80	72
	100	93	100	90
80	40	38	40	41
	80	80	80	75
	100	80	100	91
160	40	33	40	42
	80	73	80	76
	100	85	100	

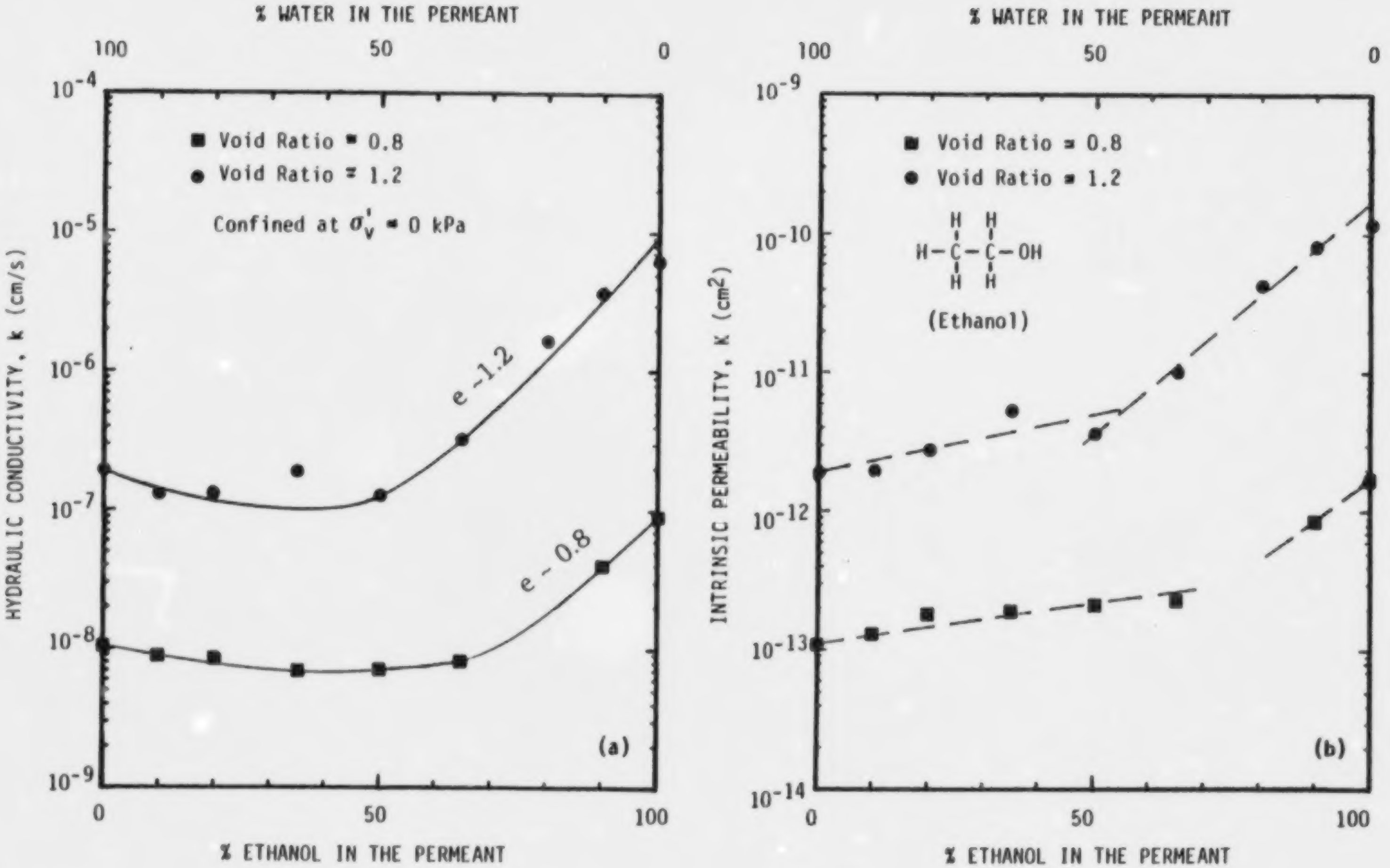

FIGURE 5.1 HYDRAULIC CONDUCTIVITY (a) AND INTRINSIC PERMEABILITY (b) OF BROWN SARNIA CLAY MOULDED AND PERMEATED WITH WATER/ETHANOL MIXTURES AT VOID RATIOS OF 0.8 AND 1.2

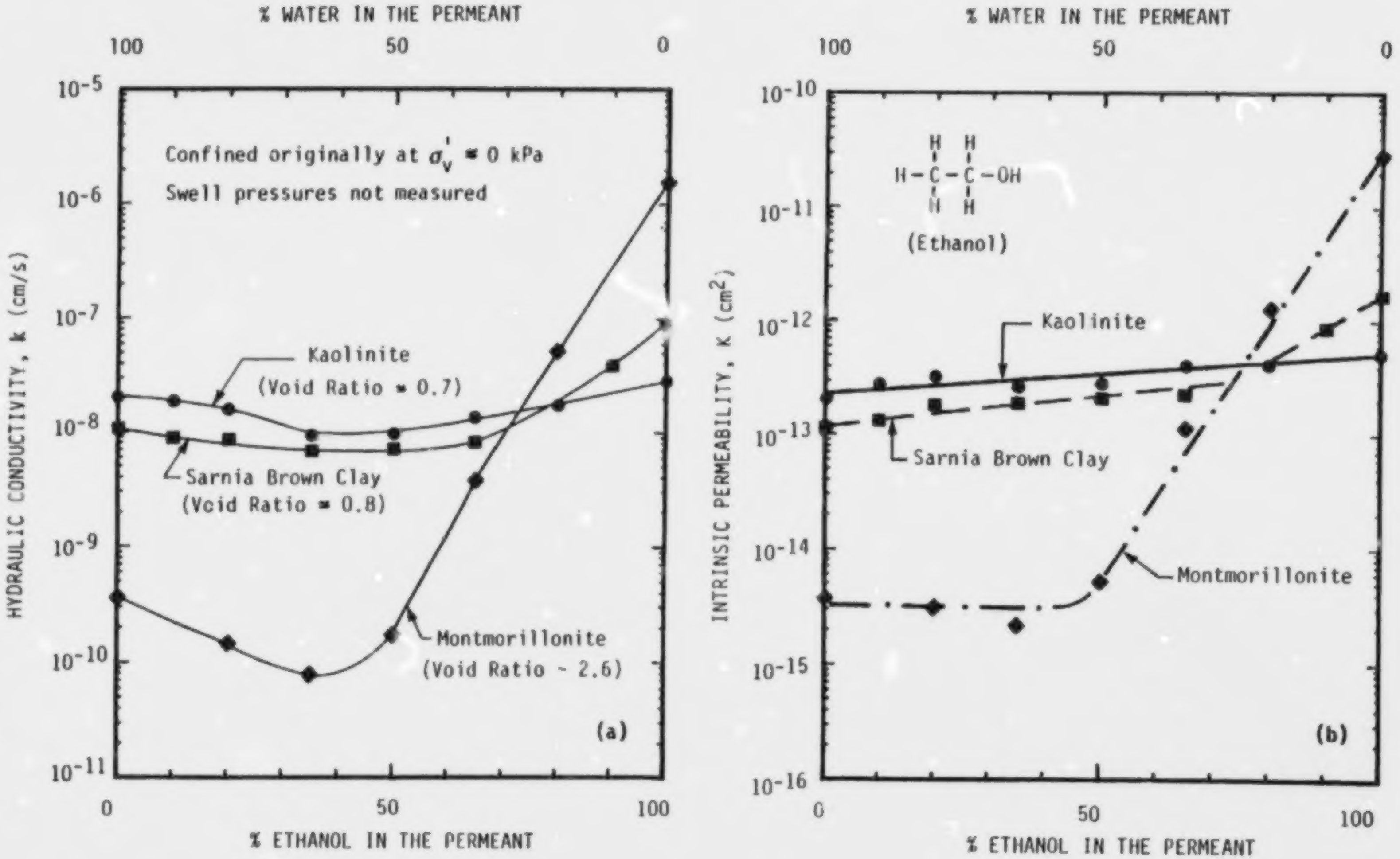

FIGURE 5.2 HYDRAULIC CONDUCTIVITY (a) AND INTRINSIC PERMEABILITY (b) OF THREE CLAYS MOULDED AND PERMEATED WITH WATER/ETHANOL MIXTURES

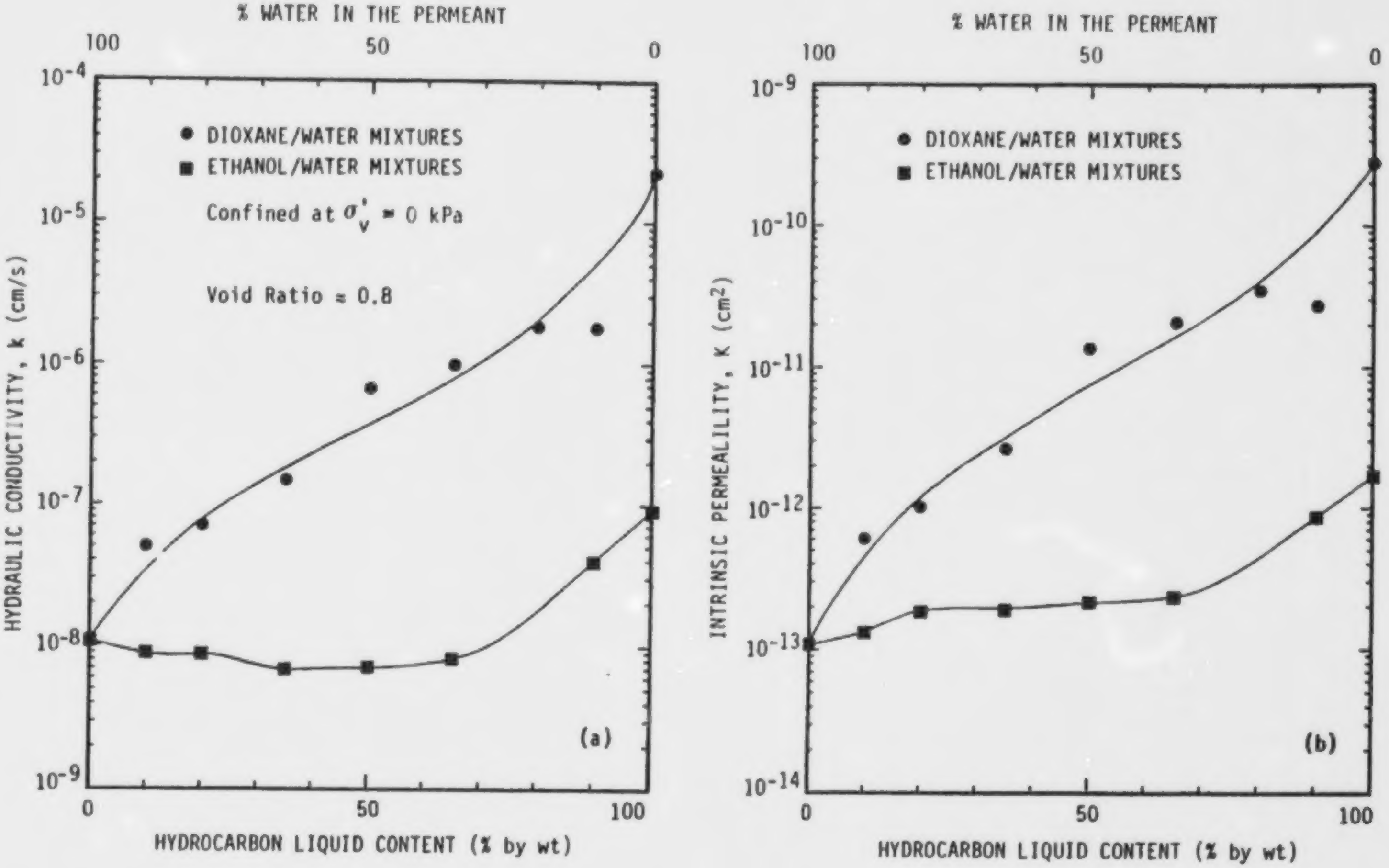

FIGURE 5.3 HYDRAULIC CONDUCTIVITY (a) AND INTRINSIC PERMEABILITY (b) OF BROWN SARNIA CLAY MOULDED AND PERMEATED WITH WATER/ETHANOL AND WATER/DIOXANE MIXTURES

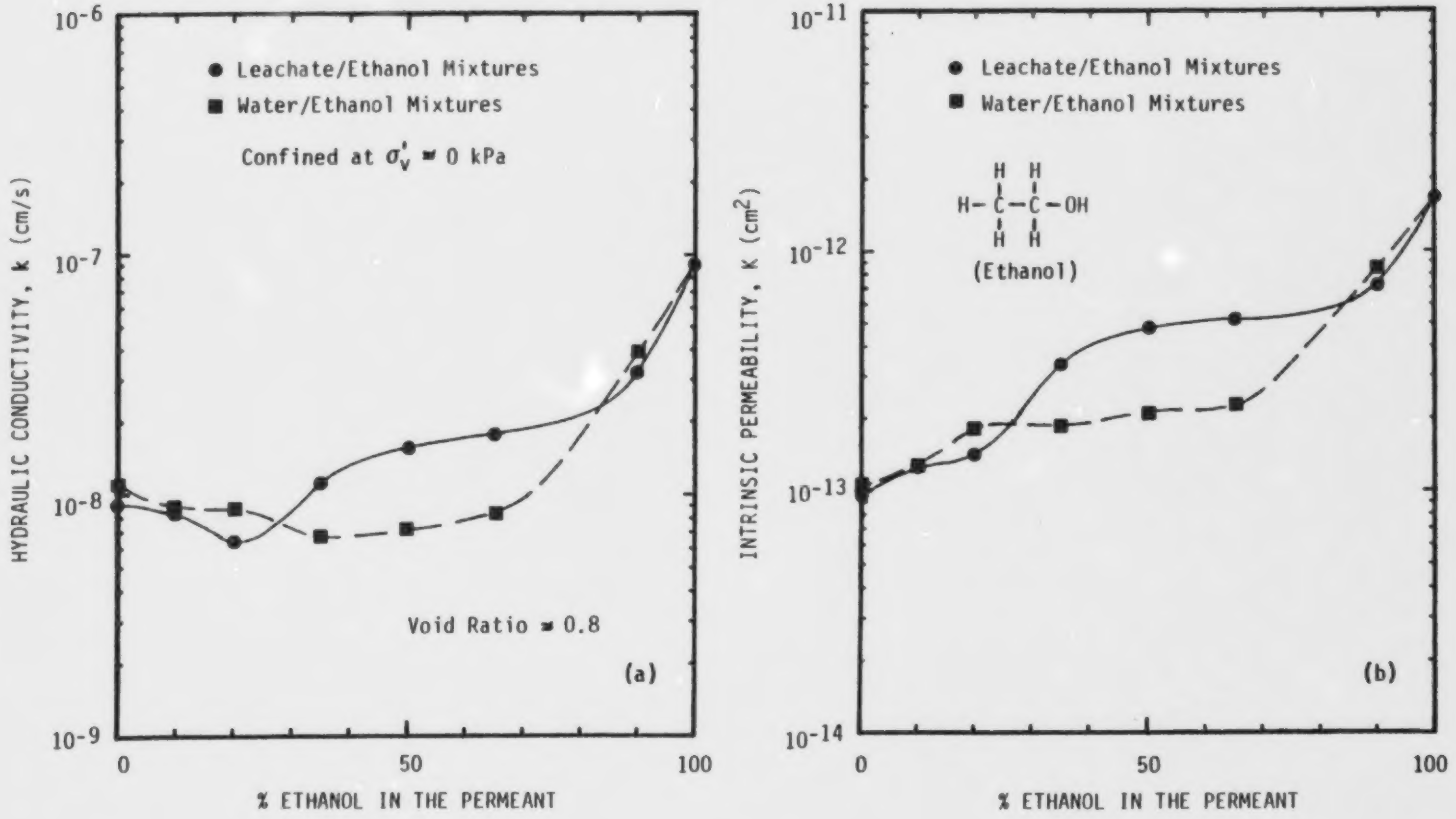

FIGURE 5.4 HYDRAULIC CONDUCTIVITY (a) AND INTRINSIC PERMEABILITY (b) OF BROWN SARNIA CLAY MOULDED AND PERMEATED WITH WATER/ETHANOL AND LEACHATE/ETHANOL MIXTURES

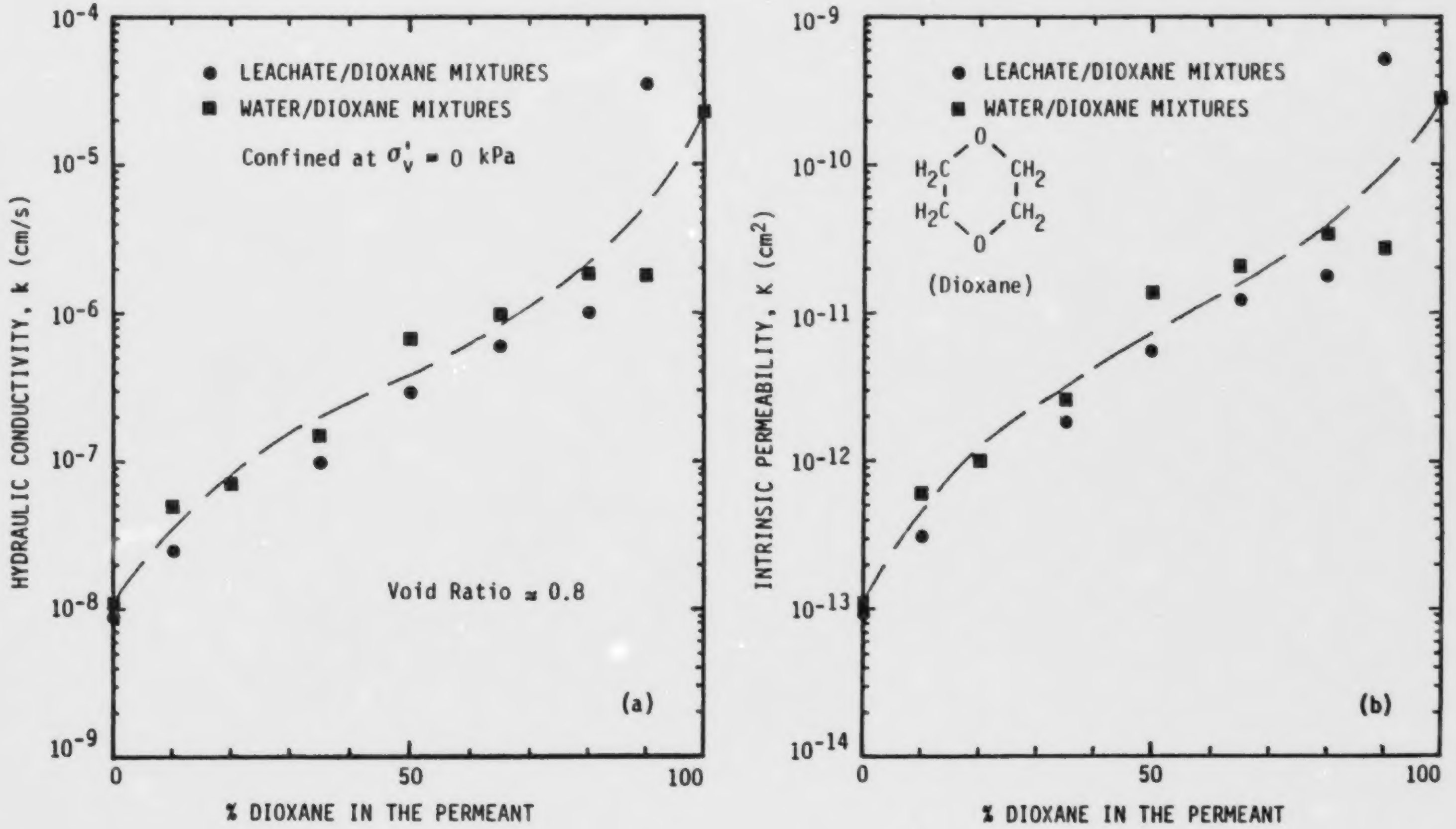

FIGURE 5.5 HYDRAULIC CONDUCTIVITY (a) AND INTRINSIC PERMEABILITY (b) OF BROWN SARNIA CLAY MOULDED AND PERMEATED WITH WATER/DIOXANE AND LEACHATE/DIOXANE MIXTURES

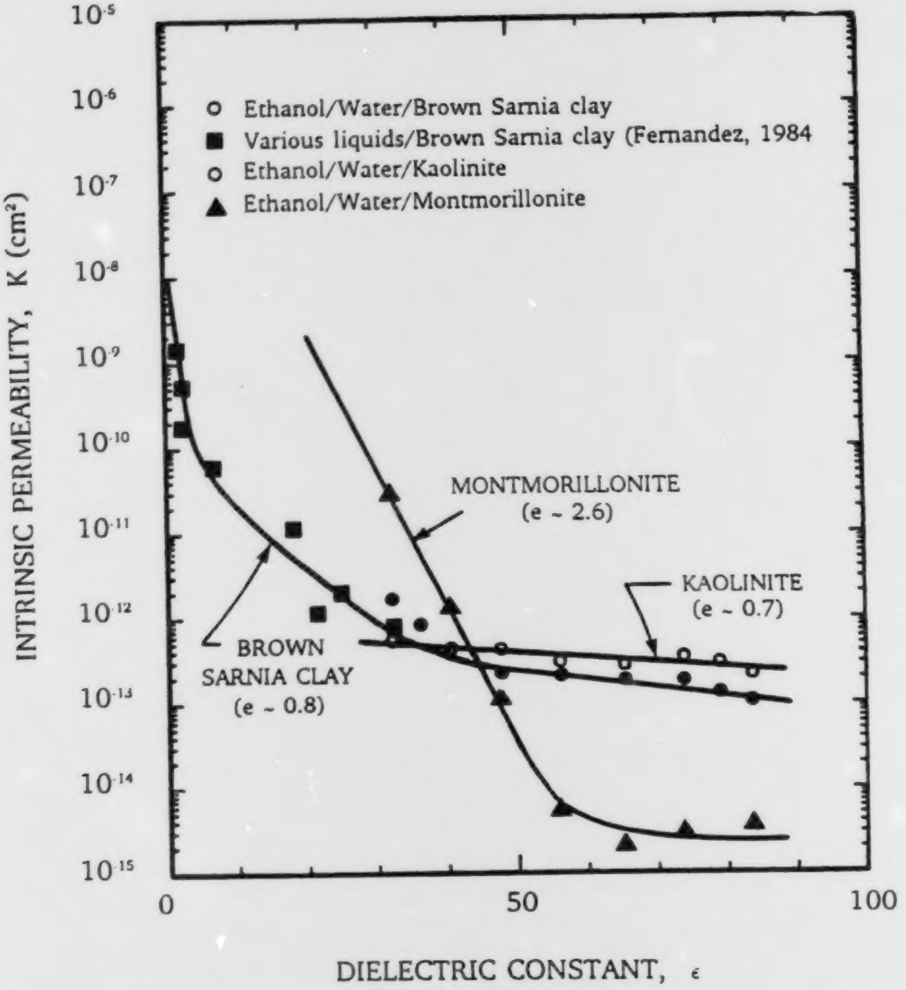

FIGURE 5.6 INTRINSIC PERMEABILITY VS DIELECTRIC CONSTANT

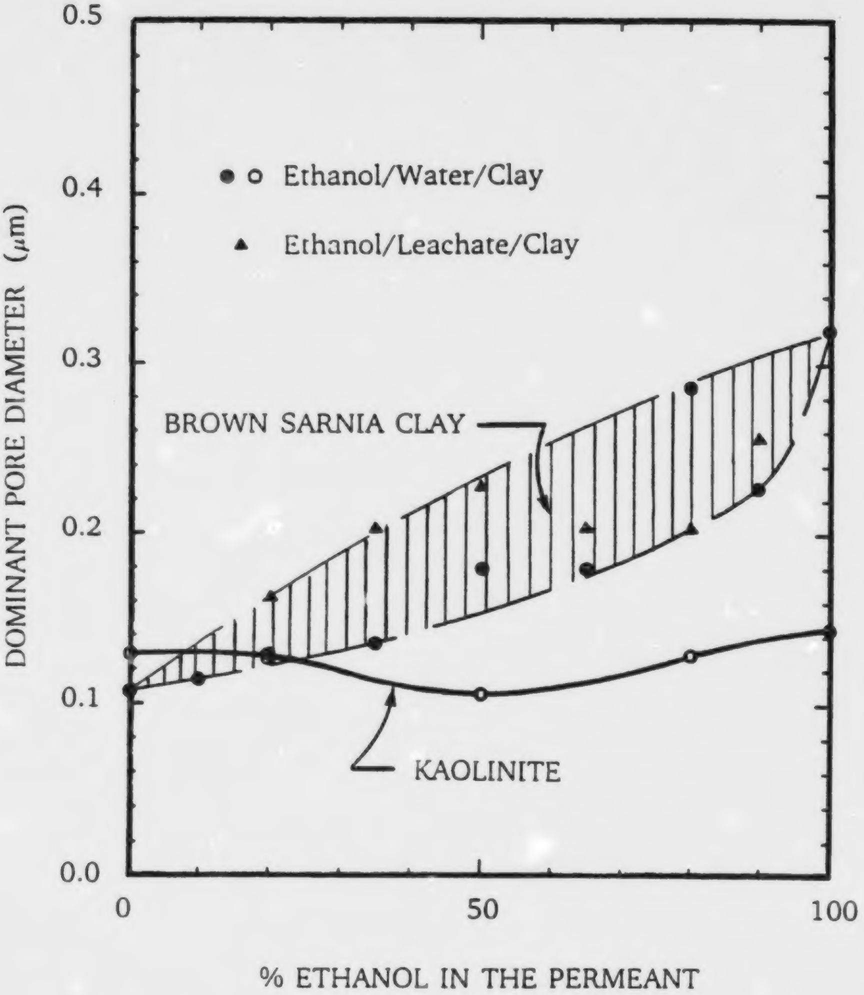

FIGURE 5.7 DOMINANT PORE DIAMETER FOR DRY CLAYS MIXED AND PERMEATED WITH AQUEOUS SOLUTIONS OF ETHANOL

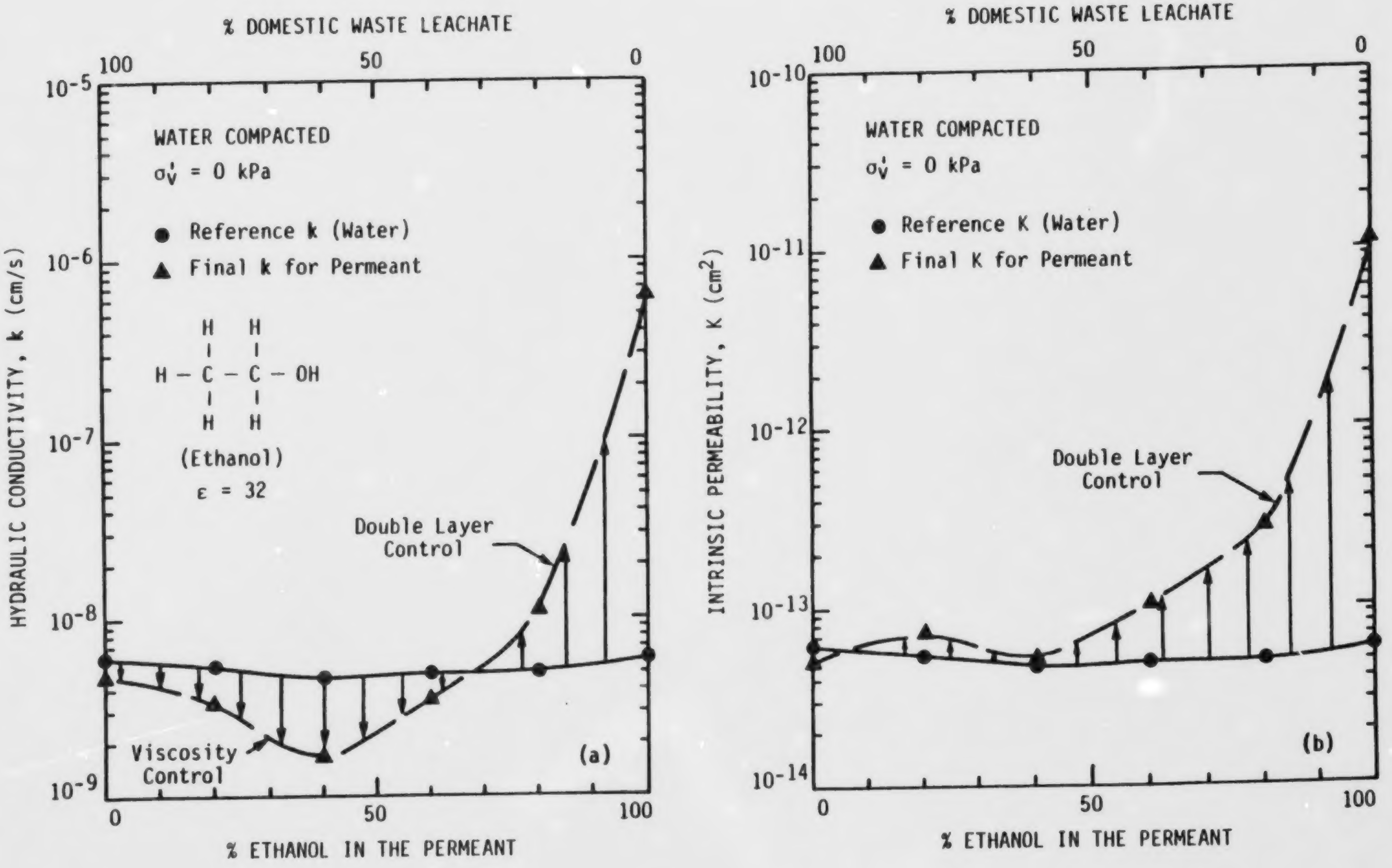

FIGURE 5.8 HYDRAULIC CONDUCTIVITY (a) AND INTRINSIC PERMEABILITY (b) OF WATER-COMPACTED BROWN SARNIA CLAY PERMEATED WITH LEACHATE/ETHANOL MIXTURES AT $\sigma'_v = 0$ kPa

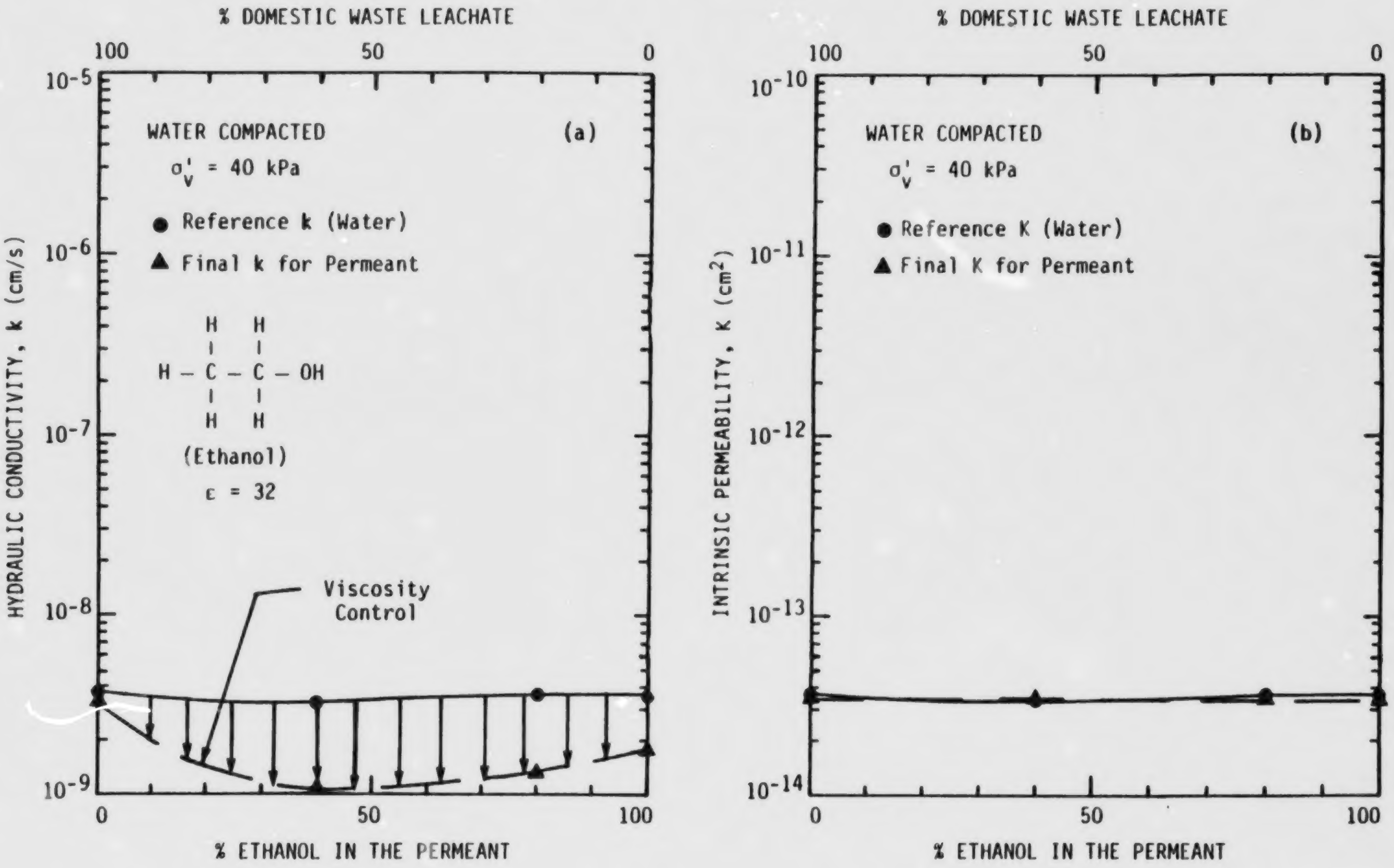

FIGURE 5.9 HYDRAULIC CONDUCTIVITY (a) AND INTRINSIC PERMEABILITY (b) OF WATER-COMPACTED BROWN SARNIA CLAY PERMEATED WITH LEACHATE/ETHANOL MIXTURES AT σ'_v = 40 kPa

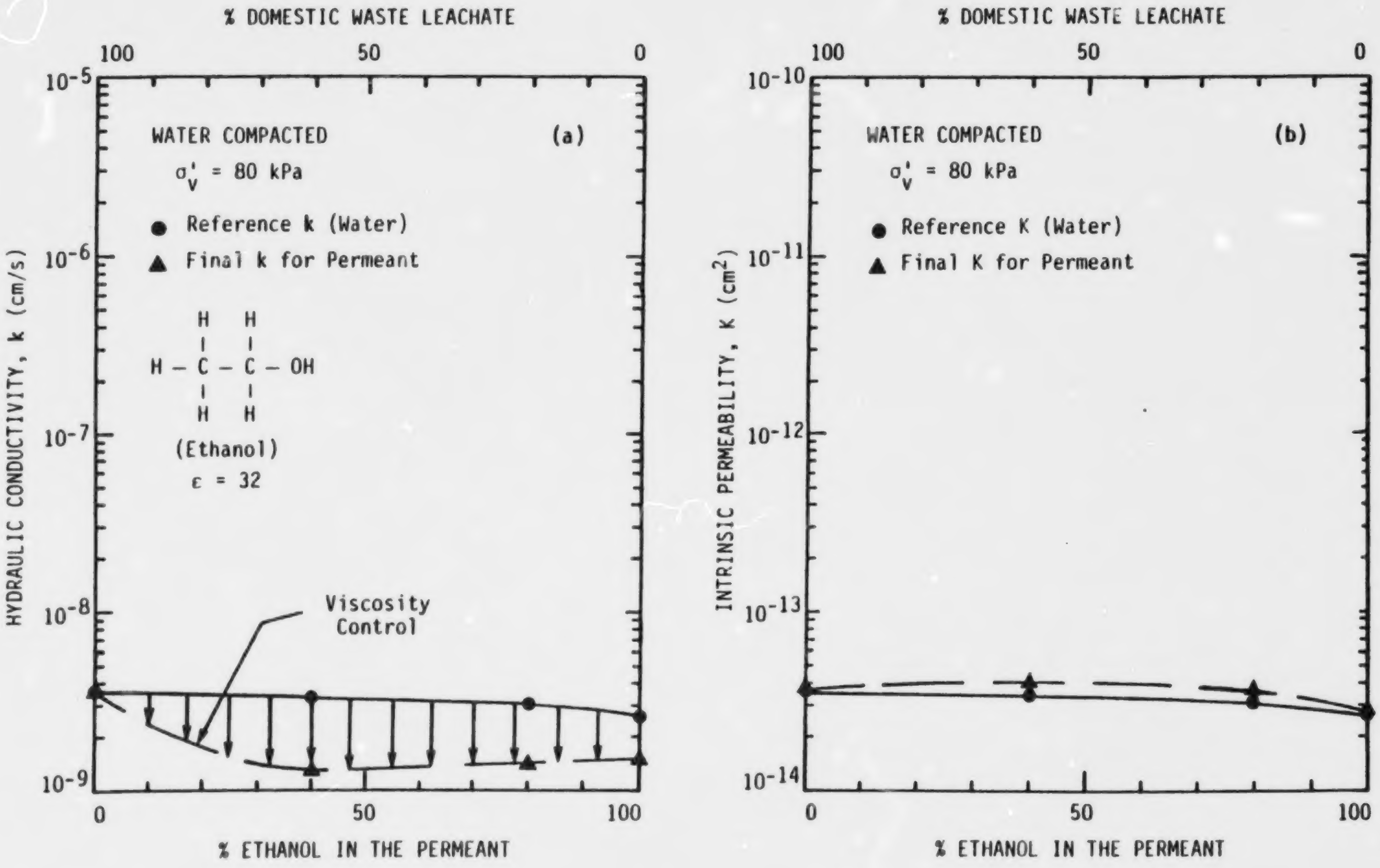

FIGURE 5.10 HYDRAULIC CONDUCTIVITY (a) AND INTRINSIC PERMEABILITY (b) OF WATER-COMPACTED BROWN SARNIA CLAY PERMEATED WITH LEACHATE/ETHANOL MIXTURES AT σ'_v = 80 kPa

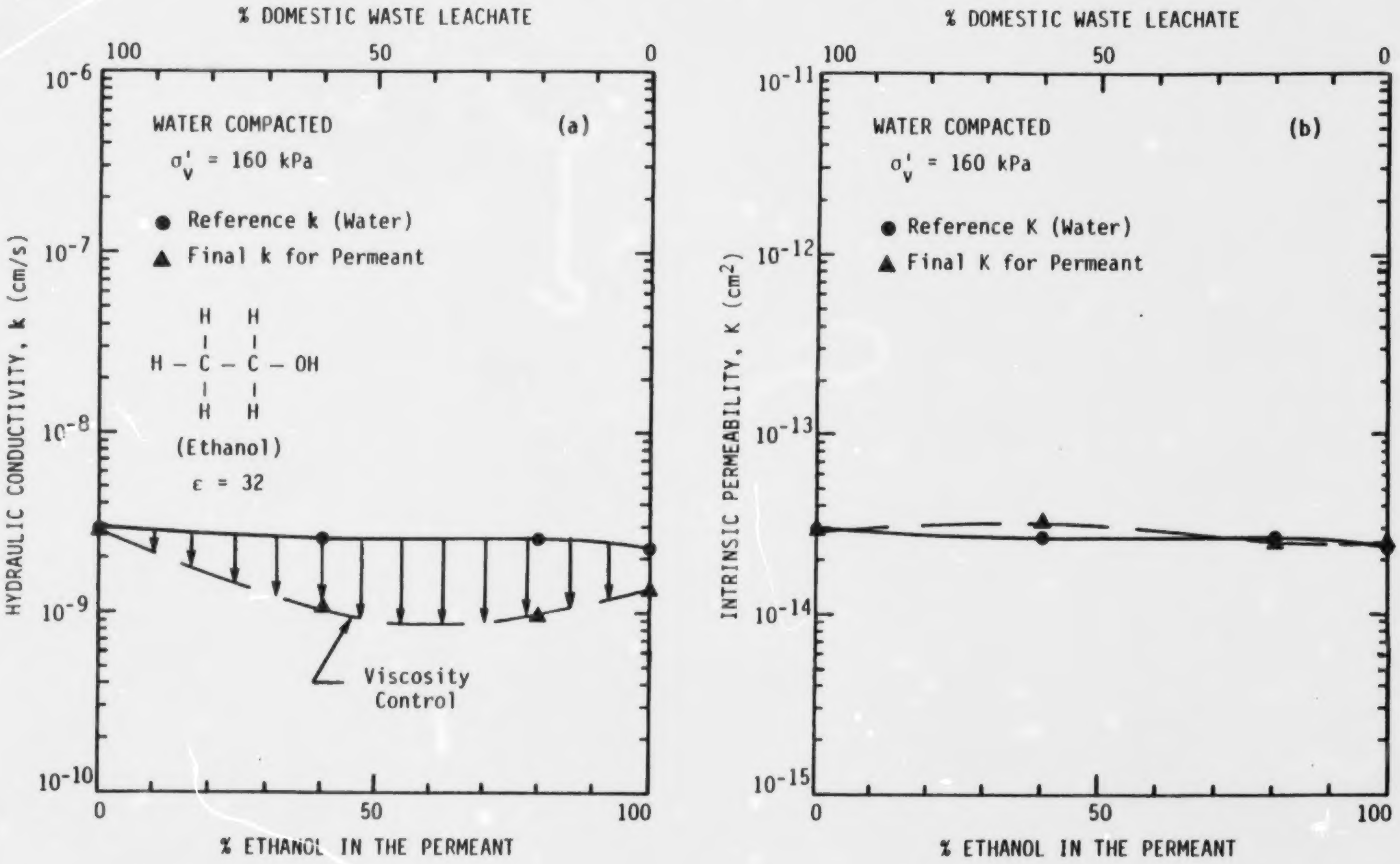

FIGURE 5.11 HYDRAULIC CONDUCTIVITY (a) AND INTRINSIC PERMEABILITY (b) OF WATER-COMPACTED BROWN SARNIA CLAY PERMEATED WITH LEACHATE/ETHANOL MIXTURES AT σ'_v = 160 kPa

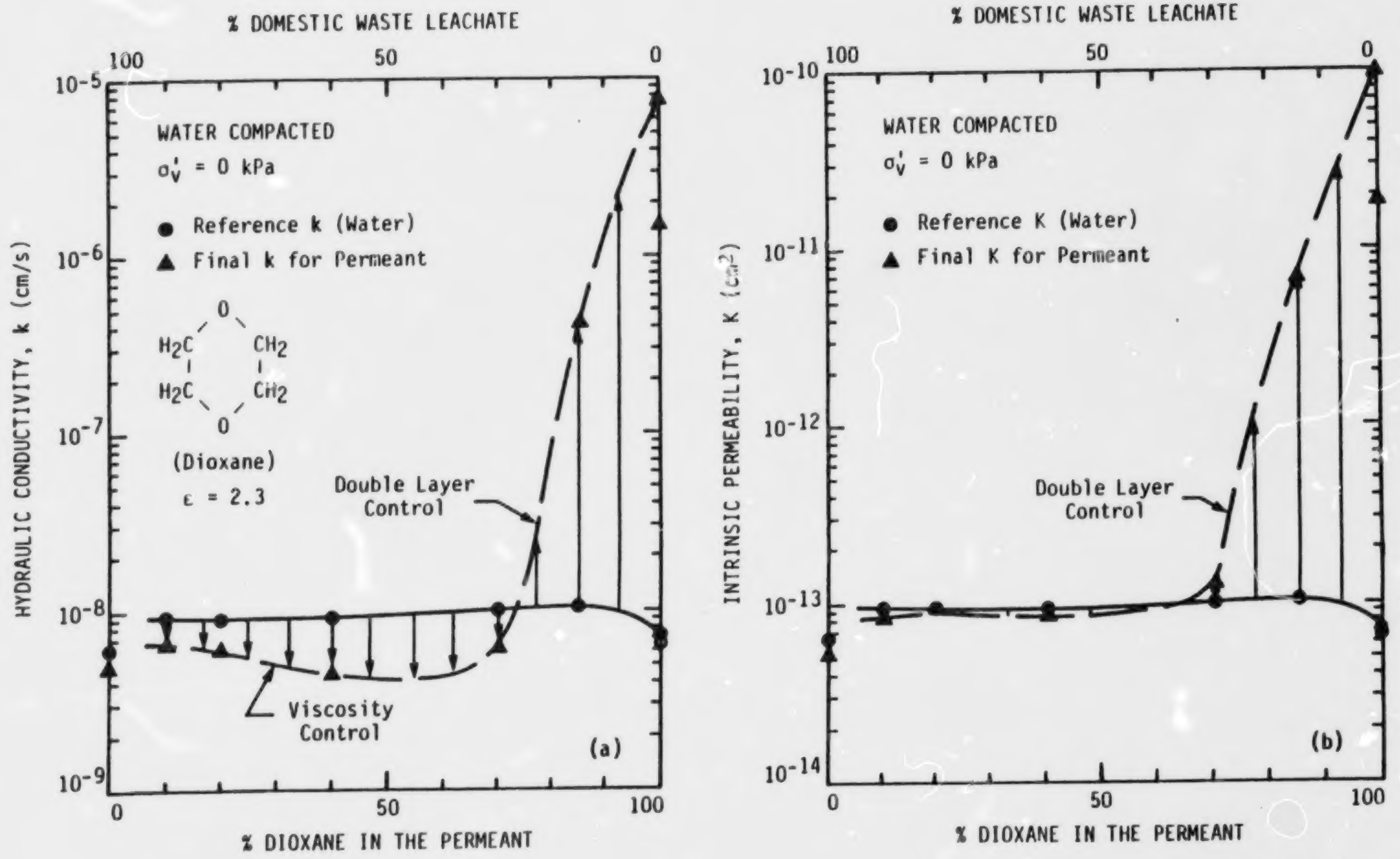

FIGURE 5.12 HYDRAULIC CONDUCTIVITY (a) AND INTRINSIC PERMEABILITY (b) OF WATER-COMPACTED BROWN SARNIA CLAY PERMEATED WITH LEACHATE/DIOXANE MIXTURES AT σ'_v = 0 kPa

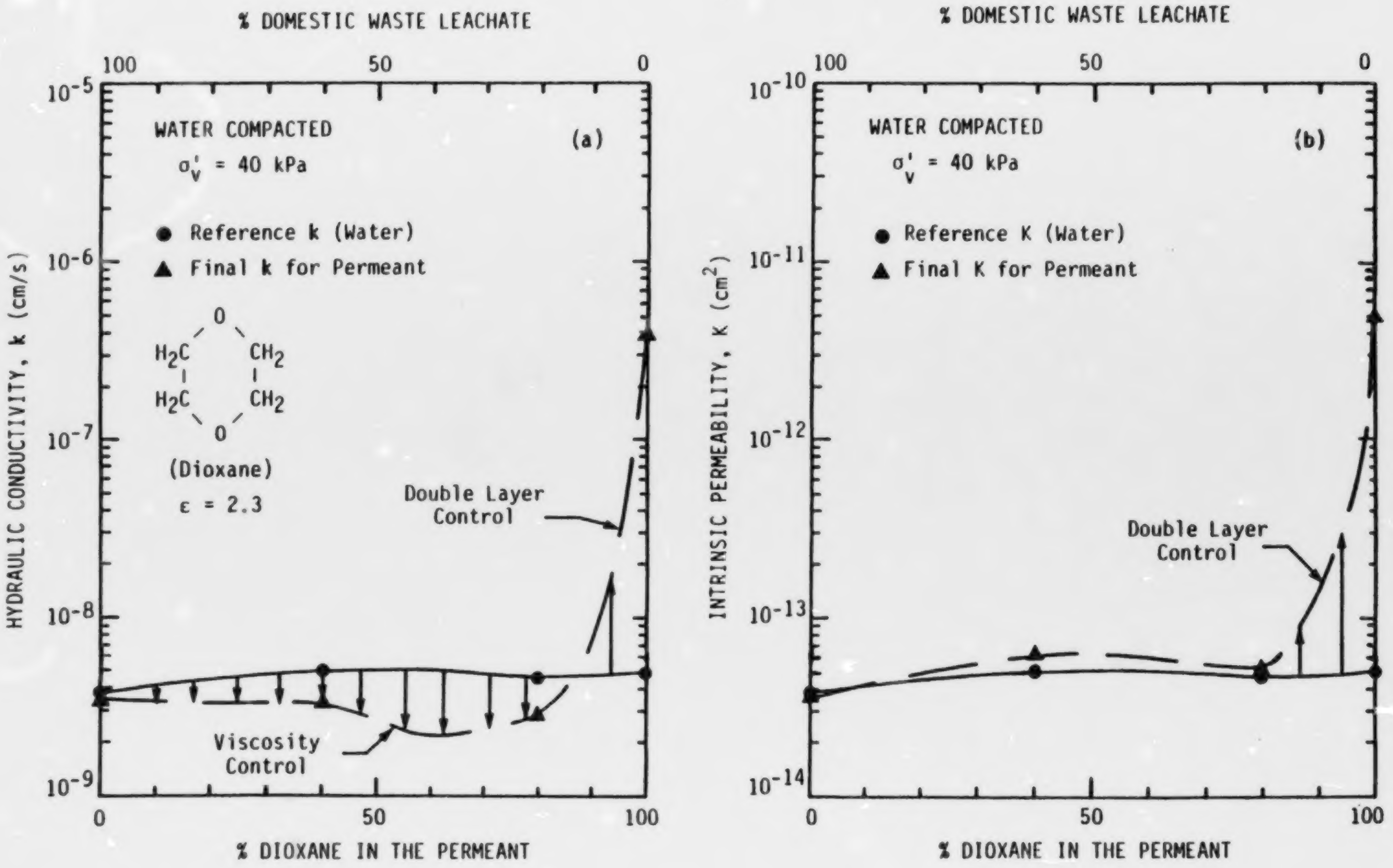

FIGURE 5.13 HYDRAULIC CONDUCTIVITY (a) AND INTRINSIC PERMEABILITY (b) OF WATER-COMPACTED BROWN SARNIA CLAY PERMEATED WITH LEACHATE/DIOXANE MIXTURES AT σ'_v = 40 kPa

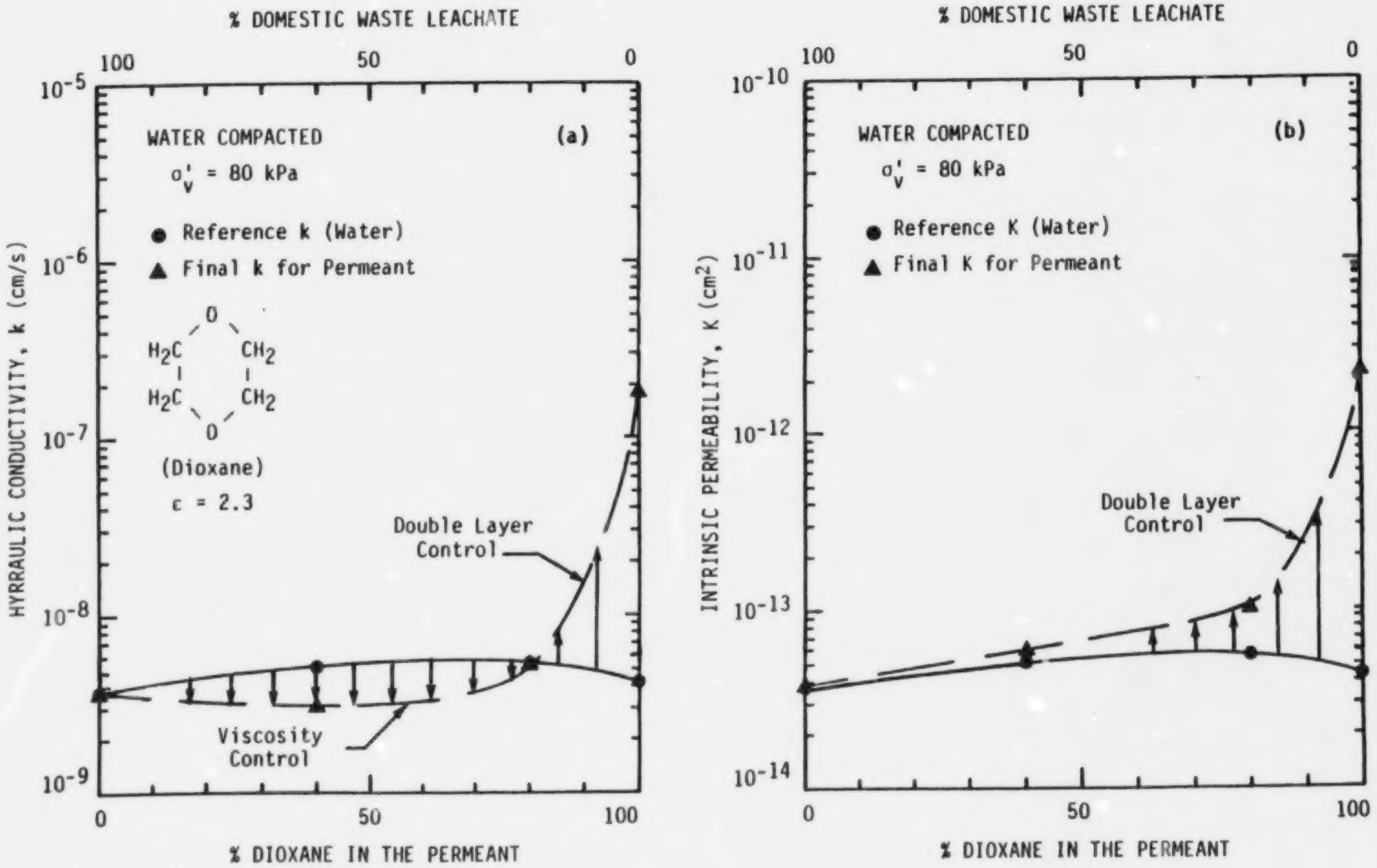

FIGURE 5.14 HYDRAULIC CONDUCTIVITY (a) AND INTRINSIC PERMEABILITY (b) OF WATER-COMPACTED BROWN SARNIA CLAY PERMEATED WITH LEACHATE/DIOXANE MIXTURES AT σ'_v = 80 kPa

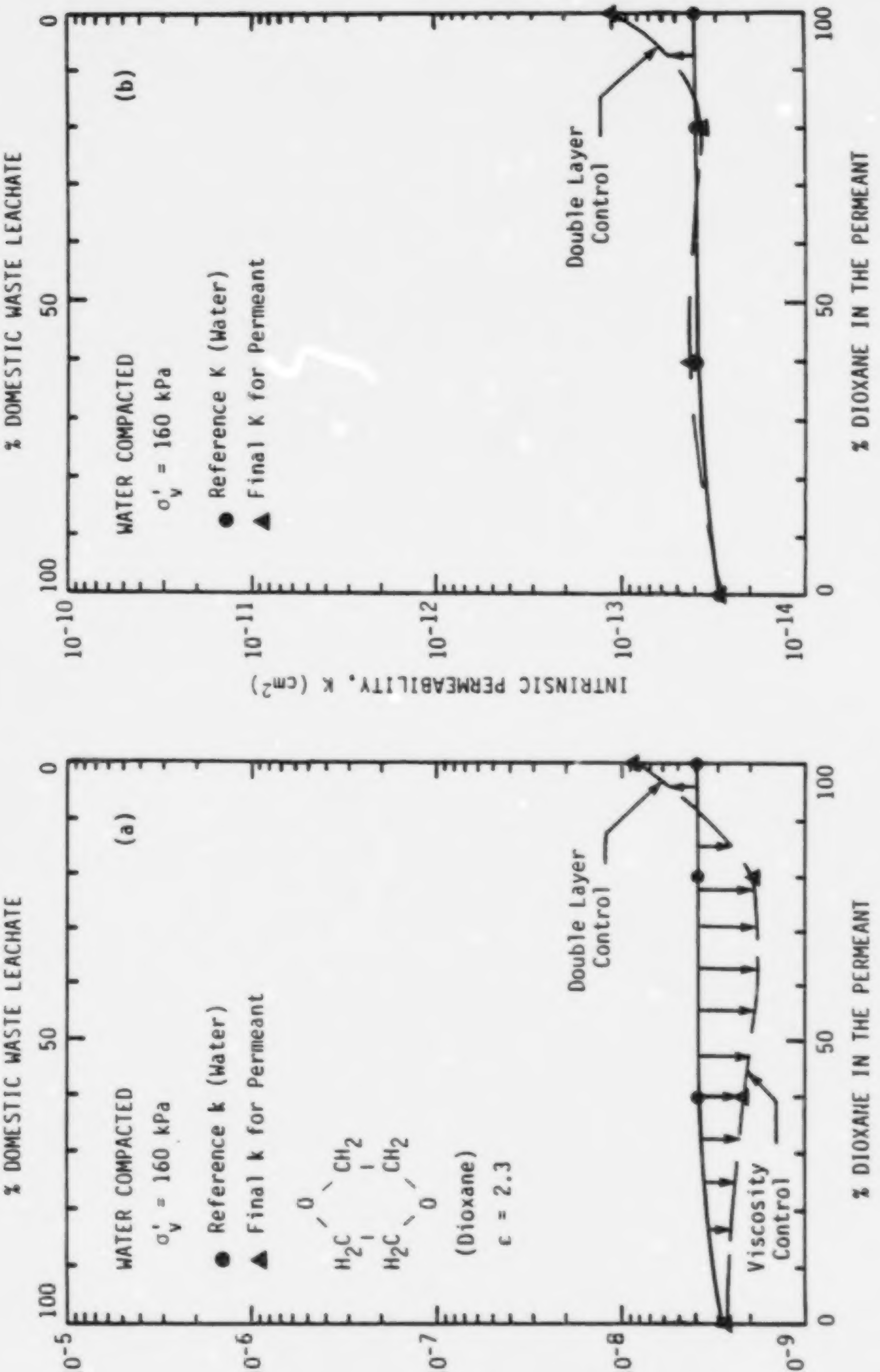

FIGURE 5.15 HYDRAULIC CONDUCTIVITY (a) AND INTRINSIC PERMEABILITY (b) OF WATER-COMPACTED BROWN SARNIA CLAY PERMEATED WITH LEACHATE/DIOXANE MIXTURES AT σ'_v = 160 kPa

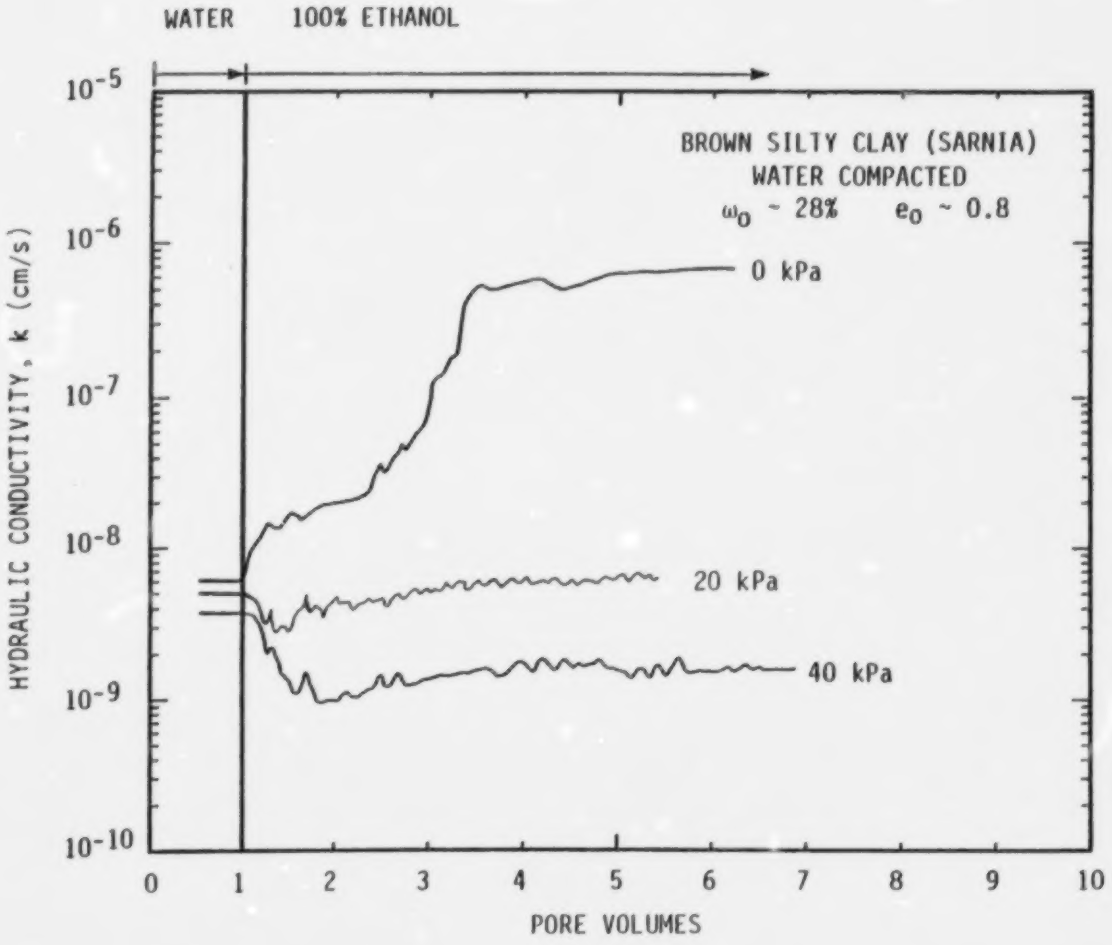

FIGURE 5.16 HYDRAULIC CONDUCTIVITY VS PORE VOLUMES FOR WATER-COMPACTED BROWN SARNIA CLAY PERMEATED WITH ETHANOL USING STATIC EFFECTIVE STRESSES OF 0, 20 AND 40 kPa

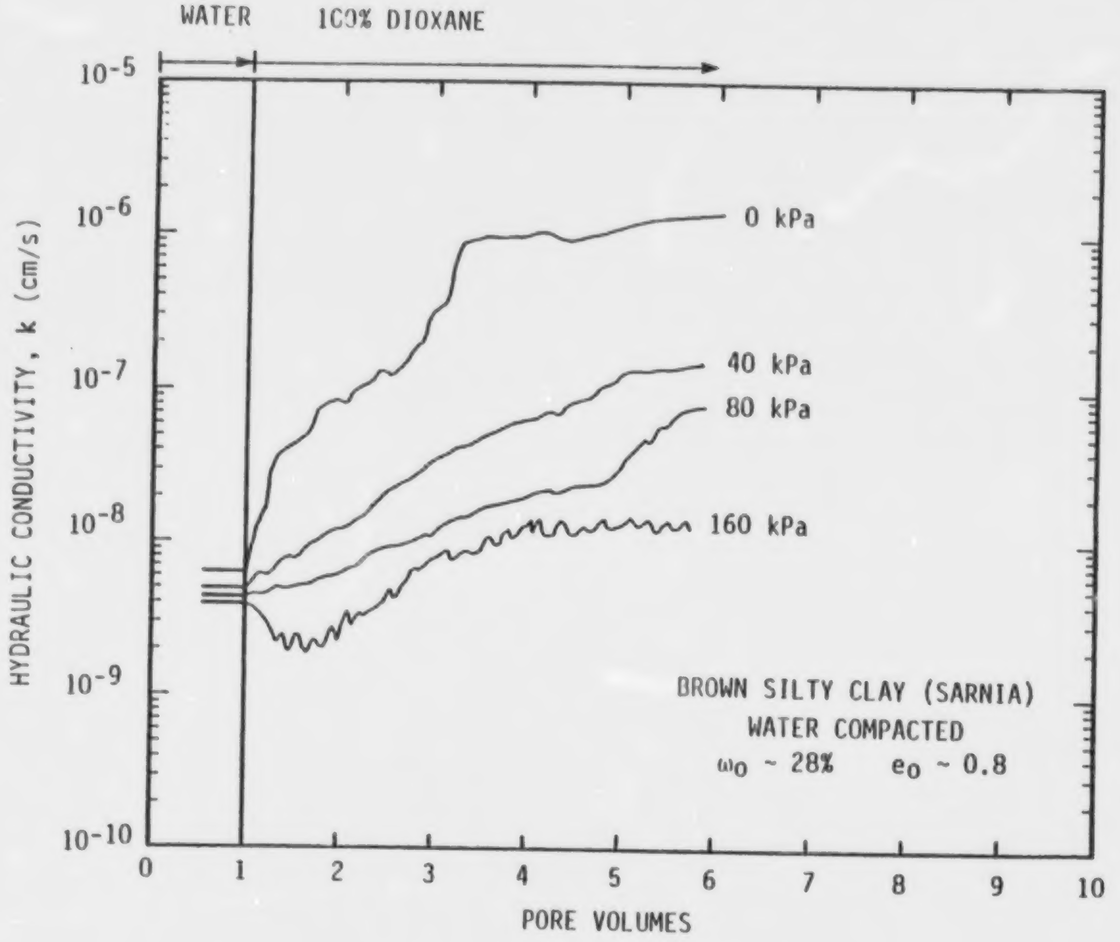

FIGURE 5.17 HYDRAULIC CONDUCTIVITY VS PORE VOLUMES FOR WATER-COMPACTED BROWN SARNIA CLAY PERMEATED WITH DIOXANE USING STATIC EFFECTIVE STRESSES OF 0, 40, 80 AND 160 kPa

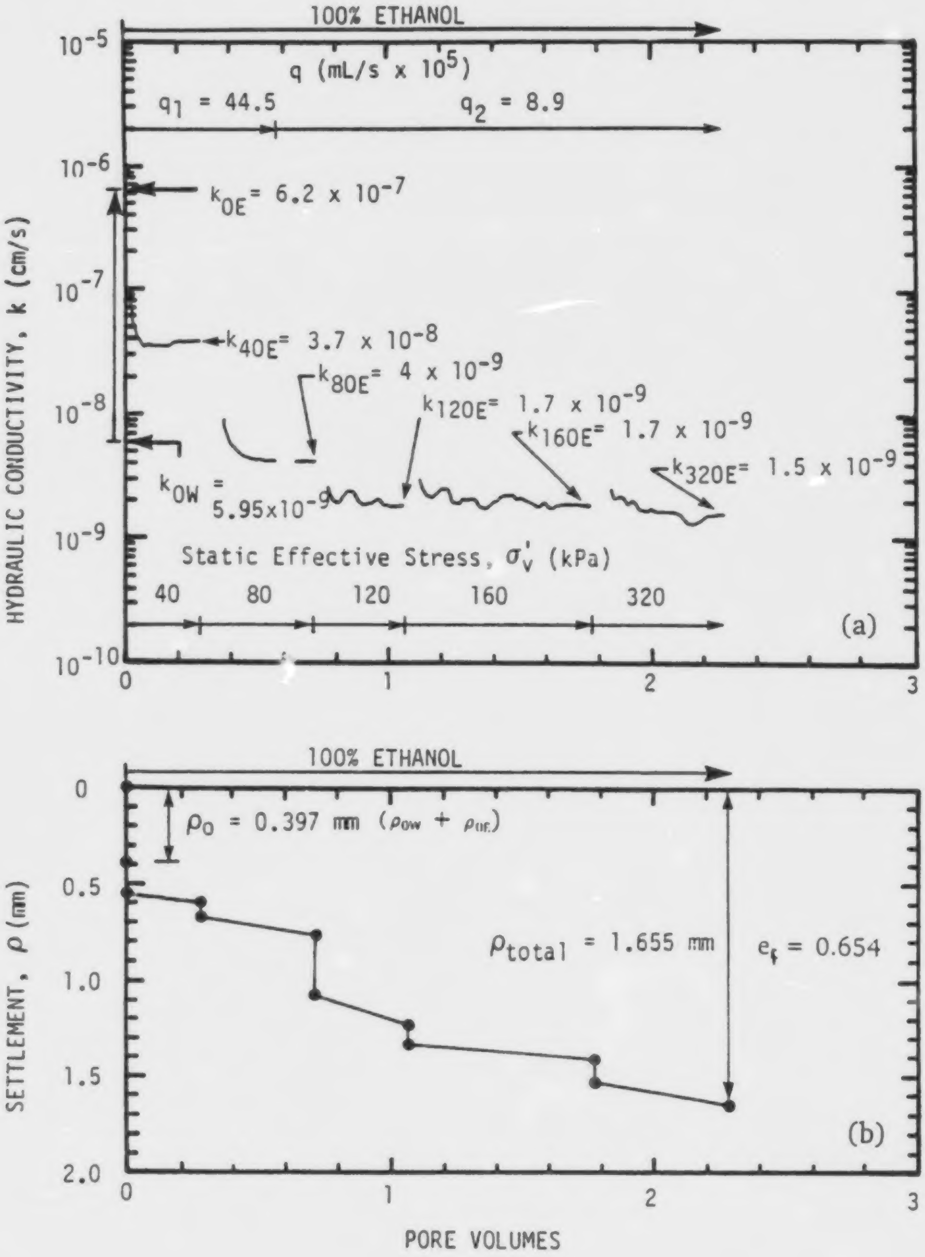

FIGURE 5.18 HYDRAULIC CONDUCTIVITY AND SETTLEMENT VS PORE VOLUMES FOR ETHANOL THROUGH WATER-COMPACTED CLAY AT POST-DAMAGE STRESSES OF 40, 80, 120, 160 AND 320 kPa [k_{i0E} = k for ethanol at 40 kPa]

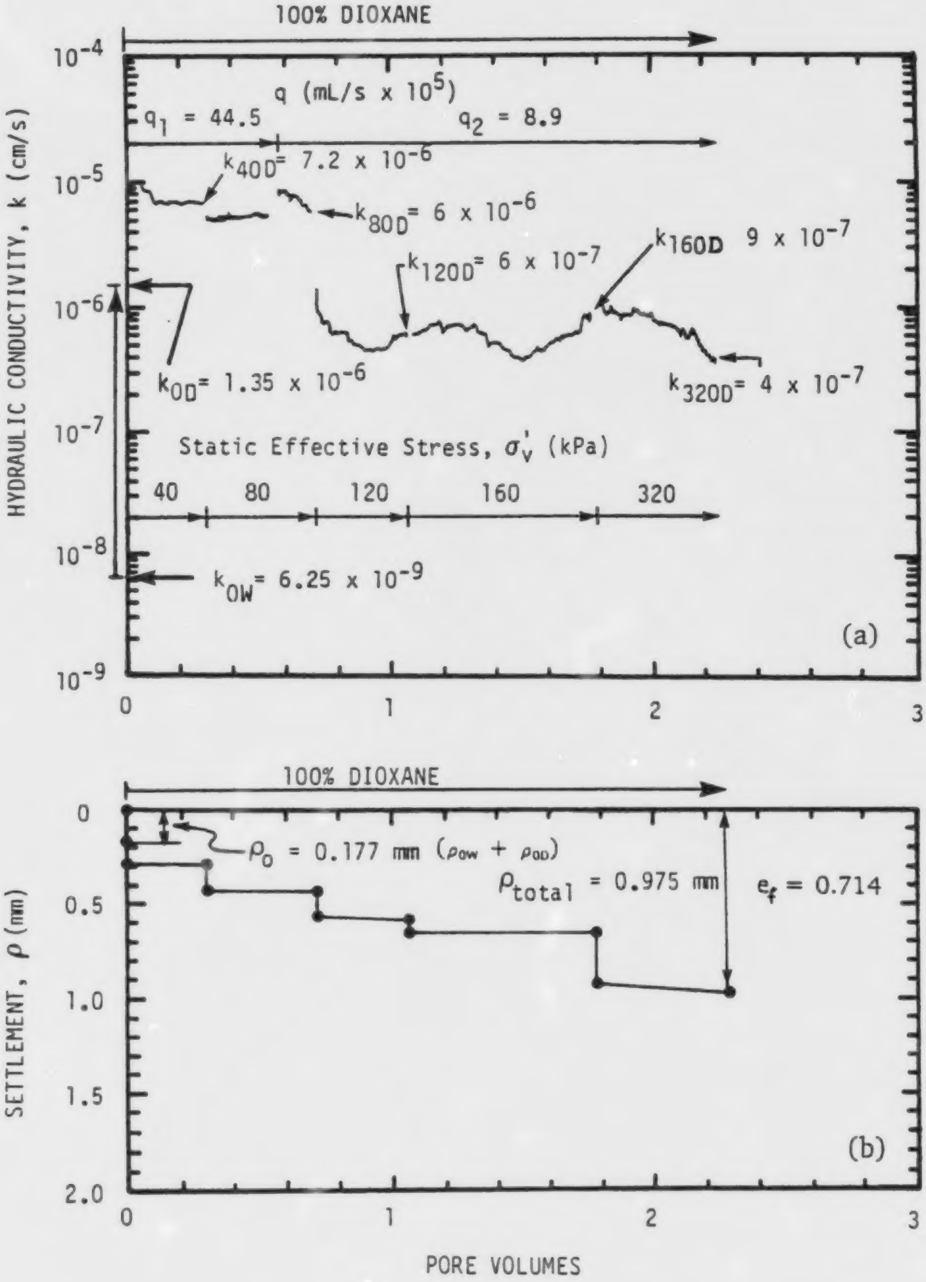

FIGURE 5.19 HYDRAULIC CONDUCTIVITY AND SETTLEMENT VS PORE VOLUMES FOR DIOXANE THROUGH WATER-COMPACTED CLAY AT POST-DAMAGE STRESSES OF 40, 80, 120, 160 AND 320 kPa [$\mathbf{k}_{40D}$ = **k** for dioxane at 40 kPa]

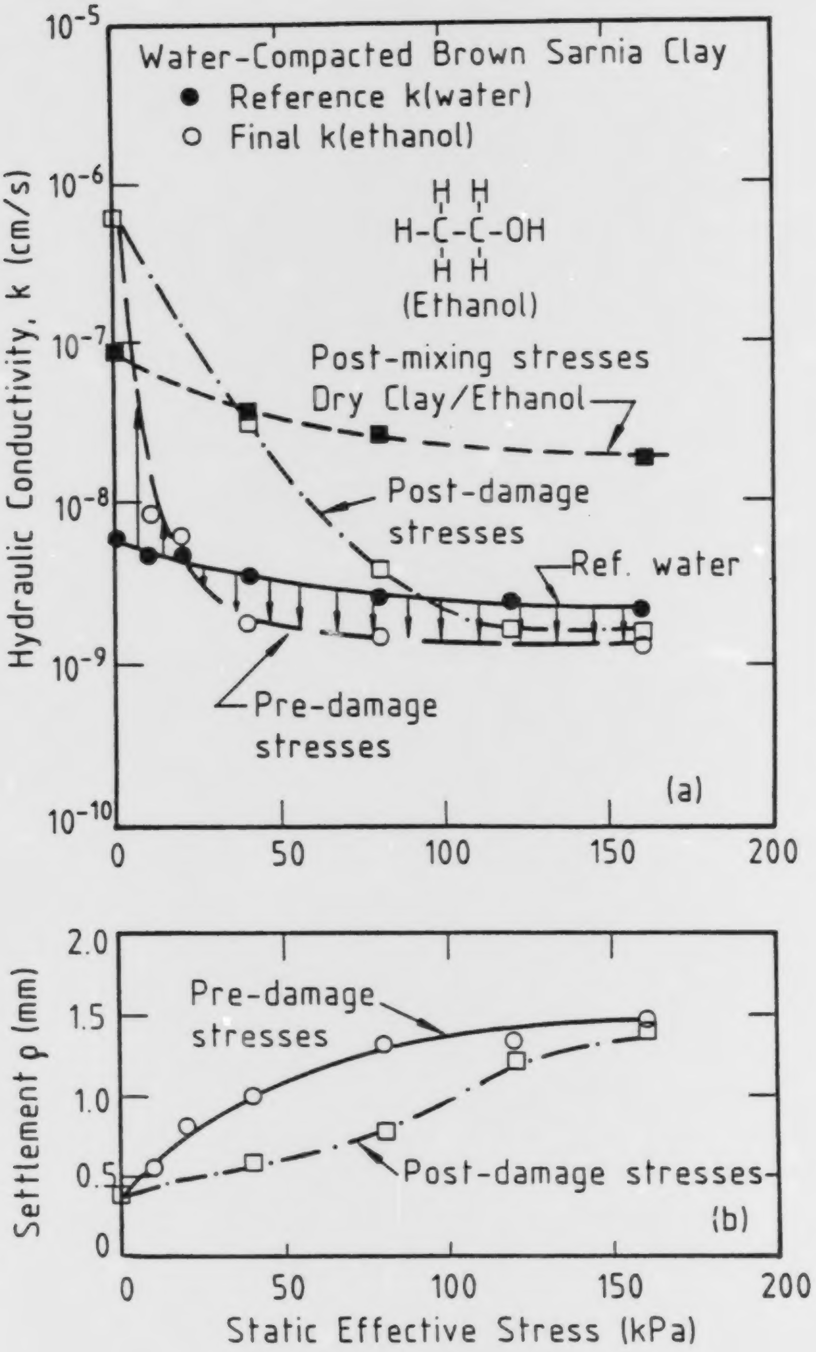

FIGURE 5.20 HYDRAULIC CONDUCTIVITY (a) AND SETTLEMENT (b) VS STATIC EFFECTIVE STRESSES FOR ETHANOL PERMEATION

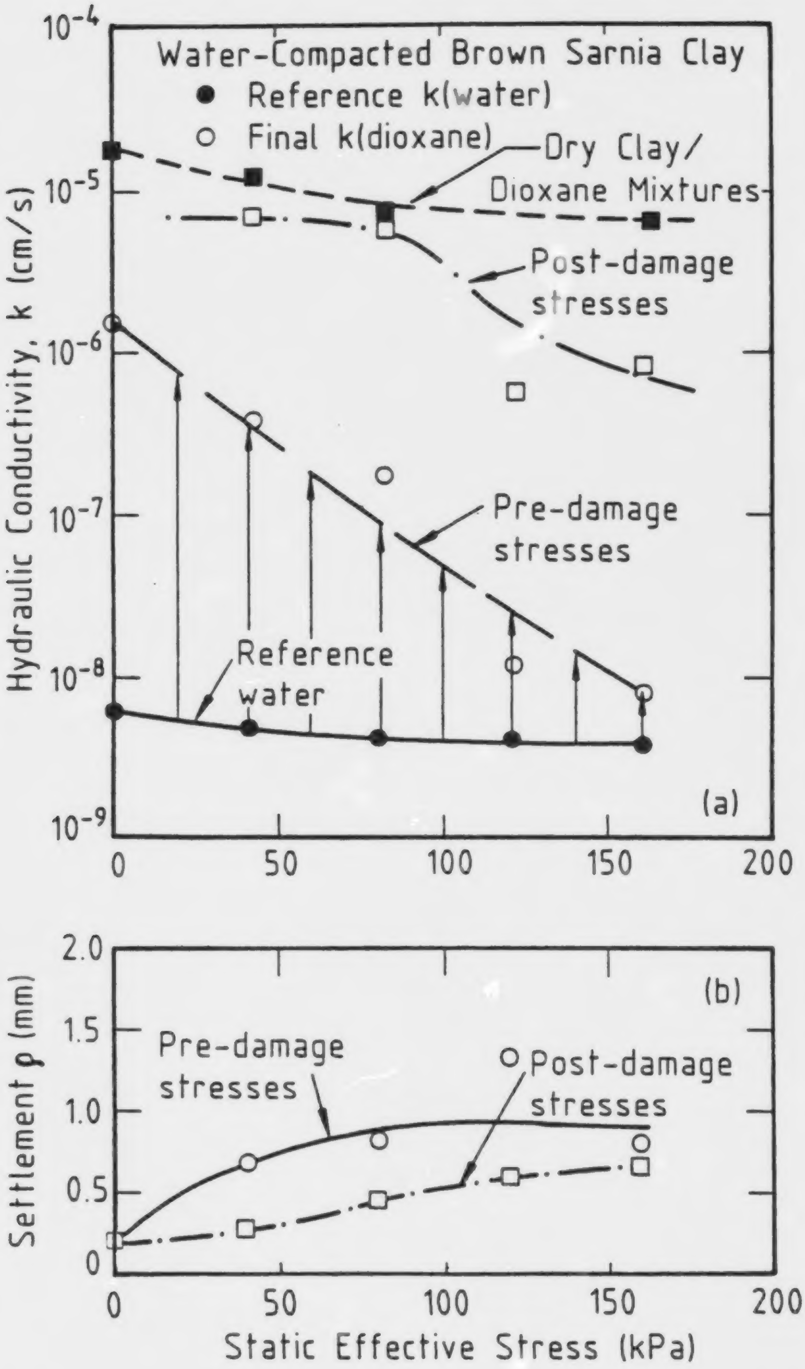

FIGURE 5.21 HYDRAULIC CONDUCTIVITY (a) AND SETTLEMENT (b) VS STATIC EFFECTIVE STRESSES FOR DIOXANE PERMEATION

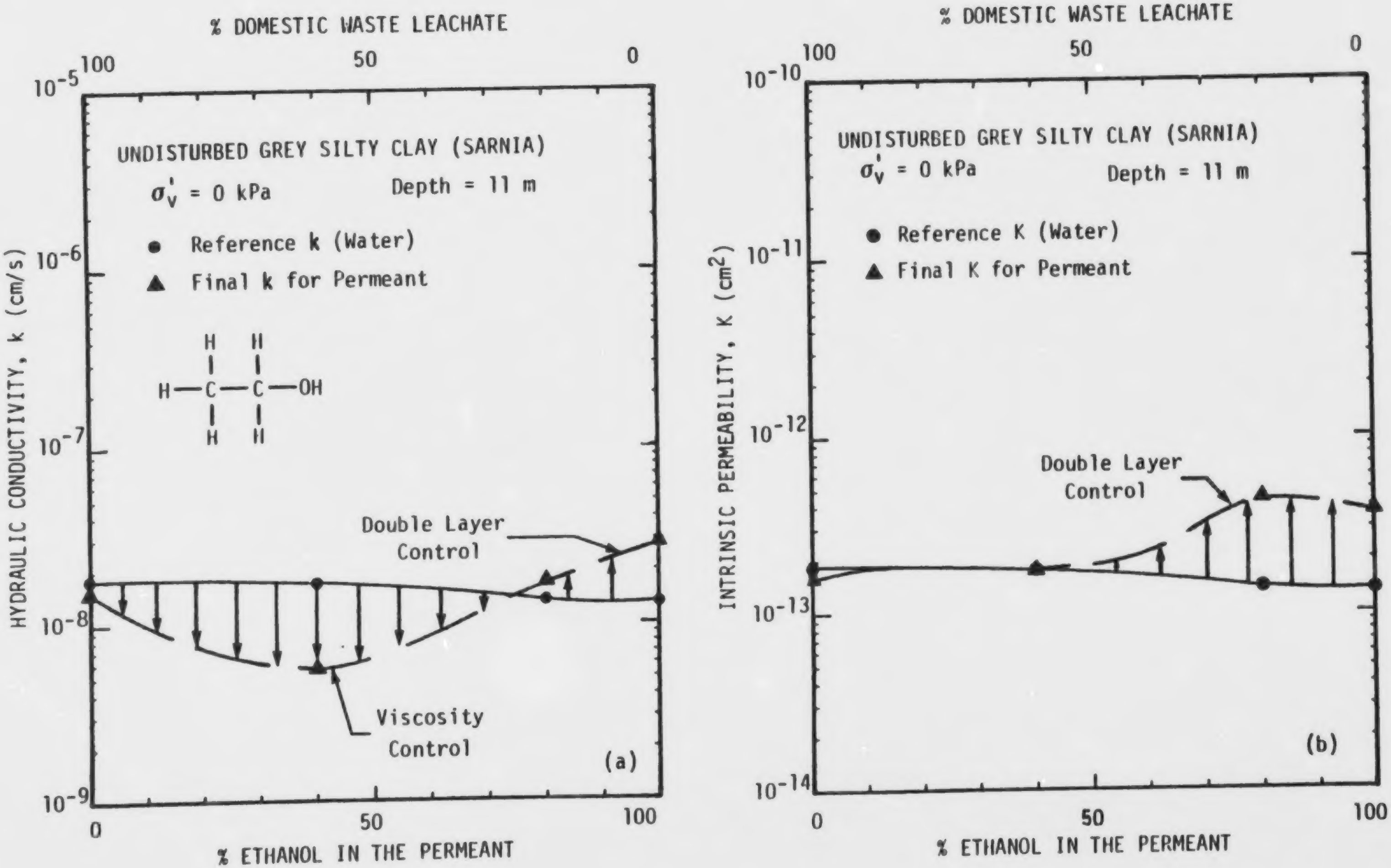

FIGURE 5.22 HYDRAULIC CONDUCTIVITY (a) AND INTRINSIC PERMEABILITY (b) OF UNDISTURBED GREY SARNIA CLAY PERMEATED WITH LEACHATE/ETHANOL MIXTURES AT $\sigma'_v = 0$ kPa

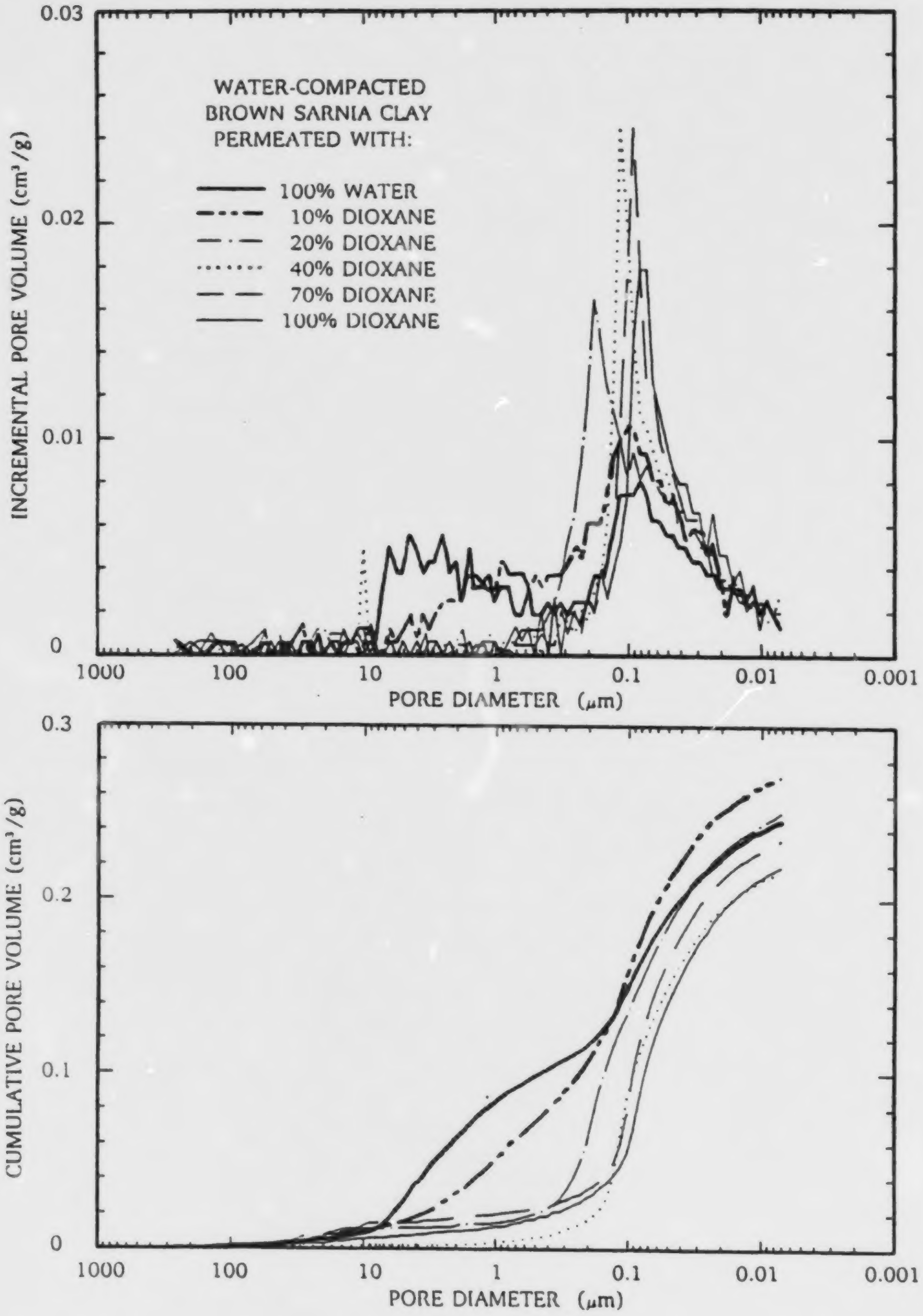

FIGURE 5.23 MERCURY INTRUSION POROSIMETRY FOR WATER-COMPACTED BROWN SARNIA CLAY PERMEATED WITH AQUEOUS SOLUTIONS OF DIOXANE

CHAPTER 6

DISCUSSION AND INTERPRETATION OF RESULTS

6.1 INTRODUCTION

Laboratory studies on the effects of domestic waste leachate containing increasing amounts of hydrocarbons on the hydraulic conductivity of clayey soils from southern Ontario were reported in the preceding chapter. This chapter presents a discussion of the work and its significance for compacted clay liners or natural clay deposits below waste disposal sites. The findings are supported by the results of a set of constant head hydraulic conductivity tests performed on larger soil samples at hydraulic gradients of 20.

6.2 THE ROLE OF PERMEANT VISCOSITY

The viscosity of permeants used to study the effects of organic liquids on the hydraulic conductivity of clays seems to have been neglected in the literature. This is probably related to the use of concentrated organic solvents which may cause very large changes in k that swamp the effects of permeant viscosity. However, mixing water-soluble hydrocarbons such as alcohols, acetone or dioxane with water (or domestic waste leachate) at intermediate concentrations results in up to 2 or 3-fold increases in viscosity (see Figure 4.5). This should cause significant decreases in hydraulic conductivity, all other variables being held constant.

Figure 6.1 shows that the variation in hydraulic conductivity reported by Bowders (1985) and Bowders et al. (1985) for compacted kaolinite permeated with water/methanol mixtures are strongly influenced by the viscosity of the permeants. For both fixed-wall and flexible-wall cells, the hydraulic conductivity decreases as the permeant becomes more viscous due to the addition of methanol (Figure 6.1a). As the alcohol content surpasses ~ 50% the viscosity of the permeant decreases and flow through the pores increases. The data is replotted on Figure 6.1b in terms of intrinsic permeability, K, which eliminates the effects of viscosity and density on **k**. Very small changes in K are observed for flexible-wall permeameters, suggesting that changes in permeant viscosity control most of the changes in hydraulic conductivity of the inactive kaolinite clay. At high concentrations, however, double layer effects may have been suppressed by chemically induced consolidation caused by the confining pressure acting on the sample through a flexible membrane. The intrinsic permeability values for fixed-wall cells exhibit little change for methanol contents up to 80%. Pure methanol is shown to cause an increase in K of over 5-fold, probably reflecting flow along the sides of the fixed-wall cell due to sample shrinkage.

Permeant viscosity may also play a dominant role in the early stages of permeation with concentrated water-soluble hydrocarbon liquids. The organics do not migrate as a uniform, piston-like front but rather, they disperse into the sample pore fluid. The resultant diffuse hydrocarbon front raises the viscosity of the pore fluid, producing initial decreases in **k**. As the test progresses the organics in the pore fluid become more concentrated and less viscous, thus leading to larger values of **k**. Figure 6.2 shows the results of two separate studies of clays permeated with concentrated acetone where viscosity effects seems to have caused the decreases in **k** observed during the early stages of acetone permeation. Similar patterns of variation in **k** were reported by various other investigators for methanol (Daniel et al., 1985; Uppot and Stephenson, 1989) and for ethylene glycol (Brown and Anderson, 1983) but the important role of permeant viscosity was not addressed.

6.3 EXCLUSION OF NON-POLAR ORGANICS FROM DOUBLE LAYERS

The hydraulic conductivity (**k**) and intrinsic permeability (**K**) results for water-compacted, brown Sarnia clay permeated with leachate/organic mixtures shown in Figures 5.8 and 5.12 are replotted as a ratio of the final permeant value to the initial water value in Figure 6.3. It is clear from Figure 6.3a that increases in **k** took place only at organic contents above 70 to 75%. At lower hydrocarbon contents (ethanol and dioxane) the increases in permeant viscosity causes decreases in **k** to values about half that for water.

The real effects of dielectric constant become apparent in Figure 6.3b, where the effects of viscosity are eliminated by plotting the data as intrinsic permeability ratios (K_f/K_w). For dioxane contents greater than 70%, K increases rapidly reaching values 1000 times greater than water for pure dioxane. However, the values of K for water ($K_w \sim 10^{-13}$ cm^2) remain practically unchanged by permeants containing less than 70% dioxane. Even though dioxane is fully soluble in water because of oxygen replacing two carbons in the benzene ring, it is also non-polar. It is believed that cations present in the double layer exhibit a strong affinity for water and reject the non-polar dioxane, thus preventing double layer collapse until dioxane concentrations of ~ 70% are reached. A somewhat different behaviour is observed in the case of ethanol, which is more polar than dioxane. Small increases in K are apparent at ethanol contents as low as 20%, suggesting partial entry of alcohol into the double layers.

Four sets of solubility tests were performed in an attempt to demonstrate the hypothesis that non-polar hydrocarbons are excluded by cations in the double layers. The tests are represented in Figure 6.4 to 6.7 and consisted of mixing 4 grams of sodium chloride with a total of 10 grams of liquid including water and hydrocarbons. The solubility of sodium chloride in each system was calculated from the dry weight of residual sodium chloride after carefully removing the liquid with a hypodermic syringe (Tables 6.1 and 6.2).

a) Salt Addition to Liquid Mixtures: The first set of tests shown in Figure 6.4 were performed by adding sodium chloride to water/ethanol mixtures containing 0, 20, 40, 60, 80 and 100% alcohol. The solubility values decreased from ~ 360 g of NaCl per kg of solvent (~ 6 Molar NaCl) for water to 2.2 g/kg (~ 0.04 Molar NaCl) for concentrated ethanol. In all cases a single liquid phase was observed.

In a similar set of tests using water/dioxane mixtures (Figure 6.5) the values of solubility decreased from ~ 360 g/kg (100% water) to 1.2 g/kg (100% dioxane). The mixtures containing 40%, 60% and 80% dioxane separated into an upper, dioxane-rich phase and a lower, water-rich phase. The upper phases contained over 95% dioxane demonstrating selective solvation of NaCl in water (lower phase).

b) Organic Addition to Brine: Another two sets of experiments are described in Figures 6.6 and 6.7, where 4 g of NaCl were added to water and after shaking for 20 hours enough ethanol or dioxane was added to the brine to form 10 g of liquid at organic contents of 0, 20, 40, 60, 80 and 100%. All mixtures containing water and hydrocarbons exhibited phase separation with the added organic liquids appearing to sit on top of the mixtures, demonstrating once again an affinity of NaCl for water and a rejection of hydrocarbons.

A photographic summary of the solvation experiments is presented in Figure 6.8 showing four bottles containing 4 g of NaCl, 4 g of organics and 6 g of water. Each of these bottles was previously represented in Figures 6.4 to 6.7. It is clear that two systems containing the exact same components can exhibit quite different arrangements, depending upon the order of mixing. In case (a), sodium chloride is added to the water/hydrocarbon mixtures and its solvation is inhibited by the presence of dissolved low dielectric organics. Case (b), on the other hand, shows that the organic liquids added to the brines are excluded into a separate (upper) phase, having little influence on NaCl solvation in the lower (water-rich) phase. This observation is confirmed by the solubility values in Table 6.2 for case (b) being consistently higher than those in Table 6.1 for case (a).

In conclusion, the solubility tests have visually demonstrated the strong preference of ions for polar water over less polar organic liquids. It is suggested that the same preference is exhibited by double layer cations, resulting in the exclusion of non-polar organics. Therefore, aqueous solutions of ethanol or dioxane have little effect on the permeability of water-compacted clays at contents below ~ 70%. Furthermore, the solubility tests have also shown that at all concentrations organic liquids inhibit the solvation of NaCl in pre-mixed solutions of hydrocarbons in water. This situation is believed to represent the solvation of salts present in dry clays moulded with pre-mixed aqueous solutions of organics. As shown in Section 5.2, double layer contraction and consequent increases in permeability with increasing organic content are apparent for all the range of concentrations.

6.4 CONFIRMATION TESTS USING LARGER CELLS AND LOWER GRADIENTS

Two hydraulic conductivity tests were carried out using low hydraulic gradients (i = 20) and larger samples (~ 9 cm diameter by ~ 2 cm thick). The two tests involved water-compacted brown Sarnia clay permeated with leachate/dioxane mixtures containing 40% and 85% dioxane, respectively. Both clay samples were compacted at a water content of ~ 30% using the Harvard miniature tamper (3 layers, 60 tamps, 32 lb or 0.142 kN per tamp).

Figure 6.9 shows one of the cells consisting of a glass cylinder, two viton stoppers and aluminum plates, all of these parts held together by four threaded rods. The inlet and outlet tubing (1/8" stainless steel) were pierced through the viton stoppers, and all the joints were sealed with silicone sealant. An air gap prevented direct contact between the influent permeant and the viton stopper. The inlet tubing was connected to the constant head equipment described in Section 3.4 and a hydraulic gradient of 20 was maintained across the samples. The influent flow was monitored by taking periodic readings of the flowmeters, while the effluent permeant was collected for chemical assessment.

The sample permeated with 40% dioxane showed little change in hydraulic conductivity throughout the 92 days of testing (Figure 6.10). The measured value of 1 x 10^{-8} cm/s was about what is expected for the brown Sarnia clay compacted at a void ratio of 0.90. Chemical assessment suggest that at the end of testing the pore fluid consists 39% dioxane and the effluent samples contain ~ 35% dioxane compared with 42% dioxane in the influent permeant. The clay sample permeated with 85% dioxane (Figure 6.11) exhibited rapid increases in **k** reaching a value of 5.5 x 10^{-6} cm/s only after 6 days of testing. The effluent chemistry demonstrates very early arrival of dioxane front (C/C_o = 0.5 at only 0.03 pore volumes), suggesting fracture flow, even at a low gradient. This is confirmed by only 66% dioxane present in the pore fluid at the end of testing, while the influent contains 80% dioxane.

The post-testing appearance of the soils is shown in Figure 6.12. The sample permeated with 40% dioxane appears uniformly brown, showing no evidence of fractures. The soil permeated with 85% dioxane, on the other hand, exhibits a single shrinkage crack (up to ~ 0.2 mm wide by ~ 50 mm long) that extends about 7 mm into the soil thickness at the side of the sample. The crack is believed to have formed as a result of double layer contraction in the presence of high dioxane contents, leading to the large values of **k** observed.

The two tests reported in this section appear to confirm the results obtained using the constant flow **k** testing equipment suggesting that no increases in **k** take place for dioxane contents below 70%. In addition, the glass cell allowed observation of the developing shrinkage crack, which was never possible for other tests presented in this reported.

TABLE 6.1 SOLUBILITY TESTS: 4 g NaCl ADDED TO 10 g SOLVENT

SOLVENT	LIQUID REMOVED (g)	RESIDUAL NaCl (g)	SOLUBILITY (g NaCl/kg solvent)
100% Water	13.24	0.50	359.3
20% Ethanol 80% Water	11.39	1.82	236.7
40% Ethanol 60% Water	10.38	2.65	149.5
60% Ethanol 40% Water	9.66	3.29	79.3
80% Ethanol 20% Water	9.09	3.78	24.8
100% Ethanol	8.97	3.98	2.2
20% Dioxane 80% Water	11.73	1.77	234.7
40% Dioxane 60% Water	10.51	2.40	170.6
60% Dioxane 40% Water	9.68	3.19	91.3
80% Dioxane 20% Water	8.75	3.77	27.0
100% Dioxane	8.56	3.99	1.2

TABLE 6.2 SOLUBILITY TESTS: HYDROCARBON ADDED TO NaCl/WATER MIXTURES

SOLVENT	LIQUID REMOVED (g)	RESIDUAL NaCl (g)	SOLUBILITY (g NaCl/kg solvent)
100% Water	13.24	0.50	359.3
20% Ethanol 80% Water	11.76	1.43	279.7
40% Ethanol 60% Water	11.18	2.22	189.4
60% Ethanol 40% Water	9.83	2.99	114.5
80% Ethanol 20% Water	9.33	3.67	36.7
100% Ethanol	8.97	3.98	2.2
20% Dioxane 80% Water	11.77	1.43	279.3
40% Dioxane 60% Water	10.25	2.35	191.9
60% Dioxane 40% Water	9.80	3.03	109.9
80% Dioxane 20% Water	9.17	3.75	28.0
100% Dioxane	8.56	3.99	1.2

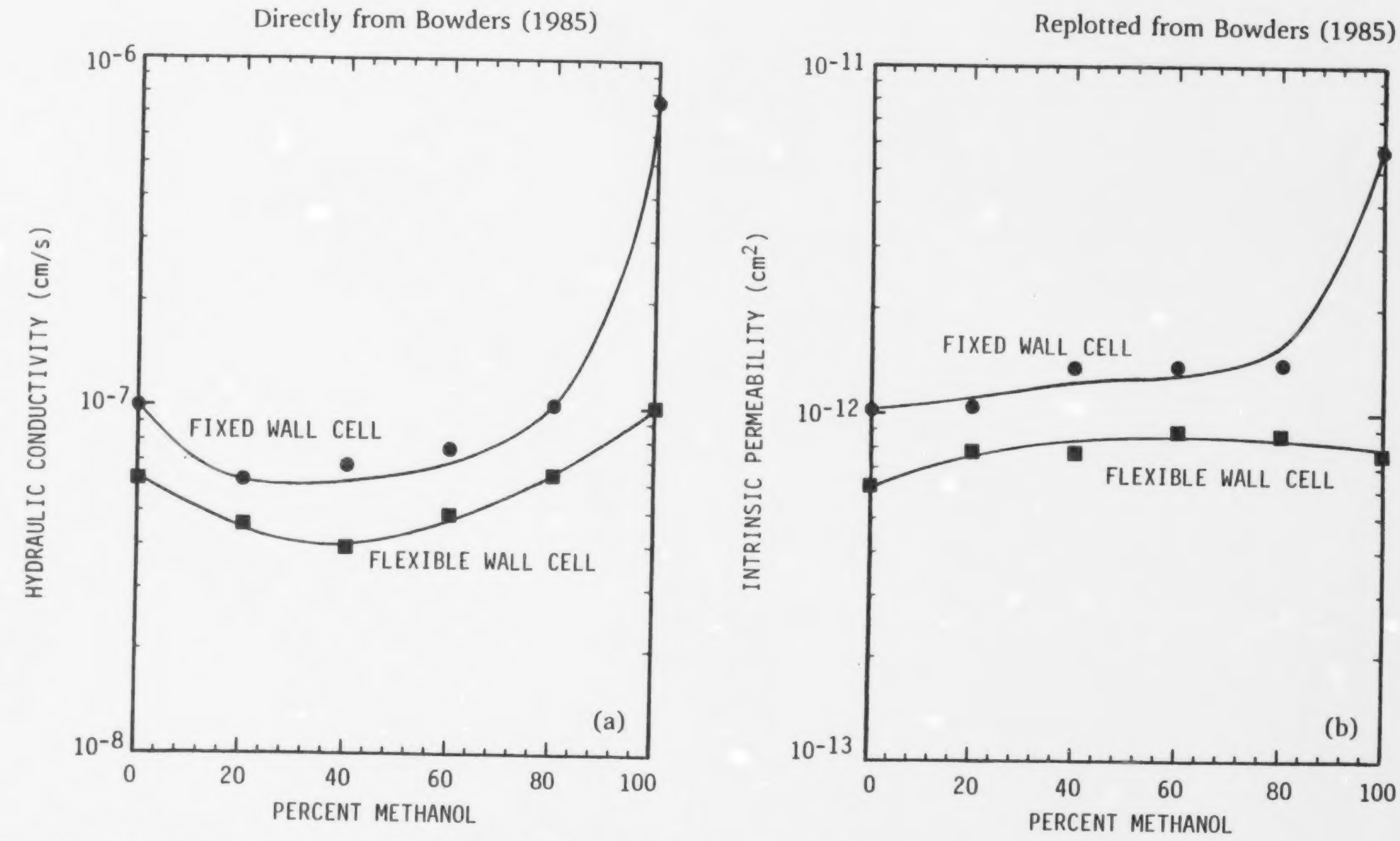

FIGURE 6.1 HYDRAULIC CONDUCTIVITY (a) AND INTRINSIC PERMEABILITY (b) FOR COMPACTED KAOLINITE PERMEATED WITH METHANOL/WATER MIXTURES (Bowders, 1985)

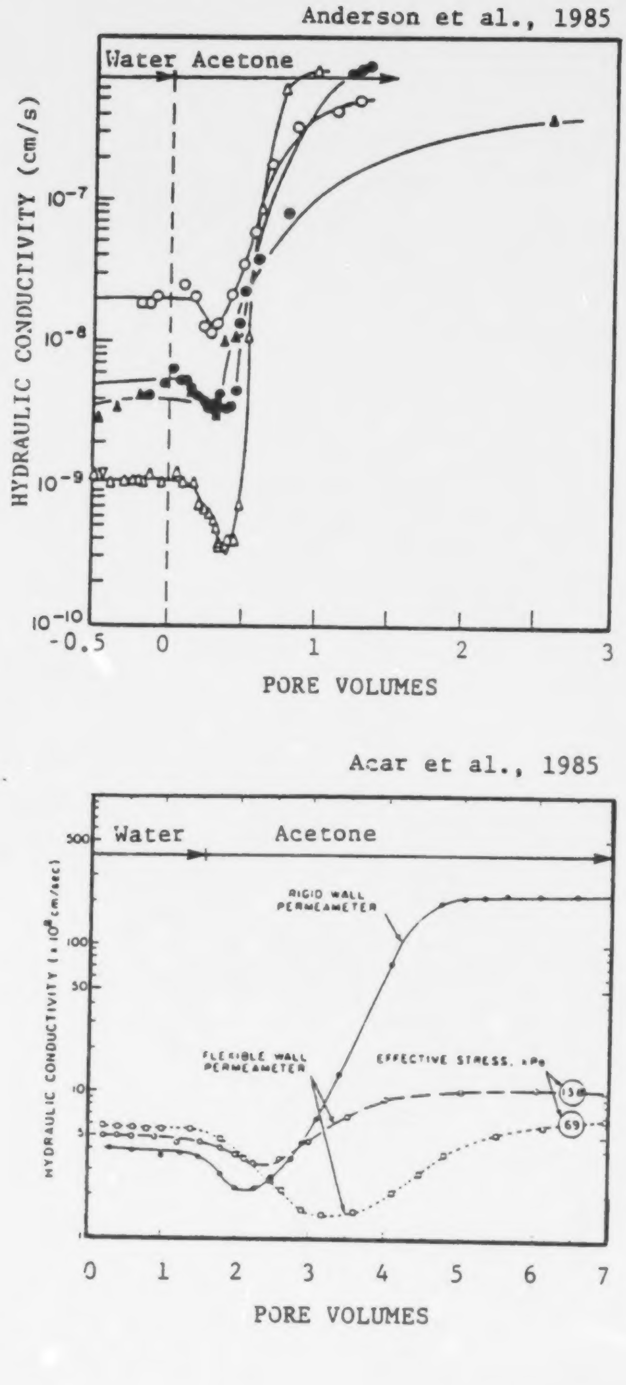

Anderson et al., 1985

Acar et al., 1985

FIGURE 6.2 HYDRAULIC CONDUCTIVITY VS PORE VOLUMES FOR ACETONE PERMEATION THROUGH WATER-COMPACTED CLAYS (Anderson et al., 1985 and Acar et al., 1985)

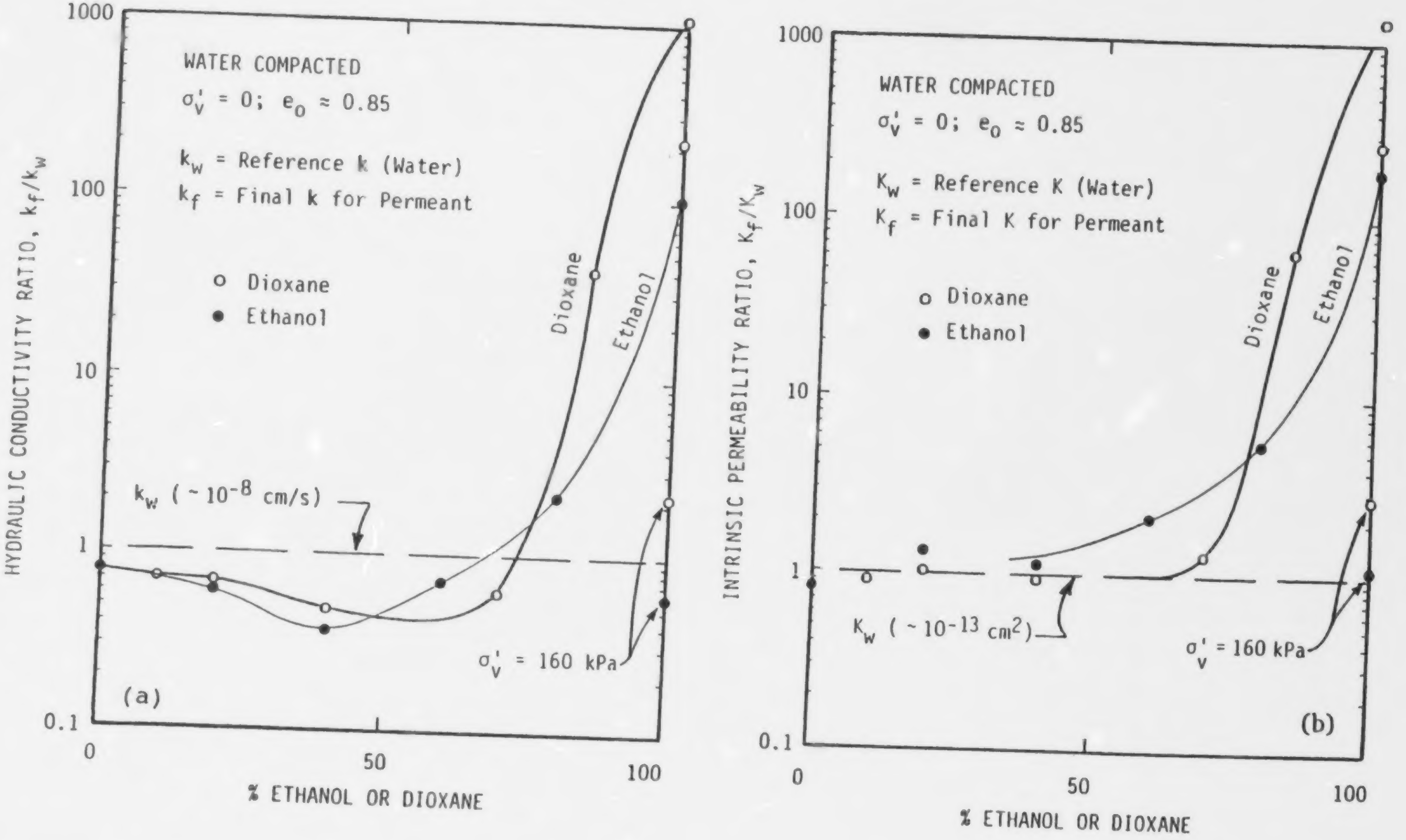

FIGURE 6.3 HYDRAULIC CONDUCTIVITY (a) AND INTRINSIC PERMEABILITY (b) OF WATER-COMPACTED BROWN SARNIA CLAY PERMEATED WITH LEACHATE/HYDROCARBON MIXTURES

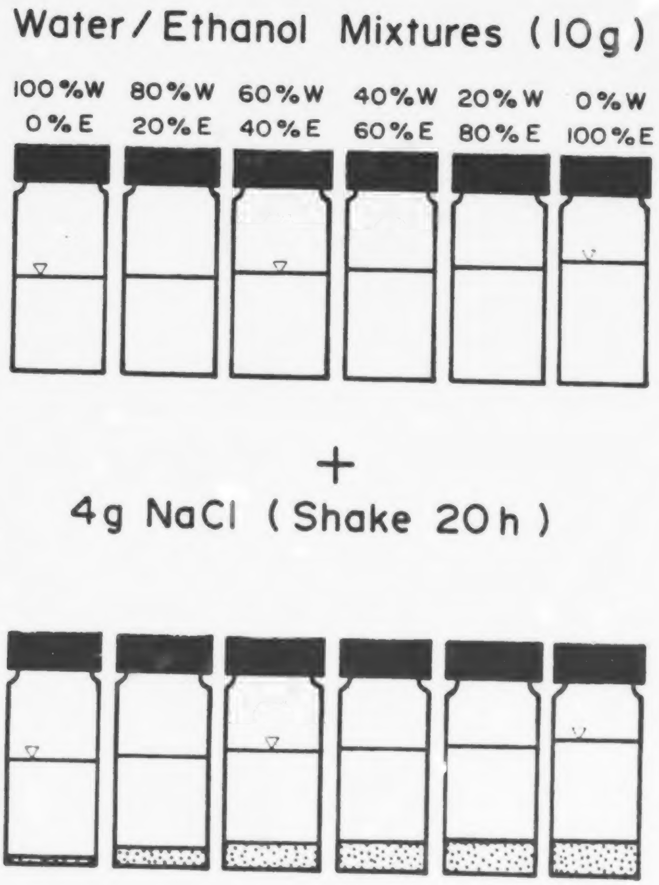
Water/Ethanol Mixtures (10g)
100%W 0%E
80%W 20%E
60%W 40%E
40%W 60%E
20%W 80%E
0%W 100%E
+
4g NaCl (Shake 20h)

FIGURE 6.4 ION SOLVATION DEMONSTRATION: [WATER/ETHANOL MIXTURES] + ADDED NaCl

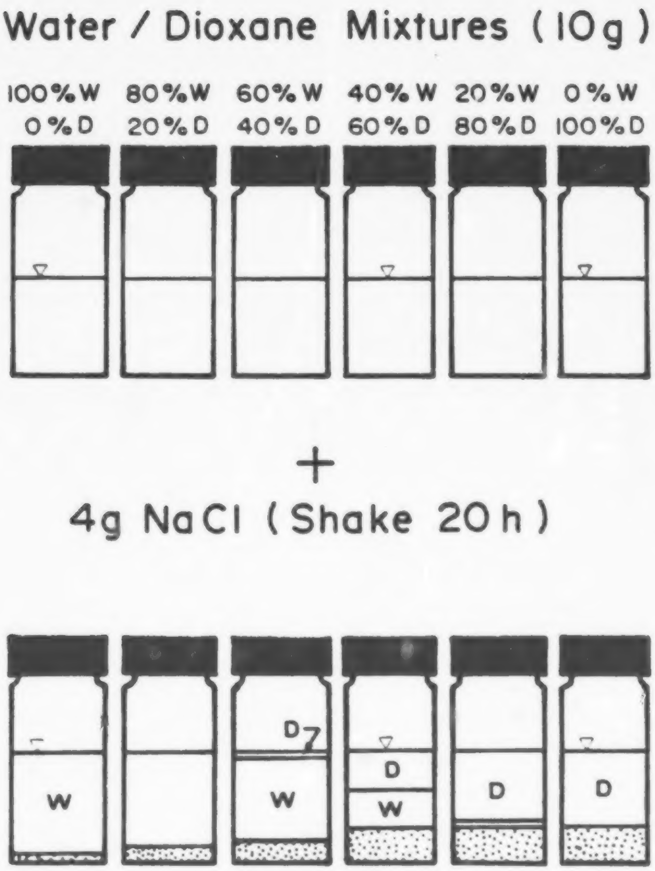
Water / Dioxane Mixtures (10g)
100% W 0% D
80% W 20% D
60% W 40% D
40% W 60% D
20% W 80% D
0% W 100% D
+
4g NaCl (Shake 20 h)
W
D
W
D
W
D
D

FIGURE 6.5 ION SOLVATION DEMONSTRATION:
[WATER/DIOXANE MIXTURES] + ADDED NaCl

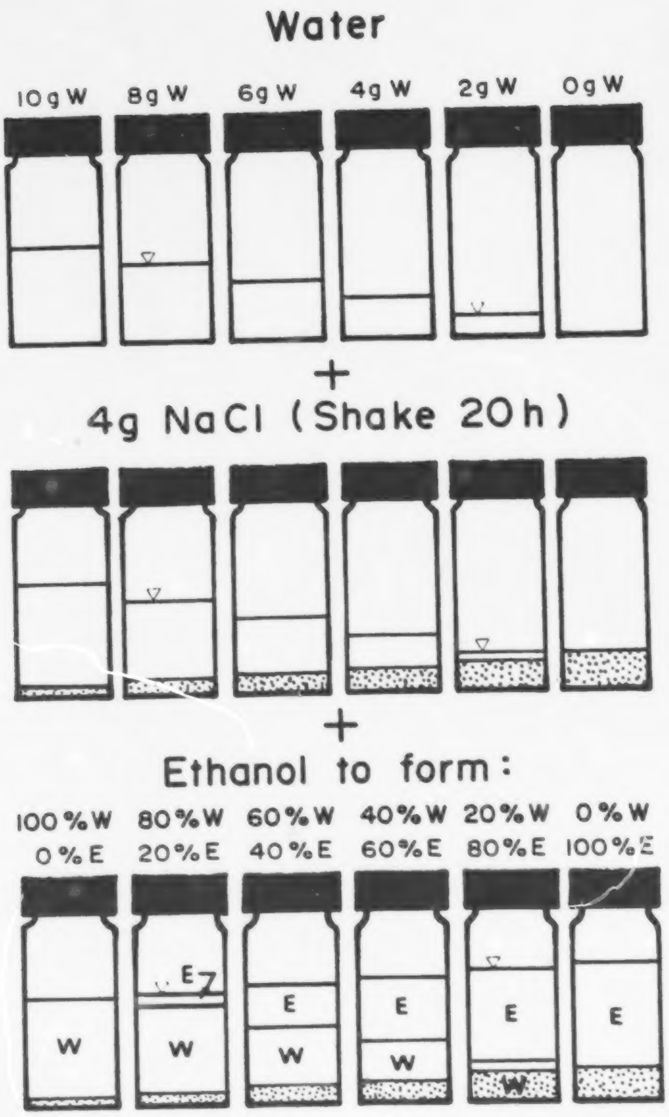
Water
10g W
8g W
6g W
4g W
2g W
0g W
+
4g NaCl (Shake 20h)
+
Ethanol to form:
100%W
0%E
80%W
20%E
60%W
40%E
40%W
60%E
20%W
80%E
0%W
100%E
E
W
E
W
E
W
E
W
E
W
E

FIGURE 6.6 ION SOLVATION DEMONSTRATION:
[WATER/NaCl MIXTURES] + ADDED ETHANOL

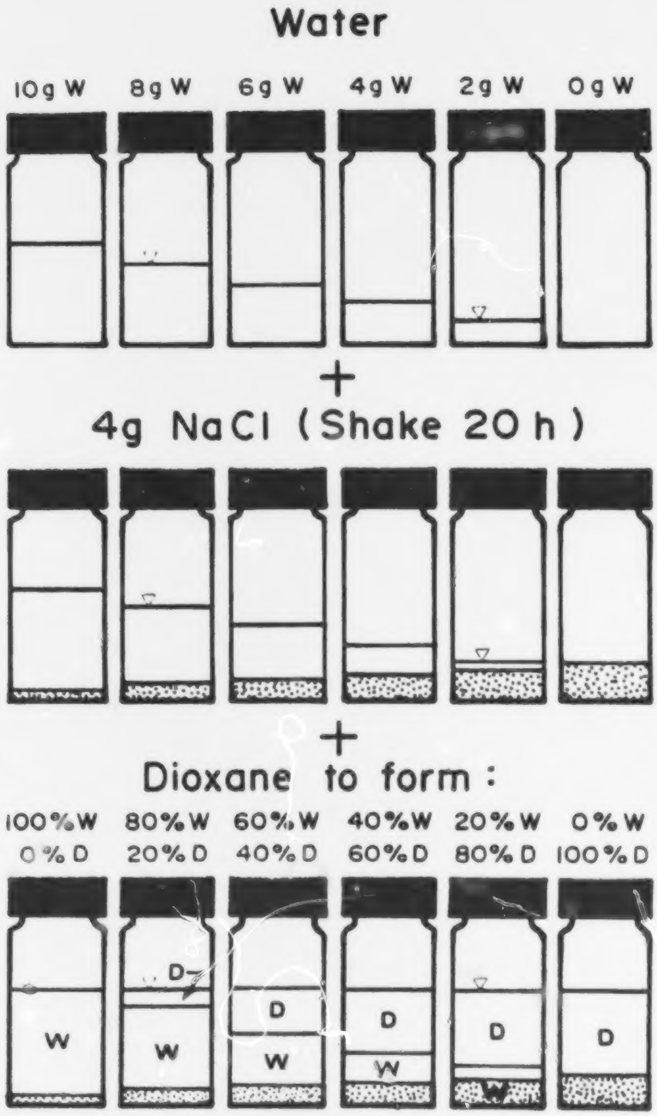
Water
10g W
8g W
6g W
4g W
2g W
0g W
+
4g NaCl (Shake 20 h)
+
Dioxane to form:
100% W
0% D
80% W
20% D
60% W
40% D
40% W
60% D
20% W
80% D
0% W
100% D
W
D
W
D
W
D
W
D
W
D

FIGURE 6.7 ION SOLVATION DEMONSTRATION:
[WATER/NaCl MIXTURES] + ADDED DIOXANE

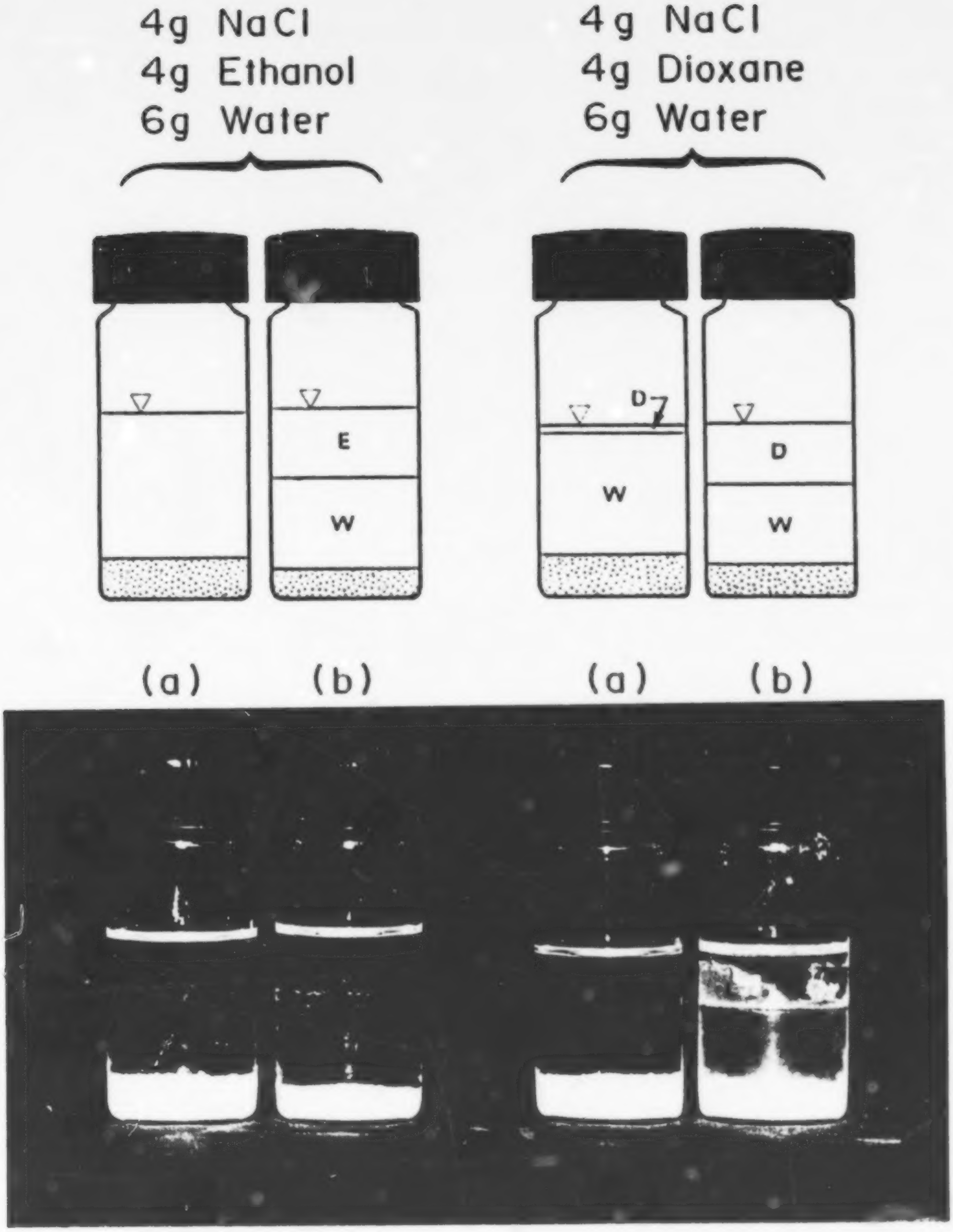
4g NaCl
4g Ethanol
6g Water
4g NaCl
4g Dioxane
6g Water
E
W
D
W
D
W
(a)
(b)
(a)
(b)

FIGURE 6.8 PHOTOGRAPHIC SUMMARY OF ION SOLVATION DEMONSTRATIONS

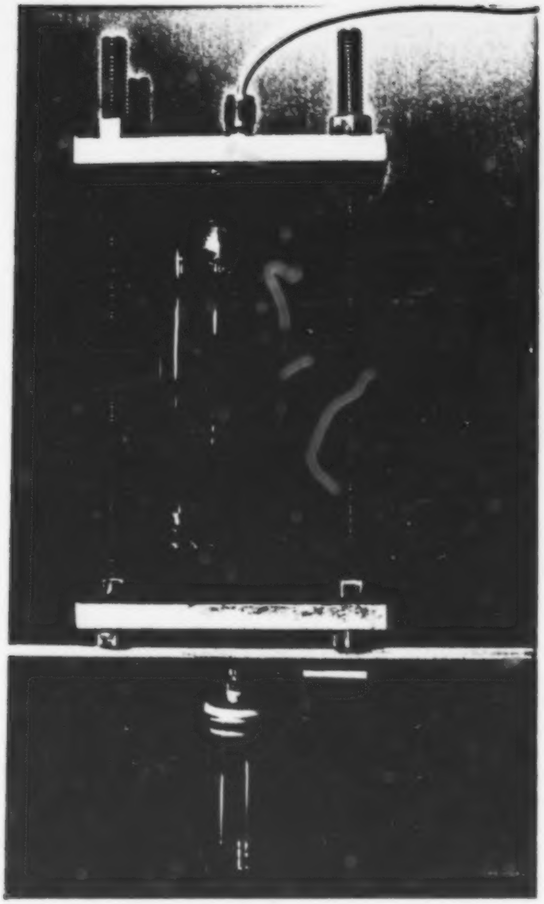

FIGURE 6.9 HYDRAULIC CONDUCTIVITY CELL

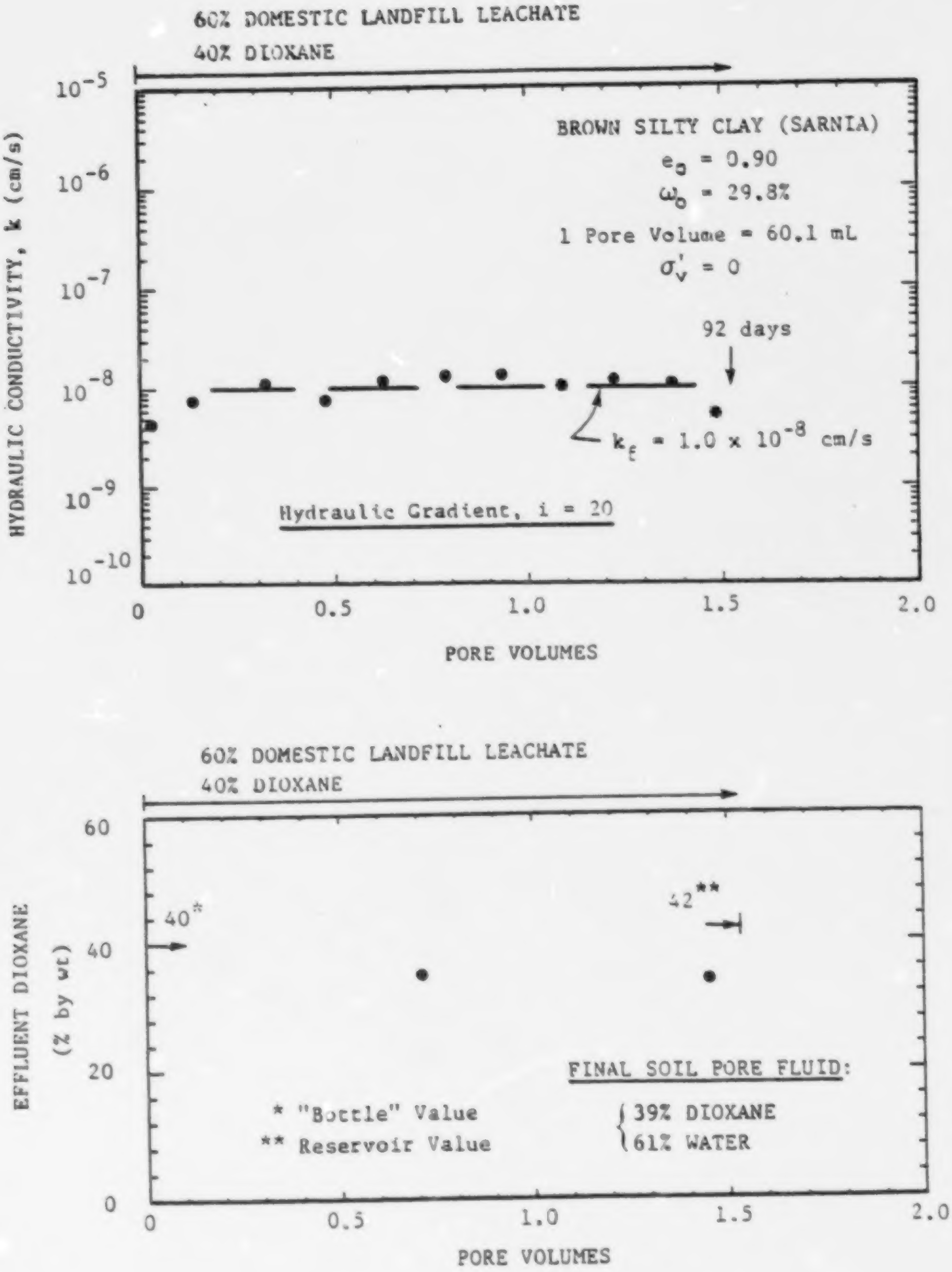

FIGURE 6.10 HYDRAULIC CONDUCTIVITY VS PORE VOLUME FOR WATER-COMPACTED BROWN SARNIA CLAY PERMEATED WITH 40% DIOXANE - 60% LEACHATE

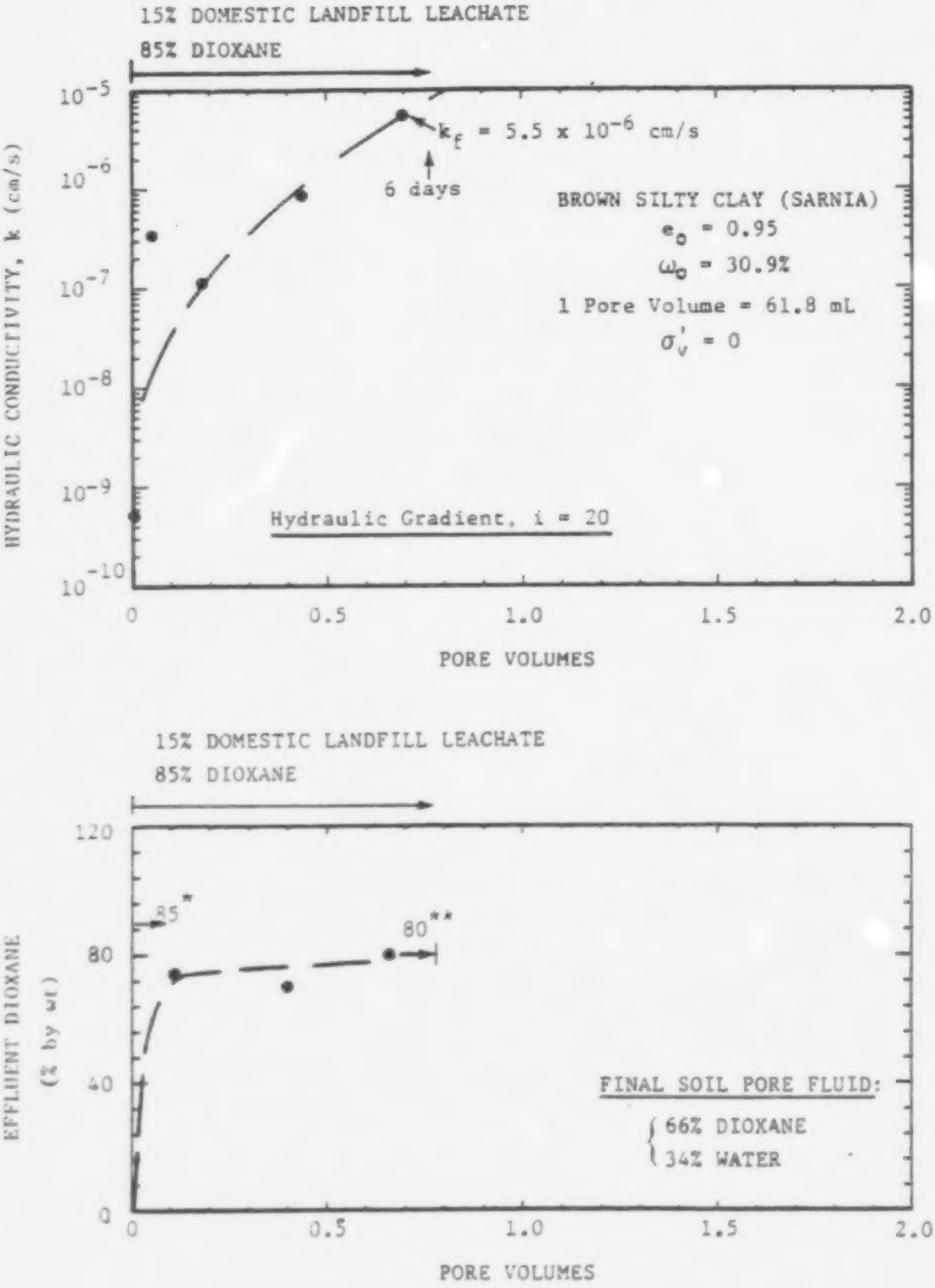

FIGURE 6.11 HYDRAULIC CONDUCTIVITY VS PORE VOLUME FOR WATER-COMPACTED BROWN SARNIA CLAY PERMEATED WITH 85% DIOXANE - 15% LEACHATE

(a) PERMEANT: 40% DIOXANE - 60% LEACHATE

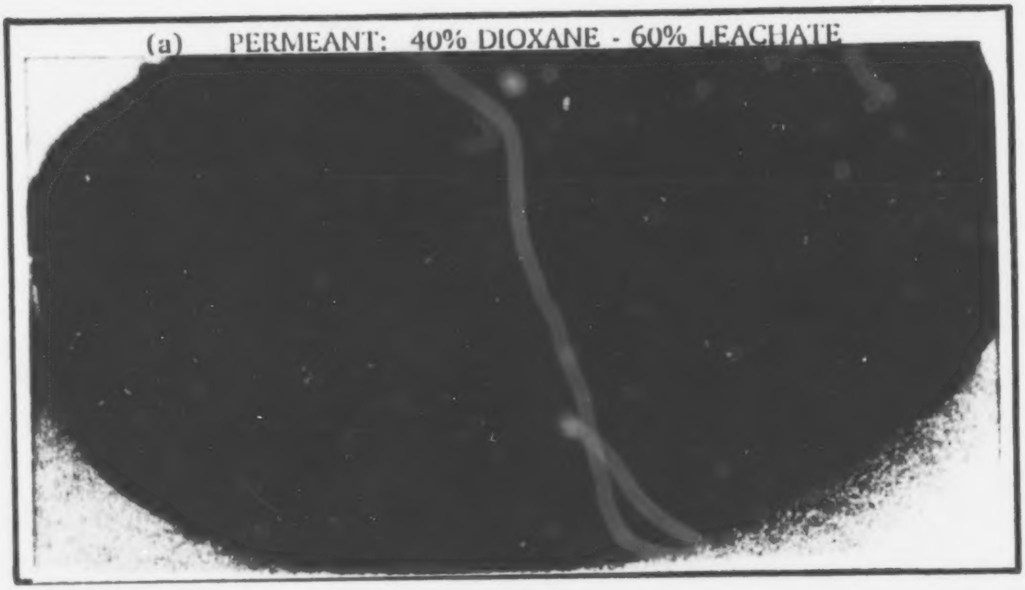

(b) PERMEANT: 85% DIOXANE - 15% LEACHATE

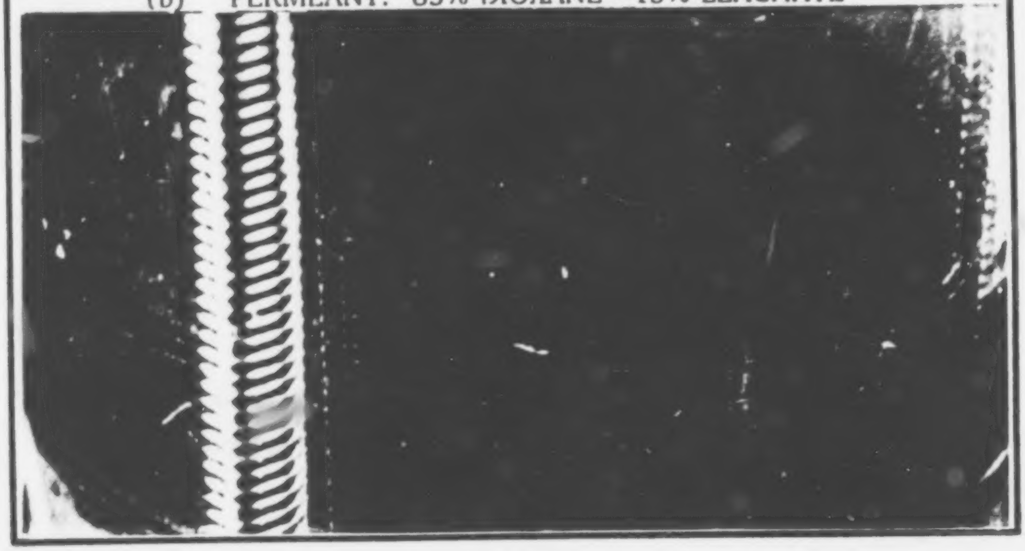

FIGURE 6.12 POST-TESTING APPEARANCE OF SOIL SAMPLES PERMEATED WITH LEACHATE CONTAINING: (a) 40% DIOXANE AND (b) 85% DIOXANE

CHAPTER 7

CONCLUSIONS

7.1 SUMMARY AND CONCLUSIONS

The effect of domestic waste leachate containing hydrocarbon liquids on the hydraulic conductivity of natural clays has been investigated. The test soils were obtained from the region of Sarnia, Ontario, and consisted of abundant illite, chlorite, quartz, feldspar, carbonate and a variable amount of smectite (up to 15%) formed by oxidation weathering of chlorite. The test permeants consisted of municipal landfill (domestic waste) leachate spiked with increasing amounts of ethanol or dioxane. This research study is based on controlled laboratory testing and has allowed good definition of some of the fundamental mechanisms of interaction between waste leachates and clayey soils to be defined. The following comments are made based on the laboratory study presented:

a) Testing equipment and material properties: The compatibility of clays with respect to waste leachates has been studied using hydraulic conductivity as the assessment tool. The fixed-ring permeameters used have been specially designed to maintain static vertical effective stresses of up to 320 kPa on the soil during testing. This condition is believed to represent the best simulation of the load of waste acting on a clay liner in a sanitary landfill facility. The permeameters are equipped to measure volume changes in the soil samples and to collect samples of the effluent permeant for chemical assessment. The hydraulic conductivity testing was performed under conditions of either constant head or constant flow rate. The computer controlled constant flow system is particularly suitable for prolonged testing involving toxic or volatile permeants because they are safely concealed in closed circuits.

The materials used in this project consist of natural clayey soils from southwestern Ontario and permeant liquids including water, domestic landfill leachate and hydrocarbon liquids. Selected properties of the soils and permeants used in this project were described in detail as they were found to bear significant effects on the test results. These properties include dielectric constant, viscosity and aqueous solubility of the permeants as well as soil composition and water content of compaction. Addition of soluble organic liquids to water (or leachate) has major effects on physico/chemical properties of the permeant: The dielectric constant decreases steadily with organic content, while the permeant viscosity increases to a maximum value (up to 3 times that of pure water) at intermediate organic contents and then decreases to values typical of the concentrated organic liquids.

b) Domestic waste leachate mixed with soluble hydrocarbons:

1) Water-soluble liquid hydrocarbons such as ethanol and dioxane mixed with leachate at concentrations below ~ 70% cause decreases in the hydraulic conductivity of water-compacted clays due to increases in permeant viscosity. These permeants cause little effects on the double layers around the clay particles, which retain their affinity for polar water and reject less polar organics.

2) At hydrocarbon contents greater than ~ 70% large increases in **k** occur as the organics enter and contract double layers, promoting the development of macropores. The increases in **k** are much greater for the brown, weathered, surface water-compacted clays than for the undisturbed, unweathered, grey clays.

3) Adequate static confining stresses may cause sufficient vertical consolidation and K_o effects to close chemically enlarged flow paths and thus prevent large increases in **k**. For ethanol, static stresses of only ~ 40 kPa are needed to eliminate the increases in **k**, whereas non-polar dioxane requires much higher stresses; small increases in **k** occur even at stresses of 160 kPa.

4) The exposure of water-compacted clays to concentrated dioxane at low stresses causes the clay structure to strengthen so that subsequent application of "corrective" stresses results in little consolidation and little

reduction in k. It is therefore beneficial that stresses be applied on the water-compacted barrier before contact with highly reactive liquid hydrocarbons.

5) Mixing dry clays with leachate/hydrocarbons mixtures prior to compaction results in flocculated soil structures and significantly higher values of permeability than water-compacted clays. It is therefore recommended that clay liners be compacted using water as the moulding fluid in order to optimize their performance.

REFERENCES

Acar, Y.B., Hamidon, A., Field, S.D., and Scott, L. 1985. The effect of organic fluids on hydraulic conductivity of kaolinite. In: Hydraulic Barriers in Soil and Rock, ASTM Special Technical Publication 874, 171-187.

Anderson,D.C., and Brown, K.W. 1981. Organic leachate effects on the permeability of clay liners. Proceedings of the 7th Annual Research Symposium, Ft. Mitchell, KY, EPA-600/9-81-002b, 119-130.

Anderson, D.C., Brown, K.W., and Green, J.W. 1982. Effect of organic fluids on the permeability of clay soil liners. In: Land Disposal of Hazardous Waste. Proceedings of the 8th Annual Research Symposium, Ft. Mitchell, KY, EPA-600/9-82-002, 179-190.

Anderson, D.C., Brown, K.W., and Thomas, J.C. 1985. Conductivity of compacted clay soils to water and organic liquids. Waste Management and Research, 3 (4), 339-349.

Barone, F.S., Yanful, E.K., Quigley, R.M. and Rowe, R.K. 1989. Effect of multiple contaminant migration on diffusion and adsorption of some domestic waste contaminants in a natural clayey soil. Canadian Geotechnical Journal, 26, in press.

Bjerrum L., and Huder, J. 1957. Proceedings of the fourth International Conference of Soil Mechanics and Foundation Engineering, London, 1, 6-10.

Bolt, G.H. 1955. Analysis of the validity of Gouy-Chapman theory of the electric double layer. Journal of Colloid Science, 10, 206-218.

Bowders, J.J., Daniel, D.E., Broderick, G.P., and Liljestrand, H.M. 1985. Methods for testing the compatibility of clay liners with landfill leachate. In: Hazardous and Industrial Solid Waste Testing: Fourth Symposium, ASTM Special Technical Publication 886, 233-250.

Brown, K.W., and Anderson, D.C. 1980. Effects of organic chemicals on clay liner permeability. Proceedings of the 6th Annual Research Symposium. Cincinnati, OH, EPA-600/9-80-010, 123-134.

Brown, K.W., Green, J.W., and Thomas, J.C. 1983. The influence of selected organic liquids on the permeability of clay liners. In: Land Disposal of Hazardous Waste. Proceedings of the 9th Annual Research Symposium, Ft. Mitchell, KY, EPA-600/9-83-018, 114-125.

Brown, K.W., and Anderson, D.C. 1983. Effects of organic solvents on permeability of clay soils. EPA-600/2-83-016. U.S. Environmental Protection Agency, Cincinnati, OH, 153 pp.

Brown, K.W., Thomas, J.C., and Green, J.W. 1984. Permeability of compacted soils to solvent mixtures and petroleum products. In: Land Disposal of Hazardous Waste. Proceedings of the 10th Annual Research Symposium, Ft. Washington, PA, EPA-600/9-84-007, 124-137.

Brunelle, T.M., Dell, L.R., and Meyer, C.J. 1987. Effect of permeameter and leachate on a clay liner. In: Geotechnical Practice for Waste Disposal'87. ASCE, Geotechnical Special Publication 13, 347-361.

Cartwright, K, Griffin, R.A., and Gilkeson, R.H. 1977. Migration of landfill leachate through glacial tills. Groundwater, 15 (4), 294-305.

Chabbra, R. 1975. The measurement of cation exchange capacity and exchangeable cations in soils: a new method. Proceedings of the International Clay Conference, 439-449.

Chian, E.S.K. 1977. Stability of organic matter in landfill leachates. Water Research, 11, 225-232.

Chian, E.S.K., and De Walle, F.B. 1976. Sanitary landfill leachates and their treatment, Journal of the Environmental Engineering Division, ASCE, 102, 411-431.

Crooks, V.E. 1981. Leachate migration through clay by combined dispersive and convective transport. M.E.Sc. Thesis, The University of Western Ontario, London, Ontario, 216 pp.

Daniel, D.E., and Liljestrand, M. 1984. Effects of landfill leachates on natural liner systems. Report to Chemical Manufacturers Association, January 1984, 85 pp.

Daniel, D.E., Anderson, D.C., and Boynton, S.S. 1985. Fixed-wall versus flexible-wall permeameters. In: Hydraulic Barriers in Soil and Rock, ASTM Special Technical Publication 874, 107-126.

Darcy, H. (1956). Les fontaines publiques de la ville de Dijon. Dalmont, Paris.

Di Nardo, L.R. 1977. Soil-cement and soil-lime stabilization of weathered surface clays in southwestern Ontario. M.E.Sc. Thesis, The University of Western Ontario, London, Ontario, 143 pp.

Dunn, R.J. 1983. Hydraulic conductivity of soils in relation to the subsurface movement of hazardous wastes. Ph.D. Thesis, The University of California, Berkeley, CA, 338 pp.

Fernandez, F. 1984. The effect of organic hydrocarbon liquids on the hydraulic conductivity of natural soils. M.E.Sc. Thesis, The University of Western Ontario, London, Ontario, 166 pp.

Fernandez, F., and Quigley, R.M. 1985. Hydraulic conductivity of natural clays permeated with simple liquid hydrocarbons. Canadian Geotechnical Journal, 22 (2), 205-214.

Fernandez, F. and Quigley, R.M. 1986. The influence of gradient, lyophobicity and void ratio on the hydraulic conductivity of a clayey soil permeated with water and cyclohexane. Proceedings 5th International Congress, International Association of Engineering Geology, Buenos Aires, Argentina, III, 965-970.

Fernandez, F., and Quigley, R.M. 1987. Effect of viscosity on the hydraulic conductivity of clayey soils permeated with water-soluble organics. Proceedings 40th Canadian Geotechnical Conference, Regina, Saskatchewan, 313-319 pp.

Fernandez, F., and Quigley, R.M. 1988. Viscosity and dielectric constant controls on the hydraulic conductivity of clayey soils permeated with water-soluble organics. Canadian Geotechnical Journal, 25 (3), 582-589.

Fernandez, F., and Quigley, R.M. 1988. Effects of increasing amounts of non-polar organic liquids in domestic waste leachate on the hydraulic conductivity of clay liners in southwestern Ontario. Proceedings Technology Transfer Conference No. 9, Ontario Ministry of the Environment, Part 3, Liquid and Solid Waste Research, paper C3, 55-79.

Fernandez, F., and Quigley, R.M. 1989. Organic liquids and the hydraulic conductivity of barrier clays. Proceedings 12th International Conference on Soil Mechanics and Foundation Engineering, Rio de Janeiro, Brazil, In press.

Flick, E.W. 1985. Industrial solvent handbook. Noyes Data Corporation, Park Ridge, NJ, 648 pp.

Foreman, D.E., and Daniel, D.E. 1986. Permeation of compacted clay with organic chemicals. Journal of Geotechnical Engineering, ASCE, 112 (7), 669-681.

Freeze, R.A., and Cherry, J.A. 1979. Groundwater. Prentice-Hall, Englewood Cliffs, NJ., 604 pp.

Goodall, D.C. 1975. Pollutant migration from sanitary landfill sites, Sarnia, Ontario. M.E.Sc. Thesis, The University of Western Ontario, London, Ontario, 135 pp.

Green, W.J., Lee, G.F., and Jones, R.A. 1981. Clay-soils permeability and hazardous waste storage. Journal of Water Pollution Control Federation, 53 (8), 1347-1354.

Griffin, R.A., Cartwright, K., Shimp, N.F., Steel, J.D., Ruch, R.R., White, W.A., Hughes, G.M., and Gilkeson, R.H. 1976. Attenuation of pollutants in municipal landfill leachate by clay minerals: Part 1 - Column leaching and field verification. Illinois State Geological Survey. Environmental Geology Notes, 78, 34 pp.

Grim, R.E. 1953. Clay mineralogy. McGraw-Hill, New York, 384 pp.

Janz, G.J. 1972. Non aqueous electrolytes handbook. Academic Press, New York, NY.

Kohn, D.L., and Pinyan, C. 1987. EPA may change trash plant rules. ENR News, February 12, p. 10.

Lambe, T.W., and Whitman, R.V. 1979. Soil mechanics. John Wiley & Sons, New York, 553 pp.

Lambe, T.W. 1954. The permeability of fine grained soils. ASTM Special Technical Publication 163, 56-67.

Lambe, T.W. 1956. The storage of oil in and earth reservoir. Journal of the Boston Society of Civil Engineers, 43, 179-241.

Marcus, Y. 1985. Ion Solvation. John Wiley & Sons, 306 pp.

Mesri, G., and Olson, R.E. 1971. Mechanisms controlling the permeability of clays. Clays and Clay Minerals, 19 (3), 151-158.

Michaels, A.S., and Lin, C.S. 1954. Permeability of kaolinite. Industrial and Engineering Chemistry, 46 (6), 1239-1246.

Mitchell, J.K. 1976. Fundamentals of soil behaviour. John Wiley & Sons, New York, 422 pp.

Mitchell, J.K., Hooper, D.R., and Campanella, R.G. 1965. Permeability of compacted clay. Journal of Geotechnical Engineering, ASCE, 91 (SM4), 41-65.

Mitchell, J.K., and Madsen, F.T., 1987. Chemical effects on clay hydraulic conductivity. In: Geotechnical Practice for Waste Disposal'87. ASCE, Geotechnical Special Publication 13, 87-116.

Montague, P. 1982. Hazardous waste landfills: some lessons from New Jersey. Civil Engineering, September 1982, 53-56.

Ogunbadejo, T.A. 1973. Physico-chemistry of weathered clay crust formation. Ph.D. Thesis, The University of Western Ontario, London, Ontario, 258 pp.

Olsen, H.W. 1965. Deviations from Darcy's law in saturated clays. Soil Science Society of America Proceedings, 29, 135-140.

Olsen, H.W. 1966. Darcy's law in saturated Kaolinite. Water Resources Research, 2 (2), 287-295.

Olsen, H.W. 1972. Liquid movement through Kaolinite under hydraulic, electric and osmotic gradients. American Association of Petroleum Geologists Bulletin, 56 (10), 2022-2028.

Olson, R.E., and Daniel, D.E. 1981. Measurement of the hydraulic conductivity of fine-grained soils. In: Permeability and Groundwater Transport, ASTM Special Technical Publication 746, 18-64.

Proctor and Redfern Limited 1982. Waste quantity studies. Report to the Ontario Waste Management Corporation, August 1982.

Quigley, R.M., Crooks, V.E., and Fernandez, F. 1984. Engineered clay liners (an overview report). Proceedings of a Working Seminar on Design and Construction of Municipal and Industrial Waste Disposal Facilities. Canadian Geotechnical Society and Consulting Engineers of Ontario. Toronto, 115-134.

Quigley, R.M., and Fernandez, F. 1986. Hydraulic conductivity of Keele Valley barrier clays permeated with domestic waste leachate. Final report to Golder Associates, Mississauga, Ontario.

Quigley, R.M., and Fernandez, F. 1985. Effects of increasing amounts of non-polar organic liquids in domestic waste leachate on the hydraulic conductivity of clay liners in southwestern Ontario. Proceedings Technology Transfer Conference No. 6, Ontario Ministry of the Environment, Part 3, Liquid and Solid Waste Research, paper 46, 244-264.

Quigley, R.M., and Fernandez, F. 1987. Effects of increasing amounts of non-polar organic liquids in domestic waste leachate on the hydraulic conductivity of clay liners in southwestern Ontario. Proceedings Technology Transfer Conference No. 8, Ontario Ministry of the Environment, Part 3, Liquid and Solid Waste Research, paper C13, 1-26.

Quigley, R.M., and Fernandez, F. 1989. Clay/organic interactions and their effect on the hydraulic conductivity of barrier clays. Proceedings International Symposium on Contaminant Transport in Groundwater. Stuttgart, Germany, In press.

Quigley, R.M., Fernandez, F., and Rowe, R.K. 1988. Clayey barrier assessment for impoundment of domestic waste leachate (southern Ontario) including clay/leachate compatibility by hydraulic conductivity testing. Canadian Geotechnical Journal, 25 (3), 574-581.

Quigley, R.M., Fernandez, F., and Yanful, E., 1986. Effects of increasing amounts of non-polar organic liquids in domestic waste leachate on the hydraulic conductivity of clay liners in southwestern Ontario. Proceedings Technology Transfer Conference No. 7, Ontario Ministry of the Environment, Part 3, Liquid and Solid Waste Research, paper 67, 1-26.

Quigley, R.M.; Fernandez, F., Yanful, E., Helgason, Th., Margaritis, A., and Whitby, J.L. 1987. Hydraulic conductivity of contaminated natural clay directly below the Confederation Road domestic waste landfill, Sarnia, Ontario. Canadian Geotechnical Journal, 24 (3), 355-383.

Quigley, R.M., Yanful, E., and Fernandez, F. 1987. Ion transfer by diffusion through clayey barriers. In: Geotechnical Practice for Waste Disposal '87. ASCE, Geotechnical Special Publication 13, 137-158.

Quigley, R.M., and Ogunbadejo, T.A. 1976. Till geology, mineralogy and geotechnical behaviour, Sarnia, Ontario. In: Glacial Till, An Inter-disciplinary Study. Ed R.F. Legget, Royal Society of Canada, Special Publication 12, 316-345.

Research Triangle Institute 1986. Design, construction and evaluation of clay liners for waste management facilities; Draft technical resource document for public comment. Prepared for the U.S. Environmental Protection Agency, Washington, DC, National Technical Information Service, U.S. Department of Commerce, Springfield, VA, PB86-184496.

Sibul, U. 1988. Liquid and solid waste research. Proceedings Technology Transfer Conference No. 9, Ontario Ministry of the Environment, Part 3, Liquid and Solid Waste Research, p. 11.

Sitting, M. 1981. Handbook of tosic and hazardous chemicals. Noyes Data Corporation, Park Ridge, NJ, 729 pp.

Taylor, D.W. 1948. Fundamentals of soil mechanics. John Wiley & Sons, New York, 700 pp.

Uppot, J.O., and Stephenson, R.W. 1989. Permeability of clays under organic permeants. Journal of Geotechnical Engineering, ASCE, 115 (1), 115-131.

van Olphen, H. 1963. An introduction to clay colloid chemistry. Wiley Interscience, New York, 302 pp.

Yanful, E.K. 1986. Heavy metal migration through clay below a domestic waste site. Ph.D. Thesis, The University of Western Ontario, London, Ontario, 357 pp.

Yanful, E., Fernandez, F., and Quigley, R.M. 1987. The chemical instability of domestic waste leachate and its geotechnical implications. Geotechnical Research Centre, The University of Western Ontario, London Ontario, Research report GEOT-15-87.

Weast, R.C. 1984. CRC handbook of chemistry and physics, 65th Ed., CRC Press, Boca Raton, Florida.

Weissberger, A., and Proskauer, E. 1935. Organic solvents: physical constants and methods of purification. Oxford University Press, London.

Volume

2

ENVIRONMENTAL RESEARCH

RESEARCH AND TECHNOLOGY BRANCH

Environment
Ontario
Jim Bradley, Minister

ISBN 0-7729-6205-7 (2 vol. set)
0-7729-6207-3 (vol. 2)

EFFECTS OF INCREASING AMOUNTS OF NON-POLAR ORGANIC LIQUIDS IN DOMESTIC WASTE LEACHATE ON THE HYDRAULIC CONDUCTIVITY OF CLAY LINERS IN SOUTHERN ONTARIO

R. A. C. PROJECT NO. 213 PL/364 G

VOLUME 2

Report prepared for Environment Ontario by:

Robert M. Quigley
and
Federico Fernandez

Faculty of Engineering Science
University of Western Ontario
London, Ontario N6A 5B9

PRINTED: OCTOBER 1989
REPRINTED: DECEMBER 1989

RECYCLABLE

Copyright: Queen's Printer for Ontario, 1989
This publication may be reproduced for non-commercial purposes with appropriate attribution.

DISCLAIMER

This report has been reviewed by the Research Advisory Committee of Environment Ontario and approved for publication. Approval does not necessarily signify that the contents reflect the views nor does mention of trade names or commercial products constitute endorsement or recommendation for use.

TABLE OF CONTENTS

Page

VOLUME 1:

FORWARD ii

EXECUTIVE SUMMARY iv

TABLE OF CONTENTS viii

CHAPTER 1 - INTRODUCTION 1

1.1 General 1
1.2 Options for Waste Management 2
1.3 Sanitary Landfills 3
1.4 Scope of the Project 5

CHAPTER 2 - HYDRAULIC CONDUCTIVITY OF CLAY BARRIERS: A REVIEW 9

2.1 General 9
2.2 Hydraulic Conductivity of Clays 10
2.2.1 Clay Minerals 10
2.2.2 Diffuse Double Layers 11
2.2.3 Soil Fabric and Hydraulic Conductivity 16
2.2.4 Hydraulic Conductivity of Compacted Clays 18
2.2.5 Laboratory Testing for Hydraulic Conductivity 21
2.2.6 The Influence of Testing Conditions on k 22
2.3 The Effect of Waste Leachates on k 24
2.3.1 Domestic Waste Leachate 27
2.3.2 Concentrated Organic Solvents 28
2.3.3 Aqueous Solutions of Organic Solvents 32
2.4 Concluding Remarks 33

CHAPTER 3 - HYDRAULIC CONDUCTIVITY TESTING EQUIPMENT .. 46

3.1 Introduction 46
3.2 Fixed-ring Permeameter 47
3.2.1 Cell Description 47
3.2.2 Soil Preparation 48
3.3 Constant Flow Hydraulic Conductivity Equipment 50
3.4 Constant Head Hydraulic Conductivity Equipment 53
3.5 Chemical Analyses of Influent and Effluent Samples 54
3.6 Post-testing Assessment 54
3.7 Concluding Remarks 55

Page

CHAPTER 4 - TESTING MATERIALS 68

4.1 Introduction 68
4.2 Soil Properties 68
4.3 Properties of the Permeants 72
4.3.1 Domestic Landfill Leachate 73
4.3.2 Aqueous Solutions of Hydrocarbons 74
4.3.3 Physico-chemical Stability of Leachate/Hydrocarbon Mixtures 76

CHAPTER 5 - PERMEATION OF CLAYS WITH DOMESTIC LEACHATE CONTAINING HYDROCARBON LIQUIDS 98

5.1 Introduction 98
5.2 Permeant Compacted Clays 99
5.2.1 Ethanol/Water/Clay Mixtures 100
5.2.2 Dioxane/Water/Clay Mixtures 101
5.2.3 Leachate/Hydrocarbon/Clay Mixtures 102
5.2.4 Discussion of the Data 102
5.3 Water-saturated Clays 105
5.3.1 Leachate/Ethanol Mixtures on Compacted Brown Clay 106
5.3.2 Leachate/Dioxane Mixtures on Compacted Brown Clay 108
5.3.3 The Importance of Effective Stress Levels 110
5.3.4 Leachate/Ethanol Mixtures on Undisturbed Grey Clay 115
5.4 Post-testing Sample Assessment 116

CHAPTER 6 - DISCUSSION AND INTERPRETATION OF RESULTS 145

6.1 Introduction 145
6.2 The Role of Permeant Viscosity 145
6.3 Exclusion of Non-polar Organics from Double Layers 147
6.4 Confirmation Tests Using Larger Cells and Lower Gradients 151

CHAPTER 7 - CONCLUSIONS 168

7.1 Summary and Conclusions 168

REFERENCES 172

* * * * * *

Page

VOLUME 2:

APPENDIX A - EVAPORATION CURVES FOR VARIOUS LIQUIDS 179

APPENDIX B - INTERCONVERSION FORMULAS FOR COMPOSITION OF LIQUID SOLUTIONS 183

APPENDIX C - MEASUREMENT OF DIELECTRIC CONSTANT OF LIQUID PERMEANTS 190

APPENDIX D - HYDRAULIC CONDUCTIVITY CURVES FOR PERMEANT/CLAY MIXTURES 194

APPENDIX E - HYDRAULIC CONDUCTIVITY CURVES FOR WATER-COMPACTED BROWN SARNIA CLAY PERMEATED WITH LEACHATE/ETHANOL MIXTURES 227

APPENDIX F - HYDRAULIC CONDUCTIVITY CURVES FOR WATER-COMPACTED BROWN SARNIA CLAY PERMEATED WITH LEACHATE/DIOXANE MIXTURES 253

APPENDIX G - HYDRAULIC CONDUCTIVITY CURVES FOR UNDISTURBED GREY SARNIA CLAY PERMEATED WITH LEACHATE/ETHANOL MIXTURES 271

APPENDIX H - EFFLUENT CONCENTRATION CURVES FOR INORGANIC SPECIES WATER-COMPACTED BROWN SARNIA CLAY PERMEATED WITH LEACHATE/ETHANOL MIXTURES 277

APPENDIX I - EFFLUENT CONCENTRATION CURVES FOR INORGANIC SPECIES WATER-COMPACTED BROWN SARNIA CLAY PERMEATED WITH LEACHATE/DIOXANE MIXTURES 285

APPENDIX J - PORE SIZE DISTRIBUTION CURVES OBTAINED BY MERCURY INTRUSION POROSIMETRY 297

APPENDIX A

EVAPORATION CURVES FOR VARIOUS LIQUIDS

The following evaporation curves were obtained by weighting the effluent collection bottles containing 3 grams of various permeants at different time intervals.

The curves shown in Figure A.1 correspond to open bottles and illustrate the high volatility of the organic liquids relative to water. Figure A.2 shows evaporation curves for cyclohexane (the most volatile liquid tested) in the effluent bottles under different venting conditions. The teflon tube tips were adopted for the design of the effluent collection bottles used in the hydraulic conductivity testing for this project.

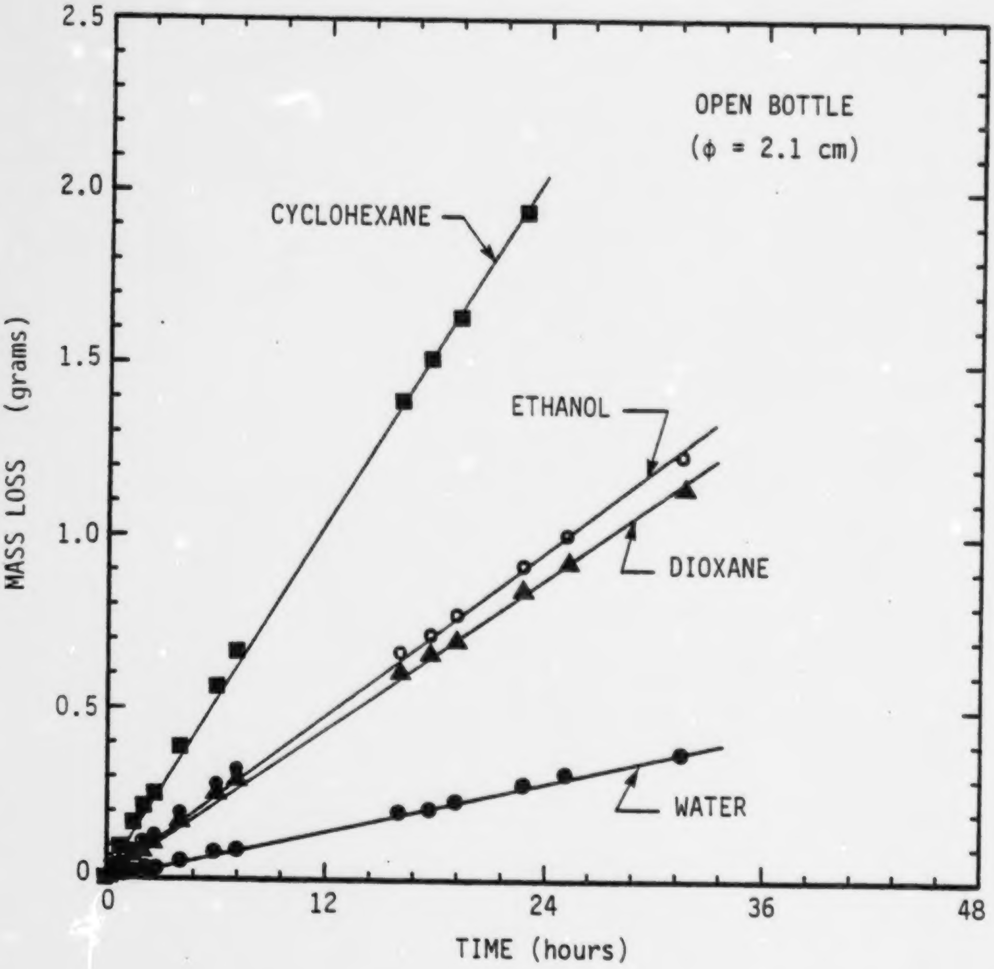

FIGURE A.1 EVAPORATION CURVES FOR VARIOUS LIQUIDS IN OPEN EFFLUENT COLLECTION BOTTLES

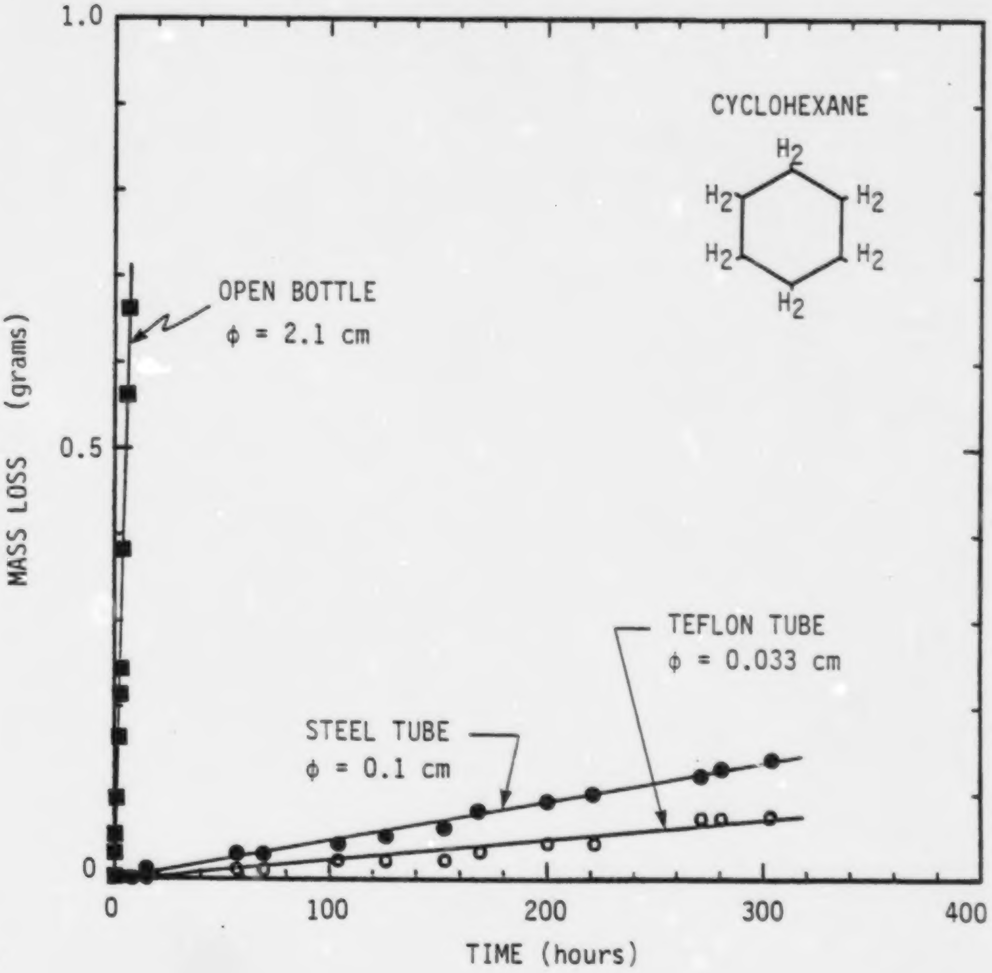

FIGURE A.2 EVAPORATION CURVES FOR CONCENTRATED CYCLOHEXANE IN EFFLUENT COLLECTION BOTTLES WITH DIFFERENT VENTING APERTURES, φ

APPENDIX B

INTERCONVERSION FORMULAS FOR COMPOSITION OF LIQUID SOLUTIONS

In a system where n_A moles of solvent A are mixed with n_B moles of solvent B the composition of the mixture can be expressed as follows:

χ_A = mole fraction of component A:

$$n_A = \frac{n_A}{n_A + n_B} \qquad ; \quad \chi_B = 1 - \chi_A$$

$\hat{w}_A$ = mass fraction (weight fraction) of component A:

$$\hat{w}_A = \frac{m_A}{m_A + m_B} = \frac{n_A}{(n_A + n_B \times M_B/M_A)} \qquad ; \quad \hat{w}_B = 1 - \hat{w}_A$$

ϕ_A = volume fraction of component A:

$$\phi_A = \frac{v_A}{v_A + v_B} = \frac{n_A}{(n_A + n_B \times V_B/V_A)} \qquad ; \quad \phi_B = 1 - \phi_A$$

where: $m_{A,B}$ = mass of n_A moles of component A,B

$M_{A,B}$ = mass of 1 mole (molar mass) of component A,B

$v_{A,B}$ = volume of $n_{A,B}$ moles of component A,B

$V_{A,B}$ = volume of 1 mole (molar volume) of component A,B

NOTE:

$$\boxed{\begin{array}{l} \hat{w} \times 100 = \text{Mass \%} = \text{\% by wt} \\ \phi \times 100 = \text{Volume \%} = \text{\% by vol} \\ \chi \times 100 = \text{Mole \%} \end{array}}$$

Neglecting the volume change on mixing the following interconversion formulas are derived:

a) Mass fraction to volume fraction: $\phi_A = \dfrac{v_A}{v_A + v_B} =$

$$= \frac{m_A/\rho_A}{m_A/\rho_A + m_B/\rho_B} = \frac{m_A}{m_A + m_B(\rho_A/\rho_B)} = \frac{\dfrac{m_A}{m_A + m_B}}{\dfrac{m_A}{m_A + m_B} + (1 - \dfrac{m_A}{m_A + m_B})\rho_A/\rho_B}$$

$$\boxed{\phi_A = \frac{\hat{w}_A}{\hat{w}_A + (1 - \hat{w}_A)\rho_A/\rho_B}}$$

b) Mass fraction to mole fraction: $\chi_A = \dfrac{n_A}{n_A + n_B} =$

$$= \frac{m_A/M_A}{m_A/M_A + m_B/M_B} = \frac{m_A}{m_A + m_B(M_A/M_B)} = \frac{\dfrac{m_A}{m_A + m_B}}{\dfrac{m_A}{m_A + m_B} + \left(1 - \dfrac{m_A}{m_A + m_B}\right)M_A/M_B}$$

$$\boxed{\chi_A = \frac{\hat{w}_A}{\hat{w}_A + (1 - \hat{w}_A)M_A/M_B}}$$

c) Volume fraction to mass fraction: $\hat{w}_A = \dfrac{m_A}{m_A + m_B} =$

$$= \frac{v_A\ \rho_A}{v_A\ \rho_A + v_B\ \rho_B} = \frac{v_A}{v_A + v_B(\rho_B/\rho_A)} = \frac{\dfrac{v_A}{v_A + v_B}}{\dfrac{v_A}{v_A + v_B} + \left(1 - \dfrac{v_A}{v_A + v_B}\right)\rho_B/\rho_A}$$

$$\boxed{\hat{w}_A = \frac{\phi_A}{\phi_A + (1 - \phi_A)\rho_B/\rho_A}}$$

d) Volume fraction to mole fraction: $\chi_A = \dfrac{n_A}{n_A + n_B} =$

$$= \frac{v_A/V_A}{v_A/V_A + v_B/V_B} = \frac{v_A}{v_A + v_B(V_A/V_B)} = \frac{\dfrac{v_A}{v_A + v_B}}{\dfrac{v_A}{v_A + v_B} + \left(1 - \dfrac{v_A}{v_A + v_B}\right)V_A/V_B}$$

$$\boxed{\chi_A = \frac{\phi_A}{\phi_A + (1 - \phi_A)V_A/V_B}}$$

e) Mole fraction to mass fraction: $\hat{w}_A = \dfrac{m_A}{m_A + m_B} =$

$$= \frac{n_A\, M_A}{n_A\, M_A + n_B\, M_B} = \frac{n_A}{n_A + n_B(M_B/M_A)} = \frac{\dfrac{n_A}{n_A + n_B}}{\dfrac{n_A}{n_A + n_B} + \left(1 - \dfrac{n_A}{n_A + n_B}\right)M_B/M_A}$$

$$\boxed{\hat{w}_A = \frac{\chi_A}{\chi_A + (1 - \chi_A)M_B/M_A}}$$

f) Mole fraction to volume fraction: $\phi_A = \dfrac{v_A}{v_A + v_B} =$

$$= \frac{n_A\, V_A}{n_A\, V_A + n_B\, V_B} = \frac{n_A}{n_A + n_B(V_B/V_A)} = \frac{\dfrac{n_A}{n_A + n_B}}{\dfrac{n_A}{n_A + n_B} + \left(1 - \dfrac{n_A}{n_A + n_B}\right)V_B/V_A}$$

$$\boxed{\phi_A = \frac{\chi_A}{\chi_A + (1 - \chi_A)V_B/V_A}}$$

where $\rho_{A,B}$ is the density of component A,B

The values of molar mass, molar volume and density of pure water, methanol, ethanol, acetone and dioxane are listed in Table B.1 as they are required to apply the conversion formulas for a particular water/hydrocarbon mixture. For example the formula to convert mass fractions to mole fractions for a water/dioxane mixture becomes:

$$\chi_{DIOX} = \frac{\hat{w}_{DIOX}}{\hat{w}_{DIOX} + (1 - \hat{w}_{DIOX})(88.06/18.02)} = \frac{\hat{w}_{DIOX}}{4.887 - 3.887\, \hat{w}_{DIOX}}$$

TABLE B.1 MOLAR MASS, MOLAR VOLUME AND DENSITY OF LIQUIDS AT 20°C

LIQUID	MOLAR MASS (g)	MOLAR VOLUME (cm^3)	DENSITY (g/cm^3)
WATER	18.02	18.05	0.99820
METHANOL	32.03	40.48	0.79133
ETHANOL	46.05	58.34	0.78934
ACETONE	58.05	73.50	0.7898
DIOXANE	88.06	85.23	1.03326

APPENDIX C

MEASUREMENT OF DIELECTRIC CONSTANT OF LIQUID PERMEANTS

The dielectric constant, ϵ, of permeant liquids was calculated from the capacitance of a the capacitor shown at the right of Figure 4.8, filled with permeant. Capacitance measurements were done using a Wayne-Kerr Autobalance Precision Bridge, model B331, at a frequency of ~ 1.6 kH. The voltages ranging from 1.2 V for water to 36 V for air.

For a given permeant the capacitance, C, equals:

$$1) \qquad C = \frac{\epsilon_o \ \epsilon \ A}{d}$$

where, ϵ_o = Permittivity of free space = 8.8542 picofarad per metre (pF/m)

A = Cross sectional area of the capacitor plates (m^2)

d = separation between capacitor plates (m)

For air ϵ = 1:

$$2) \qquad C_{air} = \frac{\epsilon_o \ 1 \ A}{d}$$

From 1) and 2):

$$C - C_{air} = \frac{\epsilon_o \ A}{d} (\epsilon - 1)$$

Therefore:

$$\boxed{\epsilon = \frac{d}{\epsilon_o \; A} (C - C_{air}) + 1}$$

This formula was used to calculate the dielectric constants of permeants from the capacitance values shown in Table C.1.

TABLE C.1 CAPACITANCE AND DIELECTRIC CONSTANTS OF PERMEANTS

MATERIAL	CAPACITANCE (pF)	DIELECTRIC CONSTANT
PURE COMPOUNDS		
Air	1.33	1.00
Water	37.4	83.6
Ethanol	14.9	32.1
Methanol	17.3	37.5
Dioxane	1.87	2.26
Cyclohexane	1.78	2.03
WATER MIXTURES		
10% Ethanol	35.4	78.9
20% Ethanol	33.1	73.8
35% Ethanol	29.4	65.3
50% Ethanol	25.4	56.1
65% Ethanol	21.7	47.7
80% Ethanol	18.6	40.5
90% Ethanol	16.7	36.2
10% Dioxane	30.9	68.8
20% Dioxane	27.3	60.5
35% Dioxane	21.5	47.1
50% Dioxane	15.5	33.5
65% Dioxane	9.85	20.5
80% Dioxane	4.84	9.06
90% Dioxane	3.51	6.02

APPENDIX D

HYDRAULIC CONDUCTIVITY CURVES FOR PERMEANT/CLAY MIXTURES

The hydraulic conductivity curves presented in this appendix correspond to dry clay samples mixed with the indicated test permeants. These permeants include water/ethanol, leachate/ethanol, water/dioxane and leachate/dioxane mixtures. The test soils are brown Sarnia clay, commercial (Black Hills) bentonite, and kaolinite.

The test results are discussed in Section 5.2 of this report.

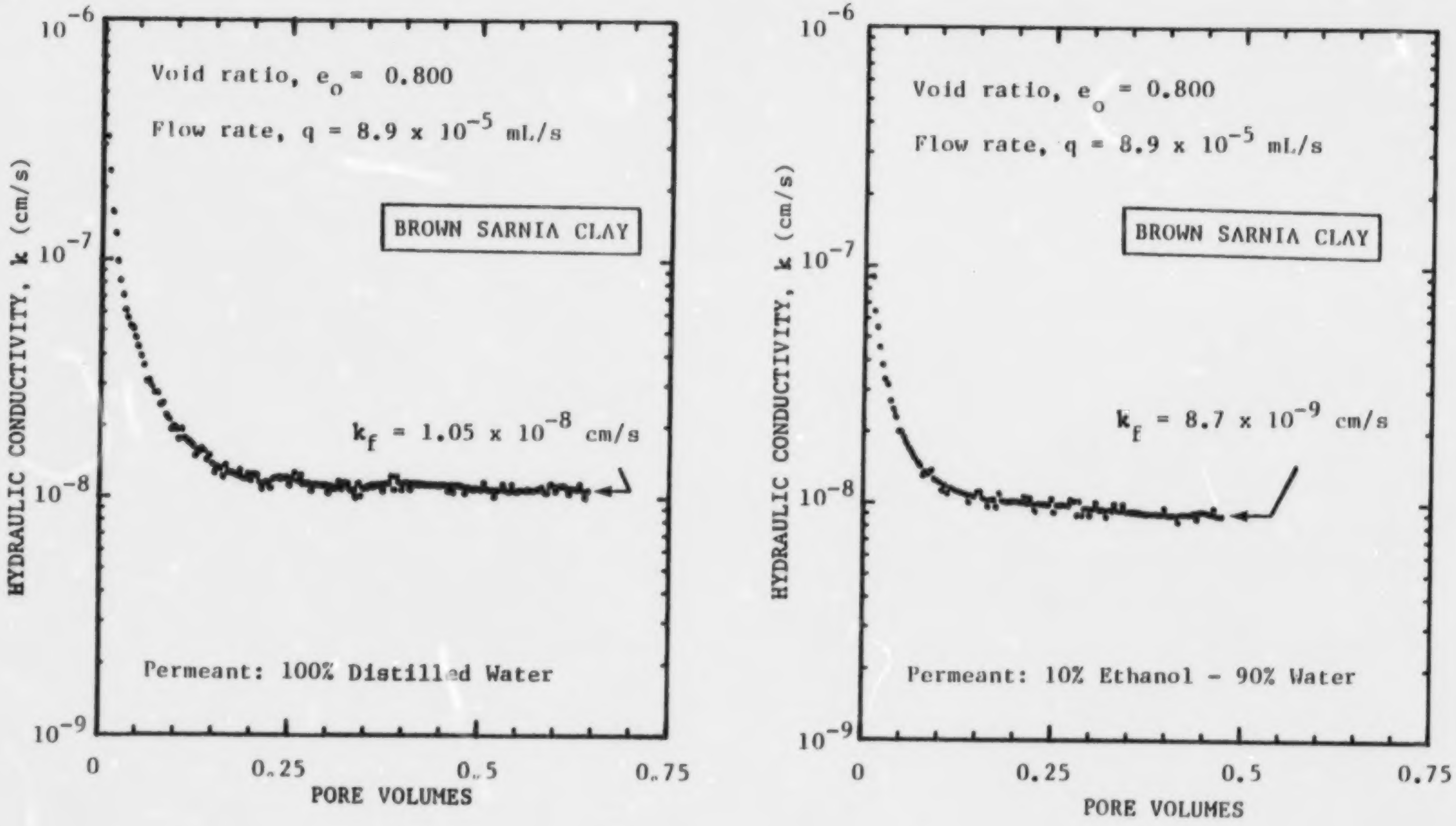

FIGURE D.1 HYDRAULIC CONDUCTIVITY VS PORE VOLUMES FOR CLAY/PERMEANT MIXTURES

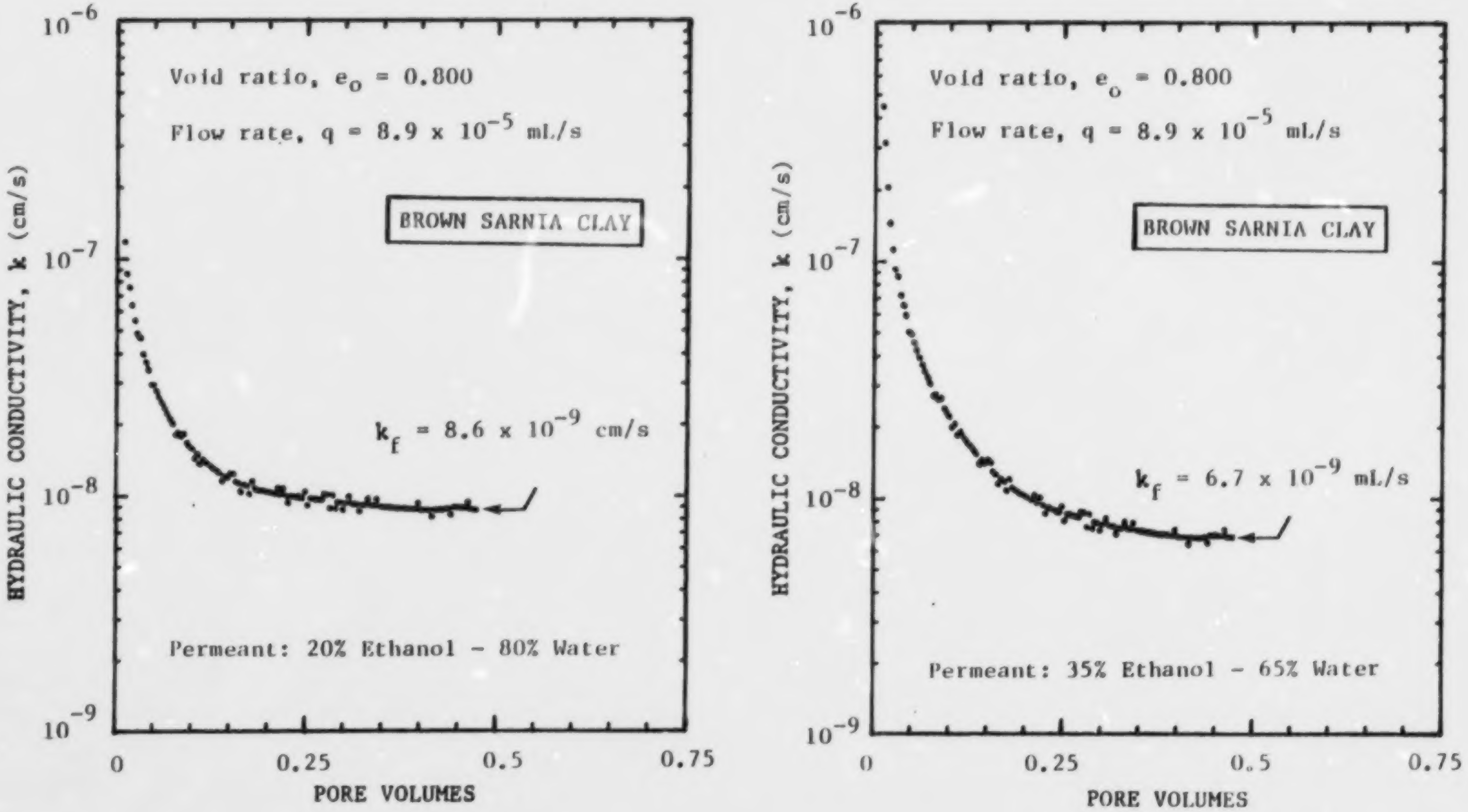

FIGURE D.2 HYDRAULIC CONDUCTIVITY VS PORE VOLUMES FOR CLAY/PERMEANT MIXTURES

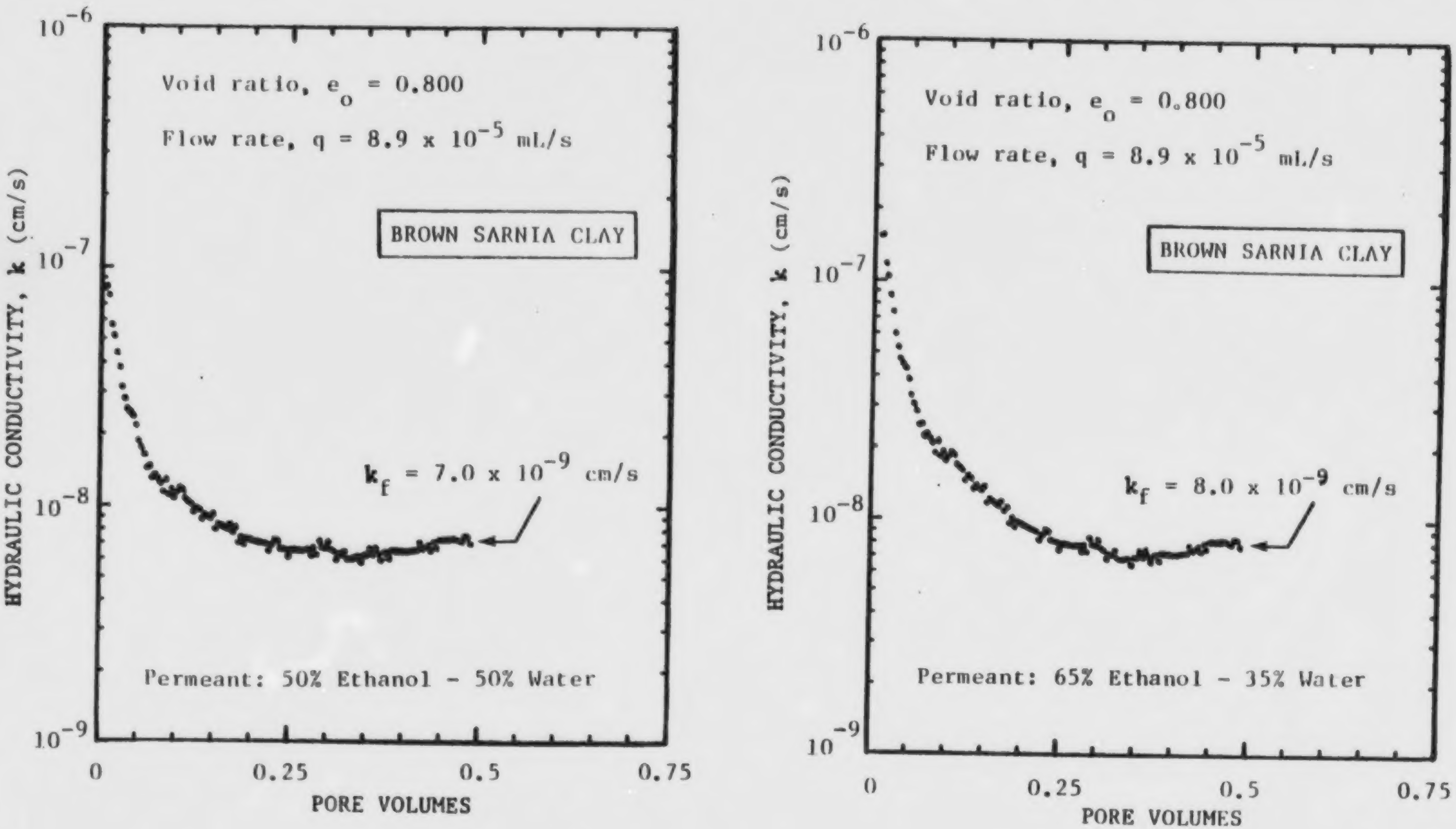

FIGURE D.3 HYDRAULIC CONDUCTIVITY VS PORE VOLUMES FOR CLAY/PERMEANT MIXTURES

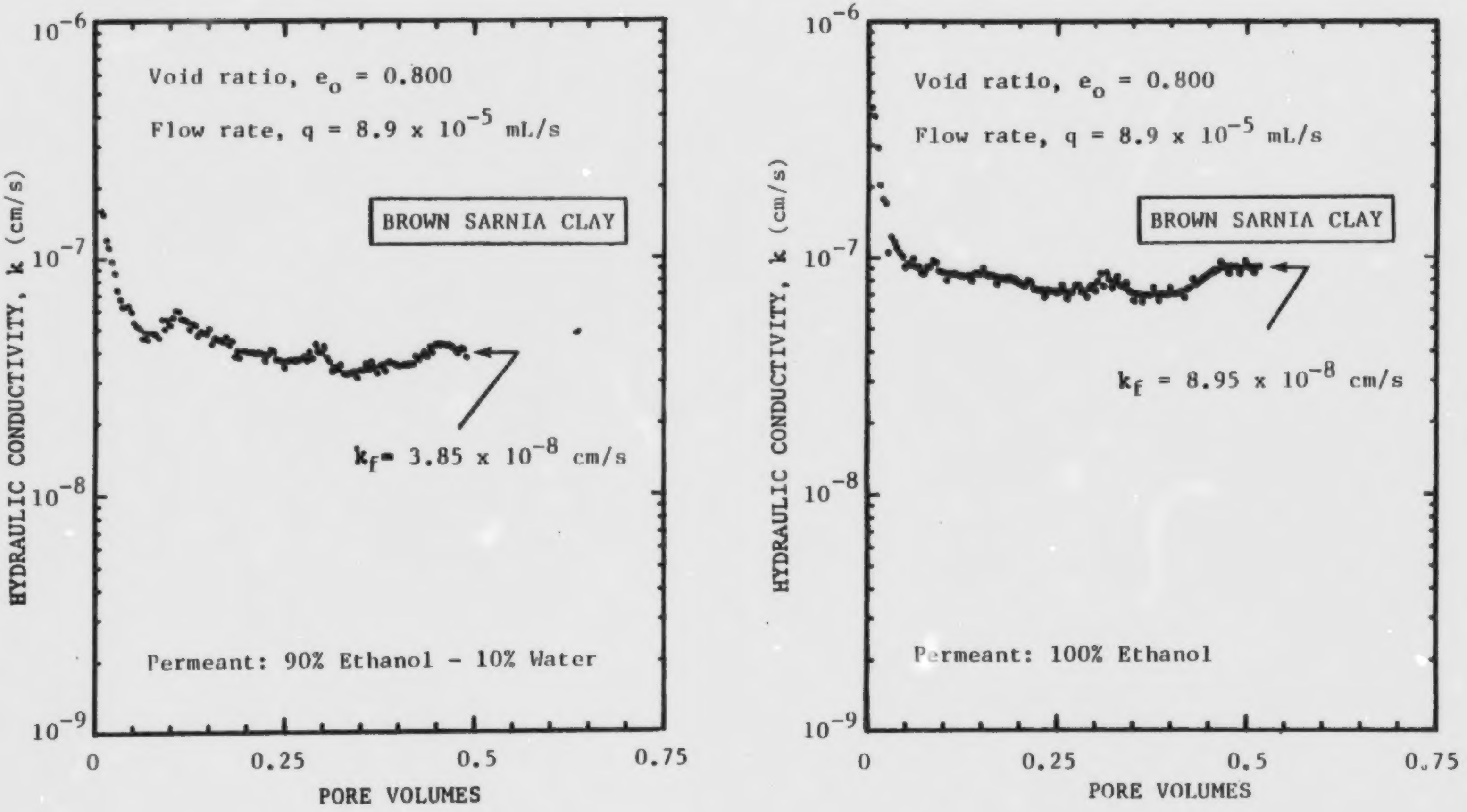

FIGURE D.4 HYDRAULIC CONDUCTIVITY VS PORE VOLUMES FOR CLAY/PERMEANT MIXTURES

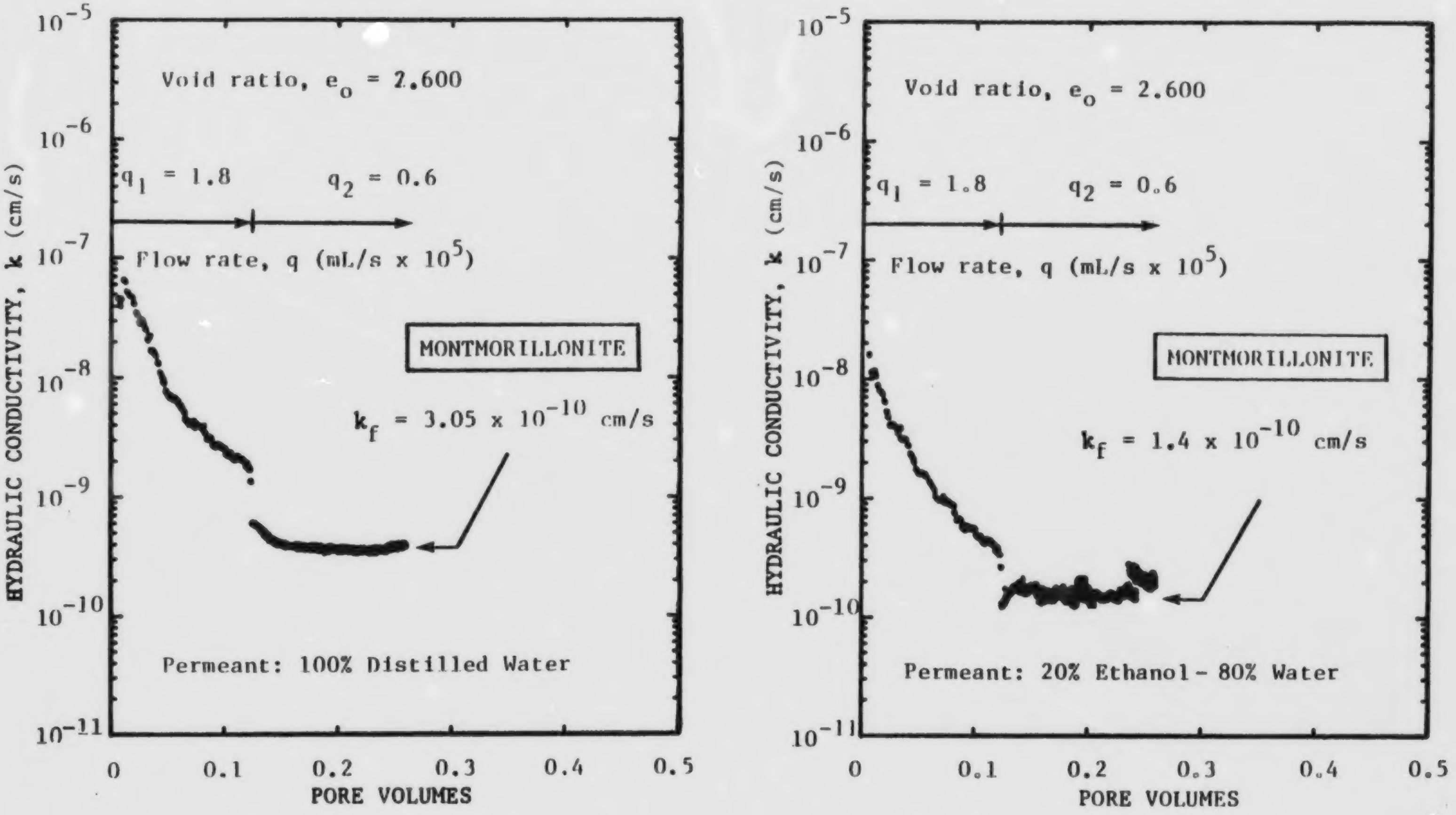

FIGURE D.5 HYDRAULIC CONDUCTIVITY VS PORE VOLUMES FOR CLAY/PERMEANT MIXTURES

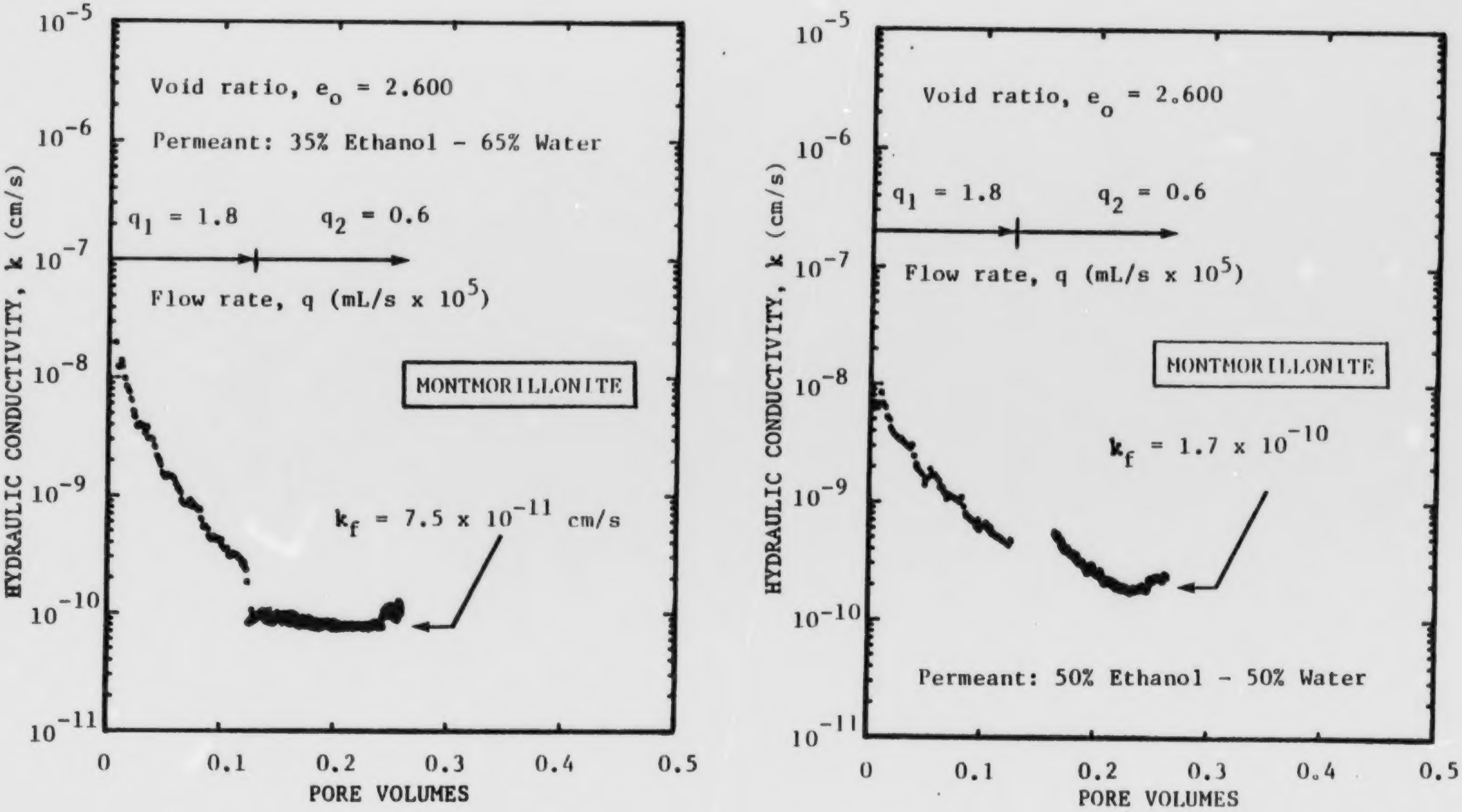

FIGURE D.6 HYDRAULIC CONDUCTIVITY VS PORE VOLUMES FOR CLAY/PERMEANT MIXTURES

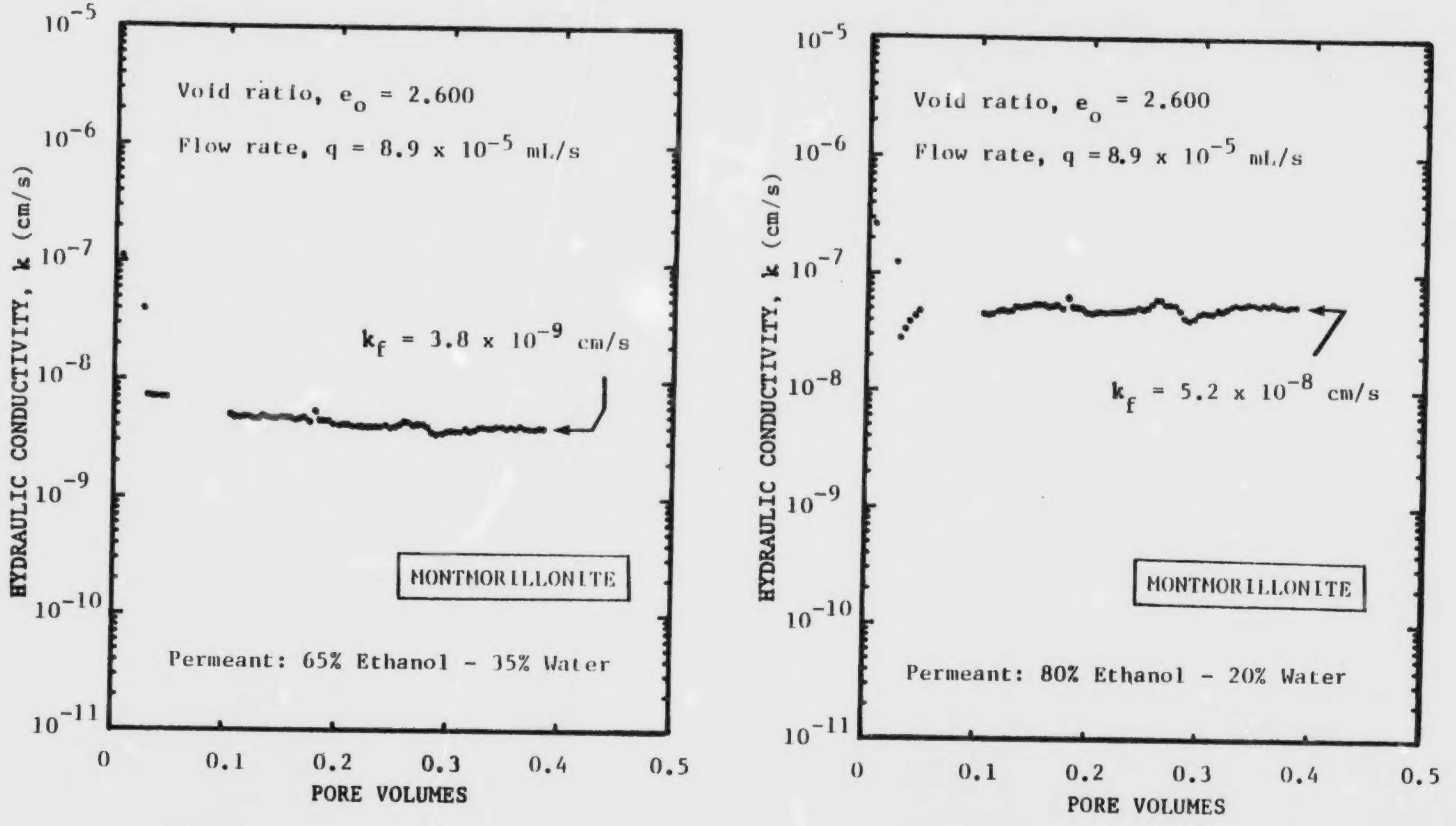

FIGURE D.7 HYDRAULIC CONDUCTIVITY VS PORE VOLUMES FOR CLAY/PERMEANT MIXTURES

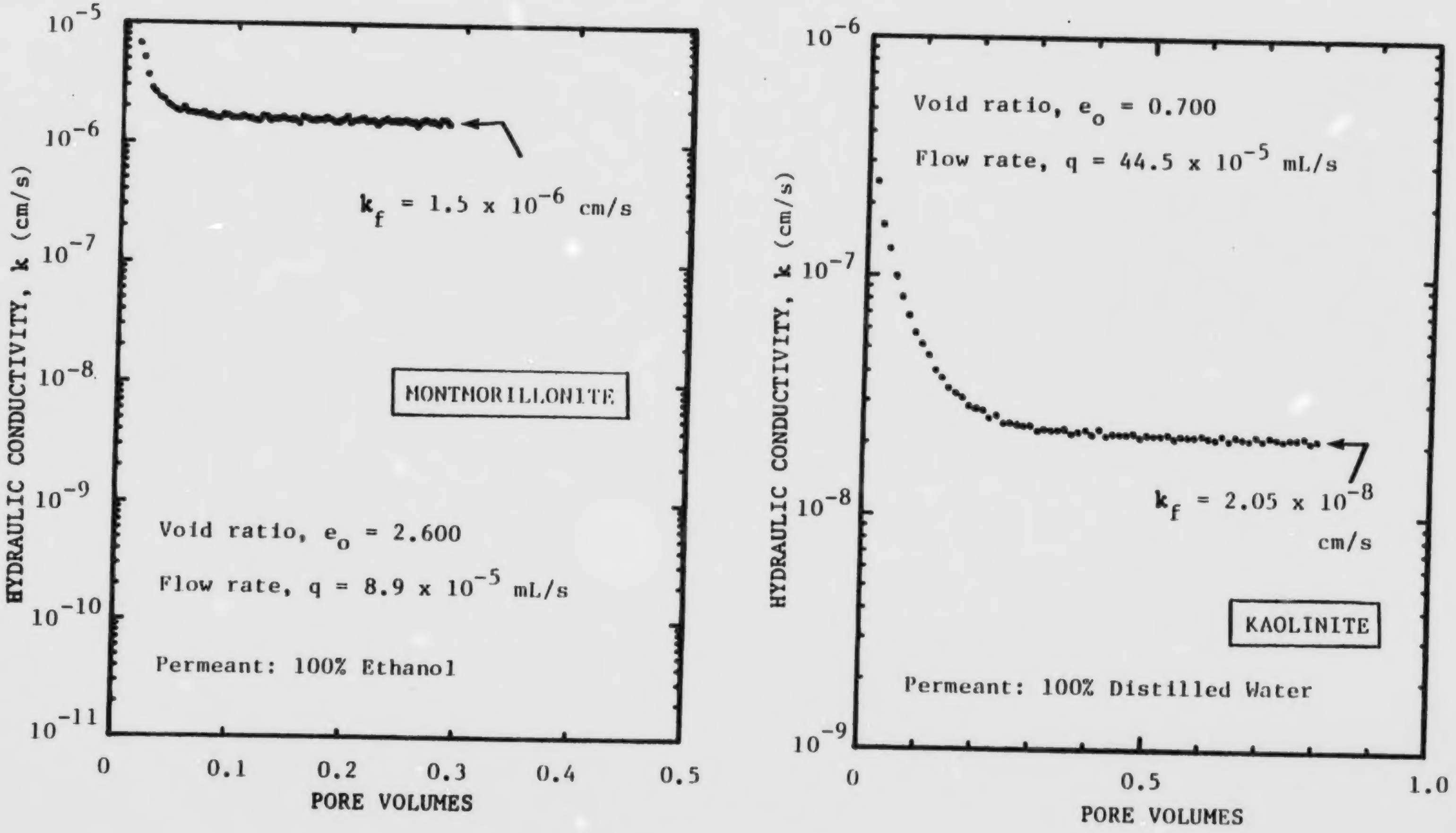

FIGURE D.8 HYDRAULIC CONDUCTIVITY VS PORE VOLUMES FOR CLAY/PERMEANT MIXTURES

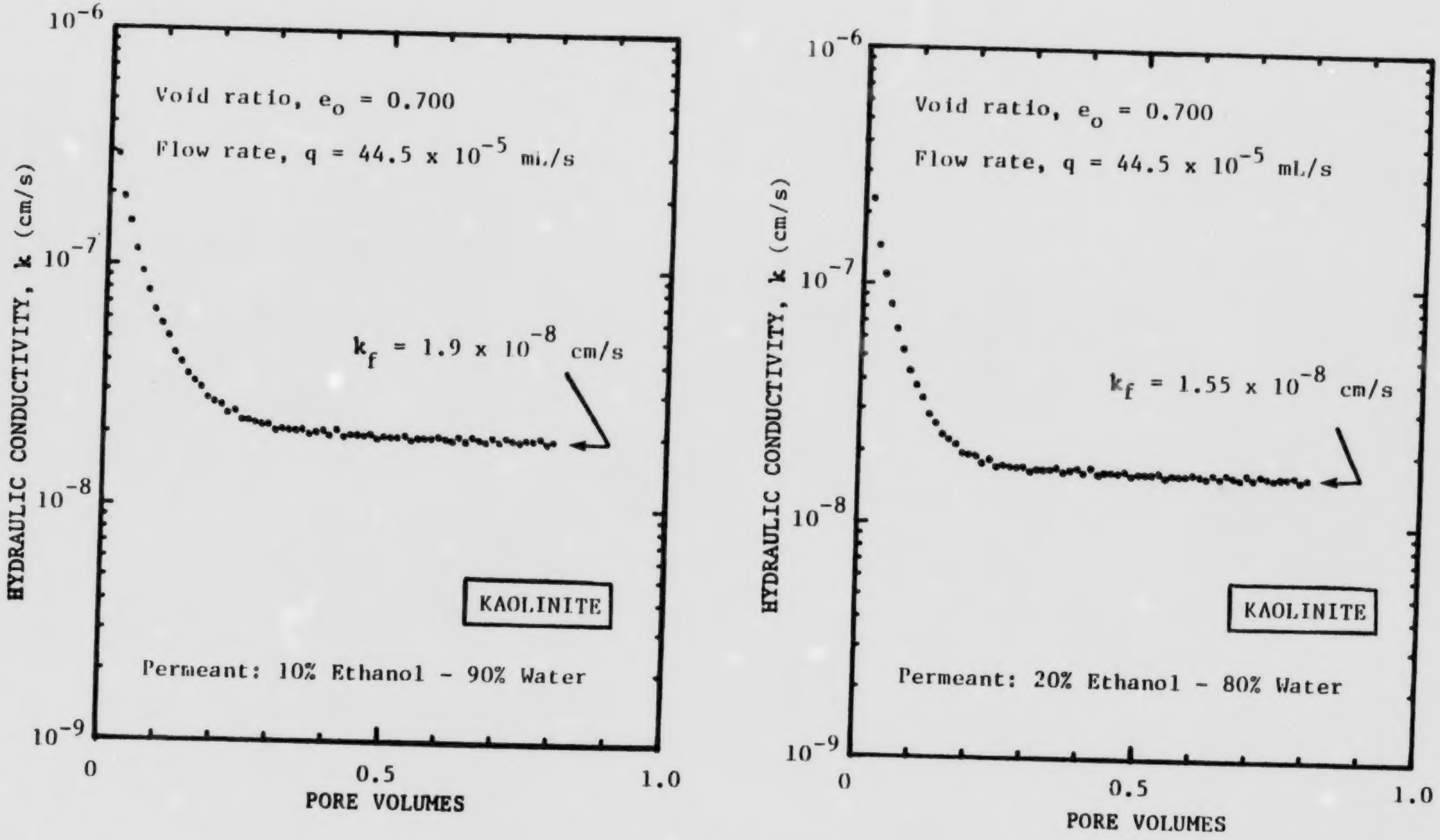

FIGURE D.9 HYDRAULIC CONDUCTIVITY VS PORE VOLUMES FOR CLAY/PERMEANT MIXTURES

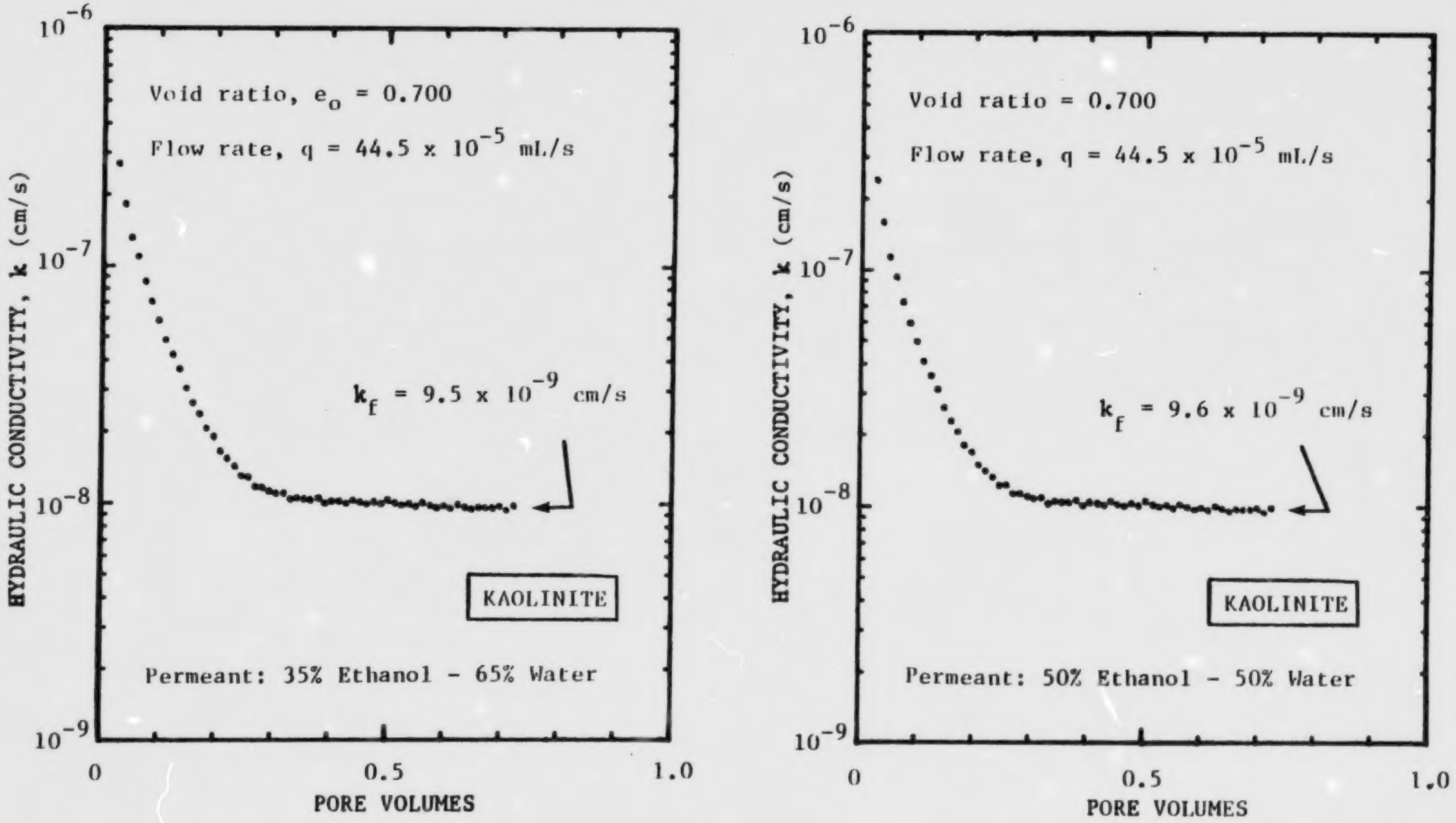

FIGURE D.10 HYDRAULIC CONDUCTIVITY VS PORE VOLUMES FOR CLAY/PERMEANT MIXTURES

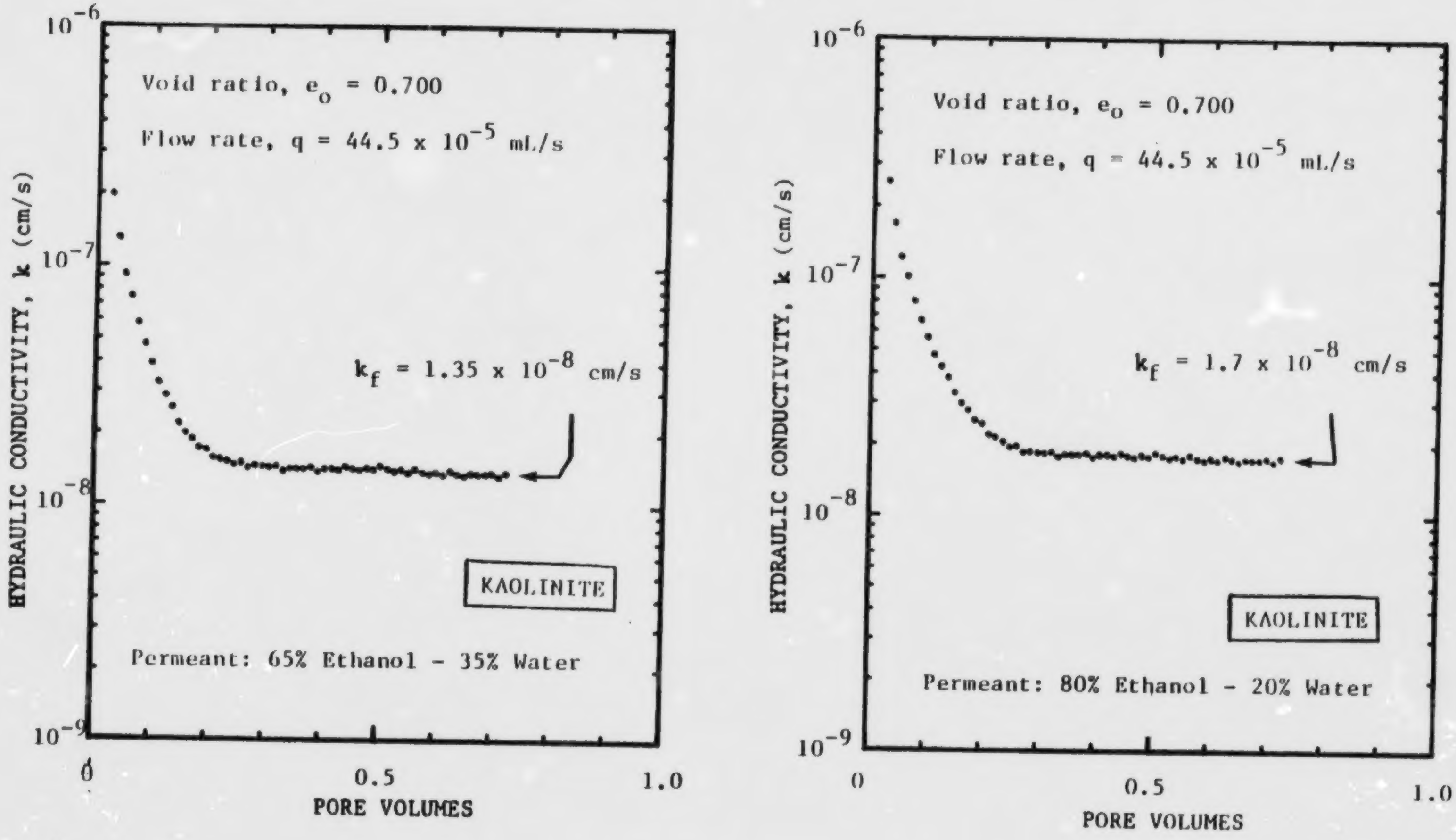

FIGURE D.11 HYDRAULIC CONDUCTIVITY VS PORE VOLUMES FOR CLAY/PERMEANT MIXTURES

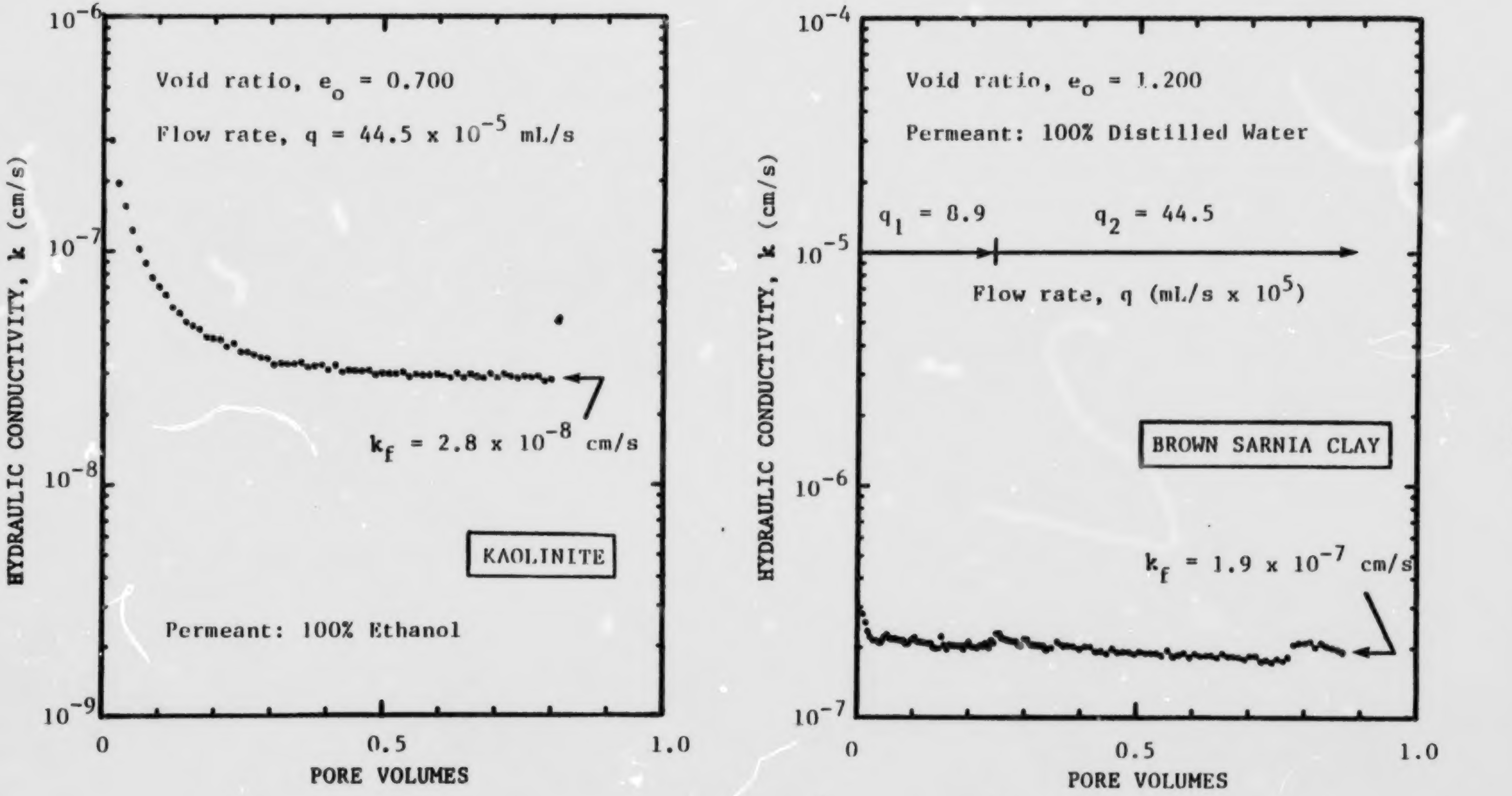

FIGURE D.12 HYDRAULIC CONDUCTIVITY VS PORE VOLUMES FOR CLAY/PERMEANT MIXTURES

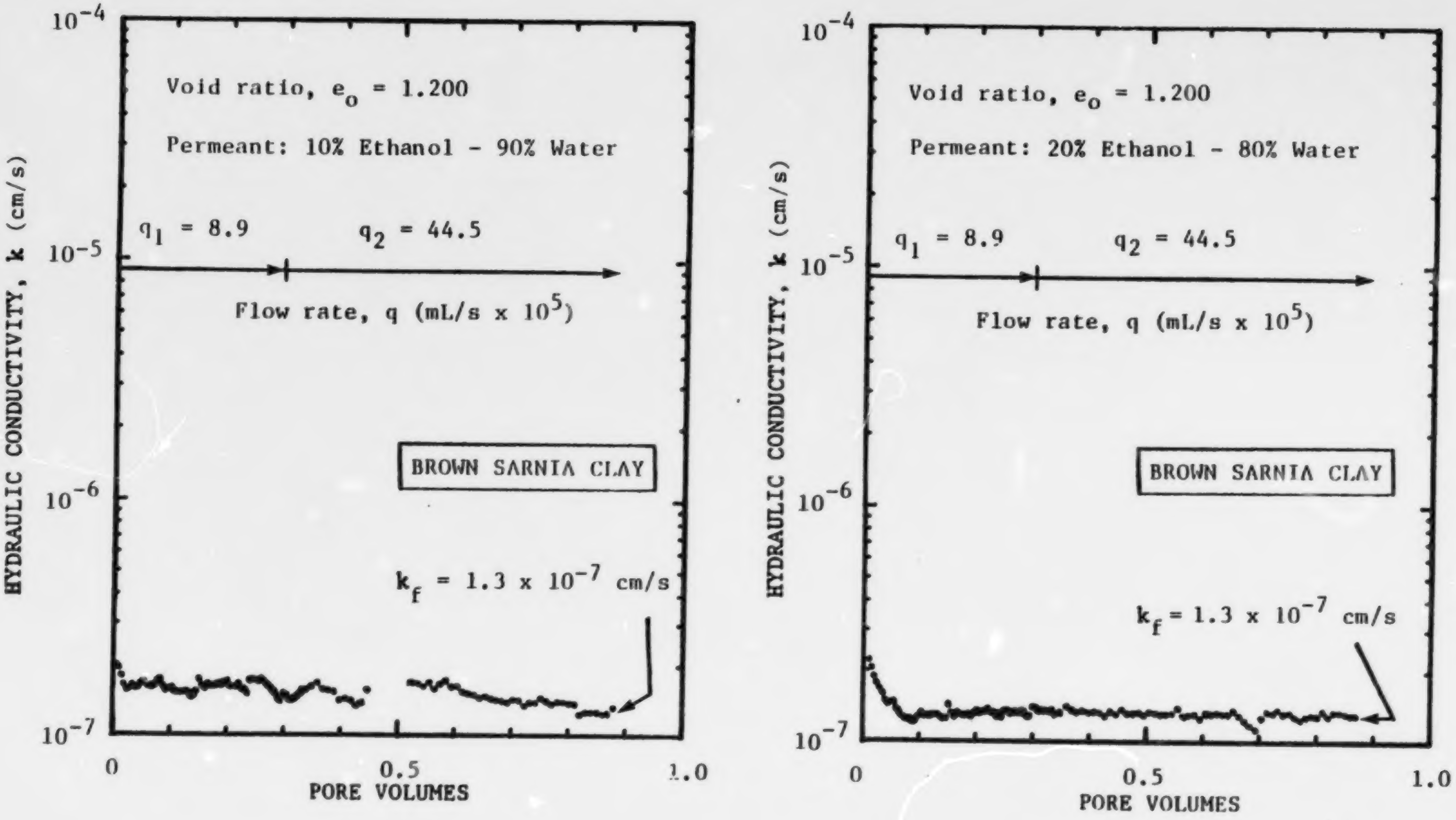

FIGURE D.13 HYDRAULIC CONDUCTIVITY VS PORE VOLUMES FOR CLAY/PERMEANT MIXTURES

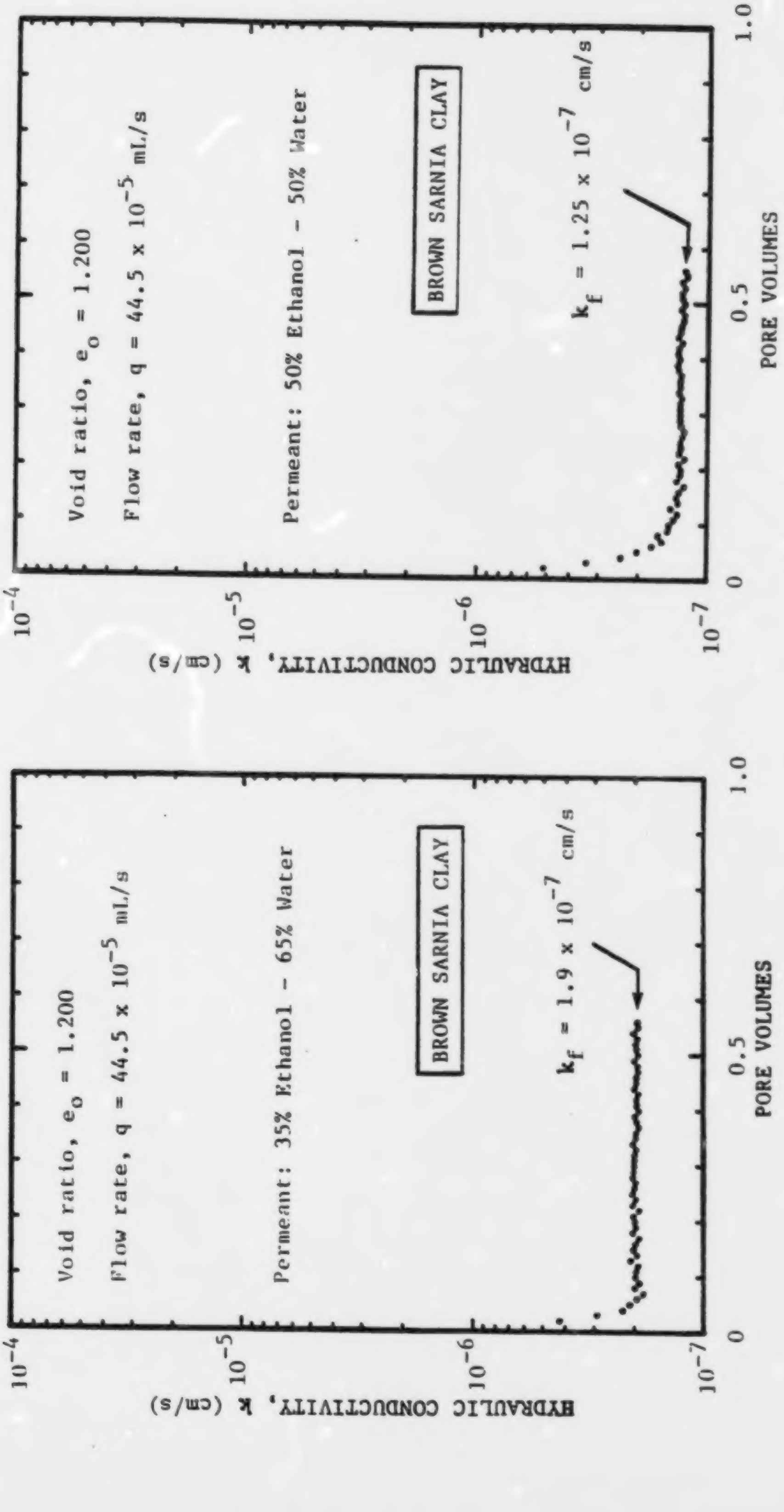

FIGURE D.14 HYDRAULIC CONDUCTIVITY VS PORE VOLUMES FOR CLAY/PERMEANT MIXTURES

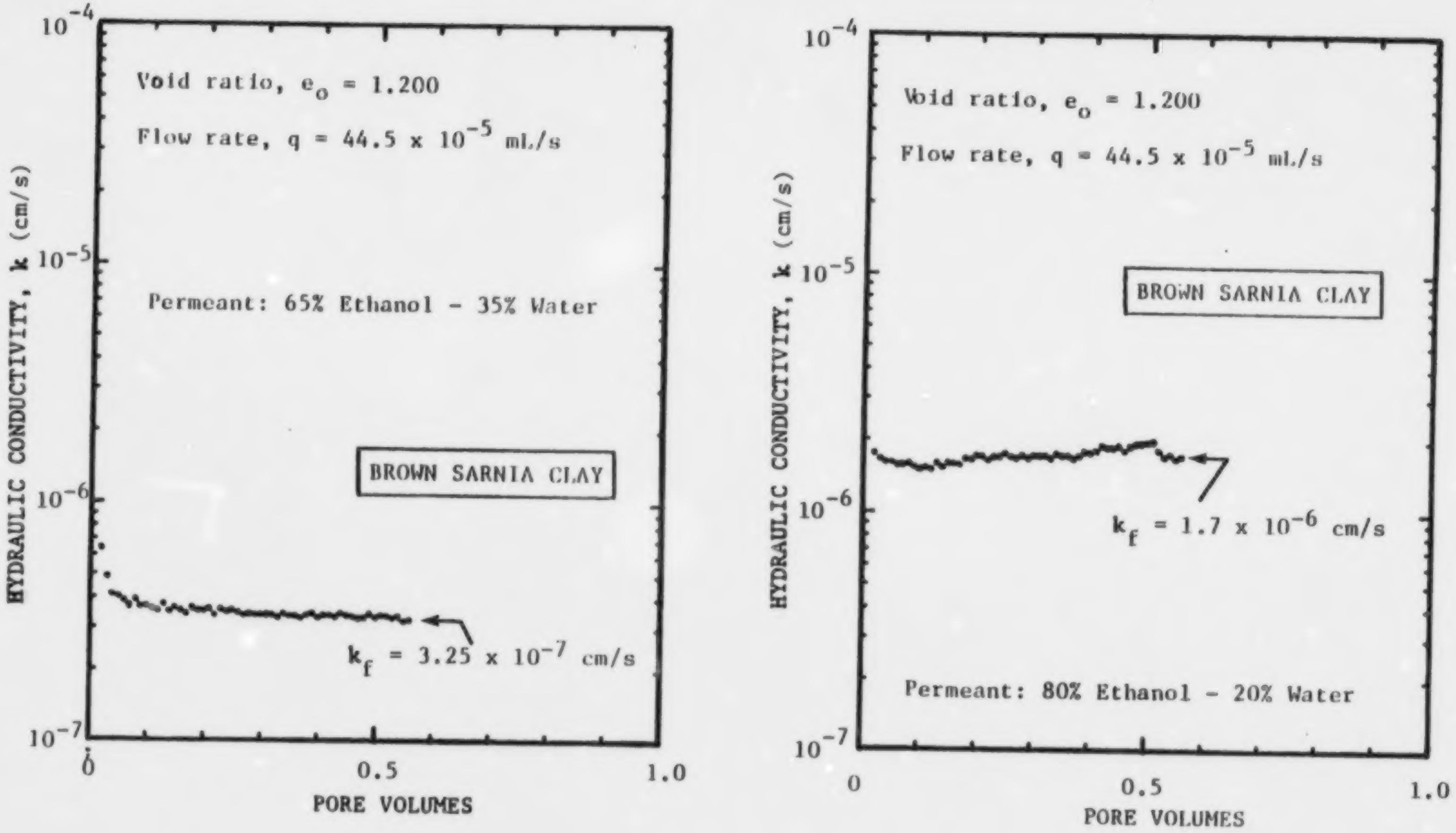

FIGURE D.15 HYDRAULIC CONDUCTIVITY VS PORE VOLUMES FOR CLAY/PERMEANT MIXTURES

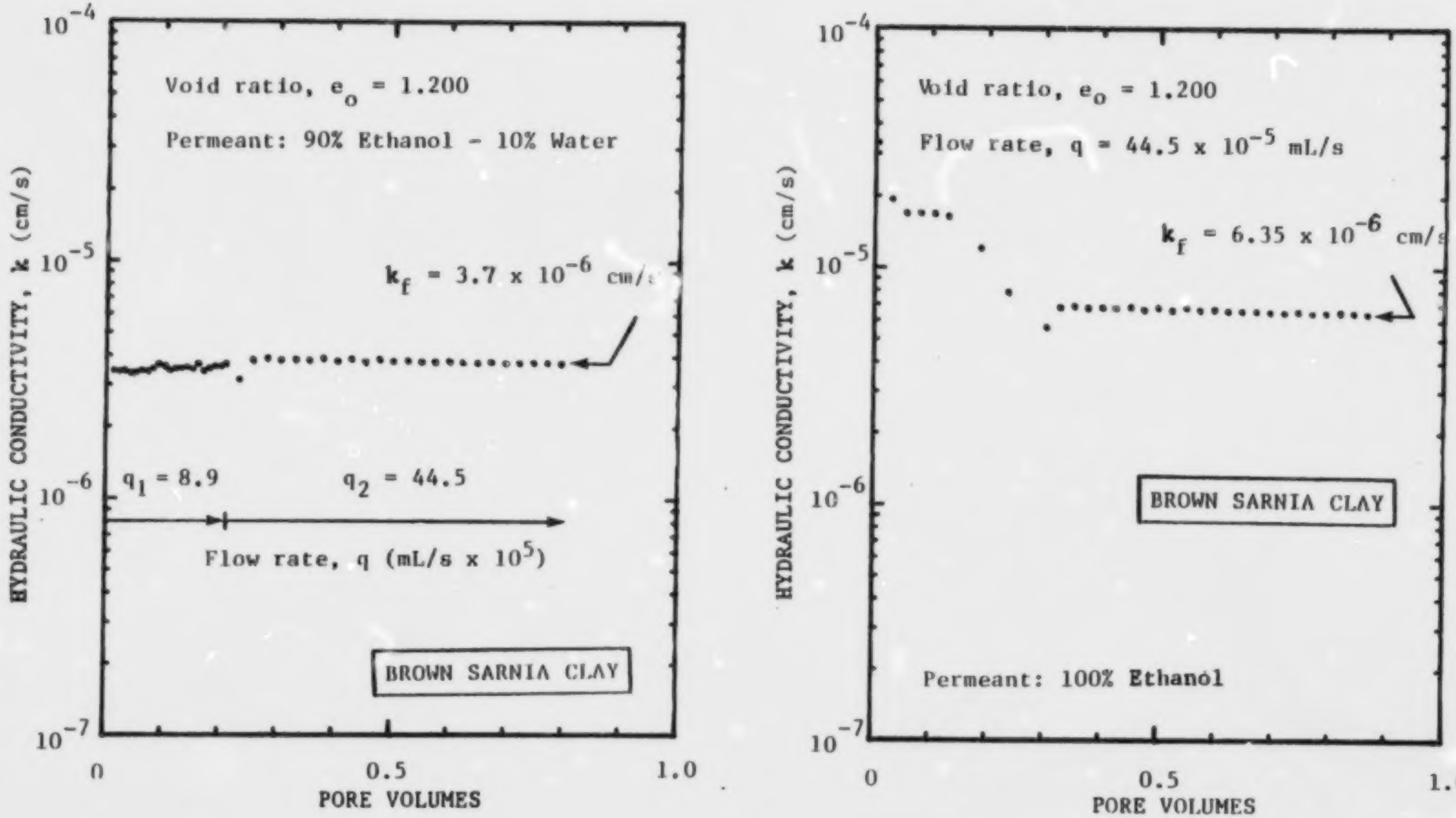

FIGURE D.16 HYDRAULIC CONDUCTIVITY VS PORE VOLUMES FOR CLAY/PERMEANT MIXTURES

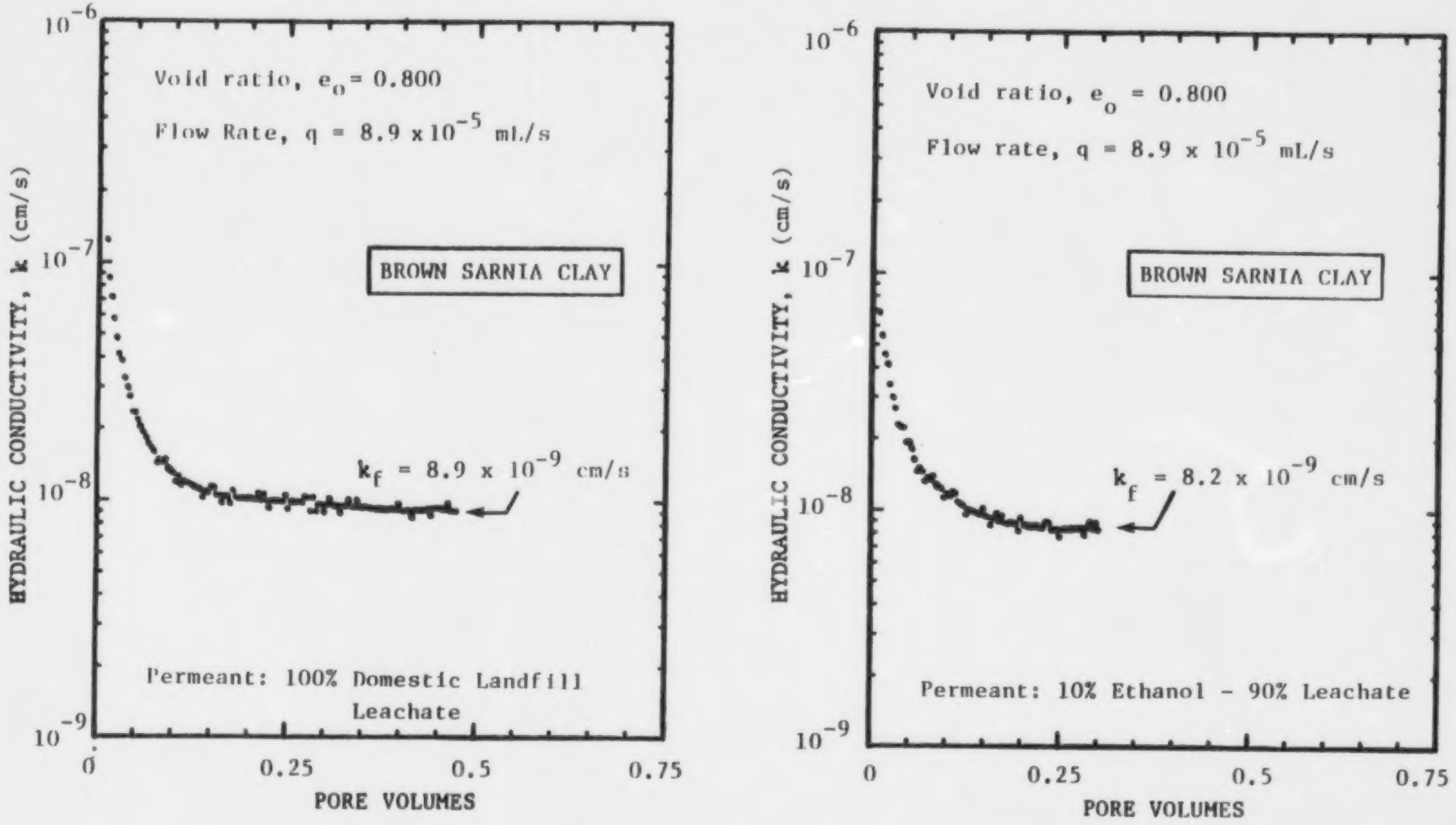

FIGURE D.17 HYDRAULIC CONDUCTIVITY VS PORE VOLUMES FOR CLAY/PERMEANT MIXTURES

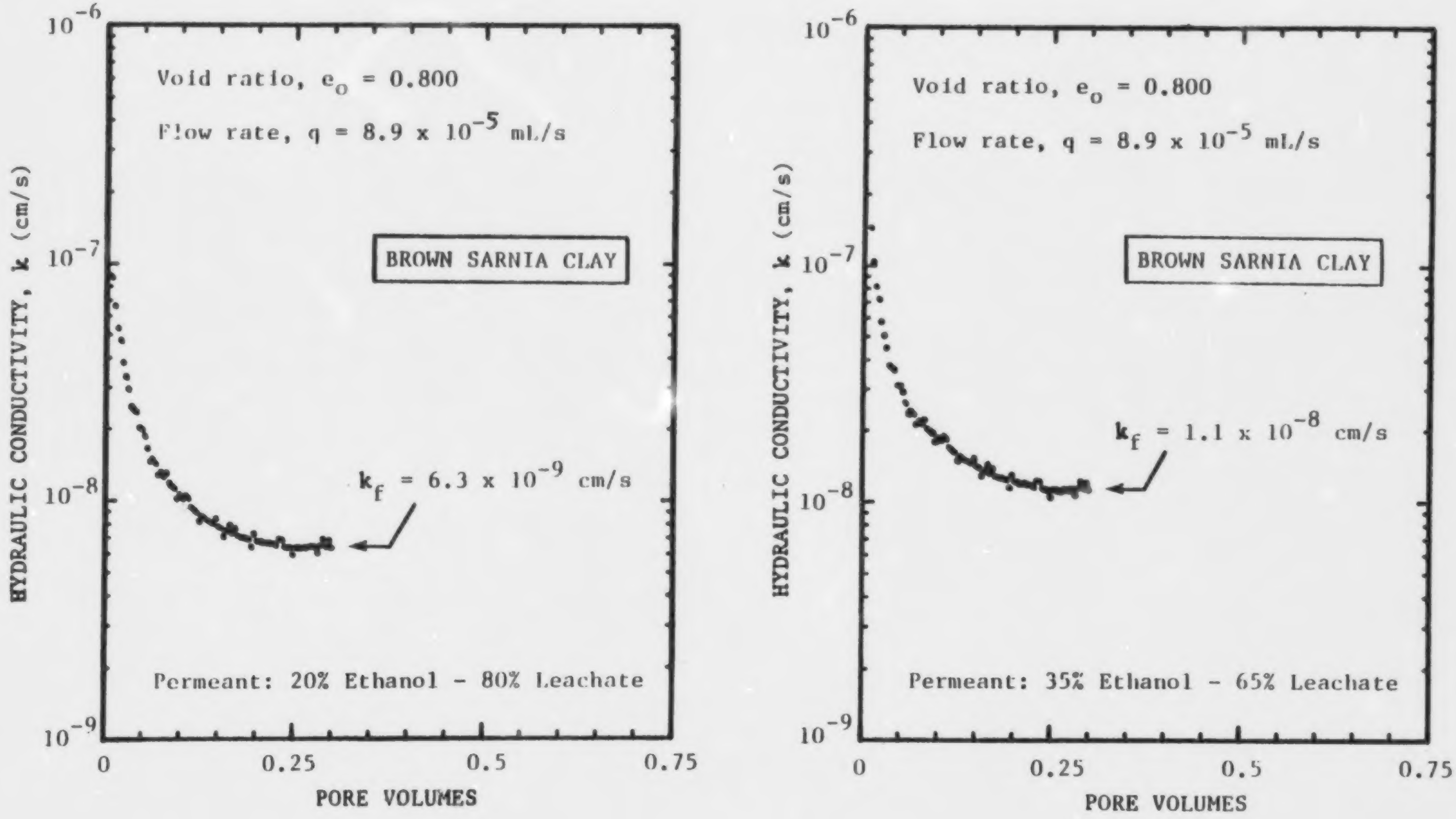

FIGURE D.18 HYDRAULIC CONDUCTIVITY VS PORE VOLUMES FOR CLAY/PERMEANT MIXTURES

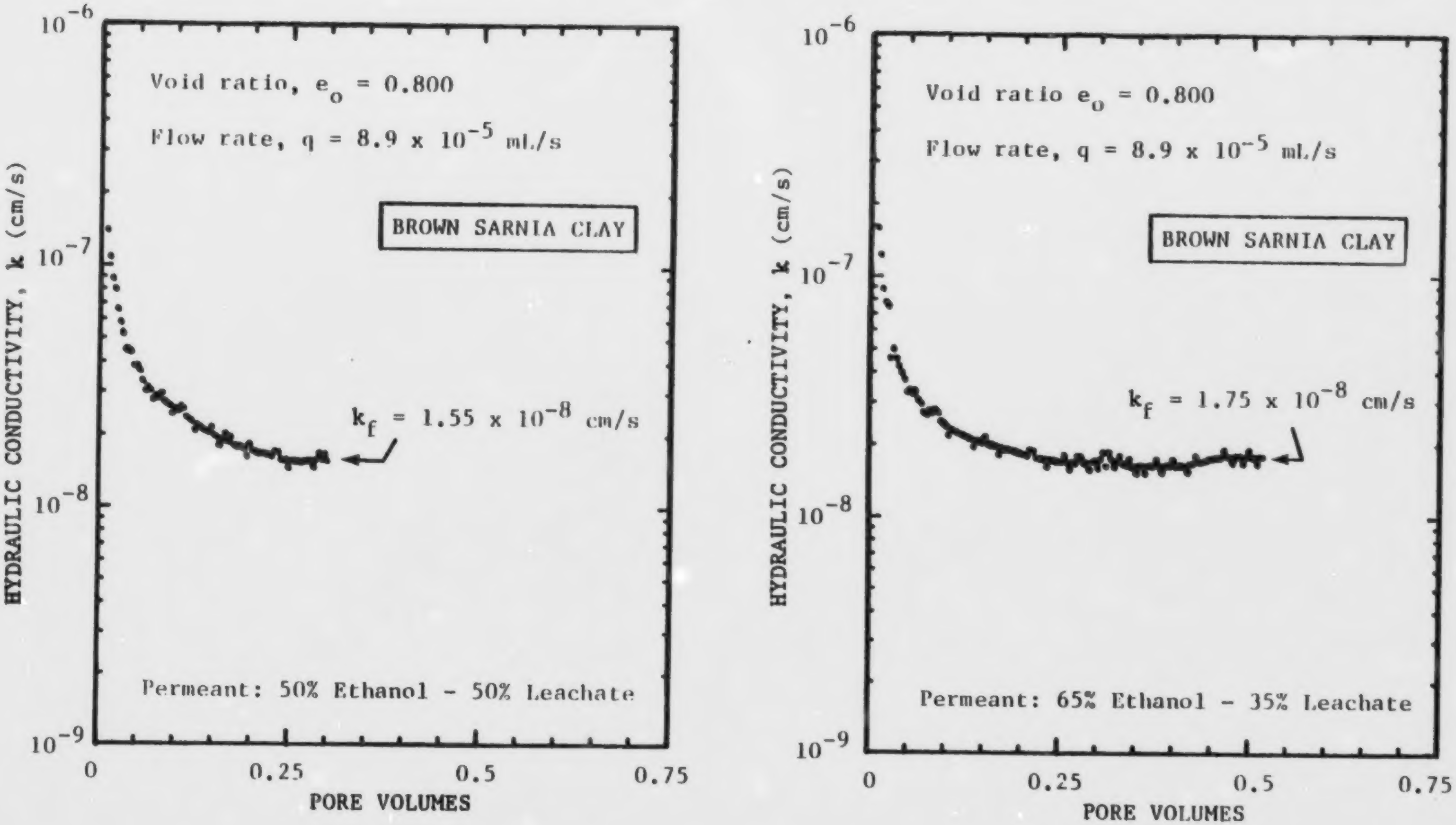

FIGURE D.19 HYDRAULIC CONDUCTIVITY VS PORE VOLUMES FOR CLAY/PERMEANT MIXTURES

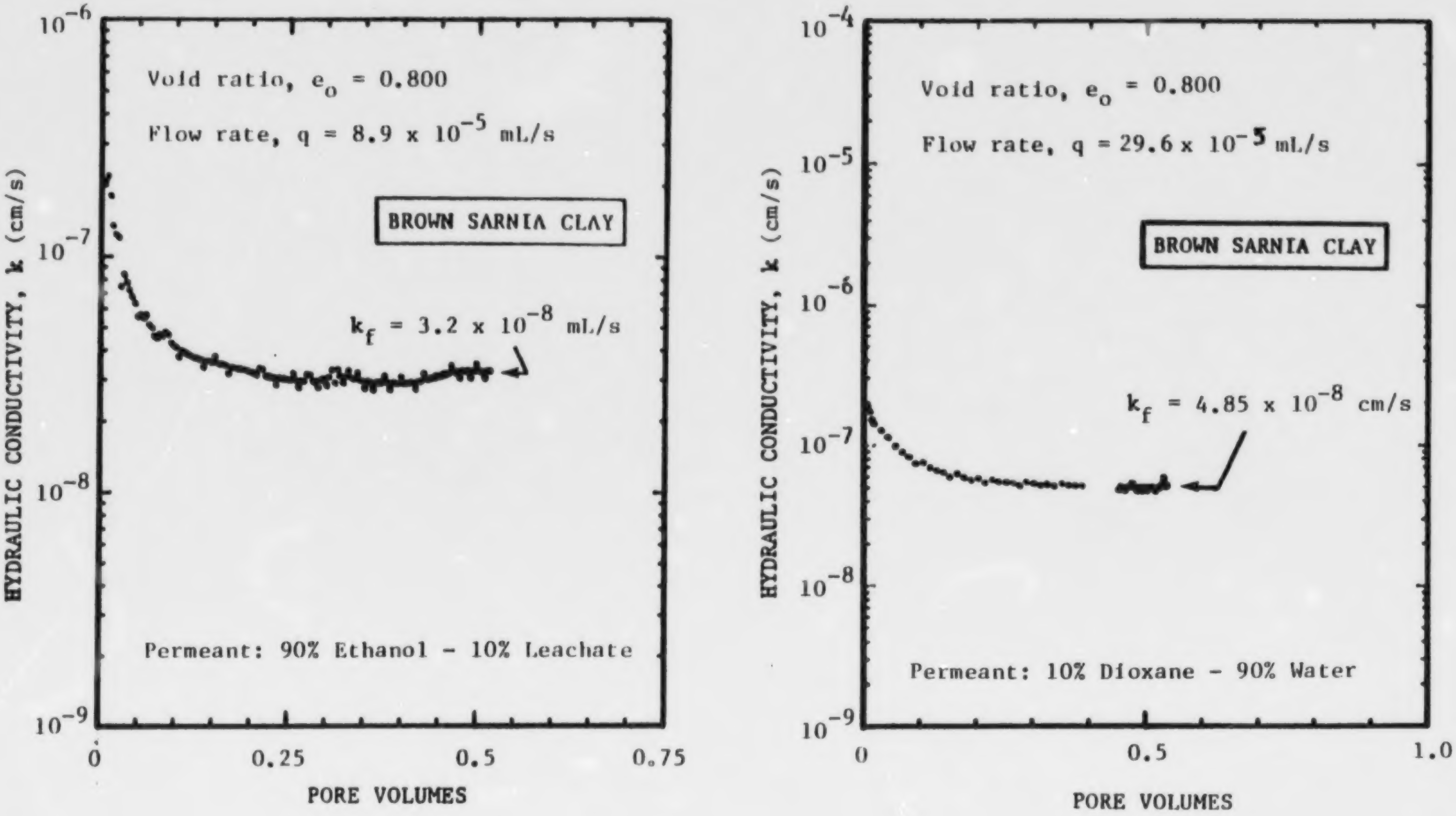

FIGURE D.20 HYDRAULIC CONDUCTIVITY VS PORE VOLUMES FOR CLAY/PERMEANT MIXTURES

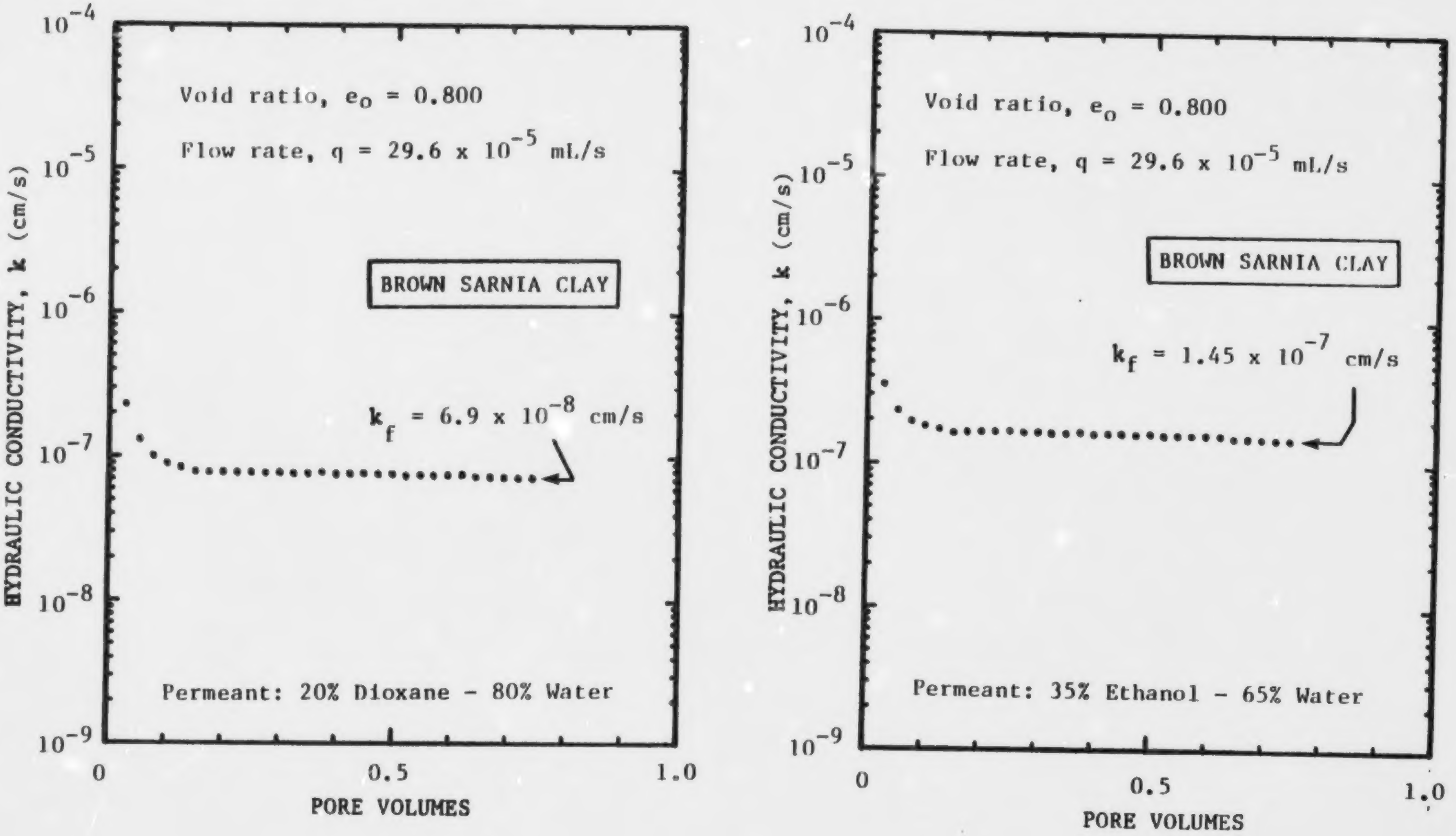

FIGURE D.21 HYDRAULIC CONDUCTIVITY VS PORE VOLUMES FOR CLAY/PERMEANT MIXTURES

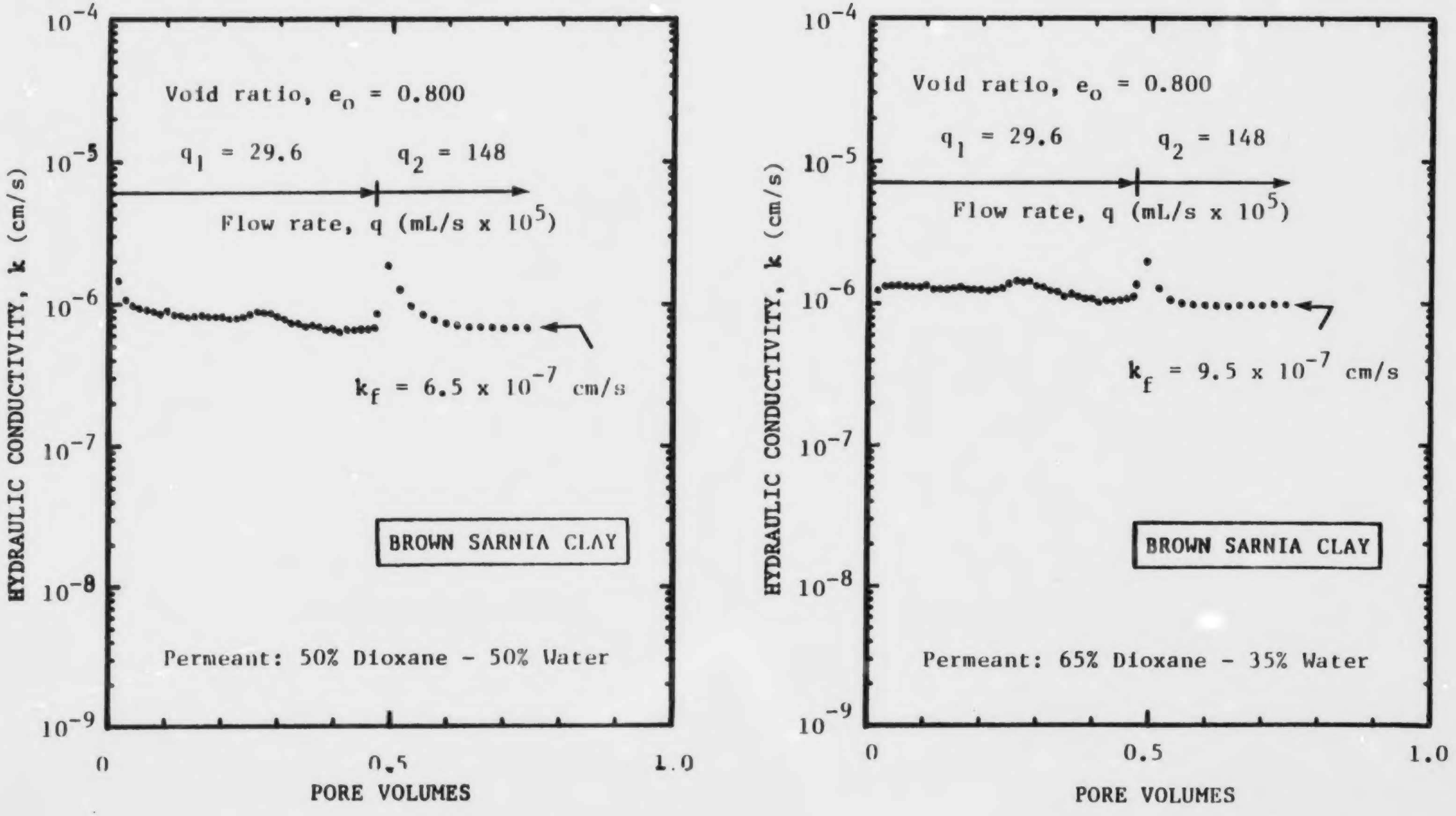

FIGURE D.22 HYDRAULIC CONDUCTIVITY VS PORE VOLUMES FOR CLAY/PERMEANT MIXTURES

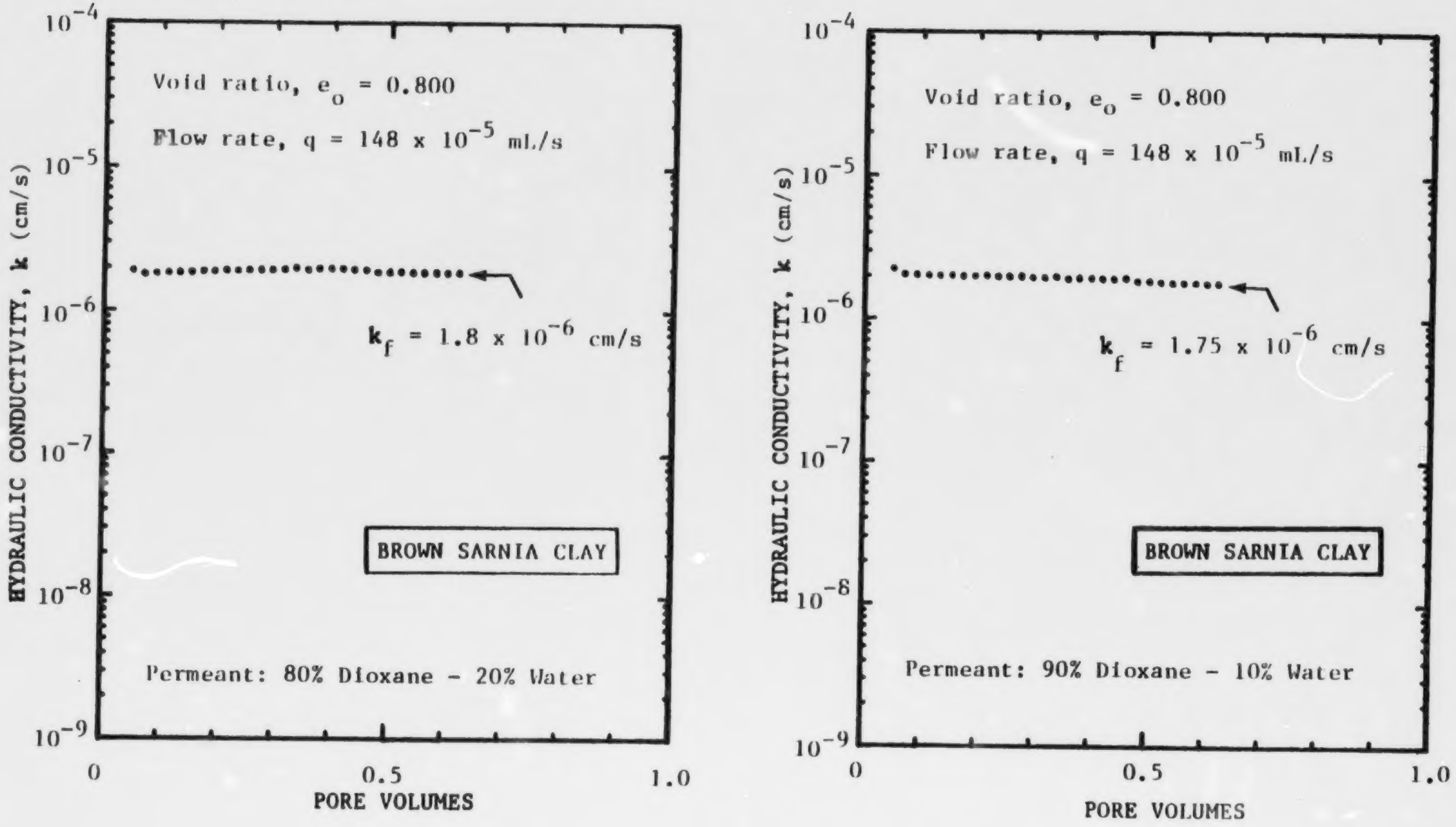

FIGURE D.23 HYDRAULIC CONDUCTIVITY VS PORE VOLUMES FOR CLAY/PERMEANT MIXTURES

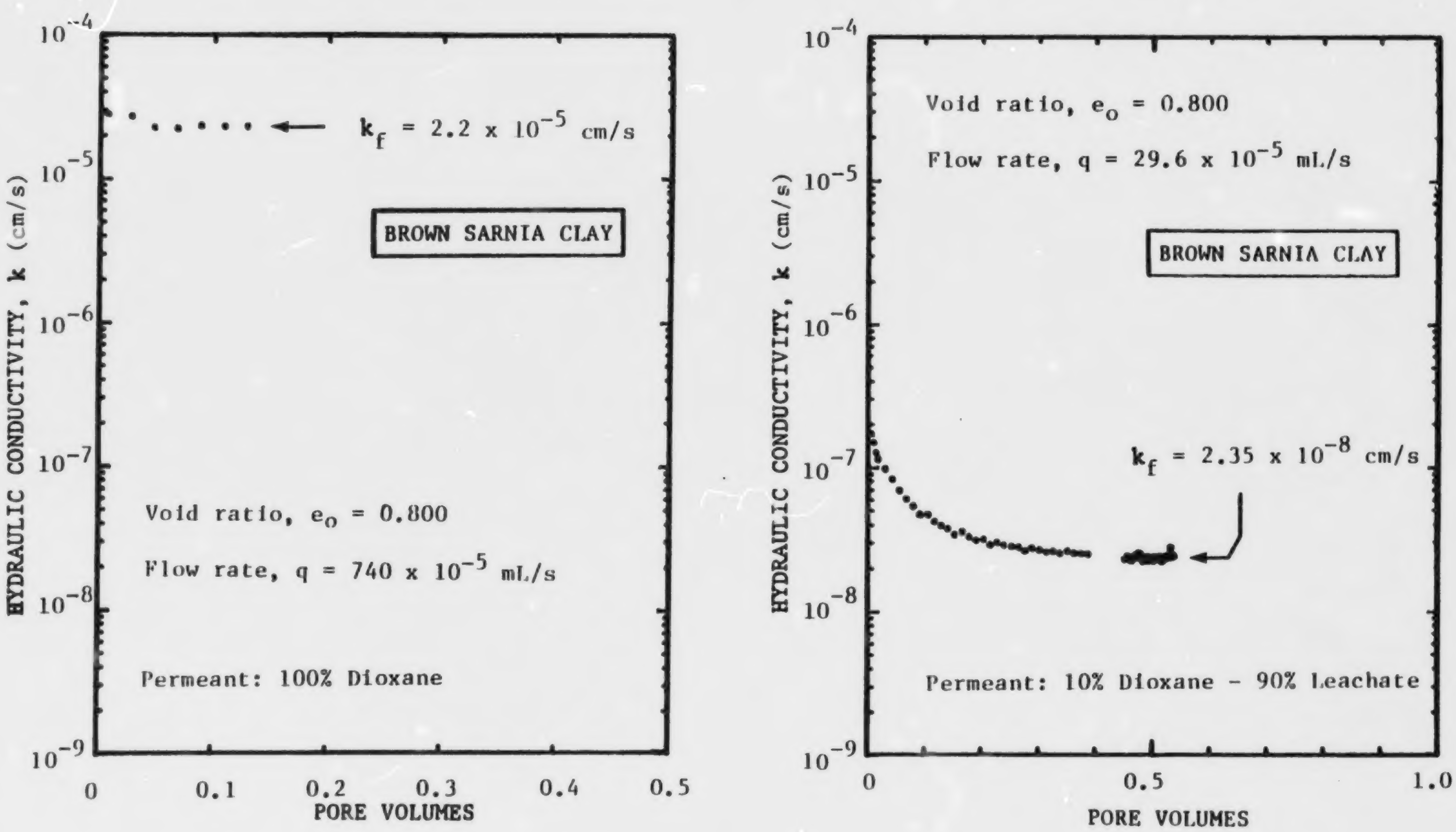

FIGURE D.24 HYDRAULIC CONDUCTIVITY VS PORE VOLUMES FOR CLAY/PERMEANT MIXTURES

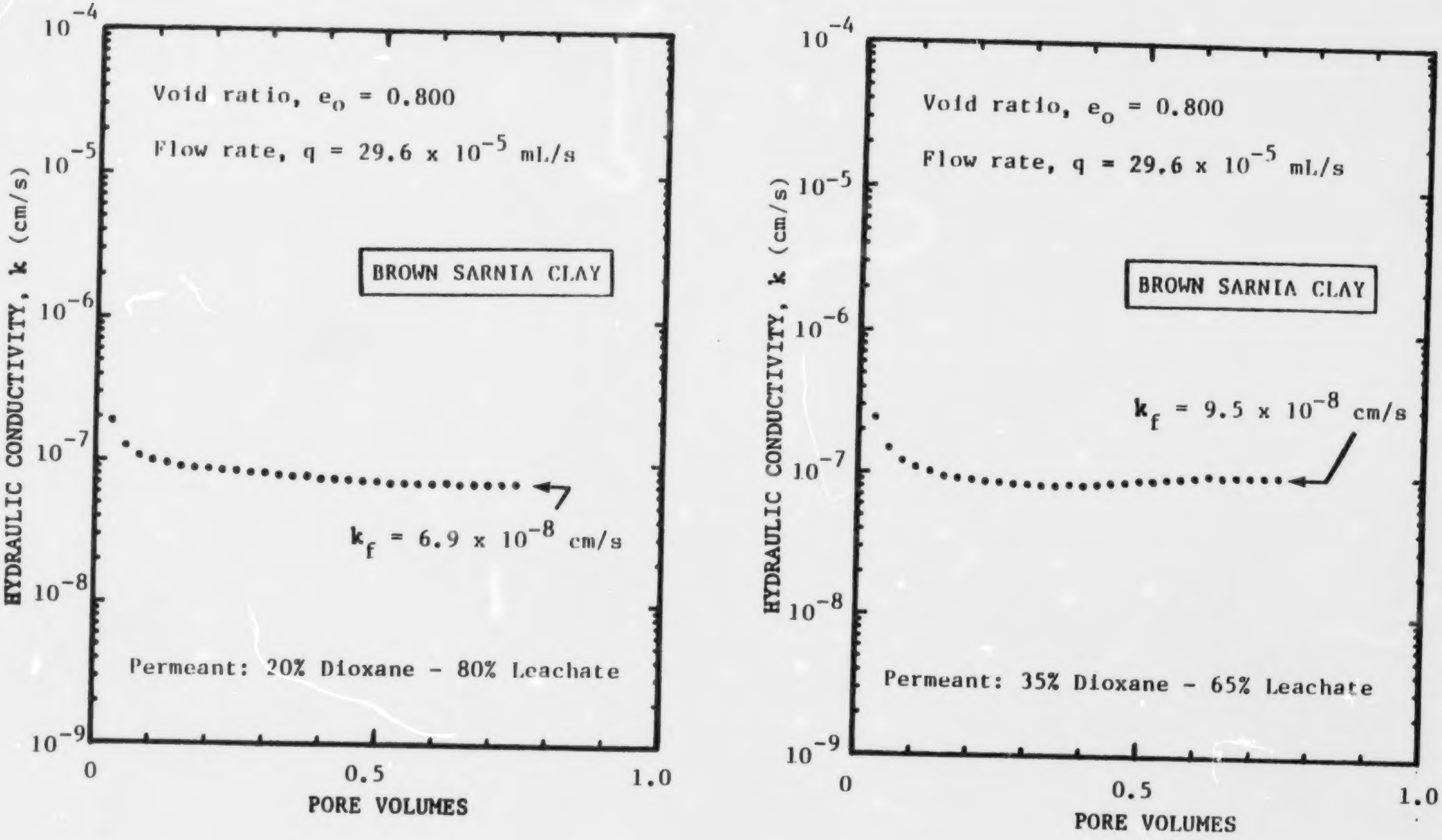

FIGURE D.25 HYDRAULIC CONDUCTIVITY VS PORE VOLUMES FOR CLAY/PERMEANT MIXTURES

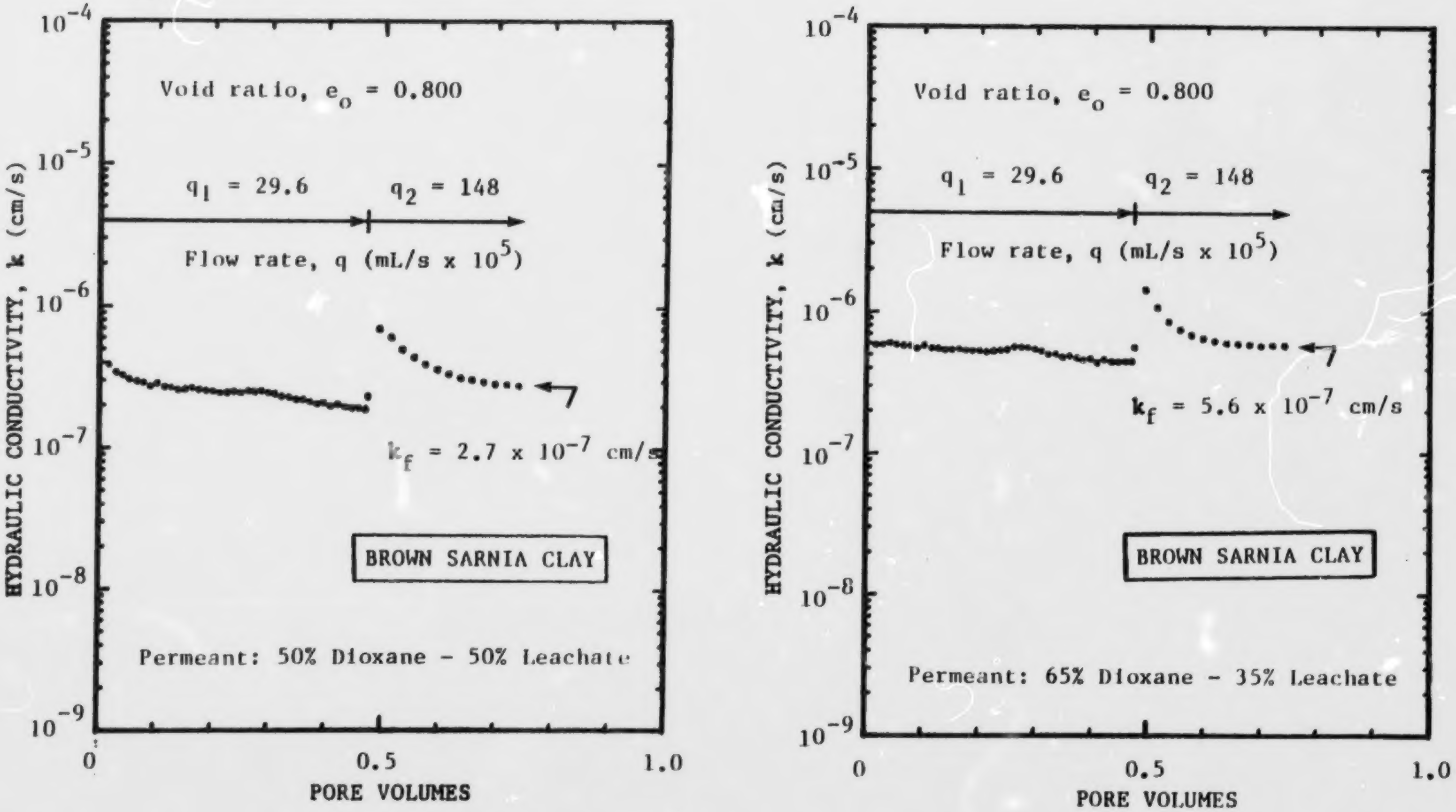

FIGURE D.26 HYDRAULIC CONDUCTIVITY VS PORE VOLUMES FOR CLAY/PERMEANT MIXTURES

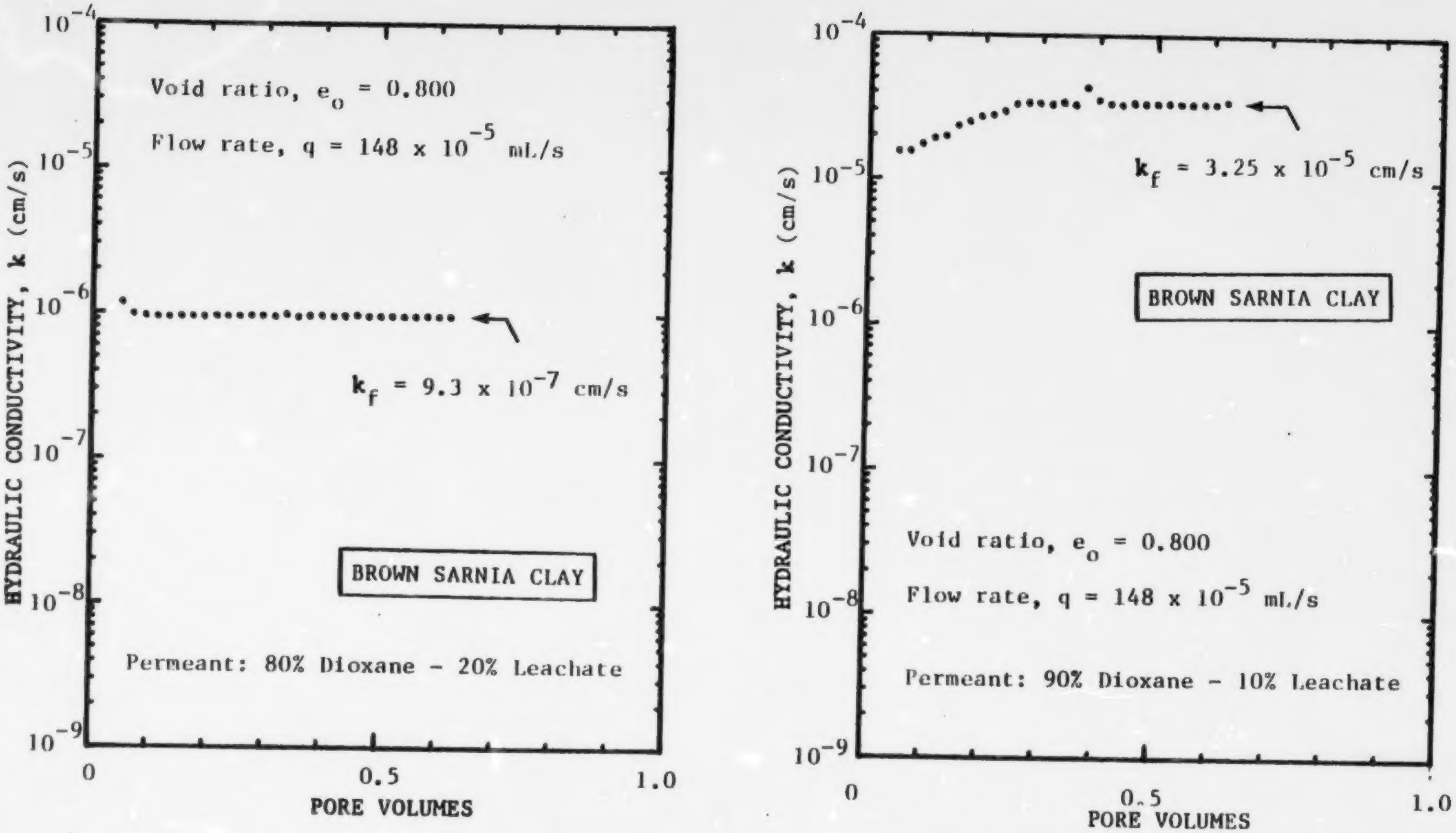

FIGURE D.27 HYDRAULIC CONDUCTIVITY VS PORE VOLUMES FOR CLAY/PERMEANT MIXTURES

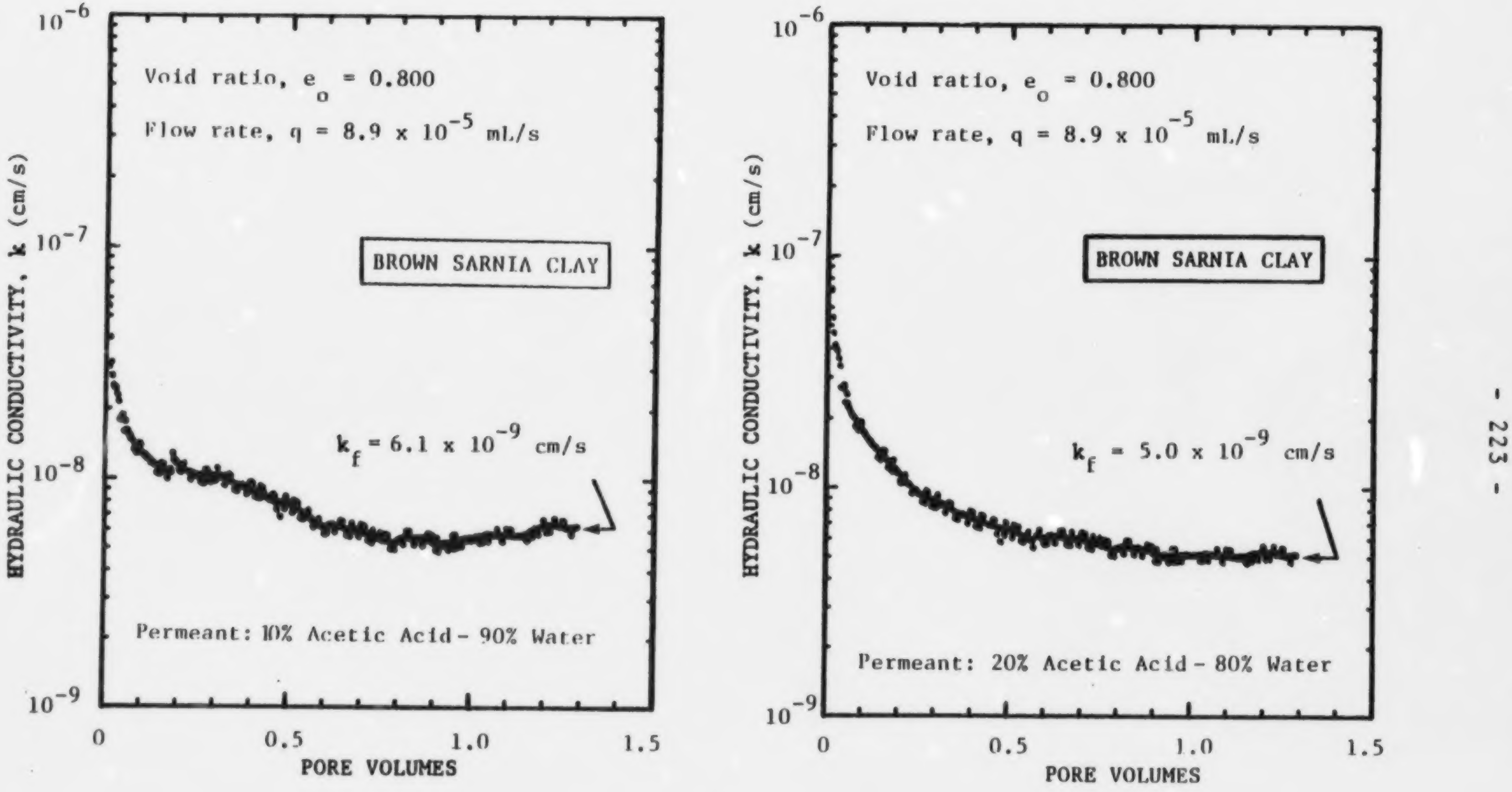

FIGURE D.28 HYDRAULIC CONDUCTIVITY VS PORE VOLUMES FOR CLAY/PERMEANT MIXTURES

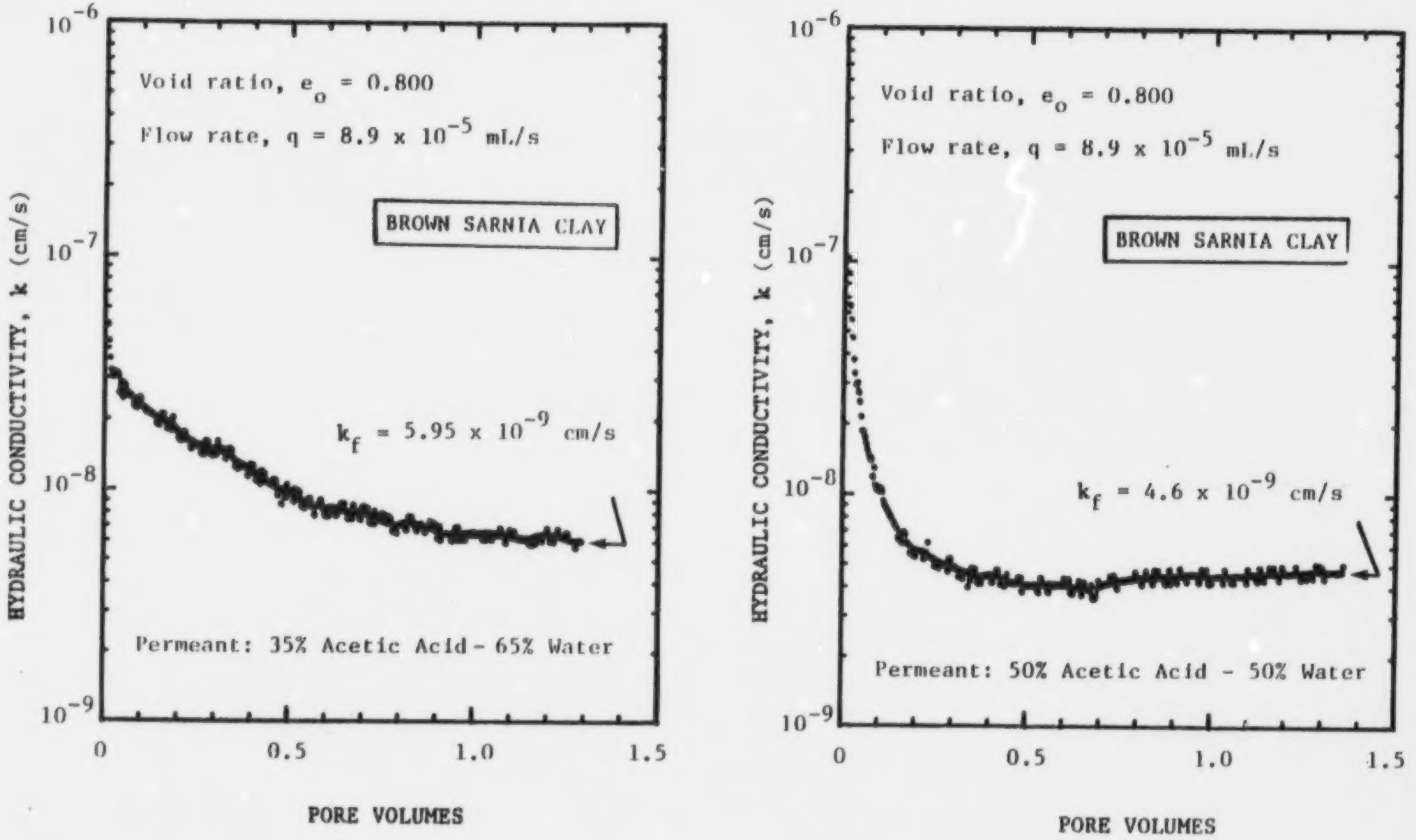

FIGURE D.29 HYDRAULIC CONDUCTIVITY VS PORE VOLUMES FOR CLAY/PERMEANT MIXTURES

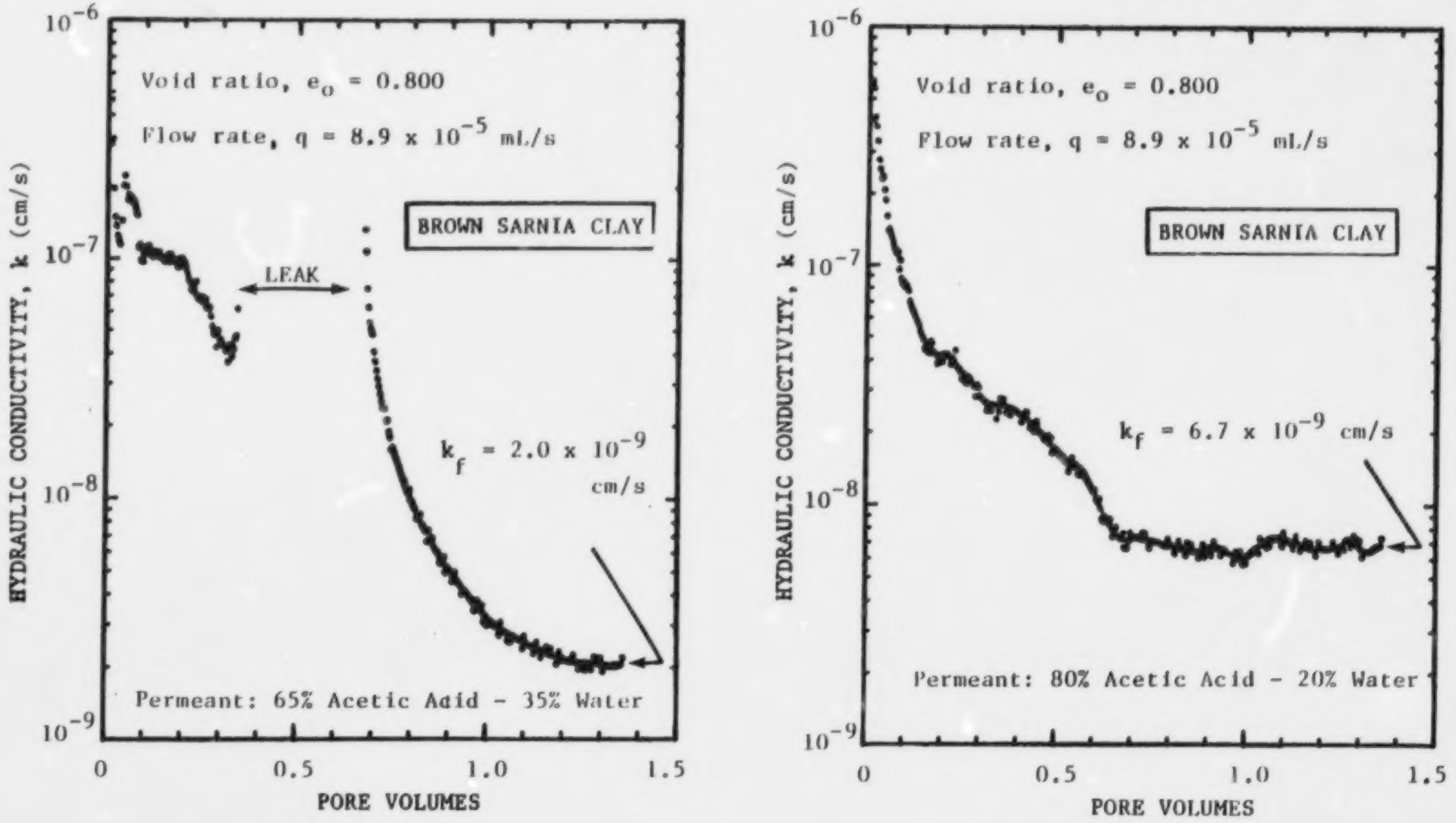

FIGURE D.30 HYDRAULIC CONDUCTIVITY VS PORE VOLUMES FOR CLAY/PERMEANT MIXTURES

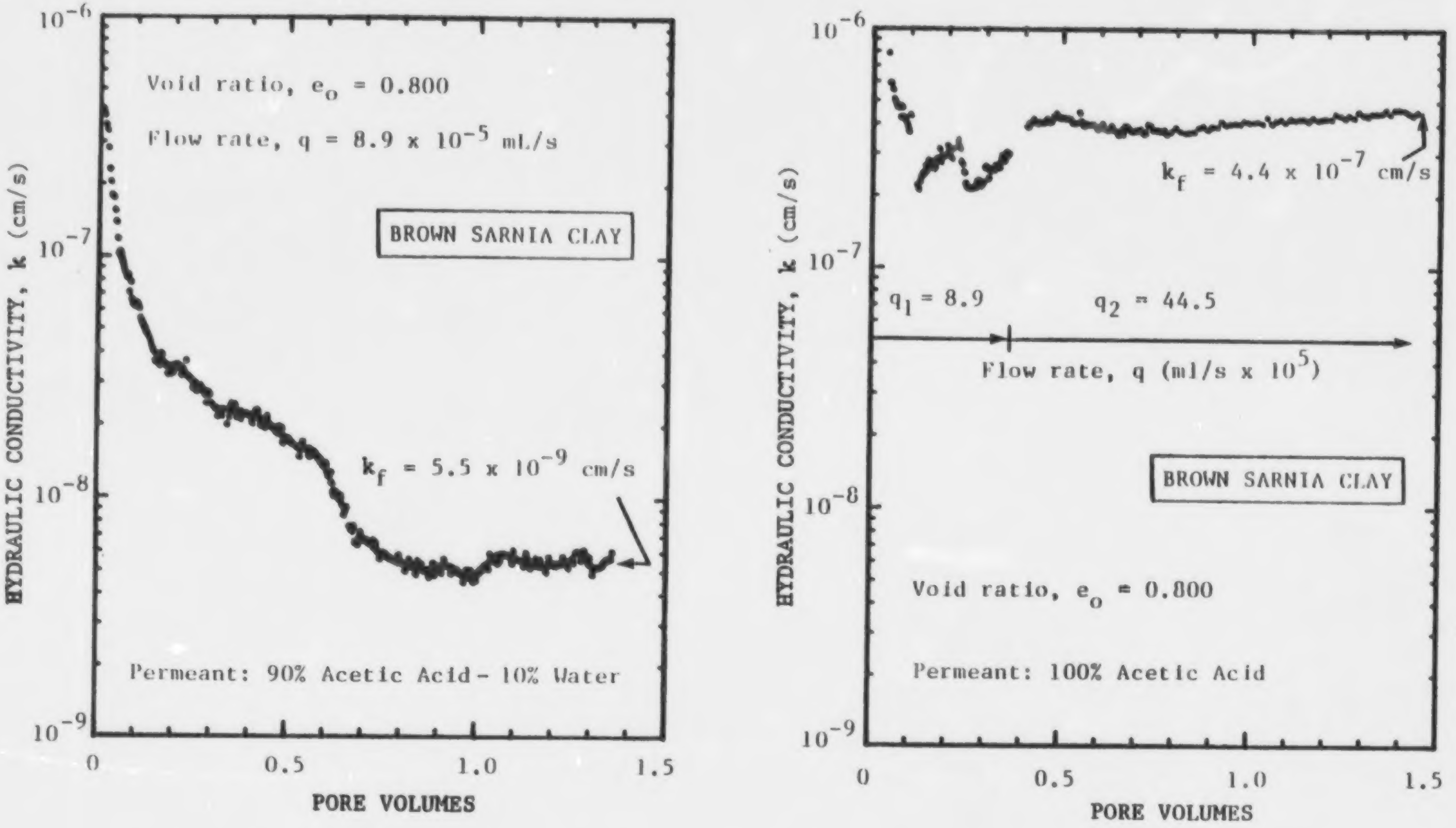

FIGURE D.31 HYDRAULIC CONDUCTIVITY VS PORE VOLUMES FOR CLAY/PERMEANT MIXTURES

APPENDIX E

HYDRAULIC CONDUCTIVITY CURVES FOR WATER-COMPACTED BROWN SARNIA CLAY PERMEATED WITH LEACHATE/ETHANOL MIXTURES

This appendix presents the results of hydraulic conductivity, settlement and effluent composition for tests performed on water-compacted brown Sarnia clays permeated with leachate/ethanol mixtures at the following static effective stresses: σ'_v = 0 kPa (Figures E.1 to E.6), σ'_v = 40 kPa (Figures E.7 to E.10), σ'_v = 80 kPa (Figures E.11 to E.14), σ'_v = 120 kPa (Figure E.15) and σ'_v = 160 kPa (Figures E.16 to E.19).

Figures E.20 and E.21 correspond to two additional tests for 100% ethanol through brown Sarnia clay at σ'_v = 10 kPa and σ'_v = 20 kPa.

Two duplicate tests for 40% ethanol and 100% ethanol at σ'_v = 0 kPa are shown in Figures E.22 and E.23).

The test results are discussed in Sections 5.3.1 of this report.

A special test carried out on water-compacted brown Sarnia clay permeated with a mixture of benzene, ethanol and leachate is shown in Figure E.24.

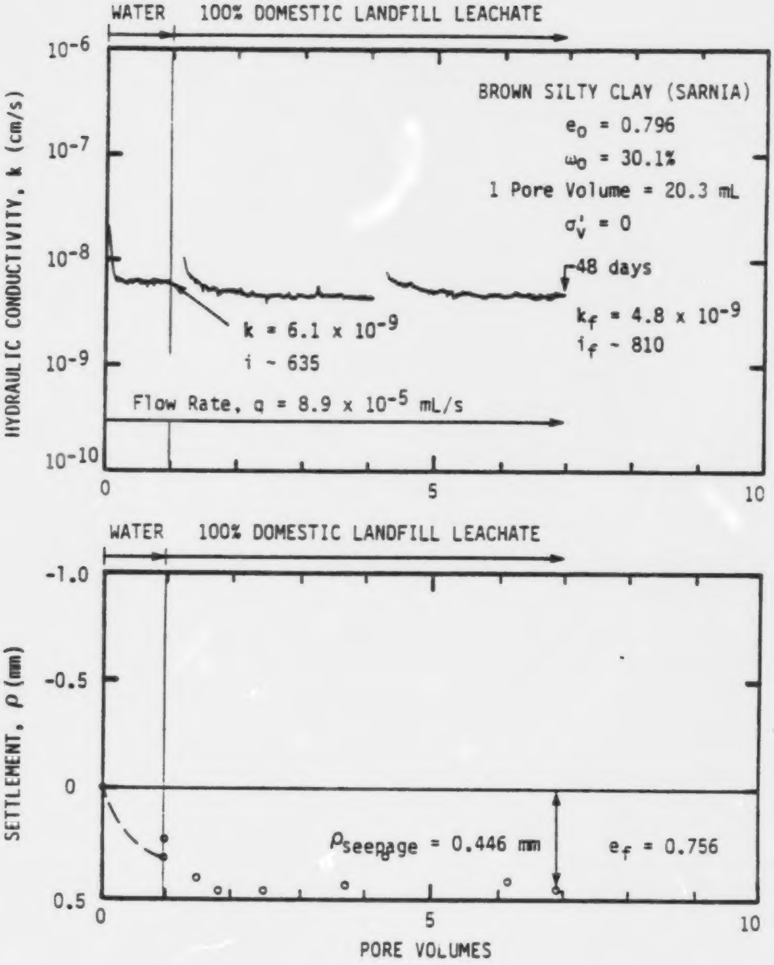

FIGURE E.1 HYDRAULIC CONDUCTIVITY, SETTLEMENT AND EFFLUENT CHEMISTRY VS PORE VOLUMES

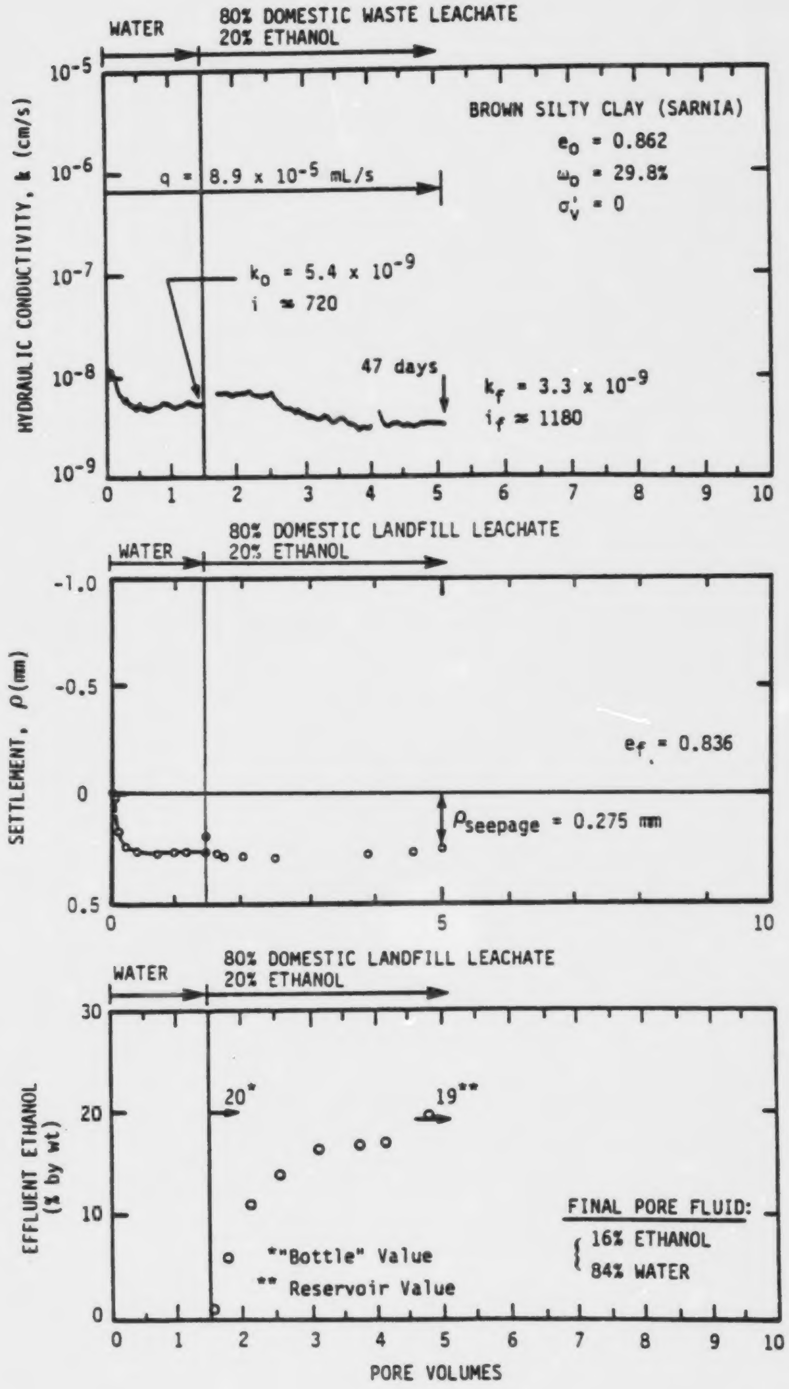

FIGURE E.2 HYDRAULIC CONDUCTIVITY, SETTLEMENT AND EFFLUENT CHEMISTRY VS PORE VOLUMES

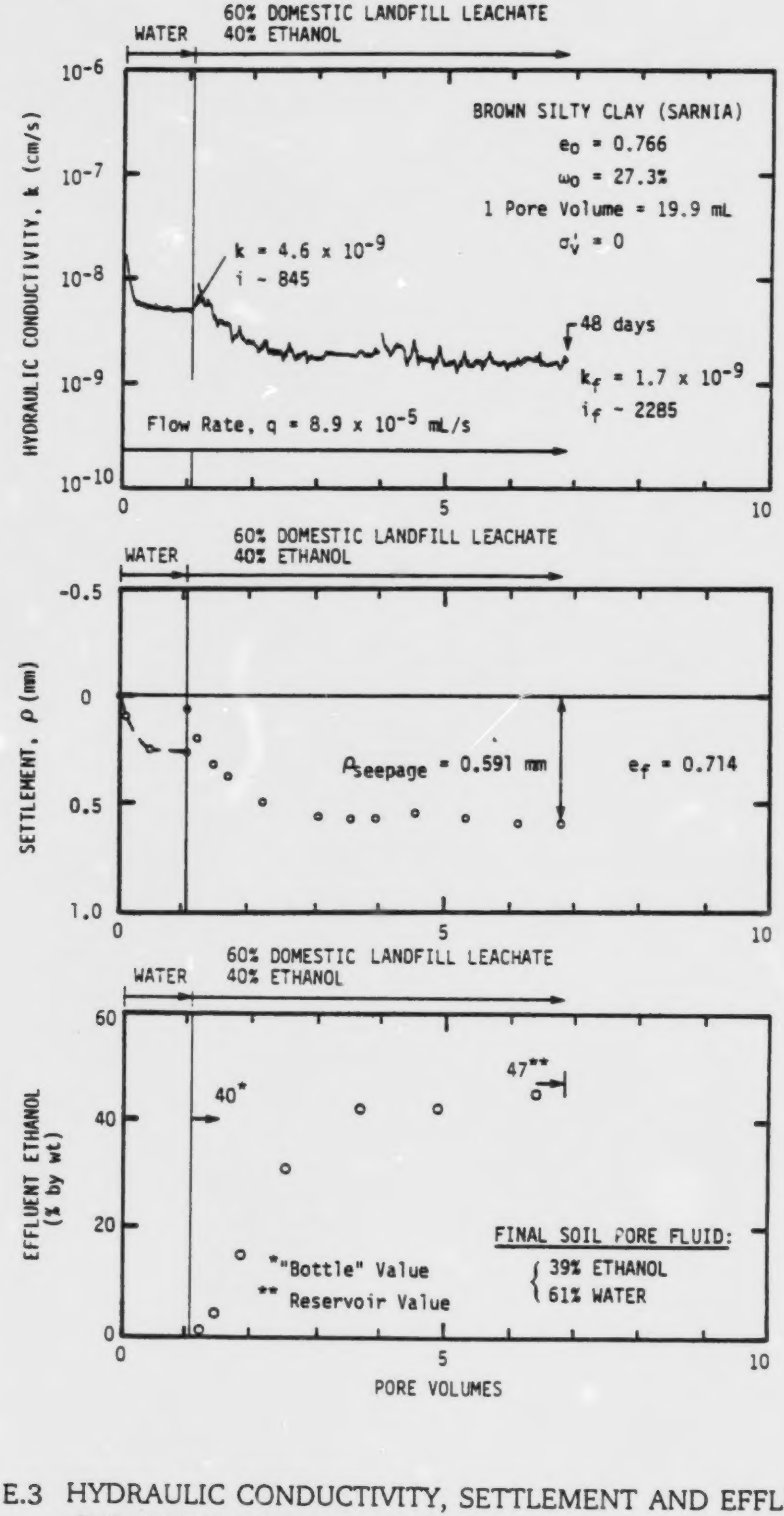

FIGURE E.3 HYDRAULIC CONDUCTIVITY, SETTLEMENT AND EFFLUENT CHEMISTRY VS PORE VOLUMES

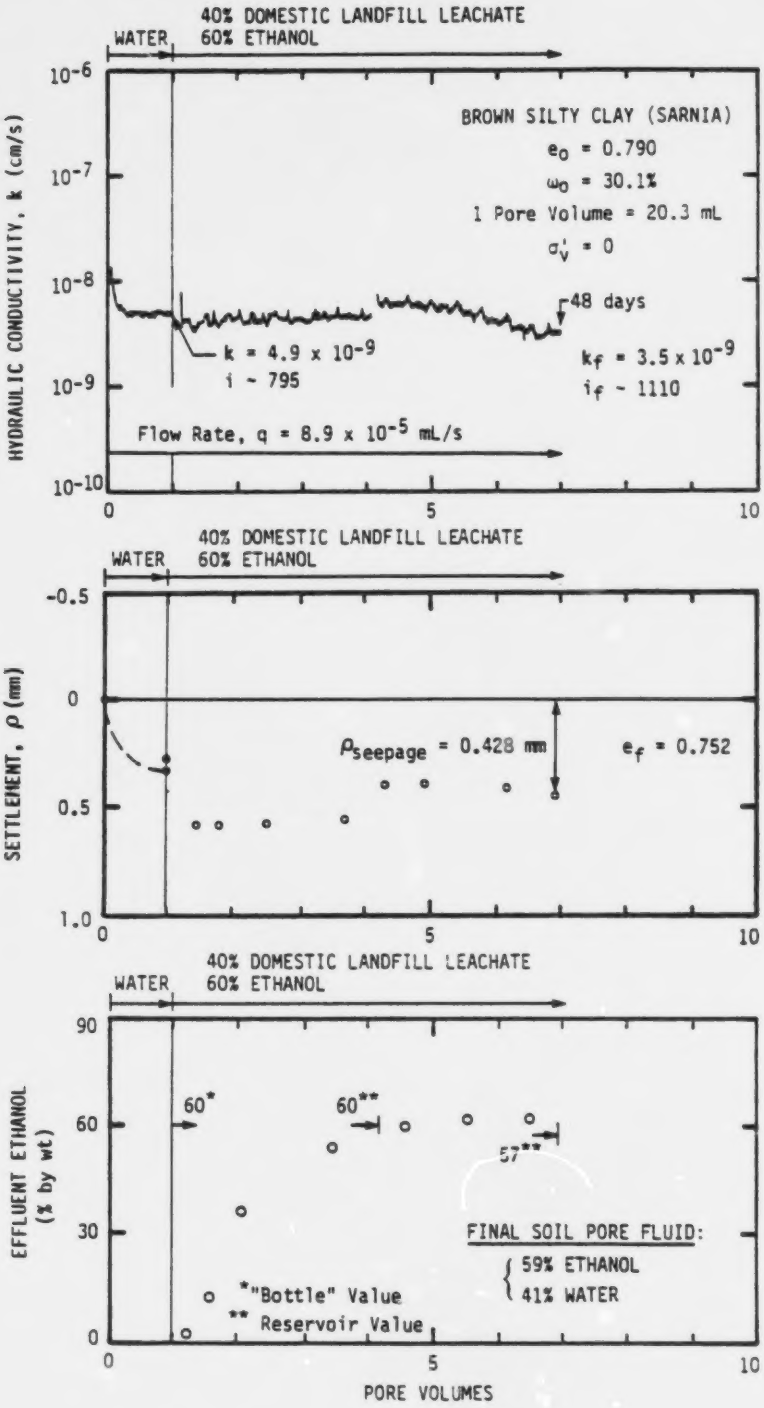

FIGURE E.4 HYDRAULIC CONDUCTIVITY, SETTLEMENT AND EFFLUENT CHEMISTRY VS PORE VOLUMES

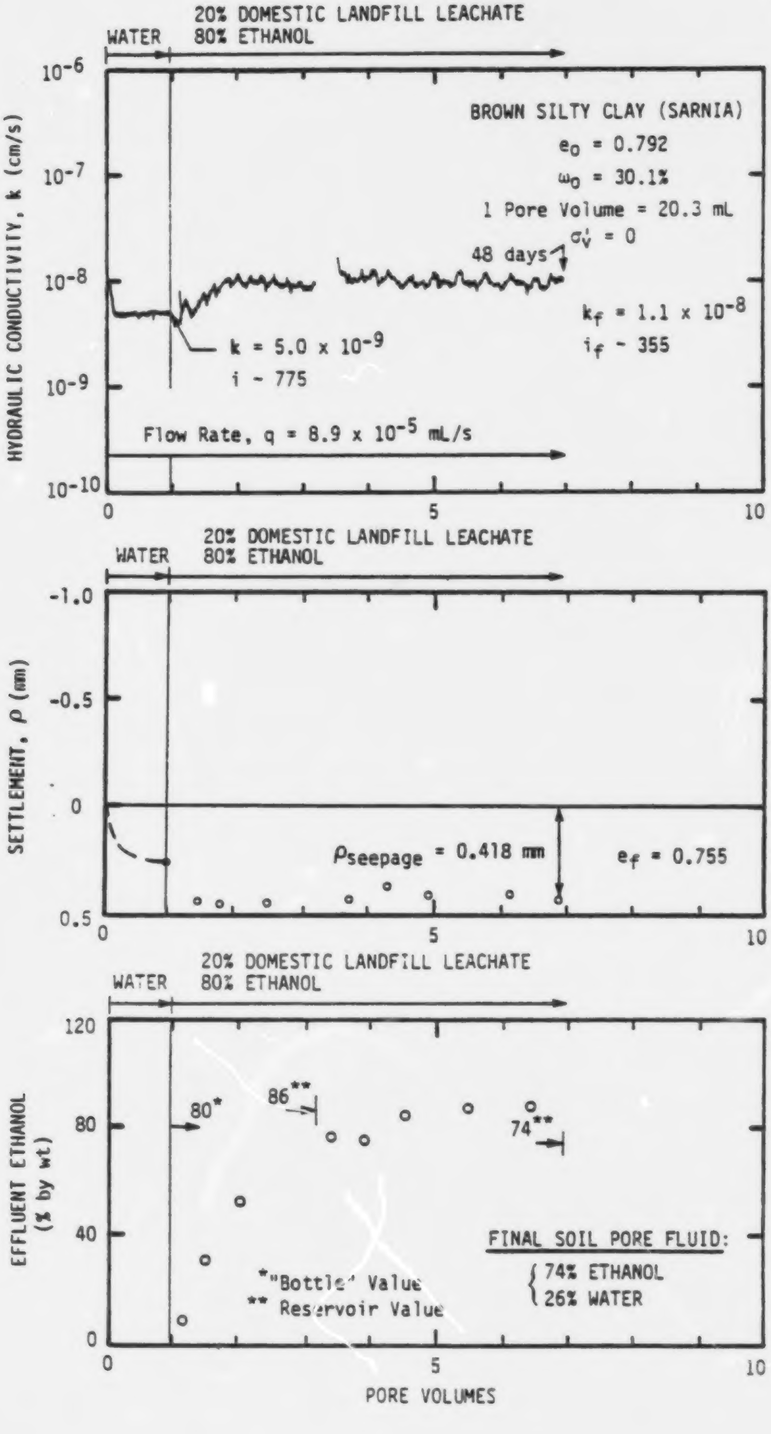

FIGURE E.5 HYDRAULIC CONDUCTIVITY, SETTLEMENT AND EFFLUENT CHEMISTRY VS PORE VOLUMES

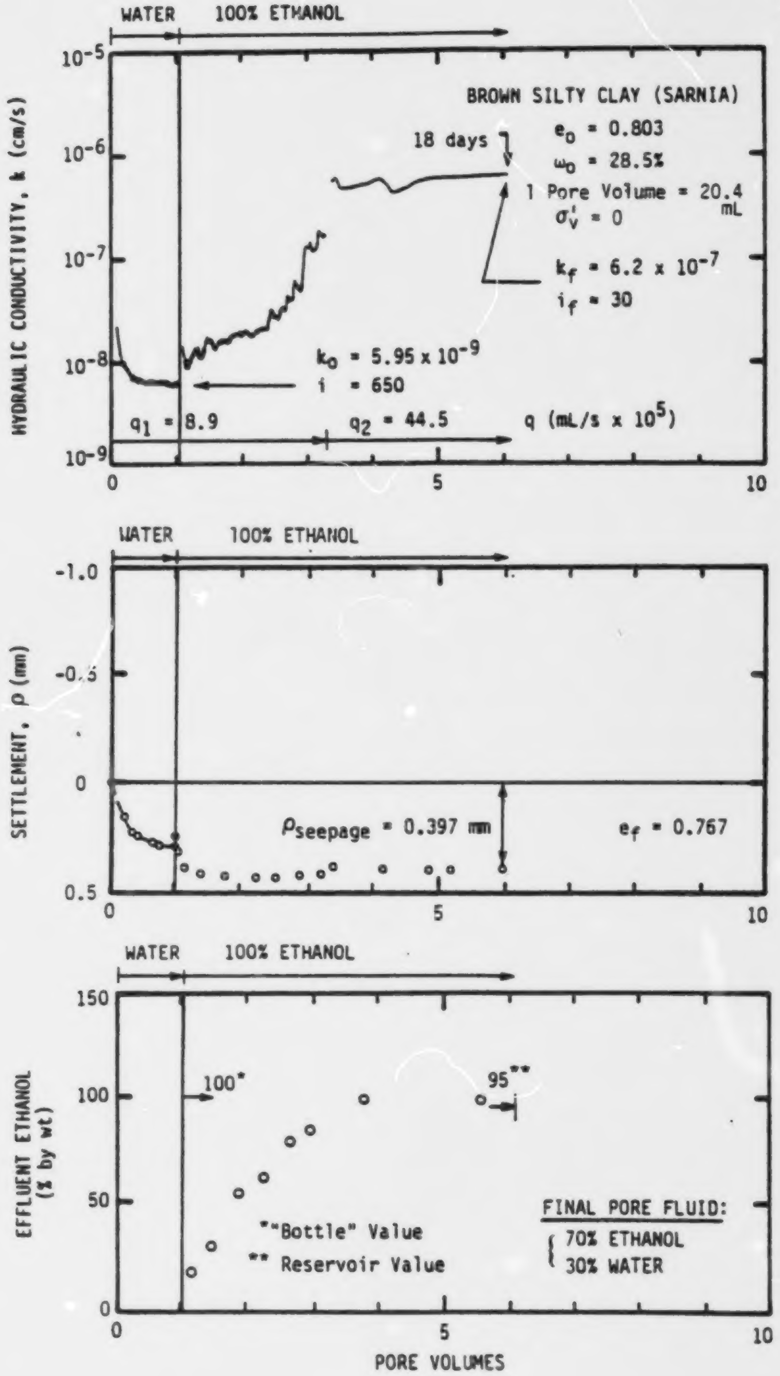

FIGURE E.6 HYDRAULIC CONDUCTIVITY, SETTLEMENT AND EFFLUENT CHEMISTRY VS PORE VOLUMES

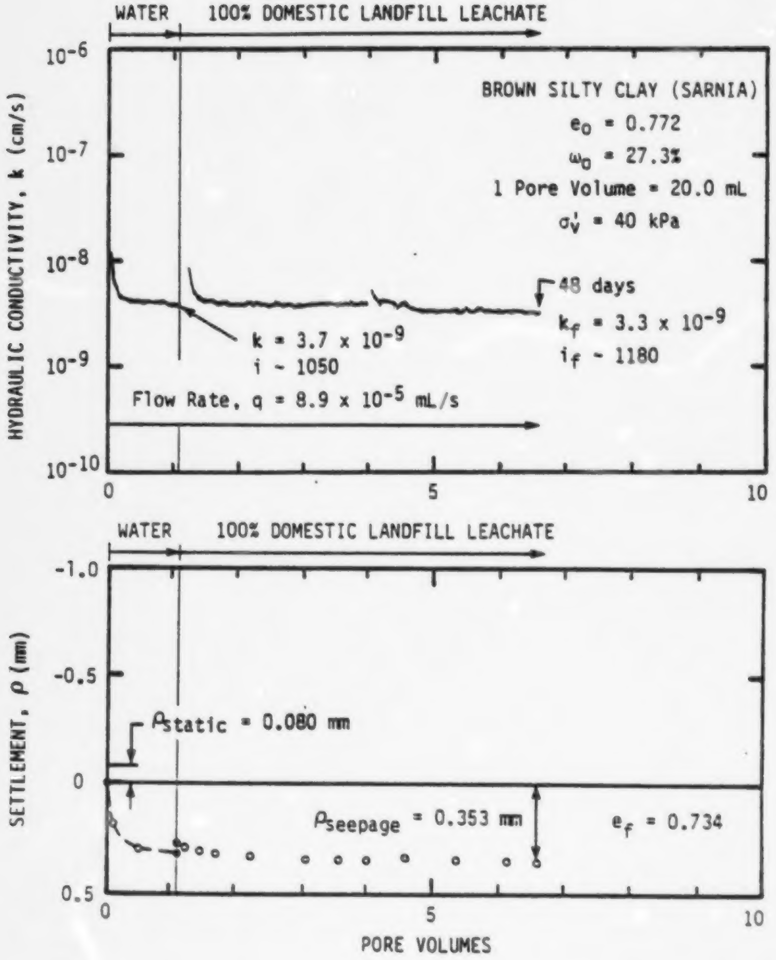

FIGURE E.7 HYDRAULIC CONDUCTIVITY, SETTLEMENT AND EFFLUENT CHEMISTRY VS PORE VOLUMES

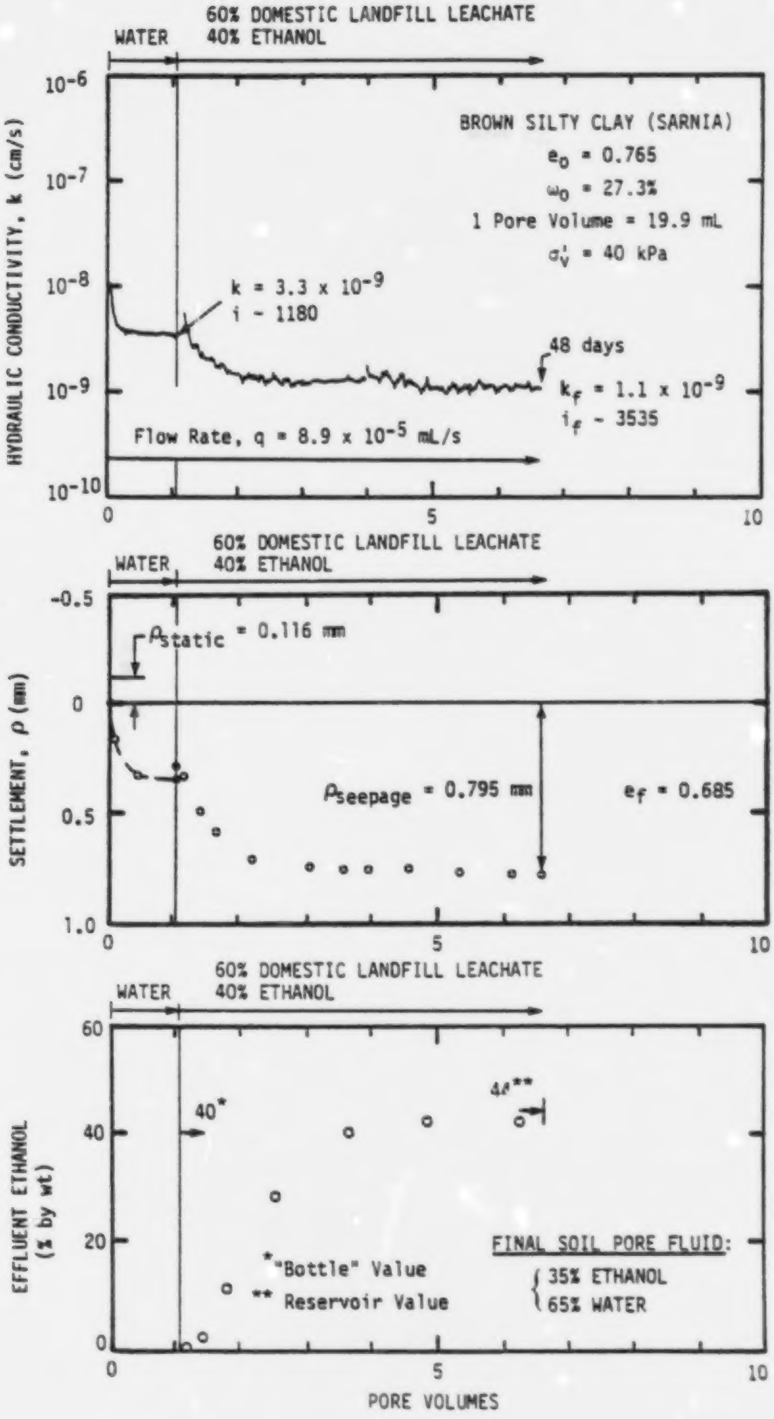

FIGURE E.8 HYDRAULIC CONDUCTIVITY, SETTLEMENT AND EFFLUENT CHEMISTRY VS PORE VOLUMES

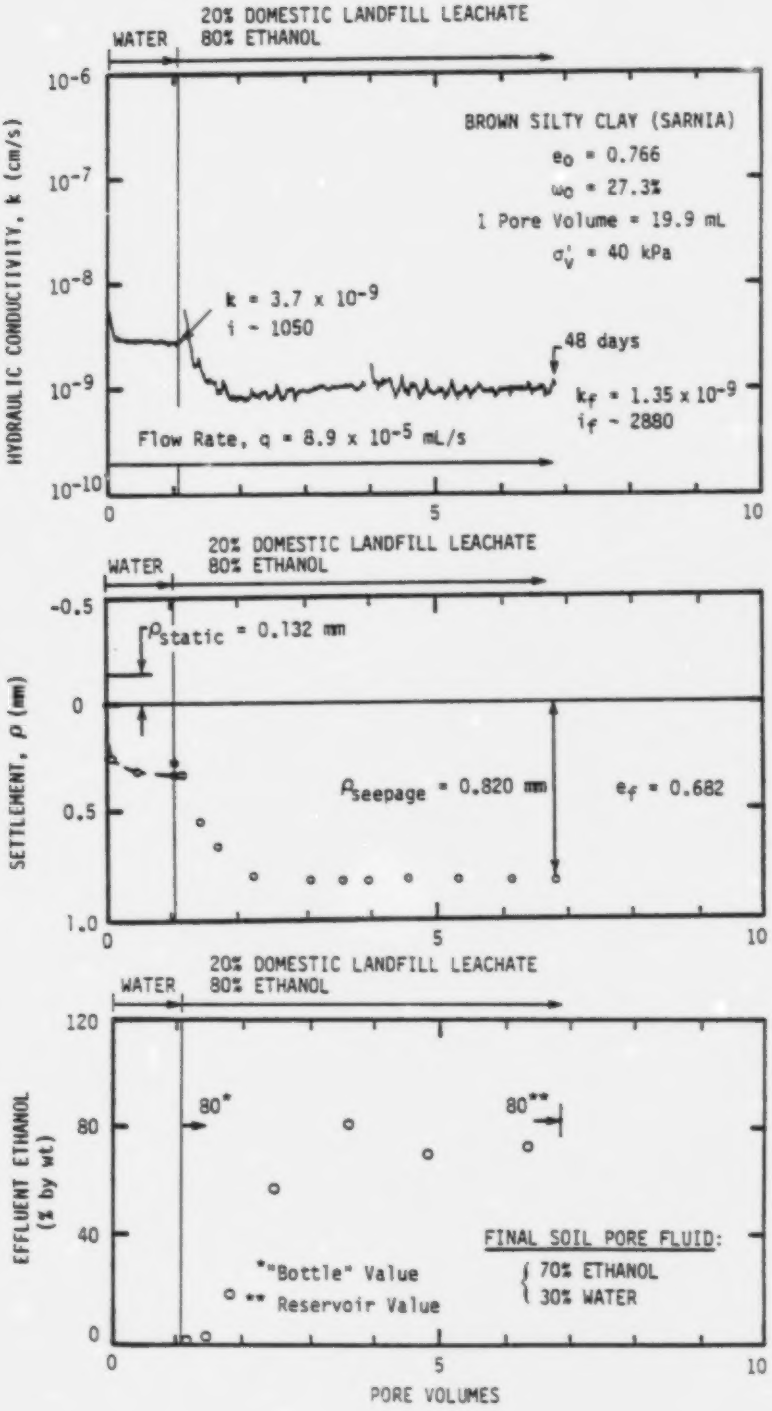

FIGURE E.9 HYDRAULIC CONDUCTIVITY, SETTLEMENT AND EFFLUENT CHEMISTRY VS PORE VOLUMES

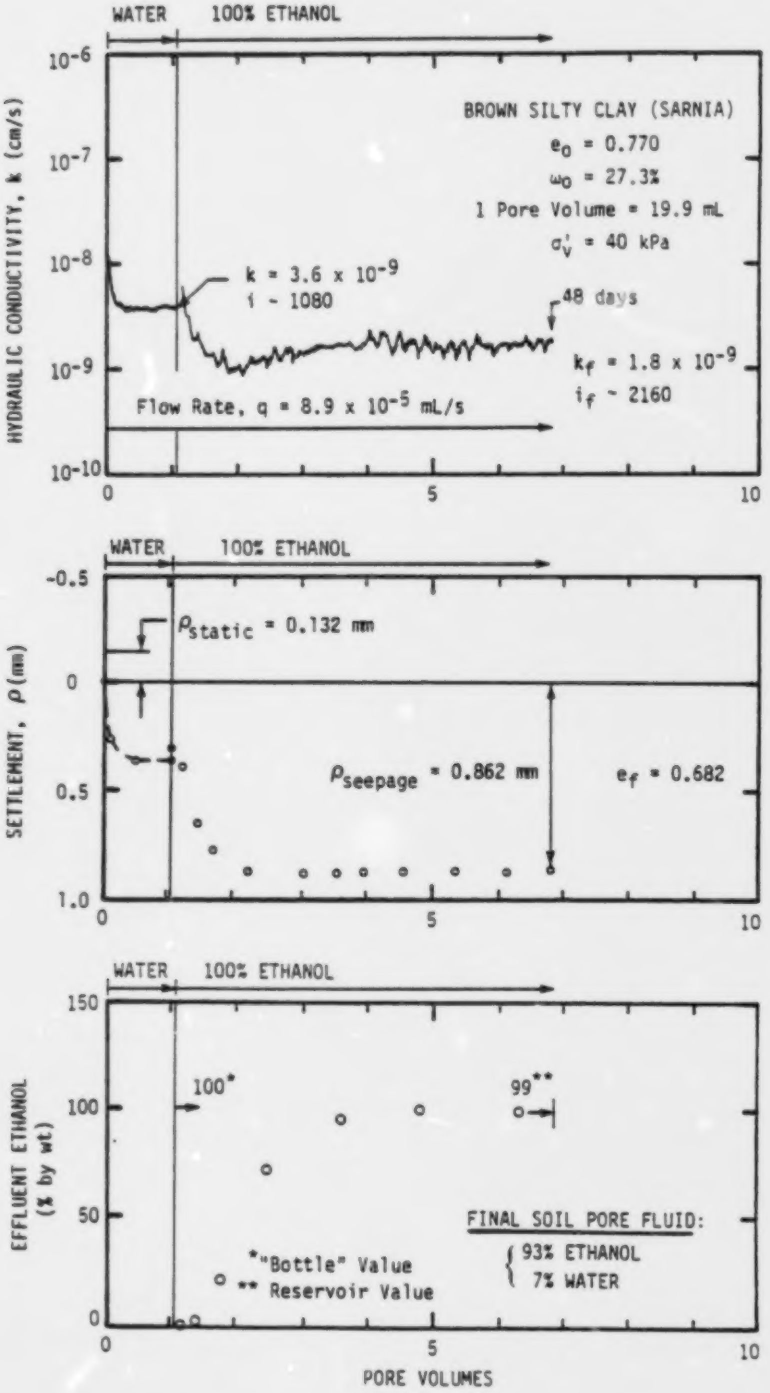

FIGURE E.10 HYDRAULIC CONDUCTIVITY, SETTLEMENT AND EFFLUENT CHEMISTRY VS PORE VOLUMES

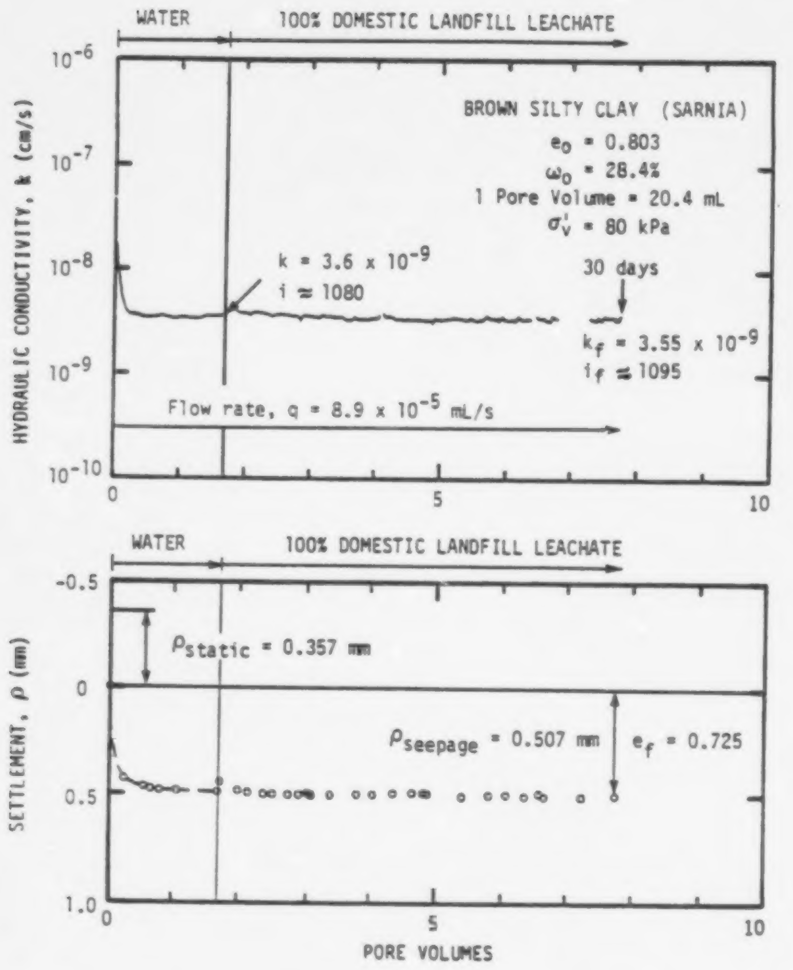

FIGURE E.11 HYDRAULIC CONDUCTIVITY, SETTLEMENT AND EFFLUENT CHEMISTRY VS PORE VOLUMES

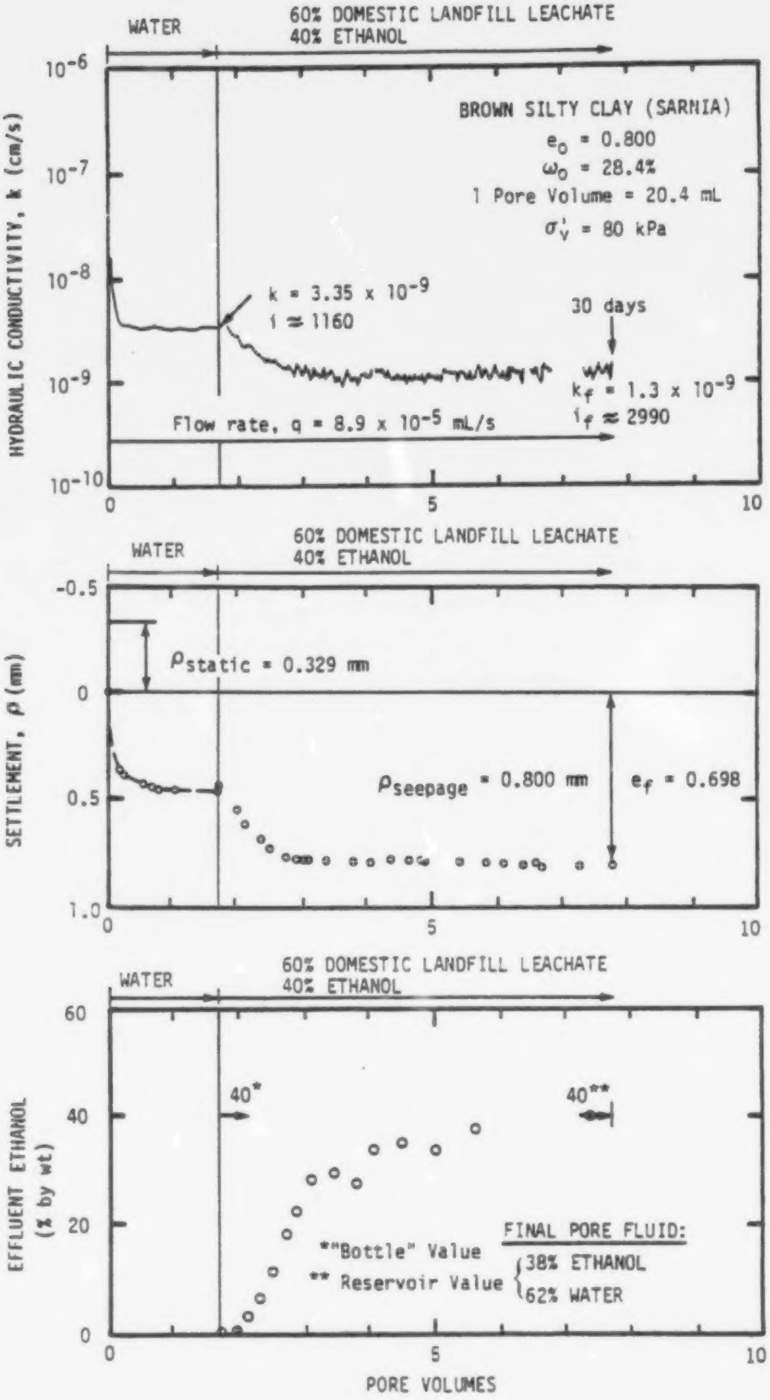

FIGURE E.12 HYDRAULIC CONDUCTIVITY, SETTLEMENT AND EFFLUENT CHEMISTRY VS PORE VOLUMES

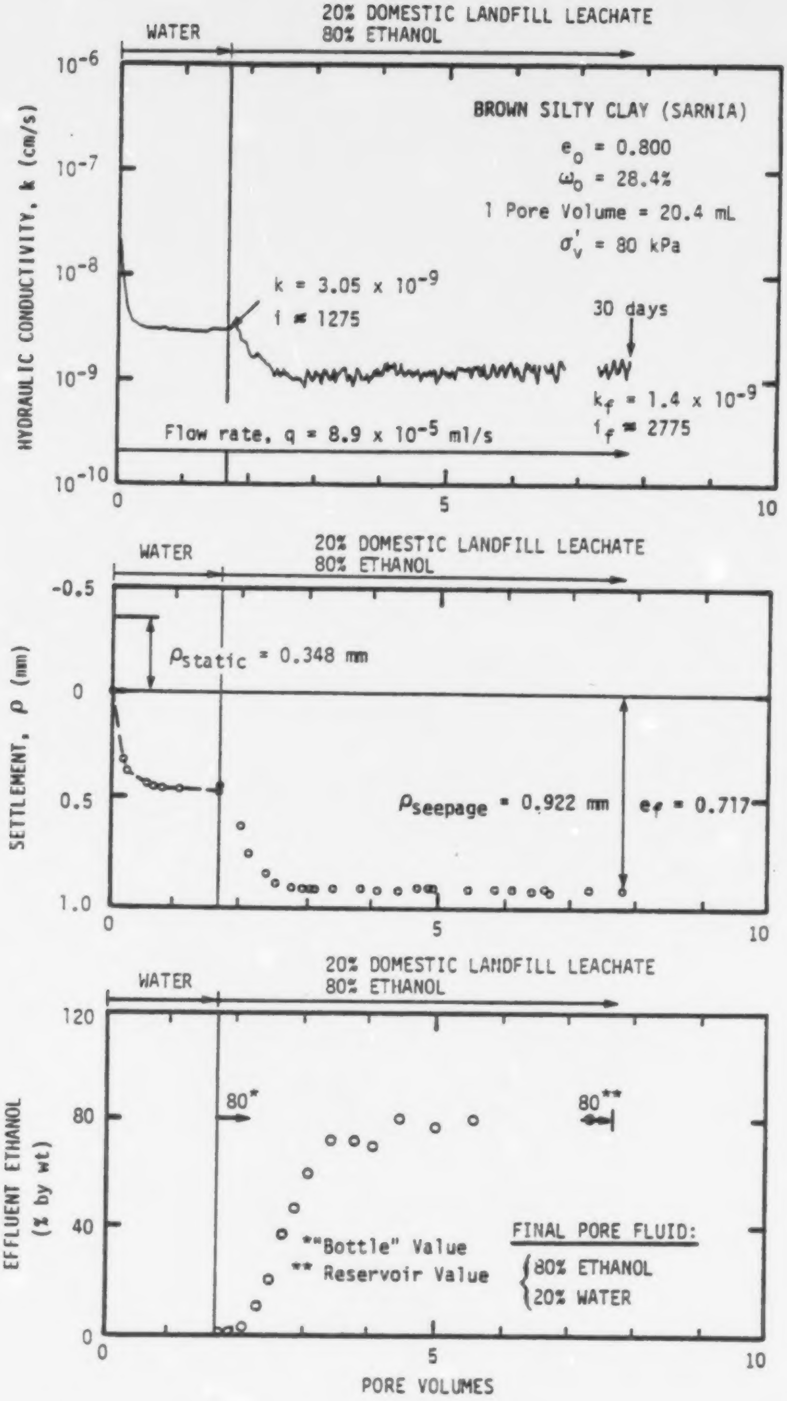

FIGURE E.13 HYDRAULIC CONDUCTIVITY, SETTLEMENT AND EFFLUENT CHEMISTRY VS PORE VOLUMES

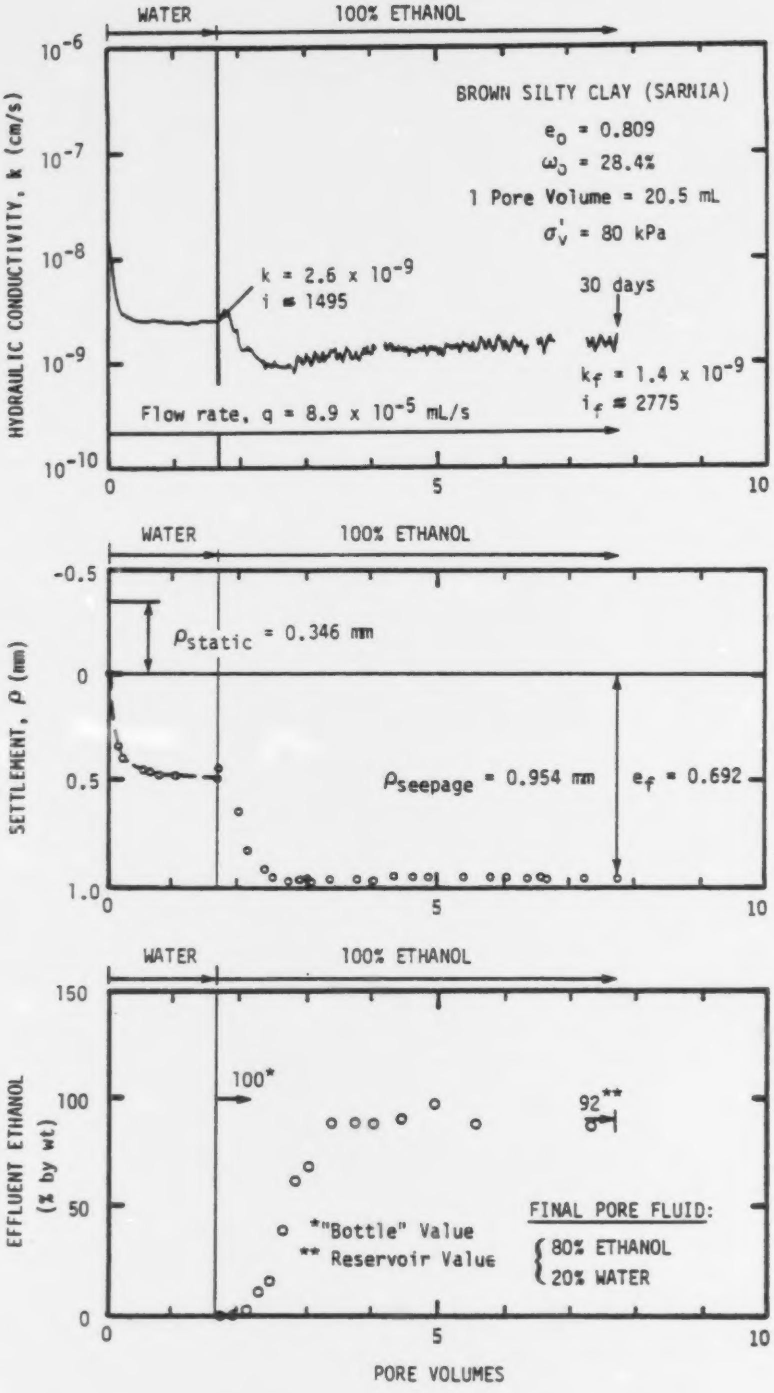

FIGURE E.14 HYDRAULIC CONDUCTIVITY, SETTLEMENT AND EFFLUENT CHEMISTRY VS PORE VOLUMES

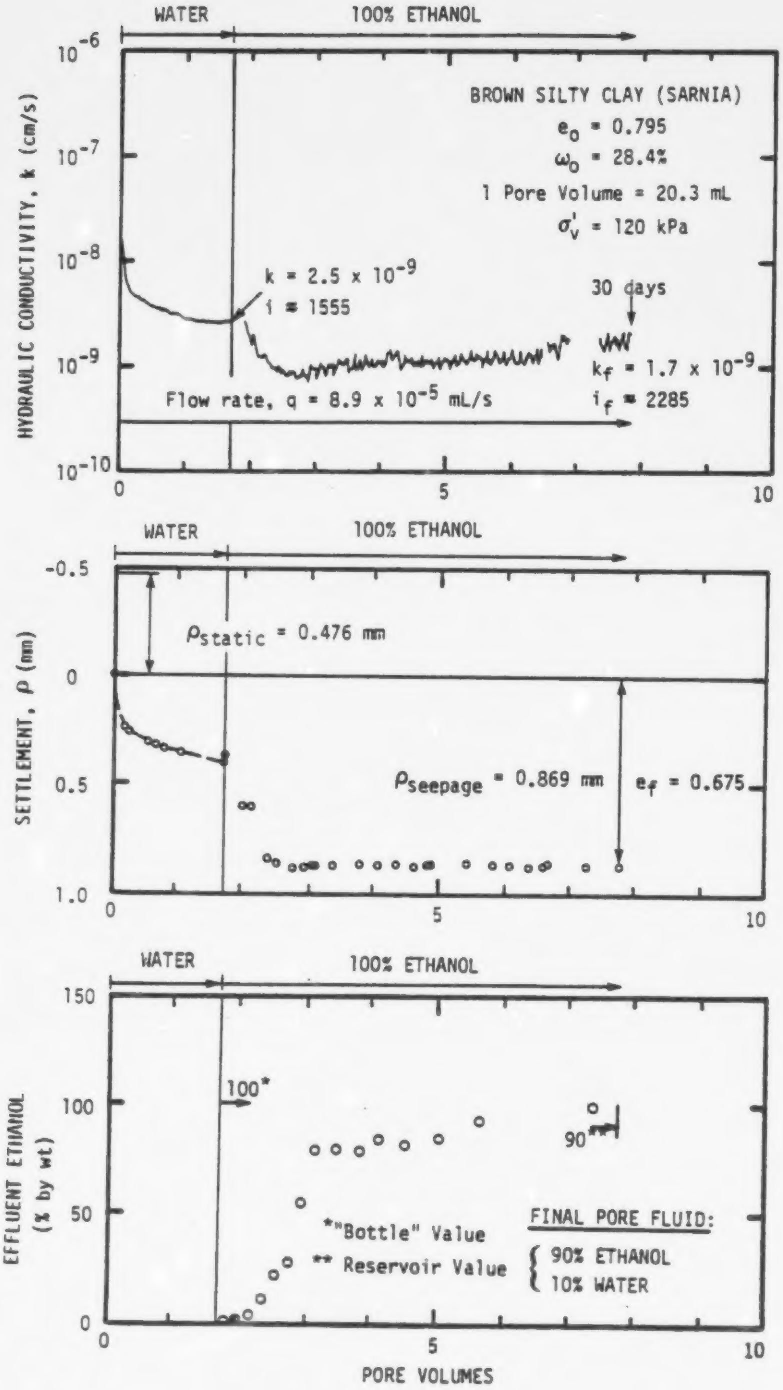

FIGURE E.15 HYDRAULIC CONDUCTIVITY, SETTLEMENT AND EFFLUENT CHEMISTRY VS PORE VOLUMES

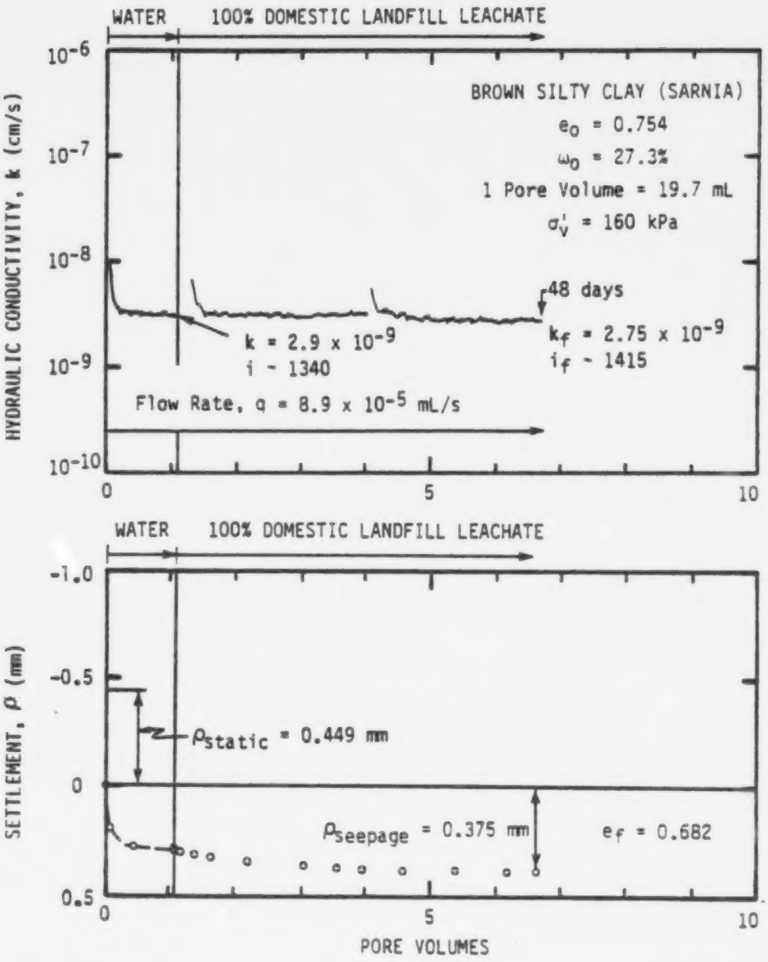

FIGURE E.16 HYDRAULIC CONDUCTIVITY, SETTLEMENT AND EFFLUENT CHEMISTRY VS PORE VOLUMES

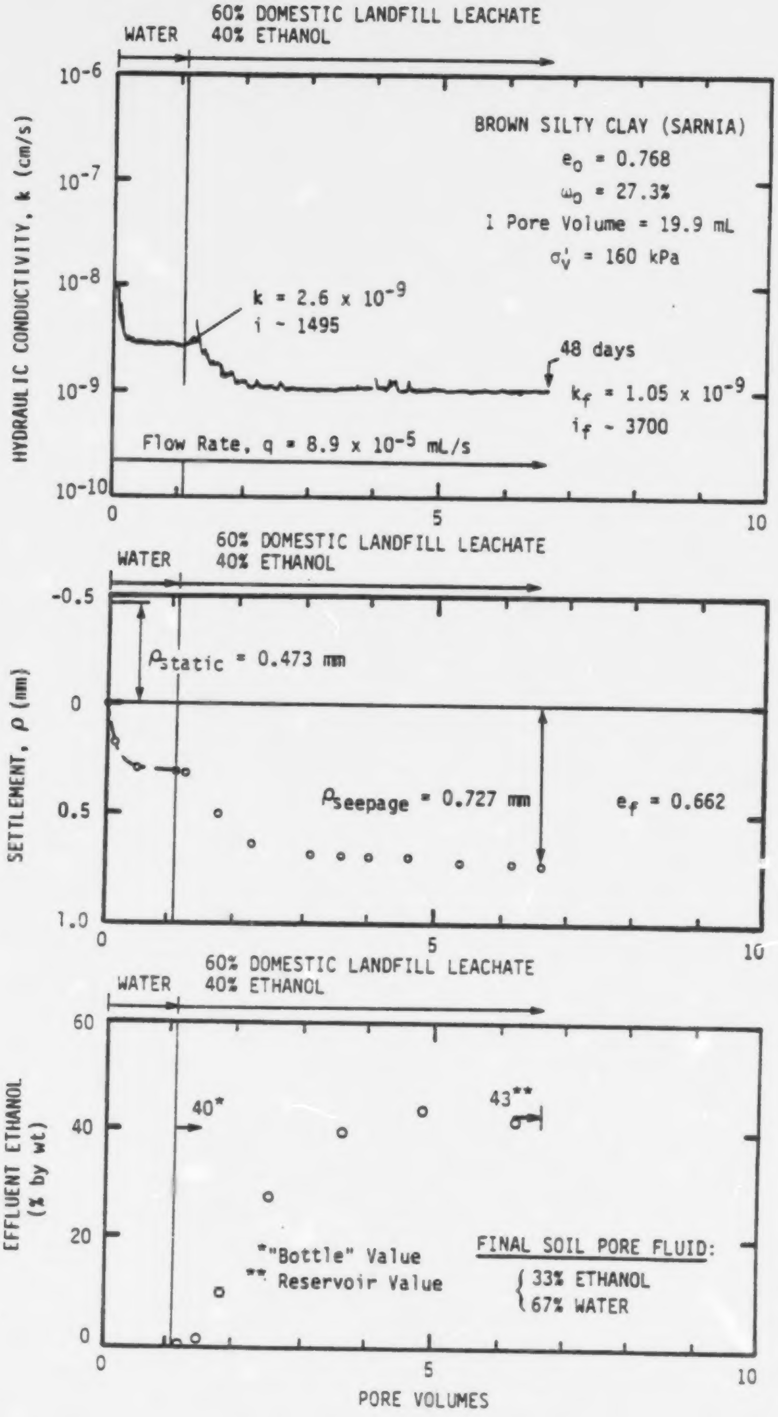

FIGURE E.17 HYDRAULIC CONDUCTIVITY, SETTLEMENT AND EFFLUENT CHEMISTRY VS PORE VOLUMES

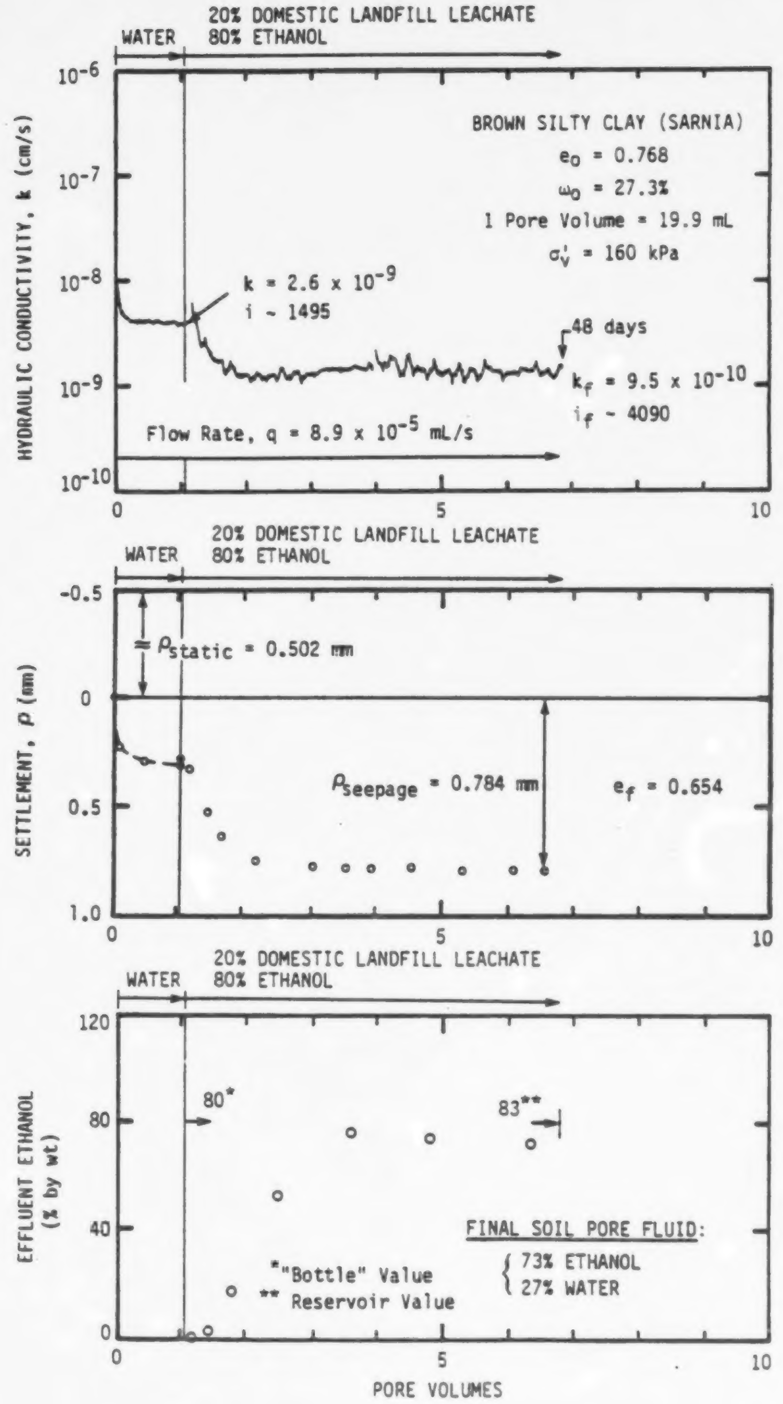

FIGURE E.18 HYDRAULIC CONDUCTIVITY, SETTLEMENT AND EFFLUENT CHEMISTRY VS PORE VOLUMES

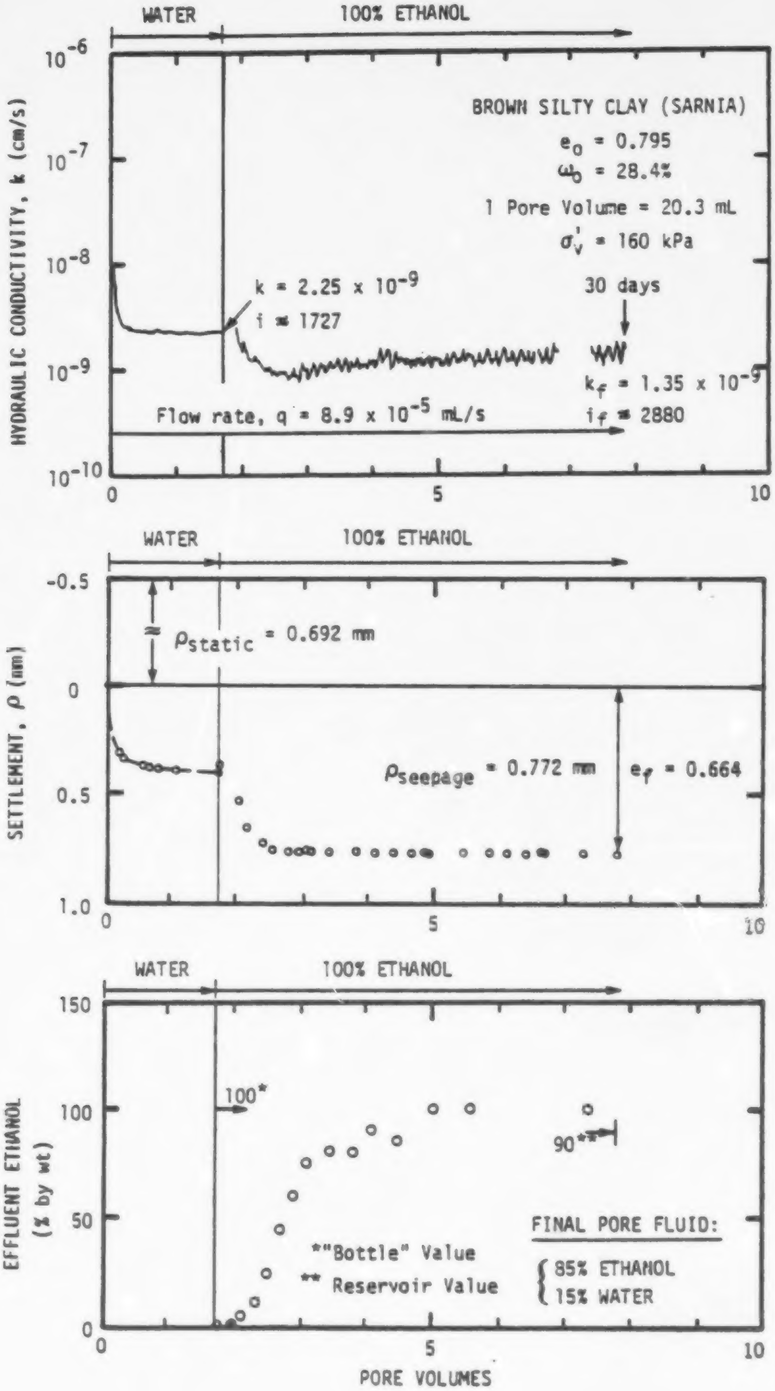

FIGURE E.19 HYDRAULIC CONDUCTIVITY, SETTLEMENT AND EFFLUENT CHEMISTRY VS PORE VOLUMES

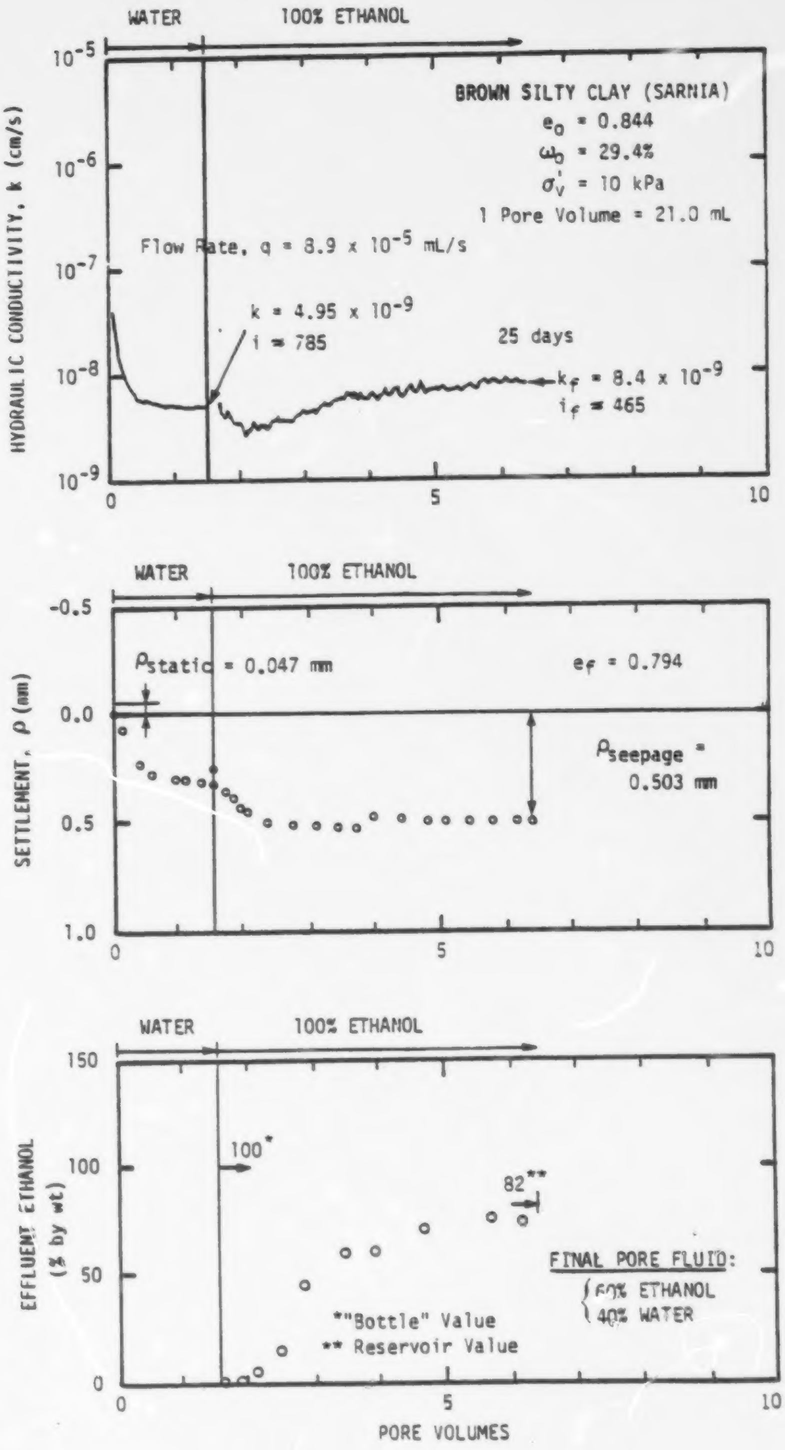

FIGURE E.20 HYDRAULIC CONDUCTIVITY, SETTLEMENT AND EFFLUENT CHEMISTRY VS PORE VOLUMES

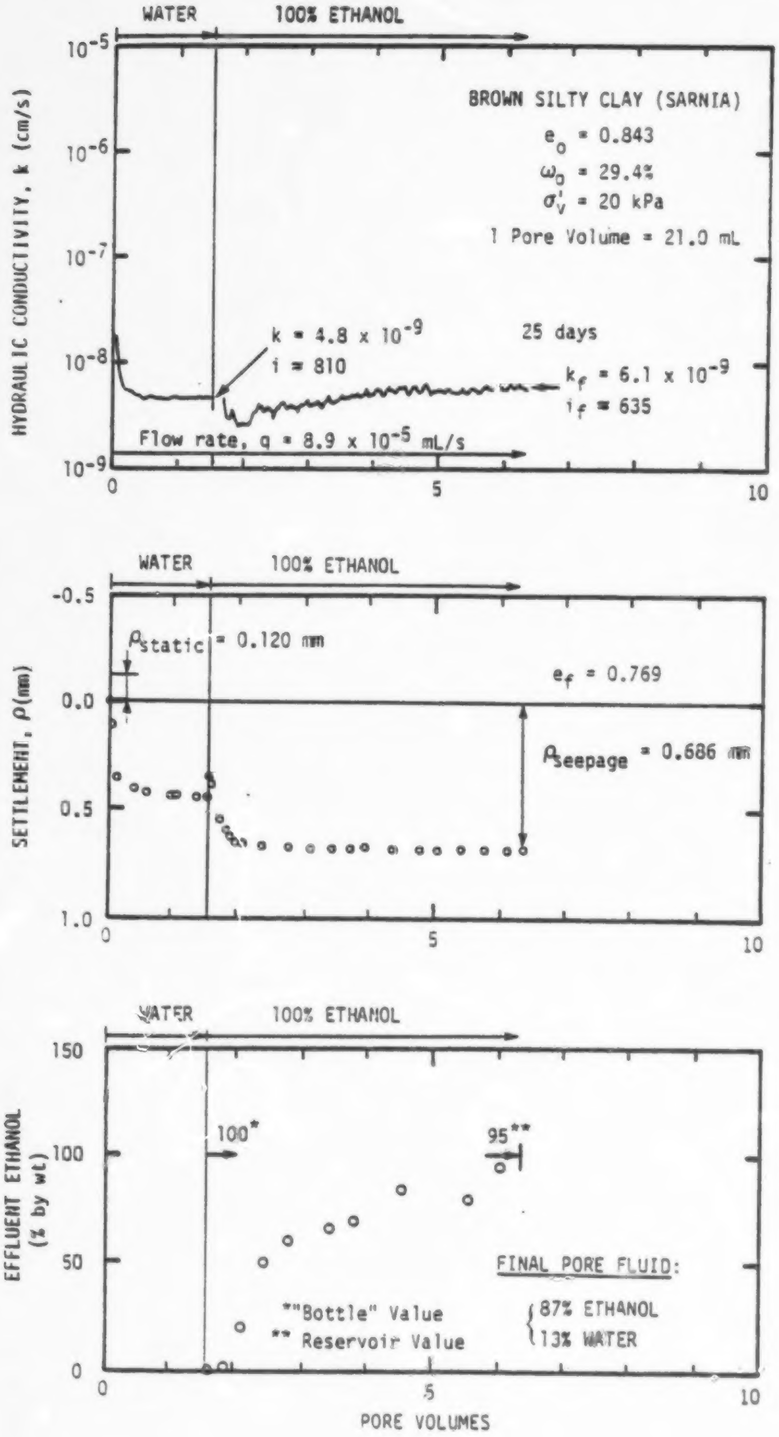

FIGURE E.21 HYDRAULIC CONDUCTIVITY, SETTLEMENT AND EFFLUENT CHEMISTRY VS PORE VOLUMES

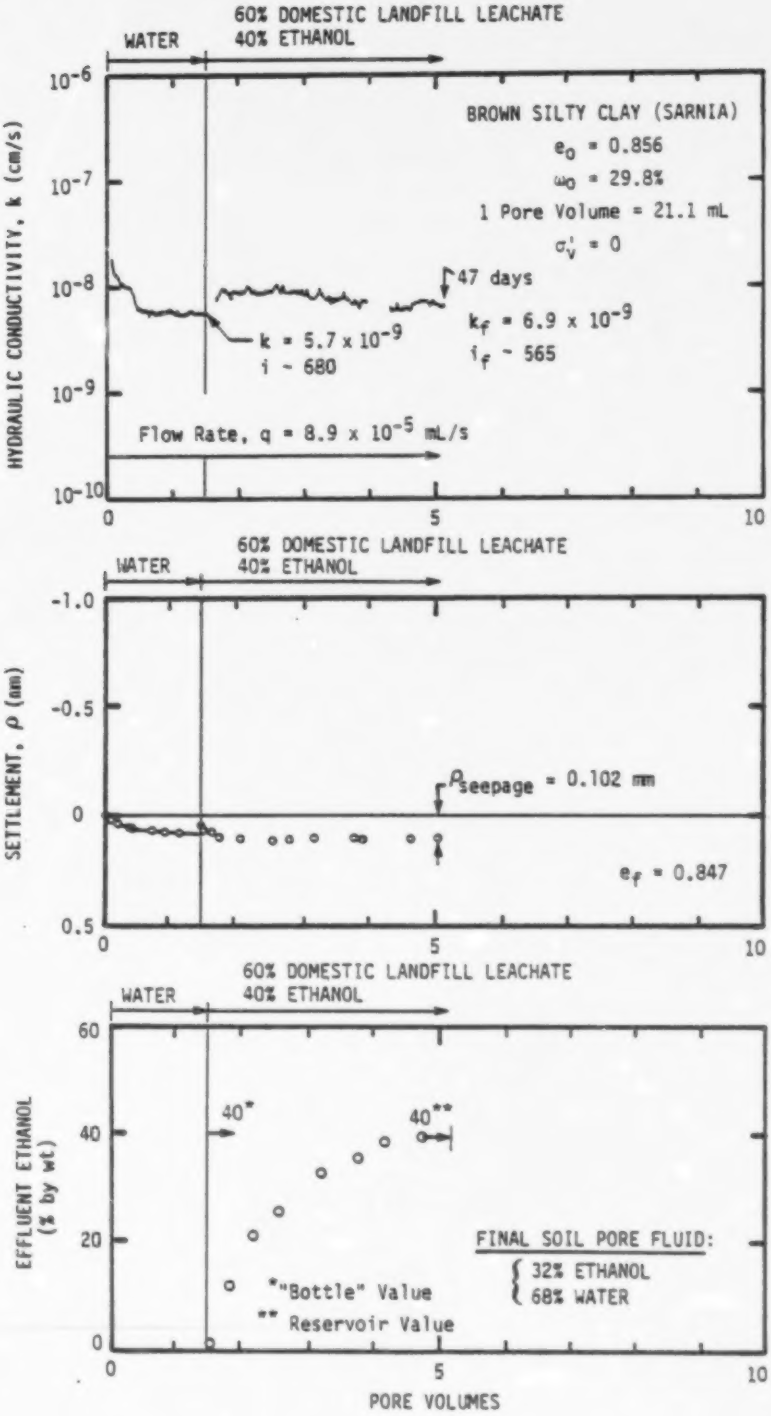

FIGURE E.22 HYDRAULIC CONDUCTIVITY, SETTLEMENT AND EFFLUENT CHEMISTRY VS PORE VOLUMES

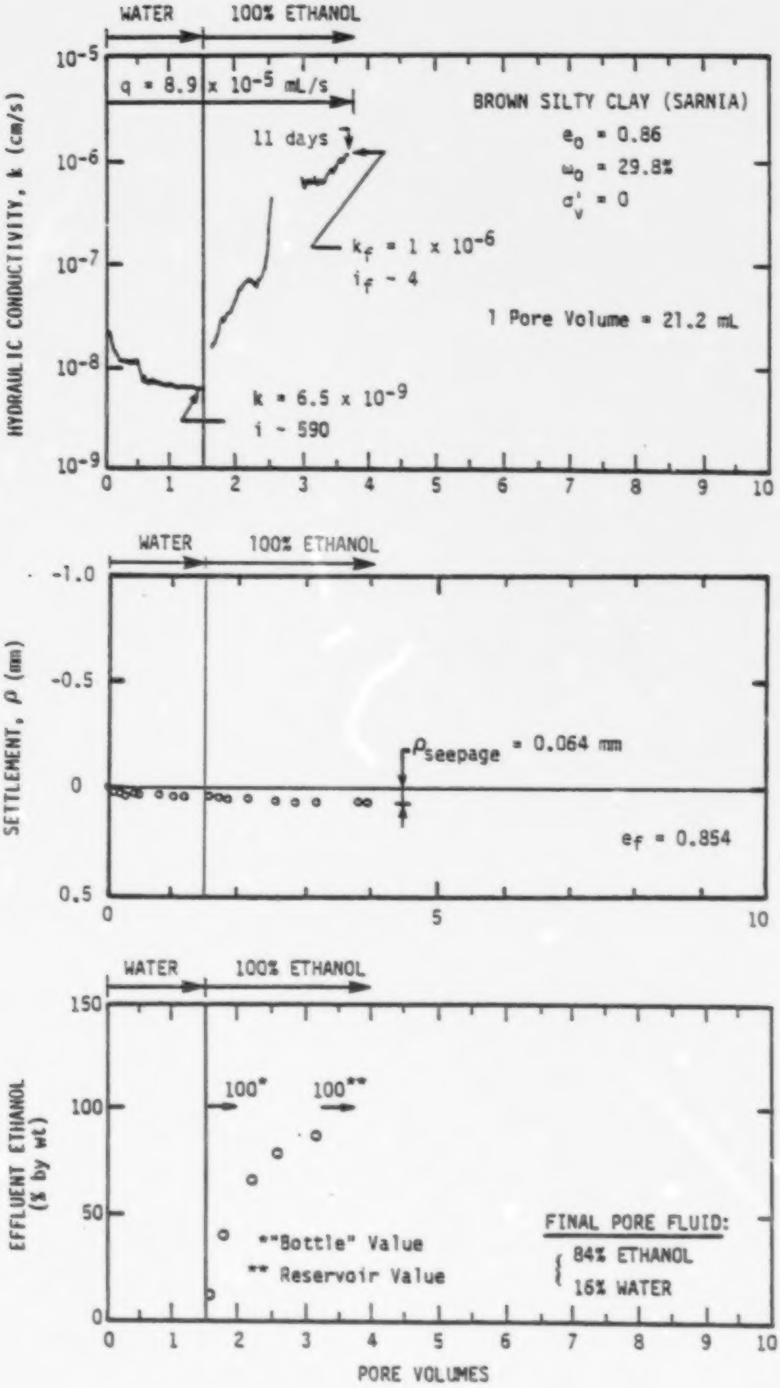

FIGURE E.23 HYDRAULIC CONDUCTIVITY, SETTLEMENT AND EFFLUENT CHEMISTRY VS PORE VOLUMES

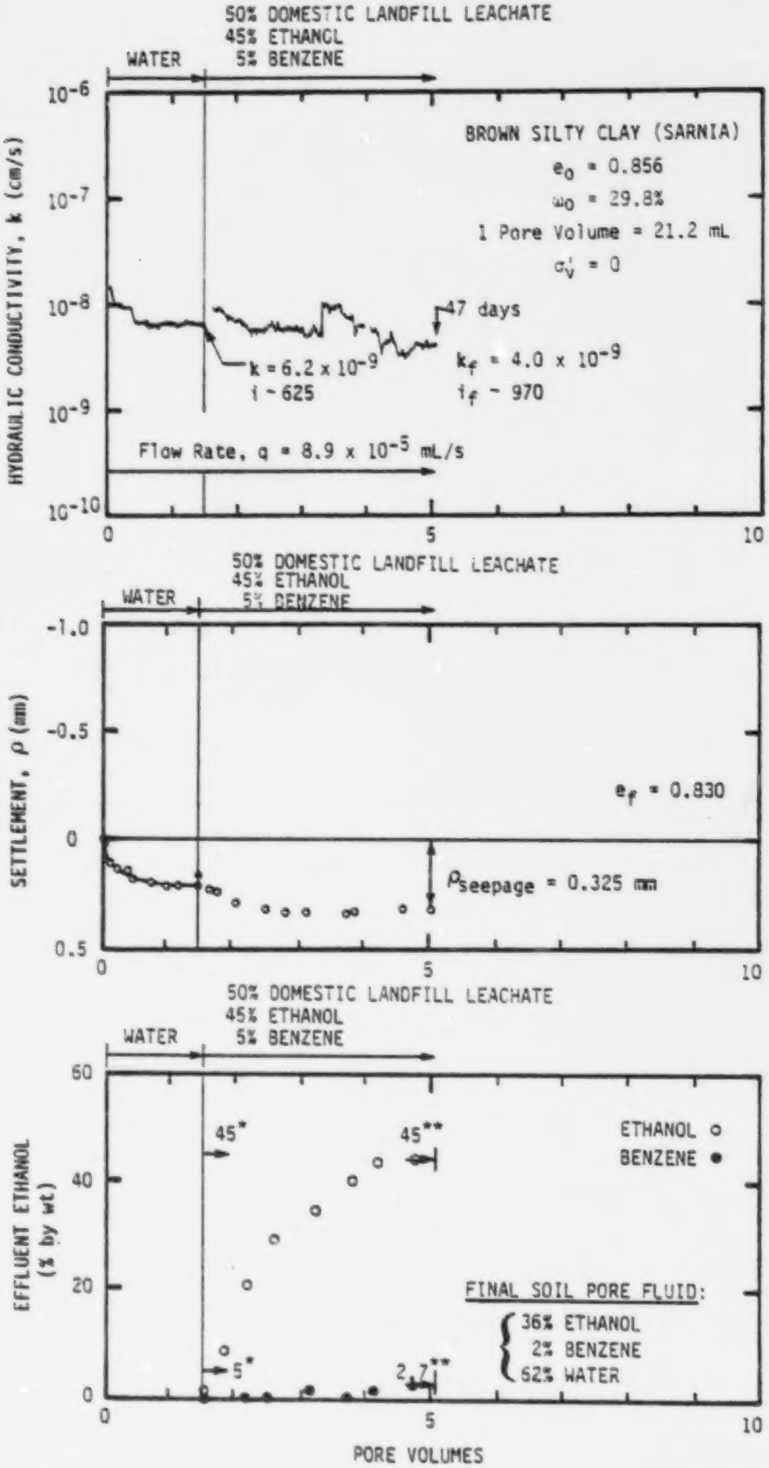

FIGURE E.24 HYDRAULIC CONDUCTIVITY, SETTLEMENT AND EFFLUENT CHEMISTRY VS PORE VOLUMES

APPENDIX F

HYDRAULIC CONDUCTIVITY CURVES FOR WATER-COMPACTED BROWN SARNIA CLAY PERMEATED WITH LEACHATE/DIOXANE MIXTURES

This figures presented in this appendix describe the results of hydraulic conductivity, settlement and effluent composition for tests performed on water-compacted brown Sarnia clays permeated with leachate/dioxane mixtures at the following static effective stresses: σ'_v = 0 kPa (Figures F.1 to F.6), σ'_v = 40 kPa (Figures F.7 to F.9), σ'_v = 80 kPa (Figures F.10 to F.12), σ'_v = 120 kPa (Figure F.13) and σ'_v = 160 kPa (Figures F.14 to F.16).

The test results are discussed in Section 5.3.2 of this report.

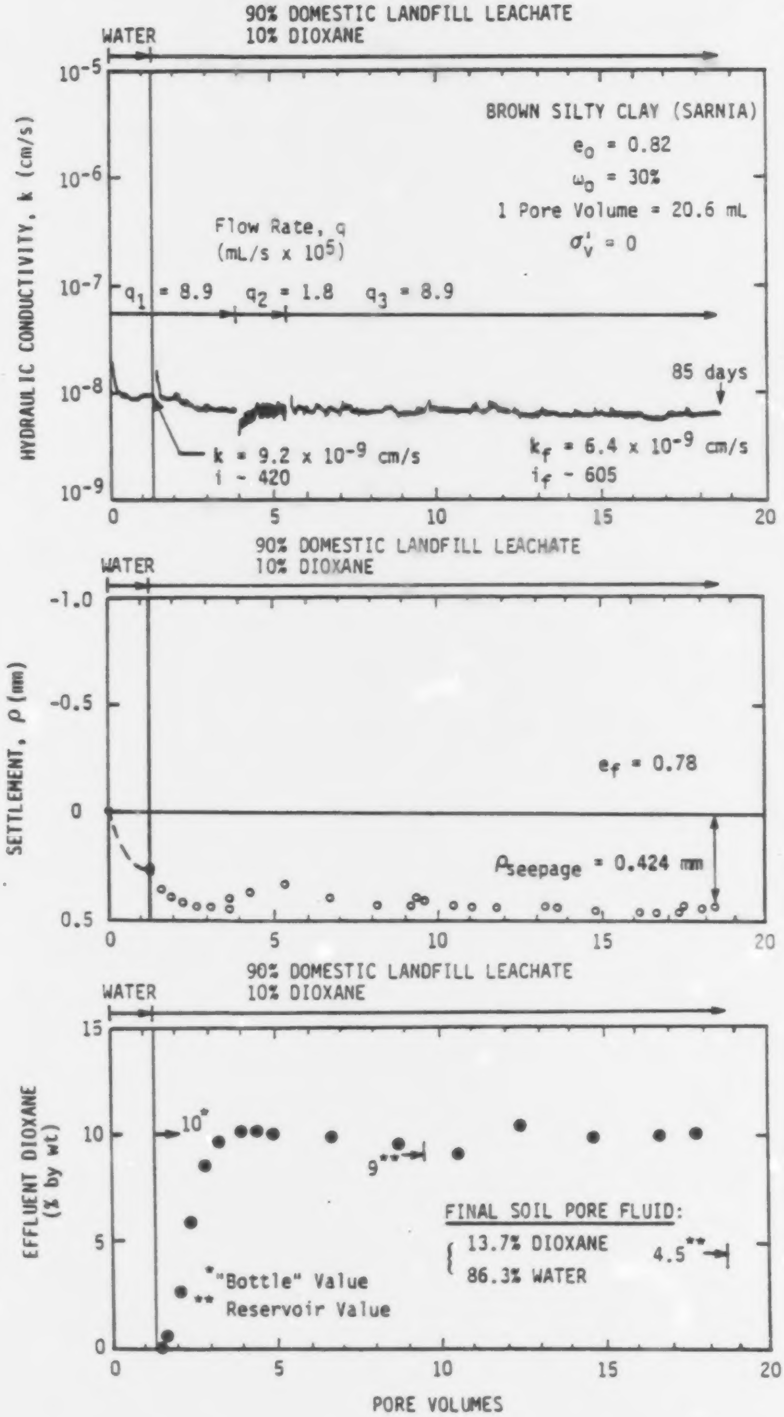

FIGURE F.1 HYDRAULIC CONDUCTIVITY, SETTLEMENT AND EFFLUENT CHEMISTRY VS PORE VOLUMES

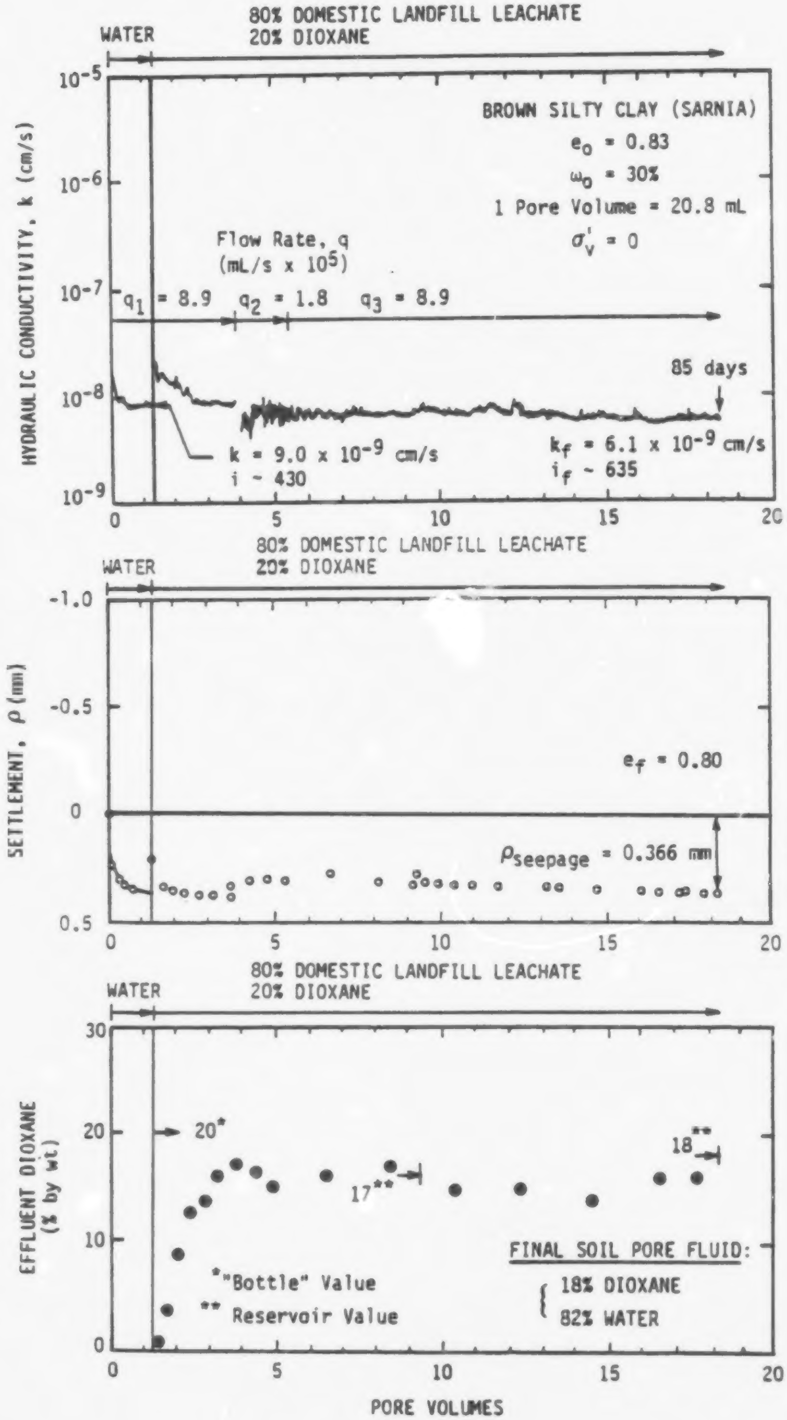

FIGURE F.2 HYDRAULIC CONDUCTIVITY, SETTLEMENT AND EFFLUENT CHEMISTRY VS PORE VOLUMES

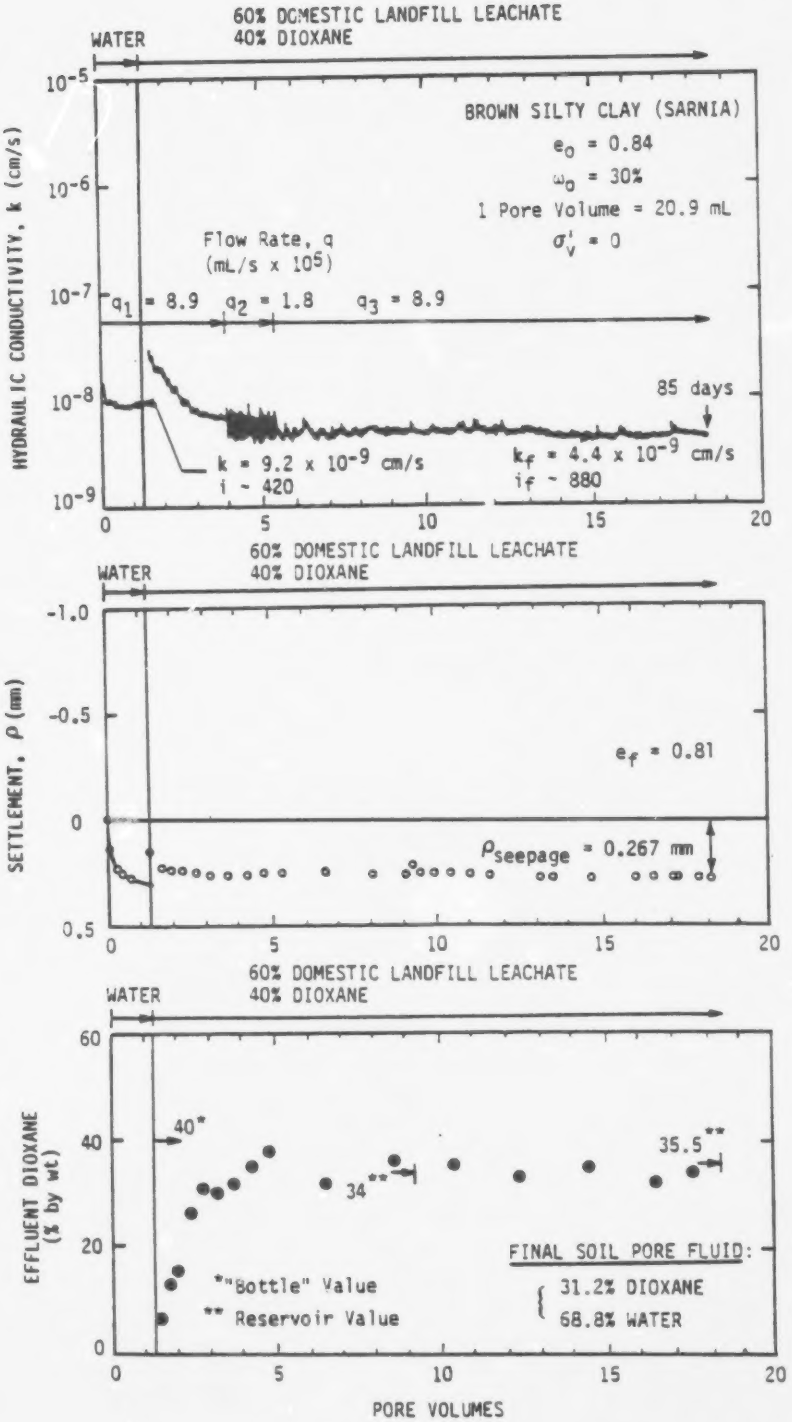

FIGURE F.3 HYDRAULIC CONDUCTIVITY, SETTLEMENT AND EFFLUENT CHEMISTRY VS PORE VOLUMES

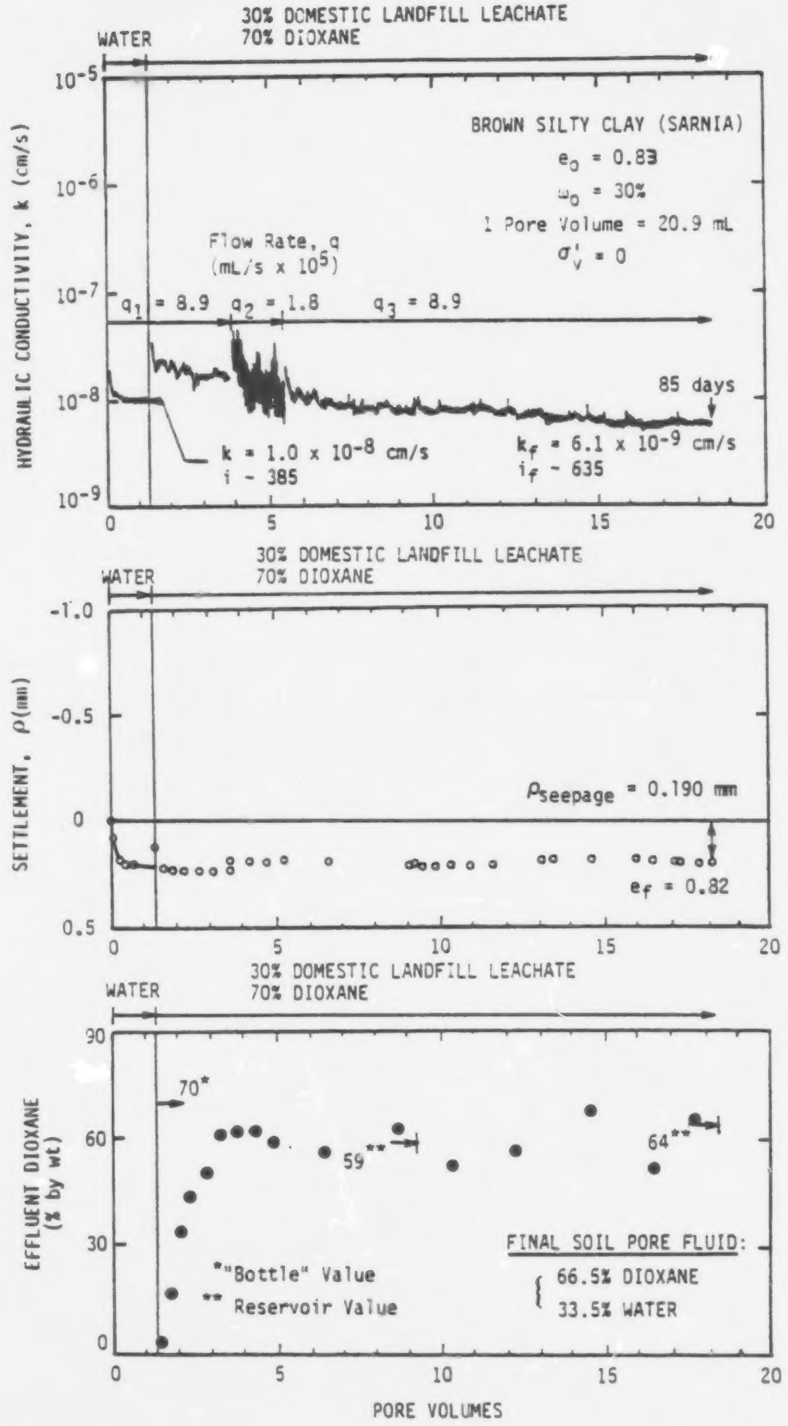

FIGURE F.4 HYDRAULIC CONDUCTIVITY, SETTLEMENT AND EFFLUENT CHEMISTRY VS PORE VOLUMES

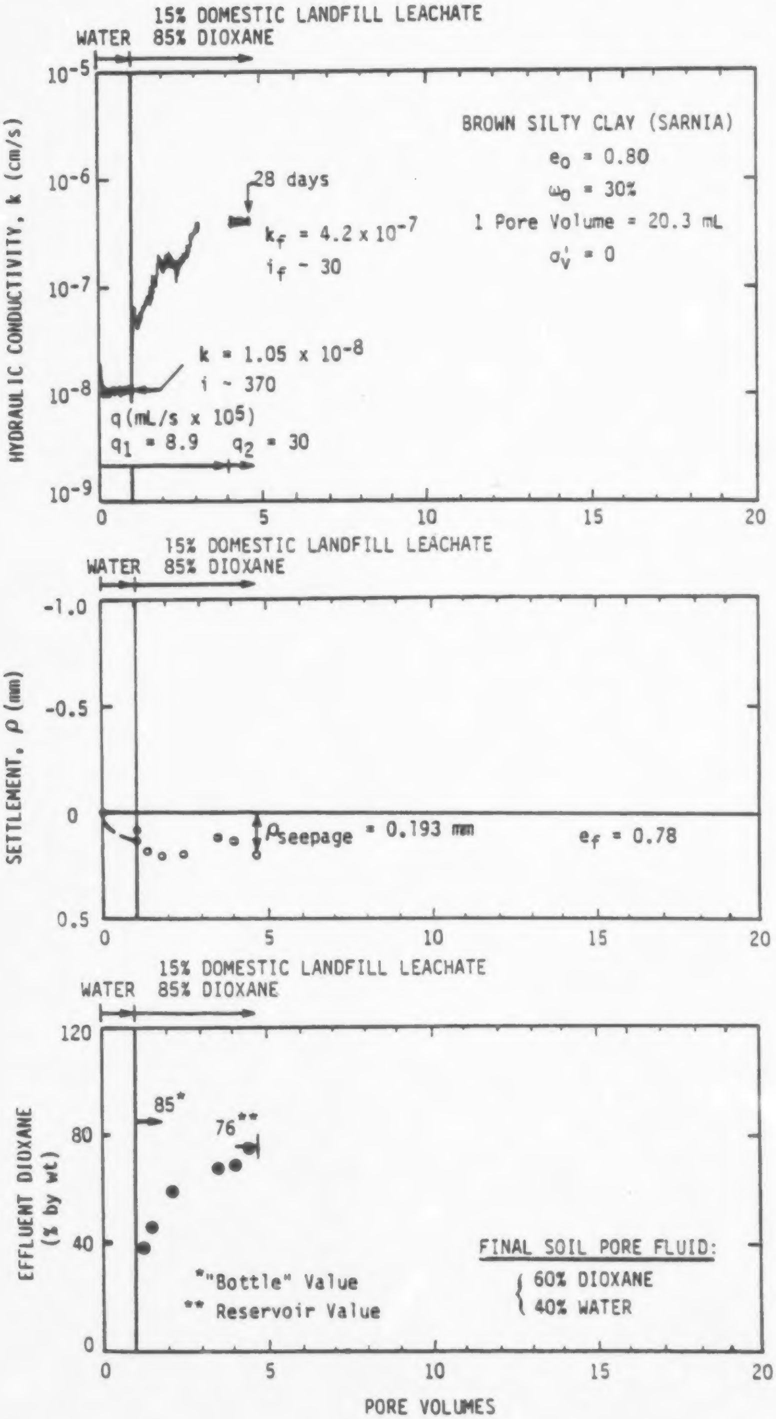

FIGURE F.5 HYDRAULIC CONDUCTIVITY, SETTLEMENT AND EFFLUENT CHEMISTRY VS PORE VOLUMES

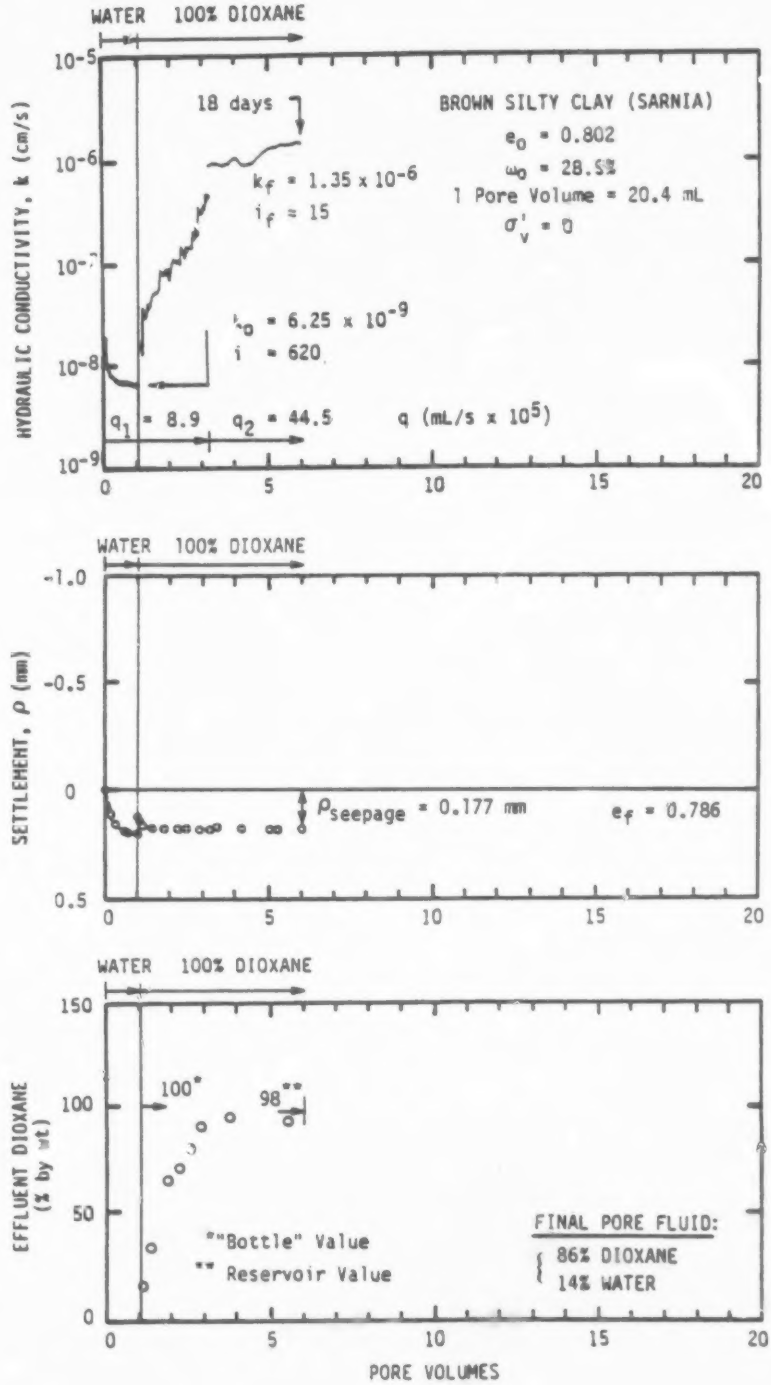

FIGURE F.6 HYDRAULIC CONDUCTIVITY, SETTLEMENT AND EFFLUENT CHEMISTRY VS PORE VOLUMES

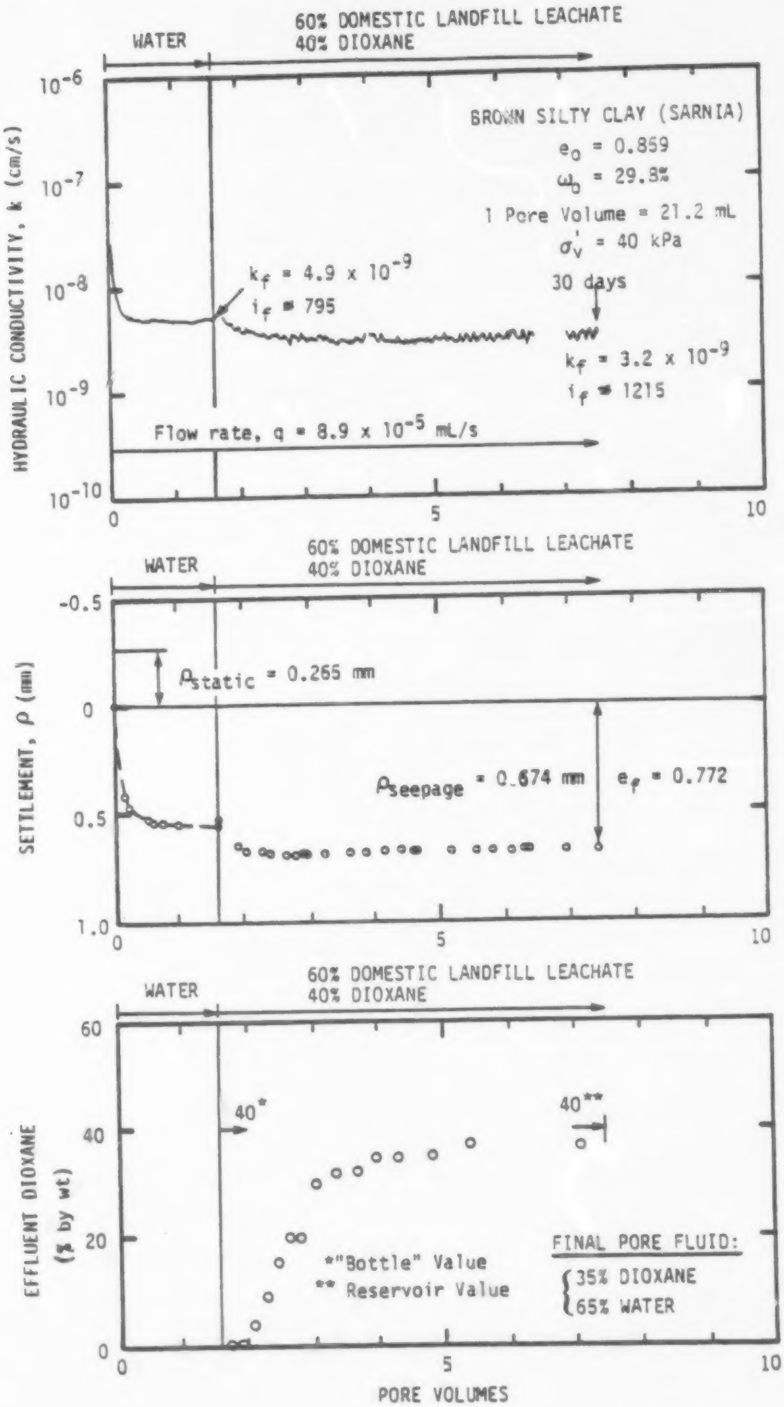

FIGURE F.7 HYDRAULIC CONDUCTIVITY, SETTLEMENT AND EFFLUENT CHEMISTRY VS PORE VOLUMES

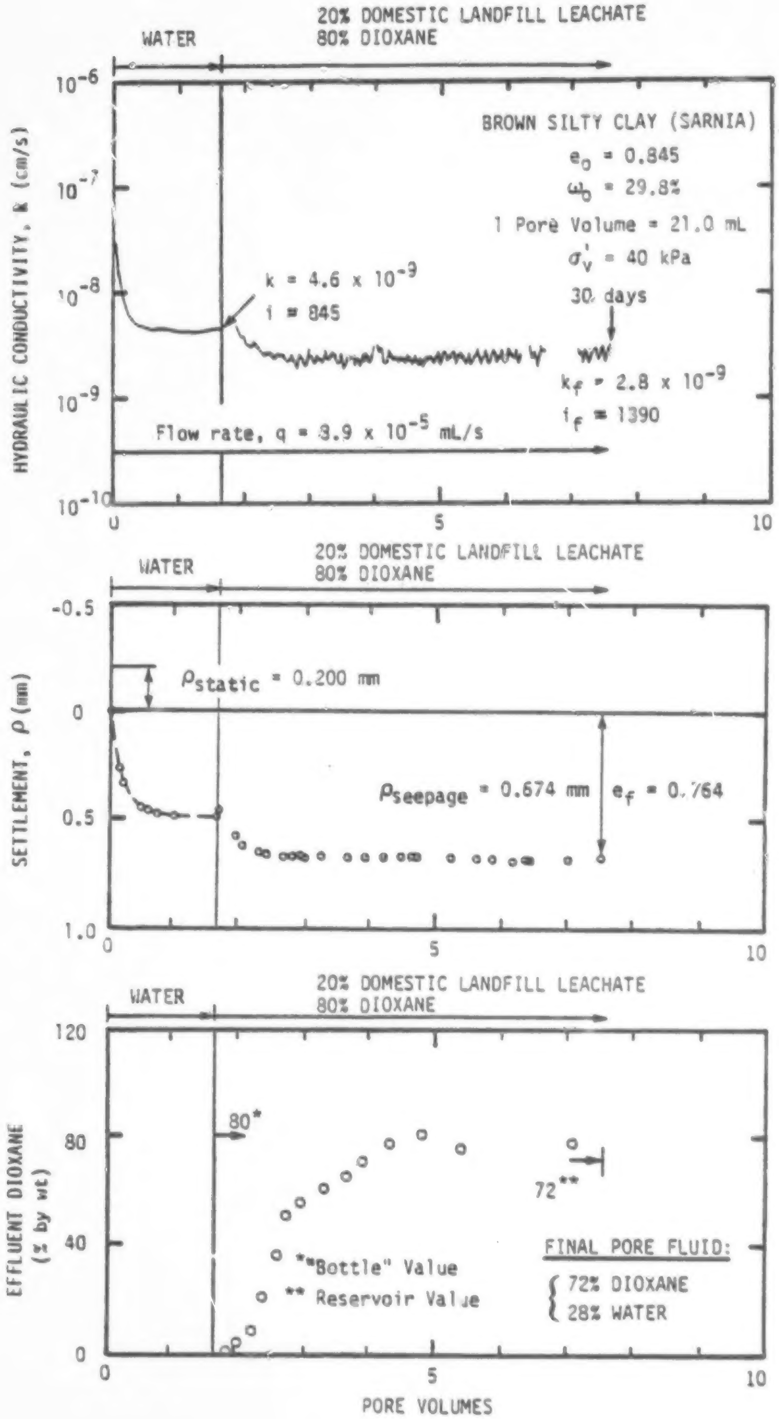

FIGURE F.8 HYDRAULIC CONDUCTIVITY, SETTLEMENT AND EFFLUENT CHEMISTRY VS PORE VOLUMES

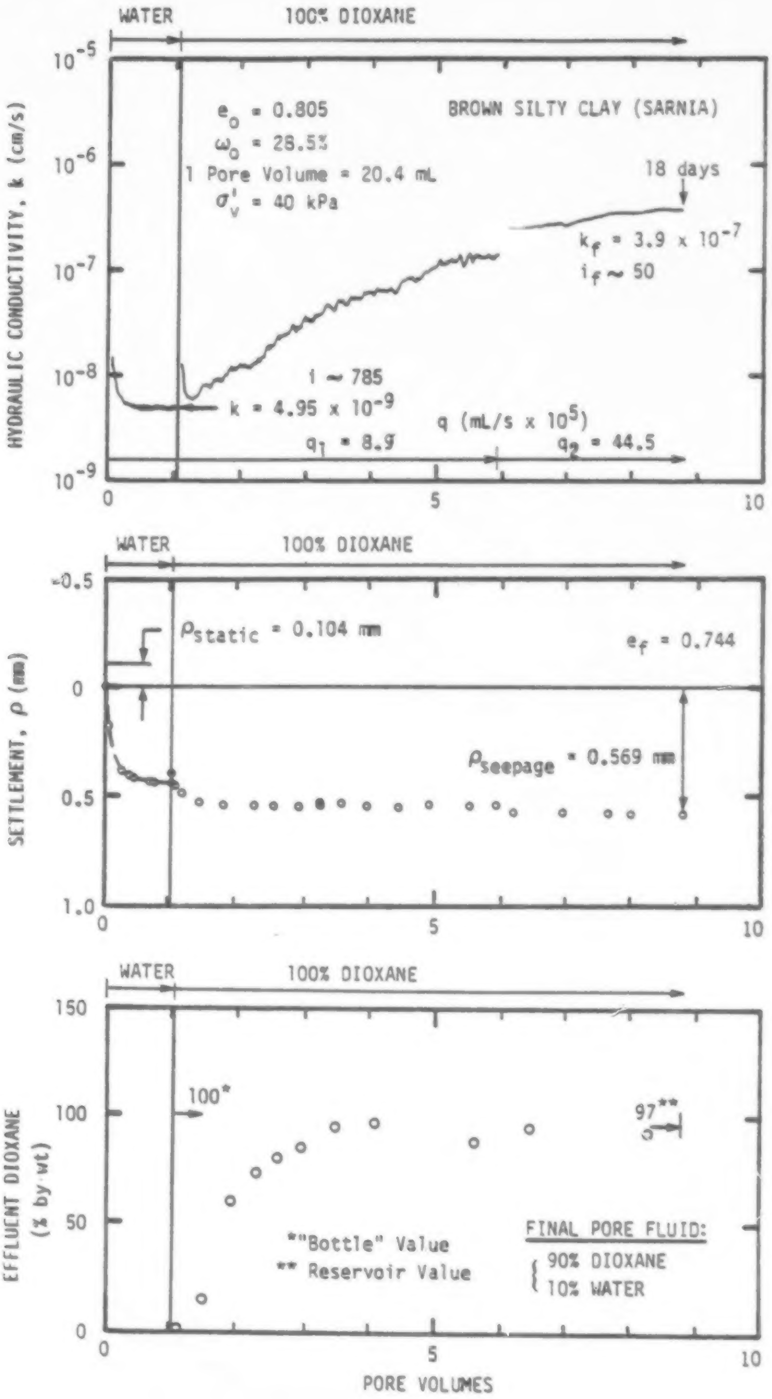

FIGURE F.9 HYDRAULIC CONDUCTIVITY, SETTLEMENT AND EFFLUENT CHEMISTRY VS PORE VOLUMES

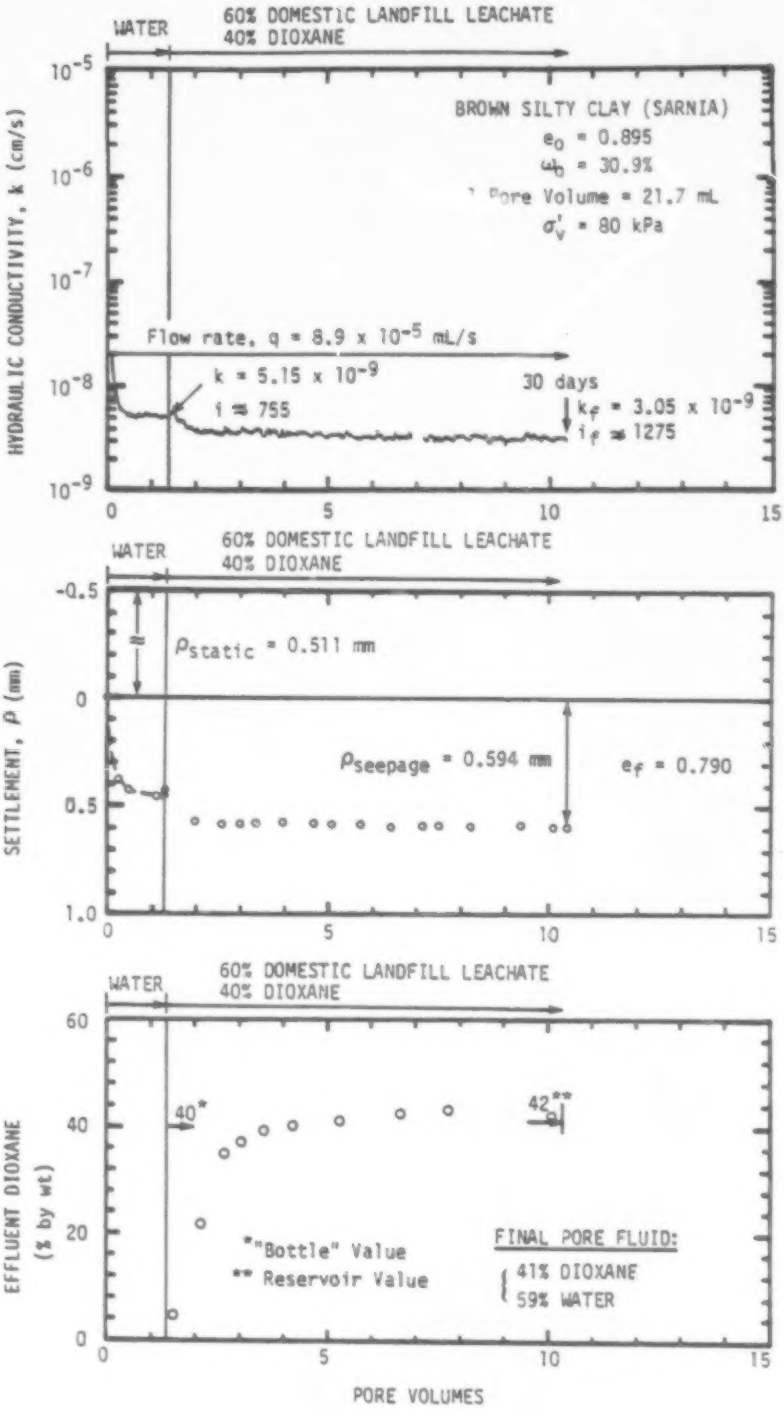

FIGURE F.10 HYDRAULIC CONDUCTIVITY, SETTLEMENT AND EFFLUENT CHEMISTRY VS PORE VOLUMES

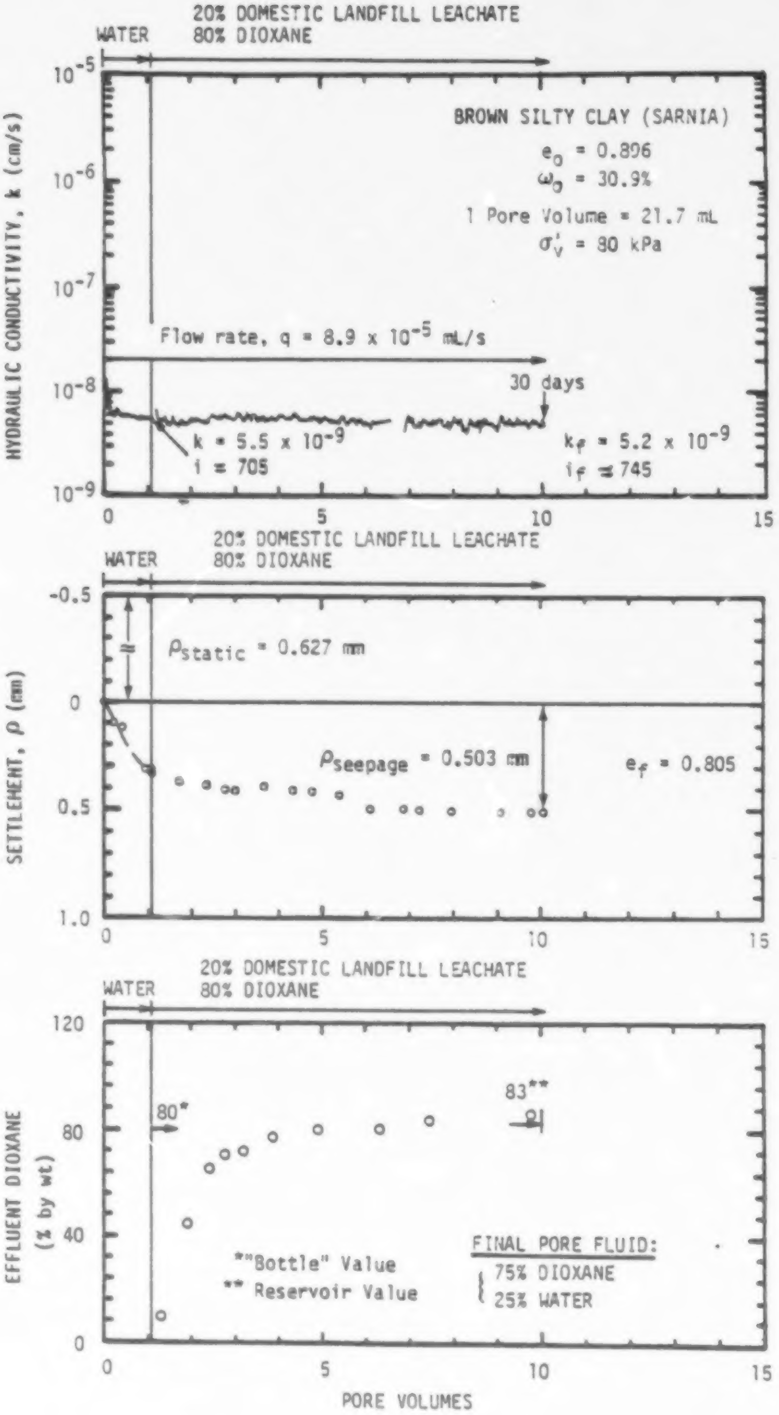

FIGURE F.11 HYDRAULIC CONDUCTIVITY, SETTLEMENT AND EFFLUENT CHEMISTRY VS PORE VOLUMES

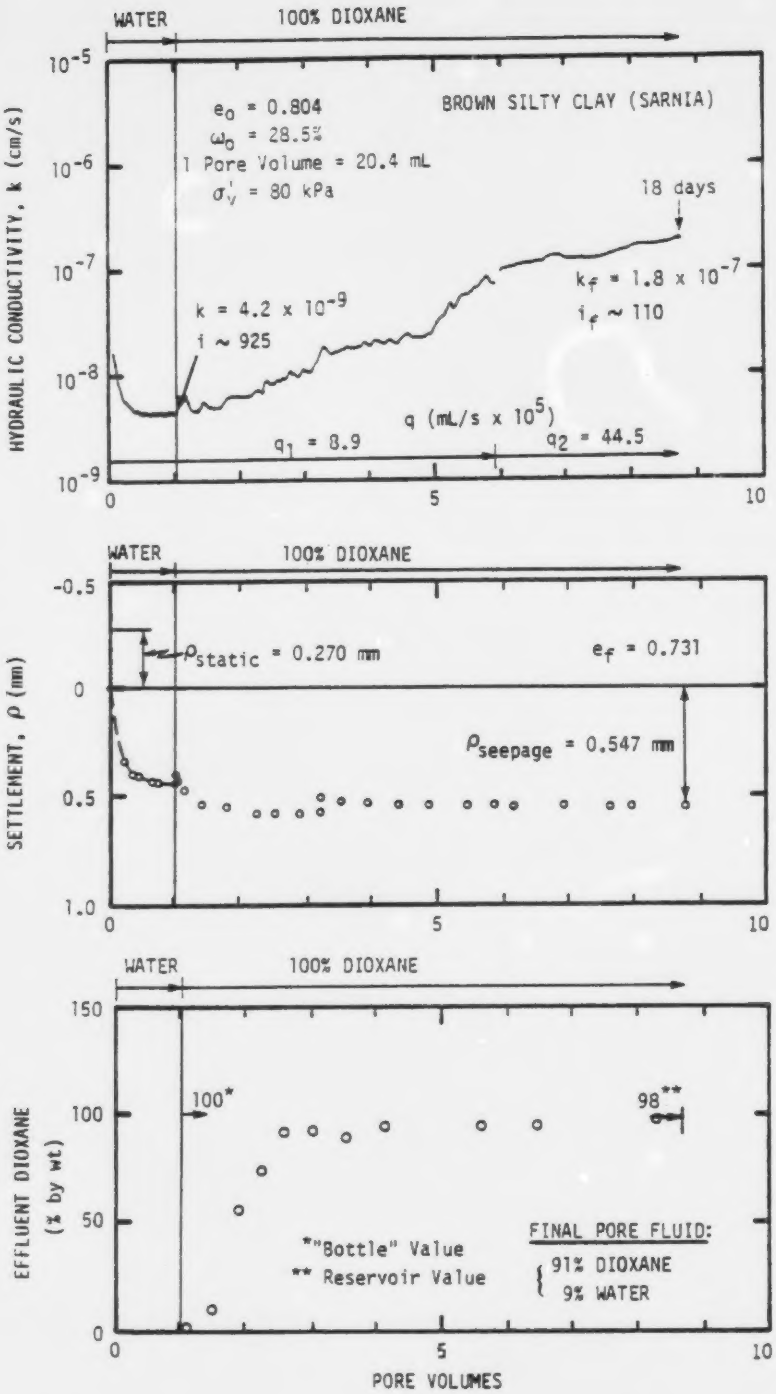

FIGURE F.12 HYDRAULIC CONDUCTIVITY, SETTLEMENT AND EFFLUENT CHEMISTRY VS PORE VOLUMES

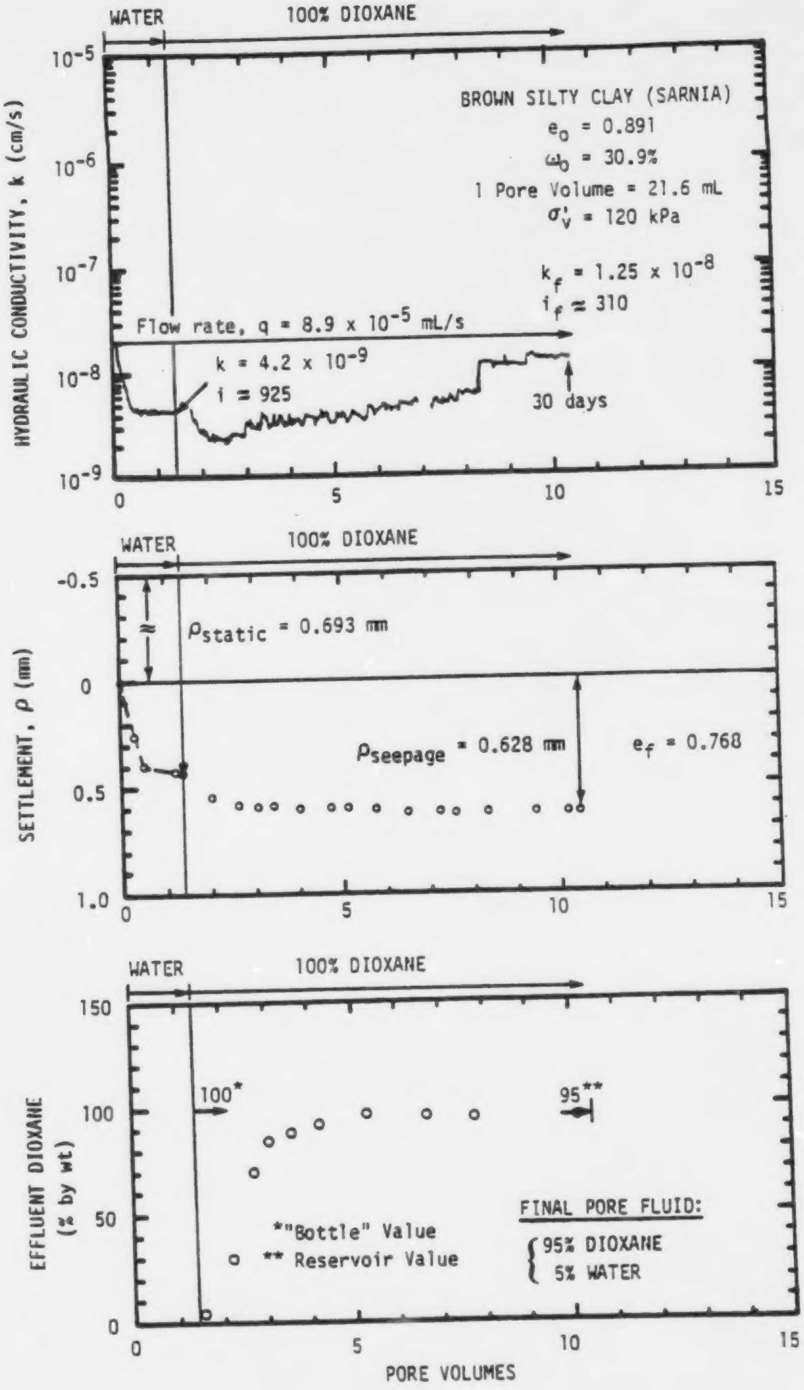

FIGURE F.13 HYDRAULIC CONDUCTIVITY, SETTLEMENT AND EFFLUENT CHEMISTRY VS PORE VOLUMES

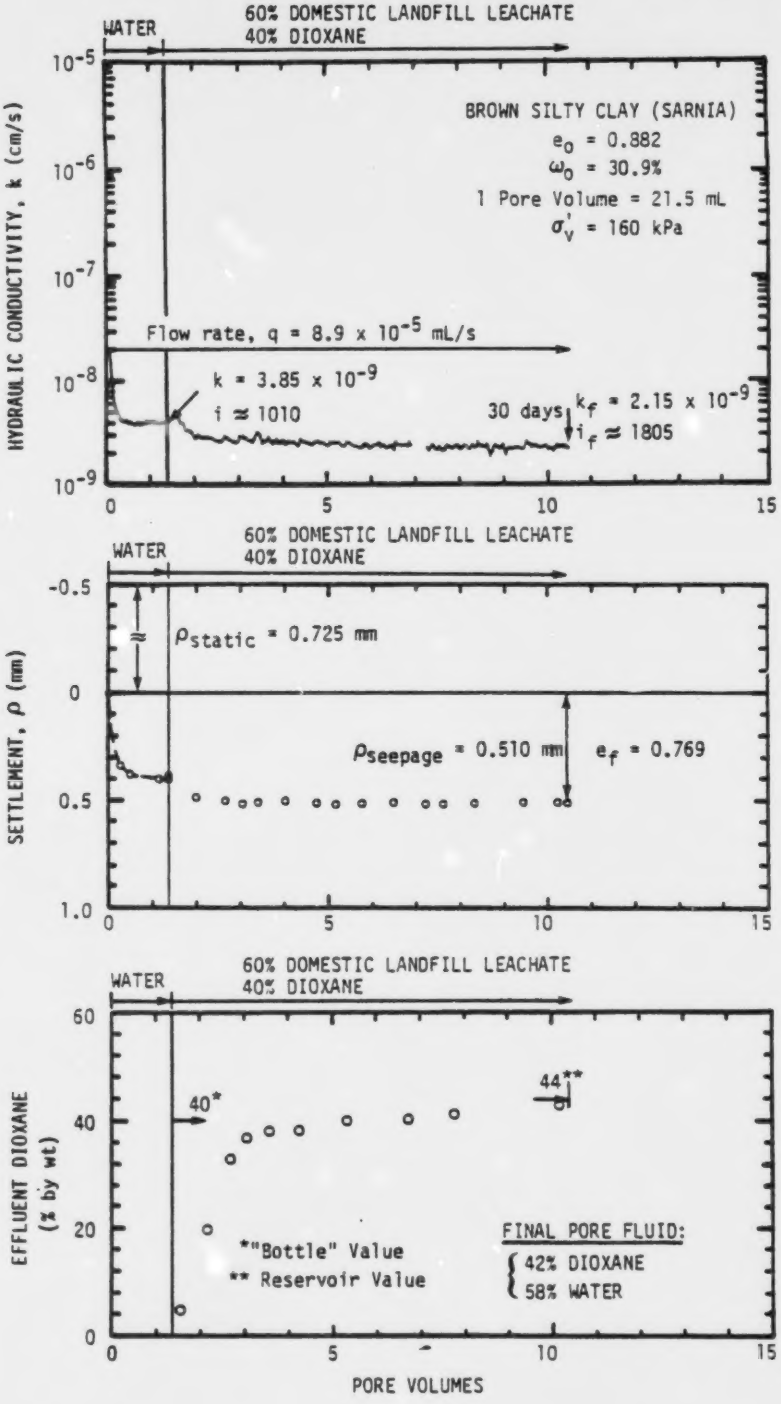

FIGURE F.14 HYDRAULIC CONDUCTIVITY, SETTLEMENT AND EFFLUENT CHEMISTRY VS PORE VOLUMES

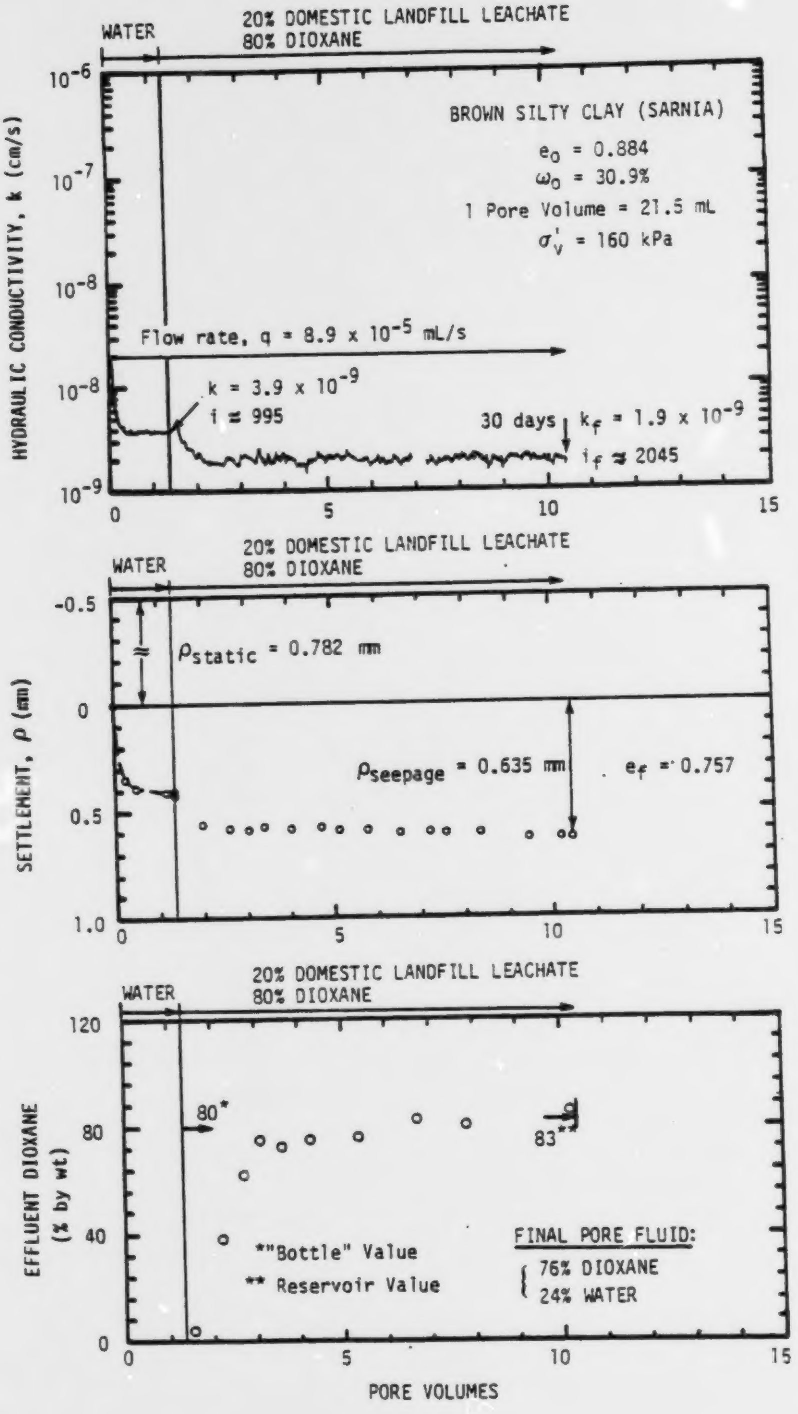

FIGURE F.15 HYDRAULIC CONDUCTIVITY, SETTLEMENT AND EFFLUENT CHEMISTRY VS PORE VOLUMES

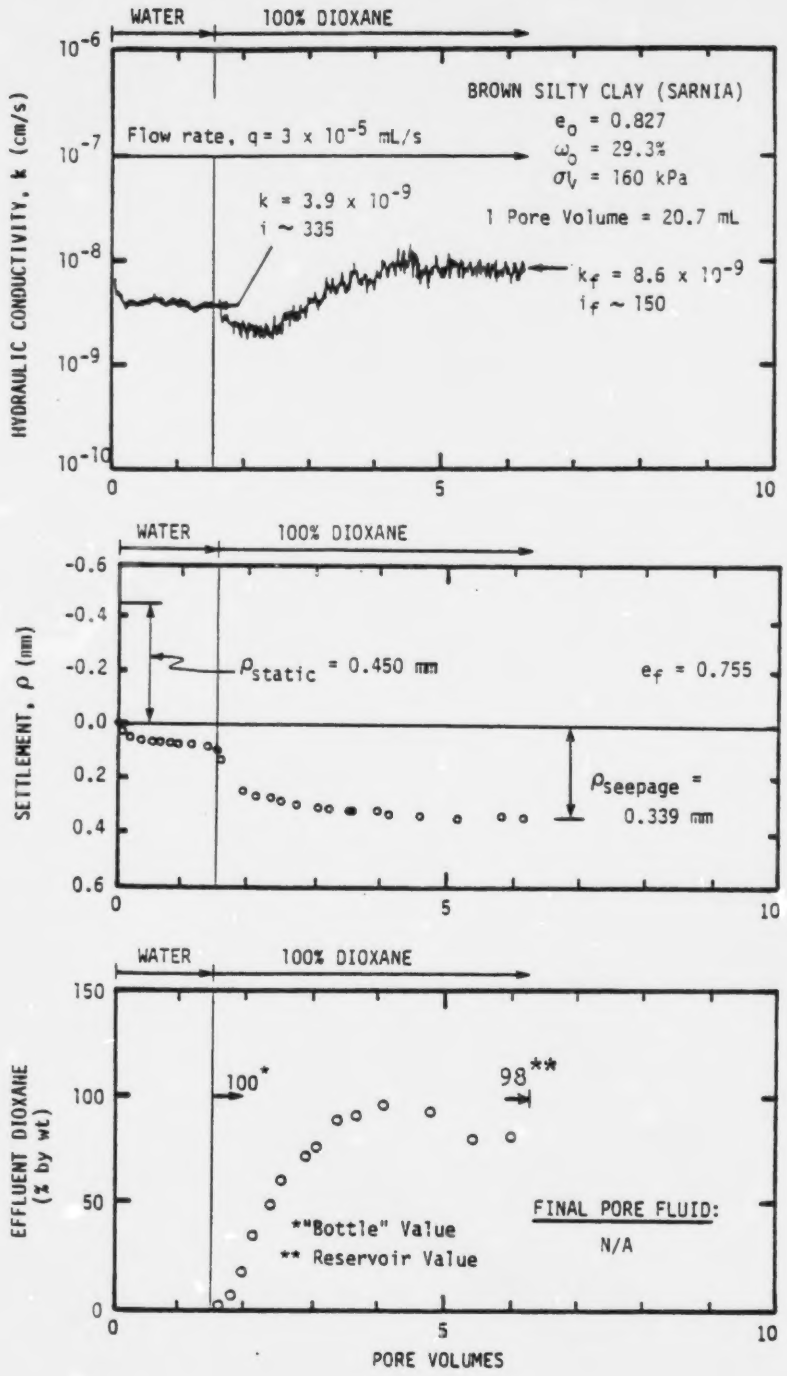

FIGURE F.16 HYDRAULIC CONDUCTIVITY, SETTLEMENT AND EFFLUENT CHEMISTRY VS PORE VOLUMES

APPENDIX G

HYDRAULIC CONDUCTIVITY CURVES FOR UNDISTURBED GREY SARNIA CLAY PERMEATED WITH LEACHATE/ETHANOL MIXTURES

This appendix presents the results of hydraulic conductivity, settlement and effluent composition for tests carried out on undisturbed samples of grey Sarnia clays permeated with leachate/ethanol mixtures at static effective stresses σ'_v = 0 kPa.

The test results are discussed in Sections 5.3.4 of this report.

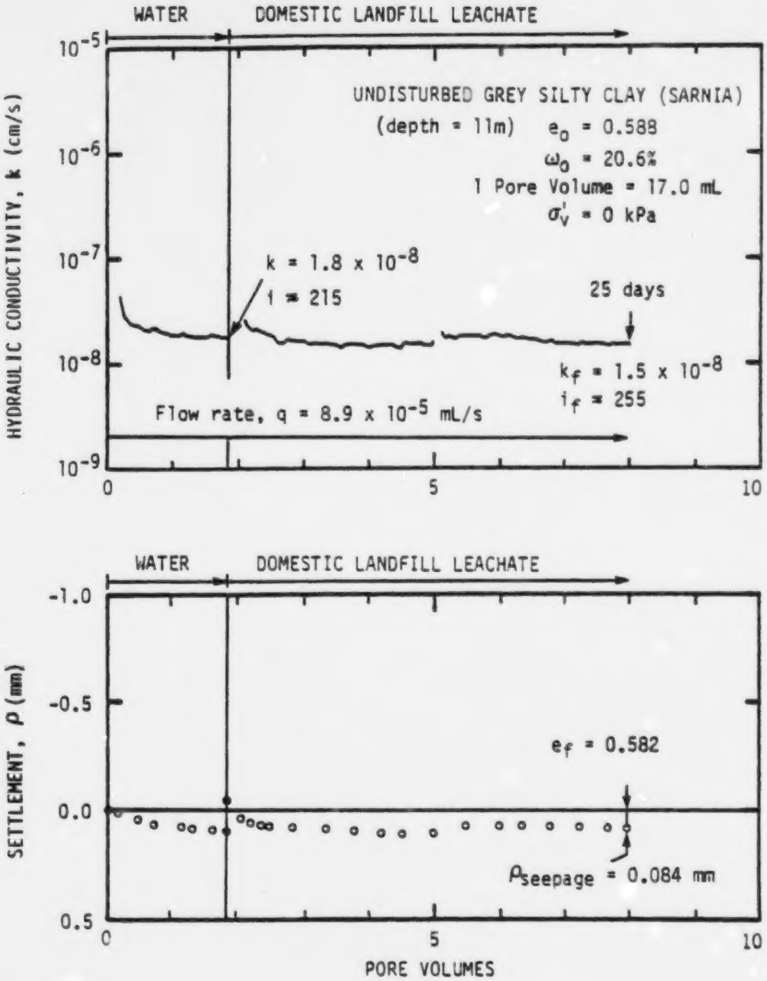

FIGURE G.1 HYDRAULIC CONDUCTIVITY, SETTLEMENT, AND EFFLUENT CHEMISTRY VS PORE VOLUMES

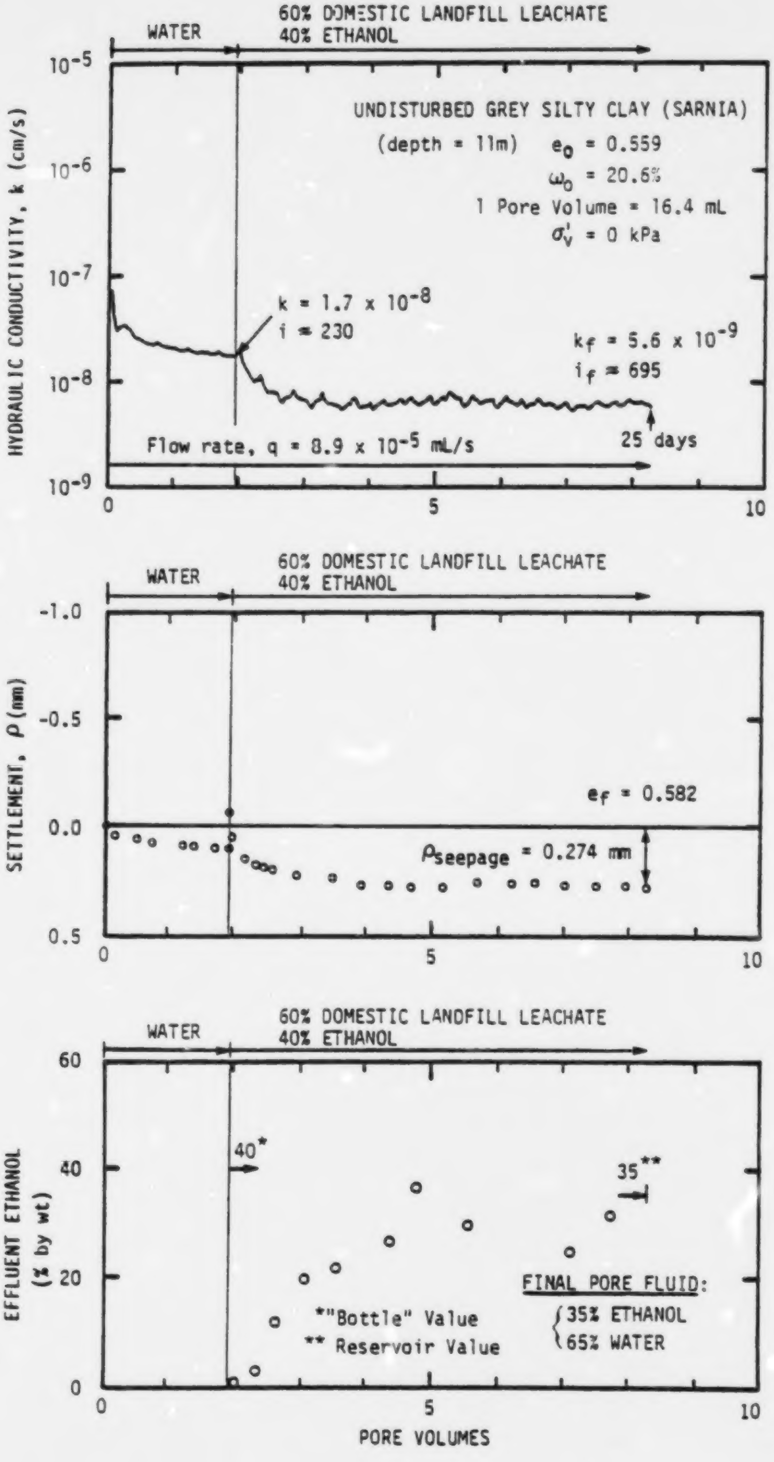

FIGURE G.2 HYDRAULIC CONDUCTIVITY, SETTLEMENT, AND EFFLUENT CHEMISTRY VS PORE VOLUMES

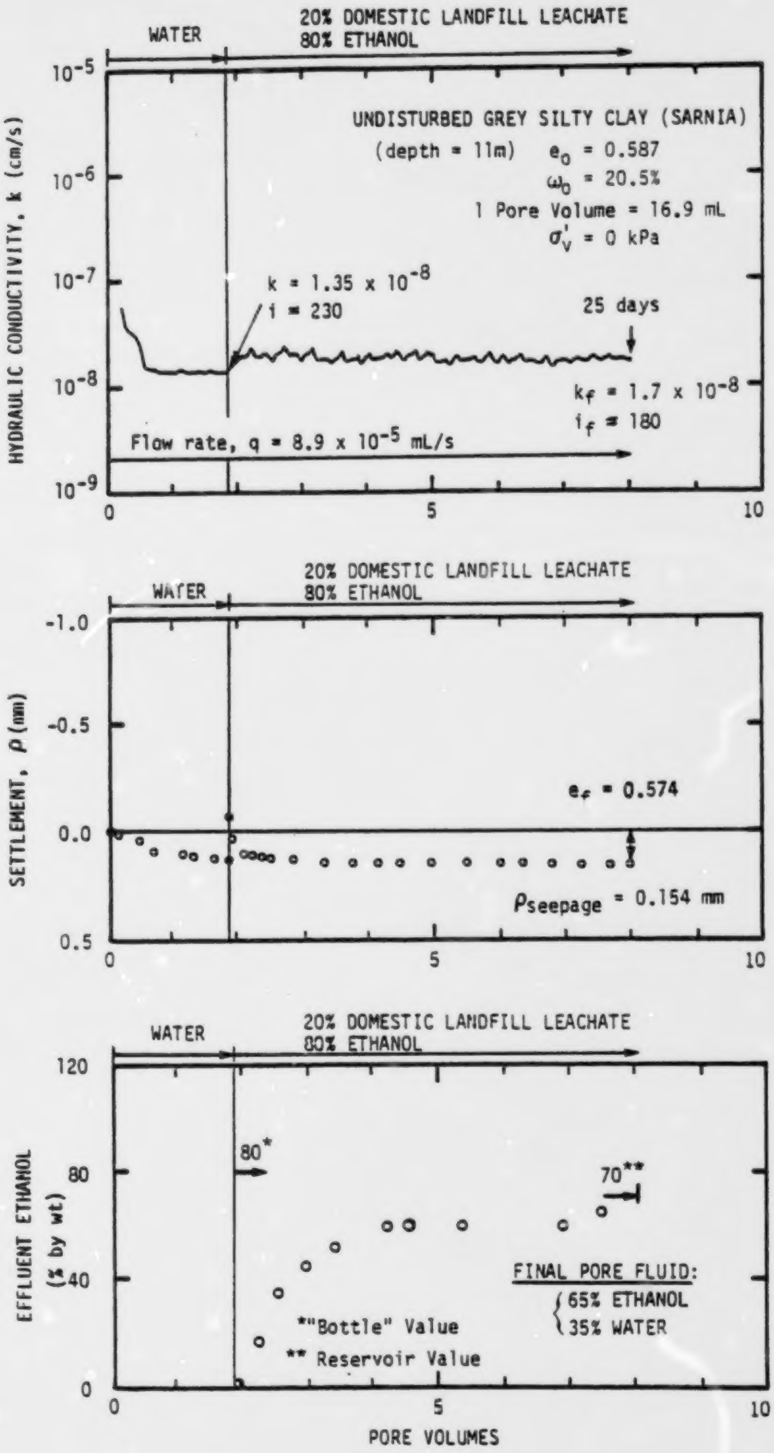

FIGURE G.3 HYDRAULIC CONDUCTIVITY, SETTLEMENT, AND EFFLUENT CHEMISTRY VS PORE VOLUMES

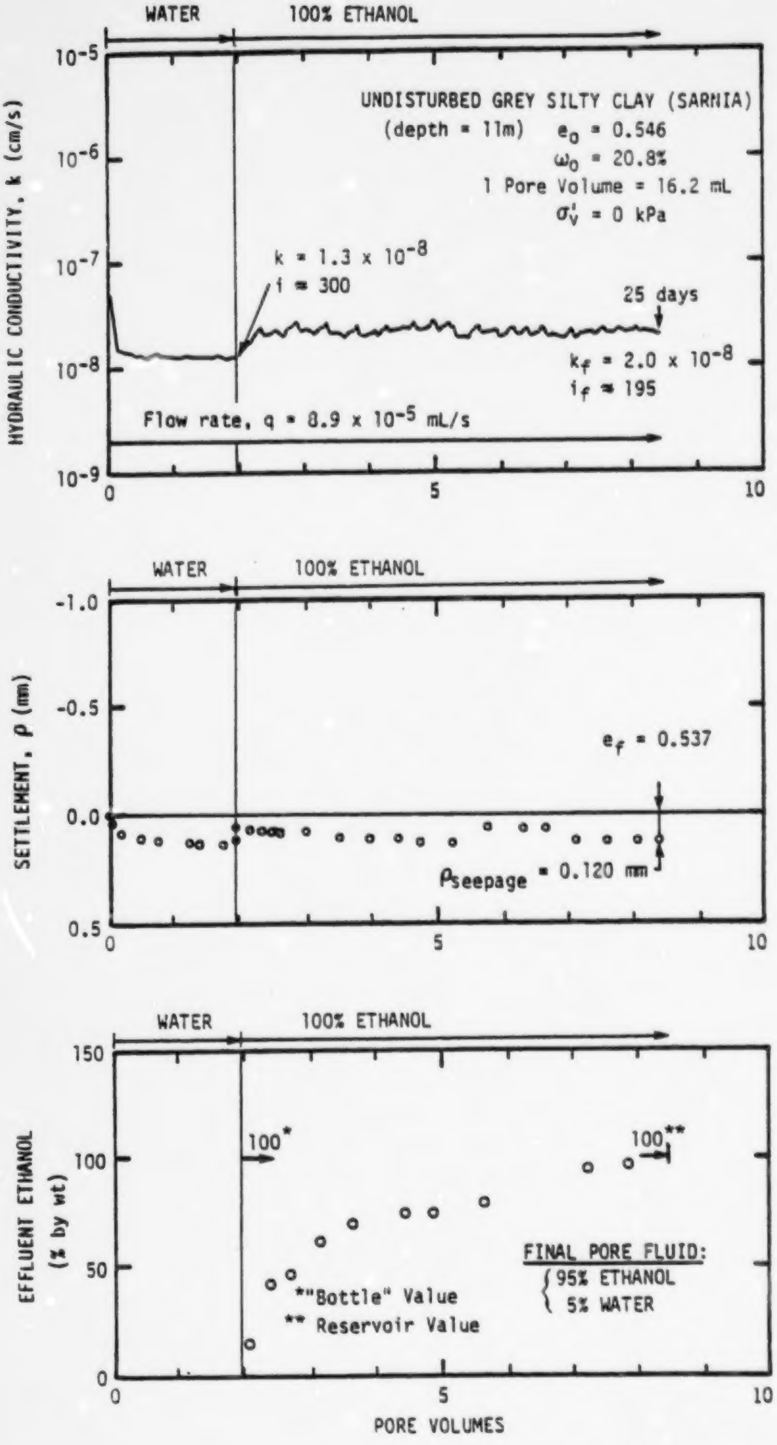

FIGURE G.4 HYDRAULIC CONDUCTIVITY, SETTLEMENT, AND EFFLUENT CHEMISTRY VS PORE VOLUMES

APPENDIX H

EFFLUENT CONCENTRATION CURVES FOR INORGANIC SPECIES WATER-COMPACTED BROWN SARNIA CLAY PERMEATED WITH LEACHATE/ETHANOL MIXTURES

The figures presented in this appendix show the effluent composition versus pore volumes for water-compacted samples of brown Sarnia clays permeated 0.01 N $CaSO_4$ (water) followed by mixtures of domestic waste leachate and ethanol. These results correspond to clay/leachate compatibility shown in Figures E.3 to E.5 and discussed in Section 5.3.1 of this thesis.

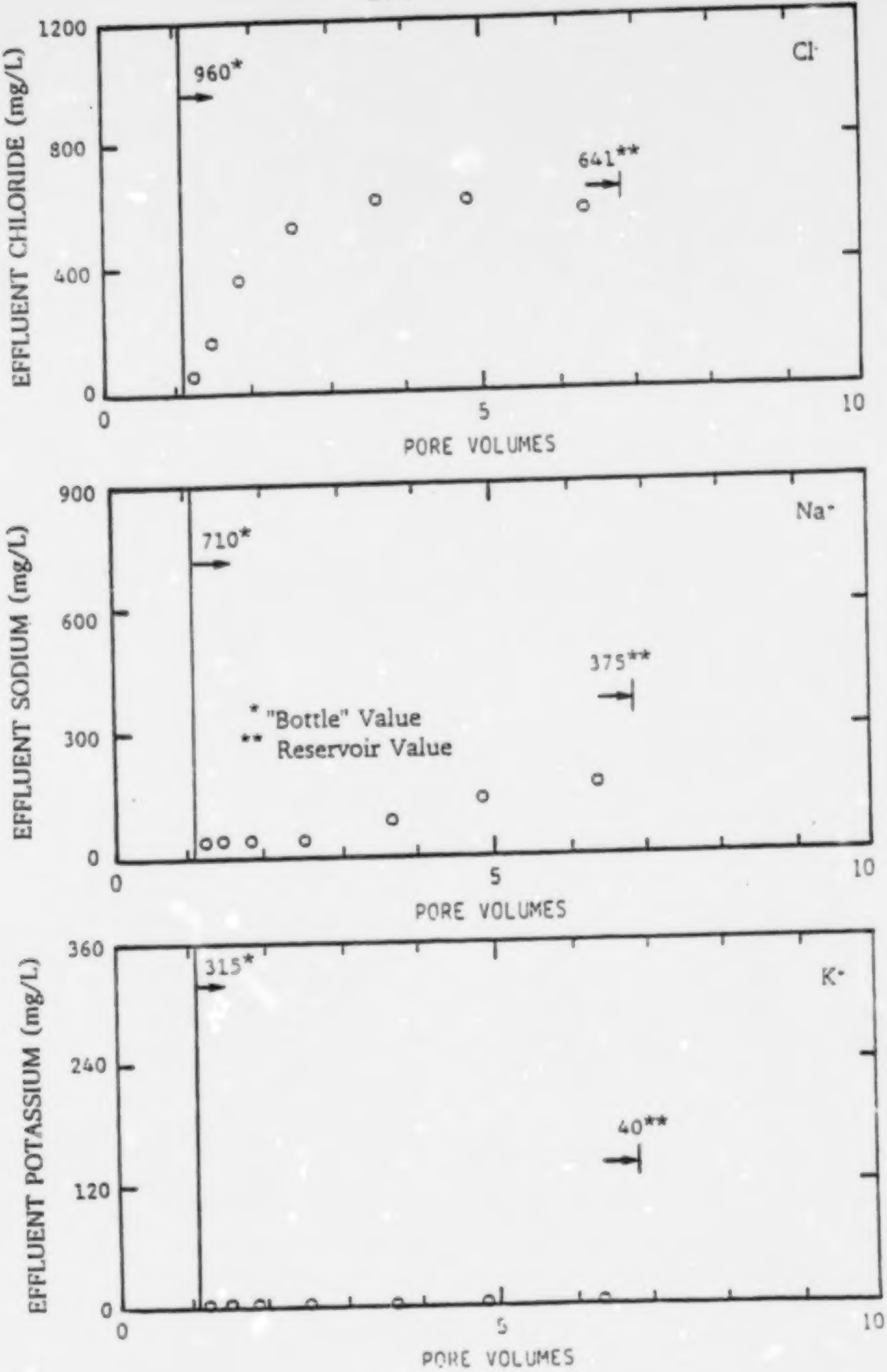

FIGURE H.1 EFFLUENT CONCENTRATION FOR INORGANIC SPECIES VS PORE VOLUMES

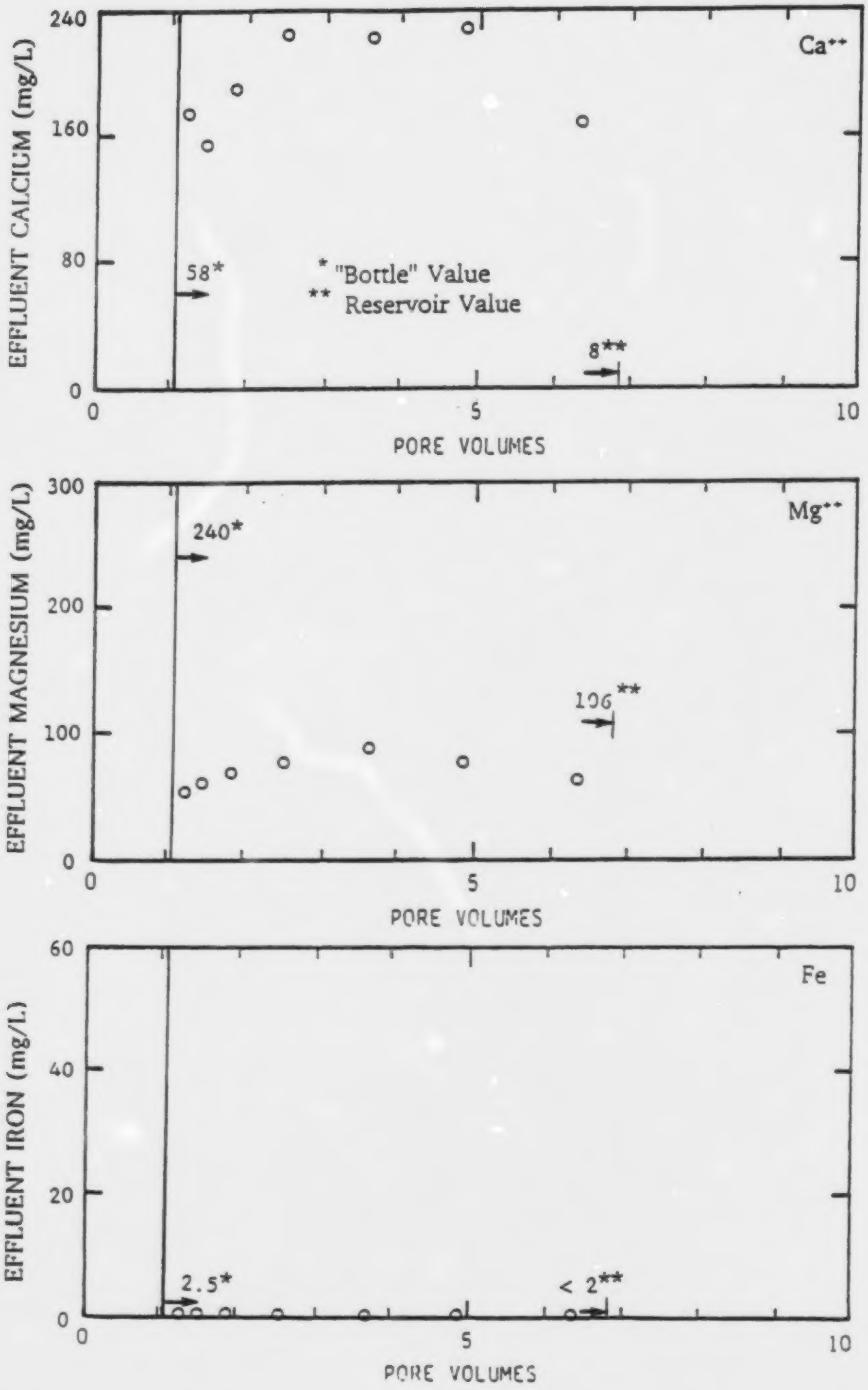

FIGURE H.2 EFFLUENT CONCENTRATION FOR INORGANIC SPECIES VS PORE VOLUMES

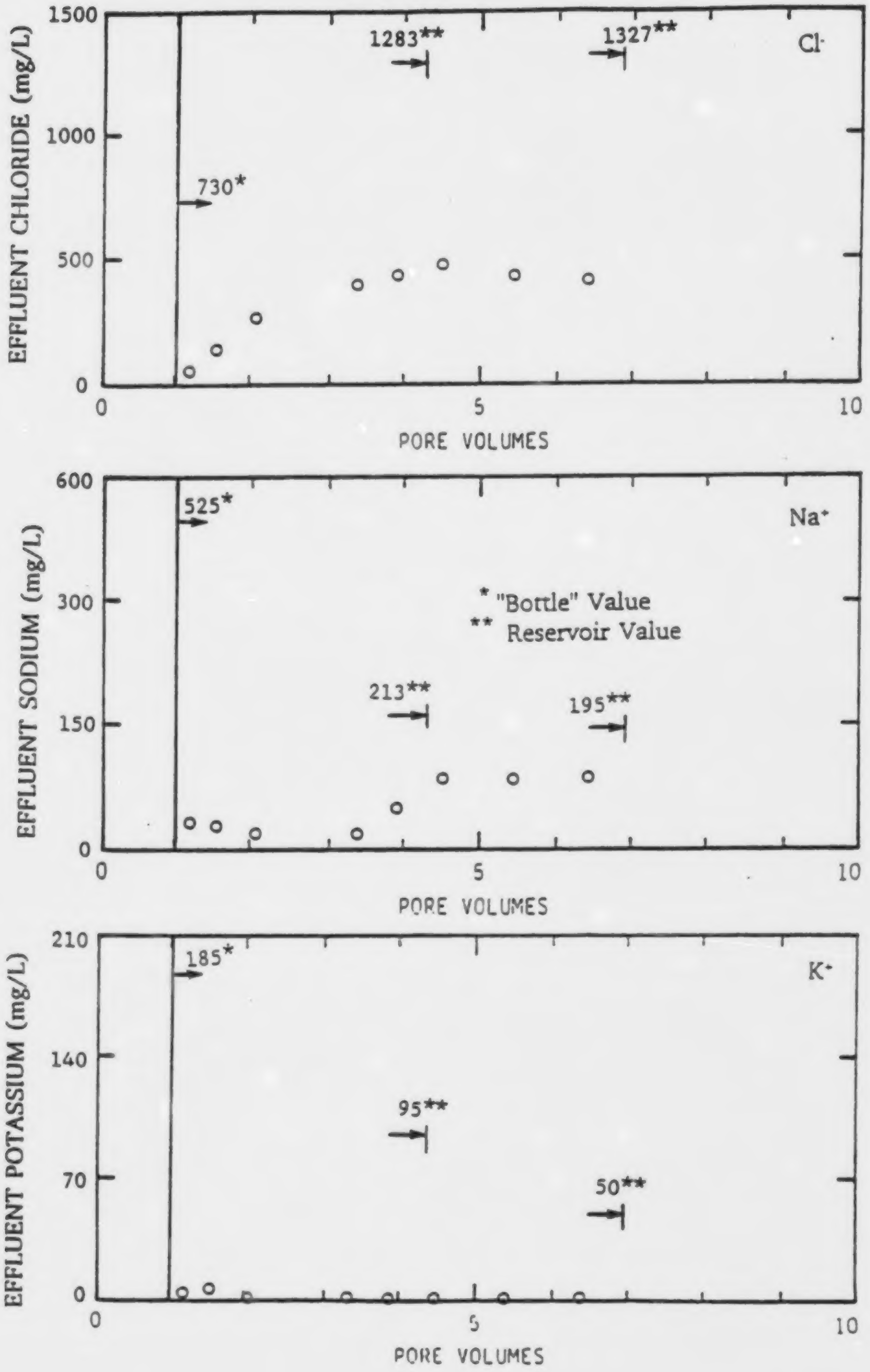

FIGURE H.3 EFFLUENT CONCENTRATION FOR INORGANIC SPECIES VS PORE VOLUMES

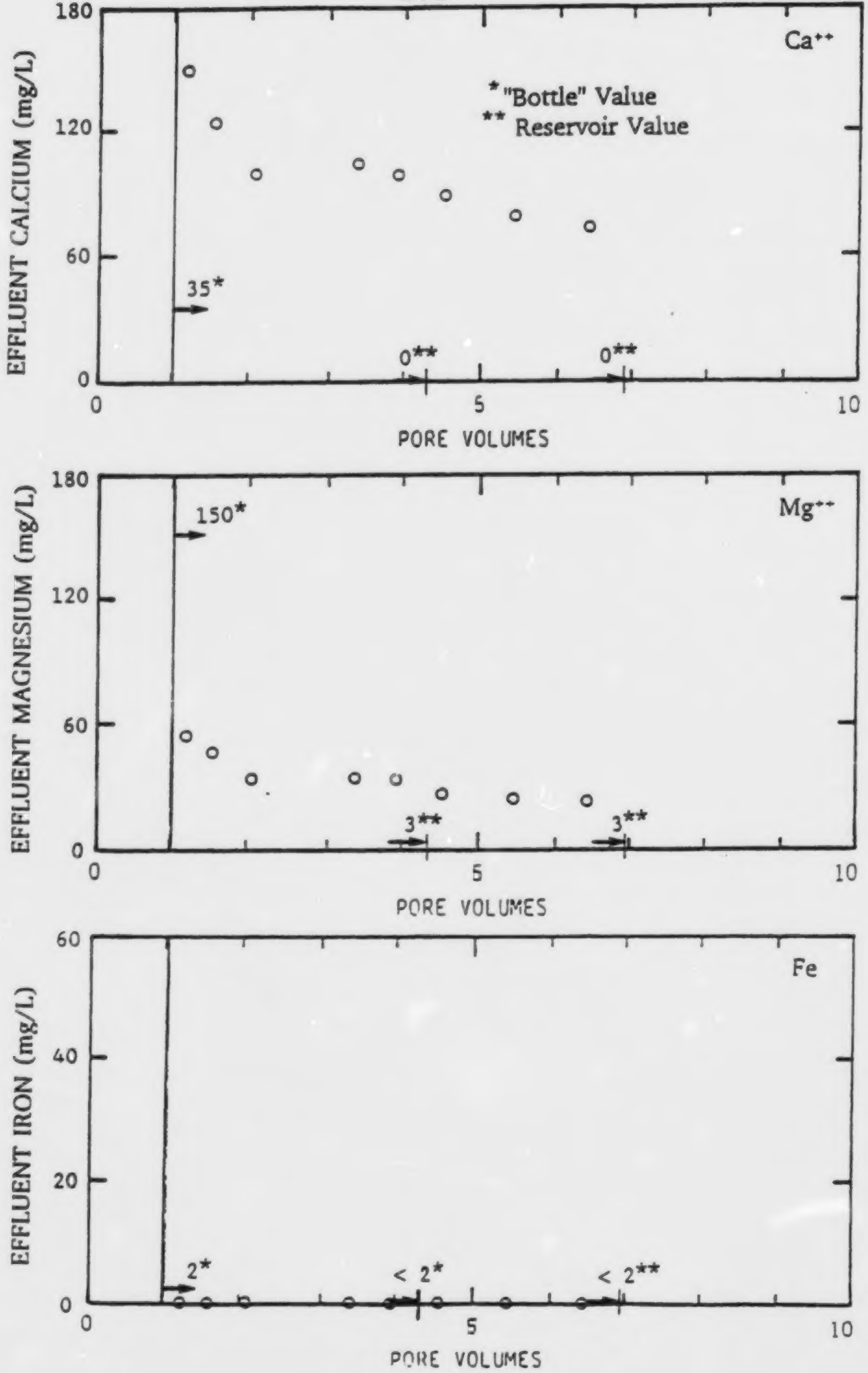

FIGURE H.4 EFFLUENT CONCENTRATION FOR INORGANIC SPECIES VS PORE VOLUMES

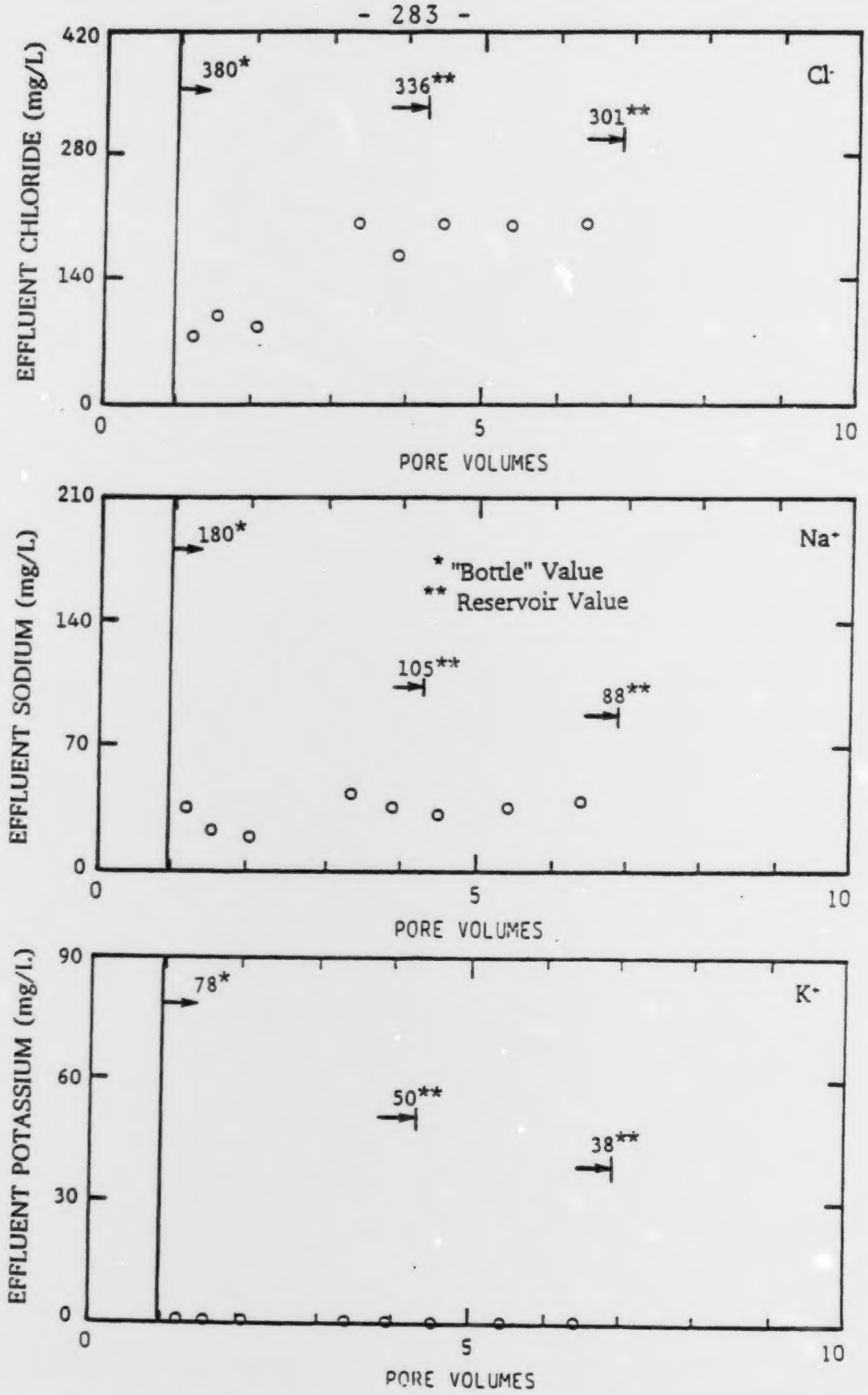

FIGURE H.5 EFFLUENT CONCENTRATION FOR INORGANIC SPECIES VS PORE VOLUMES

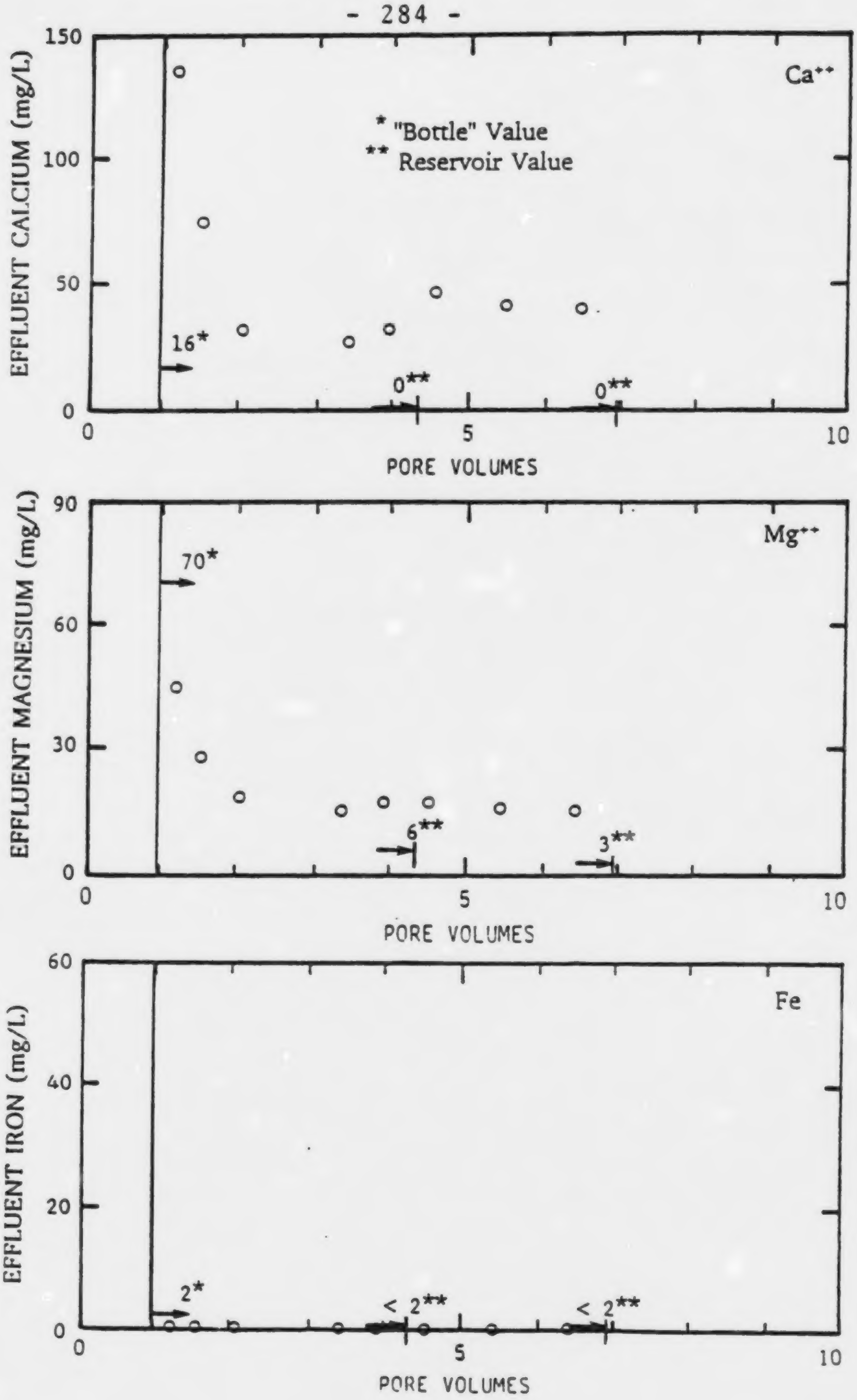

FIGURE H.6 EFFLUENT CONCENTRATION FOR INORGANIC SPECIES VS PORE VOLUMES

APPENDIX I

EFFLUENT CONCENTRATION CURVES FOR INORGANIC SPECIES WATER-COMPACTED BROWN SARNIA CLAY PERMEATED WITH LEACHATE/DIOXANE MIXTURES

The figures presented in this appendix show the effluent composition versus pore volumes for water-compacted samples of brown Sarnia clay permeated 0.01 N $CaSO_4$ (water) followed by mixtures of domestic waste leachate and dioxane. These results correspond to clay/leachate compatibility shown in Figures F.1 to F.5 and discussed in Section 5.3.2 of this thesis.

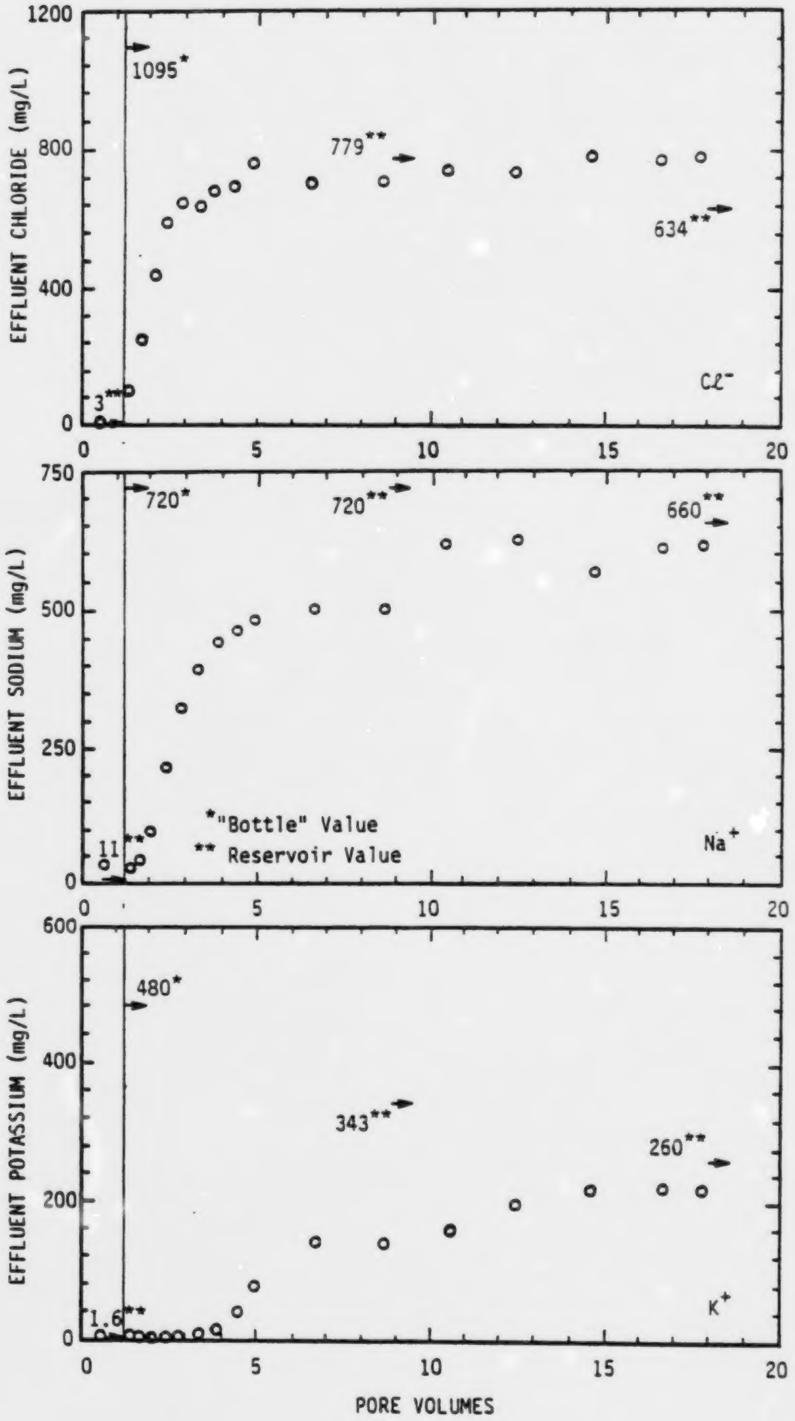

FIGURE I.1 EFFLUENT CONCENTRATION FOR INORGANIC SPECIES VS PORE VOLUMES

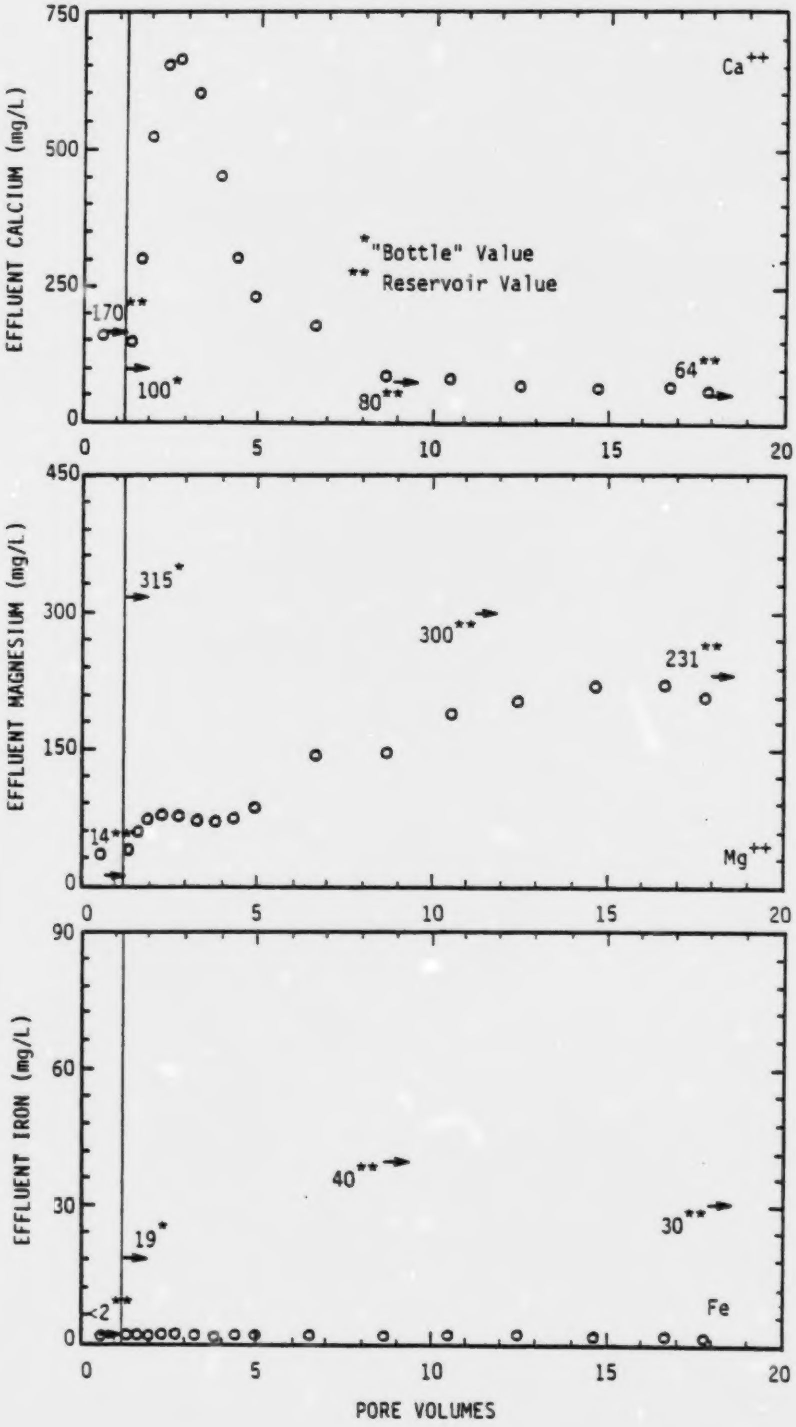

FIGURE I.2 EFFLUENT CONCENTRATION FOR INORGANIC SPECIES VS PORE VOLUMES

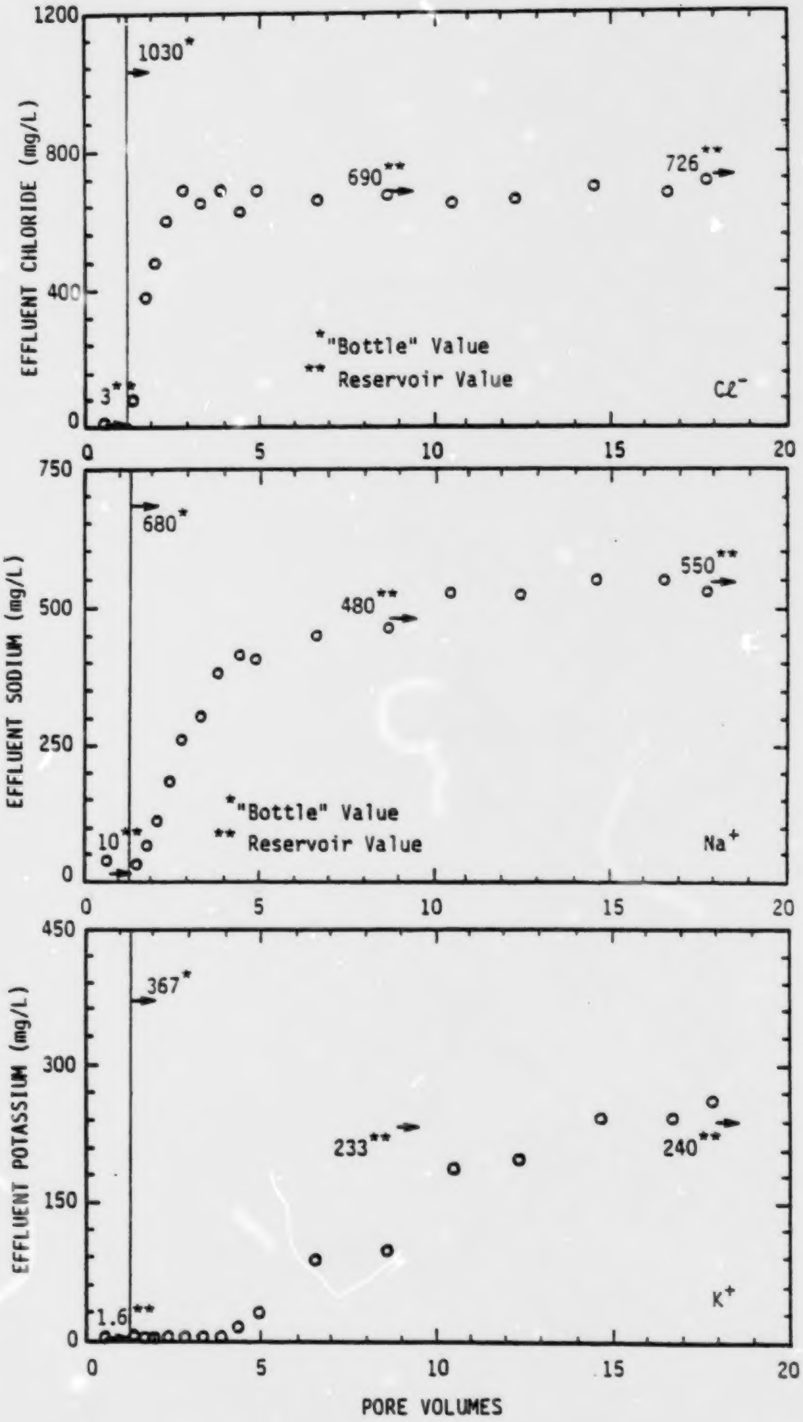

FIGURE I.3 EFFLUENT CONCENTRATION FOR INORGANIC SPECIES VS PORE VOLUMES

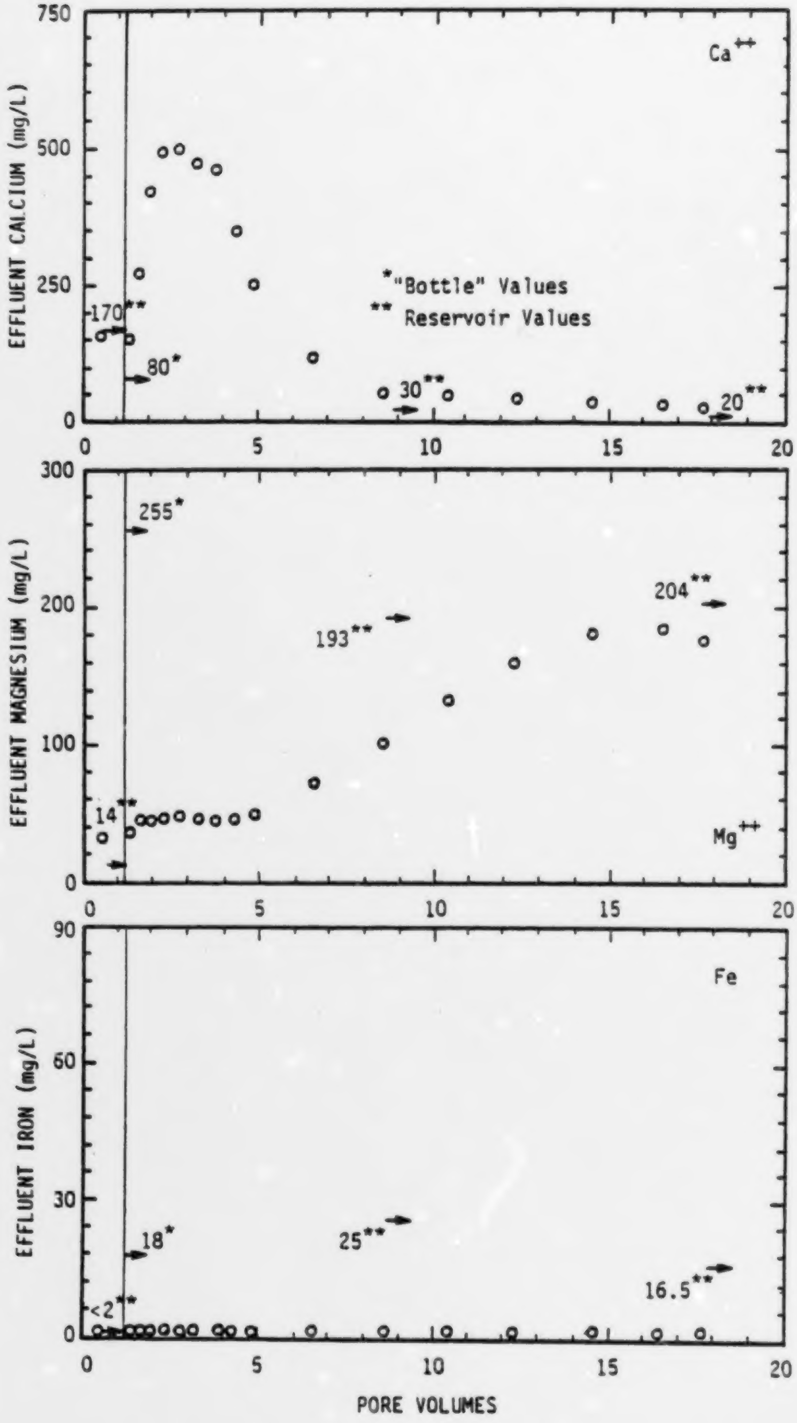

FIGURE I.4 EFFLUENT CONCENTRATION FOR INORGANIC SPECIES VS PORE VOLUMES

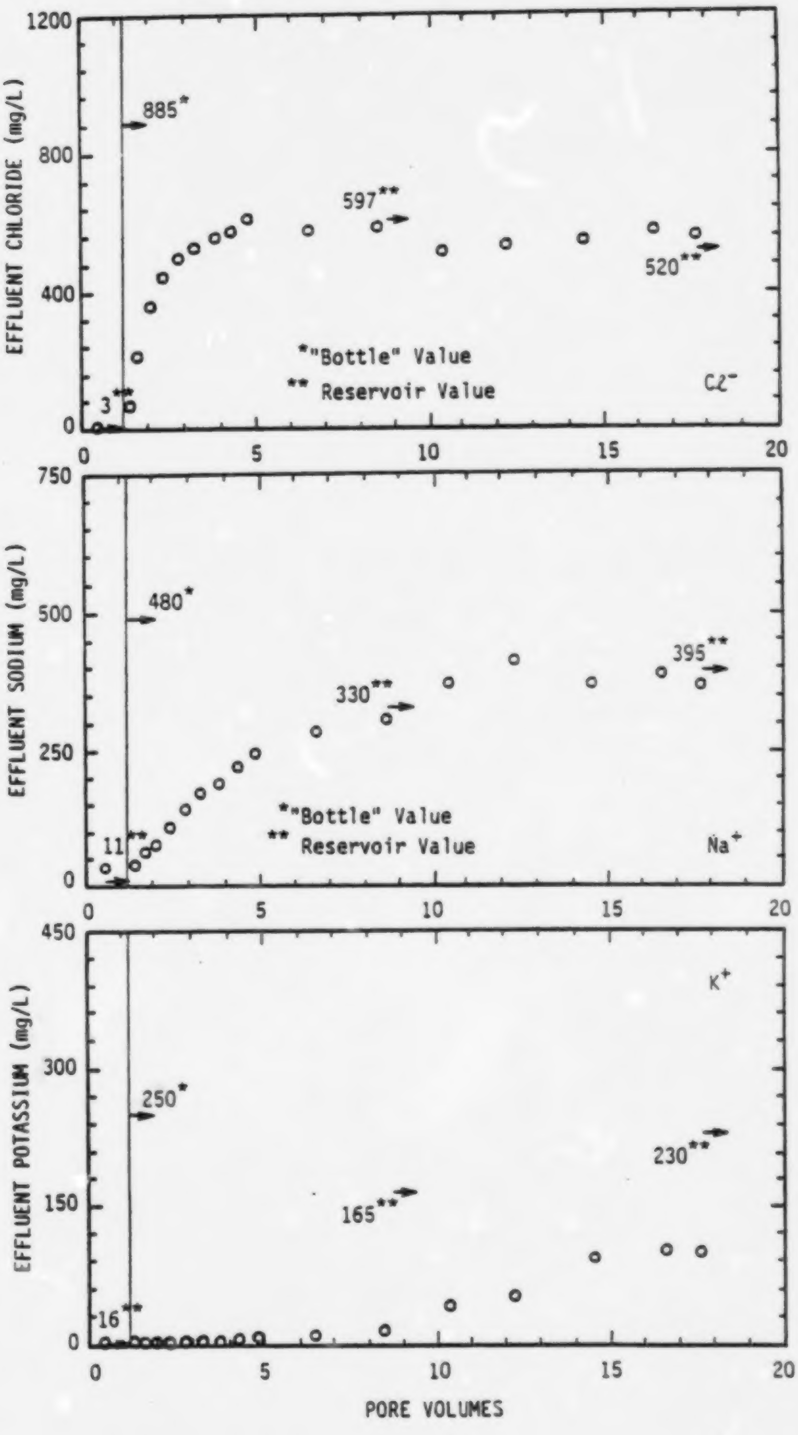

FIGURE I.5 EFFLUENT CONCENTRATION FOR INORGANIC SPECIES VS PORE VOLUMES

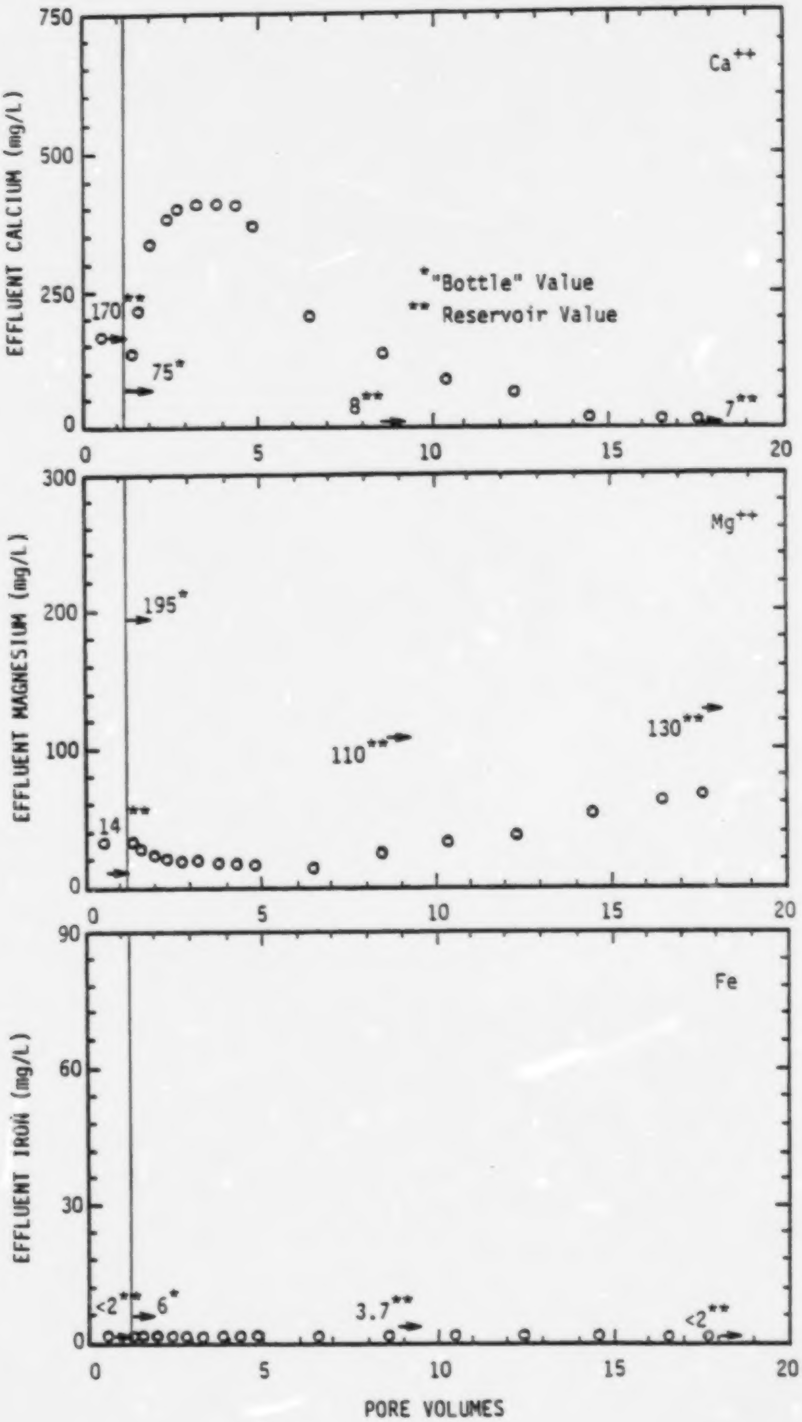

FIGURE I.6 EFFLUENT CONCENTRATION FOR INORGANIC SPECIES VS PORE VOLUMES

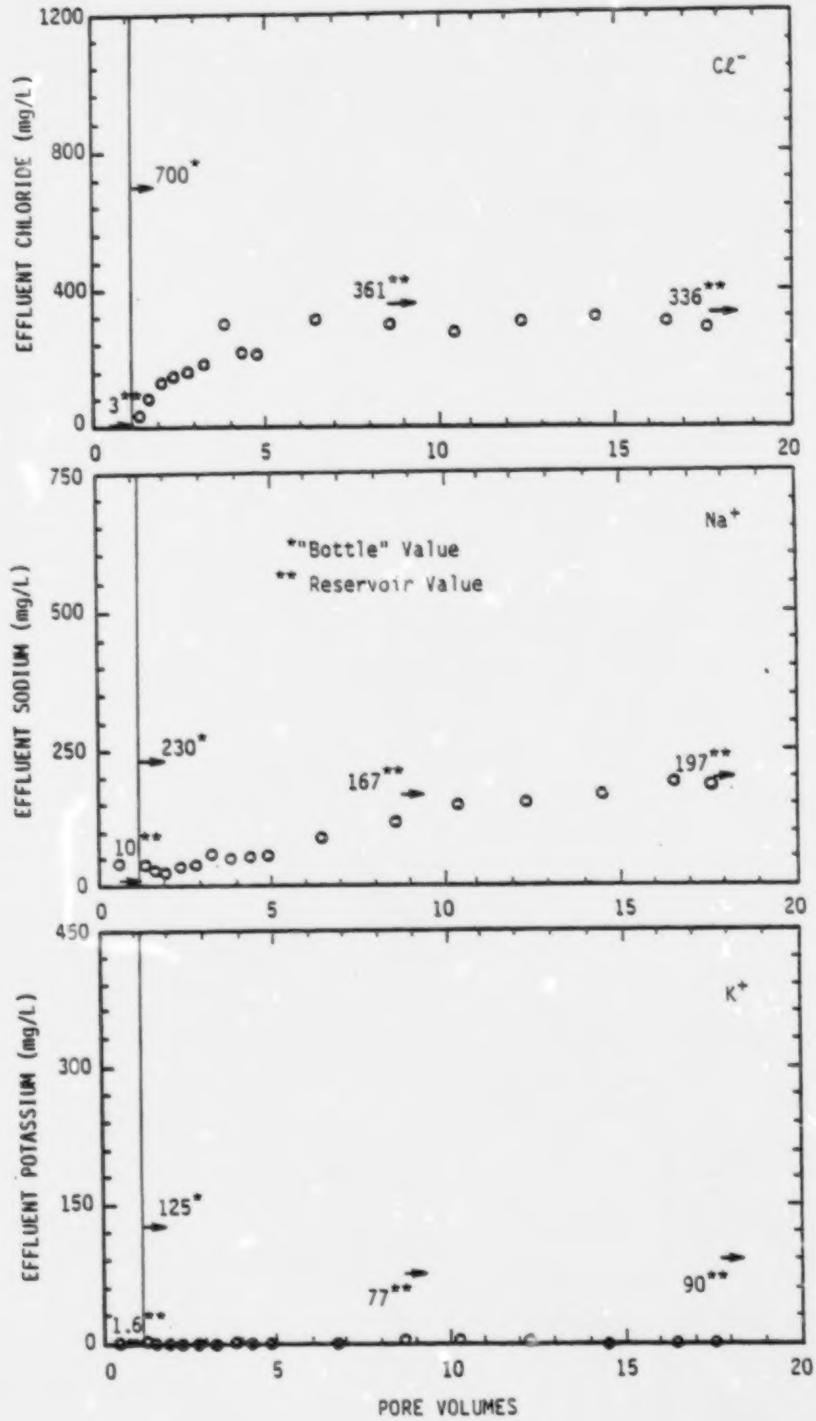

FIGURE I.7 EFFLUENT CONCENTRATION FOR INORGANIC SPECIES VS PORE VOLUMES

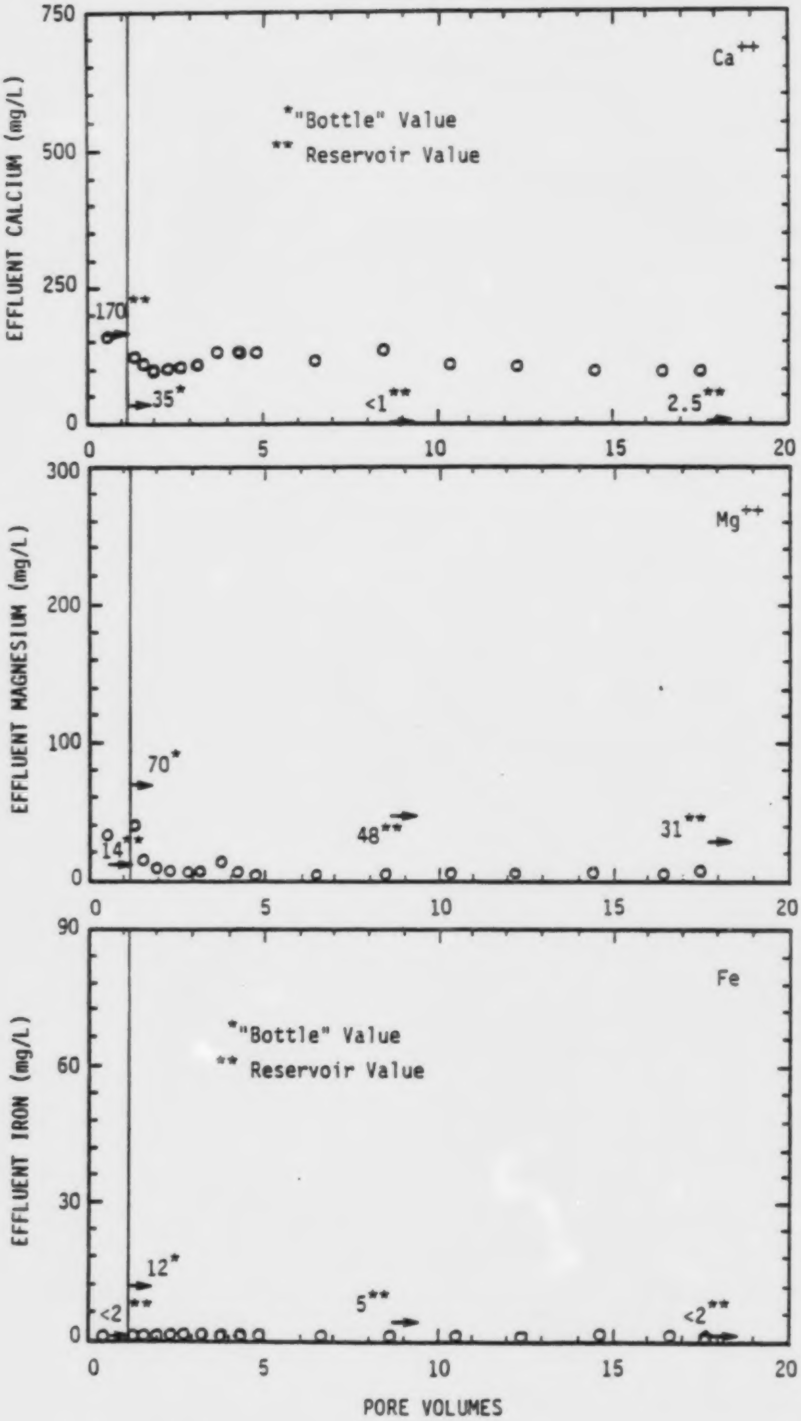

FIGURE I.8 EFFLUENT CONCENTRATION FOR INORGANIC SPECIES VS PORE VOLUMES

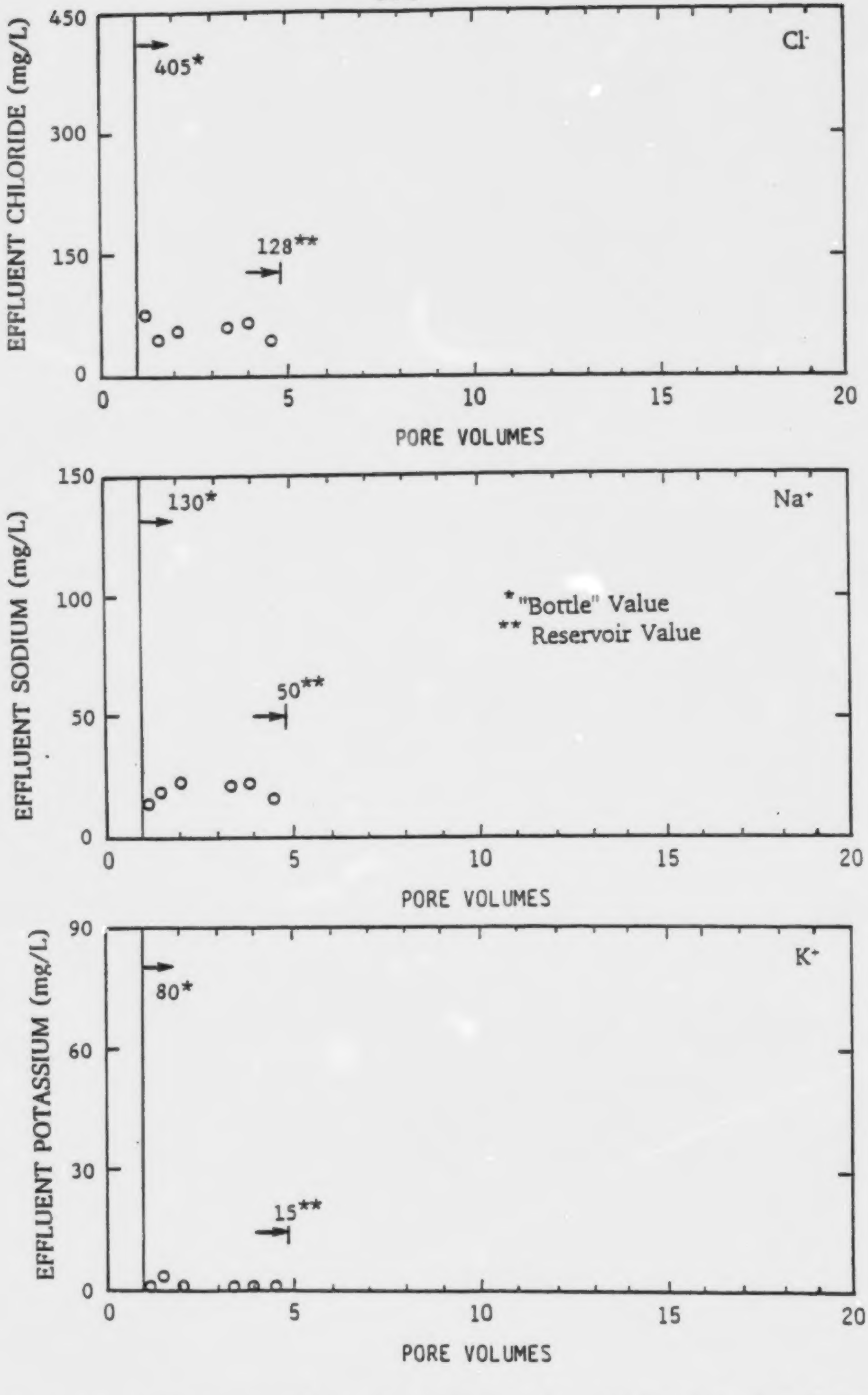

FIGURE I.9 EFFLUENT CONCENTRATION FOR INORGANIC SPECIES VS PORE VOLUMES

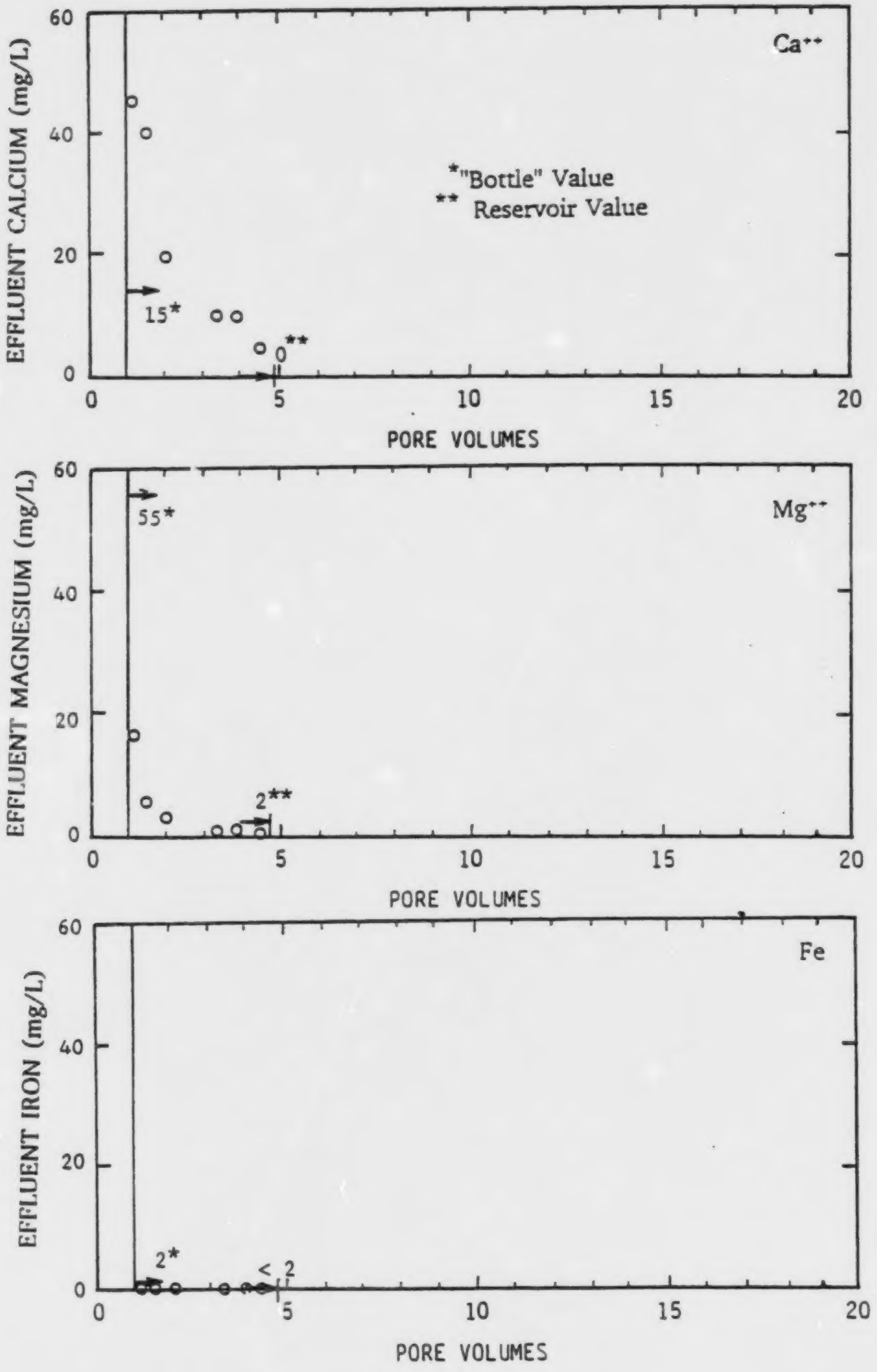

FIGURE I.10 EFFLUENT CONCENTRATION FOR INORGANIC SPECIES VS PORE VOLUMES

APPENDIX J

PORE SIZE DISTRIBUTION CURVES OBTAINED BY MERCURY INTRUSION POROSIMETRY

The results of pore size analyses by mercury intrusion porosimetry are presented in this chapter. Each figure includes an lower graph for the cumulative intruded pore volume (cubic centimetres per gram of dry soil), and an upper graph for the incremental intruded pore volume (also expressed in cm^3/g). The data in the upper graph are calculated from the measured values of pore intrusion (lower graph), and provides a clear picture of the distribution of pores in the tested specimen.

The samples were analyzed as part of the post-testing assessment of the hydraulic conductivity studies. These studies include:

Ethanol/water/brown Sarnia clay mixtures (Figures J.1 to J.9)

Ethanol/leachate/brown Sarnia clay mixtures (Figures J.10 to J.17)

Ethanol/water/kaolinite mixtures (Figures J.18 to J.22)

Dioxane/water/brown Sarnia clay mixtures (Figures J.23 to J.26)

Dioxane/leachate/brown Sarnia clay mixtures (Figures J.27 to J.29)

Water-compacted brown Sarnia clay permeated with water, σ'_v = 0 kPa (Figure J.30)

Water-compacted brown Sarnia clay permeated with water and then by leachate/ethanol mixtures, σ'_v = 0 kPa (Figures J.31 to J.34)

Water-compacted brown Sarnia clay permeated with water and then by leachate/dioxane mixtures, σ'_v = 0 kPa (Figures J.35 to J.39)

Water-compacted brown Sarnia clay permeated with water and then by leachate/dioxane mixtures, σ'_v = 40 to 160 kPa (Figures J.40 to J.47)

- Undisturbed samples of grey Sarnia clay permeated with water and then by leachate/ethanol mixtures, $\sigma'_v = 0$ kPa (Figures J.48 to J.52)

The soil specimens are trimmed by a razor blade down to a 10 mm cube and the pore fluids are removed by freeze-drying. This is done by dipping the specimens in a pentane bath for approximately one minute. The pentane bath is kept at a temperature of about -130 °C using liquid nitrogen as the cooling source. The soil specimens are subsequently placed under vacuum (< 0.07 mm Hg) and kept overnight. During this period the frozen pore fluid is removed from the soil by sublimation. The freeze-drying technique employed was found to successfully prevent volume changes for of water saturated soil samples.

The analyses were performed using a Micromeritics Poresizer 9310, which generates hydraulic pressures in excess of 30,000 psi (207 MPa). At this pressure level, mercury intrusion can reach pores of ~ 6 nm.

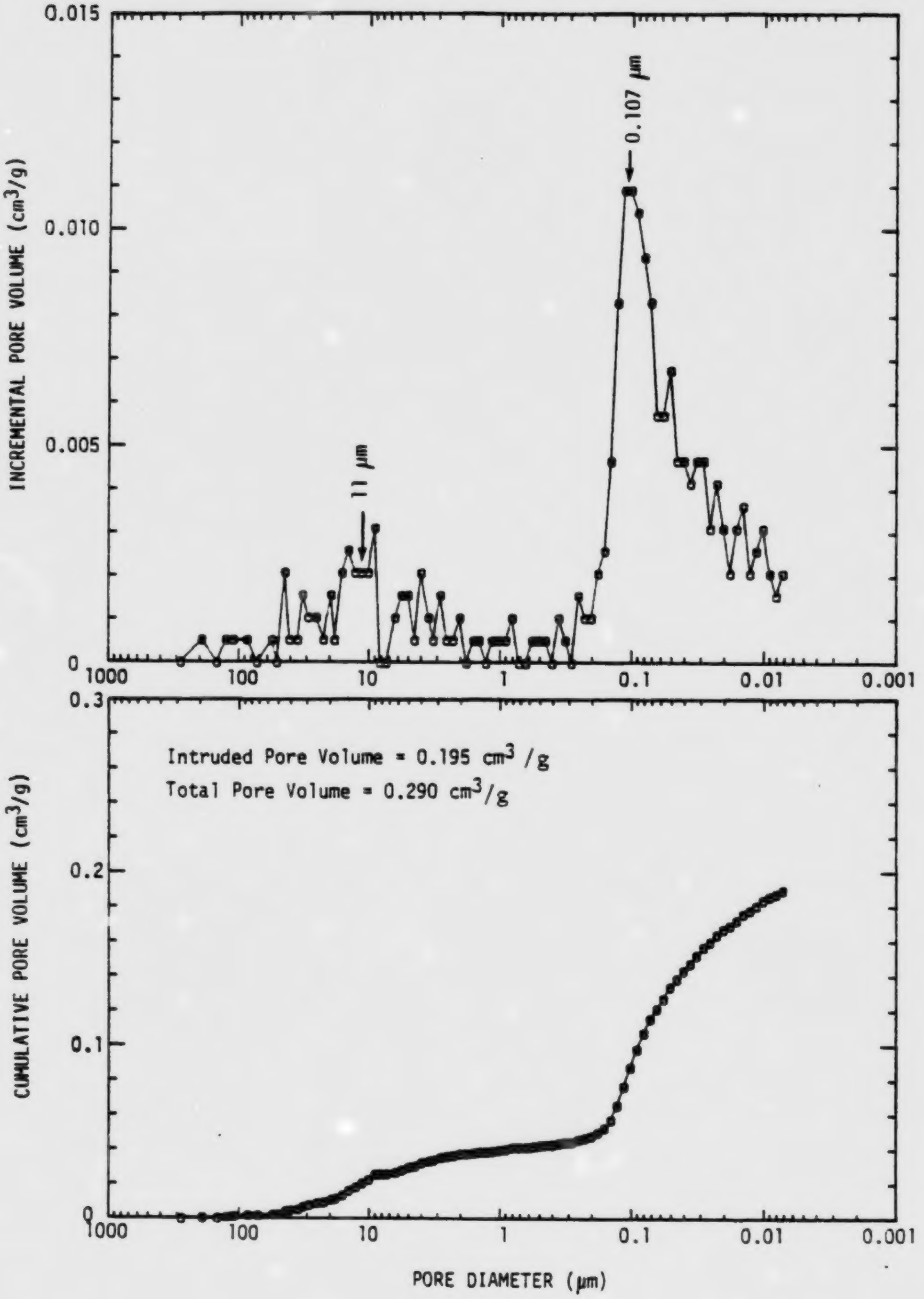

FIGURE J.1 PORE SIZE DISTRIBUTION FOR BROWN SARNIA CLAY MIXED WITH 100% WATER

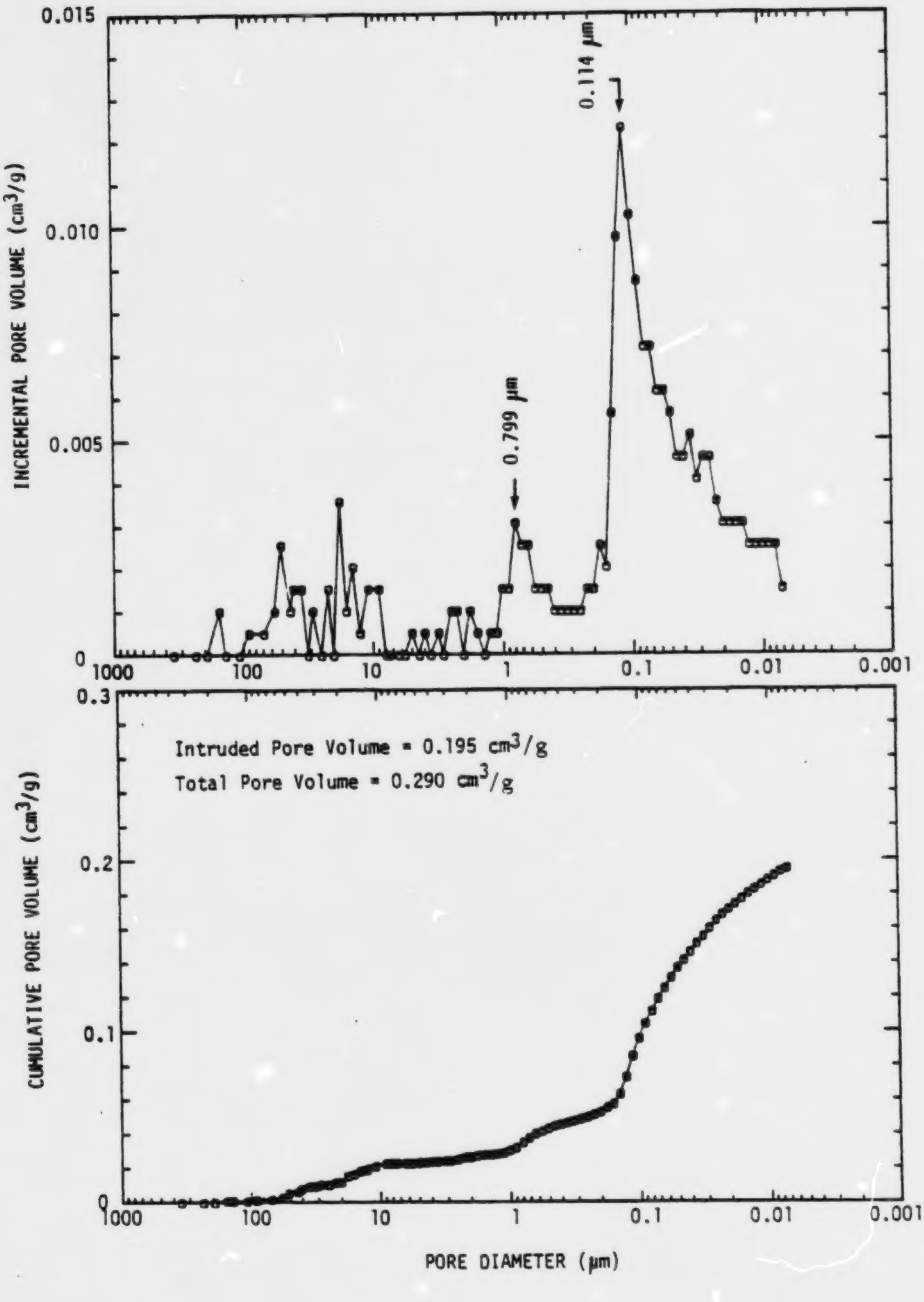

FIGURE J.2 PORE SIZE DISTRIBUTION FOR BROWN SARNIA CLAY MIXED WITH 10% ETHANOL - 90% WATER

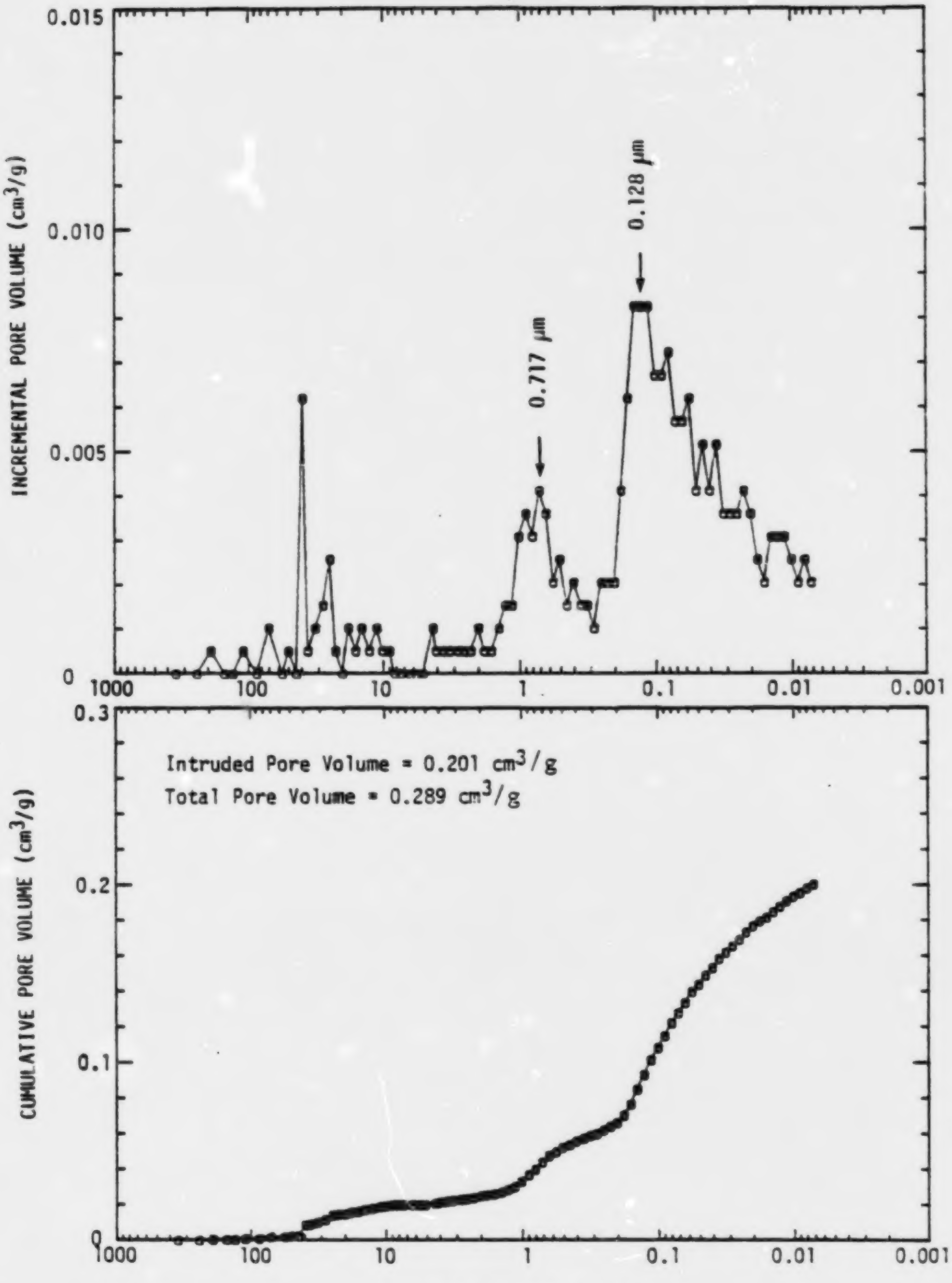

FIGURE J.3 PORE SIZE DISTRIBUTION FOR BROWN SARNIA CLAY MIXED WITH 20% ETHANOL - 80% WATER

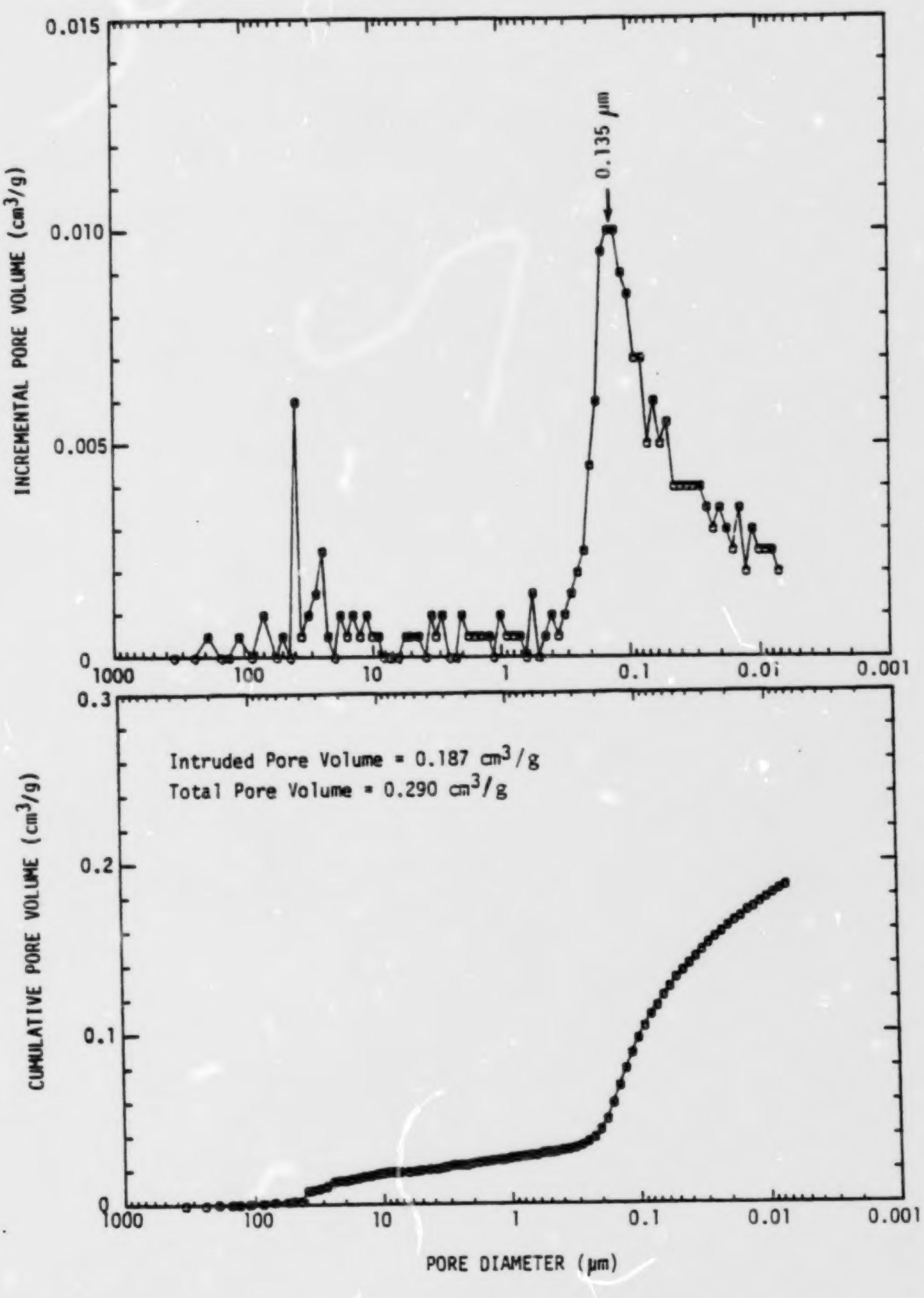

FIGURE J.4 PORE SIZE DISTRIBUTION FOR BROWN SARNIA CLAY MIXED WITH 35% ETHANOL - 65% WATER

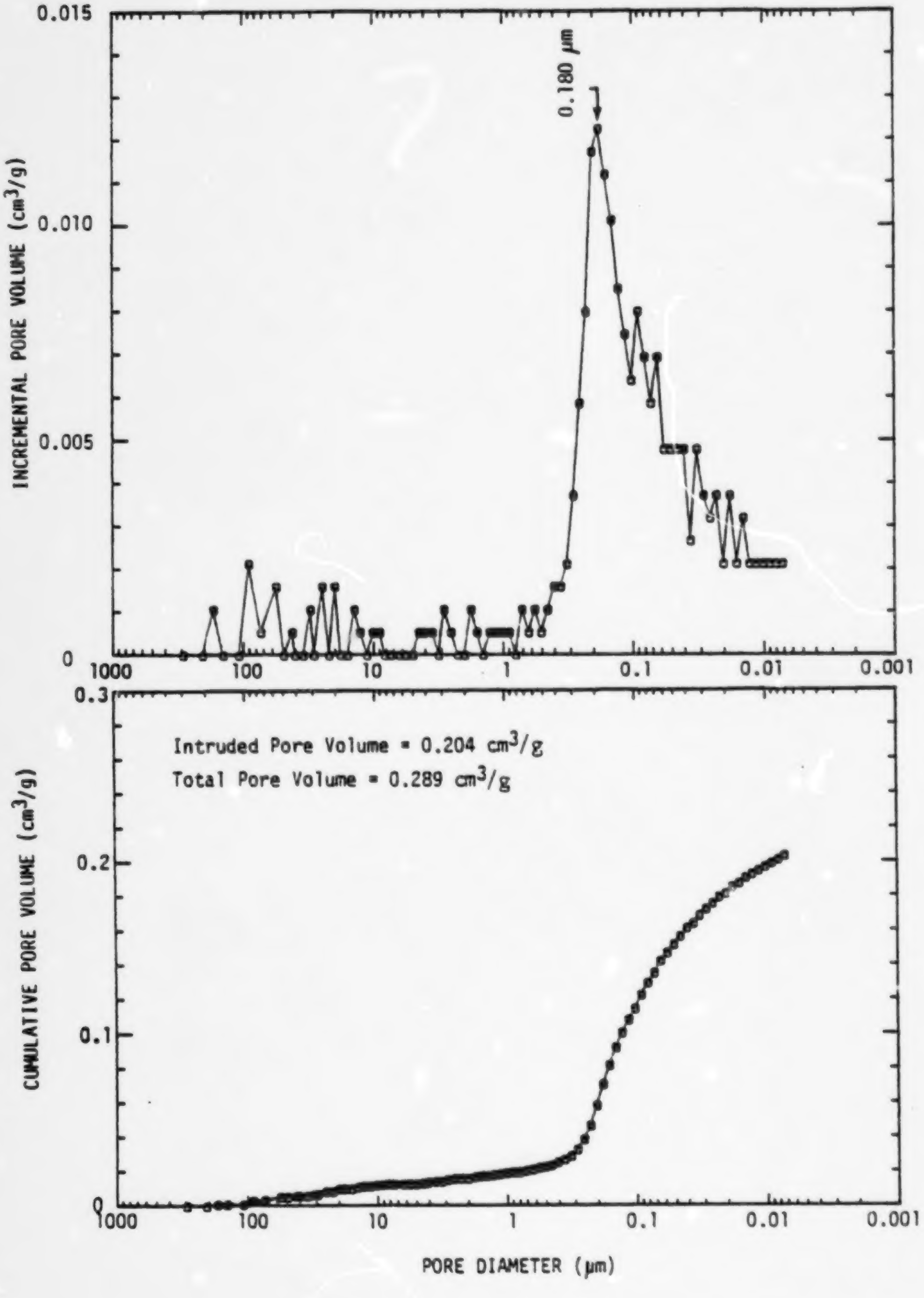

FIGURE J.5 PORE SIZE DISTRIBUTION FOR BROWN SARNIA CLAY MIXED WITH 50% ETHANOL - 50% WATER

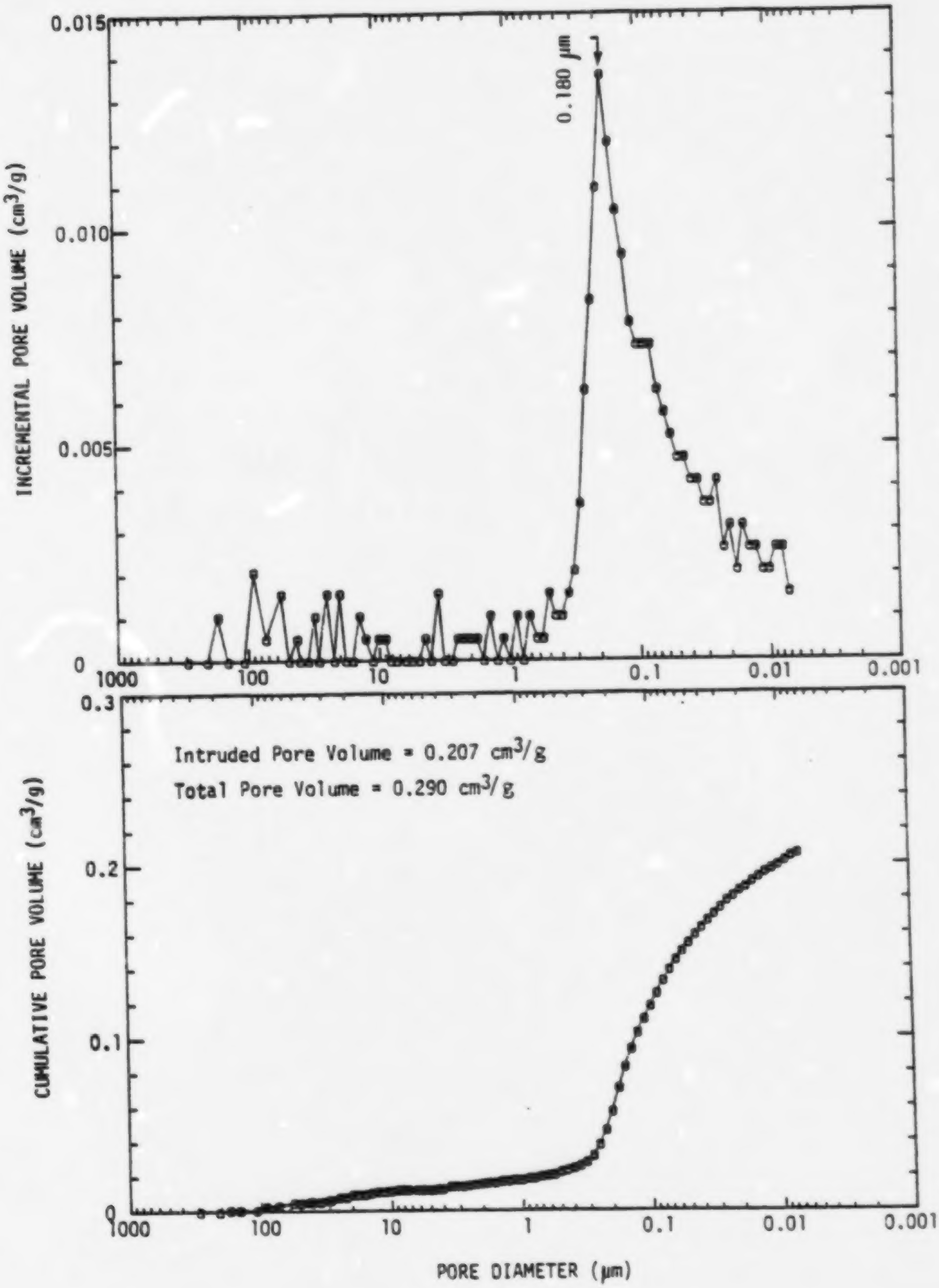

FIGURE J.6 PORE SIZE DISTRIBUTION FOR BROWN SARNIA CLAY MIXED WITH 65% ETHANOL - 35% WATER

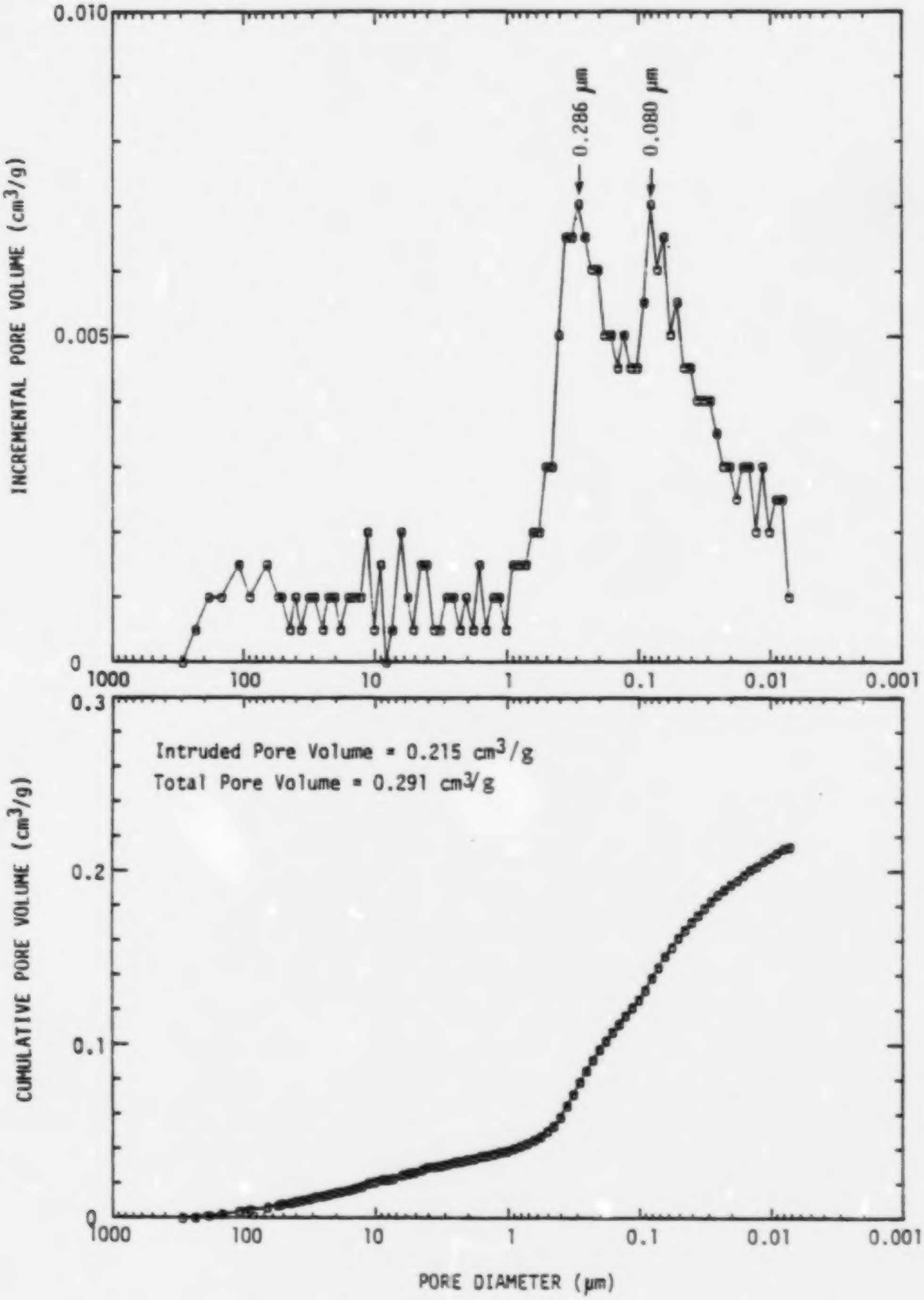

FIGURE J.7 PORE SIZE DISTRIBUTION FOR BROWN SARNIA CLAY MIXED WITH 80% ETHANOL - 20% WATER

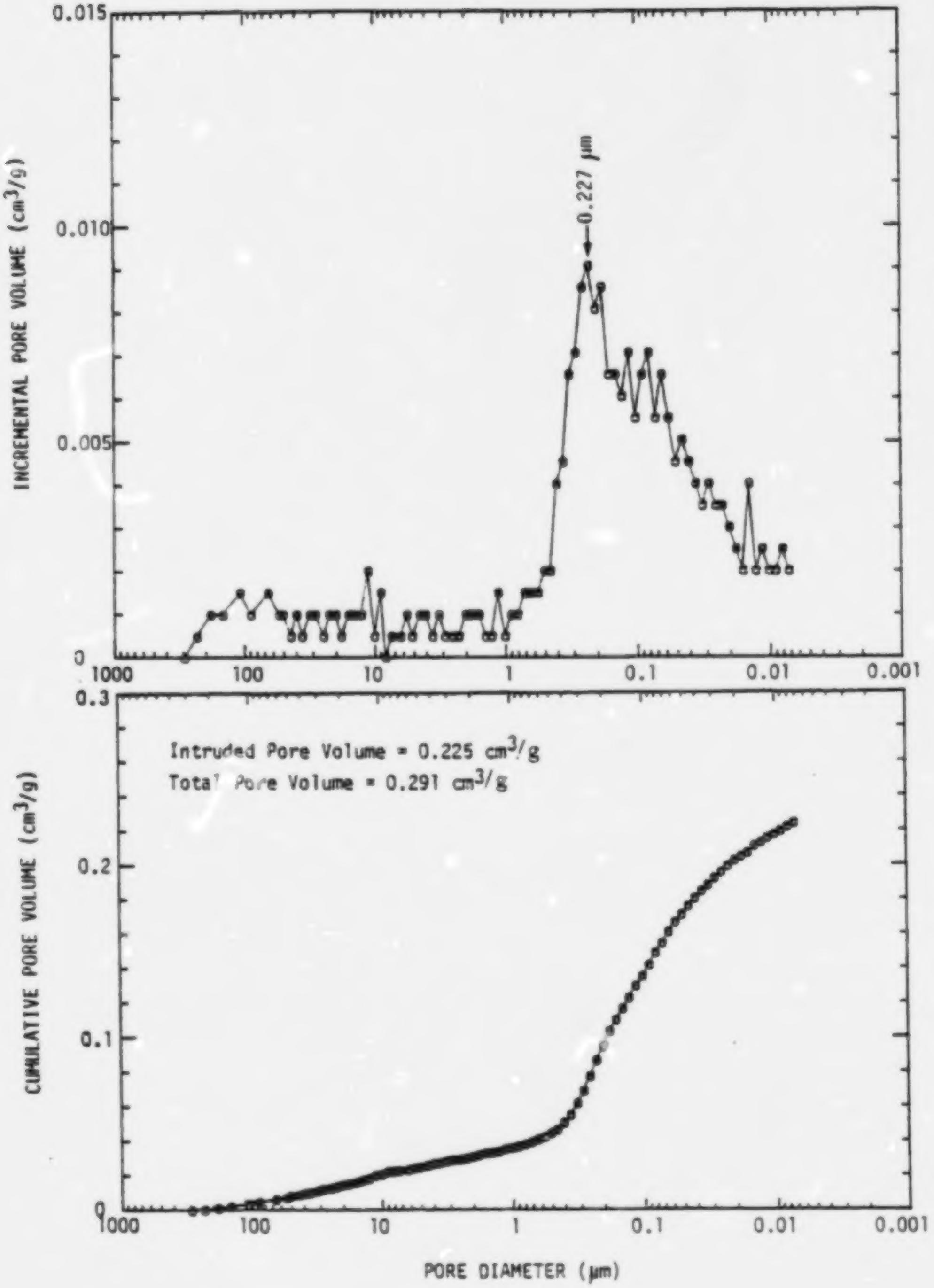

FIGURE J.8 PORE SIZE DISTRIBUTION FOR BROWN SARNIA CLAY MIXED WITH 90% ETHANOL - 10% WATER

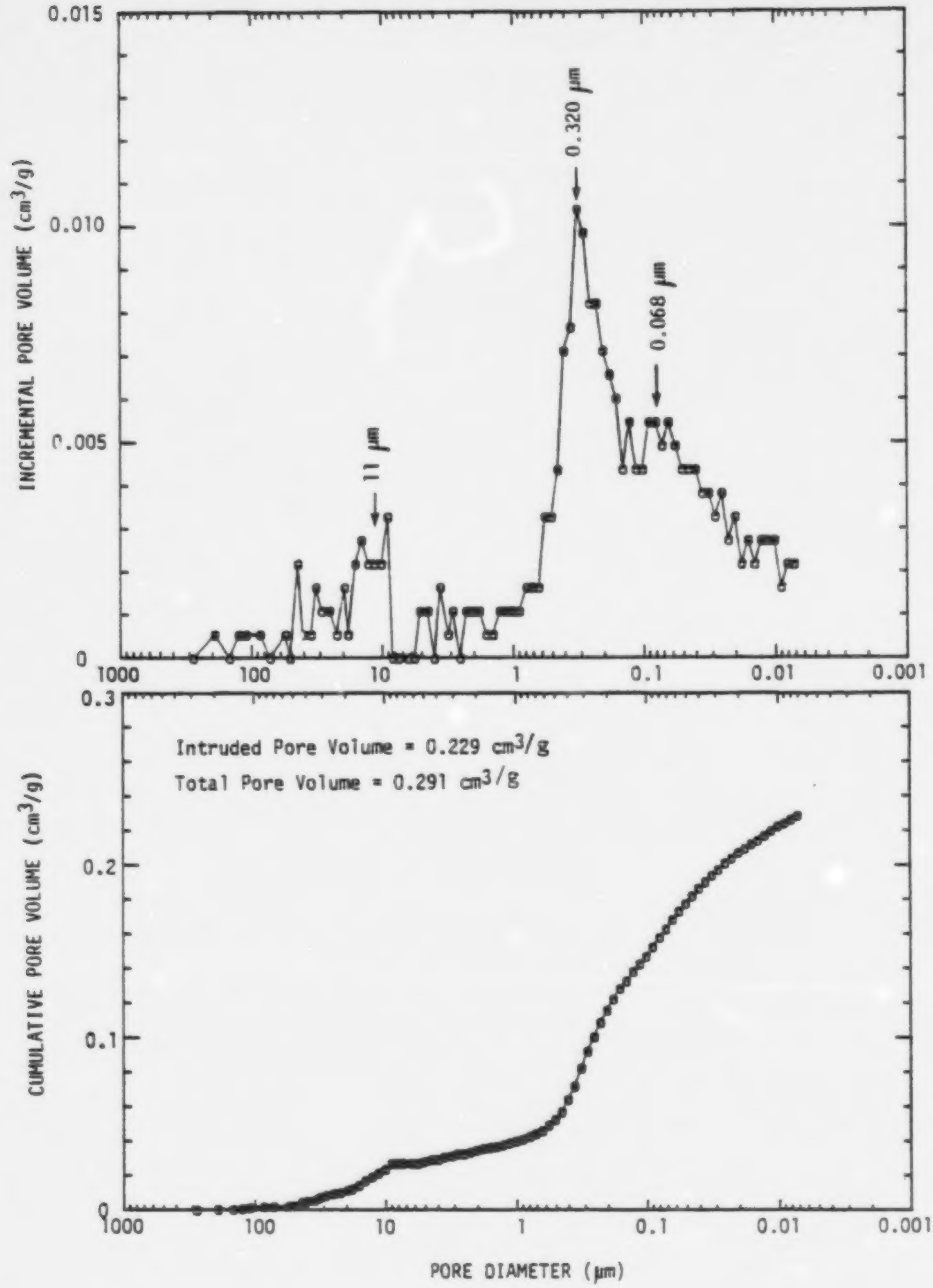

FIGURE J.9 PORE SIZE DISTRIBUTION FOR BROWN SARNIA CLAY MIXED WITH 100% ETHANOL

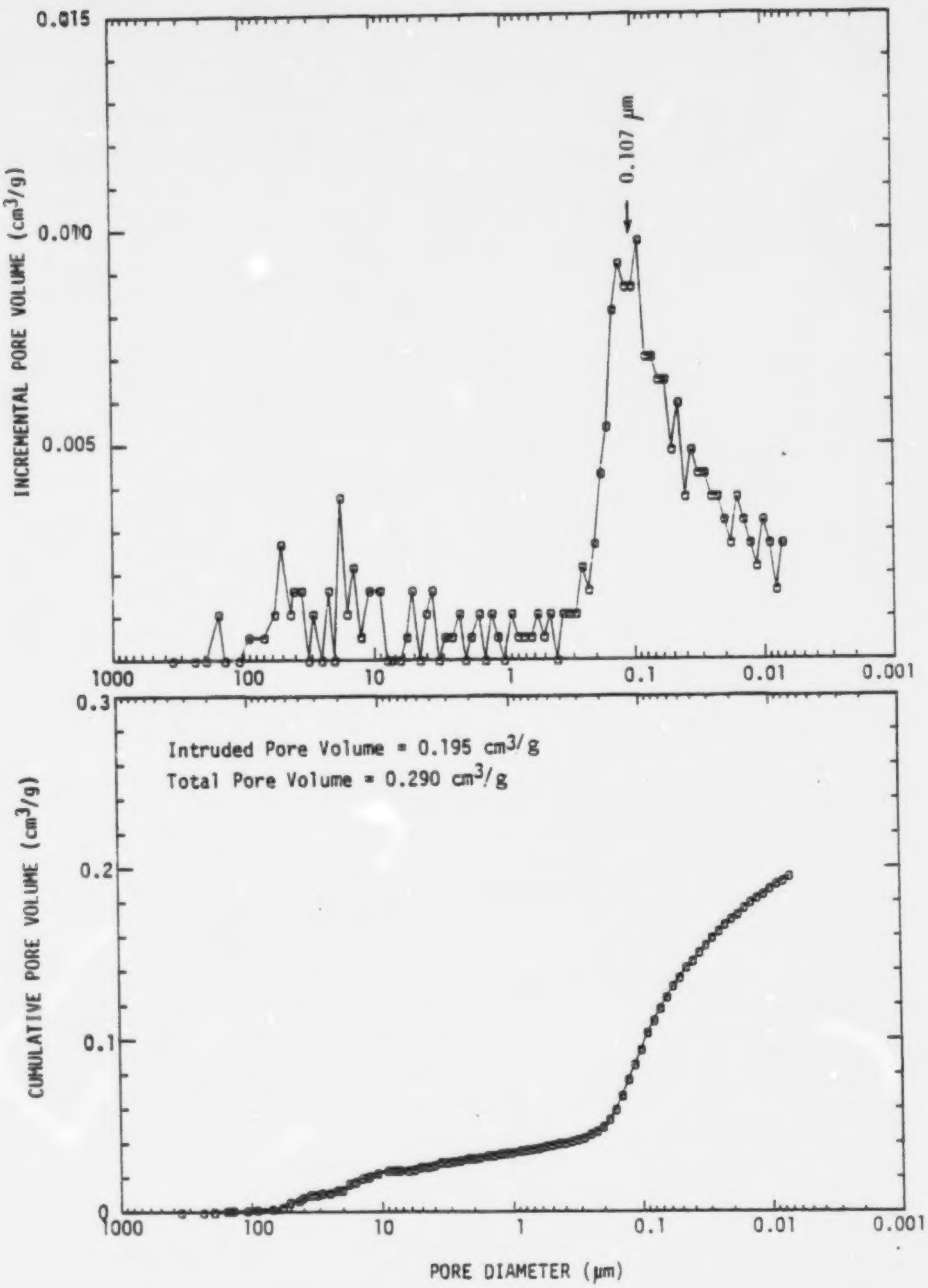

FIGURE J.10 PORE SIZE DISTRIBUTION FOR BROWN SARNIA CLAY MIXED WITH 100% LEACHATE

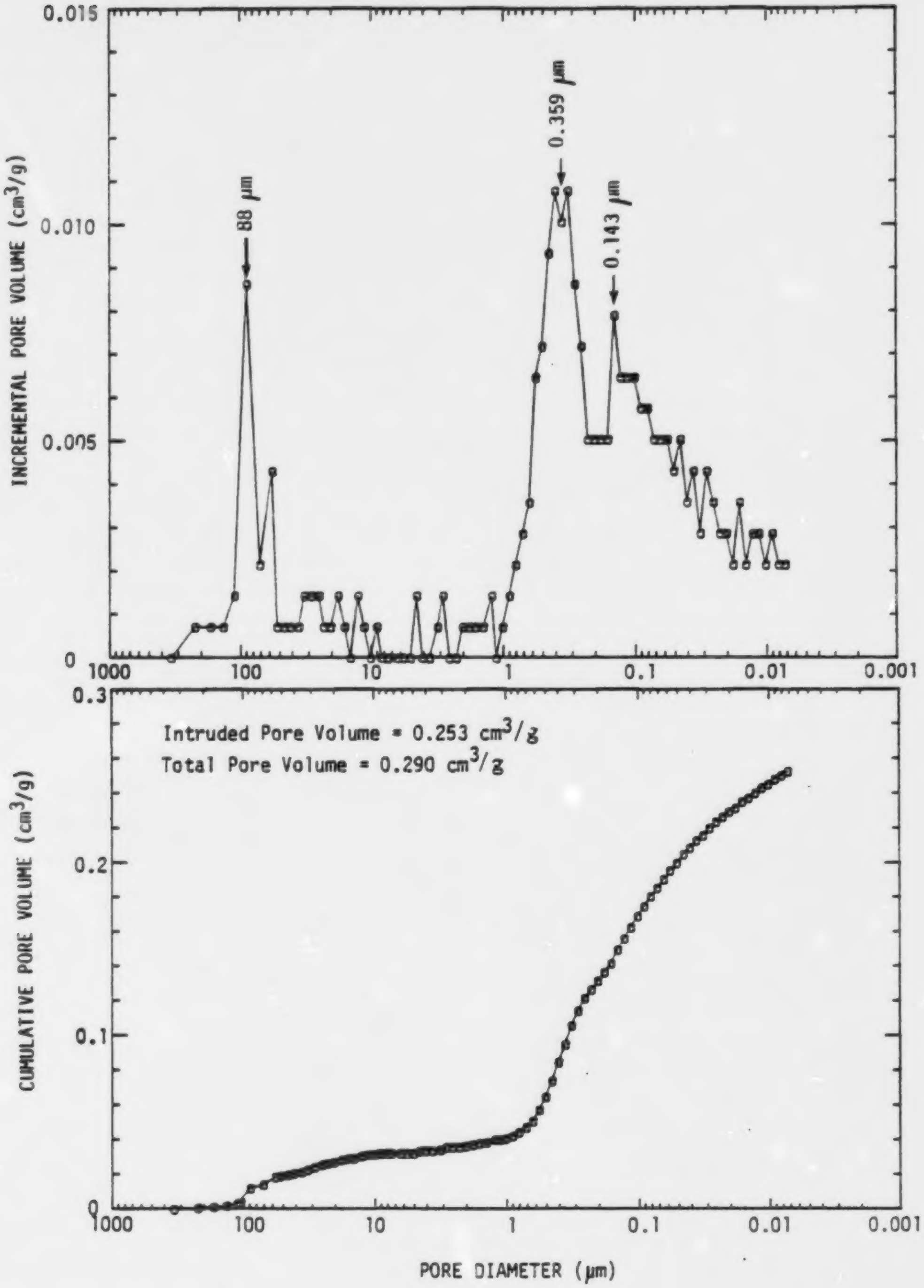

FIGURE J.11 PORE SIZE DISTRIBUTION FOR BROWN SARNIA CLAY MIXED WITH 10% ETHANOL - 90%LEACHATE

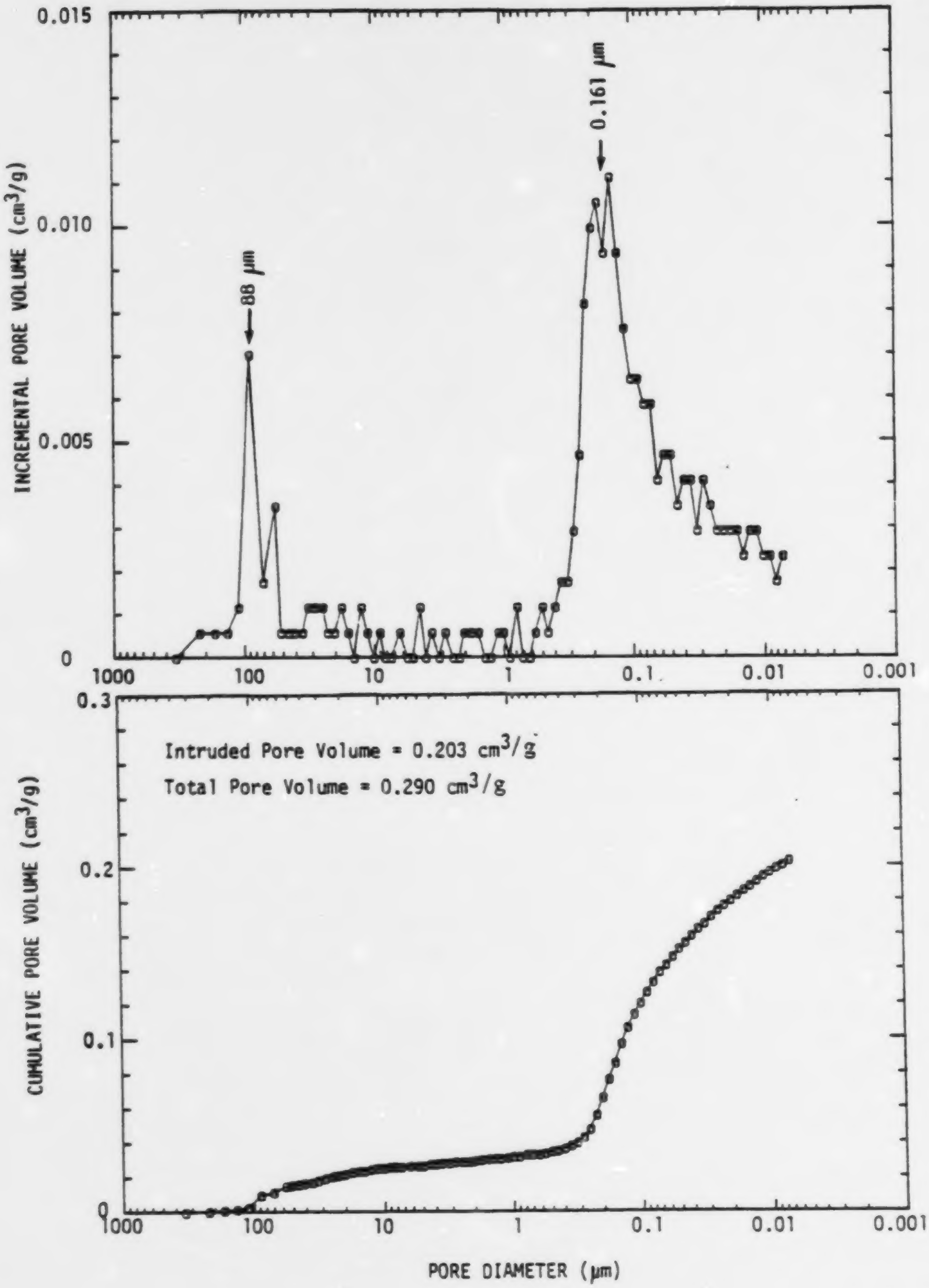

FIGURE J.12 PORE SIZE DISTRIBUTION FOR BROWN SARNIA CLAY MIXED WITH 20% ETHANOL - 80%LEACHATE

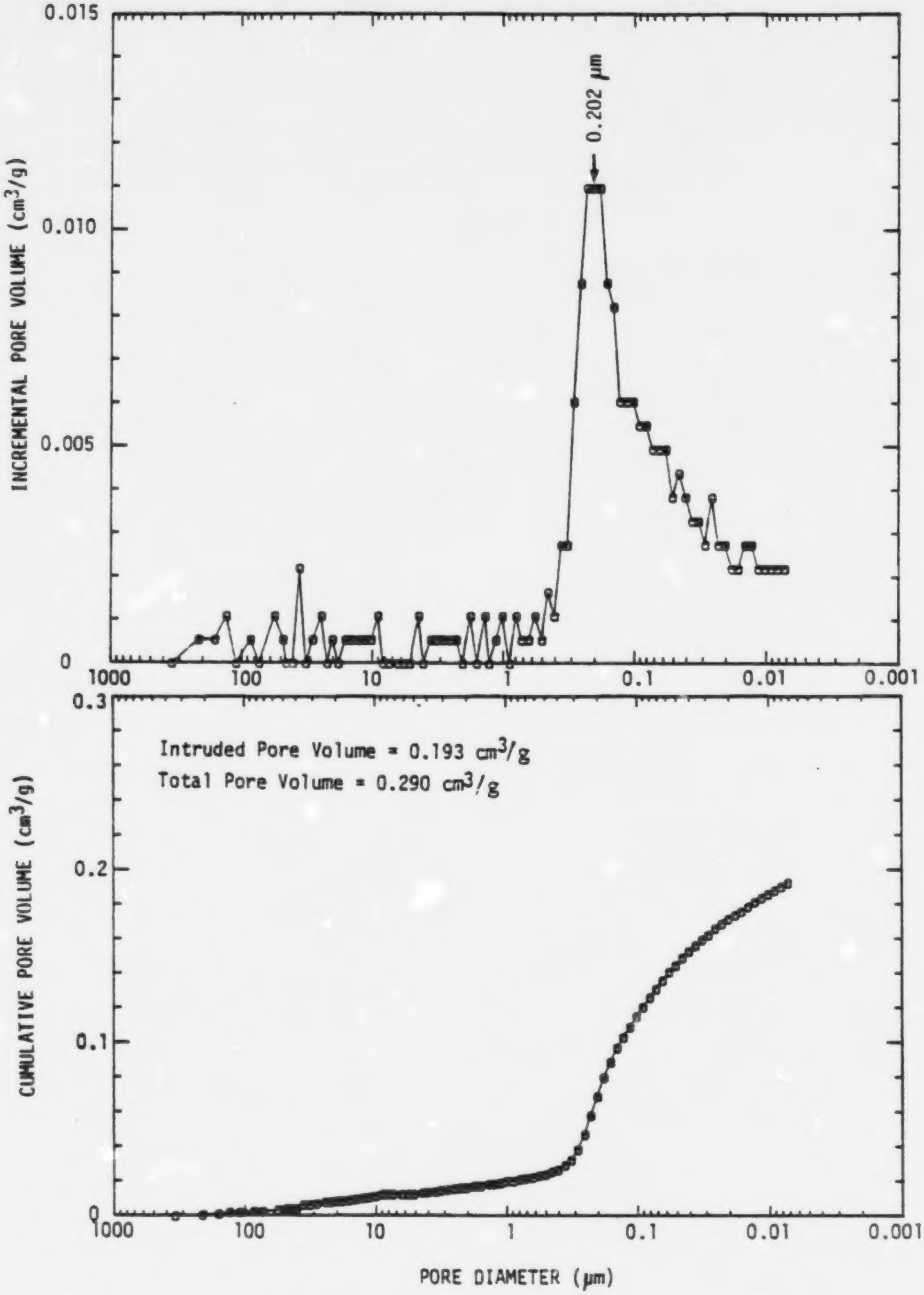

FIGURE J.13 PORE SIZE DISTRIBUTION FOR BROWN SARNIA CLAY MIXED WITH 35% ETHANOL - 65%LEACHATE

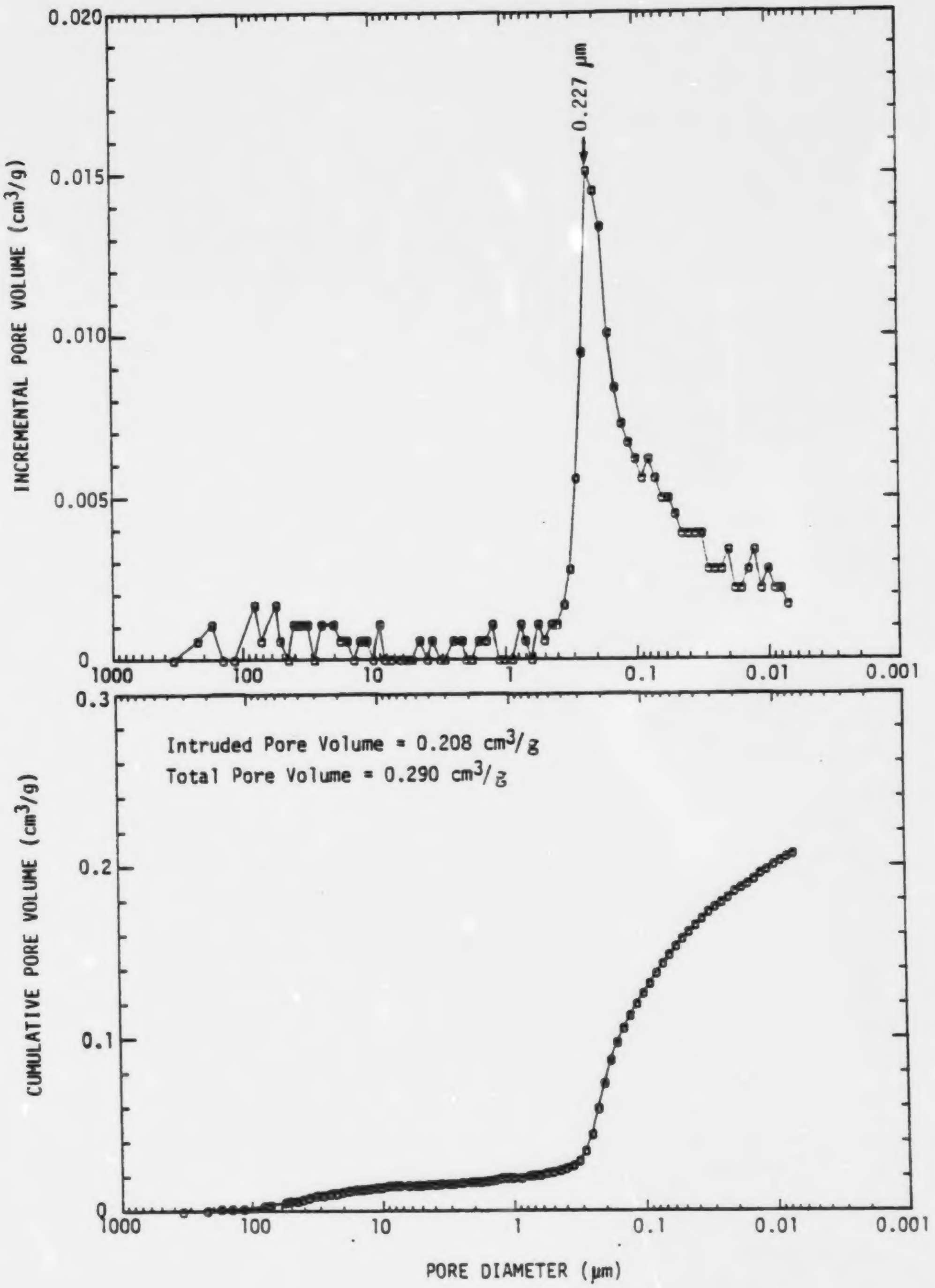

FIGURE J.14 PORE SIZE DISTRIBUTION FOR BROWN SARNIA CLAY MIXED WITH 50% ETHANOL - 50% LEACHATE

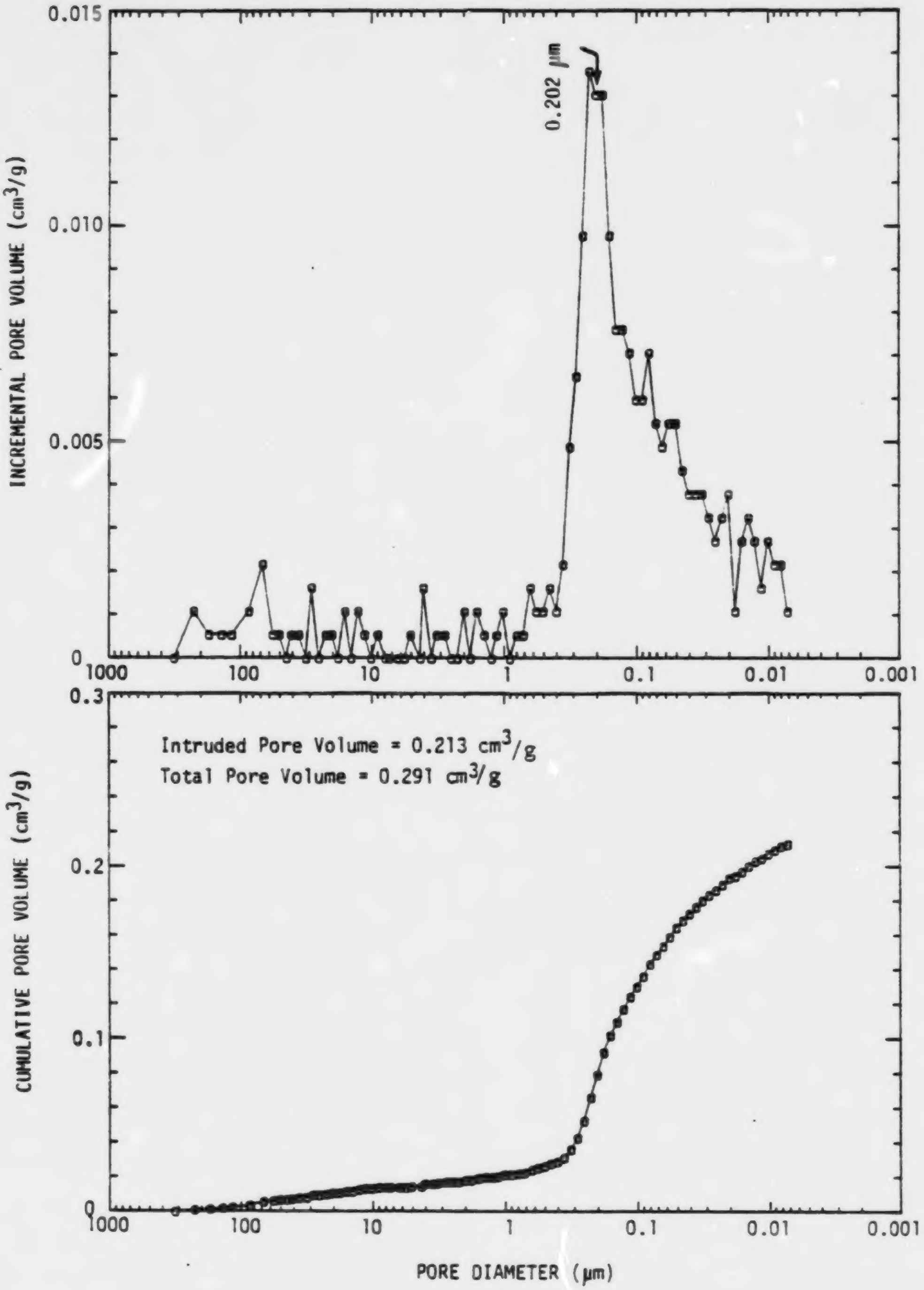

FIGURE J.15 PORE SIZE DISTRIBUTION FOR BROWN SARNIA CLAY MIXED WITH 65% ETHANOL - 35% LEACHATE

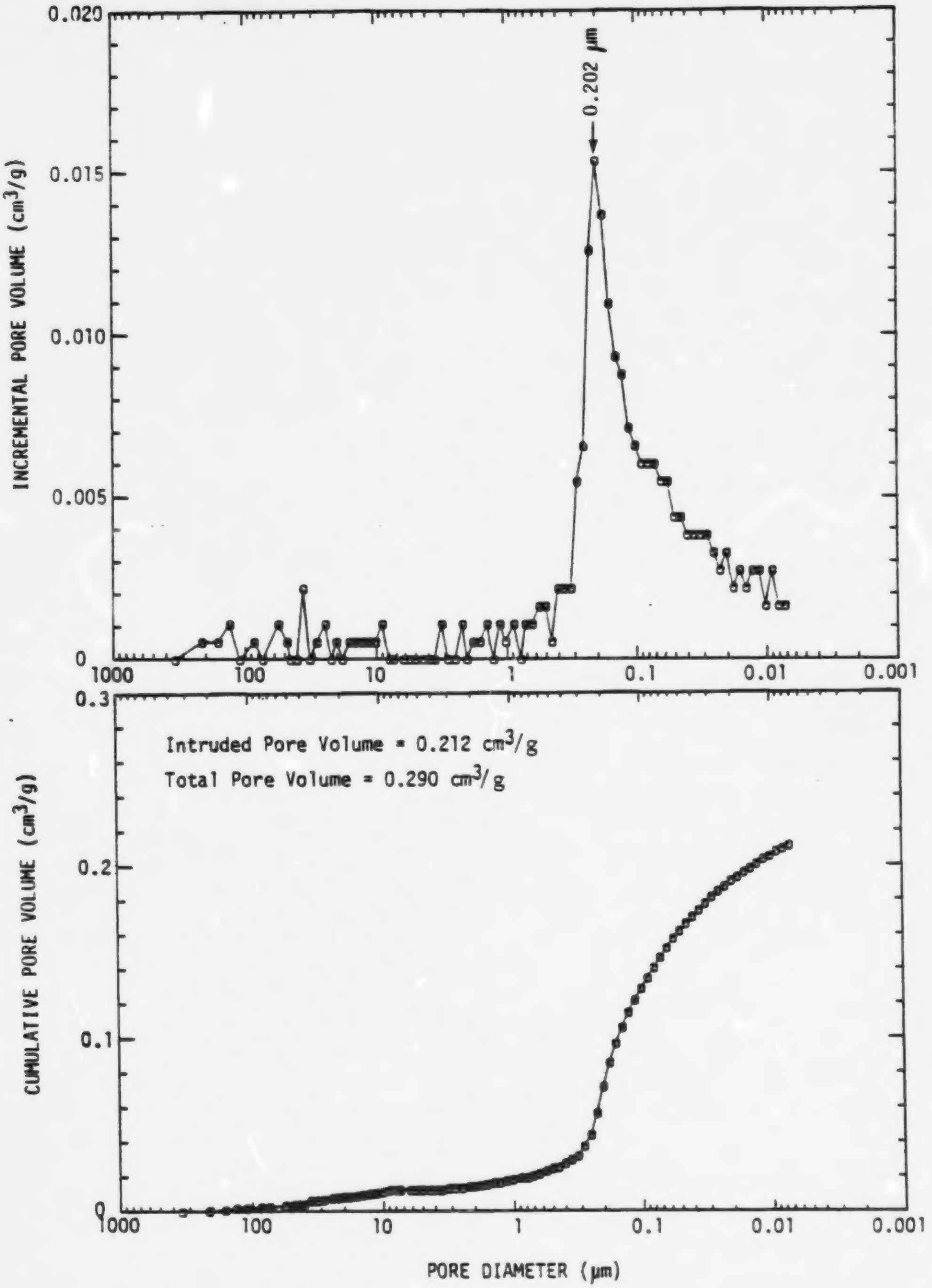

FIGURE J.16 PORE SIZE DISTRIBUTION FOR BROWN SARNIA CLAY MIXED WITH 80% ETHANOL - 20% LEACHATE

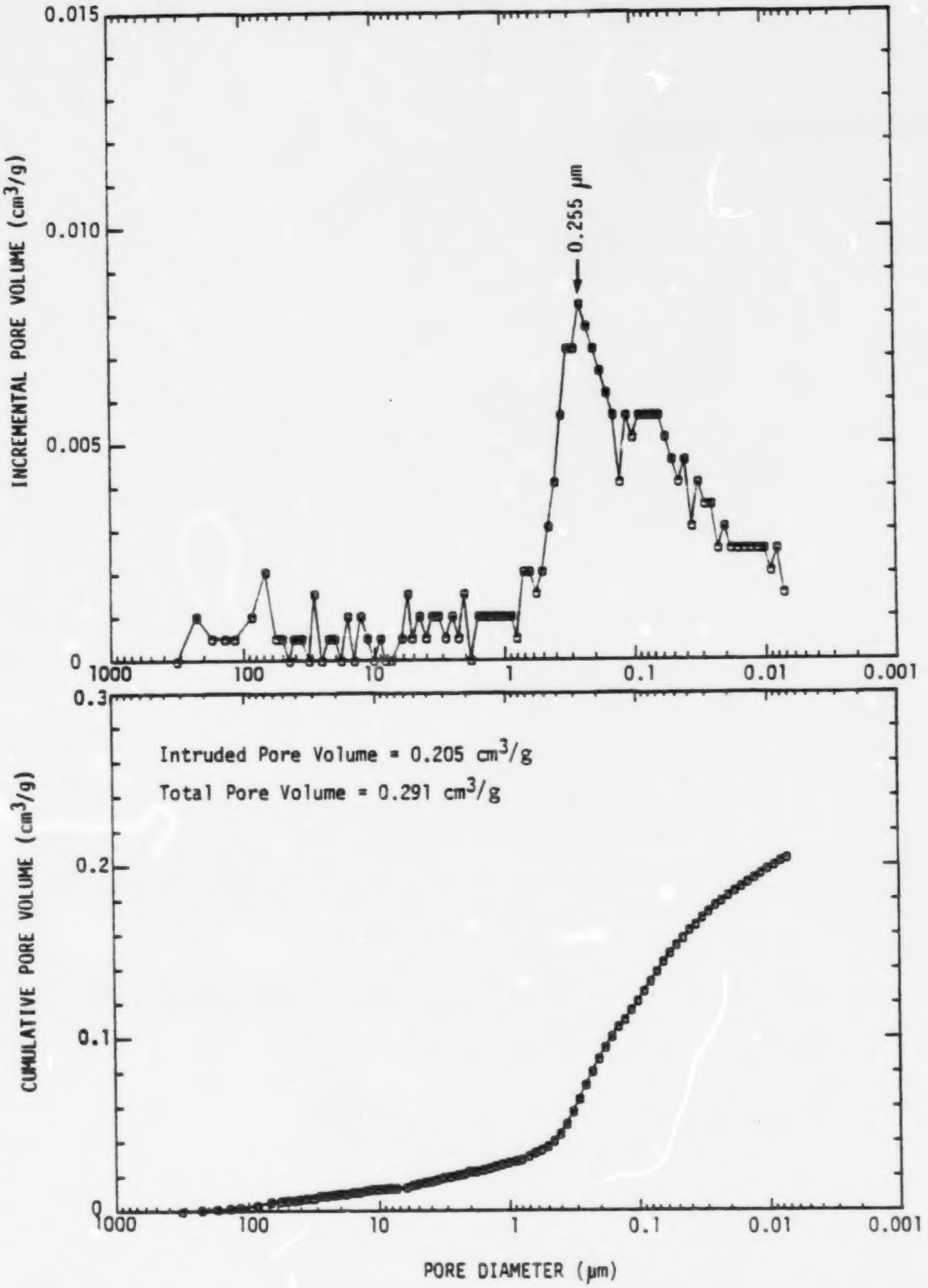

FIGURE J.17 PORE SIZE DISTRIBUTION FOR BROWN SARNIA CLAY MIXED WITH 90% ETHANOL - 10% LEACHATE .

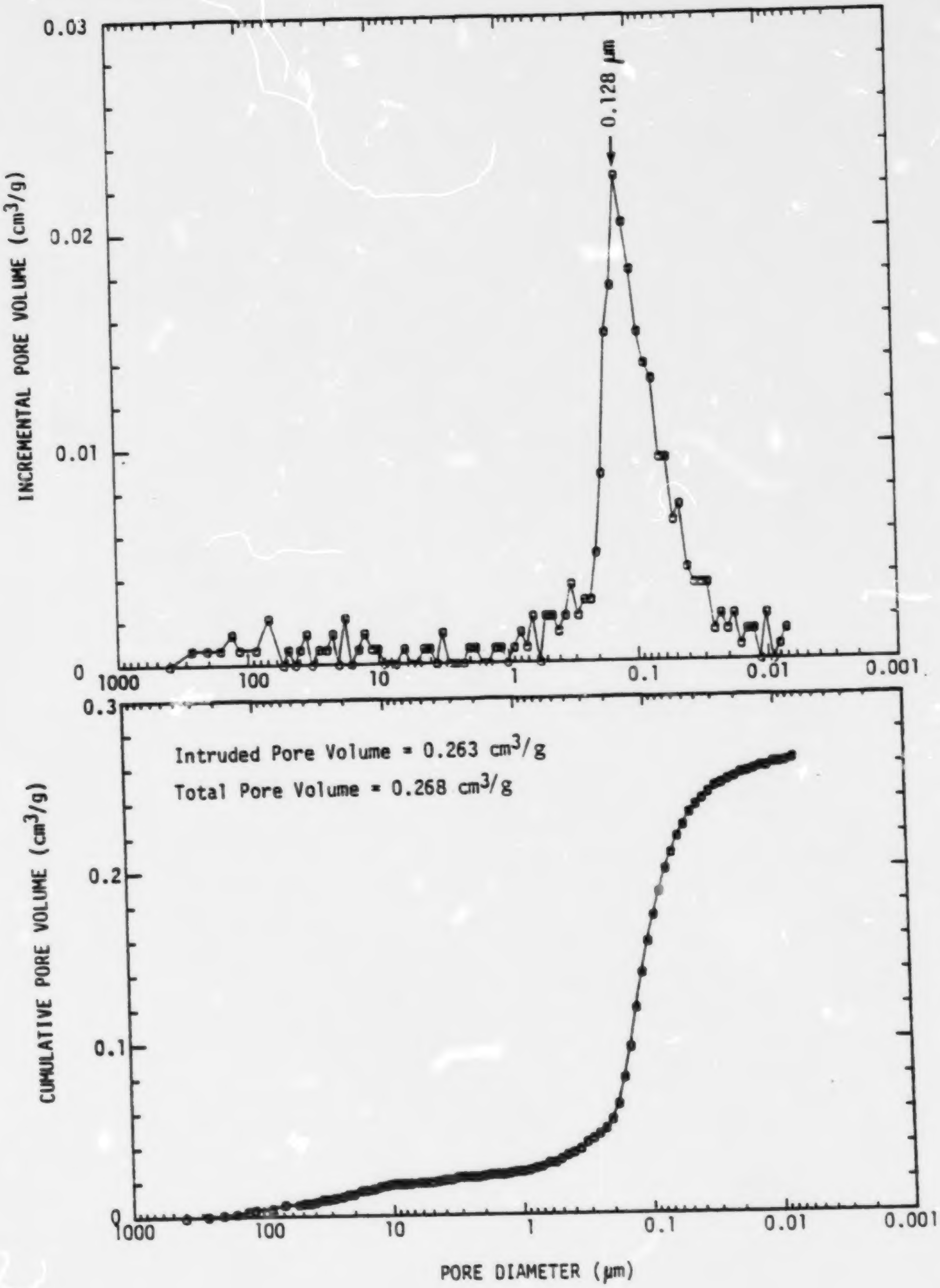

FIGURE J.18 PORE SIZE DISTRIBUTION FOR KAOLINITE MIXED WITH 100% WATER

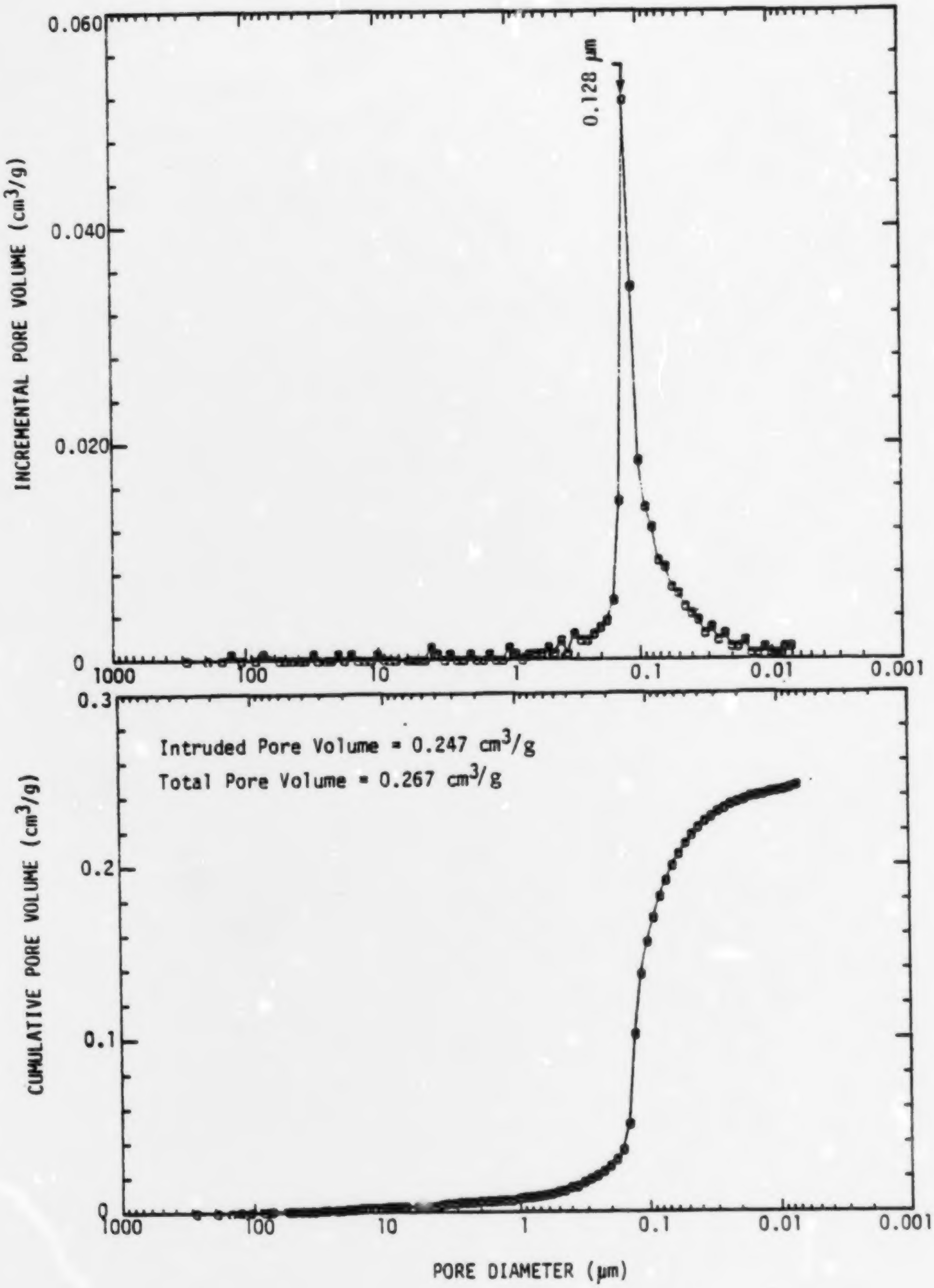

FIGURE J.19 PORE SIZE DISTRIBUTION FOR KAOLINITE MIXED WITH 20% ETHANOL - 80% WATER

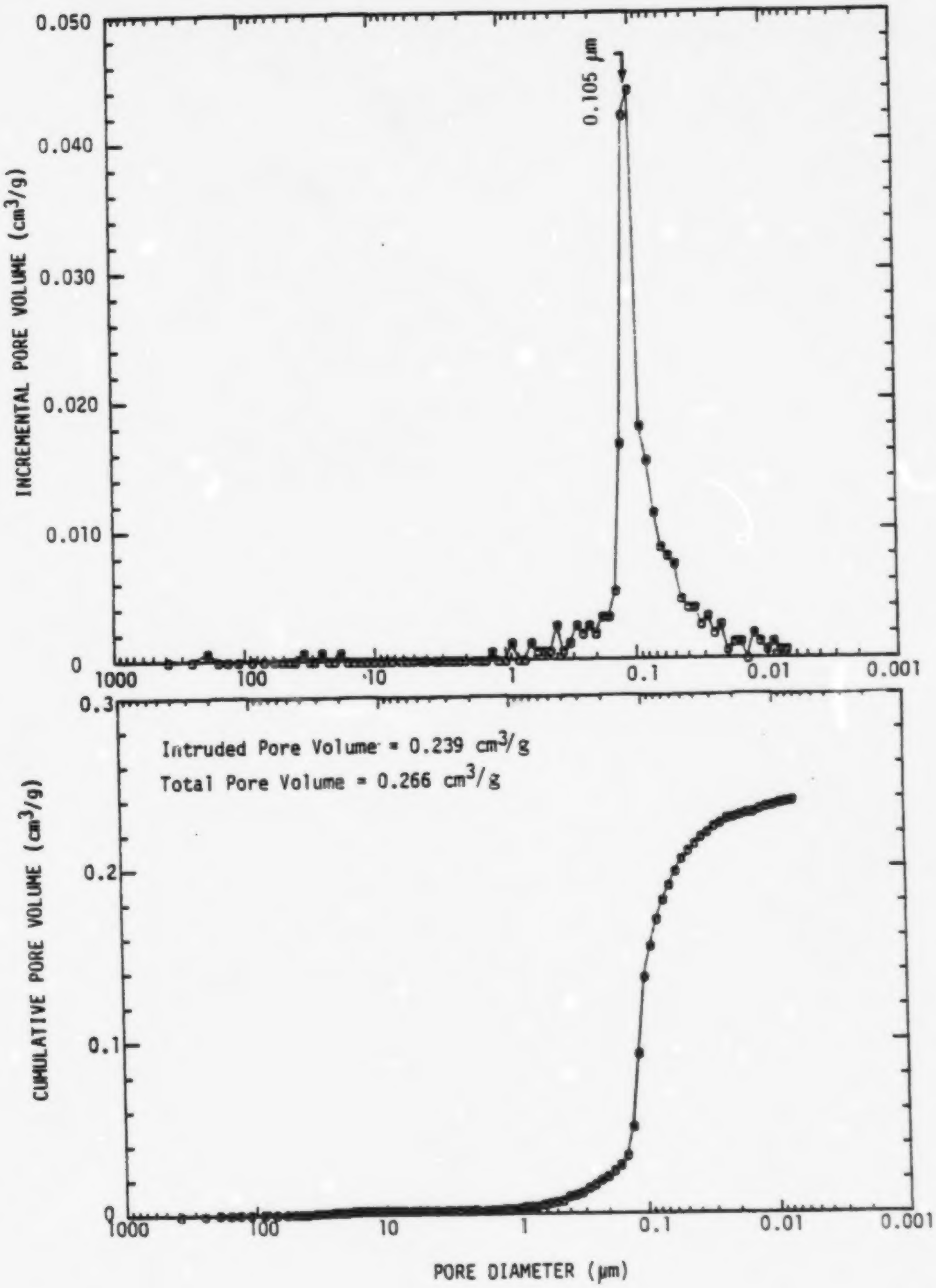

FIGURE J.20 PORE SIZE DISTRIBUTION FOR KAOLINITE MIXED WITH 50% ETHANOL - 50% WATER

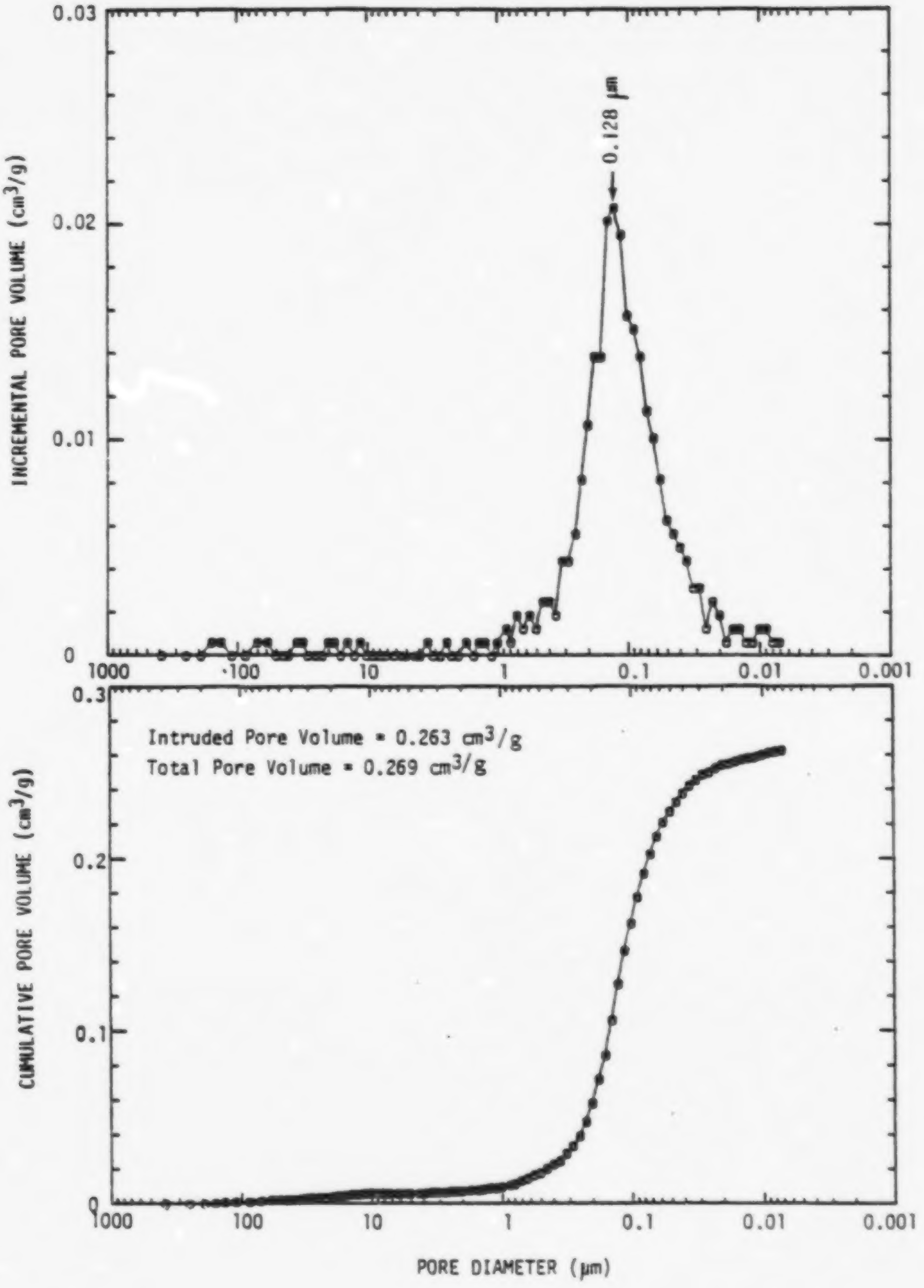

FIGURE J.21 PORE SIZE DISTRIBUTION FOR KAOLINITE MIXED WITH 80% ETHANOL - 20% WATER

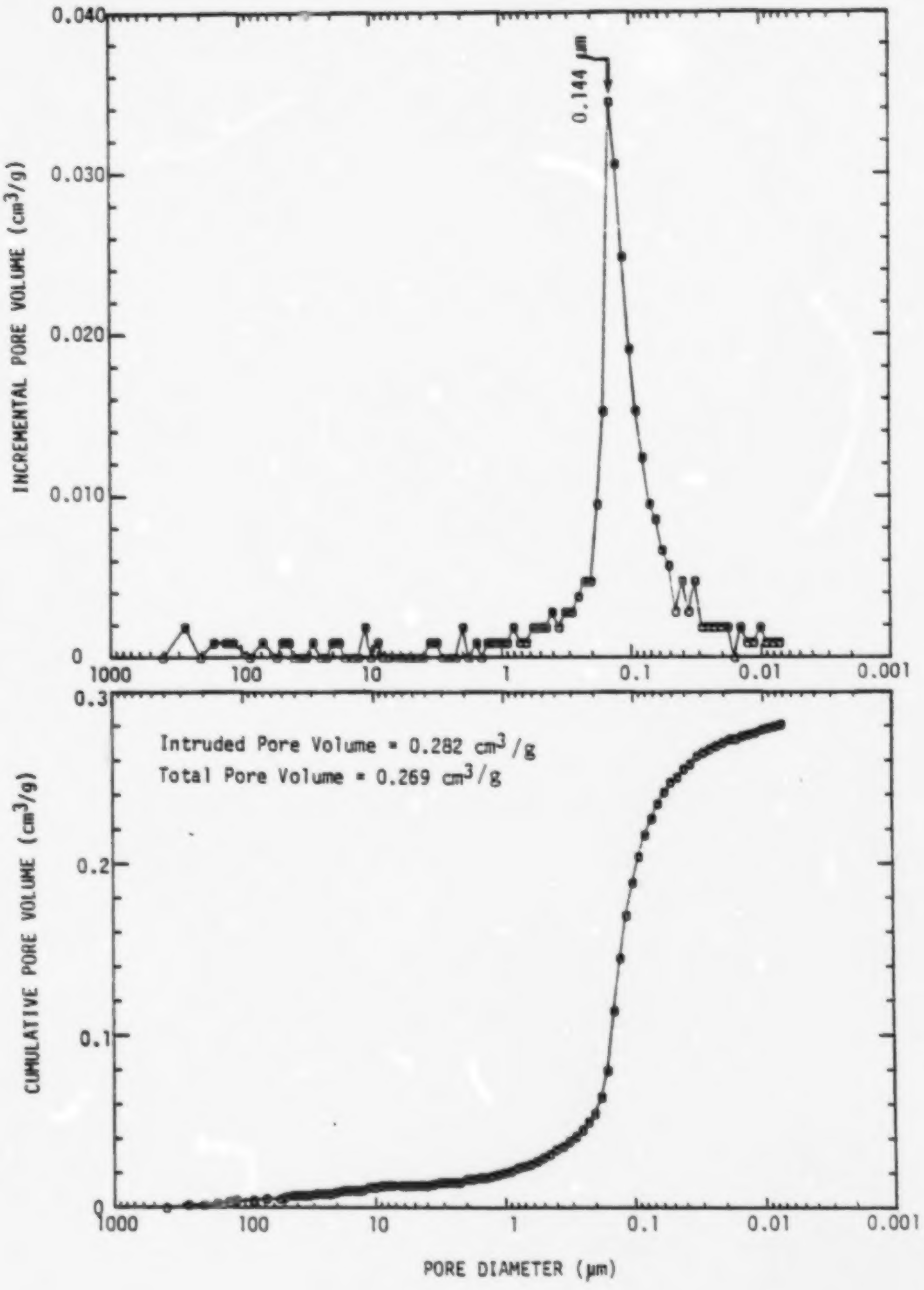

FIGURE J.22 PORE SIZE DISTRIBUTION FOR KAOLINITE MIXED WITH 100% ETHANOL

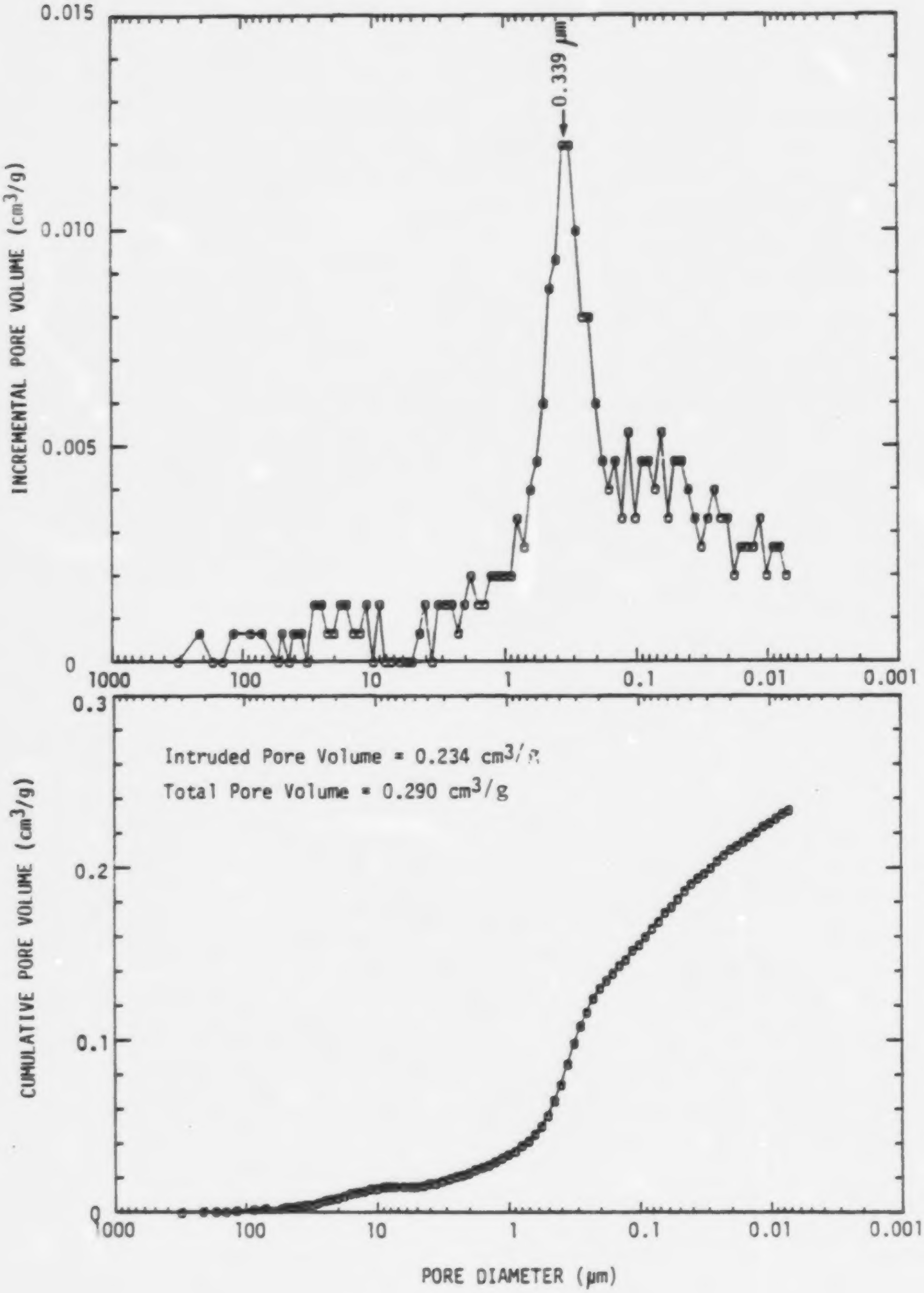

FIGURE J.23 PORE SIZE DISTRIBUTION FOR BROWN SARNIA CLAY MIXED WITH 20% DIOXANE - 80% WATER

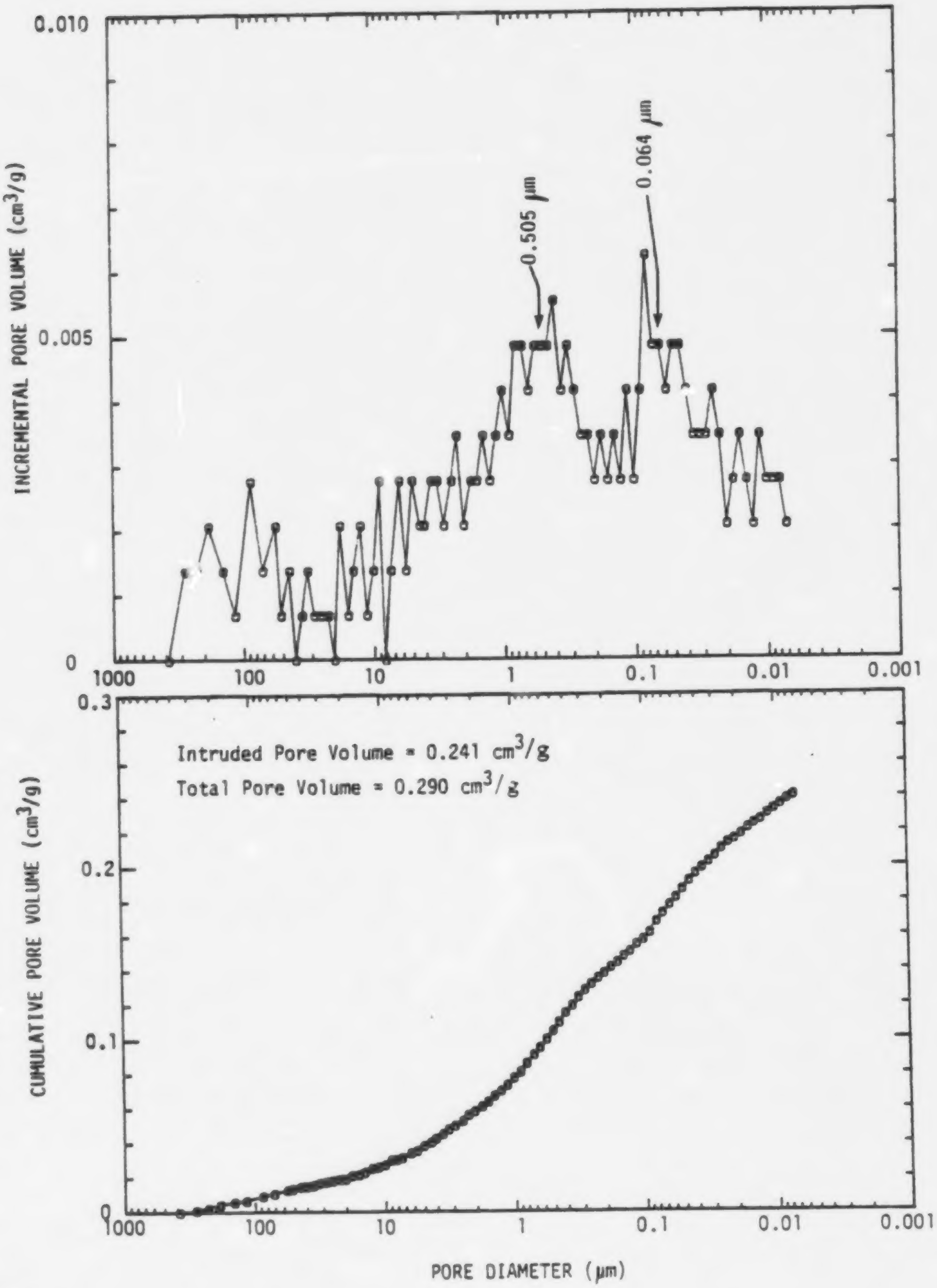

FIGURE J.24 PORE SIZE DISTRIBUTION FOR BROWN SARNIA CLAY MIXED WITH 50% DIOXANE - 50% WATER

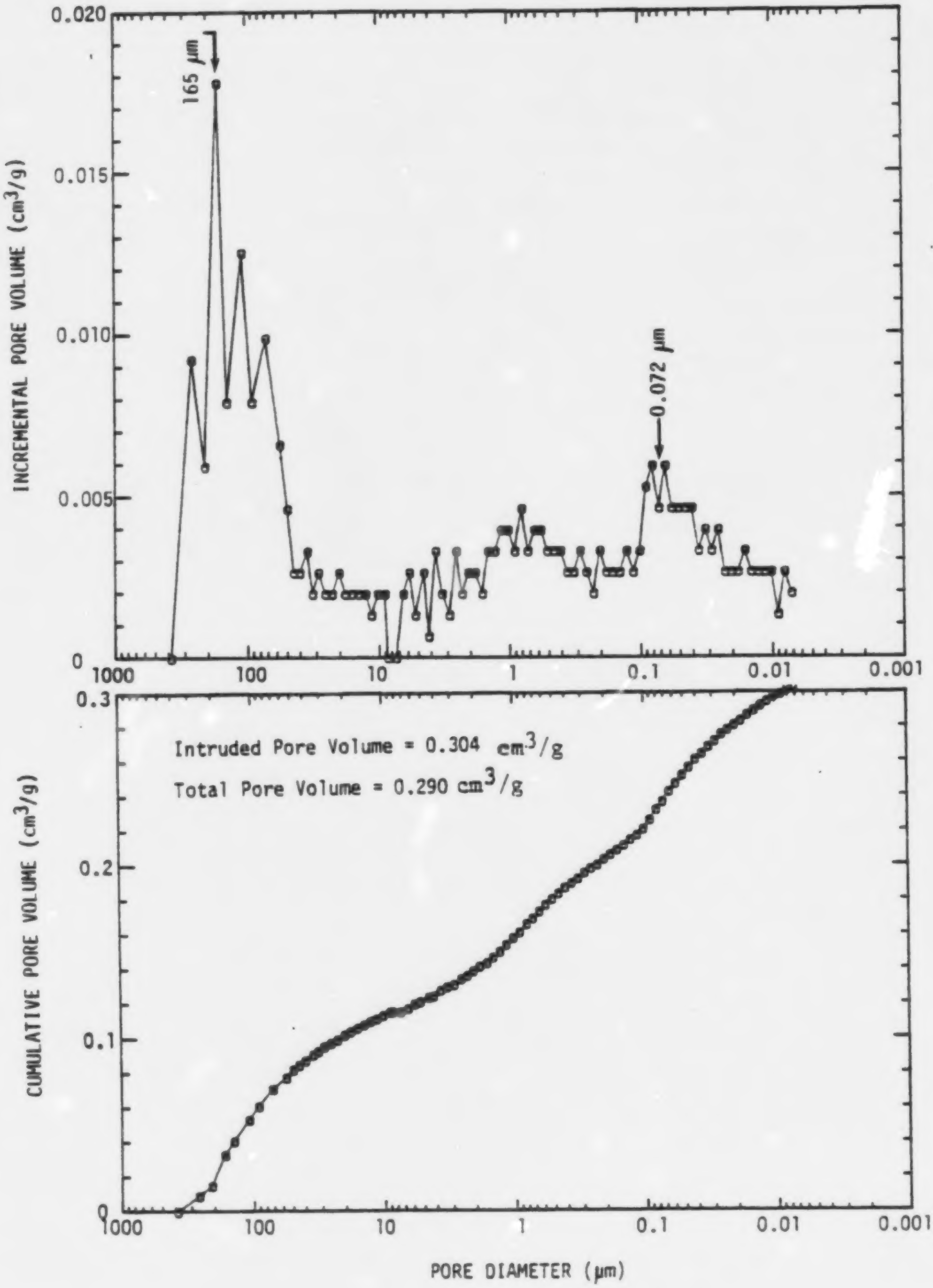

FIGURE J.25 PORE SIZE DISTRIBUTION FOR BROWN SARNIA CLAY MIXED WITH 80% DIOXANE - 20% WATER

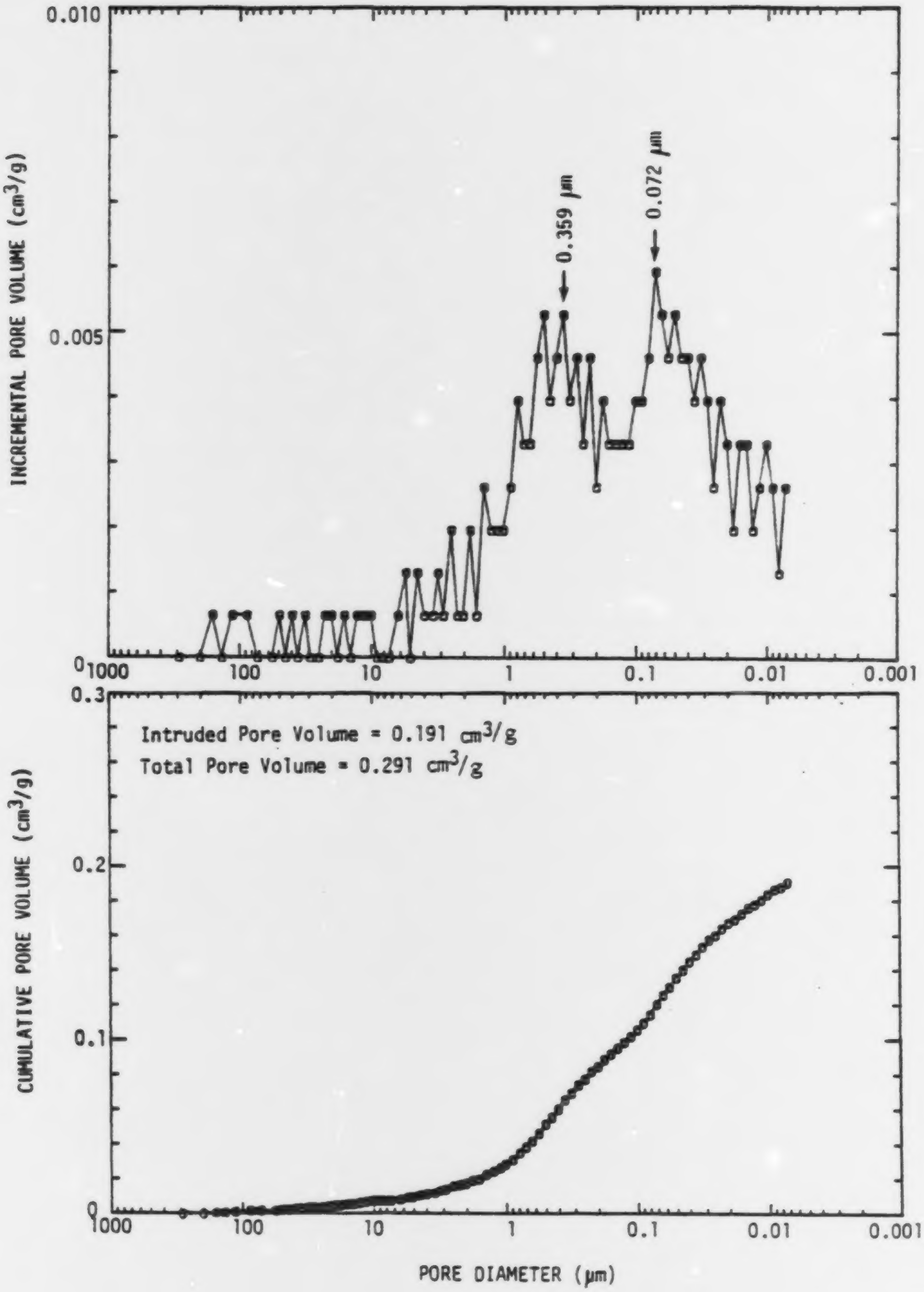

FIGURE J.26 PORE SIZE DISTRIBUTION FOR BROWN SARNIA CLAY MIXED WITH 100% DIOXANE

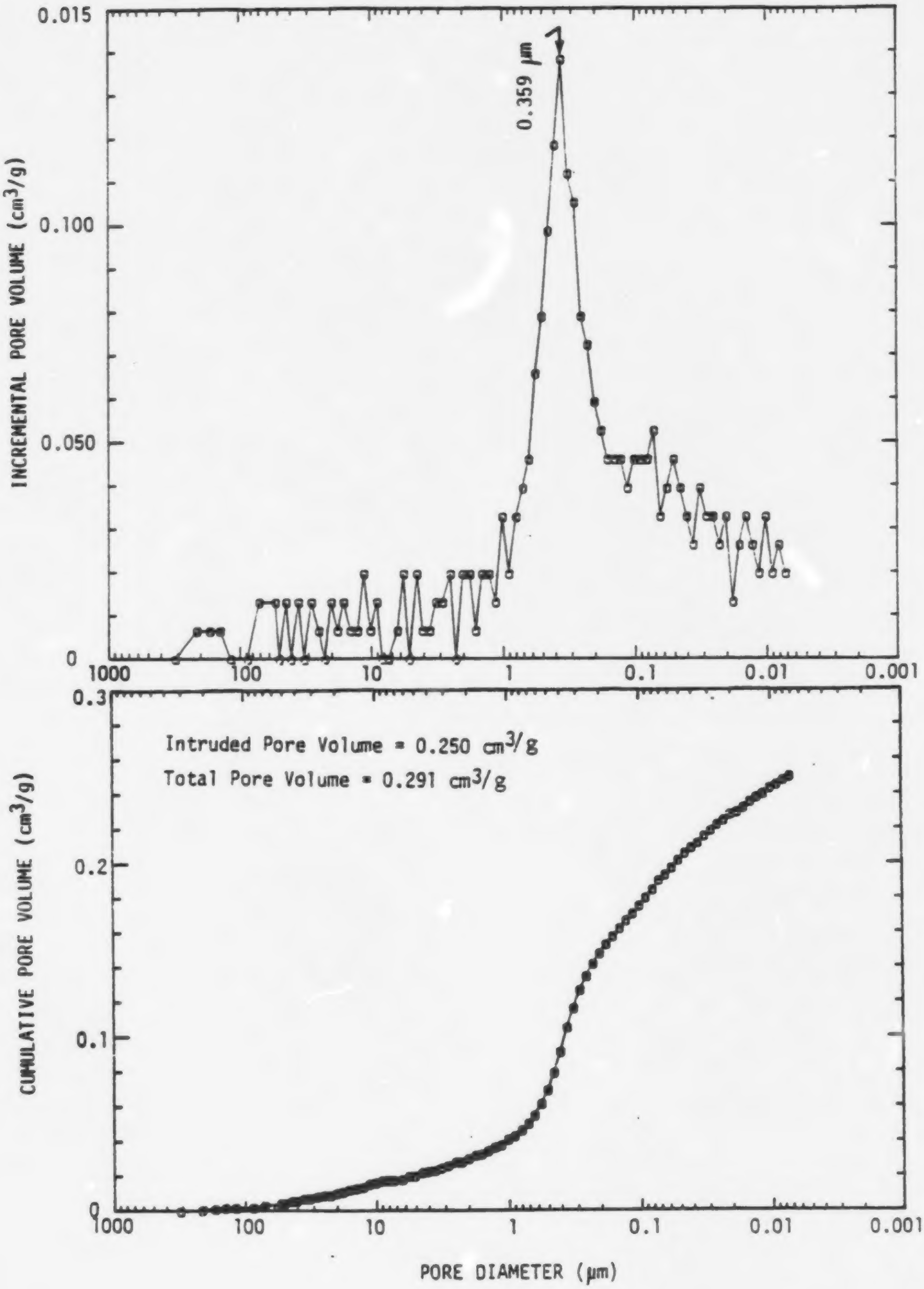

FIGURE J.27 PORE SIZE DISTRIBUTION FOR BROWN SARNIA CLAY MIXED WITH 20% DIOXANE - 80% LEACHATE

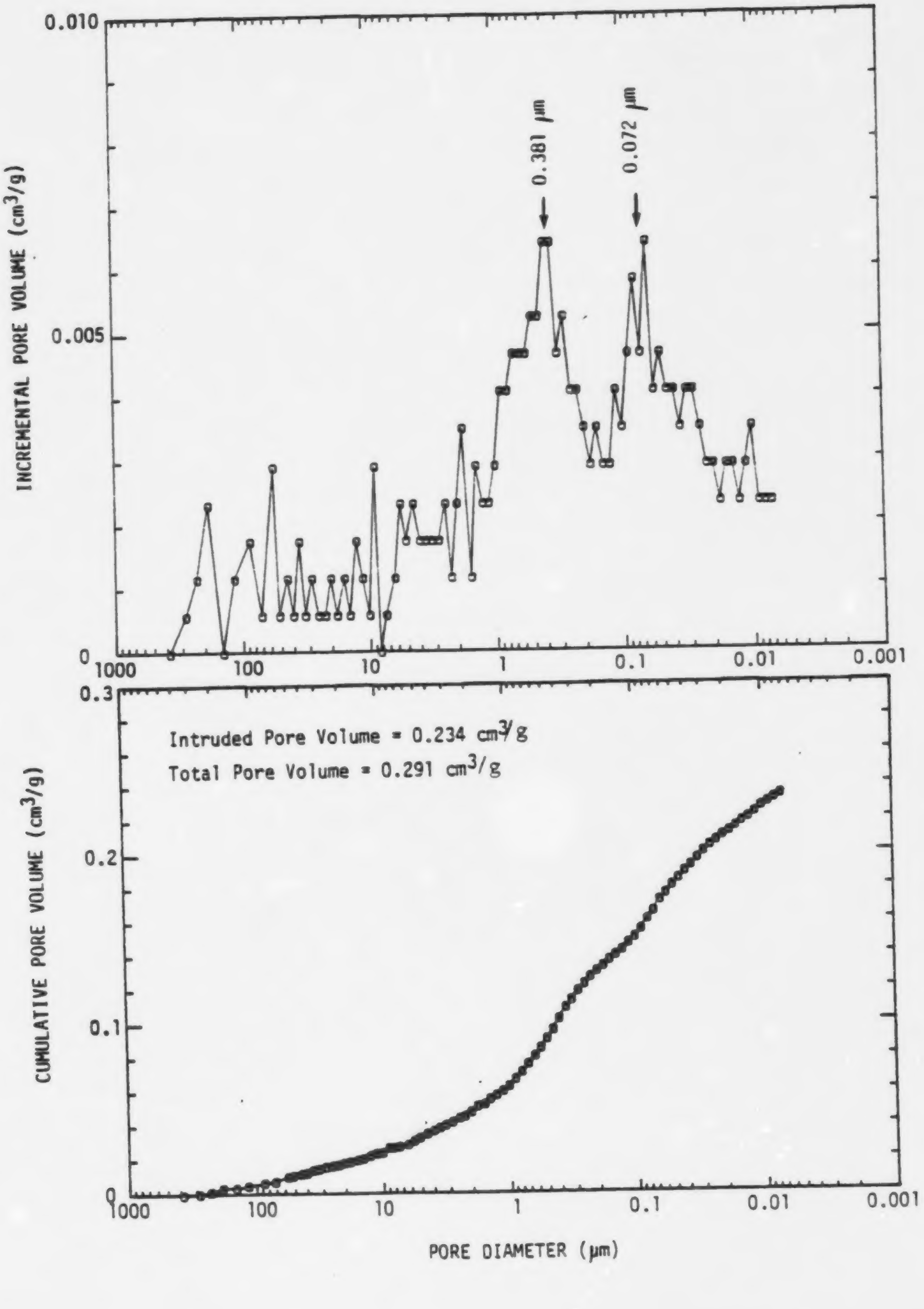

FIGURE J.28 PORE SIZE DISTRIBUTION FOR BROWN SARNIA CLAY MIXED WITH 50% DIOXANE - 50% LEACHATE

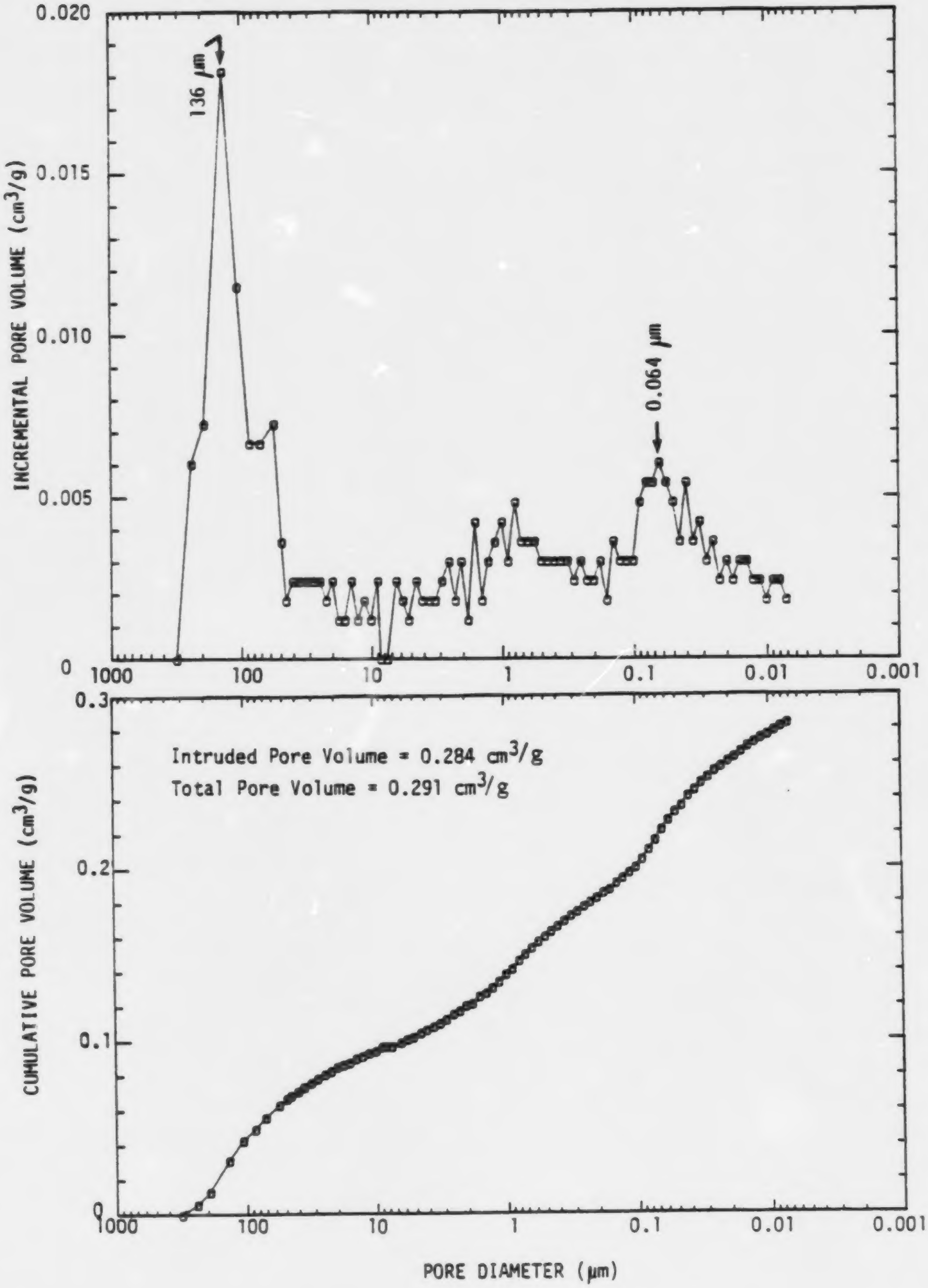

FIGURE J.29 PORE SIZE DISTRIBUTION FOR BROWN SARNIA CLAY MIXED WITH 80% DIOXANE - 20% LEACHATE

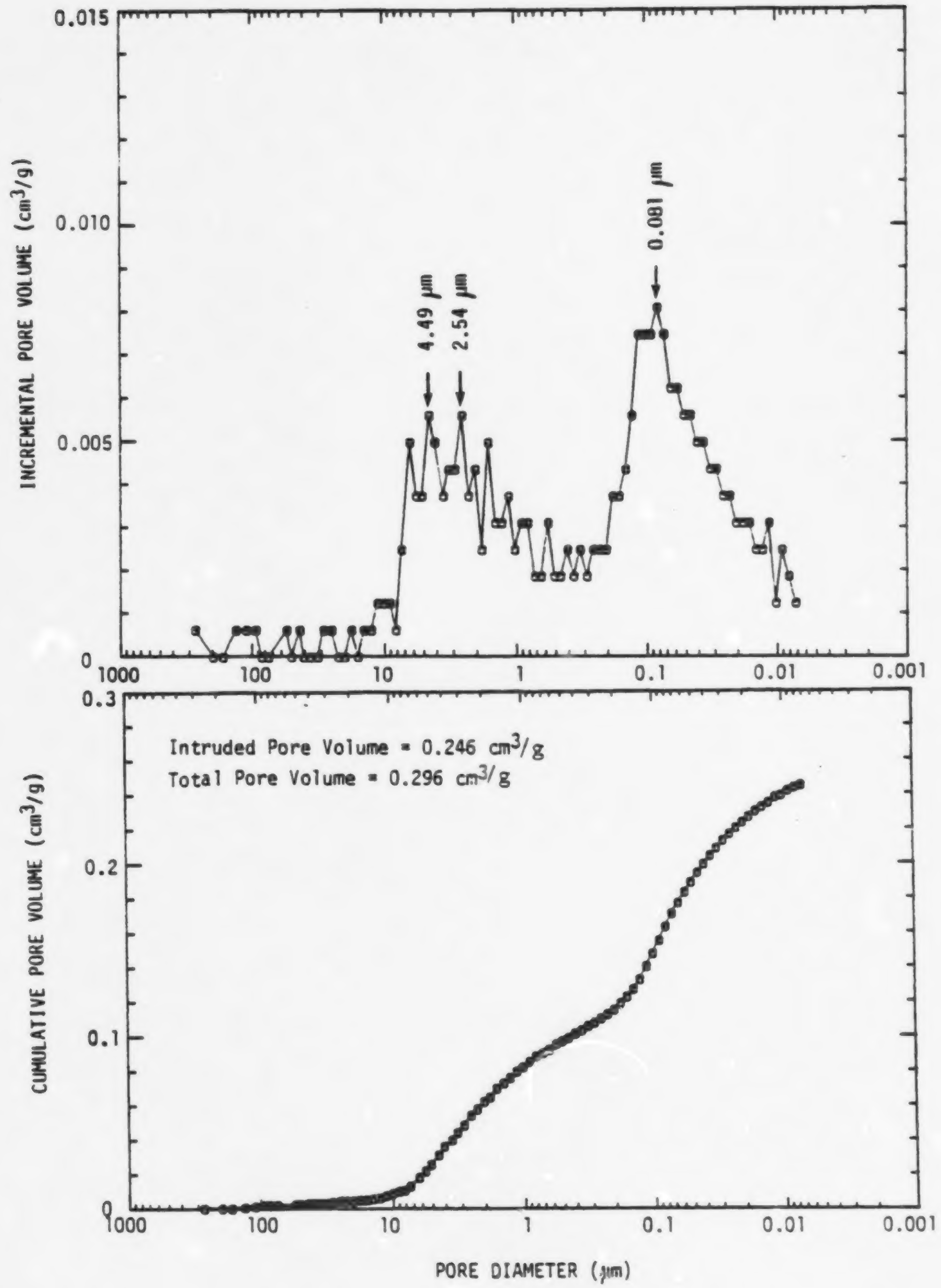

FIGURE J.30 PORE SIZE DISTRIBUTION FOR WATER-COMPACTED BROWN SARNIA CLAY

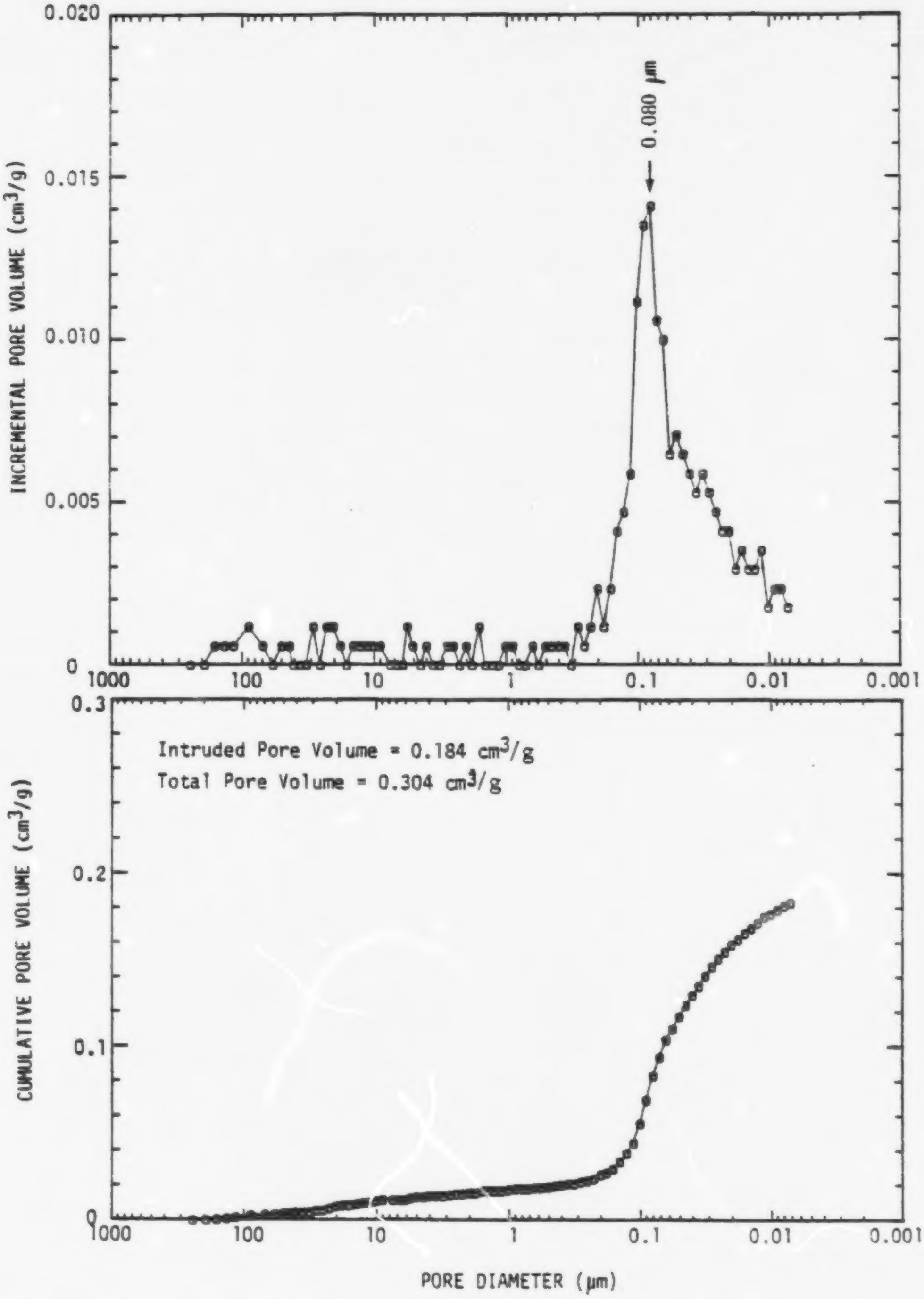

FIGURE J.31 PORE SIZE DISTRIBUTION FOR WATER-COMPACTED BROWN SARNIA CLAY PERMEATED WITH 20% ETHANOL - 80% LEACHATE

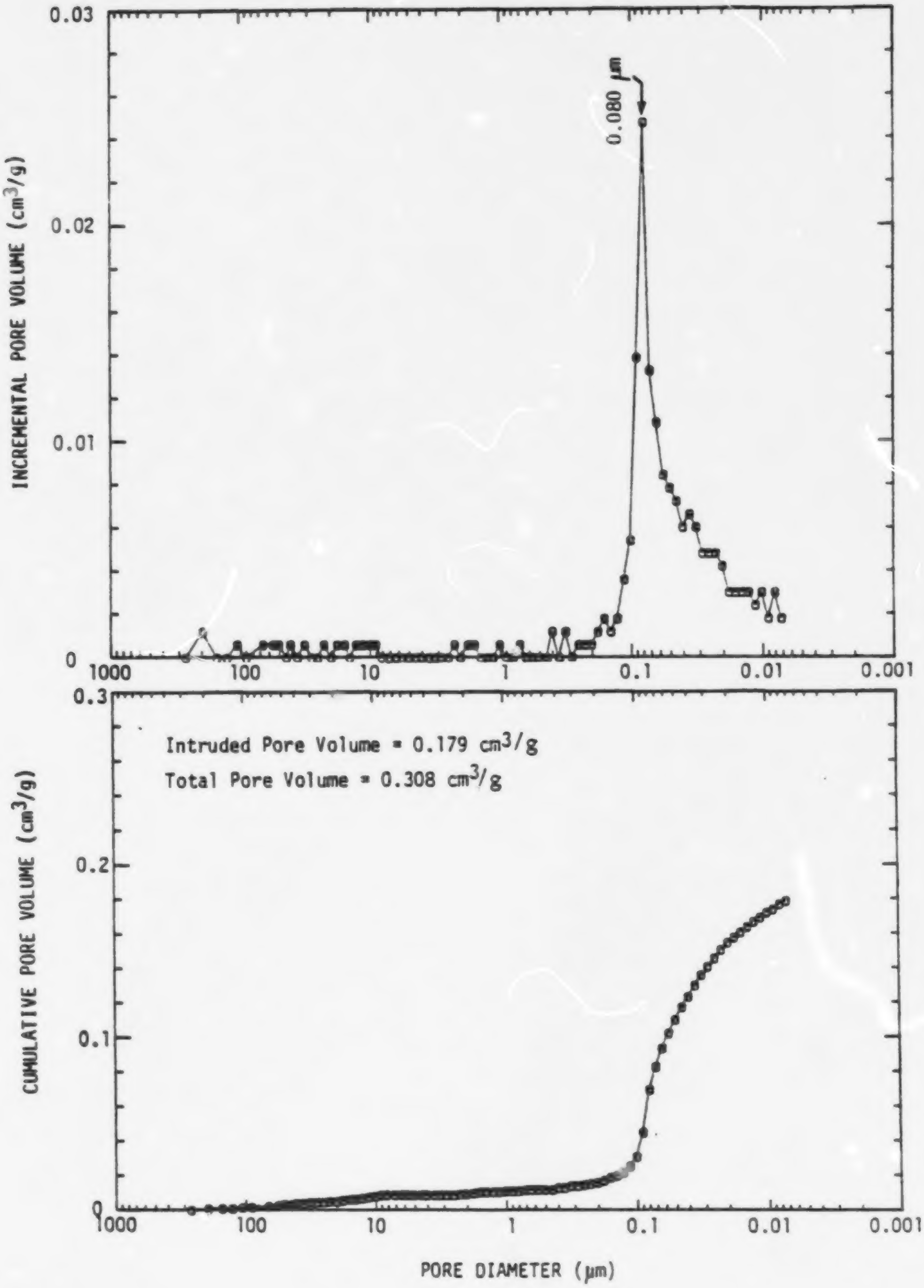

FIGURE J.32 PORE SIZE DISTRIBUTION FOR WATER-COMPACTED BROWN SARNIA CLAY PERMEATED WITH 40% ETHANOL - 60% LEACHATE

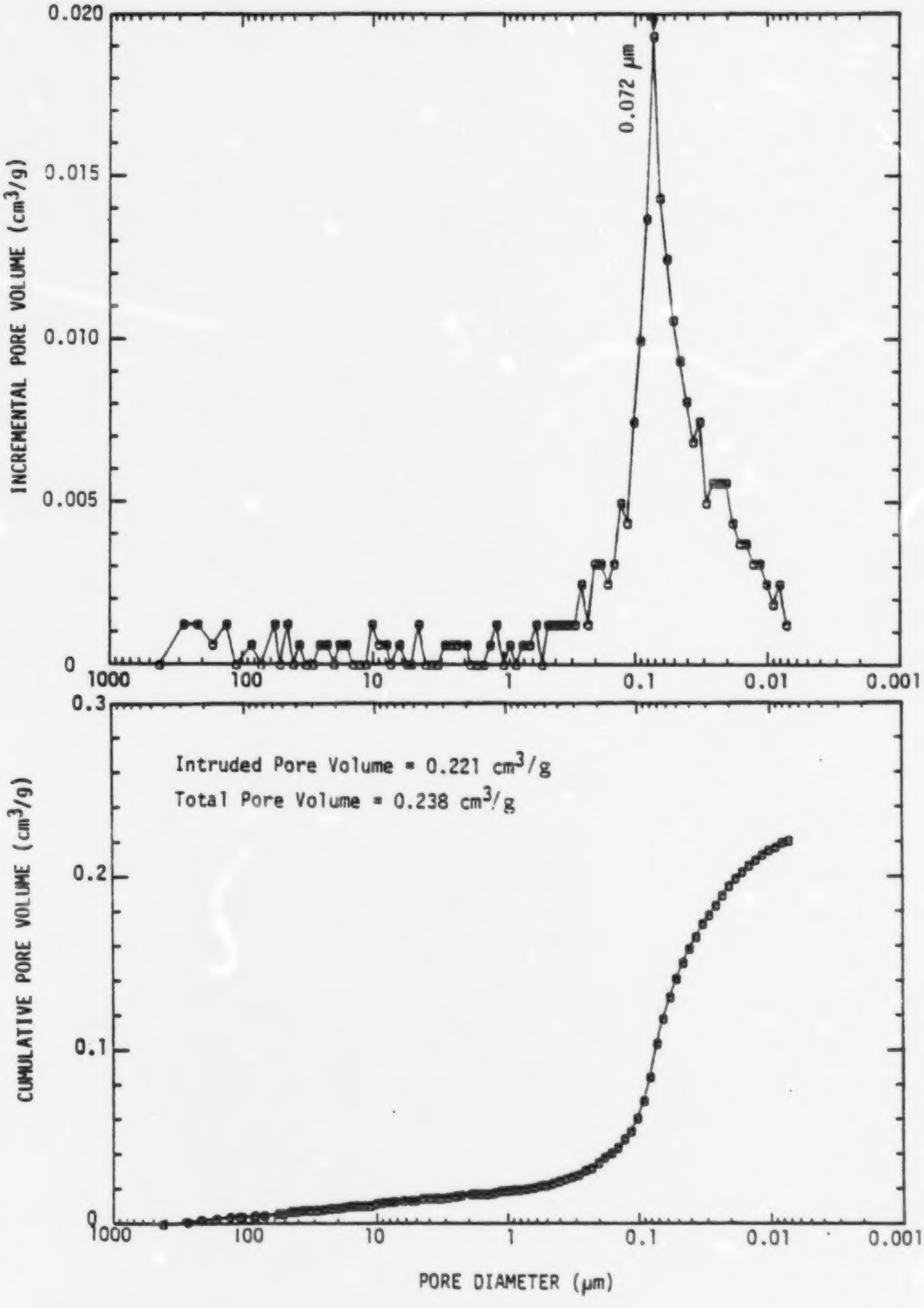

FIGURE J.33 PORE SIZE DISTRIBUTION FOR WATER-COMPACTED BROWN SARNIA CLAY PERMEATED WITH 100% ETHANOL (σ'_v = 0)

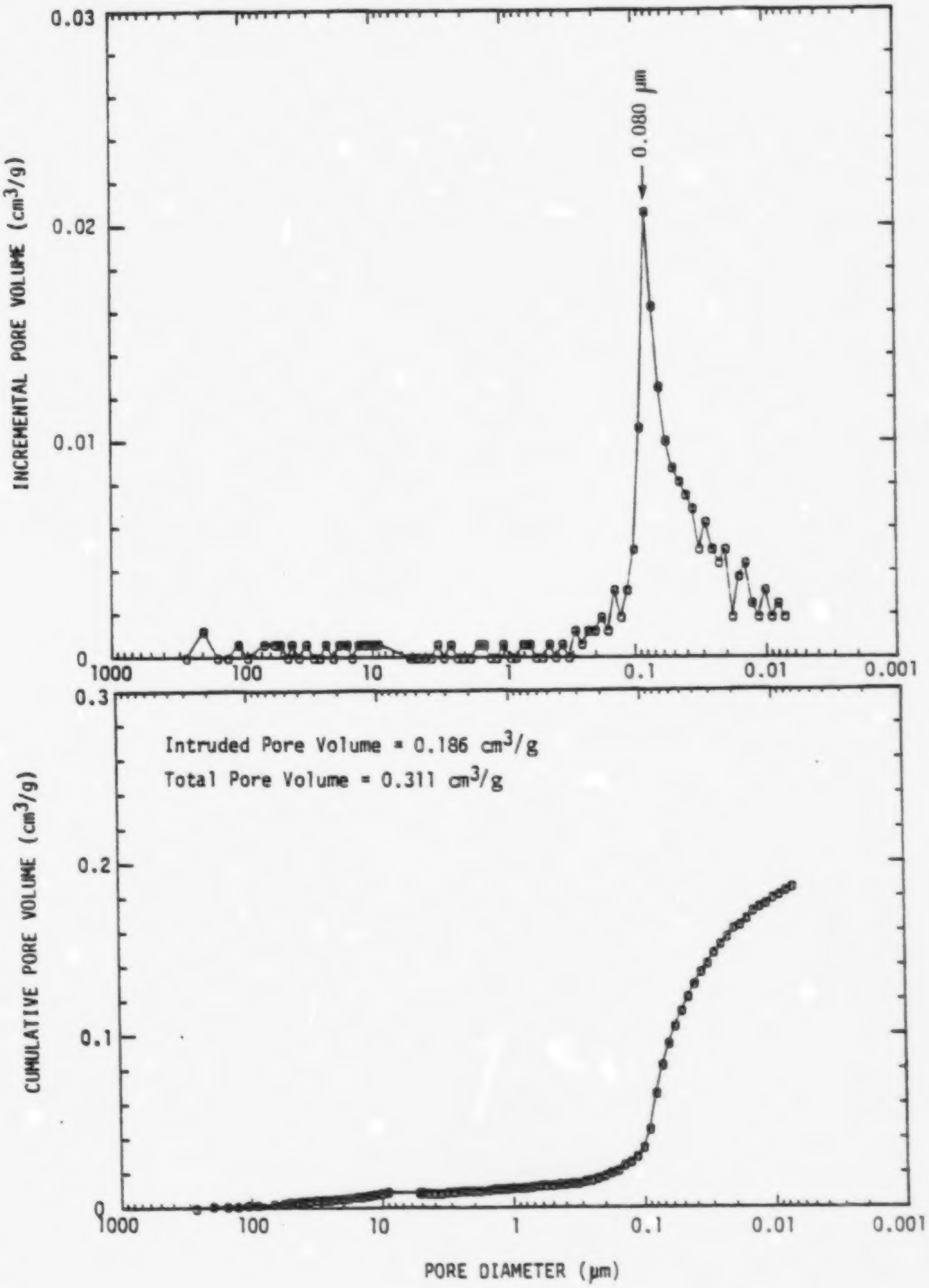

FIGURE J.34 PORE SIZE DISTRIBUTION FOR WATER-COMPACTED BROWN SARNIA CLAY PERMEATED WITH 100% ETHANOL (σ'_v = 0)

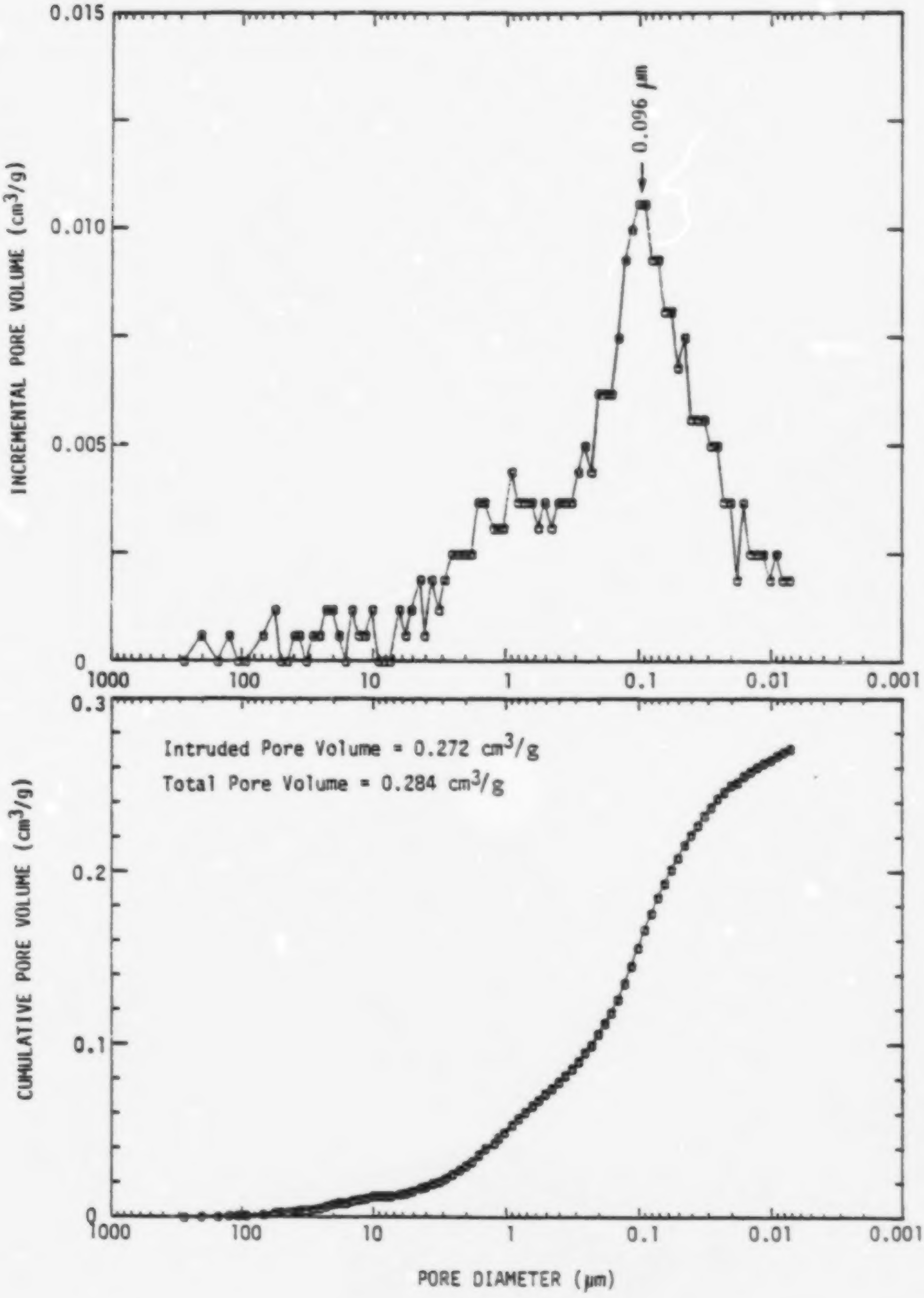

FIGURE J.35 PORE SIZE DISTRIBUTION FOR WATER-COMPACTED BROWN SARNIA CLAY PERMEATED WITH 10% DIOXANE - 90% LEACHATE

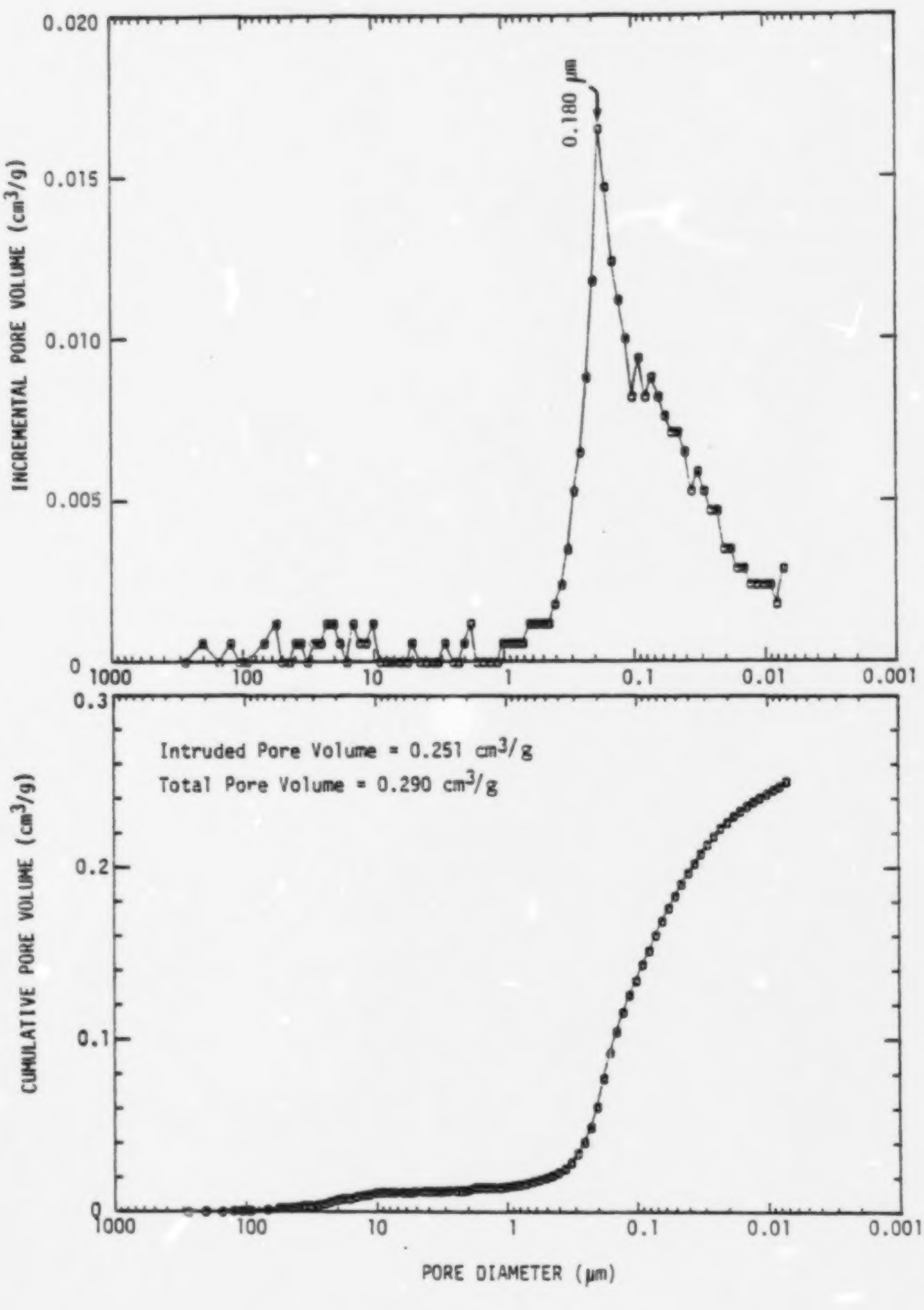

FIGURE J.36 PORE SIZE DISTRIBUTION FOR WATER-COMPACTED BROWN SARNIA CLAY PERMEATED WITH 20% DIOXANE - 80% LEACHATE

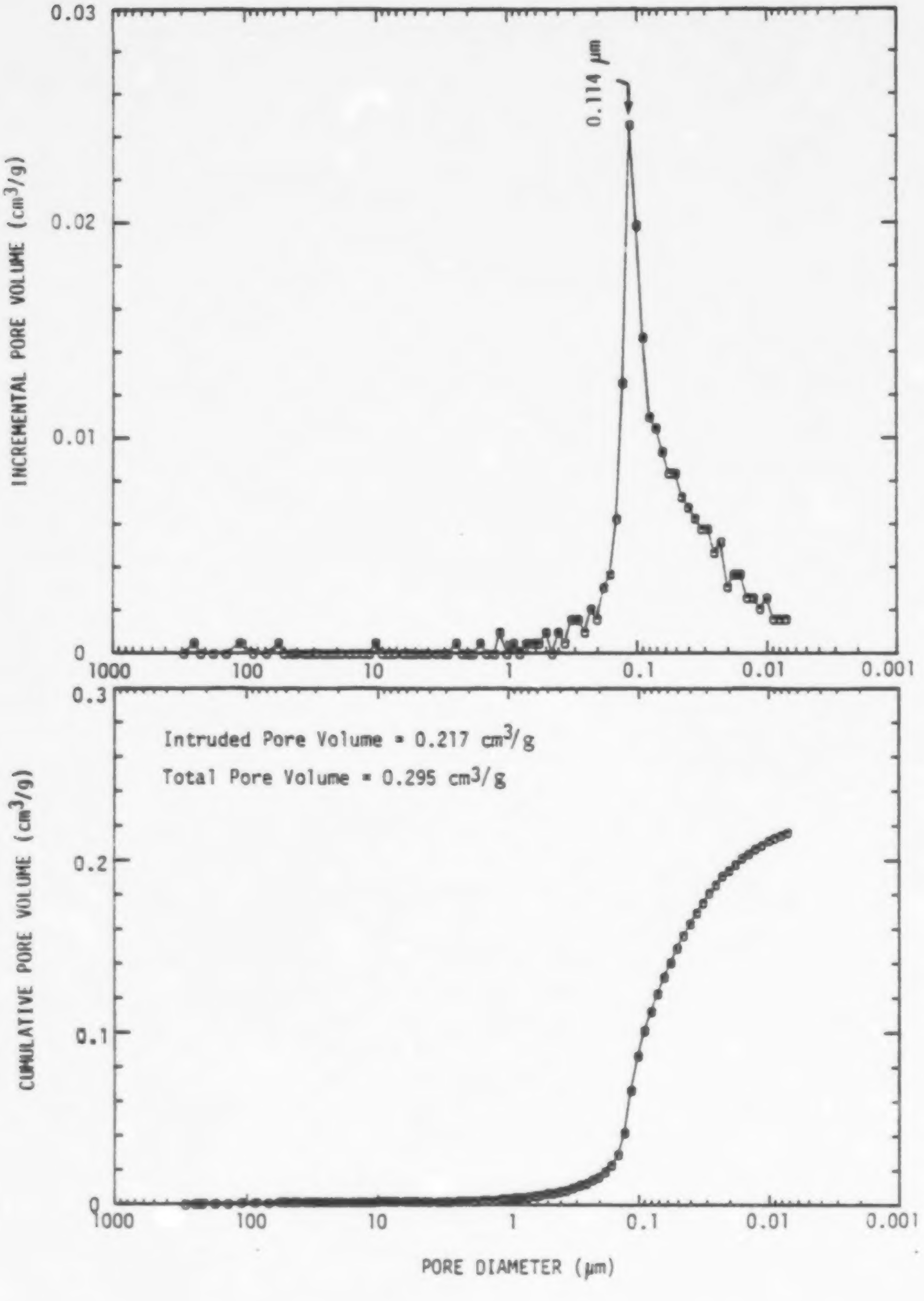

FIGURE J.37 PORE SIZE DISTRIBUTION FOR WATER-COMPACTED BROWN SARNIA CLAY PERMEATED WITH 40% DIOXANE - 60% LEACHATE

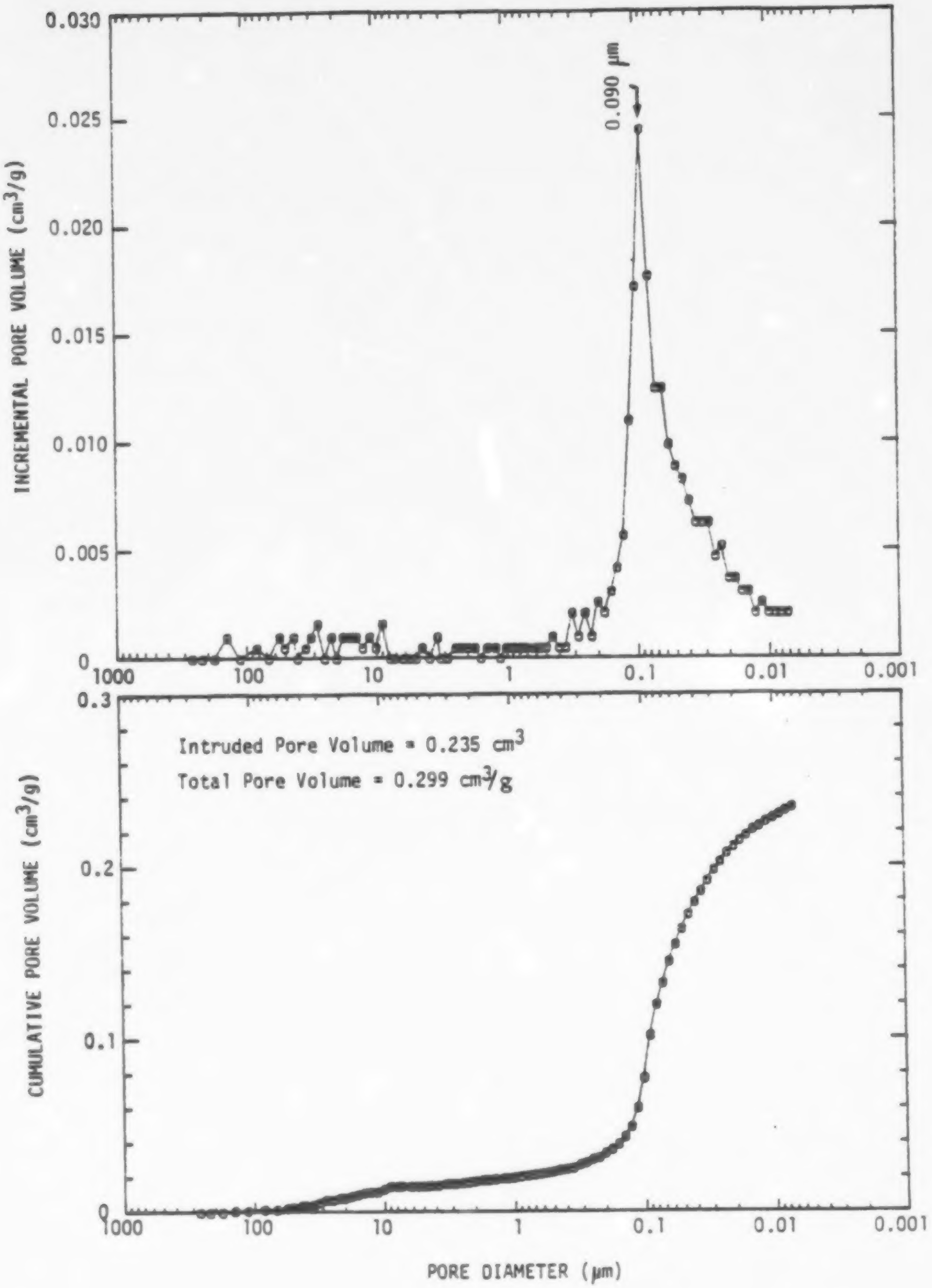

FIGURE J.38 PORE SIZE DISTRIBUTION FOR WATER-COMPACTED BROWN SARNIA CLAY PERMEATED WITH 70% DIOXANE - 30% LEACHATE

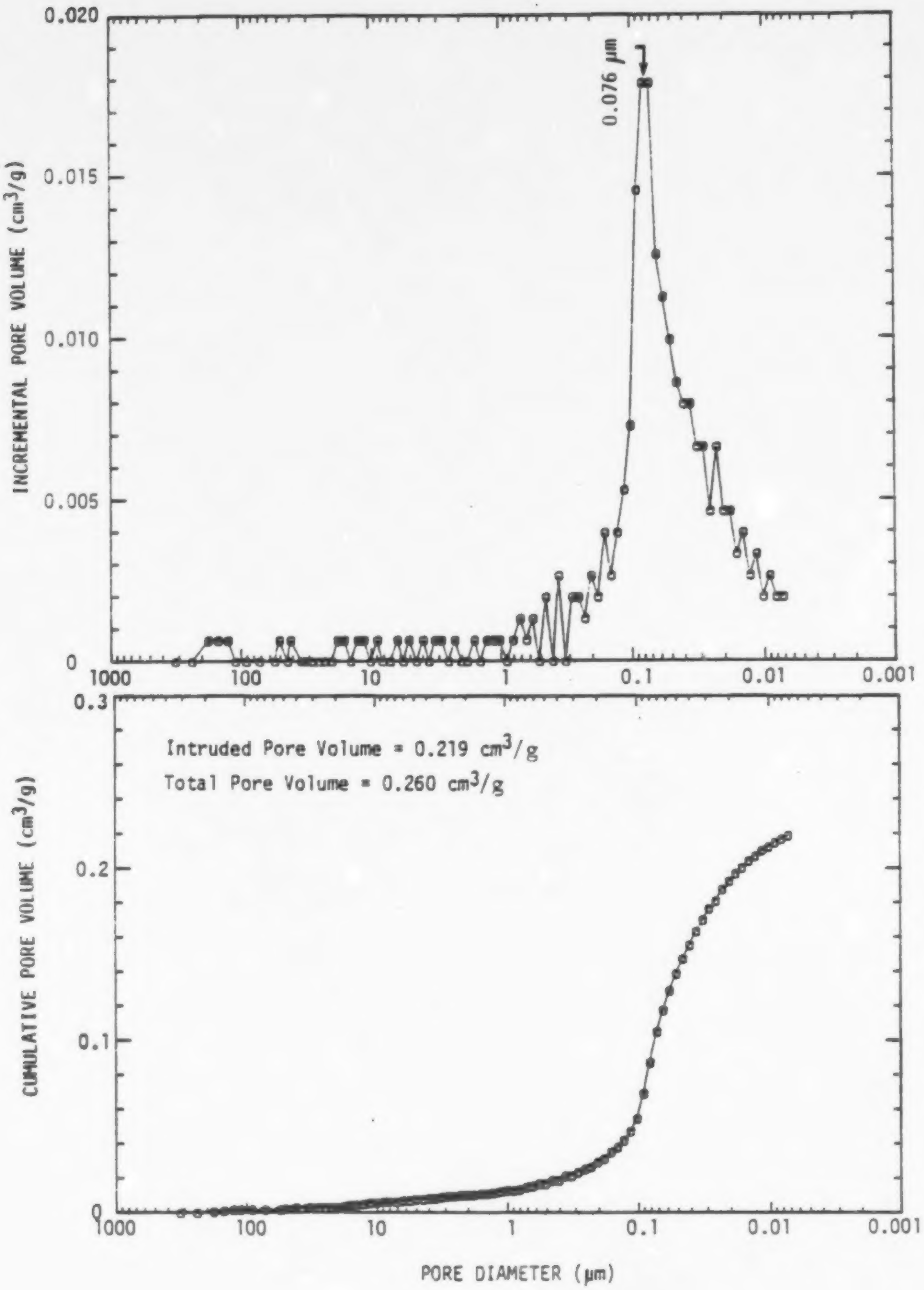

FIGURE J.39 PORE SIZE DISTRIBUTION FOR WATER-COMPACTED BROWN SARNIA CLAY PERMEATED WITH 100% DIOXANE (σ'_v = 0)

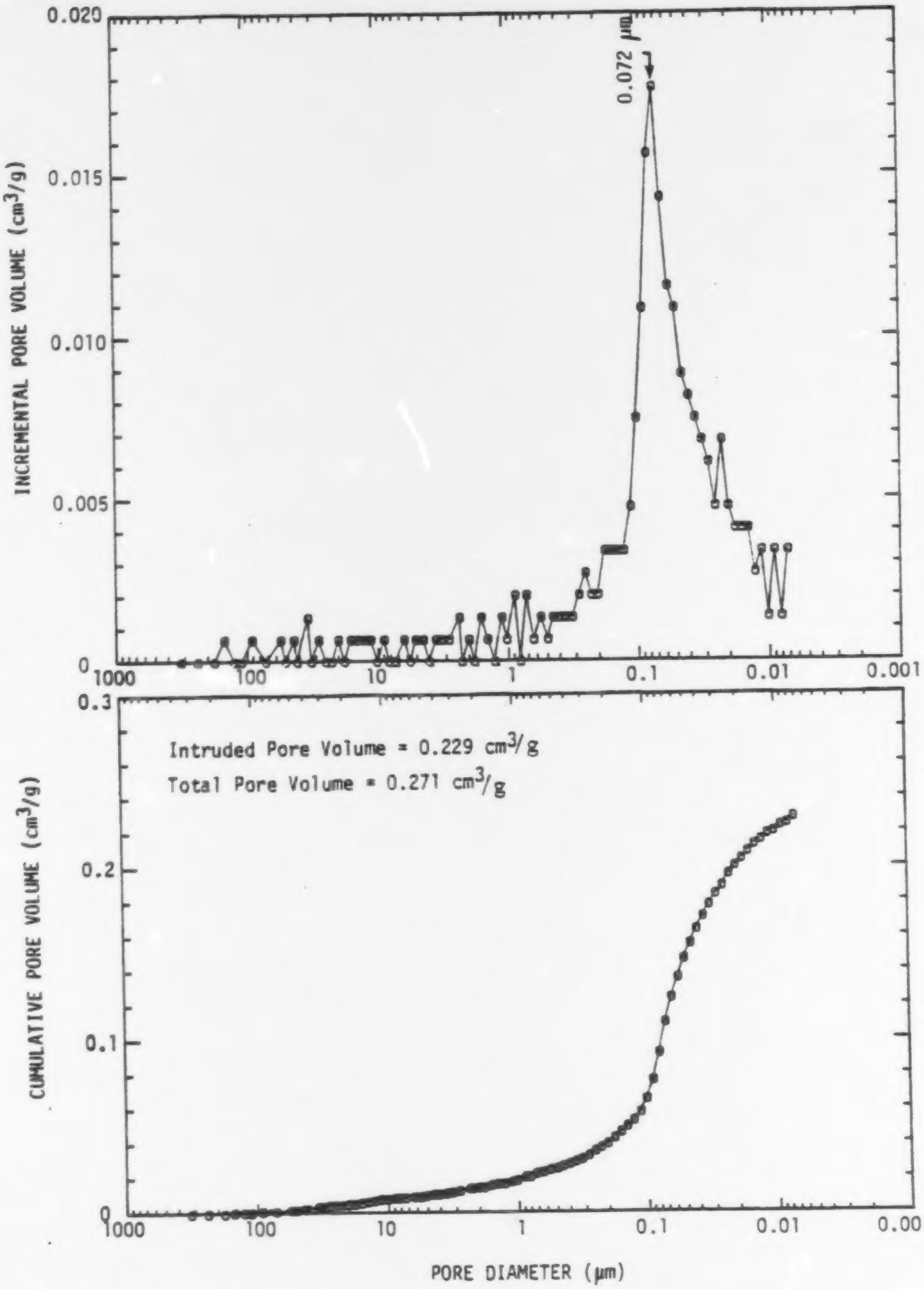

FIGURE J.40 PORE SIZE DISTRIBUTION FOR WATER-COMPACTED BROWN SARNIA CLAY PERMEATED WITH 100% DIOXANE (σ'_v = 40 kPa)

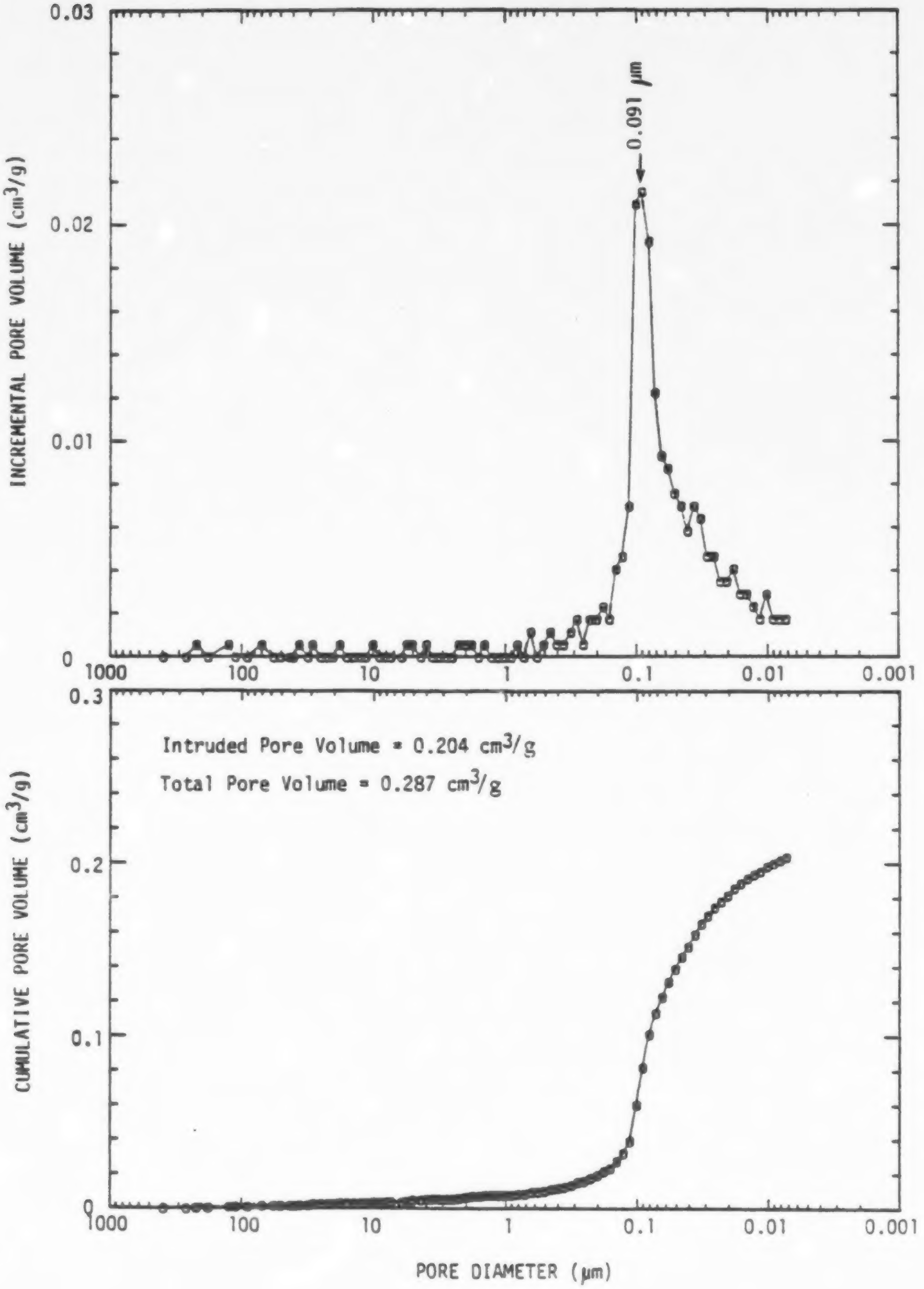

FIGURE J.41 PORE SIZE DISTRIBUTION FOR WATER-COMPACTED BROWN SARNIA CLAY PERMEATED WITH 40% DIOXANE - 60% LEACHATE (σ'_v = 80 kPa)

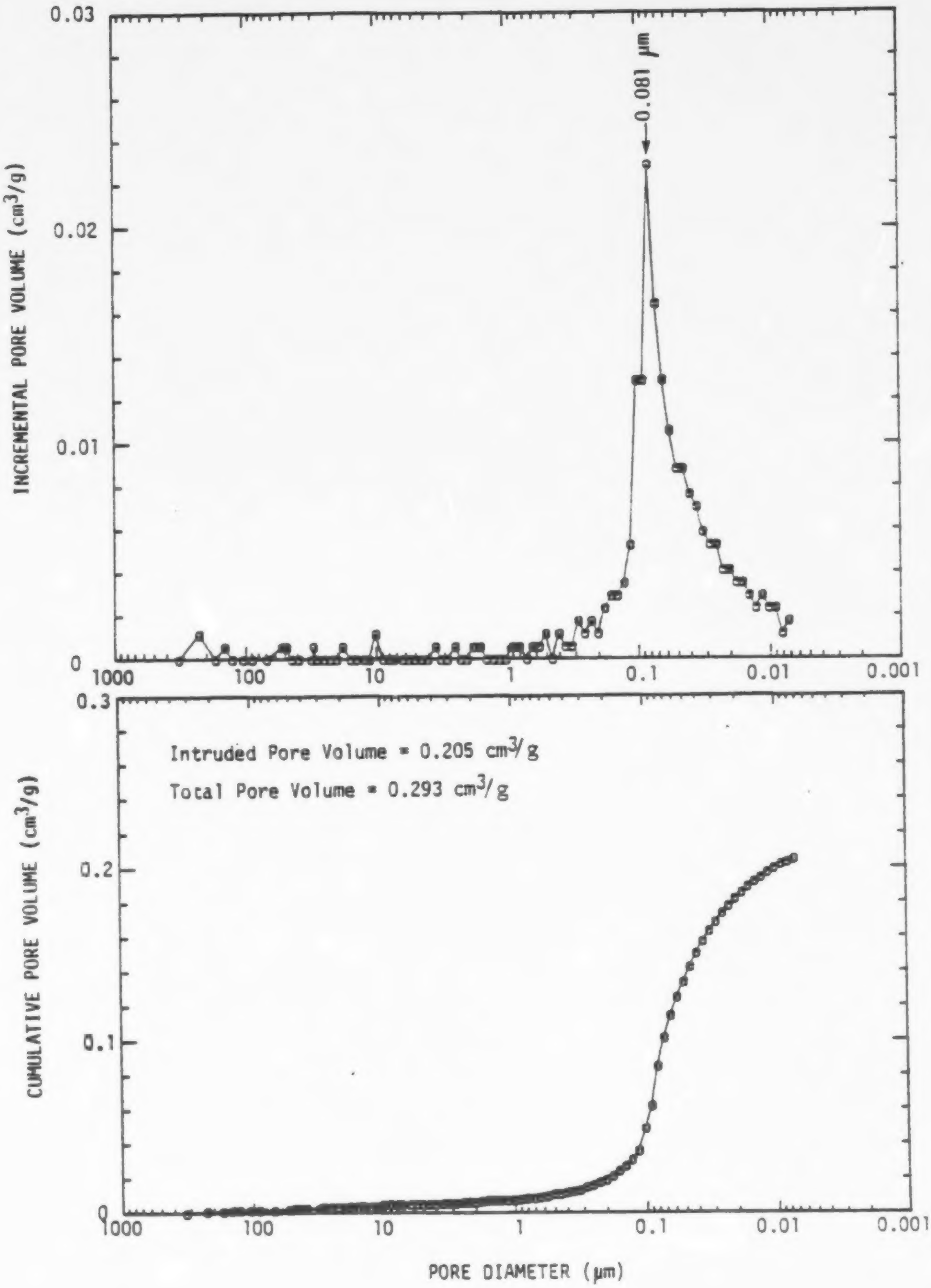

FIGURE J.42 PORE SIZE DISTRIBUTION FOR WATER-COMPACTED BROWN SARNIA CLAY PERMEATED WITH 80% DIOXANE - 20% LEACHATE (σ'_v = 80 kPa)

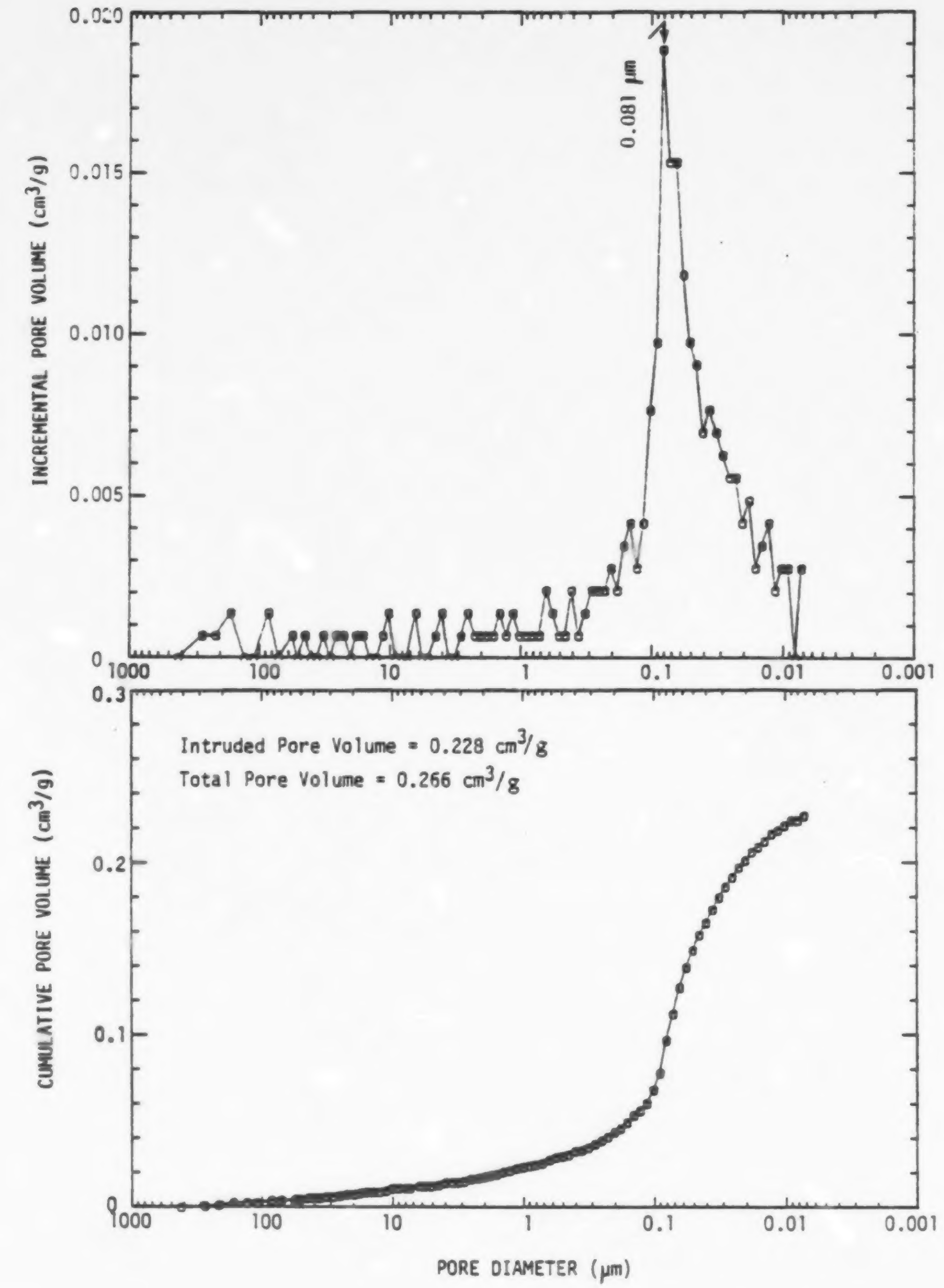

FIGURE J.43 PORE SIZE DISTRIBUTION FOR WATER-COMPACTED BROWN SARNIA CLAY PERMEATED WITH 100% DIOXANE (σ'_v = 80 kPa)

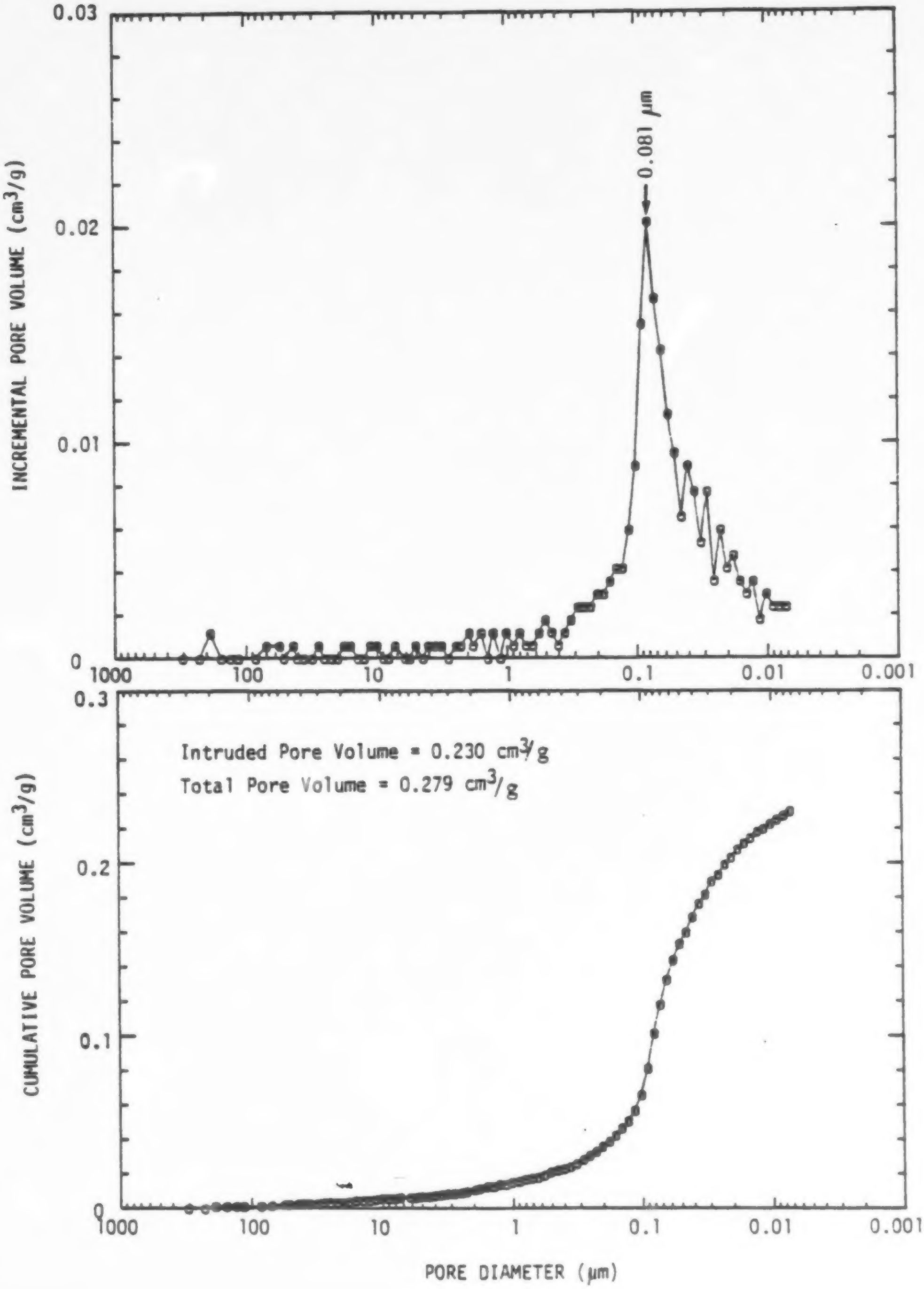

FIGURE J.44 PORE SIZE DISTRIBUTION FOR WATER-COMPACTED BROWN SARNIA CLAY PERMEATED WITH 100% DIOXANE (σ'_v = 120 kPa)

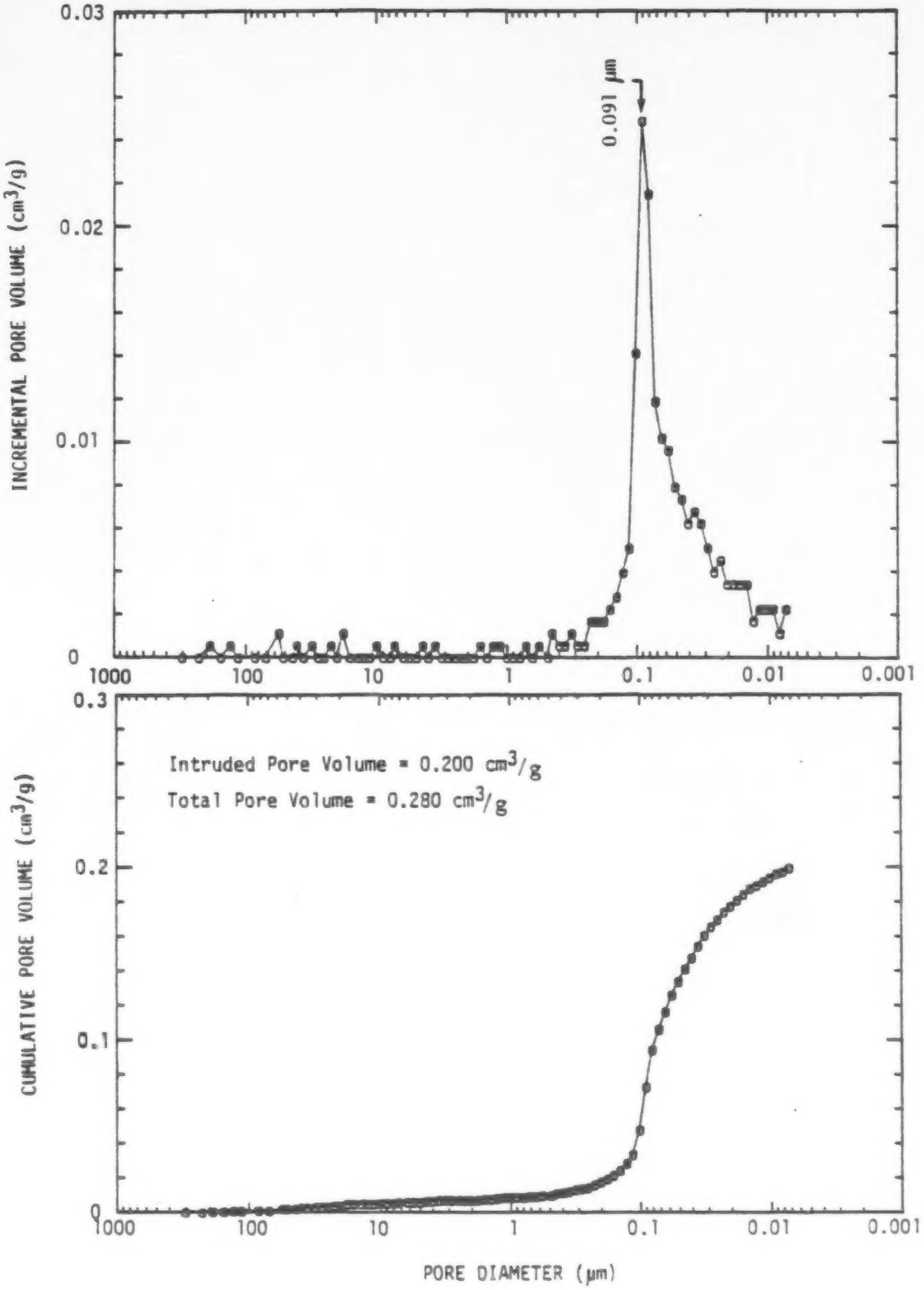

FIGURE J.45 PORE SIZE DISTRIBUTION FOR WATER-COMPACTED BROWN SARNIA CLAY PERMEATED WITH 40% DIOXANE - 60% LEACHATE (σ'_v = 160 kPa)

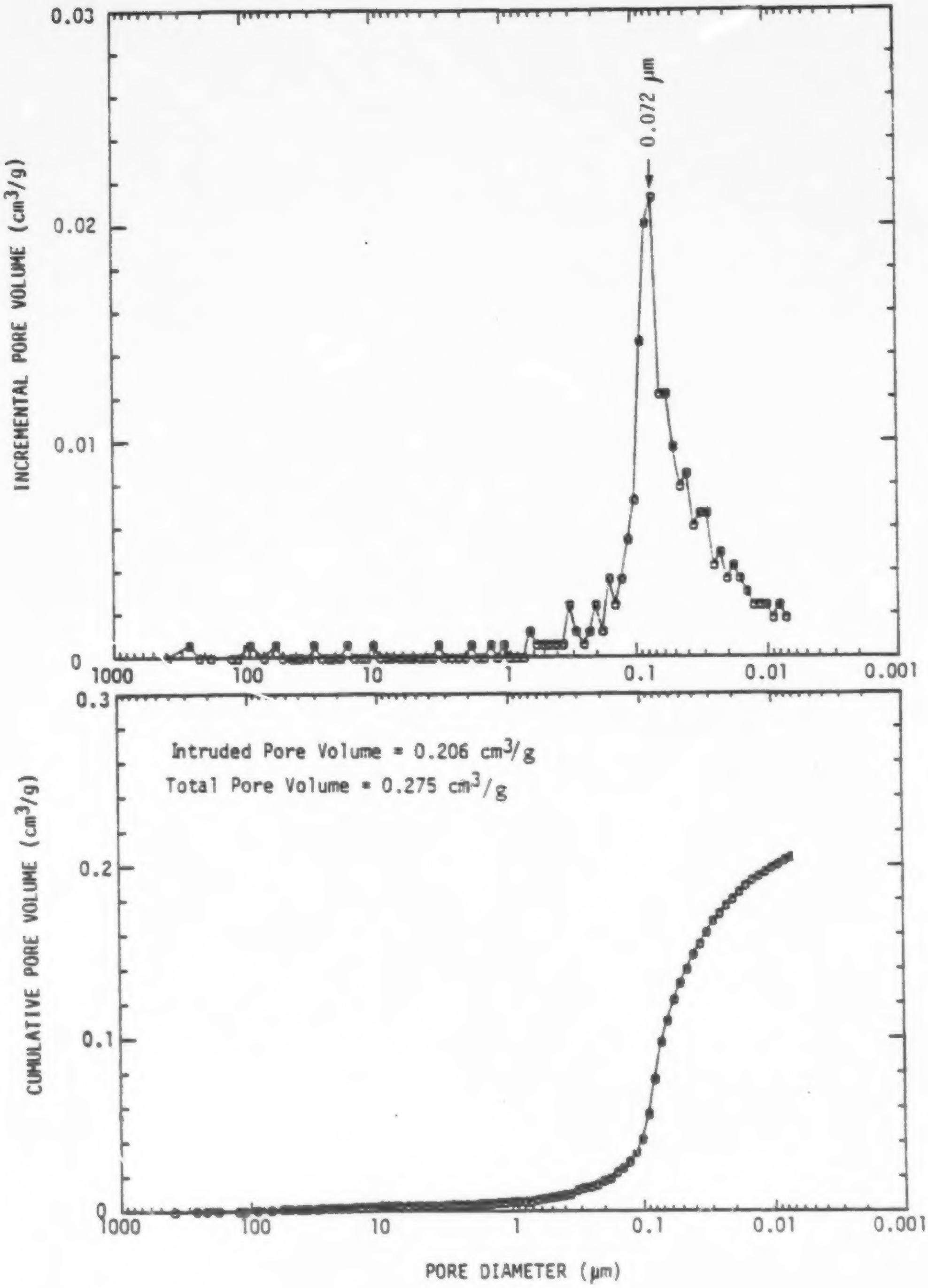

FIGURE J.46 PORE SIZE DISTRIBUTION FOR WATER-COMPACTED BROWN SARNIA CLAY PERMEATED WITH 80% DIOXANE - 20% LEACHATE (σ'_v = 160 kPa)

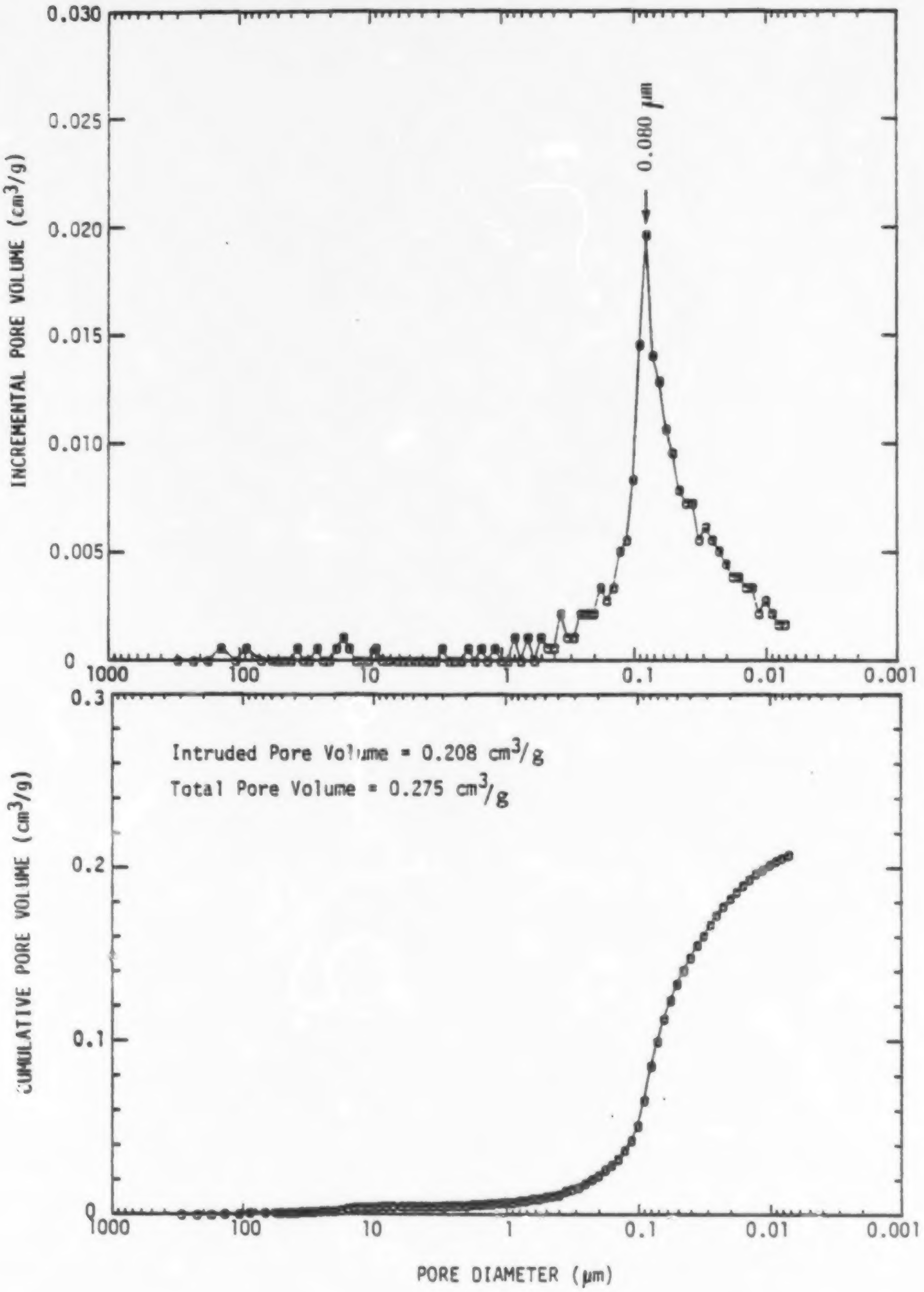

FIGURE J.47 PORE SIZE DISTRIBUTION FOR WATER-COMPACTED BROWN SARNIA CLAY PERMEATED WITH 100% DIOXANE (σ'_v = 160 kPa)

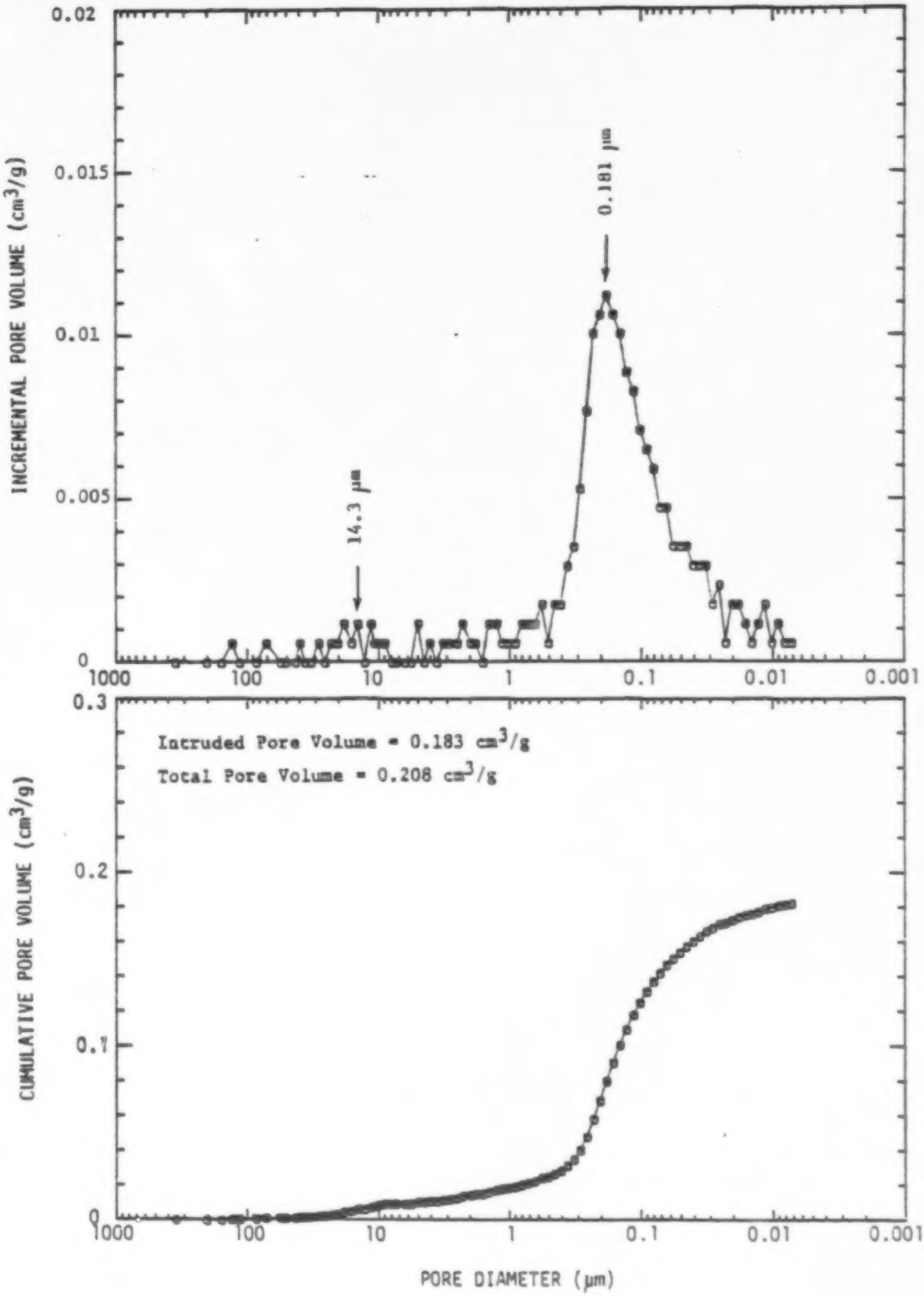

FIGURE J.48 PORE SIZE DISTRIBUTION FOR UNDISTURBED GREY SILTY CLAY (SARNIA) ($\sigma'_v = 0$)

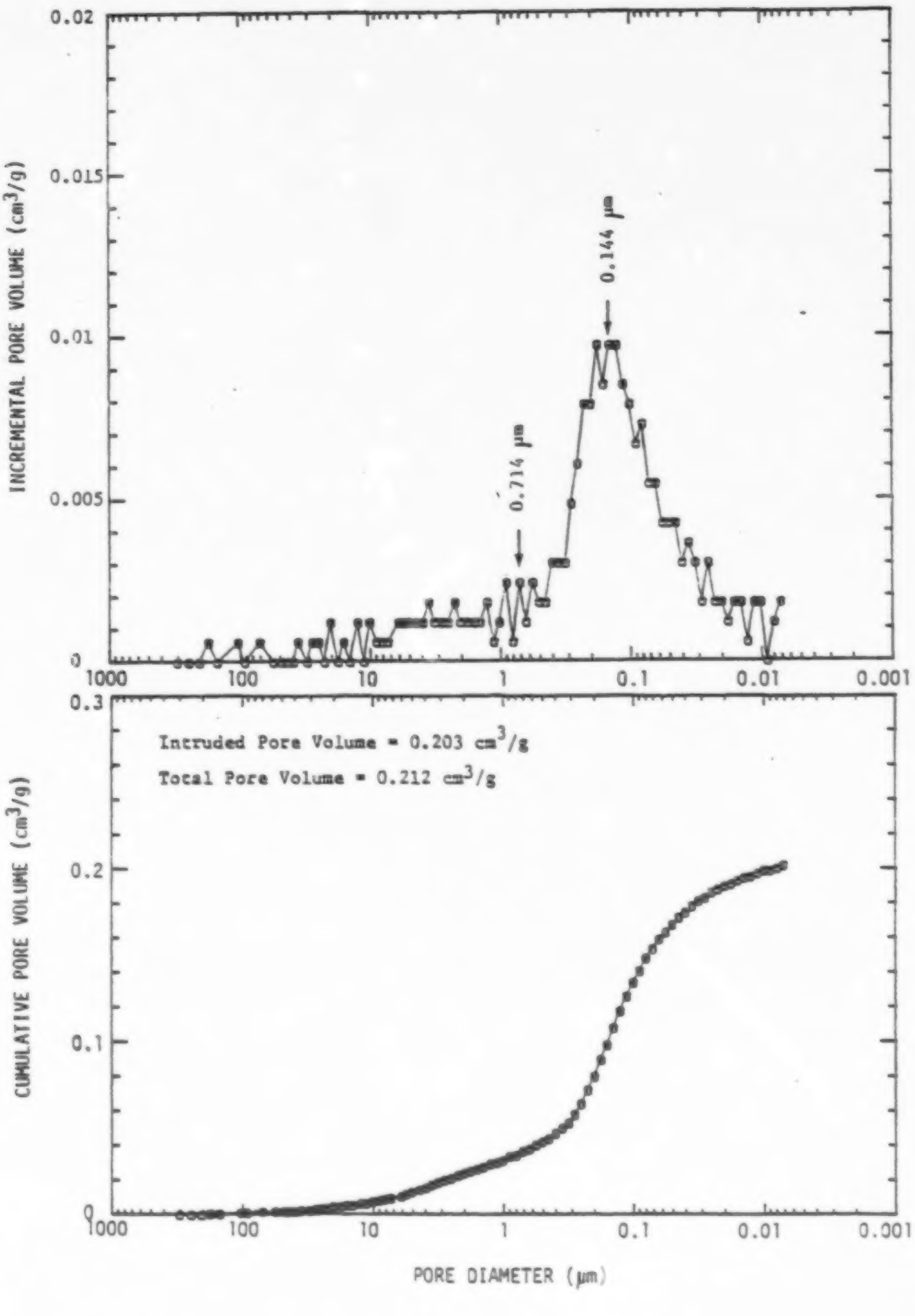

FIGURE J.49 PORE SIZE DISTRIBUTION FOR UNDISTURBED GREY SILTY CLAY (SARNIA) PERMEATED WITH 100% LEACHATE ($\sigma'_v = 0$)

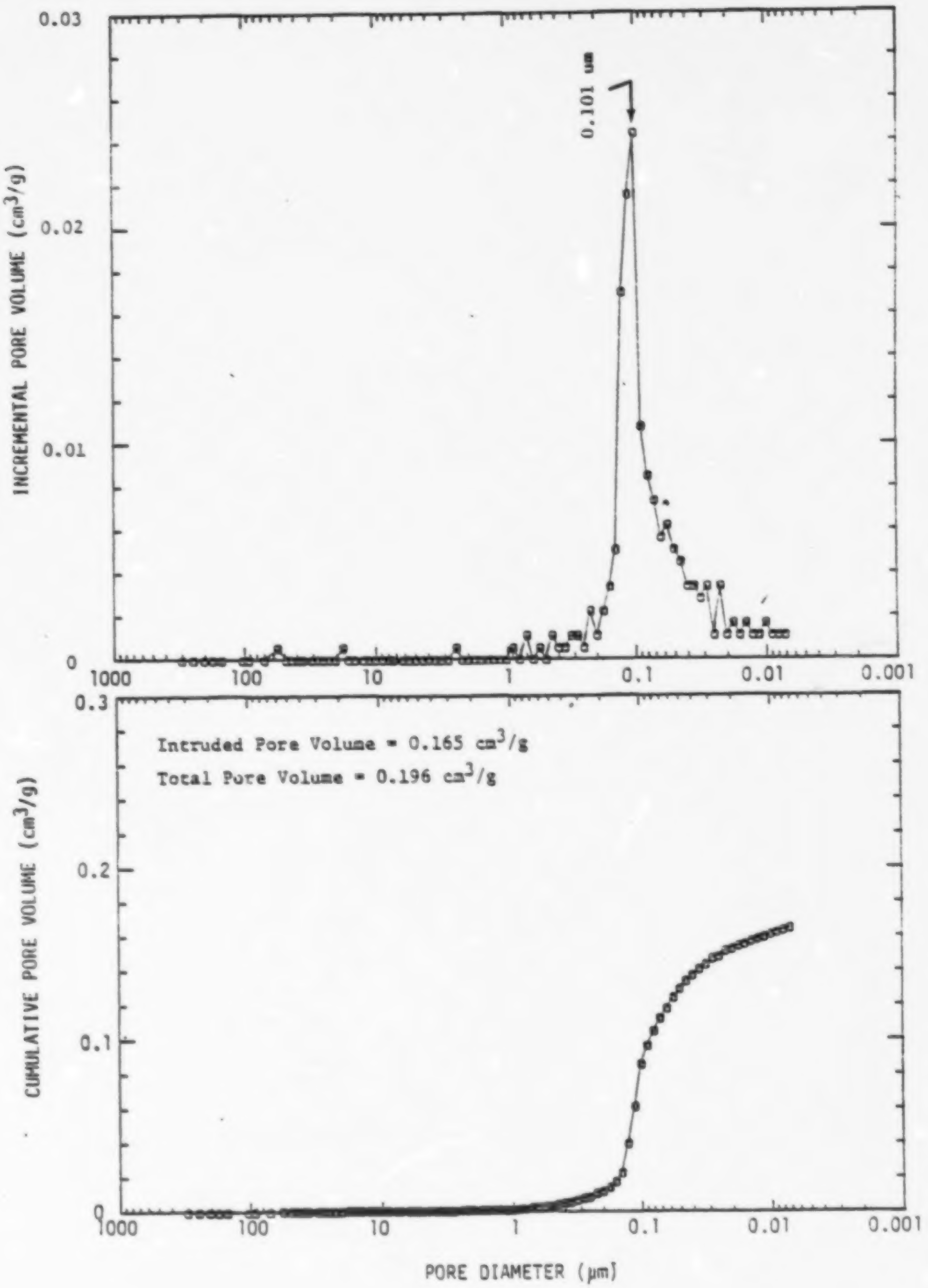

FIGURE J.50 PORE SIZE DISTRIBUTION FOR UNDISTURBED GREY SILTY CLAY (SARNIA) PERMEATED WITH 40% ETHANOL - 60% LEACHATE (σ'_v = 0)

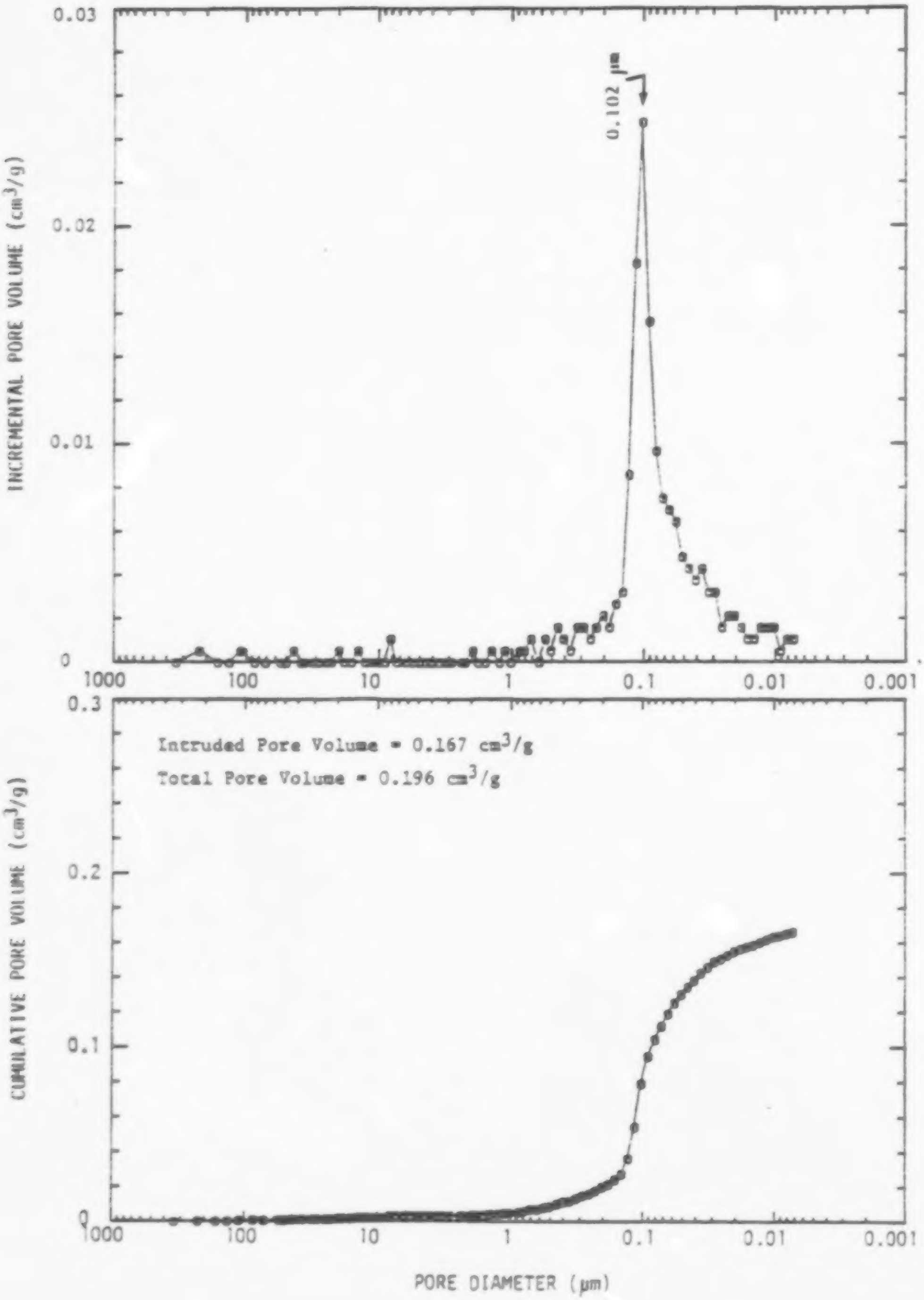

FIGURE J.51 PORE SIZE DISTRIBUTION FOR UNDISTURBED GREY SILTY CLAY (SARNIA) PERMEATED WITH 100% ETHANOL (σ'_v = 0)

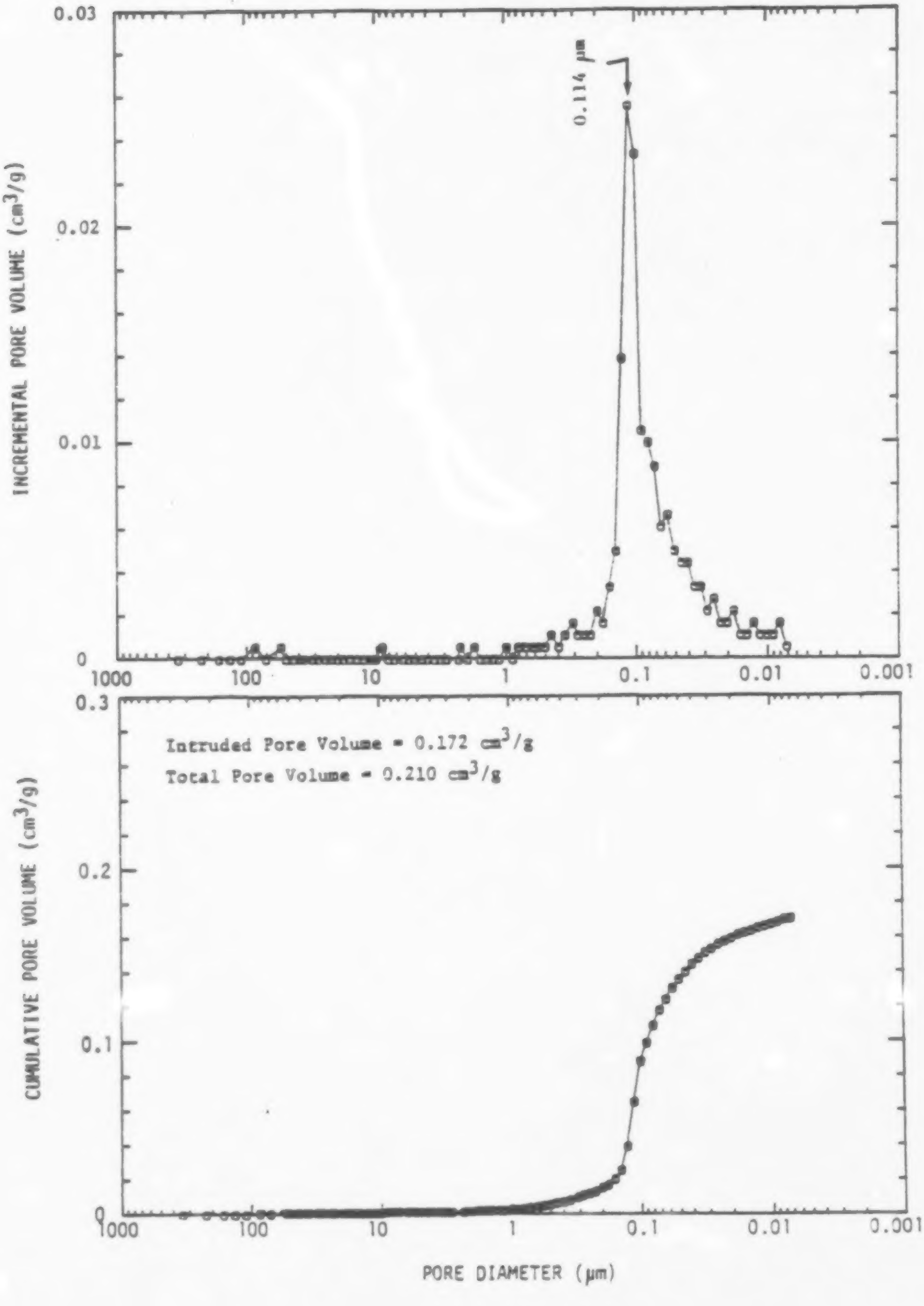

FIGURE J.52 PORE SIZE DISTRIBUTION FOR UNDISTURBED GREY SILTY CLAY (SARNIA) PERMEATED WITH 60% ETHANOL - 40% LEACHATE (σ'_v = 0)